PYRROLIDINE AND PYRROLIDINONE PEPTIDE NUCLEIC ACIDS: SYNTHESIS AND COMPARATIVE STUDIES OF THE DNA BINDING ACTIVITIES

BY

NAGENDRA KUMAR SHARMA

NATIONAL CHEMICAL LABORATORY
PUNE 411008
INDIA

OCTOBER 2005

PYRROLIDINE AND PYRROLIDINONE PEPTIDE NUCLEIC ACIDS: SYNTHESIS AND COMPARATIVE STUDIES OF THE DNA BINDING ACTIVITIES

THESIS SUBMITTED TO

THE UNIVERSITY OF PUNE

FOR THE DEGREE OF

DOCTOR OF PHILOSOPHY

IN

CHEMISTRY

BY

NAGENDRA KUMAR SHARMA

NATIONAL CHEMICAL LABORATORY
PUNE 411008
INDIA

OCTOBER 2005

CANDIDATE'S DECLARATION

I hereby declare that the thesis entitled **"Pyrrolidine and pyrrolidinone Peptide Nucleic Acids: Synthesis and Comparative studies of the DNA binding Activities"** submitted for the degree of Doctor of Philosophy in Chemistry to the University of Pune, has not been submitted by me to any other university or institution. This work was carried out at the National Chemical Laboratory, Pune, India.

Division of Organic Chemistry Synthesis

National Chemical Laboratory

Pune 411008

Nagendra Kumar Sharma

October 2005

Dr. K. N. Ganesh **FASC, FNA**
Head, Organic Chemistry division
E-MAIL: kn.ganesh@ncl.res.in

Telephone: 25902084, 25902321
Direct Telfax: 91-020-25893153

CERTIFICATE

This is to certify that the work presented in the thesis entitled **"Pyrrolidine and pyrrolidinone Peptide Nucleic Acids: Synthesis and Comparative studies of the DNA binding Activities"** submitted by Nagendra Kumar Sharma, was carried out by the candidate at the National Chemical Laboratory Pune, under my supervision. Such materials as obtained from other sources have been duly acknowledged in the thesis.

K. N. Ganesh **October 2005**

Research guide
Head of Division
Division of Organic Chemistry (Synthesis)
National Chemical Laboratory
Pune 411008

ACKNOWLEDGEMENTS

I would like to express my warmest thanks to Supervisor of this thesis-Dr. K. N. Ganesh, who fearlessly accepted me as PhD student for his project and was the main creator of the great ideas, techniques and whole background for this thesis. We experienced together all the ups and downs of routine work, the shared happiness of success and the depression of failure when (sometimes) everything went wrong. He managed to teach me how to work independently (which is very important), but at any time, his useful advice was available to me. In my opinion, this is how an ideal supervisor should be. It is a real pleasure to work and communicate with such a polite, honest and open-minded person. I would also like to acknowledge his language abilities, which were extremely useful, particularly in the beginning of my work and life in NCL.

My special thanks for Dr. (Mrs.) Vaijayanti A. Kumar, Dr. A. A. Natu, Mrs. Anita Gunjal, Dr. N. P. Argade, Dr. D. D. Dhavle and especially to Dr. Ganesh Pandey. They were always there to help me. Their encouragement, understanding and suggestions were invaluable during my stay in the NCL. Without their support, I would not have been able to complete this work.

My sincere thanks for Dr. P. R. Rajamohan, Mrs. Phalgune and Mr. Shathe for their help during NMR analysis in the course of this thesis.

I would like to thank Dr. Murugan, Dr. Kapoor, and Dr. M. Karthikeyan for being available whenever I needed their advice.

I wish to thank Dr. Vairamani, IICT, Hyderabad, Dr. Madhusudan, CDRI, Lucknow (U.P.) for their help in recording the MALDI-TOF spectra. I wish to acknowledge Mrs. Mane and Mrs. Kunte for their assistance for the HPLC analysis and Mrs. Shantakumari and Dr. Mahesh Kulkarni for the mass spectra.

This page will be incomplete without the mention of my seniors and colleagues who have gone out of their way to help in various capacities and have been my extended family throughout the tenure of my work in NCL. Thanks to my Labmates: Vallabh, Pradeep, Ramesh, Meena, Nagamani, Moneesha, Pallavi, Dinesh, Govind, Umashankar, Gaurishankar, Khirud, Ashwini, Amit, Shridhar, Sushmita, Sunil, Smita, Manashwani, Madhuri, Praveen, Gitali, Roopa, Pradnya, Sachin, Nasrin, Chitra and especially to Raman. I am lucky enough to have the support of many good friends. Life would not have been the same without them thanks to my roommate S. Easwar and my other friends: Sanjay, Subramanium (S), Jayanthi, Mallikarjun, Sankar (K), Pashupaty, Krishanaswamy, Mangal, Subramanium (U), Dumbre, Selvakanan, Devaraj, T. Suresh, R. Suresh, Dhananjoy, Anirban, Tushar, Mandar, Shinde, Mahajan, C. V. Das, Manish Chandra, Thyagrajan, Arindam, Prabal, Bidhan, Kesari, Kishor (Bhaiya), M. Baag, Sanjib,

Mhsake, Kale, Thakkar, Sivanand Pai, Kiran, Sambhaji, Nilesh, Arif, Govande, Sukhen, Praveen, Manash, Nagendra (Kondekar), Satyendra, Pushpesh, Anamitra, Kartik, Prakash, Alok, Sudhir, Joly, Nirmalaya, Ashish, Mukulesh, Sidhartha, Ramakrishana, Nagaprasad, Ekambaram, K. Mahesh, Saikat, Sumant, Yadav, Deka and also sincere thanks to Pawar and Bhumkar for their assistance in lab.

I also thank to my sisters: Aasha, Sabuja, Late Siyamani and brothers- Rabindra, Yogendra and to my family Satayandra, Dhirendra, Manoj, Rohit, Rajanikant, Rinku, Mamata, Aarti and Charu.

I am very grateful to Nikhil Gandhi, Atul Sharma, Dr. Sulekh Chandra, Dr. R. C. Srivastava, Mr. S. C. Bangiya, Late (Shri) U. K. Banerjee, Seema Banerjee, Late (Shri) Ramkrishan Gouchhawal, Joy, Sukhvir, Ajoy, Anil, Dalbir, Ashok, Gopal, Sudipto, Sudip, Debashish (Genda), Debashish (Chhotu), Tamal, Samanto, Anirudho, Amitabo, Sukanto, Deepayan, Mitali, Soma, Supriodhar, Chanchal, Satyakam, Sudhir, Naveen, Sukhpreet and Meghana without whose help it would have been impossible to reach here.

I am grateful to the Director, NCL, for giving me the opportunity to work in this institute and making all the facilities available for carrying out research.

UGC and CSIR, New Delhi is acknowledged for valuable support in the form of a fellowship.

I cannot end without thanking my Father, Shri Bigan Sharma, on whose constant encouragement and love, I have relied throughout my time at the lab.

Nagendra

CONTENTS

SUMMARY

The thesis entitled **"Pyrrolidine and pyrrolidinone Peptide Nucleic Acids: Synthesis and Comparative studies of the DNA binding Activities"** is divided into five chapter as follows

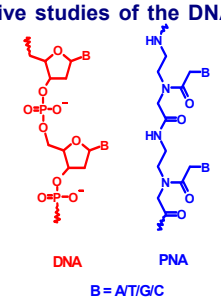

Chapter 1: **Introduction**

- PNA is Acyclic, Neutral and Achiral Mimic of DNA
- Bind to DNA/RNA both in parallel and antiparallel modes - ambiguity in binding
- PNA is promising agent for antigene and antisense in therapeutics

Chapter 2: **The Synthesis of Pyrrolidine and Pyrrolidinone Peptide nucleic acid (PNA) Monomers**

- Ragioselective oxidation at C5 in 4- and *N*-substituted pyrrolidine ring in presence of other two active position
- Synthesis of L-*cis/trans-aepone*-PNA-A/T/C/G monomer
- Synthesis of L-*cis/trans-aep*-PNA-A/T/C/G monomer
- Synthesis of L-*aeg*-PNA-A/T/C/G monomer

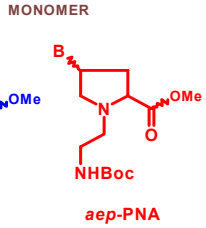

Chapter 3: **Conformational Studies of Pyrrolidine Ring Pyrrolidine PNA Monomer**

- Assignment of ring protons in pyrrolidine ring of aep-PNA monomer by 1D decoupling and 2D COSY, HETCOR and NOESY NMR techniques
- Calculation of vicinal coupling constant pyrrolidine ring of aep-PNA derivatives done
- Approximate conformation of pyrrolidine ring in *aep*-PNA monomer is calculated by use PSEUROT programe.

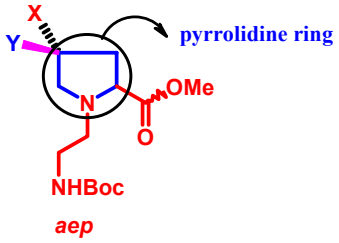

Chapter 4: **Synthesis of Pyrrolidine and pyrrolidinone PNA Oligomers and their Hybridization Studies with Complementary DNA/RNA**

- Hybridization of L-*cis/trans-aepone* PNAs with complementary DNA with UV is higher than that of control *aeg*-PNA and lower than that of *aep*-PNA
- Hybridization of L-*cis/trans-aepone* PNAs with complementary RNA is lower than that of control *aeg*-PNA and higher than that of *aep*-PNA.
- Binding stoichiometry of homoaoligomer (t_8) of *aepone*-PNA with DNA is observed by UV and CD as 2:1

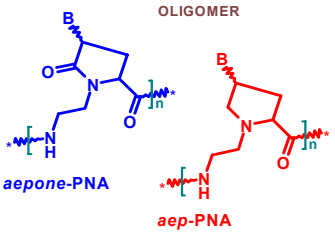

Chapter 5A: **PNA tetraplexes: Biophysical Studies of G-tetrad in *aep*- PNA**

- G-tetrad formation by G-rich sequences *aep*-PNA is observed in presence of metal ion Na^+/K^+.
- Stability of *aep*-PNA G-tetrad compare to *aeg*-PNA are almost same.
- *aep*-PNA G-tetrad does not stable at acidic pH
- short G-rich sequences of *aep*-PNA is forming stable G-tetrad structure

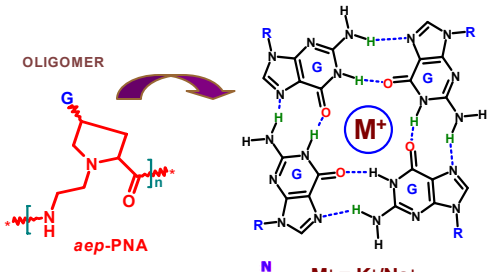

Chapter 5B: **PNA tetraplexes: Biophysical Studies *i*-motiff of PNA**

- Formation of *i*-motif by C-rich sequences of PNA in acidic pH
- Stability of *i*-motif formed by TC_8 is higher than $d(TC_8)$ at low pH

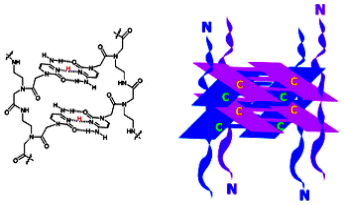

Chapter 6: **Synthesis and study of foldamer properties of unnatural *δ*-aminoethyl pyrrolidine amino acid oligomers**

- Synthesis of Unnatutral amino acid as *δ-aep* amino acid and their peptides
- Secondary structure as β-turn like in monomer and *β*-helix type in olligomers of *δ-aep* peptides is observed by CD/FT-IR

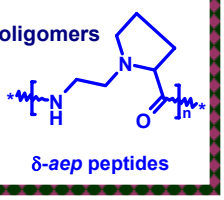

LIST OF PUBLICATIONS

1. **Sharma, N. K**.; Ganesh, K. N. Expanding the repertoire of pyrrolidyl PNA analogues for DNA/RNA hybridization selectivity: aminoethylpyrrolidinone PNA (*aepone*-PNA). *Chem. Commun.* **2003**, 2484–2485.
2. **Sharma, N. K.**; Ganesh, K. N. Regioselective oxidation of N-alkylpyrrolidines to pyrrolidin-5-ones by $RuCl_3/NaIO_4$. *Tetrahedron Letters* **2004,** *45*, 1403–1406.
3. **Sharma, N. K**.; Ganesh, K. N. PNA C–C^+ *i*-motif: superior stability of PNA TC_8 tetraplexes compared to DNA TC_8 tetraplexes at low pH. *Chem Commun* **2005**, 4330-4332.
4. **Sharma, N. K.;** Ganesh, K. N. Hybridization study of mix sequence of aminoethylpyrrolidinone PNA (*aepone*-PNA) with complementary DNA. (Manuscript is under preparation).
5. **Sharma, N. K**.; Ganesh, K. N. Comperative study of G-tetraplexes formation by modified chiral-aep-PNA over DNA and unmodified PNA. (Manuscript is under preparation).
6. **Sharma, N. K**.; Ganesh, K. N. Conformational study of prolyl ring in *aep*-PNA monomer by NMR and PSEUROT programme. (Manuscript is under preparation).
7. **Sharma, N. K**.; Ganesh, K. N. Study of secondary as Foldamer non-natural peptide δ-aminoethyl prolyl peptide by CD and IR. (Manuscript is under preparation).

Posters and Presentation:

1. **Sharma, N. K**.; Ganesh, K. N., The study 2D NMR of *aep*-PNA monomers A/T/G/C" was presented as Postre in ISBOC Symosium in Amritsar. Nov 9-11, **2001**.
2. **Sharma, N. K**.; Ganesh, K. N., Synthesis and Evaluation of Pyrrolidinone-5-one PNA; *15th IRT conferance on Nucleoitide, Nucleoside and Nucleic acid*, in Belgium Sept 10-14, **2002**.
3. **Sharma, N. K**.; Ganesh, K. N., Synthesis and Biophysical Study of Novel Aminoethylpyrrolidinone-PNA (*aepone*-PNA). *ICOB-4 & ISCNP-24 IUPAC International Conference on 26-31* January, PP. No. 317, **2004**.
4. **Sharma, N. K**.; Ganesh, K. N., "National Crystallography Symosium-2003", NCL, Pune (Maharastra)-India.
5. **Oral presentation** on OCS day -2003 of in NCL, Pune (Maharastra)-India.

Award

DR. RAJAPPA AWARD for "The Best Research Paper in Organic Chemistry-2003" by National Chemical Laboratory Research Foundation (NCLRF) on 28 February 2004.

ABSTRACT

The thesis entitled **"Pyrrolidine and pyrrolidinone Peptide Nucleic Acids: Synthesis and Comparative studies of the DNA binding Activities"** is divided into five chapter as follows

The thesis comprises of studies towards design, synthesis and DNA/RNA recognition properties of rationally designed peptide nucleic acids (PNA) with five-member pyrrolidine and pyrrolidinone ring system. The polyamide backbone of standard PNA **2** (Figure 1) is stable towards intracellular enzymes and therefore has potential applications in therapeutics. The thesis also discusses studies on tetraplexing properties of G-rich and C-rich sequences of modified and unmodified PNA and conformational studies of 4 and 5-substituted pyrrolidine ring.

The thesis is divided into five chapters. Chapter 1 introduces the background literature for undertaking the research work. Chapter 2 details the synthesis of *Pyrrolidine* and *pyrrolidinone* peptide nucleic acids (PNA) monomers. Chapter 3 describes the conformational study of 4-/5-substituted *pyrrolidine* ring in PNA monmers. Chapter 4 describes the synthesis of *aeg*, *aep* and *aepone*-PNA oligomers and their hybridization properties with complementary DNA/RNA. Chapter 5 discusses the synthesis of standard and modified PNA oligomers for studying the *tetraplexing* properties of G-rich and C-rich sequences of PNA.

Chapter 1: **Introduction**

It has been 52 years since Watson and Crick proposed the double helical structure for duplex DNA (deoxyribonucleic acid) **1** (Figure I), the genetic material of all organisms. It is built from four hetrocyclic bases Adenine (A), Cytosine (C), Guanine (G) and Thymine (T) assembled on a polymer backbone composed of deoxyribophosphodiesters. Emerging applications of oligonucleotides for various therapeutic and diagnostic purposes have necessitated the chemical modification of natural DNA/RNA. The modification of the DNA backbone has led to many different DNA analogues. PNA (peptide nucleic acid) **2** (Figure 1) is one of such DNA analogues in which the sugar phosphate bond is replaced by a neutral and achiral polyamide backbone consisting of *N*-(2-aminoethyl)-glycine units. The nucleobases are attached to the backbone through a conformationally rigid tertiary acetamide linker. Internucleobase distance in PNA is conserved as in DNA, allowing high sequence specificity and affinity for binding to complementary DNA. This along with

PNA's resistance to both proteases and nuclease under physiological conditions makes PNA a candidate with potential for use in therapeutics as antigene/antisense agents.

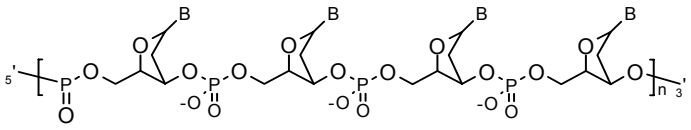

1 (DNA)

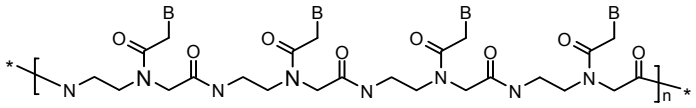

2 (PNA)

B = A, T, G, C

Figure 1: Chemical structure of DNA and

Since the first reports on PNA, several strategies for structural modifications have been explored in order to understand better the chemical and structure features that determine PNA-DNA molecular recognition. Recent structural studies by NMR and X-ray crystallography on PNA complexes (PNA-RNA, PNA-DNA, PNA_2-DNA triplex and especially PNA-PNA duplex) have indicated that flexible conformation inherently adopted by single stranded PNA, is not optimal for hybridization to complementary RNA or DNA. PNA/DNA and PNA/RNA duplex formation is accompanied by a decrease in entropy and making more rigid PNA analogues with conformations pre-organized for hybridization should reduce this entropy loss. PNAs are also achiral and therefore PNA-PNA duplexes are racemics of the doubles helices of opposite handedness. Introducing chirality in backbone of PNA may induce a preferred handedness in duplex. Several structural modifications in PNA backbone have been attempted to address these issues. This chapter summarizes the rationale and consequences of such PNA modifications on PNA-DNA hybridization.

Chapter 2: **The Synthesis of pyrrolidine and pyrrolidinone peptide nucleic acids monomers (PNA)**

In attempts to impose rigidity, chirality and conformational pre-organization in backbone of PNA **2**, pyrrolidine based PNAs are emerging as novel PNA analogues with efficient DNA/RNA hybridization properties.

One way to study the criticality of conformational feature is to design structures with frozen rotation of the side chain by locking them into rings as exemplified by the different pyrrolidine based PNA analogues (Figure 2). Remarkable stabilization of the derived PNA-DNA hybrids was achieved in the chiral and cationic aminoethylprolyl PNA (*aep*-PNA 3), in which having the neutral tertiary amide group of PNA 2 replaced by a protonatable cyclic tertiary amine. In order to avoid the dominance of non-sequence specific electrostatic component in *aep*-PNA:DNA binding and to get the best characteristics of both the normal PNA and the *aep*-PNA, we reasoned to restore the amide character to the pyrrolidine ring nitrogen.

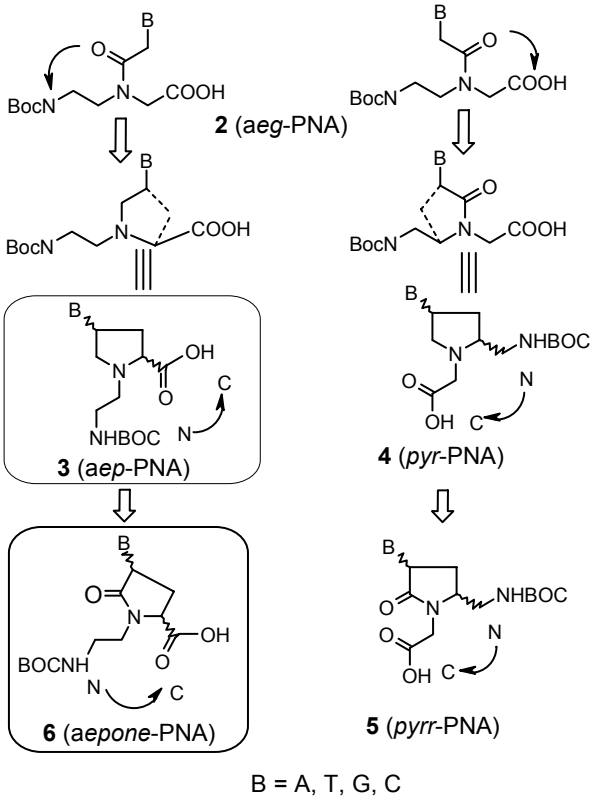

Figure 2. Structural organization of PNA

This chapter describes the synthesis and evaluation of aminoethylpyrrolidin-5-one PNA (*aepone*-PNA, 6) having the endocyclic amide CO at C5. This was done by introducing carbonyl group into the ring (endocyclic) rather than exocyclic (as in PNA) to avoid the *syn-trans* rotamer problems (Figure 3). The synthesis of A/G/C/T monomers corresponding to such PNA analogue pyrrolidinone PNA (*aepone*-PNA) was done by *regioselective oxidation* of C-5 methylene group (-CH_2-) into keto (-CO-) using RuO4.

This reagent was generated *in situ* from $RuCl_3/NaIO_4$ or $RuO_2/NaIO_4$ in water: EtOAc. During the reaction other two CH_2- (Figure 4) were not affected (Scheme 1). The isolated product was characterized by ^{13}C-NMR, PMR and IR and finally confirmed by single X-ray crystal of 9a (Figure 5). The oxidation reactions were carried out at C-5 with different 4-*O*-substituent such as mesylate, benzoate and acetate.

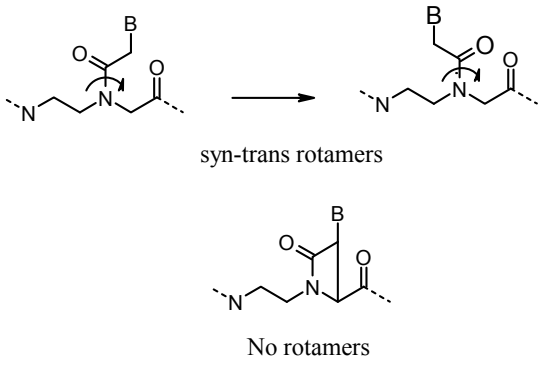

Figure 3. Freezing rotamer by bridging

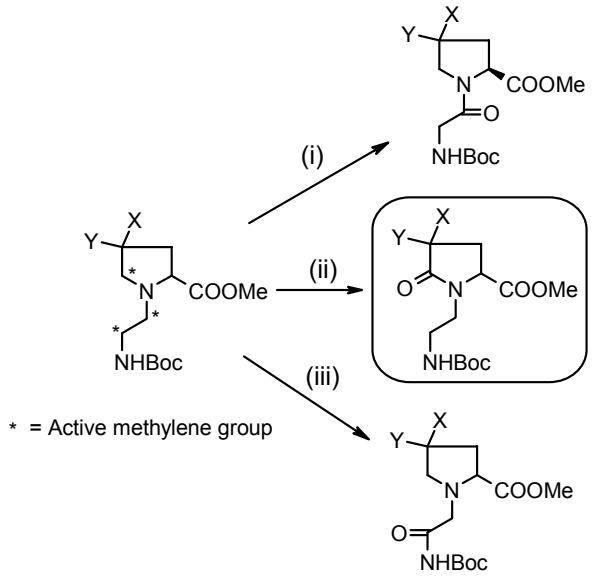

Figure 4 Active methyelene sites in pyrrolidine monomer for oxidation

Scheme 1. Regiselective Oxidation of pyrrolidine ring in pyrrolidine derivatives

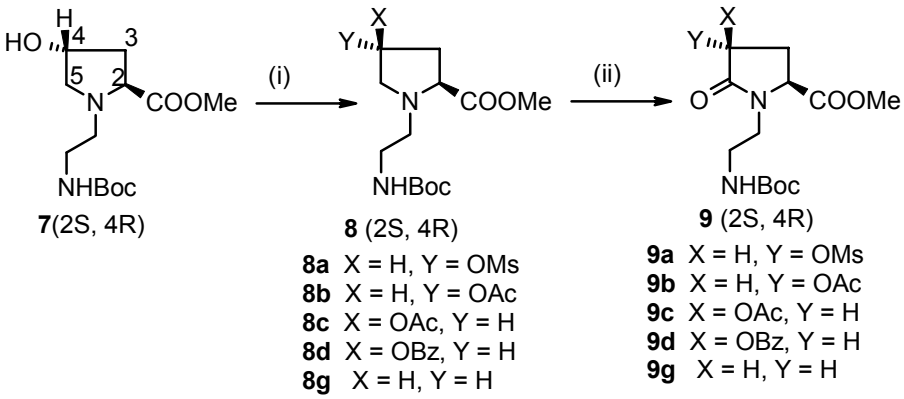

(i) $MeSO_2Cl$,, Et_3N, DCM for **8a**; Ac_2O, Py, for **8b**; Ph_3P, DIAD, CH_3COOH, THF for **8c;** p-nitrobenzoic acid**,** Ph_3P, DIAD, THF, for **8d** and **8e** is directly derived from L-proline.[10b] (ii) $NaIO_4$ /$RuCl_3.xH_2O$, AcOEt/H_2O.

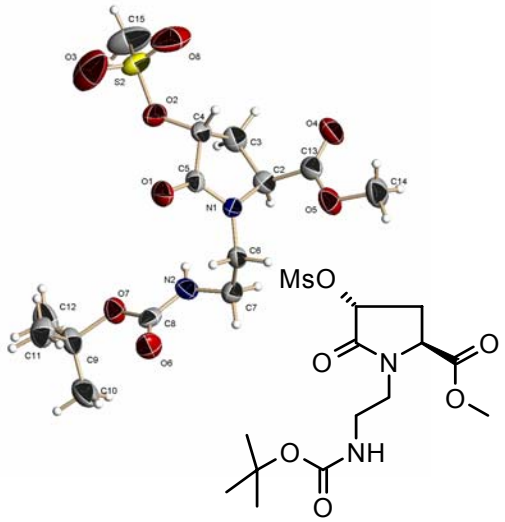

Figure 5: ORTEP diagram single X-ray cyatal of **9a**

In the absence of crystallographic data, it is necessary to unambiguously identify the site of oxidation and this was done by ^1H and ^{13}C NMR data of compound **8** and **9** (Figure 5b). In view of the similar chemical shifts of different N_α-methylene protons, the ^1H NMR was completely assigned using ^1H-^1H DQF COSY. While assignment of H5 is straightforward due to coupling with H4, assignment of βH'H" were done using

connectivity with NH followed by assignment of αH'H". The different carbons were assigned via ^{1}H-^{13}C HETCOR experiment.

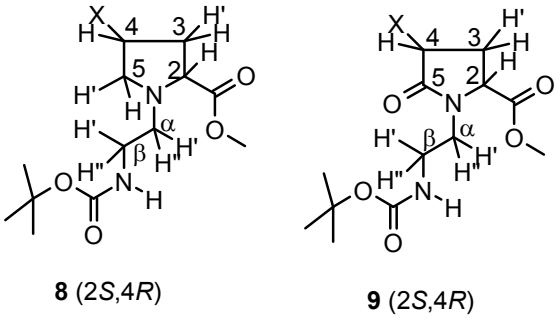

8 (2*S*,4*R*) **9** (2*S*,4*R*)

X = Oms, OAc, H

Figure 5b. Chemical Structure of **8** and **9**

2.2 The Synthesis of pyrrolidinone Peptide Nucleic Acids Monomers (PNA)

2.2.1 Synthesis of *cis*-(2*S*,4*S*)-*aepone* monomers

The synthesis of *cis*-(2*S*,4*S*)-*aepone* monomers 10, 11, 12 and 13 were achieved from the common precursor *trans*-(2*S*,4*R*)-4-*O*-mesyl pyrrolidine derivative 9a (Scheme 3a), which was reacted with different nucleobases (A/G/C/T) in presence of K_2CO_3 and catalytic amount of 18-crown-6. The esters were hydrolyzed to acids and used for oligomer PNA synthesis.

Scheme 3a. Synthesis of *cis*-(2*S*,4*S*)-*aepone*-PNA monomers

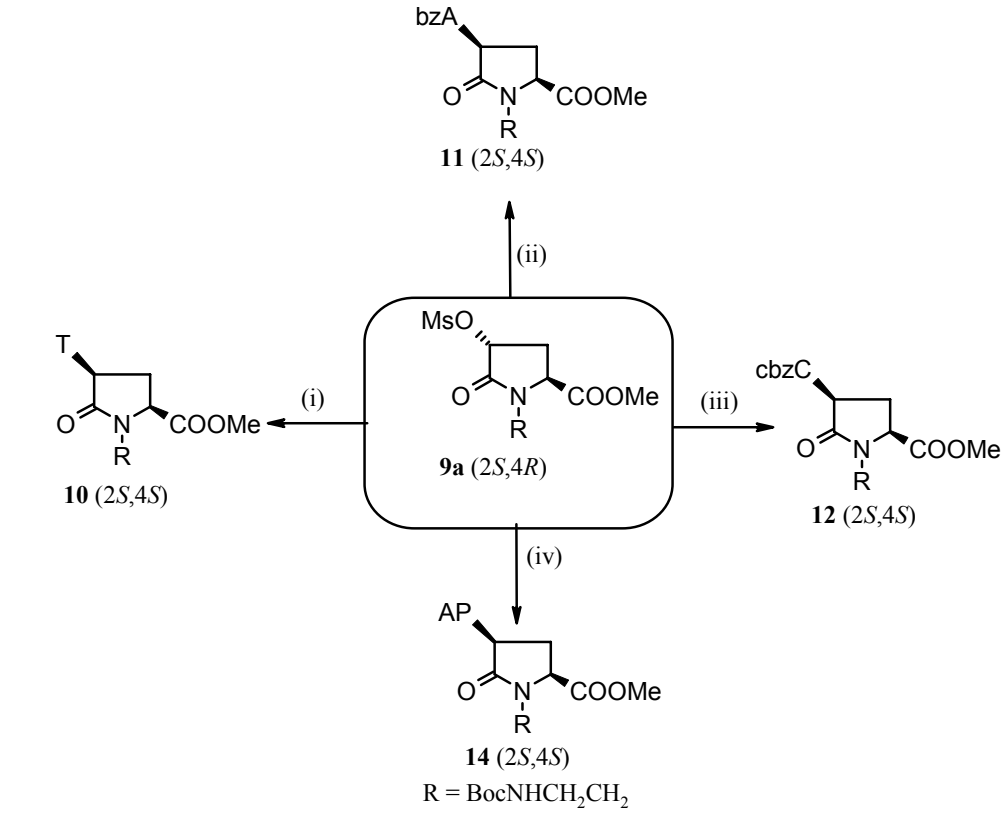

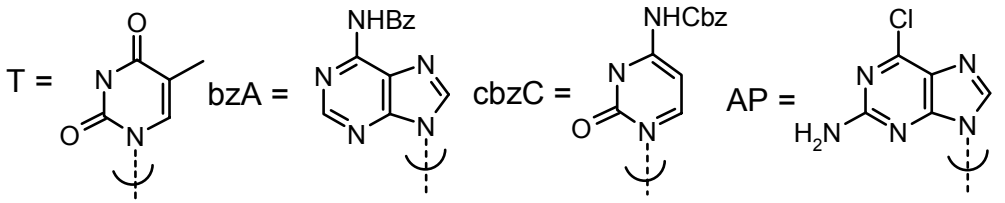

(i) Thymine (ii) N^6Bz-Adenine (iii) N^4Cbz-Cytosine (iv) 2-amino 6-chloropurine, K_2CO_3, 18-Crown-6

2.2.2 Synthesis of *trans*-(2*S*,4*S*)-*aepone* monomers

Trans-(2*S*,4*R*)-*aepone* monomers **16**, **17**, **18**, **19** were synthesized from *cis*-(2*S*,4*R*)-4-*O*-mesyl derivative **15** (Scheme 3b), obtained from compound **9c** and **9d.**

Scheme 3b. Synthesis of *trans*-(2*S*,4*S*)-*aepone*-PNA monomers

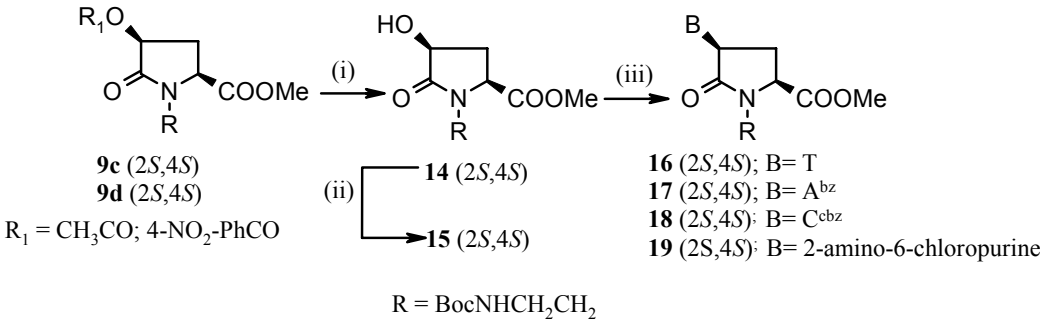

(i) K_2CO_3, dry MeOH (ii) $MeSO_2Cl$/ Et_3N/DCM (iii) Thymine /A^{bz}/C^{cbz}/2-amino 6-chloropurine, K_2CO_3, 18-Crown-6.

2.3 The synthesis of *trans*-(2S,*R*)-*aep* PNA *Pyrrolidine* and monomers

All four monomers (C/T/A/G) of *trans*-(2S,4*R*)-*aep* were made PNA from *cis*-(2*S*,4*R*)-4-hydroxy derivative **20** which was prepared by hydrolysis of *cis*-4-hydroxy protected compounds **8c** and **8d** (Scheme 4a)**.** *Trans*-(2S,4*R*)-*aep*-N^3Bz-Thymine protected monomer **21** was prepared directly from compound **20** under Mitsunobu condition in presence of N^3Bz-thymine, Ph_3P and DIAD (Scheme 4a).

Scheme 4a. Synthesis of *trans*-(2*S*,4*R*)-*aep*-PNA monomers

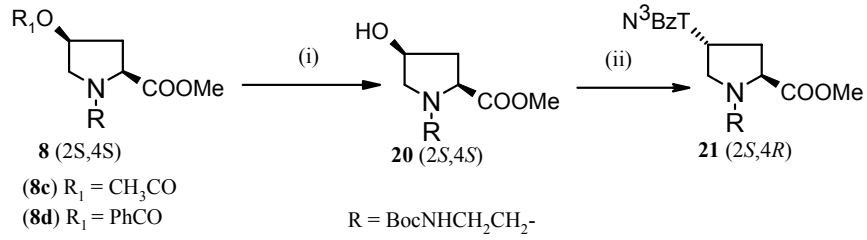

(i) NaOMe, dry MeOH (ii) N^3Bz, Ph_3P, DIAD, THF.

Other exocylic amine protected monomers of adenine, cytosine and guanine were synthesized (Scheme 4b) by alkylation from compound **22** (mesylate derivative of **20**).

Scheme 4b. Synthesis of *trans*-(2*S*,4*R*)-*aep*-PNA other monomers

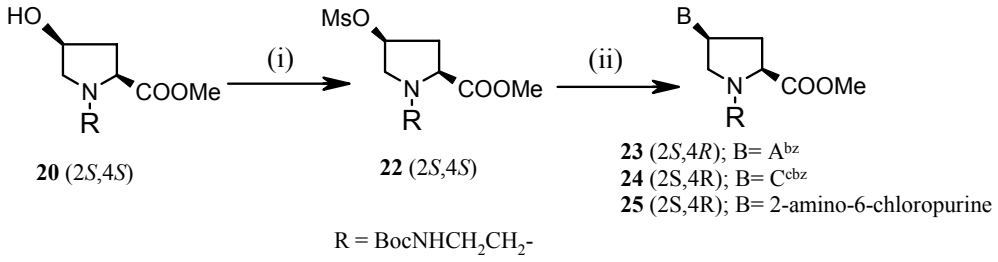

20 (2*S*,4*S*)

22 (2*S*,4*S*)

23 (2*S*,4*R*); B= A^{bz}
24 (2S,4R); B= C^{cbz}
25 (2S,4R); B= 2-amino-6-chloropurine

R = $BocNHCH_2CH_2$-

(i) MeO_2Cl/Et_3N/DCM (ii) A^{bz}/C^{cbz}/ 2-amino-6chloropurine; K_2CO_3, 18-Crown-6.

Chapter 3: Conformational studies of *pyrrolidine* Ring in *pyrrolidine* PNA-monomers

Aminoethylprolyl (*aep*) PNA **3** was found to be a promising analogue due to its higher affinity and selectivity in binding to complementary DNA sequences. *aep*-PNA is chiral, constrained and cationic in comparison with the *aeg*-PNA that is achiral, relatively flexible and neutral in nature. The PNA oligomer containing the *aep*-A/T/G/C monomers upon complexation with DNA exhibits stabilization depending upon the nucleobase, stereochemistry and binding orientation. This may arise from the fact that the nature of the 4-substituent plays an important role in defining the pucker of the pyrrolidine ring in 4-substituted prolines. The individual purines or pyrmidines differ in their group electronegativities and when present at the 4-position of the pyrrolidine ring may cause differential ring pucker. This may consequently lead to backbone conformational changes causing sequence specificity effects. In order to relate the observed binding preferences to the pyrrolidine conformational features, ^{1}H-^{1}H J_{12} coupling constants of the pyrrolidine ring were extracted from ^{1}H-NMR spectroscopic data on *aep*-PNA monomers. The complete ^{1}H-NMR assignment of all four monomers A/T/G/C of *cis*-(2*S*,4*S*)-*aep*-PNA were done by 2D COSY technique (Table 2).

Table 2. ^{1}H-NMR Spectroscopic data (Chemical Shift) of *aep* –Monomers

B	NH	H2	H3	H3'	H4	H5	H5'	a H	a H'	b H	b H'	Base Protons
T	5.2	3.4	2.0	2.9	5.2	2.8	3.3	2.7	2.9	2.6	2.8	TH6-8.1
C	5.1	3.4	1.9	2.8	5.3	2.8	3.2	2.6	2.8	3.1	3.3	H5-7.5; H6 8.5
G*	5.3	3.5	2.20	2.85	5.2	2.9	3.3	2.7	2.9	2.9	3.2	H8 8.3
A	5.2	3.4	2.2	3.0	5.4	3.1	3.4	2.7	2.9	3.2	3.3	H8 8.8; H2 8.7

G* = 2amino-6-chloropurine

NMR spectroscopic data was (J_{12}) used to derived the pseudorotation phase angle (P) and puckering amplitude (ϕ_m) of pyrrolidine ring in different compounds using Pseurot program version (5.4.1) introduced by De Leeuw and Altona.

$$\text{Phi (H-H)} = A * \phi_{Max} * \text{Cos (P + phase)} + B$$

Phi (H-H) = Torsional angle between two adjacent hydrogen; P= Phase angle of pseudorotation; ϕ_{Max} = puckering amplitude, A and B are constants

Table 8: Summary of input and output data of *aep*-derivatives*

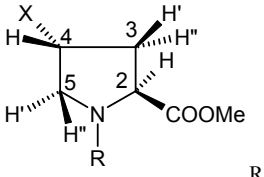

L-trans-(2*S*,4*R*)

R = CH_2CH_2NHBoc

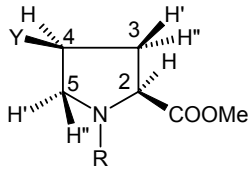

L-cis-(2*S*,4*S*)

Entry	Compound	Vicinal Proton-Pair[a]	ϕ_{H-H}[b]	J_{calcd}[c]	J_{exp}[d]	ΔJ^e	MF[f]	P_N[g]	ϕ_N[h]	rms[i]
1	**7**	$H_{2'}$-H_3'	-29.2	7.79	7.80	0.01				
	X = OH	$H_{2'}$-H_3''	-150.4	7.79	7.80	0.01				
	Y = H	H_3'-H_4	-79.7	5.40	5.40	0.00				
		H_3''-H_4	41.4	5.40	5.40	0.00				
		$H_{4'}$-H_5'	81.6	4.90	4.90	0.00				
		$H_{4'}$-H_5''	-40.0	3.39	3.40	0.01				
							0.548	15.2	44.0	0.008
2	**8a**	$H_{2'}$-H_3'	-44.9	7.02	7.30	0.28				
	X = OMs;	$H_{2'}$-H_3''	-166.1	7.25	7.40	0.15				
	Y = H	H_3'-H_4	-62.9	6.75	6.80	0.05				
		H_3''-H_4	58.2	3.39	3.20	-0.29				
		$H_{4'}$-H_5'	70.1	5.47	5.50	0.03				
		$H_{4'}$-H_5''	-51.5	2.51	2.80	0.29				
							0.503	7.7	59.7	0.216
3	**8b**	$H_{2'}$-H_3'	-35.9	7.04	7.30	0.26				
	X = OAc	$H_{2'}$-H_3''	-157.7	8.21	8.30	0.09				
	Y = H	H_3'-H_4	-77.7	3.19	3.20	0.01				
		H_3''-H_4	43.4	6.15	5.90	-025				
		$H_{4'}$-H_5'	85.0	3.19	3.20	0.01				
		$H_{4'}$-H_5''	-36.6	5.82	6.00	0.18				
							0.714	3.9	44.5	0.169
4	**8c**	$H_{2'}$-H_3'	-14.8	6.74	6.40	-0.34				
	Y= OBz	$H_{2'}$-H_3''	-136.0	6.16	5.80	-0.36				
	X = H	H_3'-H_4	-80.0	3.40	2.90	-0.50				
		H_3''-H_4	41.1	5.69	4.90	-0.79				
		$H_{4'}$-H_5'	67.6	2.24	2.00	-0.24				
		$H_{4'}$-H_5''	-54.0	4.74	4.90	0.16				
							0.756	40.3	55.2	0.448

*Proton Pair[a]: Vicinal protons pair; ϕ_{H-H}[b] Torsional angle; J_{calcd}[c] : Calculated coupling constants from pseurot program; J_{exp}[d] : Experimentally observed coupling constants; ΔJ^e : J_{exp}-J_{calcd} (in Hz); MF[f] : Mole fraction of one of the conformer (N conformer; P = 0); P_N[g]: Psuedorotaion angle for N conformer; ϕ_N[h] : Puckering amplitude for N conformer(P = 0); rms[i] : Root mean square

The results in the table indicate that pyrrolidine ring puckering is slightly affected by different 4-O-substituents at ring. Electron withdrawing groups favour *N*-type conformation (conformer-II) over S-type (conformer-I).

Chapter 4: Synthesis of pyrrolidine and pyrrolidinone PNA oligomers and their hybridization studies with complementary DNA/RNA

4.1 Synthesis of PNA Oligomers

The modified PNA monomers (*aeg*-PNA, *aep*-PNA and *aepone*-PNA) synthesized in chapter (2) were incorporated into different PNA oligomers (1-21) by solid phase peptide synthetic protocols with β-alanine as C-terminal linker. All the oligomers in the thesis work were synthesized manually on Merrifield resin (Table 4).

Table 4: PNAs Oligomers*

Name Of Sequence	Incorporated Monomer
1. BocHN–T–T–T–T–T–T–T–T-β-ala-MF	*aeg* (Control)
2. BocHN–T–T–t–T–T–T–T–T-β-ala-MF	t=*aep* 4*S*; *aepone* 4*S*; t=*aepone* 4*R*; *Aep* 4*R*
3. BocHN-T-T-t-T-T-t-T-T- βala-MF	A=*Aep*-(2S,4S), *aep* (2S, 4*R*), aepone-(2*S*, 4*S*), *aepone*-(2*S*, 4*R*)
4. BocHN–t–T–T–t–T–T–T-T-β-ala-MF	*aep* –4S
5. BocHN–T–T–T–t–T–T–T-T-β-ala-MF	*aepone* –(2*S,*4*R*)
6. BocHN–t–T–T–T–T–T–T-T-β-ala-MF	*aepone* -(2*S,*4*R*)
7. BocHN–t–T–T–T–t–T–T-T-β-ala-MF	*aepone* -(2*S,*4*R*)
8. BocNH-G-T-A-G-A-T-C-A-C-T--β-ala-MF	*aeg* (Control)
9. BocNH-g-T-A-G-A-T-C-A-C-T--β-ala-MF	g=a*ep*-(2*S*,4*S*), 4*S*, a*epone*-(2*S*,4*S*), a*ep*-(2*S,*4*R*)
10. BocNH-G-T-A-G-A-T-C-A-c-T--β-ala-MF	C=*aepone* 4*S*; a*epone*- (2*S*4*R*)
11. BocNH-G-t-A-G-A-T-C-A-C-T--β-ala-MF	*t=aepone*-(2*S*,4*R*)
12. BocNH-G-T-A-G-A-t-C-A-C-t--β-ala-MF	t=Aepone- (2*S,*4*R*)
13. BocNH-G-T-A-G-A-t-C-A-C-T--β-ala-MF	A=*aep*-(2*S*,4S), *aep*-(2S,4*R*), aepone-(2*S*, 4*S*), *aepone*-(2*S*, 4*R*)
14. BocNH-G-T-A-G-A-T-C-a-C-T--β-ala-MF	a=*Aep*-(2S,4*S*), aep-(2S,4*R*), aepone-(2*S*, 4*S*), *aepone*-(2*S*, 4*R*)
15. BocNH-T-A-T-A-T-T-A-T-T-A-T-T-β-ala-MF	*aeg*
16. BocNH-t-a-t-a-t-t-a-t-t-a-t-t-β-ala-MF	*aep*-t and *aep*-a
17. BocHN–T–T–T–T–t–T–T–T-β-ala-COO-MF	t=*aepone*- -(2*S*,4*S*),
18. BocHN–t–T–T–T–T–T–T–T-β-ala-COO-MF	t=*aepone* --(2*S*,4*S*),
19. BocHN–T–T–T-t-T–T–T-t-β-ala-COOMF	t=*aepone* --(2*S*,4*S*),
20. BocHN-t-t-t-t-t-t-t-t-β-ala-COO-MF	t=*aepone* --(2S,4*S*),
21. BocHN-t-t-t-t-t-t-t-t-β-ala-COO-MF	t=a*ep* -(2*S*,4*S*),

***aeg*-Monomer (T, A, G, C) ; modified one t, a, g,**

The PNA oligomers were purified by reverse phase HPLC and further characterized by MALDI-TOF mass spectroscopy.

4.2 Hybridization study of *cis*-(2*S*, 4*R*)-*aepone*-PNA with complementary DNA and RNA by UV-melting

The PNA: DNA/RNA complexes were constituted by stoichiometric mixing followed by annealing to obtain $(PNA)_2$:DNA triplexes. The Tm's of different triplexes were determined by temperature dependent UV absorbance at 260 nm (Table 5). It is seen that *aepone*-PNA oligomers **2–4** significantly stabilized the derived triplexes with DNA **6** as compared to that from the unmodified PNA oligomer **1** (ΔTm 16–19 °C). In comparison, the *aepone*-PNAs **2–4** affected destabilization of the triplexes formed with poly (rA), compared to the triplex from unmodified PNA **1** (ΔTm 12–15 °C). Even the completely modified *aepone*-PNA oligomer **4** binds to DNA and poly (rA) with a well-defined *T*m. Thus *aepone*-PNAs show preference for stabilization of hybrids with DNA over RNA hybrids. In comparison with unmodified PNA **1**, the opposite DNA/RNA binding selectivity was observed.

Table 5. UV-*Tm* (^oC) of PNA-DNA/RNA hybrids[a]

Sr. No.	PNA	DNA	Poly (rA)
1	H_2N–T–T–T–T–T–T–T–T-β-ala-COOH (aeg-T8)	34.8	58.0
2	H_2N–T–T–T–T–T–T–T-t- β -ala-COOH	50.7	43.1
3	H_2N–T–T–T-t-T–T–T-t- β -ala-COOH	50.9	41.8
4	H_2N-t-t-t-t-t-t-t-t- β -ala-COOH (aepone-t8)	53.3	45.6
5	H_2N-t-t-t-t-t-t-t-t- β -ala-COOH (aep-t8)	> 80	43.1

Buffer: 10 mM Sodium phosphate, 100 mM NaCl, 0.1 mM EDTA. The values quoted are the average of three experiment and are accurate to 0.5 ^oc. Value in parentheses indicate % hyperchromacities

Chapter 5A: PNA tetraplexes: Biophysical Studies of G-tetrad in *aep*-PNA

Telomeres are DNA sequences having upto thousand fold repeating guanine-rich and complementary cytosine-rich sequences. They are essential for maintenance of genome integrity and play an important role in cellular aging and cancer. Cancer cells have high levels of telomerase activity. The repeating unit in telomerase consists of two to five adjacent guanines on same strand. Human telomeric motif is (5'-TTAGGG-3'):(5'-CCCTAA-3') with repeating units as long as 50-210 bases in length at the chromosomal ends. G-rich strand can adopt a four stranded G-quadruplex (Figure 6) structure derived from guanine strands in tetrads formed by guanine donor/acceptor pairing by Watson-Crick and Hoogsteen motif. Different types of G-quaruplex structures exist, depending on the orientation and looping of the strands. Recently, G-quadruplex forming properties of PNA have been explored.

In this chapter, the modified *aep*-PNA G-oligomers (Table 7) were studied for tetraplexing properties and it is demonstrated from UV and CD studies that these modified *aep*-PNAs form able tetraplexes.

Table 7. Oligomers for the study of *Tetraplexing* of PNA*

Sr. No.	PNA oligomer
1	H2N–T–G–G–G–G–T-β-ala-COOH
2	H2N–t–g–g–g–g–t– β -ala-COOH
3	H2N–T–G–g–G–G–T-β-ala-COOH
4	H2N–T–G–G–G–G–t-β-ala-COOH
5	H2N–t–g–g–g–g– β -ala-COOH

*T,G = *aeg*-PNA; t,g = *aep*-PNA

Chapter 5B: PNA tetraplexes: Biophysical Studies i-motiff of PNA

The C-rich strands can form a four-stranded C-quadruplex via i-motif with intercalated C:C^+ base pairs (Figure 7). The self-assembling properties of the C-rich *aeg*-PNA were studied. The C-rich sequences of PNA (Table 7) were synthesized manually by solid phase method.

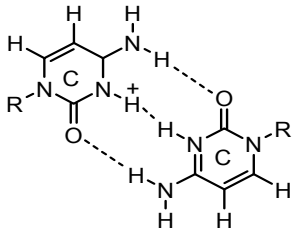

Figure 7: Hydrogen bonding Pattern in two Cytosine

The stability of i-motif depends upon pH as it requires protonated C and favoured at acidic pH. It is shown that ability of PNA-C-oligomers to form I-motiff structure is length dependent.

Table 8: Oligomers for the study of *i-motif* of PNA

Sr. No.	**PNA (*aeg*-C-PNA)**
1	H_2N-T-C-C-C-βala-COOH
3	H_2N-T-C-C-C-C-C-βala-COOH
4	H_2N-lysT-C-C-C-C-C-C-C-C-$CONH_2$

Chapter 6: Synthesis and study of foldamer properties of unnatural δ-pyrrolidine amino cid oligomers

Foldamers are oligomers that adopt well-defined conformations. The short oligomers constructed from subunits other than α-amino acids can also adopt discrete secondary structures. The ability to control molecular shape is manifested in design of foldamers with interesting function. β-peptides are among the most widely studied

unnatural foldamers (Figure 8). All three types of regular secondary structures observed in proteins, helix, sheet, and reverse turn, have been observed among short β-peptides.

δ-aminoethyl pyrrolidine (δ-*aep*) amino acid (Figure 8), a non-natural amino acid derived from L-Proline can potentially form a 8-membered or 10 membered intramolecular hydrogen boding system, thereby inducing a β-turn. The δ-*aep* amino acid monomer was used to synthesize oligomers by SSP method on MBHA resin (Table 6) followed by purification (HPLC) and characterized by ESI-MS-TOF.

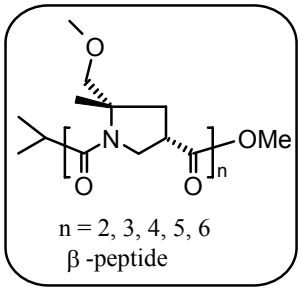

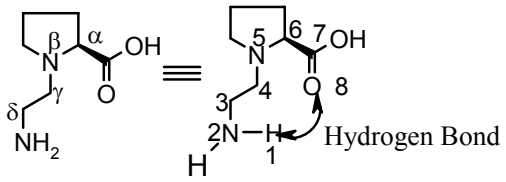

δ-Aminoethyl pyrrolidine (*aep*) amino acid monomer

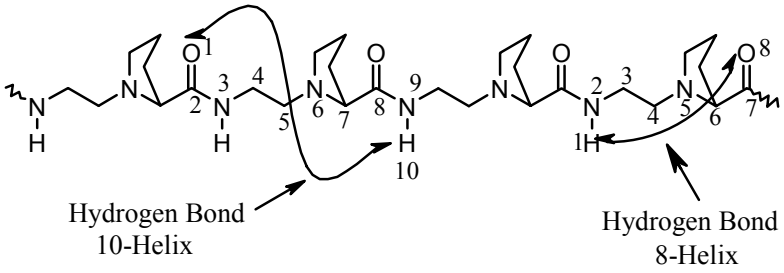

δ-Aminoethyl pyrrolidine (*aep*) amino acid oligomer

Figure 8: Chemical structure of unnatural amino acid

Table 8: Oligomers to study foladamer

Sr. No.	Peptides
1	AcHN–pr-pr -β-ala-$CONH_2$
2	AcHN–pr-pr-pr-β -ala-$CONH_2$
3	AcHN–pr-pr-pr-pr-pr- β -ala-$CONH_2$
4	AcHN-pr-pr-pr-pr-pr-pr- β -ala-$CONH_2$
5	AcHN-pr-pr-pr-pr-pr-pr-pr-β -ala-$CONH_2$

pr = δ-aminoethyl pyrrolidine (δ-*aep*) amino acid

This section describes the conformational studies of these peptides studied by CD and FT-IR.

Summary

The synthesis of *aepone*-PNA and *aep*-PNA monomers and their oligomers were completed followed by conformational study of pyrrolidine ring of intermediates of *aep*-PNA. Hybridization properties of *aepon*e and *aep* PNA with complementary DNA/RNA and self-assembly properties as tetraplexing, of *aep*-PNA are reported.

ABBREVATIONS

β-ala	β-alanine
A	Adenine
aeg	Aminothylglycine
Aep	Aminoethylprolyl
ala	Alanine
ap	Antiparallel
Boc	Tert. butyloxycarbonyl
C	Cytosine
COSY	Correlation spectroscopy
Cbz	benzyloxy carbonyl
CD	Circular Dichroism
dA	Deoxy adenine
DCC	Dicyclohexylcarbodiimide
DCM	Dichloromethane
DCU	Dicyclohexyl urea
dG	2'-deoxyguanine
DIAD	Diisopropylcarbodiimide
DIPCDI	Diisopropylcarbodiimide
DIPEA	Diisopropylethylamine
DMF	N,N-Dimethylformamide
DNA	2'-deoxynucleic acid
ds	Double stranded
EDTA	Ethylenediaminetetraacetic acid
Fmoc	9-Fluorenylmethoxycarbonyl
FPLC	Fast Protein Liquid Chromatography
g	Gram
G	Guanine
gly	Glycine

HBTU	O-Benzotriazole-N,N, N',N'-tetramethyl-uronium-hexafluoro-phosphate.
HOBt	1-Hydroxybenztriazole
HPLC	High Performance Liquid Chromatography
Hz	Hertz
IR	Infra red
MALDI-TOF	Matrix Assisted Laser Desorption Ionisation-Time Of Flight
MF	Merrifield Resin
mg	Milligram
MHz	Megahertz
μM	Micromolar
ml	Milliliter
mM	Millimolar
mmol	Millimoles
N	Normal
nm	Nanometer
NMP	N-methyl pyrrolidine
NMR	Nuclear Magnetic Resonance
NOESY	Nuclear overhauser spectroscopy
p	Parallel
PCR	Polymerase Chain Reaction
PPh3	Triphenyl phosphine
PNA	Peptide Nucleic Acid
Pro	Proline
Pyr	pyrrolidinone
RNA	Ribonucleic acid
r.t	Room temperature
ss	Single strand/ Single stranded

T	Thymine
t-Boc	Tertiarybutyloxy carbonyl
TBTU	*O*-(Benzotriazol-1-yl)-*N*,*N*,*N*',*N*'-tetramethyluronium tetrafluoroborate
TEA	Triethylamine
TFA	Trifluroacetic acid
TFAA	Trifluroacetic unhydride
TFMSA	Trifluromethanesulphonic acid
THF	Tetrahydrofuran
UV-Vis	Ultraviolet- Visible

CHAPTER 1

INTRODUCTION

CHAPTER 1: INTRODUCTION

1.1 INTRODUCTION

1.1.1 Deoxyribose nucleic acid (DNA)

DNA is present in the nucleus of organisms and contains the genetic instructions specifying the biological development of all cellular forms of life and many viruses.[1] It is 52 years since Watson and Crick proposed the double-helical structure for duplex DNA (Figure 1).[2] The molecular architecture of DNA consists of a double-stranded helix of uniform diameter, a with right handed twist. The main chemical constituents of DNA are the sugar-phosphate unit present on the outside of the helix which constitutes the backbone of each strand and the nitrogenous bases adenine (A), thymine (T), guanine (G) and cytosine (C) which are pointed towards the center of the helix. Hydrogen bonds between complementary bases pairs (A:T; G:C) hold the two strands together (Figure 1).[3]

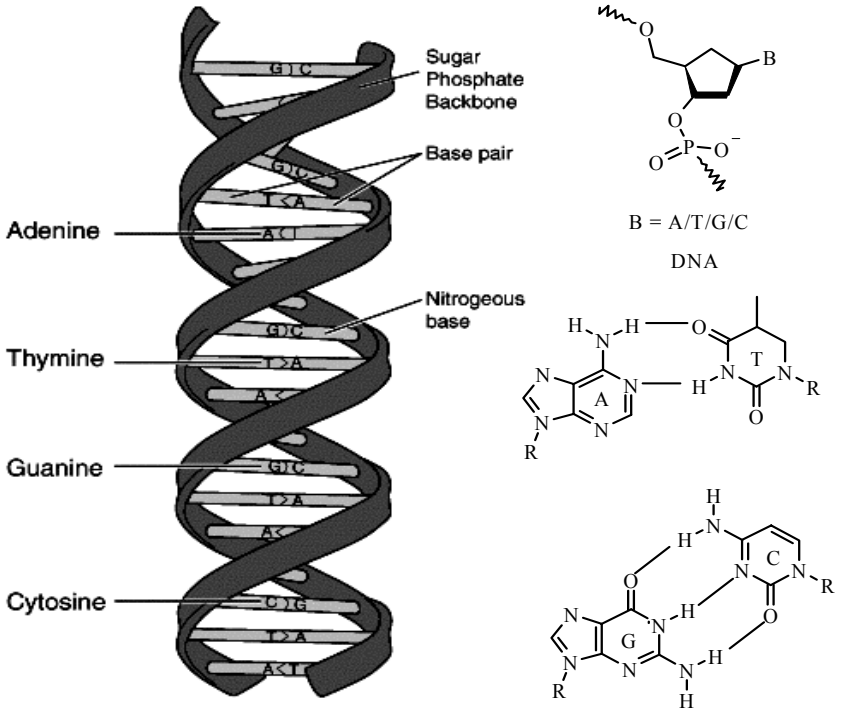

Figure 1: *Left*. DNA double helix; *Right.* Nucleotide and hydrogen bonding between nitrogenous bases.

The double helix of DNA is nature's simple and elegant solution to the problem of storing, retrieving, and communicating the genetic information of living organism.[4] The specificity and the reversibility of the hydrogen bond formation between the complementary nucleobases are one of the most important characteristic features, which allow the strands of the double helix to be unwound and then rewound in exactly the same configuration. The construction of DNA and design of its analogues for use in the recognition of specific DNA and RNA sequences has emerged as intellectual and practical assignment. The recognition of DNA and RNA sequences by complementary oligonucleotides is a central feature of biotechnology and is important for hybridization-based biological applications. The study of such complementary recognition is possible with the widely used experimental techniques and diagnostic protocols. This is vital to make antisense- or antigene-based inhibition as a practical approach to therapeutics. Zamecnik and Stephensen[5] were the first to propose the use of synthetic antisense oligonucleotides for therapeutic purposes. The specific inhibition is based on the Watson-Crick base-pairing between the heterocyclic bases of the antisense oligonucleotide and of the target nucleic acid.[6]

Various cellular processes can be inhibited depending on the site at which the antisense oligonucleotide hybridizes to the target nucleic acid (Figure 2). For an 'antisense' oligonucleotide[6] to be able to inhibit translation, it must reach the interior of the cell unaltered. The requirements for this are the stability of the oligonucleotide towards extra- and intra-cellular enzymes and equally important is its ability to traverse the cell membrane.[7] After reaching the cytoplasm, it must bind the target mRNA with sufficient affinity and high specificity. In addition, it must possess an adequate half-life inorder to elicit its action. The toxicity of the oligonucleotide should also be negligible to the cell. In the conceptually similar 'antigene' approach, the therapeutic oligonucleotide is targeted to

the complementary duplex DNA sequence to inhibit DNA replication. In order to meet all the requirements of a successful medicinal agent, it is necessary for normal oligonucleotides to be chemically modified in a suitable manner.[5,7]

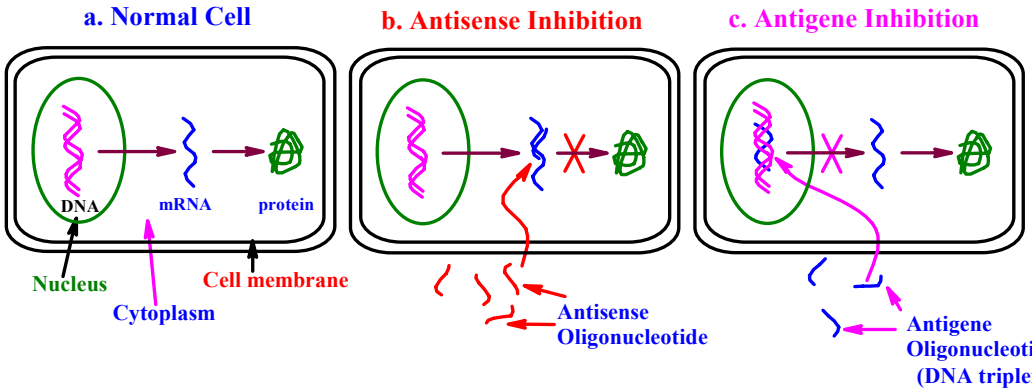

Figure 2: Principle of action of antisense and antigene oligonucleotides.

1.1.2 DNA analogues

To address the combined task of improving the rate, affinity or specificity of oligonucleotide recognition, while the enhancing membrane permeability and resistance to nuclease digestion, several chemical modifications of DNA have been attempted (Figure 3).[8] These principally include modification of the sugar-phosphate backbone and/or the nucleobases. The modifications of phosphate moiety resulting in phosphorothioates,[9] phosphorodithioates,[10] methylphosphonates,[11] phosphoramidates[12] and phosphotriesters[13] have lead to the first generation 'antisense' oligonucleotides. These have shown promising results, with one drug Vitravene (ISIS)[14] based on the phosphorothioates already approved by FDA for retinitis.

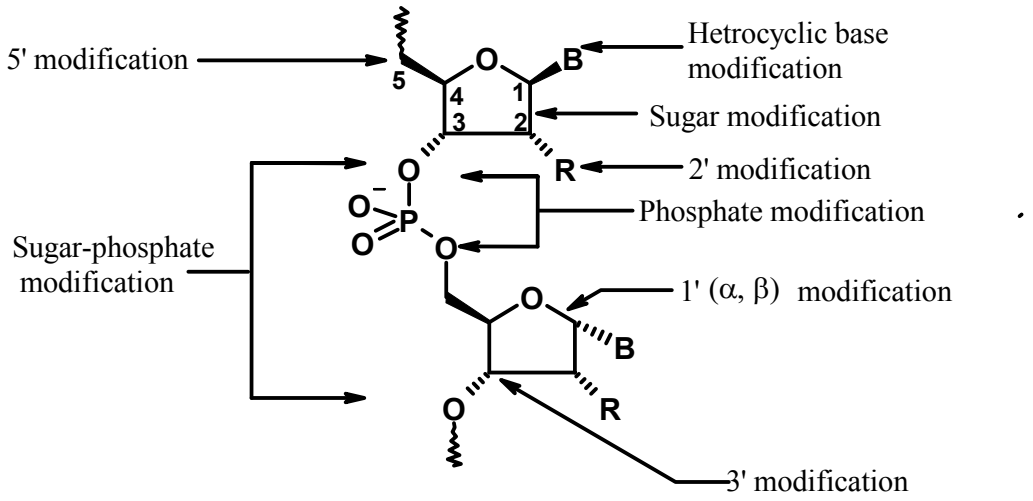

Figure 3: Structurally possible DNA modification site

Most of the chemical modifications include replacement of the phosphodiester linkage[11] by other atom W-X-Y-Z chain (Figure 4). Among these modifications, a few bind to complementary DNA/RNA fairly well, but none have exhibited the potency to be an effective drug. The replacement of the ribose sugar by hexose or carbocycles has not been very successful[15] in terms of specificity of binding/hybridization. However,

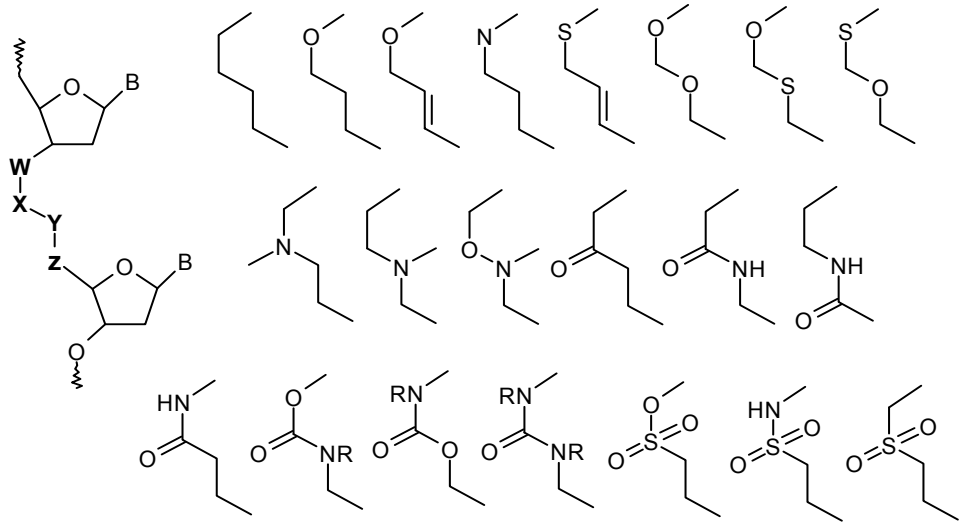

Figure 4: Phosphodiester Linkage Modifications

morpholino oligomers, where the monomers are linked through neutral carbamate linkages[16] or through phosphoramidate linkages (Figure 5a), have shown promising antisense activity as they have superior permeability properties.

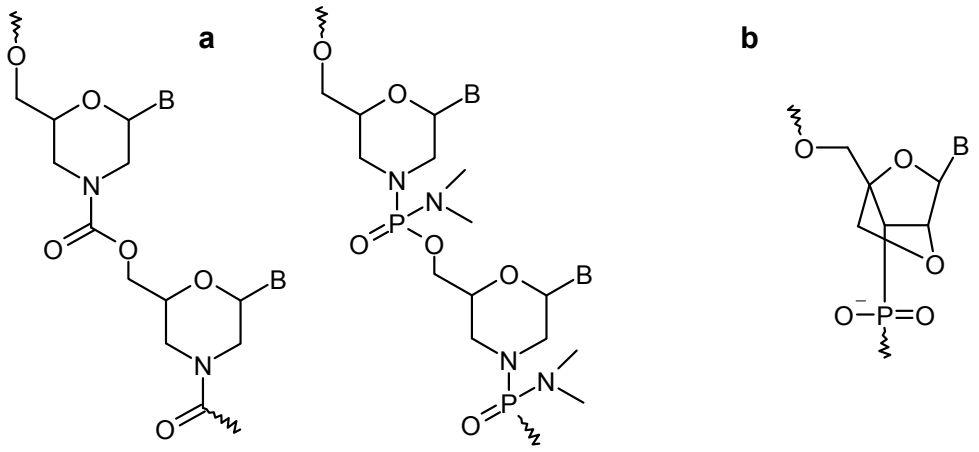

Figure 5: **a**. Morpholino oligomers and **b**. LNA

The locked nucleic acids (LNAs) invented by Wengel *et al.*[17] were found to exhibit unprecedented stability of their complexes with complementary DNA and RNA. They are also stable to 3'-exonucleolytic degradation and possess good water solubility. LNAs are oligonucleotides containing one or more 2'-*O*, 4'-*C*-methylene-β-D-ribofuranosyl nucleotides (Figure 5b).[18] The conformational preorganization of LNA is thought to be instrumental in imparting the enhanced binding affinity to DNA.

1.1.3 Peptide nucleic acid (PNA)

During the course of research on nucleic acid analogues, the novel aminoethylglycyl peptide nucleic acid (*aeg*-PNA)[19-21] **2** (Figure 6) has emerged as one of the most successful DNA mimics for potential therapeutic and diagnostic applications. PNA was originally designed and developed as a mimic of a DNA-recognizing, major groove-binding, triplex forming oligonucleotide. PNAs are neutral, achiral DNA mimics

that bind to complementary DNA/RNA sequences with high affinity and sequence specificity.[22] In PNA, the natural nucleobases are attached via methylenecarbonyl linkers to an uncharged, pseudopeptide backbone composed of repeating *N*-(2-aminoethyl)glycyl units. PNA hybridizes to complementary DNA/RNA sequences via specific base complementation to form duplexes for mixed sequences and triplexes for homopyrimidine/homopurine sequences. It is perhaps the most successful outcome of the chemical modification approach in nucleic acid analogues. The complexes of PNA with DNA/RNA sequences generally show thermal stabilities higher than the corresponding DNA-DNA/RNA complexes, depending on the sequence. PNAs and their analogues are also resistant to proteases and nucleases.[23]

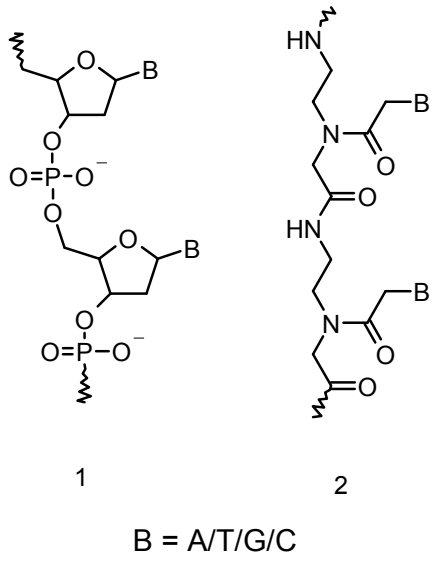

Figure 6: DNA and PNA Structure

PNAs bind to complementary DNA/RNA in either parallel or antiparallel modes, the antiparallel mode being slightly preferred over the parallel one. The antiparallel mode refers to the instance when the PNA 'N' terminus lies towards the 3'- end and the 'C' terminus, towards the 5'- end of the complementary DNA/RNA oligonucleotide. Likewise,

the parallel mode of binding is said to occur when the PNA 'N' terminus lies towards the 5'- end with the 'C' terminus towards the 3'-end of the complementary DNA/RNA oligonucleotide (Scheme 1).[24]

Scheme 1: Parallel and antiparallel modes of PNA-DNA binding

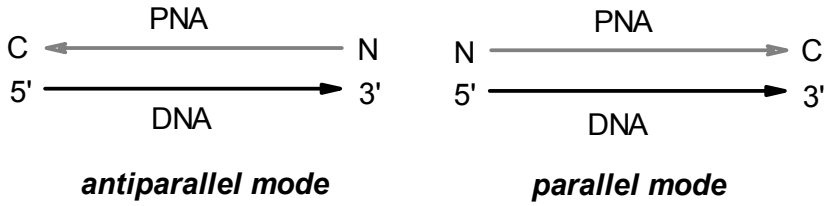

1.2 PROPERTIES OF PNA

1.2.1 Physiochemical properties

Peptide nucleic acids and DNA have no functional groups in common except for the nucleobases and the backbone linkages are quite different. Hence, the physicochemical property of PNA differs significantly from its DNA counterpart.[25]

1.2.1a Chemical Stability

In contrast to DNA, which depurinates on treatment with strong acids, while PNAs are completely acid stable.[26] It is thus possible to synthesize PNAs by using standard protecting groups from peptide chemistry. However under basic conditions, the N-terminal amino groups can initiate transamidation reactions.

1.2.1b Solubility

The PNA is a neutral molecule with a tendency for self-aggregation and limited water solubility. However, the introduction of charged groups, such as a C-terminal lysine, very much improves the properties.[24a,27] PNA solubility drops with increasing length and

purine:pyrimidine ratio and homoadenine PNA polymer is highly water soluble. Positive charges can also be introduced by modification of the PNA backbone, for instance by replacement of the glycine by a lysine unit. The incorporation of only two such groups greatly increases the solubility of the oligomers. Alternatively, negative charges can be introduced, which show enhanced water solubility.[28]

1.2.1c Binding affinity

PNAs complex efficiently to complementary DNA and RNA. The strongest binding affinity of PNA is to itself. As PNAs are uncharged, they appear to be predestined to form triple helical structures, in particular PNA_2:DNA, while PNA:$(DNA)_2$ triple helices are rarely observed for only certain sequences.[29] The formation of $(PNA)_2$:DNA hybrids is favored, through strand displacement in double-stranded DNA.[30] If the sequence is inappropriate for the formation of triple helices, then PNA:DNA, PNA:RNA[31] or, if applicable, PNA:PNA duplexes are formed.[32]

1.2.2 Structure of PNA:DNA complexes

The complexes formed by PNA with double stranded DNA targets are similar to hydrogen bonding pattern of nucleobases A/T/G/C in DNA. Homopyrimidine PNAs bind to double stranded DNA targets not by triplex formation as observed with the corresponding homomorphous DNA, but by an unusual and interesting mechanism of strand invasion (Figure 7).[33] Homopyrimidine poly-T PNA binds to the complementary poly-A DNA of poly (A:T) duplex forming a PNA_2:DNA triplex, by displacing the poly-T DNA strand which forms a P- or a D-loop structure (Figure 7a).[34] Homopurine PNA can invade a target DNA duplex (although with a lower efficiency) and form a PNA:DNA duplex, without any triplex formation, via displacement of one strand of the original DNA duplex (Figure 7b).[35] Recently, pseudo-complementary PNAs have been demonstrated to

invade the target DNA duplex by double-duplex invasion, forming two PNA:DNA duplexes wherein, each PNA strand pairs with its complementary DNA strand (Figure 7c).[36] In contrast to the strand displacement mode of binding, cytosine-rich homopyrimidine PNAs bind to target DNA duplexes as a third strand forming a PNA_2:DNA triplex (Figure 7d).[37] The complexes formed by PNA with either DNA or RNA are in general, thermally more stable than the corresponding DNA:DNA or DNA:RNA complexes. PNA:DNA duplexes are more stable when purines are in the PNA strand rather than in the DNA strand. Among the duplexes involving PNA, the generally observed thermal stability is of the order PNA:PNA > PNA:RNA > PNA:DNA.[24,38]

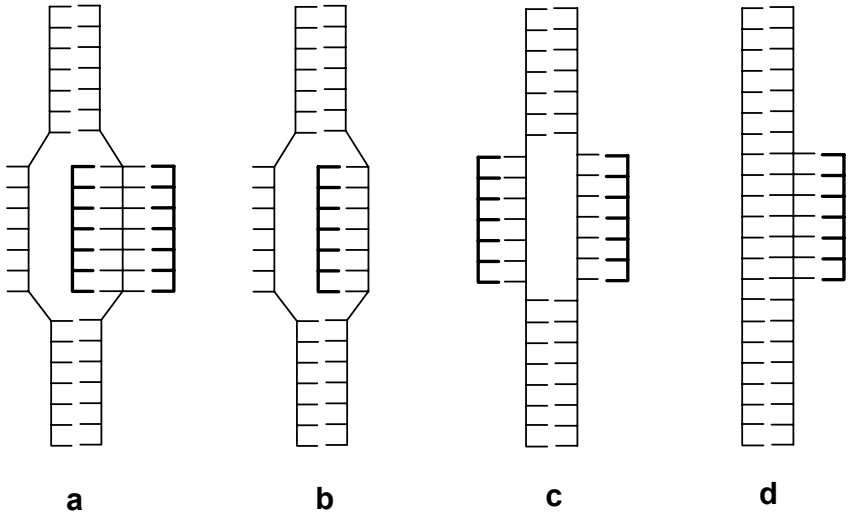

Figure 7: Strand invasion complexes of PNA-DNA: a) triplex invasion; b) duplex invasion; c) double duplex invasion; d) triplex formation.

The first report elucidating the structure of a nucleic acid-PNA hydrogen-bonded complex was put forth by Brown *et al.*[39] The NMR solution structure of a hexameric PNA, GAACTC, with complementary RNA revealed a 1:1 complex that is an antiparallel, right-handed double helix with Watson-Crick pairing similar to the 'A' form structure of RNA

duplexes. The achiral PNA backbone was found to assume a distinct conformation upon binding to the chiral RNA. This was followed by a crystal structure of a PNA_2:DNA triplex.[40] The PNA hairpin used was discovered to give a 'P-type' helix[41] that differed from previously reported nucleic acid structures. This helix was underwound, with a base tilt similar to B-form DNA. The bases were even more displaced from the helix than in A-form DNA. The deoxyribose sugars all have a C3'-*endo* conformation with an average inter-phosphate distance of 6.0Å, similar to the A-form DNA. This conformation is consistent with the observation that PNAs, including hairpins, bind more tightly to RNA than DNA. The tilt of the base triplets is however, similar to that of B-form DNA. Another structure of a PNA:DNA duplex derived from NMR[42] data and an X-ray crystal structure of a PNA:PNA duplex[43] were also subsequently reported. The PNA:DNA duplex was found to be very similar to the B-conformation of DNA, but preferred a unique different helix form, the P-form. This helix is very wide (28Å diameter) with a large pitch (18 base-pairs) and the base-pairs are almost perpendicular to the helix axis.

In general, from the crystal structure indicates that the PNA backbone seems to be flexible enough to adopt that conformation present in PNA:DNA/RNA hybrid (Figure 8).[43] The oligonucleotide in the PNA:RNA and the PNA:DNA duplexes adopts a conformation close to its natural ‘A’ and ‘B’ form respectively, in terms of sugar puckering, while the helix parameters have both ‘A’ and ‘B’ form characteristics.

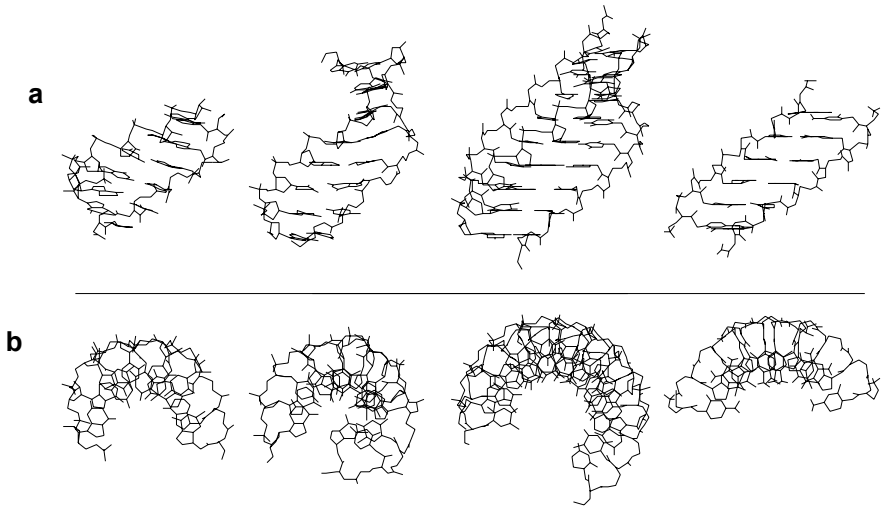

Figure 8: Structures of PNA complexes shown in side view (**a**) and top view (**b**). The complexes from left to right are PNA:RNA, PNA:DNA, PNA:DNA:PNA and PNA:PNA[43]

1.2.3 Antigene and antisense applications of PNA

Peptide nucleic acids are promising as candidates for designing gene therapeutic drugs.[44] They require well identified targets and a well-characterized mechanism for their cellular delivery. In principle, two general strategies can be adapted to design gene therapeutic drugs.[45] Oligonucleotides or their analogs are designed to recognize and hybridize to complementary sequences in a gene wherein they would interfere with the transcription of that particular gene (antigene strategy).[46] Alternatively, nucleic acid analogs can be designed to recognize and hybridize to complementary sequences in mRNA and thereby inhibit its translation (antisense strategy).[47] PNAs are chemically and biologically stable molecules and have significant effects on replication, transcription, and translation processes, as revealed from *in vitro* experiments. Moreover, no general toxicity of PNA has so far been observed. As we shall see, PNA can interfere with the translation

process, and PNA:dsDNA strand displacement complexes can inhibit protein binding and block RNA polymerase elongation.[44b]

1.2.3a Inhibition of transcription

Strand displacement complexes with DNA can create a structural hindrance to block the stable function of RNA polymerase and are thus capable of working as antigene agents. Nielsen *et al*.[48] have demonstrated that even an 8-mer PNA-T_8 is capable of blocking phage T3 polymerase activity. The presence of a PNA target within the promoter region of IL-2Ra[49] gene has been used to understand the effect of PNA binding to its target on this gene expression. The PNA_2-DNA triplex arrests transcription *in vitro* and is capable of acting as an antigene agent.[44] But one of the major obstacles to applying PNA as an antigene agent is that the strand invasion or the formation of strand displacement complex is rather slow at physiological salt concentrations. Several modifications of PNA have shown improvement in terms of binding.[50]

1.2.3b Inhibition of translation

The basic mechanism of the antisense effects by oligodeoxynucleotides is considered to be either a ribonuclease H (RNase H)-mediated cleavage of the RNA strand in oligonucleotide-RNA heteroduplex or a steric blockage in the oligonucleotide–RNA complex of the translation machinery (Figure 9).[51] Oligodeoxynucleotide analogs such as phosphorothioates activate RNase H and thus hold promise of working as antisense agents. However, they also exhibit some nonspecificity in their action. PNA/RNA duplexes, on the other hand, cannot act as substrates for RNase H. The antisense effect of the peptide nucleic acid is based on the steric blocking of either RNA processing, or translation.[52] Triplex-forming PNAs are able to hinder the translation machinery at targets in the coding region of mRNA. However, translation elongation arrest requires a

PNA_2:RNA triplex and thus needs a homopurine target of 10–15 bases. In contrast, duplex-forming PNAs are incapable of this. Triplex-forming PNAs can inhibit translation at initiation codon targets and ribosome elongation at codon region targets.

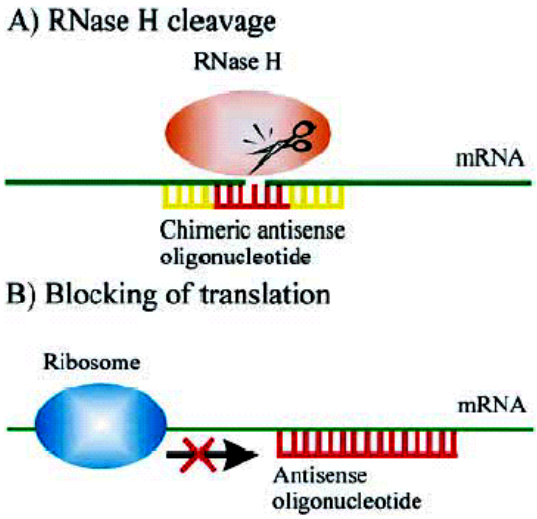

Figure 9: Mechanisms of antisense activity. (A) RNase H cleavage induced by (chimeric) antisense-oligonucleotides. (B) Translational arrest by blocking the ribosome. See the text for details.[52]

1.2.3c Inhibition of replication

It is also possible for PNA to inhibit the elongation of DNA primers by DNA polymerase. Further, the inhibition of DNA replication is feasible when the DNA duplex is subjected to strand invasion by PNA under physiological conditions or when the DNA is single stranded during the replication process.[53] Efficient inhibition of extrachromosomal mitochondrial DNA, which is largely single-stranded during replication, has been demonstrated by Taylor et al.[54] The PNA-mediated inhibition of the replication of mutant human mitochondrial DNA is a novel (and also potential) approach towards the treatment of patients suffering from ailments related to the heteroplasmy of mitochondrial DNA. Here wild-type and mutated DNA are both present in the same cell. Experiments have shown that PNA is capable of inhibiting the replication of mutated

DNA under physiological conditions without affecting the wild-type DNA in mitochondria.

1.2.4 Interaction of PNA with enzymes

1.2.4a Rnase H

The activation of the intracellular enzyme RNase H by oligonucleotides to cleave RNA bound to deoxyribonucleic acid oligomers depends on the chemical structure of Rnase H stimulating oligonucleotides. The antisense oligonucleotide with RNase H activity (e.g., phosphorothioate oligos) is considered a better antisense inhibitor than only steric block activity (methylphosphonates and hexitol nucleic acids).[55] Despite their remarkable nucleic acid binding properties, PNAs generally are not capable of stimulating RNase H activity on duplex formation with RNA. However, recent studies have shown that DNA-PNA chimeras (see in next section) are capable of stimulating Rnase H activity.[56] On formation of a chimeric RNA double strand, PNA-DNA chimera can activate the RNA cleavage activity of Rnase H.[56] Cleavage occurs at the ribonucleotide parts base paired to the DNA part of the chimera. Moreover, this cleavage is sequence specific in such a way that certain sequences of DNA-PNA chimeras are preferred over others. They are also reported to be taken up by cells to a similar extent as the corresponding oligonucleotides. Thus, PNA/DNA chimeras appear by far the best potential candidates for antisense PNA constructs.

1.2.4b Polymerase and reverse transcriptase

In general, there is no direct interaction of PNA with either DNA polymerase or reverse transcriptase.[57] However, different groups have shown indirect involvement of PNA in inhibiting these enzyme functions (activity) under *in vitro* conditions. For example, PNA oligomers are capable of terminating the elongation of oligonucleotide

primers by either binding to the template strand or directly competing with the primer for binding to the template. Primer extension by MMLV reverse transcriptase was shown to be inhibited by introducing a PNA oligomer. In another experiment, Nielsen *et al*.[37] demonstrated that the primer extension catalyzed by *Taq*-polymerase can be terminated by incorporating PNA-T_{10} oligomer into the system. The latter can bind to DNA dA_{10} sequence in the template and thereby terminate the primer extension. In addition, the reverse transcription can be completely inhibited by a pentadecameric antisense PNA, using a molar ratio of 10:1 (PNA/RNA), without any noticeable RNase H cleavage of the RNA.

1.2.4c Inhibition of human telomerase

Telomerase is a ribonucleoprotein and possesses an RNA component that can be targeted to effect inhibition of enzyme activity.[58] The designed PNAs were introduced into cells by transfection using cationic lipids. These PNAs were directed to non-template regions of the telomerase RNA. The problems due to the RNA secondary structure were overcome by intercepting the RNA component prior to holoenzyme assembly, leading to efficient inhibition of telomerase. The RNA template of telomerase was targeted by peptide conjugated derivatives of a PNA pentamer (Figure 10). It was shown that the presence of cationic peptides at the 'N' terminus of the PNA resulted in enhanced inhibition of telomerase activity. The inhibition was dependent on the specificity of PNA recognition. PNAs complementary to the 11-base template of hTR were shown to be potent inhibitors of human telomerase *in vitro* and PNAs were found to be 10-50 times more efficient inhibitors in comparison with phosphorothioate oligomers.

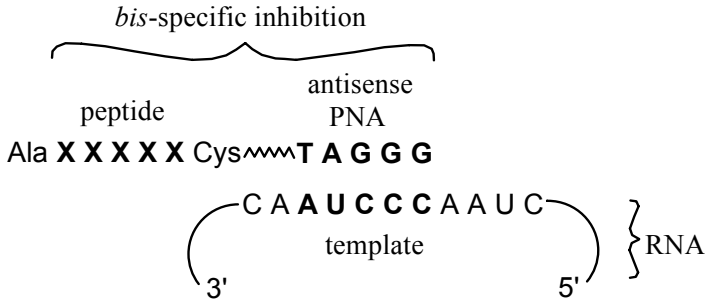

Figure 10: Design of PNA-peptide conjugates for inhibition of human telomerase.

1.3 BIOLOGICAL APPLICATIONS OF PNA

1.3.1 In situ hybridization (PNA-FISH)

The efficiency of PNAs as hybridization probes has also been demonstrated in fluorescence *in situ* hybridization (FISH) applications.[59] Because of their neutral backbone, PNA probes present *in situ* show a high specificity, require low concentrations and short hybridization times. The PNA-FISH technique was first developed for quantitative telomere analysis. Using a unique fluorescein-labelled PNA probe, Lansdorp *et al*.[60] performed the *in situ* labelling of human telomeric repeat sequences and the data obtained allowed accurate estimates of telomere lengths. Subsequently, telomeric PNA probes were used in several *in situ* studies of cancer and ageing.

1.3.2 Solid-phase hybridization techniques

PNAs can be used in many of the same hybridization applications as natural or synthetic DNA probes but with the added advantages of tighter binding and higher specificity. This leads to faster and easier procedures in most standard hybridization techniques.[61]

1.3.3 PCR and Q-PNA PCR

PNA probes have no direct interaction with DNA polymerase but PNAs can terminate the elongation of oligonucleotide primers by binding to the template or competing with the primers.[62] Furthermore, PNA-DNA chimeras can be recognized by the DNA polymerase and can thus be used as primers for PCR reactions.[63] The high affinity binding of PNAs has also been used for detecting single base pair mutations by PCR. This strategy, named PNA directed PCR clamping, uses PNAs to inhibit the amplification of a specific target by direct competition of the PNA targeted against one of the PCR primer sites and the conventional PCR primer. This PNA-DNA complex formed at one of the primer sites effectively blocks the formation of the PCR product. The procedure is so powerful that it can be used to detect single base-pair gene variants for mutation screening and gene isolation. More recently, novel automated real-time PCR has been developed using PNAs. In this method, named Q-PNA PCR, a generic quencher labelled PNA (Q-PNA)[64] is hybridized to the 5'-TAG sequence of a fluorescent dye-labelled DNA primer in order to quench the fluorescence of the primer. During PCR, the Q-PNA is displaced by incorporation of the primer into amplicons and the fluorescence of the dye label is liberated.

1.3.4 Anti-cancer agent

PNA-peptide:DNA duplexes, which can penetrates into cells, have been used in anti-cancer applications.[65] In this manner, telomerase activity in human melanoma cells and tumour specimens was inhibited by PNA conjugated with Antennapedia derived peptide (Antp) at nanomolar concentrations. Since telomerase is almost ubiquitously expressed in human tumours, the data point out the potential use of PNAs as anticancer drugs.[66] Applications of PNAs as anticancer agents were also reported with PNA complementary to various sequences of bcl-2.

1.3.5 PNA as delivery agents

A major limitation of non-viral gene therapy is the low efficiency of gene transfer into target cells. PNAs can be used as adapter to link peptides, drugs or molecular tracer to plasmid vectors.[67] According to the binding site, the coupling of PNAs to plasmids has no effect either on the transcription of genes included in the plasmid or on the plasmid's physiological activities. Thus, this approach allows circumventing such barrier to gene transfer and fixing drugs to plasmid in order to enhance the gene delivery or tissue-specific targeting. Using a triplex forming PNA as linker, Brandén *et. al*.[68] observed an eight times higher nuclear localization signal than did the free oligonucleotide.

1.4 BIOTECHNOLOGICAL APPLICATIONS OF PNA

1.4.1 PNA as a molecular-biological tool

Peptide nucleic acids also exhibit potential for use as a tool in biotechnology and molecular biology. Here we will mainly present indications of PNA becoming an important molecular biology tool.

1.4.1a Enhanced PCR amplification

The polymerase chain reaction (PCR) has been widely used for various molecular genetic applications including the amplification of variable number of tandem repeat (VNTR)[69] loci for the purpose of genetic typing. PNA has been used to achieve an enhanced amplification of VNTR locus D1S80. Small PNA oligomers are used to block the template, and the latter becomes unavailable for intra- and interstrand interaction during reassociation. On the other hand, the primer extension is not blocked; during this extension, the polymerase displaces the PNA molecules from the template and the primer is extended toward completion of reaction. This approach shows the potential of PNA

application for PCR amplification where fragments of different sizes are more accurately and evenly amplified. Since the probability of differential amplification is less, the risk of misclassification is greatly reduced.

1.4.1b PNA-assisted rare cleavage

Peptide nucleic acids, in combination with methylases and other restriction endonucleases, can act as rare genome cutters. The method is called PNA-assisted rare cleavage (PARC) technique.[70] It uses the strong sequence-selective binding of PNAs, preferably bis-PNAs, to short homopyrimidine sites on large DNA molecules, e.g., yeast or l DNA. The PNA target site is experimentally designed to overlap with the methylation/ restriction enzyme site on the DNA, so a bound PNA molecule will efficiently shield the host site from enzymatic methylation whereas the other, unprotected methylation/restriction sites will be methylated. After the removal of bis-PNA, followed by restriction digestions, it is possible to cleave the whole DNA by enzymes into limited number of pieces.

1.4.1c Determination of telomere size

The conventional method for the determination of telomere length involves Southern blot analysis of genomic DNA and provides a range for the telomere length of all chromosomes present. The modern approach uses fluorescein-labeled oligonucleotides and monitor *in situ* hybridization to telomeric repeats. However, Lansdorp *et al*.[71] shown a more delicate approach resulting in better quantitative results is possible by using fluorescein-labeled PNAs. This PNA-mediated approach permits accurate estimates of telomeric length. *In situ* hybridization of fluorescein-labeled PNA probes to telomeres is faster and requires a lower concentration of the probe compared to its DNA counterpart.

1.4.1d Nucleic acid purification

Based on its unique hybridization properties, PNAs can also be used to purify target nucleic acids. PNAs carrying six histidine residues have been used to purify target nucleic acids using nickel affinity chromatography.[72] Thus, short PNAs can also be used as generic capture probes for purification of large nucleic acids. It has been shown that a biotin tagged PNA-thymine heptamer could be used to efficiently purify human genomic DNA from whole blood by a simple and rapid procedure.

1.4.1e Isolation of mRNA

PNAs composed of *trans*-4-hydroxy-L-proline monomers and phosphono PNA monomers were utilized to achieve improved recovery of mRNA molecules with secondary structure at their 3' end as well as RNAs with short polyA tails.[73] By this method, mRNA free of genomic DNA contamination could be isolated. PNA has also been utilized to capture ds DNA of a particular sequence of interest by affinity capture in the form of linear, non-supercoiled molecules. The classical biotin-streptavidin recognition is utilized for this process (Figure 11).[73]

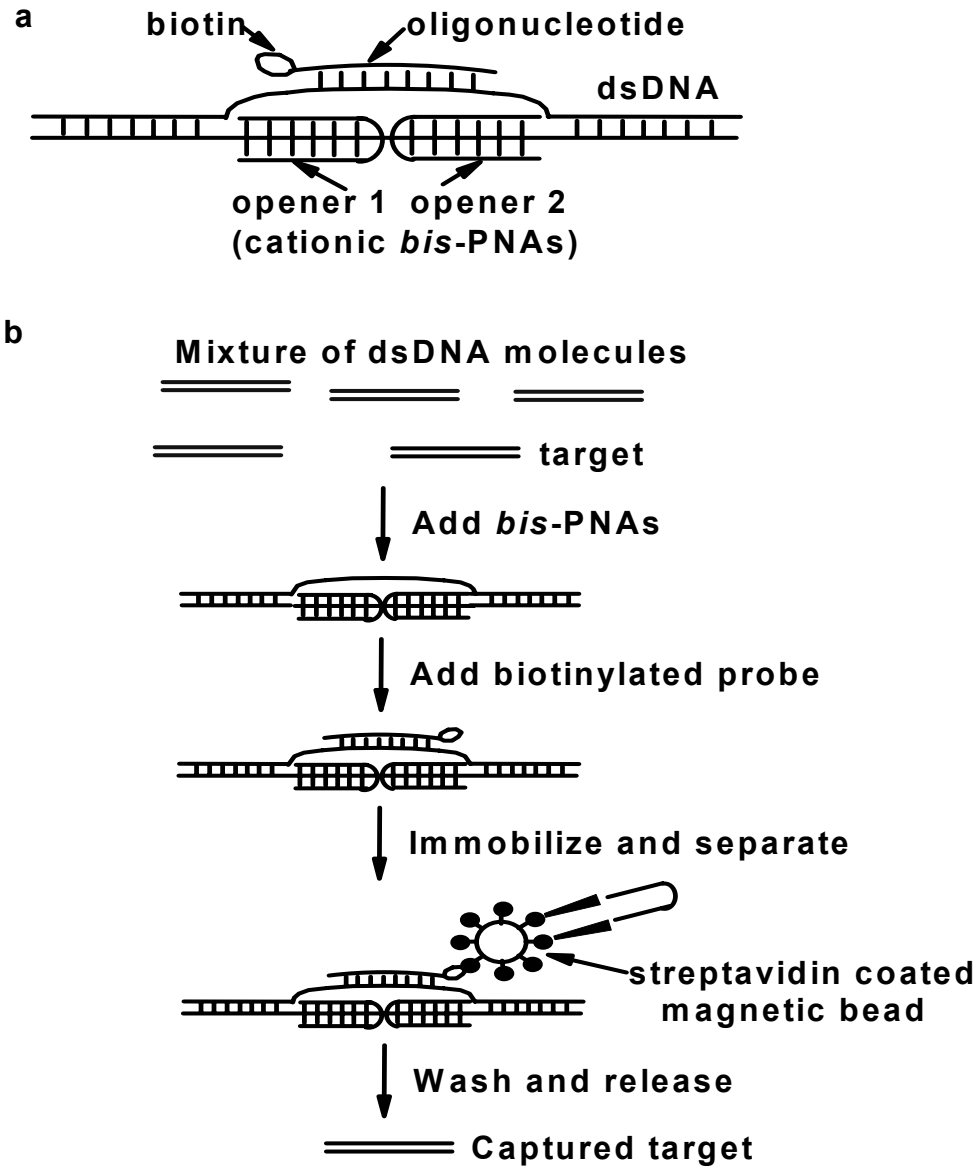

Figure 11: **a** The PD-loop consists of duplex DNA, an ODN and two PNA 'openers'. The ODN binds to the complementary DNA target *via* Watson-Crick pairing and carries biotin to provide capture on the affinity support. **b** The key steps of the procedure for dsDNA biomagnetic isolation.[73]

1.4.1f PNAs as artificial restriction enzymes

PNAs in combination with a non-specific nuclease, such as S1 nuclease, have been used as artificial restriction enzymes to cut target DNA at desired positions.[74] Double stranded DNA is cleaved at a site created by PNA strand displacement (Figure 12). This cleavage efficiency is enhanced more than 10 fold when a tandem PNA site is targeted, and additionally if this site is in *trans* rather than *cis* orientation. Thus, the single strand specific nuclease S1 behaves like a pseudo restriction endonuclease. The tethering of an artificial nuclease like Gly-Gly-His to PNA exhibits a similar effect. Binding to complementary DNA and in the presence of Ni, cleaves the DNA duplex in its *proximity.*

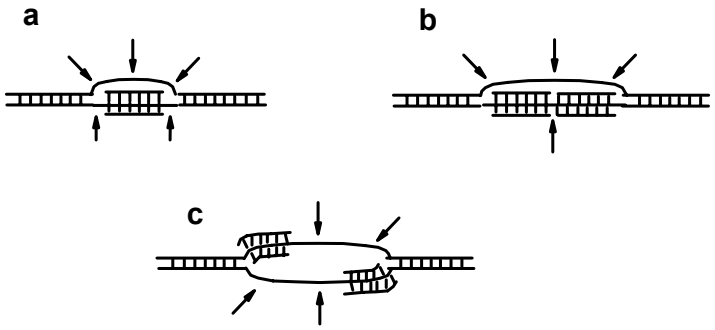

Figure 12: Schematic model for PNA-targeted S1 nuclease ds cleavage of DNA. **a** Single target . **b** Double target in *cis* orientation. **c** Double target in *trans* orientation. Arrows indicate S1 attack.

1.4.1g PNA as primordial genetic material

The currently widely-accepted theory of the origin of biomolecular life implies that RNA evolutionarily preceded all the other biomolecules, *viz*., DNA, proteins and carbohydrates.[75] The theory gained credibility because RNA provides the link between DNA and proteins. Moreover, RNAs have been discovered to possess catalytic activity (Ribozymes). However, RNA is highly unstable and it is suspectable how prebiotic life could have relied on such a fragile molecule as its genetic material. Miller[76] and Oro demonstrated that under the conditions prevailing on the primitive earth, nucleobases and

amino acids can be easily obtained, whereas, ribose and nucleosides are extremely difficult to obtain under the same conditions. Recently,[77] it was shown that the PNA precursors are possible prebiotic products. In addition, information transfer between PNA and RNA is also possible, although with low efficiency.

1.4.1h Plasmid labeling

In this approach, a highly fluorescent plasmid DNA is made by hybridizing fluorescently labeled PNA to it. Importantly, the plasmid is neither functionally nor conformationally altered. For this, a PNA homopurine binding site was cloned into a reporter gene plasmid in a region that is not involved in transcription regulation so that PNA-based probes could bind to the plasmid without affecting reporter gene expression.[78] The PNA clamp conjugated to reporter molecules like biotin, fluorescein or rhodamine did not affect the supercoiled conformation, nuclease sensitivity or transcription ability of the plasmid.[79] This method was employed to study the biodistribution of the plasmid upon transfection into cells. By using this system in a plasmid expressing green fluorescent protein (GFP), it was possible to simultaneously follow the delivery of the DNA and the expression of its transgene in real time in living cells.

1.4.2 PNA as a diagnostic tool

The high-affinity binding of PNA oligomers has led to the development of new applications of PNA, especially as a diagnostic probe for detecting genetic mutations: applications are possible for the detection of genetic mutation and mismatch analysis that can use its unique hybridization properties. The following sections will highlight some of the recent developments related to the use of PNA as a probe to detect genetic mutations and corresponding mismatch analysis confirming its potential as a diagnostic tool for clinical applications.

1.4.2a Single base pair mutation analysis using PNA directed PCR clamping

Amplification of the target nucleic acid by the PCR technique is considered an important step for detection of genetic diseases.[80] The higher specificity of PNA binding to DNA, higher stability of a PNA–DNA duplex compared to the corresponding DNA–DNA duplex, and its inability to act as a primer for DNA polymerases is the basis for this novel technique. The strategy includes a distinct annealing step involving the PNA targeted against one of the PCR primer sites.[81] This step is carried out at a higher temperature than that for conventional PCR primer annealing where the PNA is selectively bound to the DNA molecule. The PNA/DNA complex formed at one of the primer sites effectively blocks the formation of a PCR product. PNA is also able to discriminate between fully complementary and single mismatch targets in a mixed target PCR. Sequence-selective blockage by PNA allows suppression of target sequences that differ by only one base pair. Also, this PNA clamping was able to discriminate three different point mutations at a single position, as demonstrated in a model system by O'rum et al.[82] Thiede *et al*.[83] have reported a novel approach for simple and sensitive detection of mutations in the *ras* proto-oncogenes. A schematic representation of the strategy for the PCR cycle involving PNA-directed for mutation analysis using PNA-directed PCR clamping is shown in Figure 13.[75] In the case of the normal (wild-type) DNA, the bound PNA will sterically hinder annealing of a partially overlapping primer sequence, thus preventing the normal sequence from appropriate PCR amplification. In the case of mutant alleles, the melting temperature of the PNA/DNA is reduced and the primer can out-compete PNA annealing to carry on preferential amplification of mutant sequences.

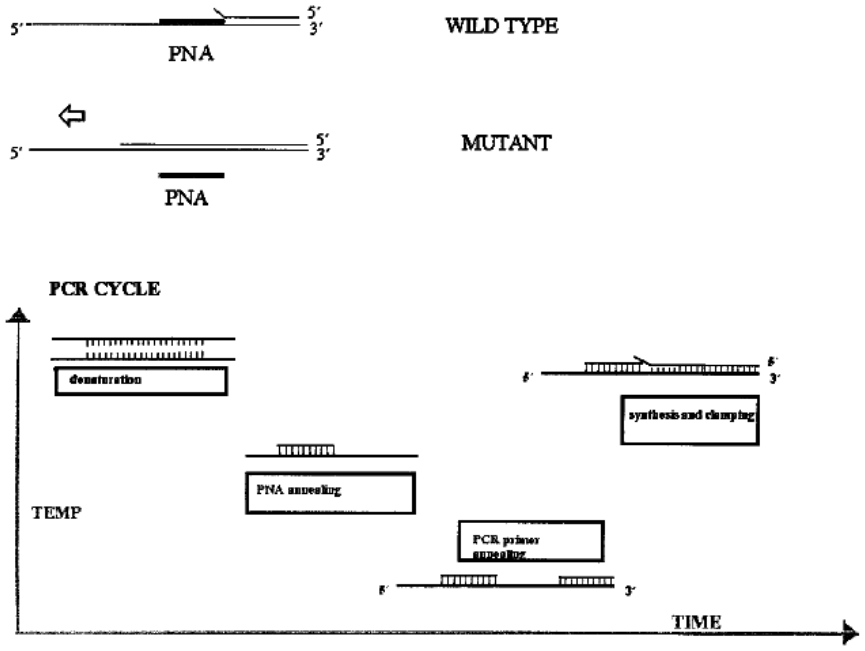

Figure 13. Mutation analysis using PNA-directed PCR clamping: schematic representation of the strategy for the PCR cycle involving PNA-directed clamping.

1.4.2b Screening for genetic mutations by capillary electrophoresis

In capillary electrophoresis,[84] the separation is generally carried out using a long, thin fused silica capillary (typically 50–80 cm long, inner diameter ; 10–300 mm). A portion of the coating, close to one end of the capillary, is removed to allow optical detection of the analyte. The analyte passes the detection window during a separation process and can be visualized by online automated UV, or laser-induced fluorescence (LIF) detection systems. A novel diagnostic method for the detection of genetic mutation using PNA as a probe for capillary electrophoresis has been reported by Carlsson *et al*.[85] The method is sensitive enough to detect a single mismatch in the sample DNA.

1.4.2c PNA as a probe for nucleic acid biosensor

The DNA biosensor technology holds promise for rapid and cost-effective detection of specific DNA sequences. A single-stranded nucleic acid probe is immobilized onto optical, electrochemical, or mass sensitive transducers to detect the complementary (or mismatch) strand in a sample solution. The response from the hybridization event is converted into a useful electrical signal by the transducer. The use of PNA as a novel probe for sequence-specific biosensors holds great promise for use as the recognition layer in DNA biosensors.[86]

1.4.2d BIAcore technique

The PNA hybridization and corresponding mismatch analysis can be studied using a BIAcore (biomolecular interaction analysis) instrument,[87] which can evaluate a real-time biomolecular interaction analysis using optical detection technology. The probe molecule is attached directly to the surface and the analyte molecule is free in solution. A biotinylated PNA [biotin-(eg1)3- TGTACGTCACAACTA-NH_2] probe was immobilized on the surface by using the strong coupling between biotin and streptavidin. Short spacer molecules, e.g., mercaptohexanol, can be used together with the ligand (probe) to form the PNA monolayer at the top of the sensor (gold) surface to prevent DNA from being nonspecifically adsorbed to the surface.

1.4.2e Quartz crystal microbalance (QCM)

The quartz crystal microbalance has been used for some time to monitor mass or thickness of thin films deposited on surfaces, study gas adsorption and deposition on surfaces in the monolayer and sub monolayer regimes.[88] A recent report by Wang and co-workers[89] on quartz crystal microbalance biosensor, based on peptide nucleic acid probes,

showed that the system can differentiate between a full complementary and single mismatch oligonucleotide.

1.4.2f MALDI-TOF mass spectrometry

MALDI-TOF mass spectrometry has been used successfully in PNA-based diagnostic research to study discrimination of single-nucleotide polymorphisms (SNPs) in human DNA.[90] Human genomic and mitochondrial DNA contains many SNPs that may be linked to diseases. Rapid and accurate screening of important SNPs, based on high-affinity binding of PNA probes to DNA, is possible by using MALDI-TOF mass spectroscopy.[91]

1.4.2g Potentiometric measurements

Wang *et al*.[92] have also reported the use of PNA as a recognition probe for the electrochemical detection of the hybridization event using chronopotentiometric measurements. The method consists of four steps: probe (PNA) immobilization onto the transducer surface, hybridization, indicator binding, and chronopotentiometric transduction.[93] A carbon paste electrode is in this process containing the immobilized DNA or PNA probe. The hybridization experiment was carried out by immersing the electrode into the stirred buffer solution containing a desired target, followed by measurement of signal.

1.4.2h PNA microarray

The basic requirement for the array system is the ability of all different probes to hybridize to their target sequences with high specificity at single temperature. As PNAs are neutral, they can hybridize with nucleic acids in absence of counter ions needed to stabilize pure nucleic acid duplexes. It has been demonstrated that PNA probes can effectively discriminate between single base mismatches in the target sequence at temperature near the optimum for hybridization.[94-95] They can also be used to analyze and

roughly quantify the amount of target molecules over a considerable concentration range. PNA arrays can be reused much more often than conventional oligonucleotide array, since the PNA molecules are extremely stable under conditions, which natural DNA cannot withstand.

1.4.2i Antiviral PNAs

One of the key enzymes in the life cycle of retroviruses (such as HIV), reverse transriptase, is very sensitive to PNA "Antisense Inhibition'. Reverse transcription of the RNA template is effectively arrested by PNA oligomers bound to the template.[96] This finding has raised hope that DNA antiviral drugs could be developed with the demonstration that HIV replication in cell culture can be inhibited by PNA targeting *gag-pol* gene.[97] However, very high PNA concentrations were required emphasizing the need of an efficient cell delivery system for PNA.[98]

1.4.2j Antibacterial PNAs

Inhibiting translation through directly interfering with the ribosome will shut down all protein synthesis, providing a very potent antibiotic strategy. Good and Nielsen[99] demonstrated that PNAs targeted to two regions of ribosomal RNA, the alpha-sarcin loop and the peptidyl transferase center, were capable of causing cell death in bacterial colonies. Homopyrimidine bisPNAs were more effective than the monoPNAs, indicating that triplex formation was important for the observed antibiotic activity. It has been reported that 9-12 mer PNAs attached to the cell wall/membrane–active peptide $(KFF)_3K$,[100] provide improvement in antisense potency in *E. Coli* amounting to two orders of magnitude while retaining target specificity. Peptide-PNA conjugates targeted to rRNA and to mRNA encoding the fatty acids biosynthesis protein Acp, prevented cell growth of *E. coli* K12 without any apparent toxicity to human cells. This indicates that the peptide

can be used to carry antisense PNA agents into bacteria. Such peptide-PNA conjugates open exciting possibilities for anti-infective drug development and provide new tools for microbial genetics. These results bear promise that PNA could be developed as 'generic antibiotics'.

1.4.3 Cellular uptake of PNA

PNAs do not readily enter cultured cells unless present at high concentrations in the media and unlike DNA/RNA, they cannot be complexed directly with cationic lipids because they are uncharged. However, Corey *et. al.*[101] have reported a novel method for *in vitro* cellular delivery of PNAs using cationc lipid. The cationic lipid is capable of associating with the negatively charged phophodiester backbone of DNA and RNA and fusion with the cell membrane allows the oligonucleotides to enter into the cell. Desired PNA oligomers are hybridized to overlapping oligonucleotides and the complex is mixed with cationic lipid. The cationic lipid-DNA-PNA complex thus formed can be internalized and the partially hybridized PNA is imported into the cell. Cellular uptake of PNAs can also be achieved by the attachment of peptide sequence that promotes translocation across cell membranes. Peptides such as Trojan peptide and penetratin have been used as carriers for cellular delivery of PNA.[98] Another strategy that has been adapted to improvise the delivery of PNA *in vitro* is to incorporate it into delivery vehicles (vesicles), e.g. liposomes. Nucleic acid- PNA chimeras are reported to be taken up even at lower extracellular concentration (1μM), so PNA-DNA chimera may be better antisense agent.[102] At higher concentrations of PNA, cytotoxic effects could also be observed.

1.5 CHEMICAL MODIFICATION OF PNA

The structure of the classical PNA monomer has been subjected to a variety of rational modifications with the aim of understanding the structure-activity relations as well as obtaining PNA oligomers with specifically improved properties for various applications in medicine, diagnostics and molecular biology.[103] The limitations of PNA for such applications include low aqueous solubility, ambiguity in DNA binding orientation and poor membrane permeability. Structurally, the analogues can be derived from modifications in the ethylenediamine or glycine part of the monomer, linker to the nucleobase, the nucleobase itself or a combination of the above. The strategic rationale behind the modifications are (i) introduction of chirality into the achiral PNA backbone to influence the orientational selectivity in complementary DNA binding, (ii) rigidification of PNA backbone *via* conformational constraint to pre-organize the PNA structure and entropically drive the duplex formation, (iii) introduction of cationic functional groups directly in the PNA backbone, in a side chain substitution or at the N or C terminus of the PNA to improve water solubility, (iv) modulate nucleobase pairing either by modification of the linker or the nucleobase itself for effective binding at physiological conditions and (v) conjugation with 'transfer' molecules for effective penetration into cells. In addition to improving the PNA structure as above for therapeutics, several modifications are directed towards their applications in diagnostics. Some of the modifications are discussed below.

1.5.1 Construction of non-bridged PNA structures

To improve the binding affinity and to enhance aqueous solubility of PNA while retaining its basic acyclic structure, various chemical modifications have been carried out. Improvement of aqueous solubility of PNAs has been achieved by the introduction of charges within the molecule or by the introduction of ether linkages in the backbone (Figure 14).[104a]

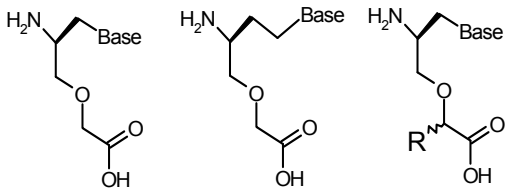

Figure 14: Ether-linked PNA (OPNA).

Making PNA anionic also aided in increasing the water solubility as in the case of the phosphonate analogs, but was accompanied by a decrease in the binding affinity to complementary nucleic acid sequence (Figure 15).[104b] The chiral versions of these analogs similar to original PNAs led to excellent aqueous solubility properties. PNAs composed of monomers derived from serine and homoserine coupled by ether linker with glycine or alanine, were able to bind sequence specifically to RNA, though with much weaker affinity.

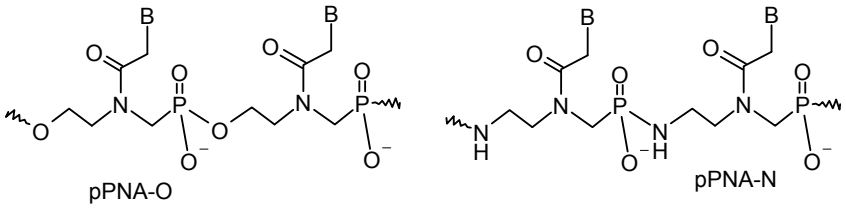

Figure 15: Phosphonate PNA.

Novel class of cationic PNA (DNG/PNA) which binds to DNA/RNA targets with high affinity has been also reported (Figure 16a).[102] In another report guanidium functional group was introduced into the PNA backbone, which exhibited remarkable cellular uptake properties while maintaining Watson-Crick recognition with complementray DNA strand (Figure16b).[103]

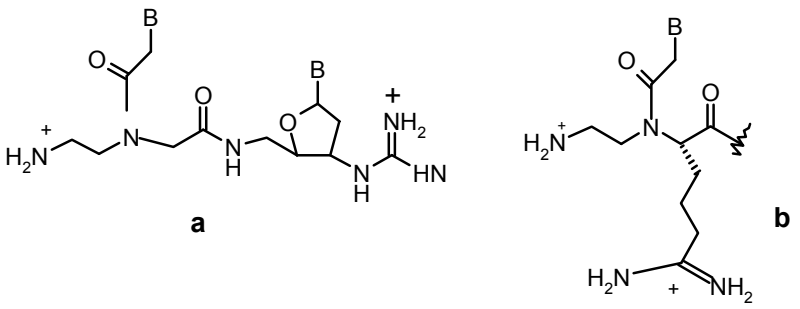

Figure 16: (a) PNA-DNG chimera. (b) GPNA.

Another type of modification involved interchange of various CO and NH groups on the peptide linkages leading to retro-inverse, peptoid and heterodimeric analogs (Figure 17).[104] Except for the heterodimer analogue (Figure 17c),[105] these exhibited a lower potency for duplex formation with complementary DNA/RNA suggesting that in addition to geometric factors, other subtle requirements such as hydration and dipole-dipole interactions that influence the environment of backbone, may be involved in effecting efficient PNA:DNA hybridization.

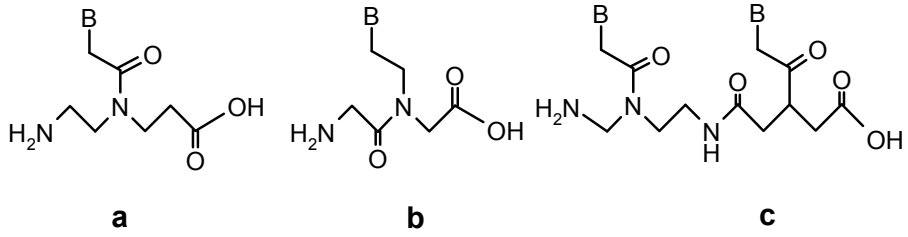

Figure 17 a: Retero-inverso, **b**. Peptoid and **c**. Heterodimeric PNA.

In another case, PNA backbone was extended by inserting a methylene group either in aminoethyl part or in the linker to the nucleobase (Figure 18).[106] The thermal stability of the hybrids between these PNA oligomers and complementary DNA oligonucleotide was significantly lower than that of the corresponding *aeg*PNA. However,

the sequence selectivity was retained. Thymidyl decamers with these modified units were unable to hybridize to the complementary dA_{10} oligonucleotide, while PNA decamer containing only ethylenecarbonyl linkers between the nucleobases showed weak affinity for complementary DNA.[107]

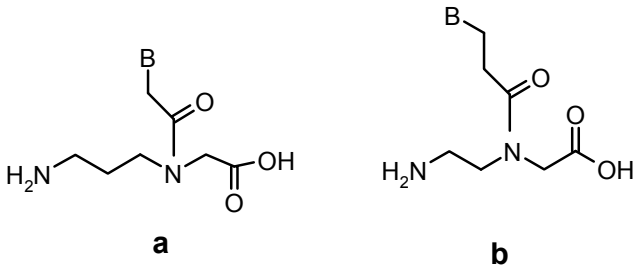

Figure 18: Backbone and side chain extended PNA.

1.5.2 Construction of bridged PNA structures

Any favorable structural reorganization of PNA may trigger a shift in equilibrium towards the desired complex formation because of the reduced entropy loss upon complex formation, provided that the enthalpic contributions suitably compensate. This may be achieved if the conformational freedom in *aeg*-PNA is curtailed by bridging the aminoethyl/glycyl acetyl linker arms to give rise to cyclic analogs with preorganized structure. Additionally, the introduction of chemical bridges into *aeg*-PNA to provide cyclic structure may help in controlling the rotameric population by fixing the nucleobase orientation. Such modifications also introduce chiral centers into PNA monomeric units with the possibility of further fine-tuning the structural features of PNA to mimic DNA.[108]

1.5.2a PNA with 5-membered nitrogen heterocycles

The naturally occurring amino acid *trans*-4-hydroxy-L-proline, a five-membered nitrogen heterocycle with useful substituents and easily manipulated stereochemistry, is a versatile, commercially available starting material amenable for creating structural diversity to mimic the DNA/PNA structures. Many researchers have exploited *trans*-4-

hydroxy-L-proline for the synthesis of a wide variety of chiral, constrained and structurally preorganized PNAs.[109] Depending on the construction strategy and the presence or absence of the tertiary amine group in monomers; the modifications afford either positively charged or uncharged cyclic PNA analogues.

***Aminoprolyl PNA*:** The introduction of a methylene bridge between β-carbon atom of the aminoethyl segment and the α'carbon atom of the glycine segment of the *aeg*PNA resulted in 4-aminoprolyl PNA, with the introduction of two chiral centers (Figure 19).[110] Upon partial substitution of these monomers into PNA oligomer, these exhibited tendency to hybridize with nucleic acids similar to that of unmodified PNA. Interestingly, inclusion of even one 4-aminoproline unit into a PNA sequence, either at the *N*-terminus or in the interior resulted in a very interesting CD profile and lead to stabilization of derived PNA-DNA hybrids simultaneously effecting significant discrimination in the orientation of binding. The stability of such complexes decreases with increasing number of chiral prolyl units and homooligomers derived from each of the diastereomers completely failed to form duplexes. In another report,[111] alternating 4-aminoprolyl and glycine units stabilize the complex suggesting that in the homo-oligomer, inter-nucleoside distances are too low.

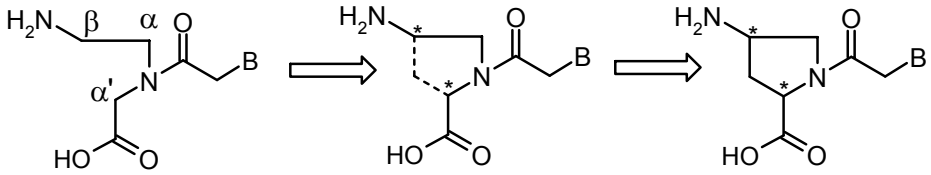

Figure 19: **A**minoprolyl PNA.

***Gly-Pro-Peptide PNA*:** The methylene bridge was inserted between the *α*-carbon atom of the glycine unit and the *β'*-carbon atom of the nucleobase linker of *aeg*-PNA (Figure

20).[111] Unlike other PNAs, this has a tertiary amide group with the amide nitrogen part of a cyclic ring system on the backbone. This leads to highly rigid structures that are not poised for effective duplex formation.

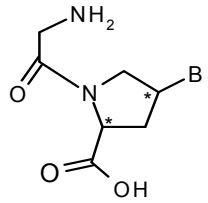

Figure 20: Gly-pro peptide PNA.

Aminoethylprolyl (aep) PNA: The replacement of the tertiary amide carbonyl on the backbone by a methylene group relieves strain to generate *aep*-PNA (Figure 21).[112, 113] These show remarkable biophysical properties in terms of triplex stabilities. Hitherto unprecedented higher melting of the derived PNA:DNA hybrids reflected very significantly enhanced DNA affinity while retaining the base pair discriminating power. The mixed pyrimidine hairpin sequences with cytosine and N-7 guanine *aep*PNA[114] units exhibited directional discrimination in binding to parallel/antiparallel DNA sequences.

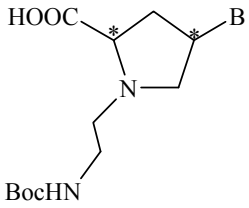

Figure 21: *aep*-PNA.

***Pyrrolidinone (pyrr) PNA*:** A methylene bridge was inserted between the α carbon atom of the aminoethyl segment and the *β*-carbon atom of the acetyl linker to the nucleobase of *aeg*PNA (Figure 22).[115] The synthesis of all the four diastereomers of adenin-9-yl-*pyr*PNA was accomplished and the oligomers incorporating the (3*S*,5*R*) isomer were shown to have highest affinity for RNA compared to DNA. The fully modified decamer bound to rU_{10} with a small decrease in the binding efficiency relative to *aeg*PNA.

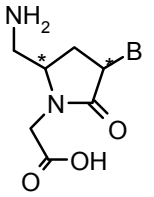

Figure 22: Pyrrolidinone PNA.

Prolyl-(β-amino acid) peptide PNA: The conformational strain in the alternating proline-glycine backbone was released by replacement of the α amino acid residue by different β amino acid spacers with appropriate rigidity. Novel pyrrolidinyl PNAs comprising alternate units of nucleobases modified with D-proline, either D/L aminopyrrolidine-2-carboxylic acid, (1*R*,2*S*)–2-aminocyclopentanecarboxylic acid or *β*-alanine were synthesized (Figure 23).[116-117]

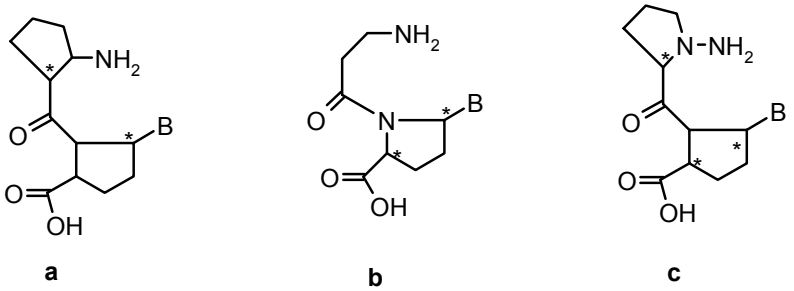

Figure 23: (a) prolyl-2-amino cyclopentanecarboxylic acid. (b) prolyl-β-alanine, c) prolyl-D/L-aminopyrrolidine carboxylic acid.

Pyrrolidine PNA and pyrrolidine PNA-DNA chimera: Insertion of a methylene bridge in *aeg*PNA, linking the α-carbon atom of the aminoethyl segment and the *β*-carbon atom of the tertiary amide linker, afforded the pyrrolidine PNA (Figure 24a).[118] A fully modified (2*R*,4*S*) pyrrolidine PNA decamer formed very stable complexes with both DNA and RNA targets. The incorporation of the (2*S*,4*S*) thymine monomer into oligomers and mixed pyrimidine oligomers resulted in a decreased binding efficiency with the target DNA/RNA sequences. The (2*R*,4*R*) isomer was incorporated into a PNA:DNA dimer amenable to the synthesis of PNA:DNA chimeras (Figure 24b). The chimeric PNA:DNA bound to the target DNA with decreased efficiency relative to the native DNA.

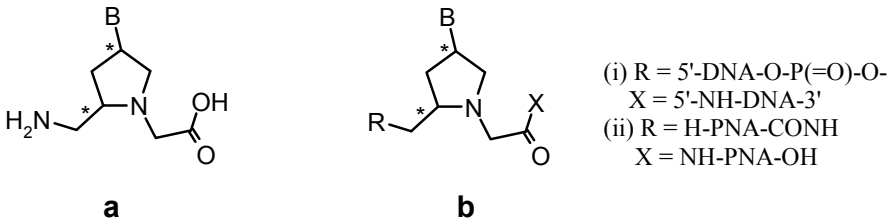

Figure 24: (a) Pyrrolidine PNA. (b) Pyrrolidine PNA-DNA chimerae.

A cyclopentane conformational restraint for a peptide nucleic: Based on molecular modelling studies (1*S*, 2*S*) cyclopentadiamine ring was used for conformational restraint of the C2-C3 dihedral angle of the PNA backbone. The *trans* cyclopentane modification improves the stability of PNA-DNA triplexes and PNA-RNA duplexes for a poly-T PNA.[119] Recently cyclopentyl PNAs having *cis* isomers have been reported (Figure 25).[120] The results suggest that these have a stereochemistry dependent stabilization effect on binding both DNA and RNA. The *cp*PNAs have a better selectivity for mismatch DNA sequence and a higher binding to complementary DNA sequence than the unmodified PNA.

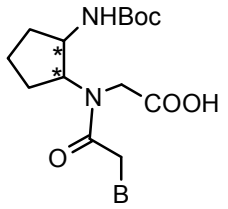

Figure 25 Cyclopentyl PNA.

***Thiazane and thiazolidine PNA*:** Bregant, *et. al*.[121] introduced rigidity by induction of ring containing thiazane and thiazolidine in the backbone of PNA (Figure 26) . With the presence of sulfur in ring, both PNAs showed improved solubility, but, the derived PNA/DNA triplexes were destabilized.

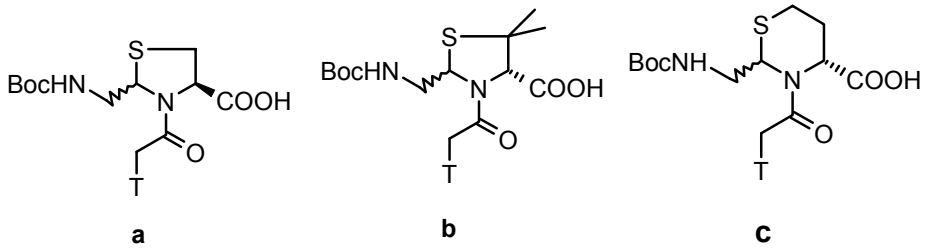

Figure 26: (a-b) Thiazane. Thiazolidine (c)

***Peptide ribonucleic Acids, PRNA*:** The synthesis of poly-L-glutamic acid in which ribonucleoside units are attached to the side chain as pendant groups through an amide linkage between the γ-carboxyl function of the side chain and the 5-amine of the 5-amino-5-deoxyribonucleoside afforded the α-peptide ribonucleic acid α-*PRNA* (Figure 27a).[122a] The strategy was to actively control the function of these oligomers through an external factor. Unfortunately, the efficiency of the external control was not very high because of the mismatched distance of the nucleobases and as a result, the complexes were all

destabilized. The strategy was further improved by the synthesis of isopoly-L-glutamic acid in which the ribonucleoside units were attached as pendant groups through an amide linkage between the α-carboxy function of the glutamic acid and the 5'-amine of the ribonucleoside. This gave rise to the γ-peptide ribonucleic acid (Figure 27b),[122b] in which the nucleobases were in the correct positions for RNA/DNA recognition. The 1:1 complex of homothymine γ-*PRNA* with complementary DNA was considerably more stable than the unmodified PNA-DNA complex. The mixed base sequence was also able to exhibit high directional selectivity, the antiparallel complex being more stable than the parallel one. The presence of the ribose sugar could favourably improve the water solubility of γ-*PRNA*. The concept of external control on DNA/RNA, recognition through duplex formation is quite interesting and may have potential in the next generation of antisense molecules.

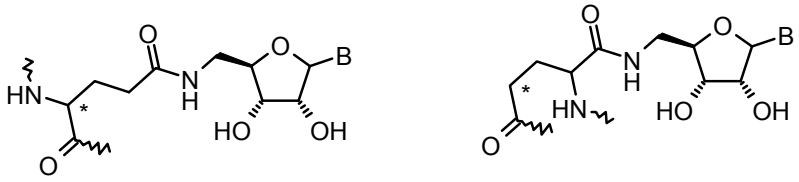

Figure 27: (a) α-PRNA with polyglutamate backbone. (b) γ-PRNAwith polyisoglutamate backbone

1.5.2b PNA with six membered ring structures

Six-membered ring structures exhibit unique conformational preferences, and the binding abilities of hexose sugar phosphate containing oligonucleotide have been extensively studied by Eschenmoser *et. al*.[123] The ability of morpholino, hexitol, and cyclohexene oligonucleotides to bind to DNA/RNA is well established and is dictated by the conformational preferences of the six membered ring structures (Figure 28). Conformations in the six membered ring structures are rigid, in contrast to the relatively

flexible five membered rings, and hence their influence on the stability of the resulting PNA-DNA/RNA complexes may be expected to make important contributions to the stabilities of the DNA/RNA complexes.

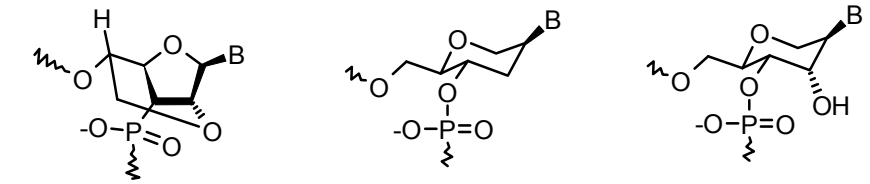

Figure 28: (a) Locked 3-*endo* conformation in LNA. (b) Frozen 3'-*endo* conformation in hexitol and altritol.

Glucosamine Nucleic Acids (GNAs): The six membered glucosamine ring appeared to fulfill the requirement of optically pure and constrained conformational scaffolding for the attachment of nucleobases (Figure 29).[124] The homopyrimidine and mixed base sequences using GNA monomer were constructed. The binding affinities and selectivities of these oligomers to DNA and RNA targets indicated selective recognition of RNA by Watson–Crick hydrogen bonding. The entropy changes were found to be smaller for GNA-DNA/RNA than for DNA-DNA/RNA, consistent with idea that the GNA oligomer was preorganized for binding to the target sequences.

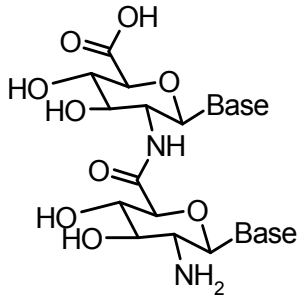

Figure 29: Dimer of GNA

Aminopipecolyl PNA, pip-PNA*:* In the quest to produce a PNA analogue with favourable geometry for optimum binding to the target DNA sequences, a PNA analogue with a six-membered ring was synthesized. This structure was arrived at by introducing a methylene bridge between the γ-carbon atom and the α-carbon atom of the aminopropylglycyl PNA (Figure 30).[125] It was envisaged that the increased conformational freedom and the internucleobase distance in the aminopropylglycyl PNA could be effectively curtailed by a bridged system in the monomeric unit. This was synthesized and incorporated into the homo-pyrimidine *aeg*PNA. The complexes with target DNA were found to be destabilized and the additional methylene groups caused reduced water solubility in the modified oligomers.

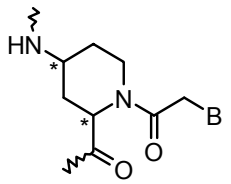

Pipecolyl PNA

Figure 30: Pipecolyl PNA based on *γ*-*α*-methylene bridge in an aminopropylglycyl backbone.

Aminoethyl pipecolyl PNA**:** The α carbon atom of the glycyl unit and β carbon atom of linker to a nucleobase are bridged by an ethylene unit to get six membered aminoethylpipecolyl PNA (Figure 31).[126] When introduced into PNA oligomers, UV-Tm studies indicated that (2*S*,5*R*)-1-(*N*-Boc-aminoethyl)-5-(thymin-1-yl)pipecolic acid, *aepip*-PNA, stabilize the resulting complex with complementary DNA.

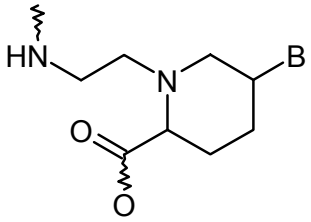

Figure 31: aminoethyl pipecolyl PNA

***Piperidinone PNA*:** Introduction of an ethylene bridge between the α carbon atom and β' carbon atom in the ethylenediamine and acetyl linker resulted in a six-membered ring structure piperidinone PNA (Figure 32).[127] (3*R*,6*R*) and (3*S*,6*R*) adenine monomers were synthesized and incorporated into *aeg*PNA which resulted in a large decrease in the duplex stability.

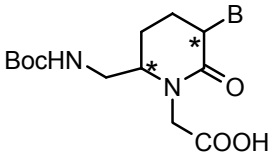

Figure 32: Piperidinone PNA

***Cyclohexyl PNA*:** Introduction of local conformational constraint in the *aeg*PNA resulted in the chiral cyclohexyl-derived backbone (Figure 33).[128] The aminoethyl segment of the *aeg*PNA was replaced with a 1,2 diaminocyclohexyl moiety, either in the (*S*,*S*) or (*R*,*R*) configuration. The oligomers with (*S*,*S*)-cyclohexyl residues were able to hybridize with DNA or RNA, with little effect on thermal stability. Molecular modeling studies revealed that (*S*,*S*) isomer can be accommodated more easily in duplex than (*R*,*R*) isomer. In contrast, incorporation of the (*R*,*R*) isomer resulted in a drastic decrease in the stability of PNA-DNA/RNA complexes. The complexes formed by the two isomers were of the opposite handedness, as evident from CD spectroscopy. The synthesis of ethyl *cis*–(1*S*,4*R*/1*R*,2*S*)-2-aminocyclohex-1-yl-*N*-(thymin-1-yl-acetyl) glycinate waws reported *via*

enzymatic resolution of the *trans*-2-azido cyclohexanols. The crystal structure of the intermediate showed an equatorial disposition of the tertiary amide group, with the torsion angle β in the range 60°-70°. UV-Tm experiments showed that (1*S*,2*R*) isomer preferred to bind RNA and (1*R*,2*S*) isomer showed higher affinity towards DNA in homothymine sequences leading to stereodiscrimination in recognition of DNA and RNA.[129]

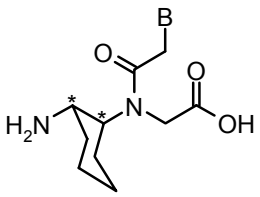

Figure 33: Cyclohexyl PNA

***Aminoethyl-amino-cyclohexanoic acid*:** Rigidity was introduced into the *aeg*-PNA by replacing the glycyl segment in the backbone by α-amino cyclohexanoic acid (Figure 34).[130] Incorporation of these monomers into oligomers and their DNA/RNA binding properties has not yet been reported.

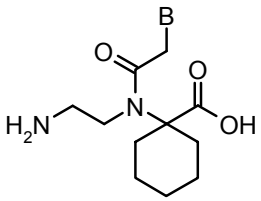

Figure 34: Aminoethyl-amino cyclohexanoic acid

***Morpholino PNA*:** The set of morpholino analogues with phosphonate esters, amide or ester linkages between the morpholino nucleoside residues was synthesized. Preliminary results indicated that amide-linked morpholino PNAs were better accommodated in the complexes than the ester or the phosphonate linked oligomers (Figure 35).[131]

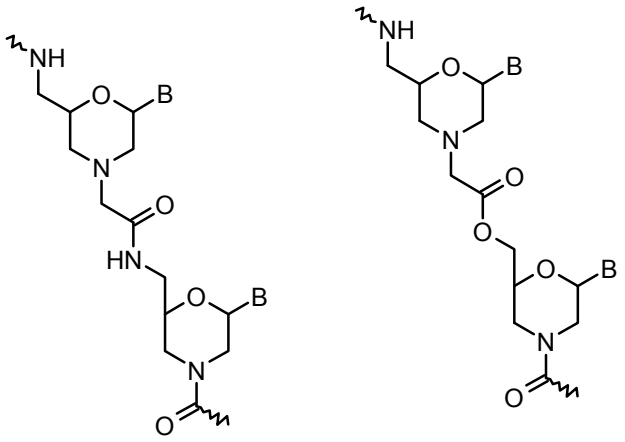

I. amide-morpholino II. ester-morpholino

Figure 35: PNA with morpholino amide and ester backbones.

***APNA and PNA-APNA chimera*:** An aromatic PNA analogue in which the backbone *O*-aminophenylbutanoic acid derivative carries the nucleobase through an ether linkage has been synthesized (Figure 35).[132] The direct incorporation of aromatic rings in the backbone renders at least three bonds in the backbone coplanar. Furthermore, the internucleobase distance was altered by additional methyl substitution in the glycyl segment, affording *N*-(2- aminobenzyl)-(*R* or *S*)-alanine or by replacing it with *β*-alanine, as in *N*-(2-aminobenzyl)-β-alanine backbones. The incorporation of these modified units in *aeg*PNA produced PNA-APNA chimera. The modified oligomers exhibited decreased binding affinities relative to the pure PNA. An *N*-(2-aminobenzyl)-glycine unit in the

*aeg*PNA resulted in the smallest decrease in the thermal stability of the triplexes with DNA and RNA while maintaining the selectivity of base pairing recognition.

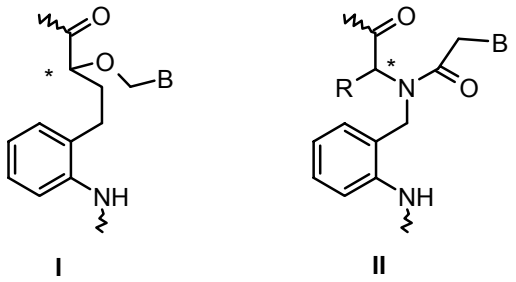

Figure 35: Aromatic peptide nucleic acid, APNA-I
APNA-II-PNA chimera.

1.5.3 Modified nucleobases

Non-natural nucleobases could aid in understanding of the recognition process between the natural nucleobase pairs in terms of factors such as hydrogen bonding and internucleobase stacking. They could also generate new recognition motifs with potential applications in diagnostics. Only a few nucleobase modifications have been reported in the PNA context (Figure 37). 2,6-Diaminopurine[133] offers increased affinity and selectivity for thymine and pseudoisocytosine mimics the C^+ recognition pattern for triplex formation. 2-Aminopurine[134] can hydrogen bond with uracil and thymine in the reverse Watson-Crick mode and being inherently fluorescent, can be used to study the kinetics of the hybridization process with complementary nucleic acids. Replacement of *aeg* PNA with thiazole orange afforded a PNA probe that fluoresced upon hybridization.[135] The E-base, hypoxanthine, N^4-benzoylcytosine and 6-thioguanine[136] represent some more examples of modified nucleobases. Thiouracil along with 2,6-diaminopurine has been utilized as a non-natural base pair in PNA-DNA recognition and was shown for the first time to lead to a phenomenon termed as ‘double duplex invasion’.

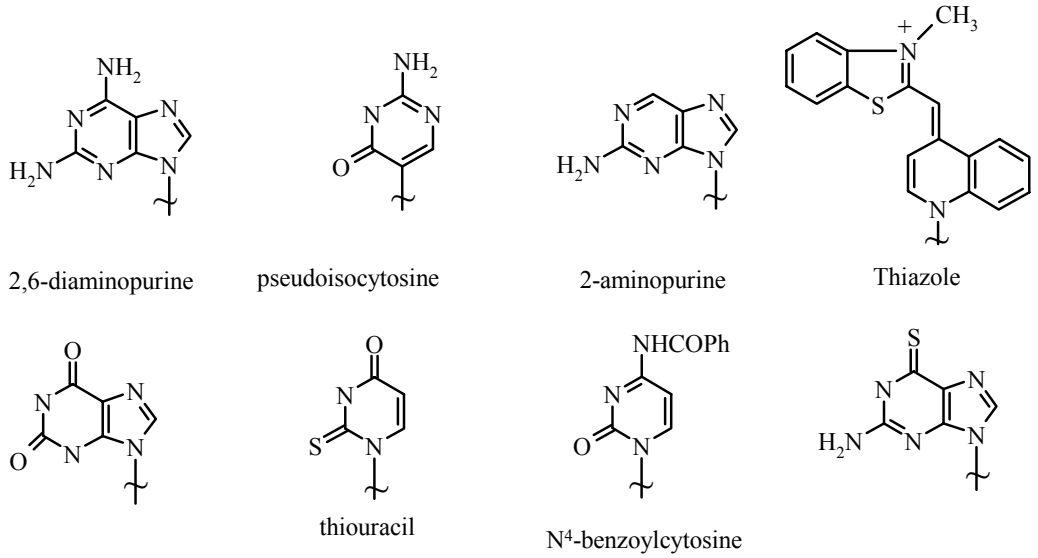

Figure 37: Modified nucleobases.

1.6 PNA CONJUGATES

Covalent hybrids of PNA with other molecules have been constructed to overcome the limitations of PNAs such as aggregation, solubility and cell uptake and to impart abilities to enable therapeutic applications like RNase H activation, cell uptake, etc.

1.6.1 PNA-DNA chimerae

Several PNA-DNA chimerae (Figure 38) have been reported till date. Conjugation of PNA to the 5'-end of DNA led to PNA-(5')-DNA chimerae while conjugation to the 3'-end led to the DNA-(3')-PNA chimerae.[137] An advantage of attaching the PNA to the 3'-end of DNA is imparting stability towards the most common 3'-exonucleases. Other advantages of such chimerae are their improved solubility in aqueous media, improved cellular uptake and a lower tendency to self-aggregate. The thermal stability of the complexes of these with complementary nucleic acids was however, lower than that of the complexes with PNA.

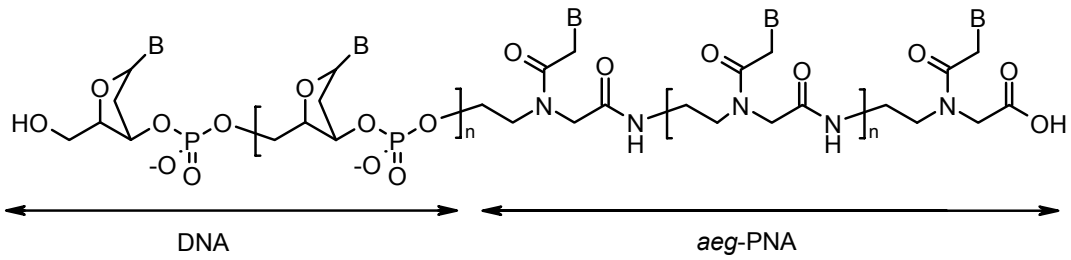

Figure 38: PNA/DNA chimeras.

Since, PNA is incredibly stable against degradation by nuclease, it constitutes serious limitations with respect to certain applications, i.e. PNA is not accepted as substrate for polymerases, DNA kinases or DNA ligases. Further, PNA cannot induce RNase H cleavage of target RNA that in many cases support biological efficacy of antisense agents. The combination of PNA and DNA in one-molecule resulted in PNA-DNA chimeras with new properties (Figure 37). The PNA-DNA chimeras obey the Watson-Crick rules on binding to complementary DNA and RNA. Binding affinity of PNA-DNA chimeras strongly depend on the PNA:DNA ratio. PNA-DNA chimeras show improved solubility in aqueous solution as compared to pure PNA. Due to the negative charges in DNA part, it can be analyzed and purified by polyacrylamide gelectrophoresis (PAGE) and ion exchange chromatography similarly to oligonucleotide. Interestingly, PNA/DNA chimeras can also assume biological function, e.g. they can serve as primers for DNA polymerases, or upon binding to RNA they can mediate RNase H cleavage.[138]

1.6.2 PNA-Peptide chimerae

There are varied reports in literature of the conjugation of PNA with peptides and proteins to gain an application advantage in biological systems. For example, the presence of cationic peptides at the N-terminus of the PNA resulted in an enhanced inhibition of

human telomerase activity.[139] Another example of PNA-peptide chimerae can be found in the PNA-NLS peptide corresponding to the SV40[140] core nuclear localization signal. This conjugate increased the nuclear uptake of oligonucleotides and enhanced the transfection efficacy of plasmids.

Shuttle proteins upon conjugation with PNA were used to 'smuggle' the target PNA into cells and across the cellular membranes.[141] This significantly increased the inhibition of target RNA expression compared to PNAs alone. Cationic peptides linked to PNAs were found to enhance the strand invasion capability of PNAs into target DNA duplexes.[142] This complex formation was also found to prime DNA strand elongation by oligonucleotide-peptide conjugates at sequences where elongation was hitherto undetected.

1.6.3 PNA-Liposome chimerae

PNAs were conjugated to lipophilic groups and incorporated into liposomes.[143] As predicted, these enhanced the cellular uptake and distribution. These favourable properties increased with the introduction of an amino side-chain into the PNA backbone.

1.6.4 PNA-Polyamine conjugates

PNAs were conjugated to polyamines like ethylene diamine and spermine in order to improve their solubility properties in aqueous media.[144] Spermine accelerated the association of PNA with anionic DNA by electrostatic interaction. It was envisaged that the conjugation of biologically relevant polyamines such as spermine would enhance the cellular uptake of PNAs through polyamine receptor mediated mechanisms. However, such studies are yet to be reported.

1.7 PRESENT WORK

The preceding sections give an overview of the peptide nucleic acids (PNA) which are DNA analogues with a homomorphous but chemically different backbone consisting of *N*-(2-aminoethyl)-glycine units in contrast to the sugar-phosphate backbone of DNA. In spite of this, PNAs bind to complementary nucleic acid oligomers obeying the Watson-Crick hydrogen bonding rules for PNA:DNA duplexes and Hoogsteen hydrogen bonding mode for third strand binding in a triplex. The attractive binding properties of PNAs, both in terms of affinity and specificity, coupled with their strand invasion potential have promoted PNA as a useful tool in molecular biology, diagnostics, and as a possible candidate for antisense/ antigene drug therapy. The major factors restricting the applications of PNA have been its poor water solubility, insufficient cell uptake, self-aggregation and ambiguity in the binding orientation. Moreover, the strand invasion phenomenon is restricted to low salt concentrations.

In order to overcome these limitations, several modifications of PNA have been carried out in literature. PNAs have also been linked to helper molecules in various chimeras in an endeavor to improve their properties. The work presented in this thesis involves the design, synthesis and biophysical evaluation of these backbone modified, chiral, ring constrained PNA analogues: *aepone*-PNA, a new isomer of *aep*-PNA, conformational study of prolyl ring of *aep*-PNA monomers, tetraplexing properties in *aep*-PNA and *i*-motif formation by *aeg*-PNA and foldamers formed by aminoethylprolyl amino acids, a new class of amino acids.

Chapter 2

Chapter 2 describes the synthesis of a novel modified PNA monomer (*aepone*-PNA), which was envisaged to confer constrained flexibility on the relatively more flexible PNA backbone (Figure 39). The modification introduces two chiral centers per

unit and retaining carbonyl group of *aeg*-PNA, which is not present in *aep*-PNA. The carbonyl group may improve orientational problems of unmodified PNA conceived by bridging the β-carbon atom of the glycine moiety in PNA and the β'-carbon of the linker to the nucleobase by a methylene group. The chiral monomers were synthesized from the naturally occurring and easily available 4(*R*)-hydroxy-2(*S*)-proline. The synthesis of the chiral monomers bearing each of the four natural nucleobases is described. In addition, a new isomer of *aep*-PNA is also synthesized. These aminoethylpyrrolidinine and prolyl PNA monomers have been incorporated into PNA oligomeric sequences by solid phase peptide synthesis. Cleavage of the synthesized oligomers from the solid support, their subsequent purification procedures, followed by suitable characterization is also detailed.

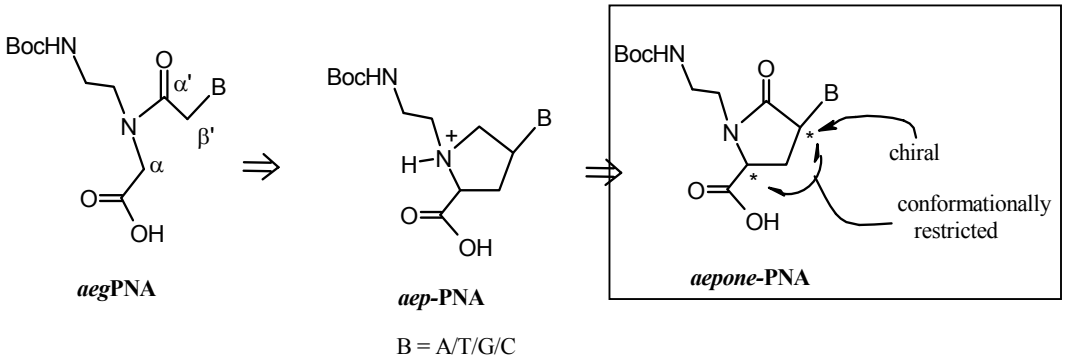

Figure 39: (a) aeg-PNA: aminoethylglycyl PNA. (b) *aep*-PNA: (Aminoethylprolyl PNA). (3) *aepone*-PNA (aminiethypyrrolidinone PNA).

Chapter 3

This Chapter presents analysis of the conformation of prolyl ring in *aep*-PNA monomers by NMR. All four monomers of *aep*-PNA were synthesized by reported procedures and fully assigned by different 2D-NMR spectroscopy techniques. The derived

vicinal coupling constants of protons in the prolyl ring were used in PSEUROT software to obtain ring-puckering information. It was seen that the conformation of prolyl ring significantly depends on the nature of the nucleobase, unlike in natural nucleosides.

Chapter 4

In this chapter, the binding properties of the synthesized PNA oligomers containing the aminoethylpyrrolidinone PNA monomers are studied. The biophysical effects of the modification have been elucidated by sequentially increasing the number of modified units in the oligomer. Temperature-dependent UV and CD spectroscopic studies were used to evaluate the binding affinities of the PNA oligomers for complementary DNA sequences. The results of the above studies are discussed along with implications and potential for future work.

Chapter 5A

This section demonstrates G-tetrad formation by *aep*-PNA. Here, the G-rich sequences of *aep*-PNA with different lengths were synthesized by solid phase synthesis and their tetraplexing properties were traced by UV spectroscopy and mass spectroscopy techniques.

Chapter 5A

This section illustrates the hitherto unknown tetraplexing properties i.e. *i*-motif formation of C-rich sequences of *aeg*-PNA by UV spectroscopy and mass spectroscopy methods and determination of pKa value of N3 in protonated cytosine in aeg-monomer monomer by UV (Figiure 40)

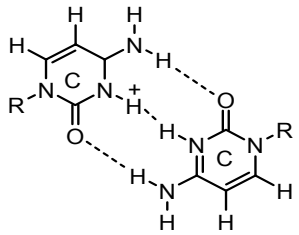

Figure 40: Hydrogen bonding Pattern in two Cytosine

Chapter 6

This section is devoted to the synthesis of a new class of amino acid δ-aminoethylproly amino acid (δ-*aep*) and their peptides (Figure 41), to study the probable secondary structure like 8-helix, 10-helix and 14-helix adopted by these molecules using CD and IR spectroscopic techniques.

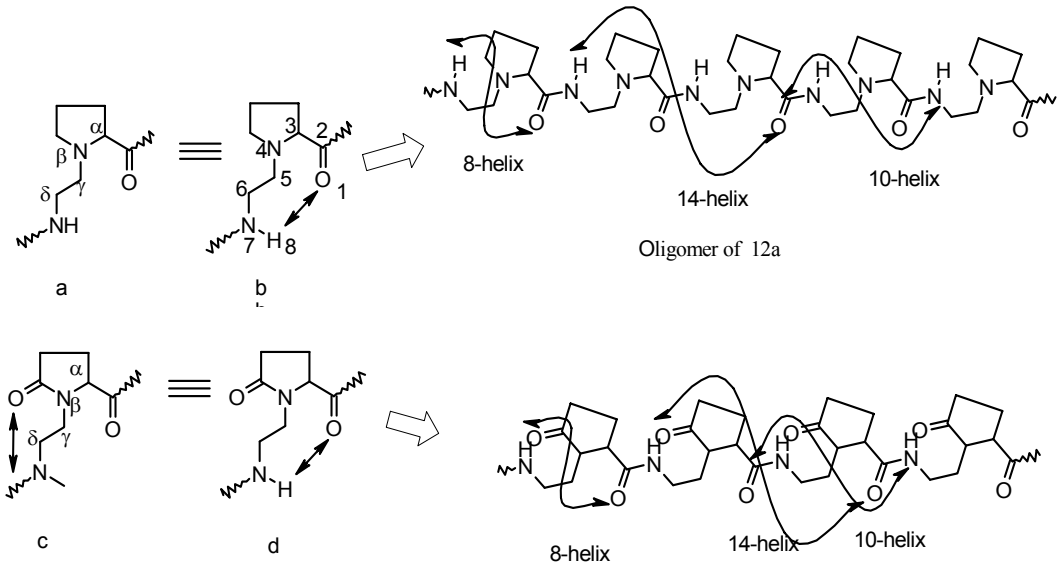

Figure 41: *Left*. Chemical structure of δ-*aep* and (δ-*aepone*); *Right*. Their proposed secondary structure.

1.8 REFERENCES

1. Blackburn, G. M.; Gait, M. J. Nucleic acids in chemistry and biology. Oxford University Press **1990**.
2. Watson, J. D.; Crick, F. H. C. Molecular structure for nucleic acids: A structure for deoxyribose nucleic acid. *Nature* **1953**, *171*, 737–738.
3. Soyfer, V. N.; Potman, V. N. Triple-Helical Nucleic Acids, **1996**, Springer-Verlag: NewYork.
4. Crooke, S. T. Therapeutic Applications of oligonucleotides, Springer-Verlag: Heidolbery **1995**.
5. Zamecnik, P. C.; Stephenson, M. L. Inhibition of Rous sarcoma virus replication and cell transformation by a specific oligodeoxynucleotide. *Proc. Natl. Acad. Sci.* **1978**, *75*, 280-284.
6. Uhlmann, E.; Peyman, A. Antisense Oligonucleotides: A new therapeutic principle. *Chem. Rev*. **1990**, *90*, 544-584.
7. (a) De Mesmaeker, A.; Waldner, A.; Sanghvi, Y. S.; Lebreton, J. *Bioorg. Med. Chem. Lett.* **1994**, *4*, 395-8. (b) De Mesmaeker, A.; Haner, R.; Martin, P.; Moser, H. E. Antisense Oligonucleotides. *Acc. Chem. Res.* **1995**, *28*, 366-374.
8. Dagel, J. M.; Walder, J.; Weeks, D. L. Targeted degradation of mRNA in *xenopus oocytes* and embryos directed by modified oligonucleotides: Studies of An2 and Cyclin in embryogenesis. *Nucleic Acids Res.* **1990**, *18*, 4751-4757.
9. (a) Eckstein, F. Phosphorothioates oligonucleotides: What is their origin and what is unique about them? *Antisense Nucleic acid drug Dev*. **2000**, *10*, 117-121. (b) Matsukura, M.; Shinozuka, K.; Zon G.; Mitsuya, H.; Reitz, M.; Cohen, J. S. & Broder , S. Phosphorothioate analogs of oligodeoxynucleotides: inhibitors of replication and cytopathic effects human immunodeficiency virus. *Proc. Natl Acad Sci.* USA. **1987**, *84,* 7706-7719.
10. (a) Cummins, L.; Graff, D.; Beaton, G.; Marshall, W. S.; Caruthers, M. H. Biochemical and physicochemical properties of phosphorodithioate DNA. *Biochemistry* **1996**, *35*, 8734-41. (b) Kodra, J. T.; Kehler, J.; Dahl, O. Stability of oligodeoxynucleoside phosphorodithioates and phosphorothioates in aqueous ammonia. *Nucleic Acids Res*. **1995,** *23*, 3349-50.
11. Mahajna, M.; Quistad, G. B.; Casida, J. E. S-methylation of O, O-dialkyl phosphorodithioic acids: O,O,S-trimethyl phosphorodithioate and phosphorothiolate as metabolites of dimethoate in mice.*Chem. Res. Toxicol*. **1996**, *9*, 1202-6.
12. (a) Awad, A. M.; Sobkowski, M.; Seliger, H. Enzymatic and hybridization properties of oligonucleotide analogs containing novel phosphoramidate internucleotide linkages. *Nucleosides Nucleotides Nucleic Acids* **2004**, *23*, 777-87.
13. (a) Muller, H. C.; Meier, C.; Balzarini, J.; Reinstein, J. Novel nucleotide analogues as potential substrates for TMPK, a key enzyme in the metabolism of AZT. *Nucleosides Nucleotides Nucleic Acids* **2003,** *22*, 821-3. (b) Sujikawa L.; Weinfield, M.; Reha-Krantz, L. J. Differences in replication of a DNA template containing an ethyl phosphotriester by T_4 DNA polymerase and Escherichia coli DNA polymerase I. Nucleic Acids Res. **2003**, *31,* 4965-72.
14. Zambarakji, H. J.; Mitchell, S. M.; Lightman, S.; Holder, G. E. Electrophysiological abnormalities following intravitreal vitravene (ISIS 2922) in two patients with CMV retinitis. *Br. J. Ophthalmol*. **2001,** *85*, 1142.

15. Eschenmoser, A.; Dobler, M. Why pentose and not hexose nucleic acids? *Helv. Chim. Acta.* **1992,** *75*, 218-259. (b) Summerton, J.; Weller, D. Morpholino antisense oligomer: Design, preparation and properties. *Antisense Nucleic Drug Dev*. **1997**, *7*, 187-190.
16. Stirchak, E. P.; Summerton, J. E.; Weller, D. D. Uncharged stereoregular nucleic acid analogs: 2. Morpholino nucleoside oligomers with carbamate internucleoside linkages. *Nucleic Acids Res.* **1989**, *17*, 6129-6141
17. (a) Vester, B.; Wengel, J. LNA (locked nucleic acid): high-affinity targeting of complementary RNA and DNA. *Biochemistry*. **2004**, *43*, 13233-13241. (b) Petersen, M.; Wengel. J. LNA: a versatile tool for therapeutics and genomics. *Trends in Biotechnology,* **2003**, *21*, 74-81. (c) Kurreck, J.; Wyszko, E.; Gillen, C.; Erdmann, V. A. Design of antisense oligonucleotides by locked nucleic acids. *Nucleic acid Res*. **2002**, *30*, 1911-1918.
18. (a) Petersen, M.; Bondensgaard, K.; Wengel, J.; Jacobsen, J. P. Locked nucleic acid (LNA) recognition of RNA: NMR solution structures of LNA:RNA hybrids. *J. Am. Chem. Soc*. **2002**, *124*, 5974-82. (b) Kumar, R.; Singh, S. K.; Koshkin A. A.; Rajwanshi, V. K.; Meldgaard, M.; Wengel, J. The first analogues of LNA (locked nucleic acids): phosphorothioate-LNA and 2'-thio LNA. *Bioorg. Med. Chem. Lett*. **1998**, *8*, 2219-22.
19. (a) Nielsen, P. E.; Egholm, M.; Berg, R. H.; Buchardt, O. Sequence selective recognition of DNA by strand displacement with a thymine-substituted polyamide. *Science* **1991**, *254*, 1497-150. (b) Hanvey, J. C.; Peffer, N. J.; Bisi. J. E.; Thomson, S. A.; Cadilla, R.; Josey, J. A. Antisense and antigen properties of peptide nucleic acids. *Science,* **1992**, *258*, 1481-1485. (c) Egholm, M.; Buchardt, O.; Nielsen, P. E.; Berg, R. H. Peptide nucleic acids (PNA). Oligonucleotide analogues with an achiral peptide backbone. *J. Am. Chem. Soc.* **1992**, *114*, 1895-1897.
20. (a) Patel, D. J. Marriage of convenience. *Nature* **1993**, 365: 490-492. (b) Ganesh, K. N.; Nielsen, P. E. Peptide nucleic acids: analogs and derivatives. *Current Org. Chem.* **2000**, 931-943. (d) Nielsen, P. E.; Egholm, M.; Buchardt, O. Peptide nucleic acid (PNA): A DNA mimic with a peptide backbone. *Bioconjugate Chem*. **1994**, *5*, 3-7.
21. Egholm, M.; Buchardt, O.; Christensen, L.; Behrens, C.; Frier, S. M.; Driver, D. A.; Berg, R. H.; Kim, S. K.; Norde´n, B.; Nielsen, P. E. PNA hybridizes to complementary oligonucleotides obeying the Watson-Crick hydrogen bonding rules. *Nature* **1993**, *365***,** 566–568.
22. Nielsen, P. E. Sequence-specific recognition of doublestranded DNA by peptide nucleic acids. *Adv. DNA Sequence-Specific Agents* **1998**, *3,* 267–278.
23. Nielsen, P. E.; Egholm, M.; Berg, R.; Buchardt, O. Sequence specific inhibition of DNA restriction enzyme clevage by PNA. *Nucleic Acid Res*. **1993**, *21*, 197-200.
24. (a) Nielsen, P. E. DNA analogs with nonphosphodiester backbones. *Annu. Rev. Biophys. Biomol. Struct*. **1995**, 167-183. (b) Nielsen, P. E. Applications of PNA. *Current Opinion in Biotechnology* **1999**, *10,* 71-75.
25. Corey, D. R. Peptide nucleic acids: expanding the scope of nucleic acid recognition. *Trends Biotechnol.* **1997**, *15*, 224–229. (d) Eriksson, M.; Nielsen, P. E. PNA-nucleic acid complexes: Structure, stability and dynamics. *Q. Rev. Biophys.* **1996**, *29,* 369–394

26. (a) Eriksson, M.; Christensen, L.; Schmidt, J.; Haaima, G.; Orgel, L.; and Nielsen, P. E. Sequence dependent N-terminal rearrangement and degradation of peptide nucleic acid (PNA) in aqueous solution. *New J. Chem.* **1998**, 1055–1059. (b) Tomac, S.; Sarkar, M.; Ratilainen, T.; Wittung, P.; Nielsen, P. E.; Nordén, B.; Gräslund, A.Ionic effects on the stability and conformation of PNA complexes. *J. Am. Chem. Soc.* **1996**, *118*, 5544-5552.
27. Hyrup, B.; and Nielsen, P. E. Peptide nucleic acids (PNA): synthesis, properties and potential applications. *Bioorg. Med. Chem.* **1996**, *4*, 5–23
28. Gildea, B. D.; Casey, S.; Mac Neill, J.; Perry-O'Keefe, H.; Sørensen, D.; Coull, J. M. PNA solubility enhancers. *Tetrahedron Lett.* **1998**, *39*, 7255-7258.
29. Betts, L.; Josey, J. A.; Veal, J. M.; Jordan, S. R. A nucleic acid triple helix formed by a peptide nucleic acid-DNA complex. *Science,* **1995**, *270*, 1838-1841.
30. Wittung, P.; Nielsen, P. E.; Buchardt, O.; Egholm, M.; Norde´n, B. DNA like double helix formed by peptide nucleic acid. *Nature (London)* **1994**, *368,* 561–563
31. Lesignoli, F.; Germini, A.; Corradini, R.; Sforza, S.; Galaverna, G.; Dossena, A. Recognition and strand displacement of DNA oligonucleotides by peptide nucleic acids (PNAs). Highperformance ion-exchange chromatographic analysis. *Journal of Chromatography, A 2001*, *922*, 177-185.
32. Vernille, J. P.; Kovell, L. C.; Schneider, J. W. Peptide nucleic acid (PNA) amphiphiles: Synthesis, selfassembly, and duplex stability. *Bioconjugate Chemistry* **2004**, *15*, 1314-1321.
33. (a) Peffer, N. J.; Hanvey, J. C.; Bisi, J. E., Thomson, S. A., Hassman, C. F., Noble, S. A.; Babiss, L. E. Strand-invasion of duplex DNA by peptide nucleic acid oligomers. *Proc. Natl.Acad. Sci. USA* 1993, *90,* 10648–10652. (b) Ishihara, T.; Corey, D. R. Rules for Strand Invasion by Chemically Modified Oligonucleotides. *Journal of the American Chemical Society* **1999**, *121*: 2012-2020. (c) Wittung, P.; Nielsen, P. E.; Norde´n, B. Direct observation of strand invasion by peptide nucleic acid (PNA) into double-stranded DNA. *J. Am. Chem. Soc.* **1996**, *118*, 7049–7054
34. Demidov, V. V. PD-loop technology: PNA openers at work. *Expert. Rev. Mol. Diagn.* **2001**, *1*, 343-351.
35. Nielsen, P. E.; Egholm, M.; Buchardt, O. Evidence for $(PNA)_2$/DNA triplex structure upon binding of PNA to dsDNA by strand displacement. *J. Mol. Recog.* **1994**, *7***,** 164–170.
36. (a) Kim, S. K.; Nielsen, P. E.; Egholm, M.; Buchardt, O.; Berg, R. H.; Nord, B. Right-handed triplex formed between peptide nucleic acid PNA-Ts and Poly(dA) shown by linear and circular dichroism spectroscopy. *J. Am. Chem. Soc.* **1993**, *115*, 6477-6481.
37. Lohse, T.; Dahl, O.; Nielsen, P. Double duplex invasion by PNA: A general principle for sequence-specific targeting double stranded DNA. *Proc. Natl. Acad. Sci.* **1999**, *96*, 11804-11808.
38. Wittung, P.; Nielsen, P. E.; Nordén, B. Observation of a PNA-PNA-PNA triplex . *J. Am. Chem. Soc.* **1997**, *119*, 3189-3190.
39. (a) Brown, S. C.; Thomson, S. A.; Veal, J. M.; Davis, D. G. NMR Solution structure of a Peptide nucleic acid complexed with RNA. *Science* **1994**, *265*, 777-780. (b) Cherney, D. Y.; Belotserkovskii, B. P.; Frank-Kamenetskii, M. D.; Egholm, M.; Buchardt, O., Berg, R. H.; Nielsen, P. E. DNA unwinding upon strand displacement binding of a thymine-substituted polyamide to double-stranded DNA. *Proc. Natl. Acad. Sci. USA* **1993,** *90,* 1667–1670.

40. Sen, S.; Nilsson, L. MD simulations of homomorphous PNA, DNA, and RNA single strands: characterization and comparison of conformations and dynamics. *J. Am. Chem. Soc*. **2001**, *123*, 7414-7422. (b) Griffith, M. C.; Risen, L. M.; Greig, M. J.; Lesnik, E. A.; Sprankle, K. G.; Griffey, R. H.; Kiely, J. S.; Freier, S. M. Single. Bis PNA as triplexing agents, Binding and stoichiometry. *J. Am. Chem. Soc*. **1995**, *117*, 831-832.

41. Okamoto, A.; Tanabe, K.; Saito, I. P-loop DNA. *Bioorg. Med. Chem.* **2003**, *11*, 3747-3751.

42. Eriksson, M.; Nielsen, P. E. Solution structure of a peptide Nucleic Acid-DNA duplex. *Nature Structural Biology* **1996**, *3*, 410-413.

43. (a) Menchise, V.; De Simone, G.; Tedeschi, T.; Corradini, R.; Sforza, S.; Marchelli, R.; Capasso, D.; Saviano, M.; Pedone, C. Insights into peptide nucleic acid (PNA) structural features: the crystal structure of a D-lysine-based chiral PNA-DNA duplex. *Proc. Natl. Acad. Sci. U S A*. **2003,** *100*, 12021-12026. (b) Rasmussen, H.; Kastrup, J. S.; Nielsen, J. N.; Nielsen, J. M.; Nielsen, P. E. Crystal structure of a Peptide Nucleic acid (PNA) duplex at 1.7 A Resolution. *Nature Structural Biology* **1997**, *4*, 98-101.

44. (a) Knudsen, H.; Nielsen, P. E. Antisense properties of duplex and triplex forming Peptide nucleic Acids. *Nucleic Acid Res*. **1996**, *24*, 494-500. (b) Bentin, T.; Larsen, H. J.; Nielsen, P. E. Combined triplex/duplex invasion of double-stranded DNA by "tail-clamp" peptide nucleic acid. *Biochemistry* **2003**, *42*, 13987-13995.

45. Jensen, K. K.; Orum, H.; Nielsen, P. E., Nordén, B. Kinetics for hybridization of peptide nucleic acids (PNA) with DNA and RNA studied with the BIAcore technique. *Biochemistry* **1997**, *36*, 5072–5077

46. (a) Praseuth, D.; Guieysse, A. L.; Helene, C. Triple helix formation and the antigene strategy for sequence-specific control of gene expression. *Biochim. Biophys. Acta*. **1999**, *489*, 181-206. (b) Helene, C.; Thuong, N. T.; Harel-Bellan, A. Control of gene expression by triple helix-forming oligonucleotides. The antigene strategy. *Ann. N. Y. Acad. Sci*. **1992**, *660*, 27-36.

47. Noble, S. A.; Bonham, M. A.; Bisi, J. E.; Bruckenstein, D. A.; Brown P. H.; Brown, S. C *et al*.: Impact of biophysical parameters on the biological assessment of peptide nucleic acids, antisense inhibitors of gene expression. *Drug Dev. Res*. **1995**, *34*, 184-195.

48. Nielsen, P. E.; Egholm, M.; Berg, R. H.; Buchardt, O. Peptide nucleic acids (PNAs): potential antisense and anti-gene agents. *Anticancer Drug Des*. **1993**, *8*, 53-63.

49. Dieci, G.; Corradini, R; Sforza, S.; Marchelli, R.; Ottonello, S. Inhibition of RNA polymerase III elongation by a T_{10} peptide nucleic acid. *J. Biol. Chem*. **2001**, *276*, 5720-5725.

50. (a) Uhlmann, E.; Pcyman, A.; Brcipohl, G.; Will, D. W. PNA: Synthetic polyamide nucleic acid with unusal binding properties. *Angew Chem. Int. Ed*. **1998**, *37*, 2796-2823. (b) Mesmaeker, A.; Waldner A.; Lebreton, J.; Hoffmann, P.; Fritsch, V.; Wolf, R. M. Amide bridging, a new type of modification of oligonucleotide backbones. *Angew. Chem.* **1994**, *106,* 237-240

51. Walder, R. Y.; Walder, J. A. Role of RNase H in hybrid arrested translation by antisense oligonucleotides. *Proc. Natl. Acad. Sci.U.S.A,* **1988**, *85*, 5011-5015.

52. Bonham, M. A.; Brown, S.; Boyd, A. L. Brown, P. H.; Bruckenstein, D. A.; Hanvey, J. C. An assessment of the antisense properties of RNase H-competent and steric-blocking oligomers. *Nucleic Acids Res* **1995**, *23*, 1197-1203

53. Diviacco, S.; Rapozzi, V.; Xodo, L.; Helene, C.; Quadrifoglio, F.; Giovannangeli, C. Site-directed inhibition of DNA replication by triple helix formation. *FASEB J*. **2001,** *15,* 2660-2668.
54. Taylor, R. W.; Chinnery, P. F.; Turnbull, D. M.; Lightowlers, R. N. Selective inhibition of mutant human mitochondrial DNA replication in vitro bypeptide nucleic acids. *Nat. Genet.* **1997**, 212-215
55. Crooke, S. T.; Lemonidis, K. M.; Neeilson, L.; Griffey, R.; Lesnik, E. A.; Monia, B. P. Kinetic characteristics of Escherichia colli RNase H1: cleavage of various antisense oligonucleotide-RNA duplexes. *Biochem*. *J*. **1995**, *312*, 599-607.
56. Uhlmann, E. Peptide nucleic acids (PNA) and PNA-DNA chimeras: from high binding affinity towards biological function. *Biol Chem*. **1998**, *379*, 1045-52
57. (a) Koppelhus, U.; Zacher, V.; Nielsen, P. E.; Liu, X.; Eugen-olsen, J.; Ebbesen, P. Efficient invitro inhibition of HIV-1 gag reverse transription by peptide nucleic acid (PNA) at minimal ratios of PNA/RNA. *Nucleic Acids Res*. **1997**, *25*, 2167-2173. (b) Lutz, M. J.; Benner, S. A.; Hein, S.; Breipohl, G.; Uhlmann, E. Recognition of uncharged polyamide-linked nucleic acid analogs by DNA polymerases and reverse transcriptases. *J*. *Am*. *Chem*. *Soc*. **1997**, *119***,** 3177–3178
58. Norton, J.; Platyszec, M.; Wright, W.; Shay, J.; Corey, D.R. Inhibition of human telomerase activity by Peptide Nucleic Acids. *Nat*. *Biotech*. **1996**, *14*, 615-620.
59. Chen, C.; Hong, Y. K.; Ontiveros, S. D.; Egholm, M.; Strauss, W. M. Single base discrimination of CENP-B repeats on mouse and human Chromosomes with PNA-FISH. *Mammalian Genome* **1999**, *10*, 13-18.
60. Lansdorp, P. M. Close encounters of the PNA kind. *Nature Biotechnology* **1996**, 14: 1653
61. Stender, H.; Mollerup, T. A.; Lund, K.; Petersen, K. H.; Hongmanee, P.; Godtfredsen, S. E. Direct detection and identification of Mycobacterium tuberculosis in smear-positive sputum samples by fluorescence *in situ* hybridization (FISH) using peptide nucleic acid (PNA) probes. *Int*. *J*. *Tuberc. Lung*. *Dis*. **1999**, *3*, 830-837. Larsen, R. D.; Schonau, A.; Thisted, M.; Petersen, K. H.; Lohse, J.; Christensen, B.; Philip, J.; Pluzek, K. J. Detection of gamma-globin mRNA in fetal nucleated red blood cells by PNA fluorescence in situ hybridization. *Prenat Diagn*. **2003**, *23*, 52-9.
62. Ørum, H. PCR clamping. *Curr*. *Issues*. *Mol*. *Biol*. **2000**, *2*, 27-30.
63. Drewe, L. J.; Brightwell, G.; Hall, E.A H.Detection of PCR products using PNA strand invasion. *Mol Cell Probes* **2000**, *14*, 269-283. 476. Isacsson, J.; Cao, H.; Ohlsson, L.; Nordgren, S.; Svanvik, N.; Westman, G. Rapid and specific detection of PCR products using light-up probes. *Molecular and Cellular Probes* **2000**, *14*, 321- 328.
64. Fiandaca, M. J.; Hyldig-Nielsen, J. J; Gildea, B. D.; Coull, J. M. Self-reporting PNA/DNA primers for PCR analysis. *Genome Res*. **2001**, *11,* 609-13
65. Kelland, L. R. Telomerase inhibitors: targeting the vulnerable end of cancer? *Anti-Cancer Drugs* **2000**, *11*, 503-513
66. (a) Knudsen H, Nielsen PE. Application of peptide nucleic acid in cancer therapy. *Anticancer Drugs*. **1997**, *8*, 113-8. (b) Taneja, K. L.; Chavez E. A.; Coull, J.; Lansdorp, P. M. Multicolor fluorescence in situ hybridization with peptide nucleic acid probes for enumeration of specific chromosomes in human cells. *Genes, Chromosomes & Cancer* **2001**, *30*, 57-63.

67. Kim, D-. H.; Hong, Y-. K.; Egholm, M.; Strauss, W. M. Non-disruptive PNA-FISH protocol for formalinfixed and paraffin-embedded tissue sections. *Bio. Techniques* **2001**, *31*, 475-476
68. Brandén, L. J.; Christensson, B.; Smith, C. I. E. In vivo nuclear delivery of oligonucleotides via hybridizing bifunctional peptides. *Gene Therapy* **2001**, *8*, 84-87.
69. Demers, D. B.; Curry, E. T.; Egholm, M.; Sozer, A. C. Enhanced PCR amplification of VNTR locus D1S80 using peptide nucleic acid (PNA). *Nucleic Acids Res*. **1995**, *23*, 3050-3055.
70. Veselkov, A. G.; Demidov, V.; Nielsen, P. E.; Frank-Kamenetskii, M. D. A new class of genome rare cutters. *Nucleic Acids Res.* **1996**, *24,* 2483–2487
71. Lansdorp, P. M.; Verwoerd, N. P.; Van de Rijke, F. M.; Dragowska, V.; Little, M. T.; Dirks, R. W. Heterogeneity in telomere length of human chromosomes. *Human Molecular Genetics* **1996**, *5*, 685-691.
72. Isacsson, J.; Cao, H.; Ohlsson, L.; Nordgren, S.; Svanvik, N.; Westman, G. Rapid and specific detection of PCR products using light-up probes. *Molecular and Cellular Probes* **2000**, *14*, 321-328
73. Phelan, D.; Hondorp, K.; Choob, M.; Efimov, V.; Fernandez, J. Messenger RNA isolation using novel PNA analogues. *Nucleosides Nucleotides Nucleic Acids*. **2001**, *20*, 1107-11.
74. Buryakova, A.; Phelan, D.; Chakhmakhcheva, O.; PNA-related oligonucleotide mimics and their evaluation for nucleic acid hybridization studies and analysis. *Nucleosides Nucleotides Nucleic Acids* **2001**, *20*, 419-28.
75. Ray A, Nordén B: Peptide nucleic acid (PNA): its medical and biotechnical applications and promise for the future. *FASEB J.* **2000**, *14*, 1041-1060.
76. Miller S. L: Peptide nucleic acids and prebiotic chemistry. *Nature Struct. Bio.* **1997**, *4*, 167-169
77. Kaihatsu, K.; Huffman, K. E.; Corey, D. R. Intracellular uptake and inhibition of gene expression by PNAs and PNA-peptide conjugates. *Biochemistry* **2004**, *43*, 14340-14347.
78. Simmons, C. G.; Pitts, A. E.; Mayfield, L. D.; Stay, J. W.; Corey, D. R. Synthesis and membrane permeability of PNA-Peptide. *Bioorg. Med. Chem. Lett*. **1997**, *7*, 3001-3006.
79. (a) Liebling, M. R.; Jou, N. T.; Fang, W.; Louie, J. S. Blockade of plasmid replication mediated by peptide nucleic acids. *Mol Biotechnol*. **2003**, *25*, 229-40. (b) Rufer N, Dragowska W, Thornbury G, Roosnek E, Lansdorp, P. M: Telomere length dynamics in human lymphocyte subpopulations measured by flow cytometry. *Nature Biotechnology* **1998**, *16*, 743-747.
80. Liang, X.; Zelphati, O.; Nguyen, C.; Felgner, P. Plasmid labeling using PNA. In *Peptide Nucleic Acids: Protocols and Applications*. Edited by Nielsen, P. E.; Egholm, M.; Horizon scientific press; **1999**, 201-211
81. Mrozikiewicz, P. M. Cascorbi, I.; Brockmöller, J.; Roots, I. *CYP1A1* mutations 4887A, 4889G,5639C and 6235C in the Polish popylation and their allelic linkage, determined by peptide nucleic acidmediated PCR clamping. *Pharmacogenomics* **1997**, *7*, 303-307.
82. Seeger C, Batz H-G, Ørum H: PNA-mediated purification of PCR amplifiable human genomic DNA from whole blood. *BioTechniques* **1997**, *23*, 512-516
83. Thiede, C.; Bayerdorffer, E.; Blasczyk, R.; Wittig, B.; Neubauer, A. Simple and sensitive detection of mutations in the ras proto-oncogenes using PNA-mediated PCR clamping. *Nucleic Acids Res*. **1996, *24*,** 983–984.

84. Ørum, H.; Nielsen, P. E.; Egholm, M.; Berg, R. H.; Buchardt, O.; Stanley, C. Single base pair mutation analysis by PNA directed PCR clamping. *Nucleic Acids* Res. **1993**, *21***,** 5332–5336.

85. Carlsson, C.; Jonsson, M.; Norde´n, B.; Dulay, M. T.; Zare, R. N.; Noolandi, J.; Nielsen, P. E.; Tsui, L-C.; Zielenski, J. Screening for genetic mutations. *Nature (London)* **1996**, *380,* 207

86. Wang, J.; Palecek, E.; Nielsen, P. E.; Rivas, G.; Cai, X.; Shirashi, H.; Dontha, N.; Luo, D.; Farias, P. A. M. Peptide nucleic acid probes for sequence-specific DNA biosensors. *J. Am. Chem. Soc*. **1996**, *118***,** 7667–7670

87. Jensen, K. K.; Ørum, H.; Nielsen, P. E.; Norden, B. Kinetics for hybridisation of Peptide Nucleic Acids (PNA) with DNA and RNA studied with the BIAcore technique. *Biochemistry* **1997**, *36*, 5072.

88. (a) Wang, J. DNA biosensors based on peptide nucleic acid (PNA) recognition layers. A review. *Biosens. Bioelectron*. **1998**, *13*, 757-62. (b) Okahata, Y.; Matsunobo, Y.; Ijiro, K.; Mukae, M.; Murakami, A.; Makino, K. Hybridization of nucleic-acids immobilized on a quartz crystal microbalance. *J. Am. Chem. Soc.* **1992**, *114*, 8299–8300. (c) Lu, C.; Czanderna, A. W.; *Applications of Piezoelectric Quartz Crystal Microbalances*, **1984** Elsevier, Amsterdam.

89. Wang, J.; Nielsen, P.E.; Jiang, M.; Cai, X.; Fernandes, J. R.; Grant, D. H.; Ozsoz, M.; Beglieter, A.; Mowat, M.; Mismatch-sensitive hybridization detection by peptide nucleic acids immobilized on a quartz crystal microbalance. *Anal. Chem*. ***1997***, *69*, 5200-5202.

90. (a) Jiang-Baucom, P.; Girard, J. E.; DNA typing of Human Leukocyte Antigen Sequence Polymorphisms by Peptide Nucleic Acid Probes and MALDI-TOF Mass Spectrometry. *Analytical Chemistry* **1997**, *69*, 4894-4898. (b) Butler, J. M.; Jiang-Baucom, P.; Huang, M.; Belgrader, P.; Girard, J. Peptide nucleic Acid Characterization by MALDI-TOF Mass Spectrometry. *Analytical Chemistry* **1996**, *68*, 3283-3287. Griffin, T. J.; Tang, W.; Smith, L. M. MALDI-TOF mass spectrometric detection of PNA hybrids for genetic analysis. In *Peptide Nucleic Acids: Protocols and applications.* Edited by Nielsen PE, Egholm M. Horizon scientific press, **1999**, 143-154.

91. Ross, P. L.; Lee, K.; Belgrader, P. Discrimination of single-nucleotide polymorphisms in human DNA using peptide nucleic acid probes detected by MALDI-TOF mass spectrometry. *Anal. Chem.* **1997** *69,* 4197–4202.

92. Fojta, M.; Vetterl, V.; Tomschik, M.; Jelen, F.; Nielsen, P.; Wang, J.; Palecek, E. Adsorption of peptide nucleic acid and DNA decamers at electrically charged surfaces. *Biophys. J*. **1997,** *72*, 2285-93.

93. Germini, A.; Mezzelani, A.; Lesignoli, F.; Corradini, R.; Marchelli, R.; Bordoni, R. Detection of genetically modified soybean using peptide nucleic acids (PNAs) and microarray technology. *Journal of Agricultural and Food Chemistry* **2004**, *52*, 4535-4540.

94. Jain, K. K. Applications of biochip and microarray systems in pharmacogenomics. *Pharmacogenomics* **2000**, *1*, 289-307.

95. Brandt, O.; Feldner, J.; Stephan, A.; Schroder, M.; Schnolzer, M.; Arlinghaus, H. F.; Hoheisel J. D.; Jacob, A. PNA microarrays for hybridisation of unlabelled DNA samples. *Nucleic Acids Res.* **2003**, *31*, 119.

96. Yamasaki, T.; Abdel-Aziz, M.; Kiyota, N.; Maruyama, T.; Otsuka, M. New strategy to antiviral agents from peptide nucleic acid derivatives. *Heterocycles* **2003**, *60*, 1561-1566.

97. (a) Righetti, P. G.; Gelfi, C. Capillary electrophoresis of DNA. In *CRC Series in Analytical Bio/Technology, Capillary Electrophoresis in Analytical Bio/Technology* (*Righetti, P. G., ed),* **1996**, 431–476.

98. Igloi, G. L. Variability in the stability of DNA-peptide nucleic acid (PNA) single-base mismatched duplexes: real-time hybridization during affinity electrophoresis in PNA containing gels. *Proc. Natl. Acad. Sci. USA* **1998**, *95***,** 8562–8567

99. Good, L.; Nielsen, P. E. Inhibition of translation and bacterial growth by peptide nucleic acid targeted to ribosomal RNA. *Proc. Natl. Acad. Sci.* USA **1998**, *95*, 2073-2076.

100. Romanelli, A.; Pedone, C.; Saviano, M.; Bianchi, N.; Borgatti, M.; Mischiati, C.; Gambari, R. Molecular interactions with nuclear factor kappaB (NF-kappaB) transcription factors of a PNA-DNA chimera mimicking NF-kappaB binding sites. *Eur. J. Biochem*. **2001**, *268,* 6066-75.

101. Hamilton, S. E.; Simmons, C. G, Kathiriya I. S, Corey D. R.: Cellular delivery of peptide nucleic acids and inhibition of human telomerase. *Chem. Biol*. **1999**, *6*, 343-351.

102. (a) Rose, D. J. Characterization of antisense binding properties of peptide nucleic acids by capillary gel electrophoresis. *Anal. Chem.* **1993**, *65***,** 3545–3549. (b) Hoffmann R, Ertl HCJ, Pease AM, He Z, Rovera G, Otvos L, Jr.: Low scale multiple array synthesis and DNA hybridization of peptide nucleic acids. In: *Peptides: Frontiers of Peptide Science, Proceedings of the American Peptide Symposium, 15th, Nashville, June 14-19, 1997*.

103. Kitamatsu, M; Shigeyasu, M.; Okada,; T, Nakai, T.; Saitou, M.; Sisido, M.; Thermodynamic analysis of hybridization between POPNA and DNA. *Nucleic Acids Research Supplement* **2002**, *2*, 261-262.

104. Efimov, V. A.; Choob, M. V.; Buryakova, A. A.; Chakhmakhcheva, O. G. Synthesis and binding study of phosphonate analogues of PNAs and their hybrids with PNA. *Nucleosides Nucleotides* **1998**, *17*, 1671-1679.

105. (a) Slaitas, A.; Yeheskiely, E. A novel *N*-(pyrrolidinyl-2-methyl)glycine-based PNA with a strong preference for RNA over DNA. *Eur. J. Org Chem*. **2002**, 2391-2399. (b) Veselkov, A. G.; Demidov, V.; Nielsen, P. E.; Frank-Kamenetskii, M. D. A new class of genome rare cutters. *Nucleic Acids Res.* **1996**, *24*, 2483–2487

106. Efimov, V.; Choob, M.; Buryakova, A.; Phelan, D.; Chakhmakhcheva, O. PNA-related oligonucleotide mimics and their evaluation for nucleic acid hybridization studies and analysis. *Nucleosides Nucleotides Nucleic Acids*. **2001**, *20*, 419-28.

107. (a) van der Laan, A. C.; Havenaar, P.; Oosting, R. S.; Kuyl-Yeheskiely, E.; Uhlmann, E.; van Boom J. H. Optimization of the binding properties of PNA-(5')-DNA chimerae. *Bioorg Med Chem Lett*. **1998**, *8*, 663-668. (b) Kehler, J.; Henriksen, U. Vejbjerg, H.; Dahl, O. Synthesis and hybridization properties of an acyclic achiral phosphonate DNA analogue. *Bioorg Med Chem*. **1998**, *3*, l 315-22.

108. (a) Dempcy, R. O.; Browne, K. A.; Bruice, T. C. Synthesis of the Polycation Thymidyl DNG, its fidelity in binding polyanionic DNA/RNA, and the stability and nature of the hybrid complexes. *J. Am. Chem. Soc.* **1995**, *117*, 6140-6141. (b) Blasko, A.; Dempcy, R. O.; Minyat, E. E.; Bruice, T. Association of short-strand DNA oligomers with guanidinium-linked nucleosides. A kinetic and thermodynamic study. *J. Am. Chem. Soc.* **1996**, *118*, 7892-7899.

109. (a) Barawkar, D. and Bruice, T. **1999**, Deoxynucleic Guanidines/PNA (DNG/PNA) Chimeras: Oligonucleoside Analogue Containing Cationic Guanidinium and Neutral Amide Linkages*J. Am. Chem. Soc. 121*, 10418-10419. (b) Zhou, P; Wang, M.; Du, L.; Fisher, G. W.; Waggoner, A.; Ly, D. H. Novel binding and efficient cellular uptake of guanidine-based peptide nucleic acids (GPNA). *J. Am. Chem. Soc*. **2003**, *125*, 6878-6879

110. (a) Krotz, A. H.; Buchardt, O.; Nielsen P. E. Synthesis of retro-inverso peptide nucleic acids: 1chracterisation of the monomer. *Tetrahedron Lett.* **1995**, *36*, 6937-6940. (b) Jordan, S.; Schwemler, C.; Kosch, W.; Kretschmer, A.; Schwenner, E.; Stropp, U.; Mielke, B. New hetero-oligomeric peptide nucleic acids with improved binding properties to complementary DNA, *Bioorg. Med. Chem. Lett.* **1997**, *7*, 687-690.

111. (a) Kumar, V. A.; Ganesh, K. N. Conformationally constrained PNA analogues: structural evolution toward DNA/RNA binding selectivity. *Acc. Chem. Res*. **2005**, *38*, 404-412. (b) Kumar, V. A. Structural preorganization of peptide nucleic acids: chiral cationic analogues with five- or six-membered ring structures. *Eur. J. Org. Chem*. **2002**, 2021-2032

112. (a) Gangamani. B. P.; Kumar, V. A.; Ganesh, K. N. Synthesis of N-(purinyl/pyrimidinyl acetyl)-4-aminoproline diastereomers with potential use in PNA synthesis. *Tetrahedron* **1996**, *52*, 15017-15030. (b) Lowe, G.; Vilaivan, T. Amino acids bearing nucleobases for the synthesis of novel peptide nucleic acids. *J. Chem. Soc. Perkin Trans 1* **1997**, 539-546. (c) Samuel, T. H.; David, T.; Hickman, T.; Morral, J.; Beadham, I. G.; Micklefield, J. Nucleic acid binding properties of thyminyl and adeninyl pyrrolidine-amide oligonucleotide mimics (POM) *Chem. Comm*. **2004**, 516-517.

113. (a) D'Costa, M.; Kumar, V. A.; Ganesh, K. N. Aminoethylprolyl (*aep*) PNA: mixed purine/pyrimidine oligomers and binding orientation preferences for PNA:DNA duplex formation. *Org. Lett*. **2001**, *3*, 1281-1284. (b) D'Costa, M.; Kumar, V. A.; Ganesh, K. N. Aminoethylprolyl peptide nucleic acids (*aep*-PNA): chiral PNA analogues that form highly stable DNA:(*aep*-PNA)$_2$ triplexes. *Org. Lett*. **1999,** *1*, 513-1516.

114. D'Costa, M.; Kumar, V. A.; Ganesh, K. N. N7-Guanine as a C^+ Mimic in Hairpin *aeg*/*aep*PNA-DNA Triplex: Probing Binding Selectivity by UV-T*m* and Kinetics by Fluorescence-Based Strand-Invasion Assay. *J. Org. Chem*. **2003**, *68*, 4439-4445.

115. Puschl, A.; Boesn, G.; Zuccarello, G.; Dahl, O.; Pitsch, S.; Nielsen, P. E. Synthesis of pyrrolidinone PNA: A novel conformationally restricted peptide nucleic acid analogues *J. Org. Chem.* **2001**, *66*, 707-712.

116. Willams M. A.; Rapoport H. Synthesis of conformationally constrained DTPA analogs Incorporation of the ethylene diamine units as aminopyrrolidines. *J. Org. Chem*. **1994**, *59*, 3616-3625.

117. (a) Puschl, A.; Tedeschi, T.; Nielsen, P. E. Pyrrolidine PNA: A novel conformationally restricted PNA analogues. *Org. Lett.* **2000**, *2*, 4161-4163. (b) Kumar, V. A.; Meena. Pyrrolidine PNA-DNA chimeric oligonucleotides with extended backbone. *Nucleosides Nucleotides Nucleic Acids*. **2003**, *22*, 1101-4.

118. Kumar, V.; Pallan, P. S.; Meena, M.; Ganesh, K. N. Pyrrolidine nucleic acids: DNA/PNA oligomers with 2-hydroxy/aminomethyl-4-(thymin-1-yl)pyrrolidine-N-acetic acid. *Org Lett*. **2001**, *3*, 1269-1272.

119. (a) Michael, C. Mark, M.; Witschi, A.; Larionova, N.; John, M.; Russell; Haynes, D.; Toshiaki Hara, Grajkowski, A.; Appella, D. H. A cyclopentane conformational restraint for a Peptide Nucleic Acid:

Design, asymmetric synthesis and improved binding affinity to DNA & RNA. *Org. Lett.* **2003**, *5*, 2695-2698.

120. Govindaraju, T.; Kumar, V. A.; Ganesh, K. N. *cis*-Cyclopentyl PNA (*cp*PNA) as constrained chiral PNA analogues: stereochemical dependence of DNA/RNA hybridization. *Chemm. Comm*. **2004**, *7*, 860-861. (c) Govindaraju, T.; Kumar, V. A.; Ganesh, K. N. *cis*-Cyclopentyl PNA (*cp*PNA) as constrained chiral PNA analogues:stereochemical dependence of DNA/RNA hybridization *Chemm.Comm*. **2004**, 860-861.
121. Bregant, S.; Burlina, F.; Chassaing, G. New thiazane and thiazolidine PNA monomers: synthesis, incorporation into PNAs and hybridization studies. *Bioorg*. *Med*. *Chem*. *Lett*. **2002,** *12*, 1047-50.
122. (a) Wada, T.; Sato, H.; Inoue, Y. External reversible control of recognition behavior of alpha-peptide ribonucleic acid (alpha-PRNA) through anti-syn orientational switching of the nucleobase induced by borate esterification of the cis-2',3'-diol. *Biopolymers*. **2004**, *76*, 15-20. (b) Sato, H.; Wada, T.; Inoue, Y. Conformation and recognition control of peptide ribonucleic acid containing pyrimidine/purine mixed sequence. *Nucleic Acids Res*. *Suppl*. **2001**, 229-230. (c) Sato, H.; Hashimoto, Y.; Kikkawa, M.; Wada, T.; Inoue, Y.; DNA recognition control of gamma-PRNA and mismatched base effects upon complex stability. *Nucleic Acids Res*. *Suppl*. **2002**, 159-160.
123. (a) Schoning, K.; Scholz, P.; Guntha, S.; Wu, X.; Krishnamurthy, R.; Eschenmoser, A. Chemical etiology of nucleic acid structure: The–threofuranosyl (3'-2;) oligonucleotide system. *Science* **2000**, *290*, 1347-1351. (b) Miculka, C.; Windhab, N.; Eschenmoser, A.; Sherer, S.; Quinkert, G. PCT Int. Appl. WO 9915509 A2 **1999**, 43. (c) Kozlov, A.; Politis, K.; Van, A.; Busson, R.; Herdewijn, P.; Orgel, E. Nonenzymatic synthesis of RNA and DNA oligomers on hexitol nucleic acids templates: The importance of the A-structure. *J. Amer. Chem. Soc.* **1999,** *121***,** 2653-2656
124. Goodnow, R. A.; Jr., Tam, S.; Pruess, D. L.; Mc. Comas, W. W: Oligomer synthesis and DNA/RNA recognition properties of a novel oligonucleotide backbone analog: glucopyranosyl nucleic amide (GNA). *Tetrahedron Letters* **1997**, *38*, 3199-3202.
125. Lonkar, P. S.; Kumar, V. A. trans-5-aminopipecolyl-aegPNA chimera: design, synthesis, and study of binding preferences with DNA/RNA in duplex/triplex mode. *J. Org*. *Chem*. **2005**, *70*, 6956-6959.
126. Shirude, P.; Kumar, V. A.; Ganesh, K. N. Chimeric peptide nucleic acids incorporating (2*S*,5*R*)-aminoethyl pipecolyl units : synthesis and DNA binding studies. *Tettrahedron Lett*. **2004**, *45*, 3085-88.
127. Püschl, A.; Boesen, T.; Tedeschi, T.; Dahl, O.; Nielsen, P. E. Synthesis of (3*R*,6*R*)- and (3*S*,6*R*)-piperidinone PNA *J. Chem. Soc. Perkin Trans. 1*, **2001**, *21*, 2757 – 2763.
128. Lagriffoule, P.; Wittung, P.; Eriksson, M.; Jensen, K. K.; Norden, P.; Buchardt, O.; Nielsen, P. E. Peptide nucleic acids with a conformationally constrained chiral cyclohexyl-derived backbone. *Chem. Eur. J.* **1997**, *3*, 912-919.
129. (a) Govindaraju, T. G.; Ganesh, K. N.; Kumar, V. A. Synthesis and evaluation of (1*S*,2*R*/1*R*,2*S*)-aminocyclohexylglycyl PNAs as conformationally preorganised PNA analogues for DNA/RNA recognition. *J. Org. Chem.* **2003**, *69*, 1858-1865. (b) Govindaraju, T.; Gonnade, R. G.; Bhadbhade, M. M.; Kumar, V. A.; Ganesh, K. N.; 1*S*,2*R*/1*R*,2*S*)-Aminocyclohexyl Glycyl Thymine PNA: Synthesis, Monomer Crystal Structures, and DNA/RNA Hybridization Studies. *Organic Lett*. **2003**, *5*, 3013-3016.

130. Maison, W.; Schlemminger, I.; Westerhoff, O.; Martens, J. Modified PNAs: a simple method for the synthesis of monomeric building blocks. *Bioorg. Med. Chem. Lett.* **1999**, *9*, 581-584.

131. Sazani, P.; Kang, S. H.; Maier, M. A.; Wei, C.; Dillman, J.; Summerton, J.; Manoharan, M.; Kole, R. Nuclear antisense effects of neutral, anionic and cationic oligonucleotide analogs. Nucleic Acids Res. **2001**, *29*, 3965-74.

132. Fader, L. D.; Tsantrizos, Y. S. Hybridization properties of aromatic peptide nucleic acids: a novel class of oligonucleotide analogues. *Org Lett*. **2002**, *4*, 63-66. (b) Ferrer, E.; Shevchenko, A.; Eritja, R. Synthesis and hybridization properties of DNA-PNA chimeras carrying 5-bromouracil and 5-methylcytosine. *Bioorg*. *Med*. *Chem*. **2000**, *8*, 291-297.

133. Hansen, H. F.; Christensen, L.; Dahl, O.; Nielsen, P. E. 6-thioguanine in peptide nucleic acids: synthesis and hybridization properties. *Nucleosides Nucleotides* **1999**, *18***,** 5–9

134. Gangamani, B. P.; Kumar, V. A.; Ganesh, K. N. 2-Aminopurine peptide nucleic acids (2-*ap*PNA): intrisis fluorescent PNA analoges for probing PNA-DNA interaction dynamics. *Chem*. *Commun*. **1997**, 1913-1914

135. Haaima, G.; Hansen, H. F.; Christensen, L.; Dahl, O.; Nielsen, P. E. Increased DNA binding and sequence discrimination of PNA oligomers containing 2,6-diaminopurine. *Nucleic Acids Res*. **1997**, *25*, 4639

136. Finn, P. J.; Gibson, N. J.; Fallon, R.; Hamilton, A.; Brown, T. Synthesis and properties of DNA-PNA chimeric oligomers. *Nucleic Acids Res* **1996**, *24*, 3357-3363.

137. Borgatti, M.; Lampronti, I.; Romanelli, A.; Pedone, C.; Saviano, M.; Bianchi, N.; Mischiati, C.; Gambari, R. Transcription factor decoy molecules based on a peptide nucleic acid (PNA)-DNA chimera mimicking Sp1 binding sites. *J Biol Chem*. **2003**, *278*, 7500-7509

138. (a) Uhlmann E. Peptide nucleic acids (PNA) and PNA-DNA chimeras: from high binding affinity towards biological function. *Biol Chem*. **1998**, *379*, 1045-52. (b) Bajor, Z.; Sagi, G.; Tegyey, Z.; Otvos, L. Synthesis, biophysical, and biochemical properties of PNA-DNA chimeras. *Nucleosides Nucleotides Nucleic Acids*. **2003**, *22*, 1215-7. (c) Barone, G.; De Napoli, L.; Di Fabio, G.; Erra, E.; Giancola, C.; Messere, A.; Montesarchio, D.; Petraccone, L.; Piccialli, G. Synthesis and DNA binding properties of DNA-PNA chimeras. *Nucleosides Nucleotides Nucleic Acids*. **2003,** *22*, 1089-91. (d) Uhlmann, E.; Greiner, B.; Breipohl, G. PNA/DNA chimeras. In *Peptide Nucleic Acids: Protocols and Applications*. Edited by Nielsen, P. E.; Egholm, M. Horizon scientific press, **1999**, 51-70.

139. Norton, J.; Platyszec, M.; Wright, W.; Shay, J.; Corey, D.R. Inhibition of human telomerase activity by Peptide Nucleic Acids. *Nat*. *Biotech*. **1996**, *14*, 615-620.

140. (a) Nielsen, P. E.; Egholm, M.; Berg, R. H. Buchardt, O. Sequence specific inhibition of DNA restriction enzyme cleavage by PNA. *Nucleic Acids Res*. **1993**, *21*, 197-200. (b) Gambari, R. Peptide-nucleic acids (PNAs): a tool for the development of gene expression modifiers. *Curr Pharm Des*. **2001**, *7*, 1839-62

141. Borgatti, M.; Romanelli, A.; Saviano, M.; Pedone, C.; Lampronti, I.; Breda, L. Resistance of decoy PNA-DNA chimeras to enzymatic degradation in cellular extracts and serum. *Oncology Research* **2003**, *13,* 279-287.

142. Gallazzi, F.; Wang, Y.; Jia, F.; Shenoy, N.; Landon, L. A.; Hannink, M.; Lever, S. Z.; Lewis, M. R. Synthesis of radiometal-labeled and fluorescent cell-permeating peptide-PNA conjugates for targeting the bcl-2 proto-oncogene. Bioconjug Chem. **2003**, *14*, 1083-1095.

143. Nielsen, P. E.; Knudsen, H. *PCT Int. Appl. WO 9853801* A1 *3*, **1998**, 60

144. (a) Gangamani, B. P.; Kumar, V. A.; Ganesh, K. N. Chiral analogues of peptide nucleic acids:synthesis of 4-aminoprolyl nucleic acids and DNA complementation studies using UV-CD spectroscopy. *Tetrahedron* **1999**, *55*, 177-192. (b) Gangamani, B. P.; Kumar, V. A.; Ganesh, K. N. Spermine conjugated Peptide Nucleic Acids (*sp*PNA): UV and fluorescence studies of PNA-DNA hybrids with improved stability. *Biochemical andBiophysical Research Communications* **1997**, *240*, 778-782.

CHAPTER 2

THE SYNTHESIS OF PYRROLIDINE AND PYRROLIDINONE PEPTIDE NUCLEIC ACIDS (PNA) MONOMERS

CHAPTER 2: THE SYNTHESIS OF PYRROLIDINE AND PYRROLIDINONE PEPTIDE NUCLEIC ACIDS (PNA) MONOMERS

2.1 INTRODUCTION

Highly stable analogs of DNA or RNA are the promising candidates for inhibiting gene expression.[1-2] When introduced into cells, these analogs seek complementary sequences on target DNA duplex (antigene) or single stranded mRNA (antisense) and bind to inhibit the production of corresponding coded functional protein in a cell.[3-6] Chemical modifications of the sugar, nucleobase or the phosphodiester linkage may improve the entry of these analogs into cells and also prevent their intracellular degradation.[7-18] To achieve these requirements, Nielsen and his colleagues used computer modeling to design a new nucleic acid analog, peptide nucleic acid (PNA).[19-25] In this analog, the entire negatively charged sugar-phosphate backbone of DNA is replaced by a neutral and achiral polyamide backbone consisting of *N*-(2-aminoethyl)-glycine units and the four standard nucleobases as side chains. The nucleobases are attached to the backbone through a conformationally rigid tertiary acetamide linker (Figure 1). The internucleobase distances

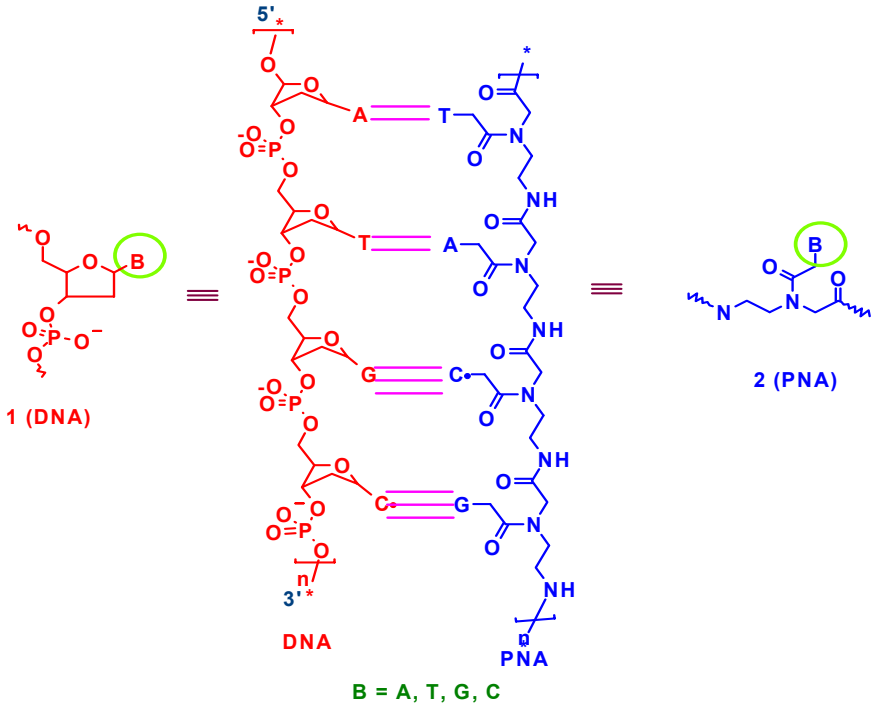

Figure 1: Chemical structure of DNA and *aeg*-PNA

in PNA are conserved as in DNA, which allows its binding to the target DNA/RNA sequences with high sequence specificity and affinity.[26-30] Moreover, PNA is stable to cellular enzymes like nucleases and proteases. However, major limitations of the therapeutic applications of PNA are their poor solubility in aqueous media due to self-aggregation, insufficient cellular uptake and ambiguity in orientational selectivity of binding.[31]

In the recent past, there have been many attempts to address these problems in a effective manner by introduction of chirality into PNA. This has been done by linking chiral amino acids, peptides and oligonucleotides in the PNA backbone to improve the orientational selectivity of binding with natural oligonucleotides. Chirality was also imparted to PNA by using chiral amino acids in the backbone itself.[33] Most of these efforts had only marginal desired effects on the hybridization properties of PNA. Recently, the five-membered prolyl ring was introduced into PNA to impart the necessary structural rigidity and chirality for orientational selectivity (Figure 2a).[34] But, it was found to be unsatisfactory in improving the PNA:DNA binding in the desired manner. However, alternating units with glycine enhanced the binding affinity for DNA. In another attempt, introduction of positive charges in the PNA backbone[35] was found to improve its aqueous solubility. Considerable interest is emerging in making positively charged PNAs as they are expected to possess superior ability to strand invade complementary DNA sequences.

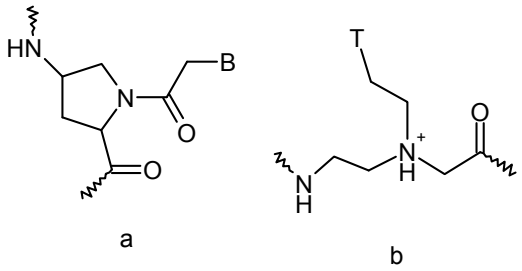

Figure 2: a. 4-Aminoprolyl PNA; **b**. Eth-T PNA; **c**. *aep*-PNA; **d**. *pyrr*-PNA

Hyrup *et al.*[36] have introduced a positive charge in the PNA backbone at the expense of the conformational rigidity of the tertiary amide linkage. The nucleobase is attached to the polyamide backbone *via* a flexible ethylene linker instead of an acetamide linker (Figure 2b). Although this improved the aqueous solubility of PNA, the detrimental effect on stability of the PNA:DNA complexes stressed the importance of rigid preorganization of the PNA structure for effective binding to ss/ds DNA.

Very recently, Hickman *et al.*[37] reported the synthesis and binding properties of a T_5-pentamer pyrrolidine-amide oligonucleotide mimic (Figure 3). In this mimic, the nucleobase is attached to the C4 position of the pyrrolidine ring and the ring nitrogen is alkylated to yield a tertiary amine that is positively charged. This report was followed by that of Püschl *et al.*[38] who prepared its (2*R*,4*S*) adenine analogue. In this case, the homooligomer of this nucleotide was found to form a $(DNA)_2$:PNA triplex. These oligomers also formed stable triplexes with DNA and RNA and exhibited binding selectivity for RNA over DNA. Though the pyrrolidine ring nitrogen is positively charged, increasing the salt concentration resulted in only slightly higher Tm values. This is in contrast to other cationic modified oligonucleotides that show a marked decrease in the stability of their complexes with RNA and DNA at higher salt concentration. This was attributed to a reduction in the electrostatic attraction between the oppositely charged backbones owing to the charge compensation by the salt.

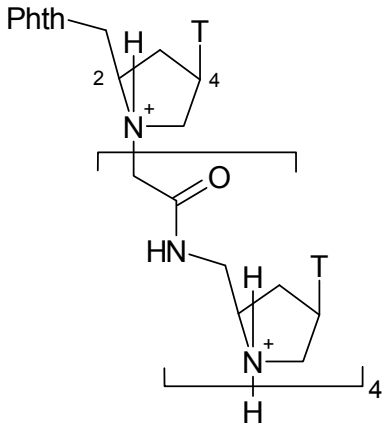

Figure 3: Pyrrolidine-amide oligonucleotide mimic

Recently, D'Costa *et. al*.[39] reported the synthesis of (2*S*,4*S*) and (2*S*,4*R*) "aminoethylprolyl PNAs", (*aep*-PNA), in which the glycyl component of PNA backbone has been substituted by a prolyl unit, to which all four nucleobases base are singularly attached at position C4 (Figure 4a). Interestingly, these chiral and cationic PNA analogues did show increased binding strength toward DNA, but further data is required to fully evaluate the properties of these interesting analogues. In preorganizing the PNA backbone for duplex formation, a new cyclic pyrrolidinone PNA (*pyrr*-PNA) analogue has been designed (Figure 4b).[40] In this analogue the aminoethylglycine backbone and the methylenecarbonyl linker are connected, introducing two chiral centers into otherwise non-chiral PNA. The four diastereoisomers of the adenine analogue were synthesized, and the hybridization properties of PNA decamers containing one of the analogues were measured against complementary DNA, RNA, and PNA strands. The (3*S*,5*R*) isomer containing PNA was shown to have the highest affinity toward RNA, and recognized RNA better than DNA. The (3*S*,5*R*) isomer was used to prepare a fully modified decamer which bound to $r(U)_{10}$ with only a small decrease in Tm (ΔTm/mod = 1 °C) relative to aminoethylglycine PNA.

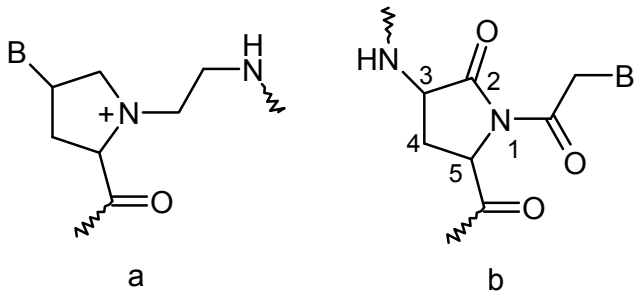

Figure 4: (a) *aep*-PNA (b) *pyrr*-PNA

A somewhat similar approach using olefinic PNA analogues was recently reported, where the methylene ketone function in the linker was replaced by a configurationally stable carbon-carbon double bond to give *E*-OPA and *Z*-OPA (Figure 5).[41] Incorporation

of one unit of OPA monomer (B = T) in the middle of a PNA sequence showed that the *E* isomer, which has a configuration similar to the PNA rotamer preferred in duplexes, gave a higher affinity to anti-parallel complementary DNA than the *Z*-isomer. However, both OPA isomers resulted in a substantial decrease in affinity of the modified PNA toward DNA (by ΔTm) = -6.5 and -14.2 °C for a decamer PNA containing one central *E*- and *Z*-OPA unit respectively).

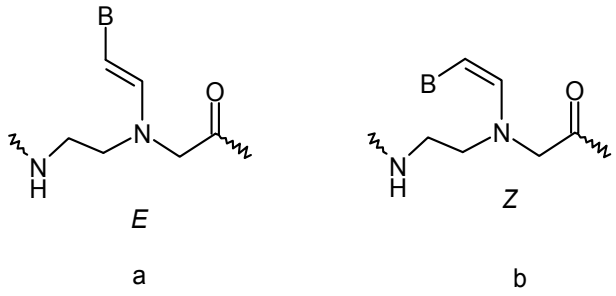

Figure 5: (a) *E*-OPNA; (b) Z-OPNA

2.2 RATIONALE AND OBJECTIVES OF PRESENT WORK

While attempting to impose the chirality and rigidity (conformational constrain) for pre-organization of backbone in *aeg*-PNA, the pyrrolidine based PNAs are growing as novel PNA analogues with efficient DNA/RNA hybridization properties.[42] Figure 6 describes a simple a preorganization of backbone in PNA, depending upon the direction of side chain carbonyl group of backbone in unmodified *aeg*-PNA. There are two possibilities in orientation of the carbonyl group in *aeg*-PNA unit, either toward the N-terminus or to the C-terminus of the peptide backbone. Such type of preorganization leads to various types of constrained, rigid, cyclic and chiral modified PNA analogues (Figure 6). As a result, the *aep*-[39] and *prolyl*-[34] are the most successful and the simplest constrained PNAs derived by locking the side chain with backbone methylene group from the C-terminal or *N*-terminal part (Figure 6b and 6c).[34] In both cases, the modified PNAs

do not have tertiary carbonyl group in the backbone, in contrast to the *aeg*-PNA. The properties of PNA and various PNA analogues have recently been reviewed.

In a recent report, PNA/DNA or PNA/RNA duplex formation is shown to be accompanied by a decrease in entropy. It should be possible to structurally effect entropy loss by using more rigid, preorganised PNA analogues. This is possible by use of conformationally constrained backbones. The NMR studies of single stranded PNA oligomers clearly show a rotameric equilibrium, in which tertiary amide bond leading to a presence of complex mixture (up to 2^n; n = 1, 2, 3….) of isomers.[43] It is also reported that PNA hybridization is disfavored by a slow rotamer equilibrium of the linker-backbone

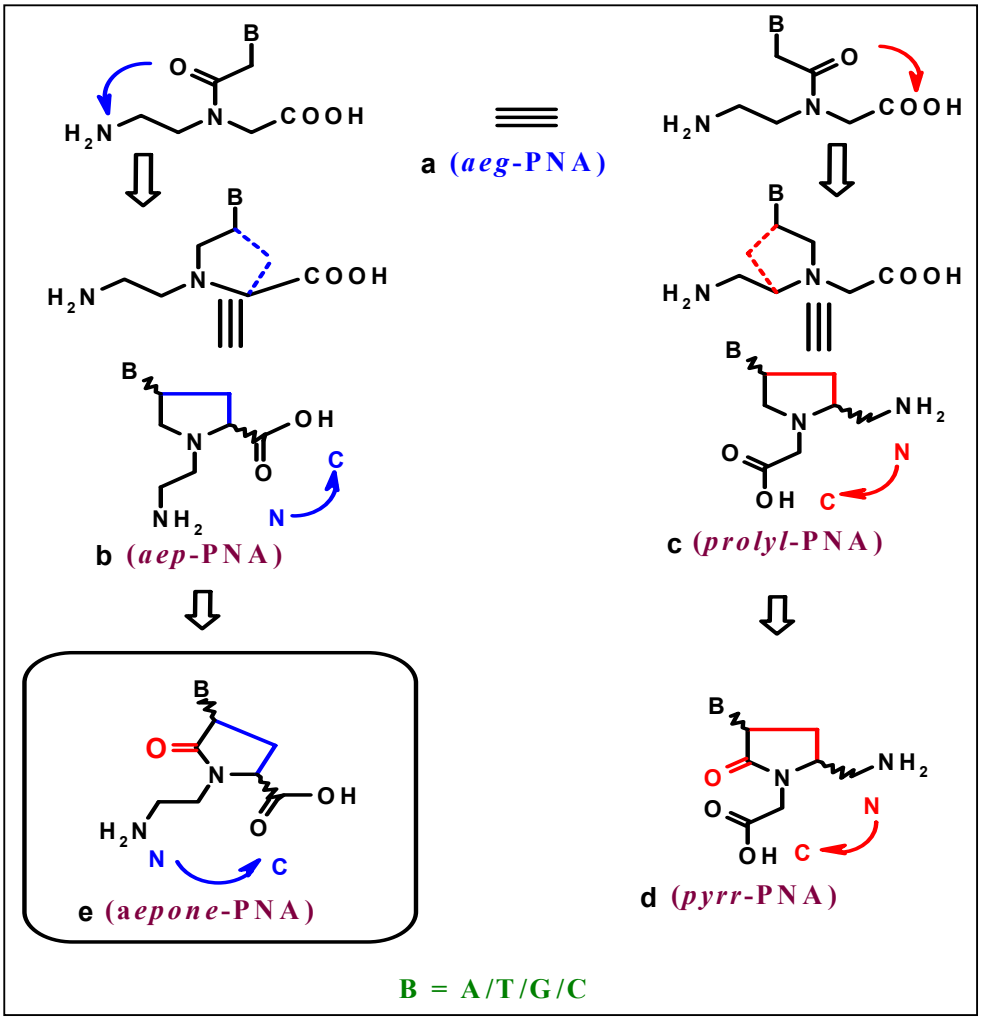

Figure 6: Structural organization in PNA

amide.[34] Thus shifting the equilibrium to enrich one of the rotamer population, should stabilize duplex formation by preorganizing single stranded PNA to its conformation in duplex, leading to entropy loss upon duplex formation. In another report, the examination of PNA/DNA, PNA/RNA and PNA/PNA duplexes as well as PNA_2/DNA triplexes reveals that the base linker-carbonyl points toward the carboxyl end of PNA.[44] The rotation around the methylene carbonyl linker in single stranded PNA can be prevented by connecting the linker to the backbone through a methylene bridge in a cyclic structure.

In *pyrr*-PNA (Figure 6d)[40] the linker-carbonyl is fixed to one direction by locking the *aeg*-PNA via bridging methylene group. In other words, this modification can be derived in the existing *prolyl*-PNA (Figure 6c) by addition of *carbonyl group* at C5 position of its *prolyl*-ring. Out of the four possible diastereomers, the (3*S*,5*R*) was shown to recognize RNA better than DNA.[17] The marginally satisfactory results of these PNAs, encouraged us to look for the alternative possibility of fixing the carbonyl group orientation toward the *N*-terminal side of peptide backbone of *aeg*-PNA and examine its effect on binding affinity toward DNA/RNA. This modification is equivalent to introduction of carbonyl group at C5 position in *aep*-PNA (Figure 6b), which leads to pyrrolidinone ring. As a result, the newly designed PNA is termed *N*-aminoethylpyrrolidinone PNA (*aepone*-PNA).

The specific objectives of this chapter are:

1. To develop methodologies for introduction carbonyl group at C5 in pyrrolidine ring of of *aep*-PNA monomer.
2. Synthesis of 1-*N*-(Boc-aminoethyl)-4(*S*)-(A/T/G/C)-2(*S*)-pyrrolidin-5-one (*cis*-*aepone*) (Figure 7).
3. Synthesis of 1-*N*-(Boc-aminoethyl)-4(*R*)-(A/T/G/C)-2(*S*)-pyrrolidin-5-one (*trans*-*aepone*) monomers for use in PNA synthesis (Figure 7).

4. Synthesis of 1-*N*-(Boc-aminoethyl)-4(*R*)-(A/T/G/C)-2(*S*)-pyrrolidine (*cis*/*trans*-*aep*) monomers for comparative studies with *aepone*-PNA (Figure 7).

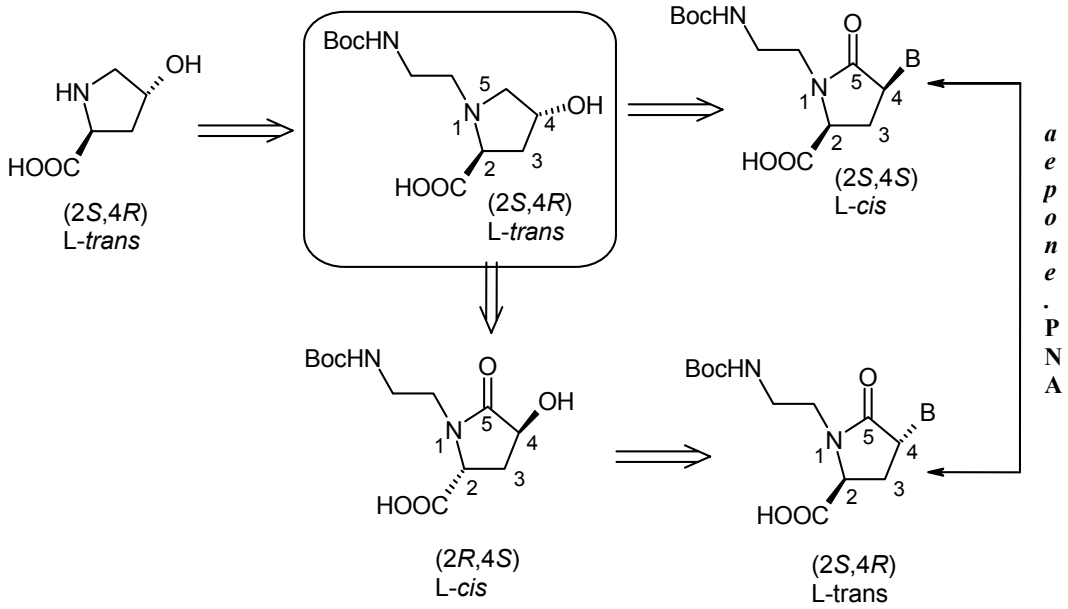

Figure 7: Schematic proposal for synthesis *aepone*-PNA

2.3 PRESENT WORK: RESULTS AND DISCUSSION

2.3.1 Conversion of pyrrolidine ring of *aep*-PNA into pyrrolidinone ring

2.3.1a Synthesis of 1-N-(t-Boc-aminoethyl)-4-hydroxy-prolyl methyl ester (6)

Compound **6** is a common intermediate for synthesis of *aep*- and *aepone*-PNA monomers (Scheme 1) and this compound was synthesized from the commercial available starting materials aminoethanol **1** and 4-hydroxy-L-*trans*-proline **4**. *N*-Boc-protected aminoethanol **2** was synthesized from 2-aminoethanol **1** by reaction with 1 eq. of Boc-anhydride. The protected alcohol **2** was converted into its *O*-mesylate derivative **3,** which was used to *alkylate* the ring nitrogen of methyl ester of 4-hydroxy-L-*trans*-proline **5** under mild basic conditions in presence of DIPEA and DMAP to get the reported[39]

compound 1-*N*-*(*Boc-aminoethyl)-4*S*-hydroxyl-2*R*-proline methyl ester **6**. The methyl ester of 4-hydroxy-L-proline **5** was synthesized by esterification of 4-hydroxy-L-Proline (**4**).

2.3.1b Introduction of carbonyl group at C-5 position of prolyl ring

In Figure 6, the synthesis of proposed *aepone*-PNA monomers (**d**) requires the conversion of pyrrolidine ring of *aep*-PNA monomer[40] (**c**) into a pyrrlidinone ring. This was achieved by the introduction of carbonyl group at C-5 position of prolyl ring of *aep*-PNA monomer (**c**) by two routes A and B, that differ in the order in which *N*-alkylation and C-5 oxidation are carried out.

Scheme 1: Synthesis of 4-Hydroxyl Intermediate of *aep*- and *aepone*-PNA Monomers

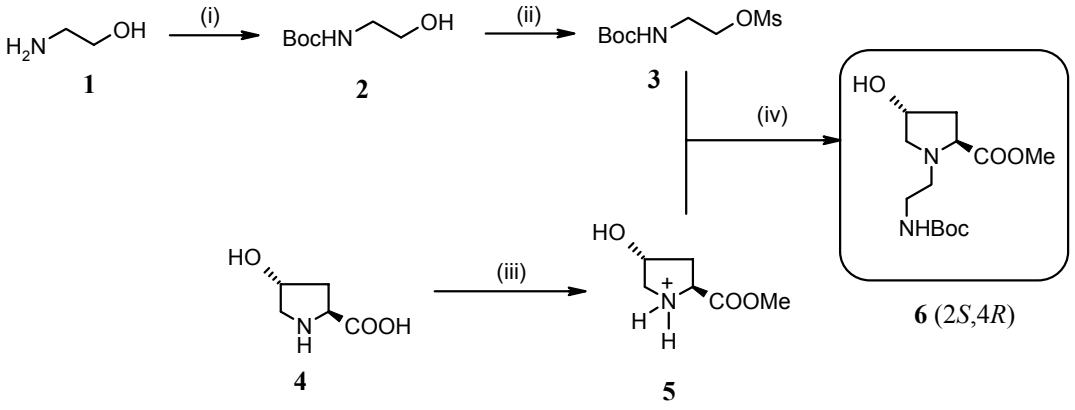

Reagents: (i) Boc_2O, Et_3N, Dioxane:H_2O, rt, 90%; (ii) $MeSO_2Cl$, Et_3N, 0 ^oC-rt 8 hr,% (iii) $SOCl_2$, MeOH, reflux, 85%; (iv) Compound **3**, DIPEA, DMAP, DMF: CH_3CN (1:1), 70%.

Most reported methods to obtain C4-functionalized pyroglutamates involve asymmetric 1,3-dipolar cycloadditions[45] or *N*-alkylation of pyroglutamates using lithium enolates.[46] In a recent report, C-4 substituted *N*-Boc pyrrolidin-5-one derivatives were synthesized from 4-(*R*)-hydroxy-L-proline through direct oxidation of 4-substituted-*N*-Boc proline.[47] This was done using the versatile oxidizing agent RuO_4 generated *in situ* from $RuO_2/NaIO_4$.[48]

Our intention was to prepare C4 functionalized N1-alkylated pyroglutamate derivatives (**d**) of Figure 8 as intermediates for the synthesis of modified peptide nucleic acids (PNA) monomers. This can be achieved by *N*-alkylation of suitable pyroglutamates (route A, Figure 8); however, the use of strong bases in *N*-alkylation is accompanied by a facile opening of the pyrrolidine ring. This can also be achieved by first *N*-alkylation of suitable followed by oxidation to get substituted pyroglutamates (route A, Figure 8) to avoid the use of strong bases in *N*-alkylation to retain the pyrrolidine ring.

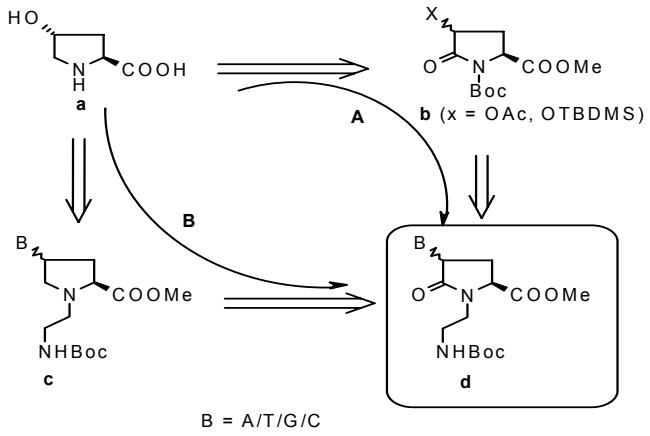

Figure 8: Proposed synthetic route of intermediate of *aepone*-PNA

To overcome this, we attempted the hitherto unknown direct oxidation of various N1-alkylated C4-substituted pyrrolidine derivatives [Figure 9 (**a**)] by using the another oxidizing agent $RuCl_3/NaIO_4$. This reagent also generates the same oxidizing agent RuO_4 *in situ* by following the similar procedure of $RuO_2/NaIO_4$. In principle RuO_4 oxidized the active CH_2 groups which are adjacent to hetro-atoms (N, O etc.); therefore the pyrrolidine derivatives (**a**) [Figure 9] may give three oxidation products as (**b**), (**c**) and (**d**) (Figure 9) because there are three oxidizable Nα-CH_2 sites. Herein, it was interestingly observed that only regioselective oxidation of the endocyclic Nα-methylene (at C5) occurs, in

preference to the oxidation of other Nα-methylenes such as the exocyclic N-CH_2 or CH_2-NHBoc to yield the desired monomers for *aepone*-PNA synthesis.

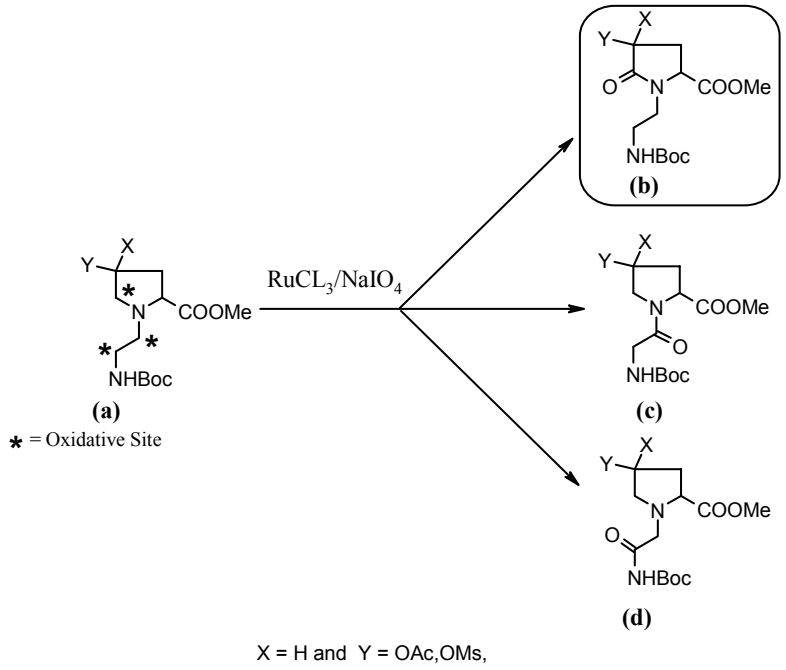

Figure 9: Active methyelene sites in pyrrolidine monomer for oxidation

2.3.1c Testing the efficacy of $RuCl_3/NaIO_4$

It was reported that oxidation of C5 of compound **4a** into **4b** is possible by the reagent RuO_4 generated *in situ* by $RuO_2/NaIO_4$. The efficacy of the oxidizing reagent $RuCl_3/NaIO_4$ for a similar kind of reaction was checked by reaction of compound **4a** with

Scheme 2: Oxidation on 4-subsituted derivative of *N*-Boc-hydroxyl-L-*trans*-proline

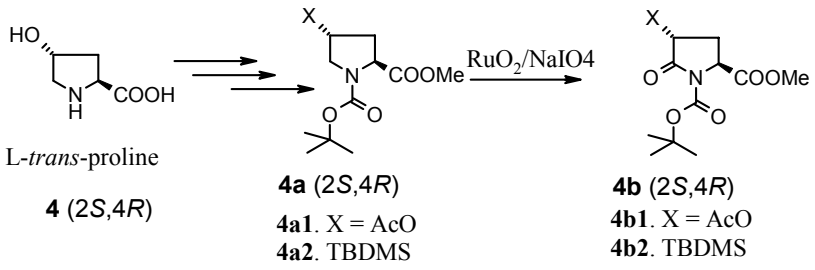

$RuCl_3/NaIO_4$ (Scheme 2). N1-Boc-4-acetoxy (**4a1**) and 4-*O*-TBDMS (**4a2**) proline methyl esters were treated with the $RuCl_3/NaIO_4$ in two different biphasic solvent systems CCl_4:CH_3CN:H_2O (1:1:1.5) and EtOAc/H_2O. The reaction gave the corresponding C5-one products **4b** in 70% yield. The identity of these compounds was established by appropriate spectral data.[48] Thus, $RuCl_3/NaIO_4$ is as efficient and equivalent reagent as $RuO_2/NaIO_4$ for the present substrates.

2.3.1d Synthesis of 4-substituted proline derivatives

Scheme 3 shows various 1-*N*-(Boc-a*minoethyl*)-4-(*R*/*S*)-substituted-2*S*-proline methyl esters (**7**) prepared from 4-(*R*)-hydroxyproline derivative **6** directly or via a Mitsunobu reaction[49] at C4 of prolyl compound **6**.[35,40] These were synthesized to examine the effect of 4-substituents on the oxidation reaction.

Scheme 3: Synthesis of Pyrrolidine deerivatives

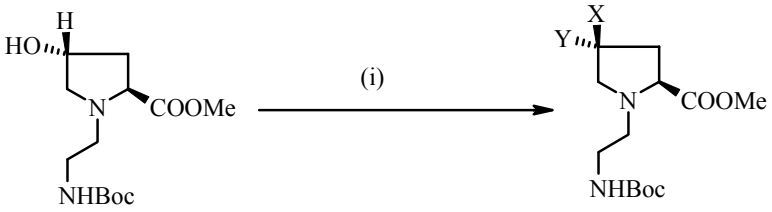

6 (2*S*,4*R*)

7 (2*S*,4*R*)

7a X = H, Y = OMs
7b X = H, Y = OAc
7c X = H, Y = OTBDMS
7d X = OAc, Y = H
7e X = OBz, Y = H
7f X = OTs, Y = H
7g X = OPNB, Y = H
7h X = H, Y = H

Reagents: (i) $MeSO_2Cl$, Et_3N, DCM, 0 ^oC, 2h, 85% for **7a**; Ac_2O, Py, rt 5 h for 7**b**; TBDMSCl, DMF, imidazole 6 h for 7**c**; Ph_3P, DIAD, AcOH for **7d** Ph_3P, DIAD, PhCOOH for **7e,** THF, 5 hr, 80%**;** Ph_3P, DIAD, methyl tosylate for **7f,** THF, 8 h, 65%**;** Ph_3P, DIAD, 4-nitro-benzoic acid for **7g** THF, 10 h, 70%. **7h** (see in chapter 4b)

1-*N*-(Boc-aminoethyl)-4*R*-*O*-mesyl-2*S*-proline methyl ester (**7a**) was prepared directly from 1-*N*-(Boc-aminoethyl)-4*R*-hydroxy-2*S*-proline methyl ester **6** by *O*-mesylation reaction with methanesufonyl chloride ($MeSO_2Cl$) in presence of mild organic base Et_3N and DCM under anhydrous conditions. The compound was characterized by ^{1}H-NMR, which showed appearance of a singlet for 3H at δ (ppm) 3.0, characteristic of the CH_3 of mesylate function.

1-*N*-(Boc-aminoethyl)-4*R*-*O*-acetyl-2*S*-proline methyl ester (**7b**) was synthesized directly from 1-*N*-(Boc-aminoethyl)-4-(R)-hydroxy-2-(S)-proline methyl ester **6** by reaction of 4-hydroxyl group with Ac_2O in presence of anhydrous pyridine. The product was confirmed by ^{1}H-NMR, with appearance of singlet at δ 2.0 due to CH_3 of the acetyl group. 1-*N*-(Boc-aminoethyl)-4*S*-*O*-acetyl-2*S*-proline methyl ester (**7d**) was obtained from 1-*N*-(Boc-aminoethyl)-4*R*-hydroxy-2*S*-proline methyl ester **6**, by reaction with acetic acid in presence of Ph_3P and DIAD under Mitsunobu conditions. The reaction is accompanied by inversion at C4 to obtain compound **7d.** This compound was confirmed by ^{1}H-NMR, exhibiting a singlet δ 2.0 due to CH_3 of acetyl residue.

1-*N*-(Boc-aminoethyl)-4*R*-(*tert*-butyldimethylsilyloxy)-2*S*-proline methyl ester (**7c**) was derived directly from 1-*N*-(Boc-aminoethyl)-4*R*-hydroxy-2*S*-proline methyl ester **6** by reaction of 4-hydroxyl group by silylating reagent *tert*-butyldimethylsilyl chloride (TBDMS) in presence of imidazole and DMAP under anhydrous conditions. The product was characterized by ^{1}H-NMR having a singlet at 0.87 (9H, *t*-butyl) and 0.16 (6H, dimethyl silyl) corresponding to the presence of TBDMS residue.

1-*N*-(Boc-aminoethyl)-4*S*-*O*-benzoyl-2*S*-proline methyl ester (**7e**) was prepared from 1-*N*-(Boc-aminoethyl)-4-(*R*)-hydroxy-2-(*S*)-proline methyl ester **6** by a similar Mitsunobu reaction with benzoic acid in presence of Ph_3P and DIAD, involving inversion at C4**.**

Compound **7e** was characterized by appearance of a multiplet in aromatic region at δ 8-7.4 with (m, 5H) due to phenyl residue of benzoate.

1-*N*-(Boc-aminoethyl)-4*S*-*O*-tosyl-2*S*-proline methyl ester (**7f**) was derived from 1-*N*-(Boc-aminoethyl)-4*R*-hydroxy-2*S*-proline methyl ester **6** by reaction with methyltosylate in presence of Ph_3P and DIAD under Mitsunobu conditions with inversion at C4.

1-*N*-(Boc-aminoethyl)-4*S*-*O*-(p-nitro-benzoyl)-2*S*-proline methyl ester (**7g**) was synthesised from reaction of 1-*N*-(Boc-aminoethyl)-4*R*-hydroxy-2*S*-proline methyl ester **6** with *p-nitro-benzoic acid* under Mitsunobu rection conditions. The identity of product was confirmed by ^{1}H-NMR consisting of a singlet for 3H at δ 2.4 and two doublets for 2H each at δ 7.8 and 7.3 due to aromatic H's of p-nitrobenzoate residue**.**

2.3.1d Oxidation reactions: Synthesis of 4-substituted 5-prolinones

1-*N*-(Boc-aminoethyl)-4*R*-(*O*-mesyl)-5-one-2*S*-proline methyl ester (**8a**) was prepared directly from 1-*N*-(Boc-aminoethyl)-4*R*-*O*-mesyl-2*S*-proline methyl ester (**7a**) (Scheme 4) by oxidation with $RuCl_3/NaIO_4$ in either CCl_4:CH_3CN:H_2O (1:1:1.5) or EtOAc:H_2O (1:1) at room temperature. As followed by TLC analysis, the starting material disappeared with the appearance of a major product during a 30–60 min period. The product was isolated after usual aqueous work up, followed by purification. The spectral characterization suggested the structure to be **8**, arising from oxidation occurring at C5. In ^{1}H-NMR of **8a,** the signals due to H5',5" seen at in **7a** disappeared as expected. Further, the chemical shift of NH was upfield shifted from δ 5.2 to 4.8, and that of H2 downfield shifted from δ 3.4 to3.8. In ^{13}C-NMR, the appearance of one additional peak at δ 169.0 (CONR) and disappearance of a peak from a region δ 78-79 (CH_2N), supported the assigned structure with oxidation at C5. The assignments were confirmed by 2D and HETCOR experiments and finally proved by single X-ray crystal structure.

Scheme 4: Synthesis of Pyrrolidinone derivatives by oxidation reaction

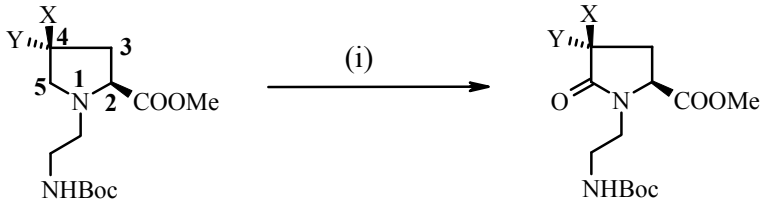

7 (2*S*,4*R*)

7a X = H, Y = OMs
7b X = H, Y = OAc
7c X = H, Y = OTBDMS
7d X = OAc, Y = H
7e X = OBz, Y = H
7f X = OTs, Y = H
7g X = OPNB, Y = H
7h X = H, Y = H

8 (2*S*,4*R*)

8a X = H, Y = OMs
8b X = H, Y = OAc
8c X = H, Y = OTBDMS
8d X = OAc, Y = H
8e X = OBz, Y = H
8f X = OTs, Y = H
8g X = OPNB, Y = H
8h X = H, Y = H

Reagents: (i) $NaIO_4$ /$RuCl_3.xH_2O$, AcOEt/H_2O, rt , 30 min-1 h., Yields 30-45%. Details **a-g** is given in footnote of Table 1.

Table 1. Reaction yields for RuCl3/NaIO4 oxidation of substrates **7***

Entry	Substrate	Product	EtOAc:H2O (% Yield)	CH3CN:CCl4:H2O (1:1:1.5)	Time min
1	**7a**	**8a**	45	45	60
2	**7b**	**8b**	38	30	30
3	**7c**	**8c**	39	32	45
4	**7d**	**8d**	45	36	30
5	**7e**	**8e**	35	30	75
6	**7f**	**8f**	40	37	45
7	**7g**	**8g**	35	41	45
8	**7h**	**8h**	45	40	60

* For a-c, X=H; d-f, Y=H; a, Y= OMs; b, Y= OAc; c, Y= OTBDMS, d, X= OBz; e, X = OTs; f, X = OPNB; g, X=H; Y= H

1-*N*-(Boc-aminoethyl)-4*R*-(*O*-acetyl)-5-one-2*S*-proline methyl ester (**8b**) was synthesized from 1-*N*-(Boc-aminoethyl)-4*R*-*O*-acetyl-2*S*-proline methyl ester (**7b**) by a similar oxidation procedure. The disappearance of H5'/H5" signals of substrate in ^{1}H-NMR, downfield chemical shift of H2 from δ 3.5 to 4.4, the appearance of a peak at δ 170.0 of amide, disappearance of C5 from δ 42.7 in ^{13}C-NMR suggested the formation of oxidized product **8b**.

1-*N*-(Boc-aminoethyl)-4*R*-(*tert*-butyldimethylsilyloxy)-5-one-2*S*-proline methyl ester (**8c**) was obtained from 1-*N*-(Boc-aminoethyl)-4*R*-(*tert*-butyldimethylsilyloxy)-2*S*-proline methyl ester (**7c**) by a similar oxidation procedure of **8a**. The disappearance of signals due to H5'/H5" in ^{1}H-NMR, downfield in chemical shift of H2 from δ 3.4 to 4.4, the appearance a peak at δ 170.5 of amide and disappearance of C5 from δ 42.9 in ^{13}C-NMR suggested the formation of oxidized product **8c.**

1-*N*-(Boc-aminoethyl)-4*S*-(*O*-acetyl)-5-one-2*S*-proline methyl ester (**8d**) was prepared from 1-*N*-(Boc-aminoethyl)-4*S*-*O*-acetyl-2*S*-proline methyl ester (**7d**) by a similar oxidation procedure of **8a**. The disappearance of H5'/H5" signals, downfield in chemical shift of H2 from δ 3.6 to 4.8 in ^{1}H-NMR and the appearance a peak at δ 171.5 of amide and disappearance of C5 from δ 41.9 in ^{13}C-NMR of substrate suggested the formation of oxidized product **8d.**

1-*N*-(Boc-aminoethyl)-4*S*-(*O*-benzoyl)-5-one-2*S*-proline methyl ester (**8e**): This benzoate derivative **8e** was prepared from 1-*N*-(Boc-aminoethyl)-4*S*-*O*-benzoyl-2*S*-proline methyl ester (**7e**). The disappearance of H5'/H5", downfield in chemical shift of H2 from δ 3.5 to 4.5 in ^{1}H-NMR and the appearance a peak at δ 171.2 of amide and disappearance of C5 from δ 42.7 in ^{13}C-NMR suggested the formation of oxidized product **8e.** Finally the structure of oxidized product **8e** was confirmed by single X-ray crystal.

1-*N*-(Boc-aminoethyl)-4*S*-(*O*-tosyl)-5-one-2*S*-proline methyl ester (**8f**) was derived from oxidation of 11-*N*-(Boc-aminoethyl)-4*S*-*O*-tosyl-2*S*-proline methyl ester (**7f**). 1-*N*-(Boc-aminoethyl)-4*S*-*O*-(p-nitro-benzoyl)-5-one-2*S*-proline methyl ester (**8g**) was derived from oxidation of 1-*N*-(Boc-aminoethyl)-4*S*-*O*-(*p*-nitro-benzoyl)-2*S*-proline methyl ester (**7g)** 1-(N-Boc-aminoethyl)-5-one-2*S*-proline methyl ester (**8h**) was synthesized from 1-(N-

Boc-aminoethyl)-proline methyl ester (**7h**) by a similar oxidation procedure. The spectral data are given in experimental section .

In all oxidation reactions, the isolated yields of the products were in the range 30-45% and the solvent system EtOAc:H_2O (1:1) gave slightly better yields (Table 1). Among the different C4 substituents OMs, OBz, OAc, TBDMS, OTs, OPNB and H, the reaction gave best yields with the 4-OMs derivative. There was no particular dependence of the yields on the stereochemistry of C4 substituents, with *R* and *S* isomers behaving similarly. The same C5-one product was obtained even with proline substrate **7h** lacking any C4 substituents.[63] The reactions of N1-alkyl substrates **7** were also found to be faster than that of N1-Boc analogues **1.**

The oxidizing agent RuO_4 generated *in-situ* from $RuCl_3/NaIO_4$ is well-known to oxidise methylene groups α to heteroatoms N or O into carbonyl goups.[64,51] In the substrates used here (**7**a-**7**h), there are three Nα-methylene groups–endocyclic C5, exocyclic N1-CH_2 and BocHN-CH_2. Of the different possible oxidation products (see Figure 9) including *N*-oxide formation, it was found that the major products (**8**a-**8**h) obtained were from a regioselective oxidation of the endocyclic CH_2 at C5 of pyrrolidine ring to give the lactam derivatives (**8**a-**8**h) (Scheme 4). The identity of the oxidation product was unambiguously confirmed by single crystal X-ray data for **8a** and **8e** and finally supported by NMR spectral evidence. The present method is therefore convenient as it gave intermediates for transformation into other C4 substituted pyrrolidin-5-ones, and timally into the *aepone*-PNA analogues.

2.3.1e Crystal Structure

Single crystals of compounds **8a** and **8e** were obtained from a mixture of CH_2Cl_2 and CH_3OH and a good quality crystal was selected using a Leica Polarizing Microscope. X-

ray intensity data were collected on a Bruker SMART APEX CCD diffractometer at room temperature. All the data were corrected for Lorentzian, polarisation and absorption effects using Bruker's SAINT and SADABS programs. SHELX-97 (G. M. Sheldrick, SHELX-97 program for crystal structure solution and refinement, university of Gottingen, Germany, 1997) was used for structure solution and full matrix least squares refinement on F^2. Hydrogen atoms were included in the refinement as per the riding model. The X-ray crystal structure (ORTEP diagram) and packing diagram of compound **8a** and **8e** are given in Figure 10.

Crystal data of 8a: Crystallised from CH_2Cl_2-MeOH, $C_{14}H_{24}N_2O_8S$, M = 380.41, crystal dimensions 0.61 x 0.09 x 0.05 mm, crystal system: monoclinic, space group P21, a = 12.739(5), b = 9.294(4) c = 15.994(6) Å, β = 103.419(8)°, V= 1841.9(13) Å3, Z = 4, Dc = 1.372 g.cm-3, μ (Mo-Kα) = 0.219 mm–1, T = 293(2) K, F(000) = 808, Max. and min. transmission 0.9885 and 0.8780, 9094 reflections collected, 6134 unique [I>2σ (I)], S=1.109, R value 0.0652, wR2 = 0.1213 (all data R = 0.0816, wR2 = 0.1283). ***CCDC No***. 213533.

Crystal data of 8e: $C_{20}H_{26}N_2O_7$, M = 406.43, crystal dimensions 0.61 x 0.59 x 0.14 mm, crystal system Monoclinic, space group $P2_1$, a = 9.2779(15), b = 8.9289(14), c = 13.239(2)Å, β = 96.512(3)°, V=1089.7(3) Å^3, Z = 2, D_c = 1.239 g cm^{-3}, μ (Mo-K_α) = 0.094 mm^{-1}, T = 293(2) K, F(000) = 432, 5493 reflections collected, 3634 unique [I>2σ (I)], S = 1.053, R value 0.0393, $wR2$ = 0.1116 (all data R = 0.0416, $wR2$ = 0.1135). ***CCDC No***. 221794.

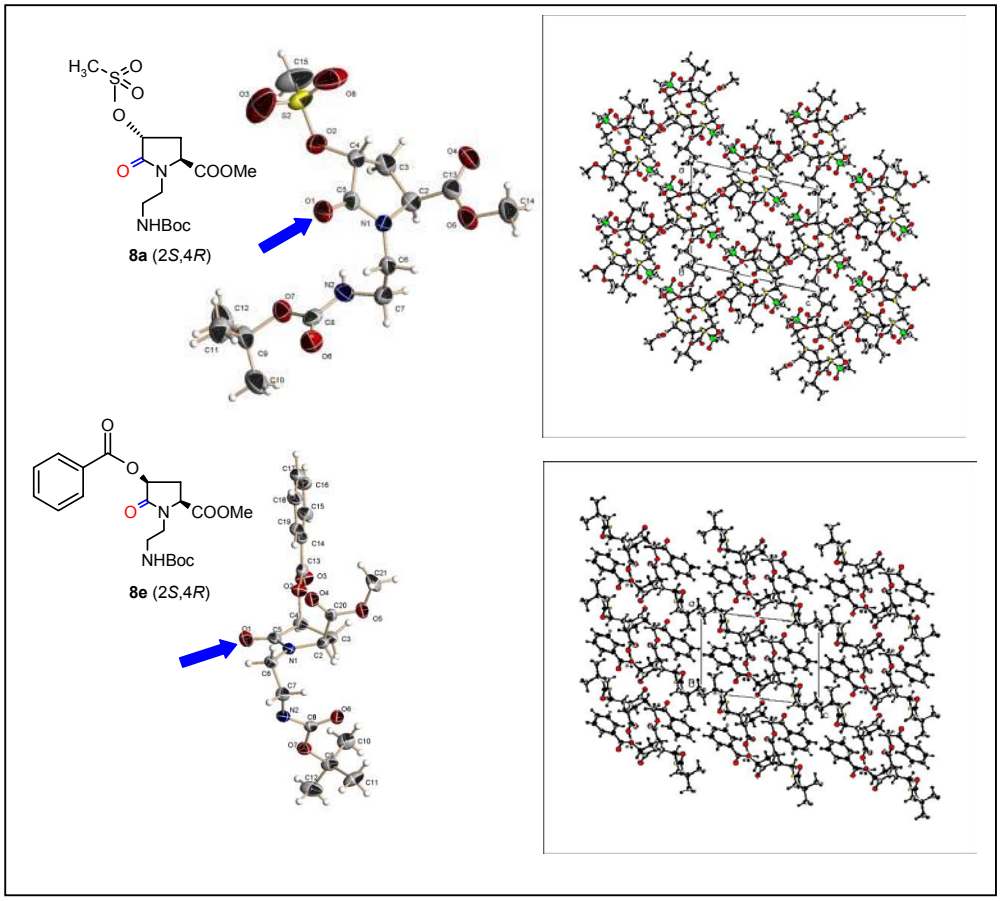

Figure 10: X-ray crystal structure (ORTEP diagram) and packing diagram of compound **8a** and **8e**

The crystal structure unambiguously established the oxidation site to be C5 irrespective of the nature of 4-substituent. Packing diagram gives approximate orientation of carbonyl group .

2.3.1f Spectroscopic Characterization

In the absence of any crystallographic data, it is necessary to unambiguously identify the site of oxidation and this was done by ^{1}H and ^{13}C NMR spectroscopic analysis. The spectroscopic data is shown in Tables 2 and 3. In view of the similar chemical shifts of different Nα-methylene protons, the ^{1}H NMR was completely assigned using ^{1}H-^{1}H DQF COSY. While assignment of H5 in **7a**, **7b** and **7h** is straightforward

due to coupling with H4, assignment of side chain βH'H" (adjacent to BocNH of side chain) were done using connectivity with BocNH followed by assignment of side chain αH'H" (adjacent to N of prolyl ring). The different carbons were assigned via ^{1}H-^{13}C HETCOR experiment (Figure 11-12).

Table 2 : Chemical Shift of pyrrolidinone ring protons (determined 2D COSY /HETCOR NMR)

Monomer	H2	H3	H3'	H4	H5	H5'	αH	α H'	βH	β H'	NH
8a	4.4	2.5	2.7	5.3	-	-	2.6	2.7	3.5	3.7	4.8
8b	4.4	2.3	2.7	5.4	-	-	2.6	2.7	3.5	3.7	4.9
8e	4.6	2.3	2.7	5.2	-	-	2.4	2.3	3.1	3.4	4.5

Table 3: Selected ^{1}H and ^{13}C chemical shifts

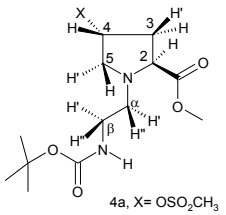

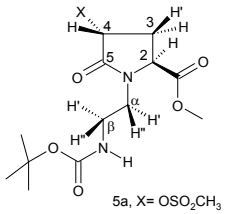

Compound	7a	8a	7b	8b	7h	8h
H4	5.2	5.3	5.3	5.4	1.8, 1.9	2.1
H5'	2.8	-	2.6	-	2.4	-
H5"	3.4	-	3.5	-	3.1	-
αH'	2.6	3.0	2.6	3.1	2.6	3.1
αH''	2.7	3.1	2.7	3.1	2.7	3.2
βH'	3.1	3.5	3.1	3.5	3.1	3.1
βH''	3.1	3.7	3.2	3.7	3.1	3.4
NH	5.1	4.8	5.2	4.9	5.2	4.9
C4	79.0	75.6	73.0	69.6	23.3	23.0
C5	58.4	169.8	58.6	171.2	53.4	172.4
Cα	53.5	42.0	53.2	42.9	54.8	42.1
Cβ	39.0	37.4	39.0	37.5	39.0	38.2

*All spectra recorded at 500 MHz for ^{1}H and 125 MHz for ^{13}C in $CDCl_3$

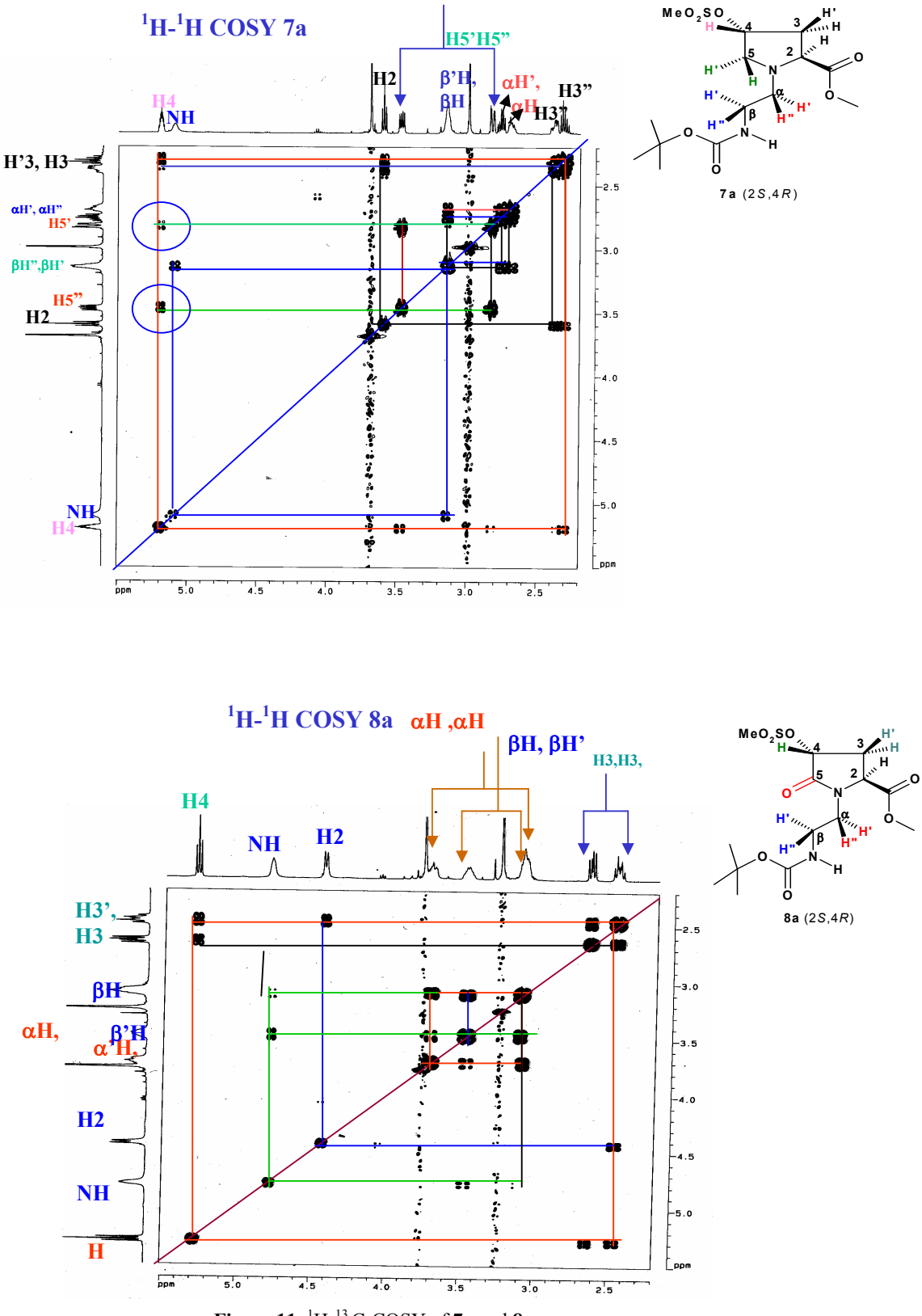

Figure 11: ^{1}H-^{13}C-COSY of **7a** and **8a**

^{1}H-^{13} C-HETCOR of **7a**

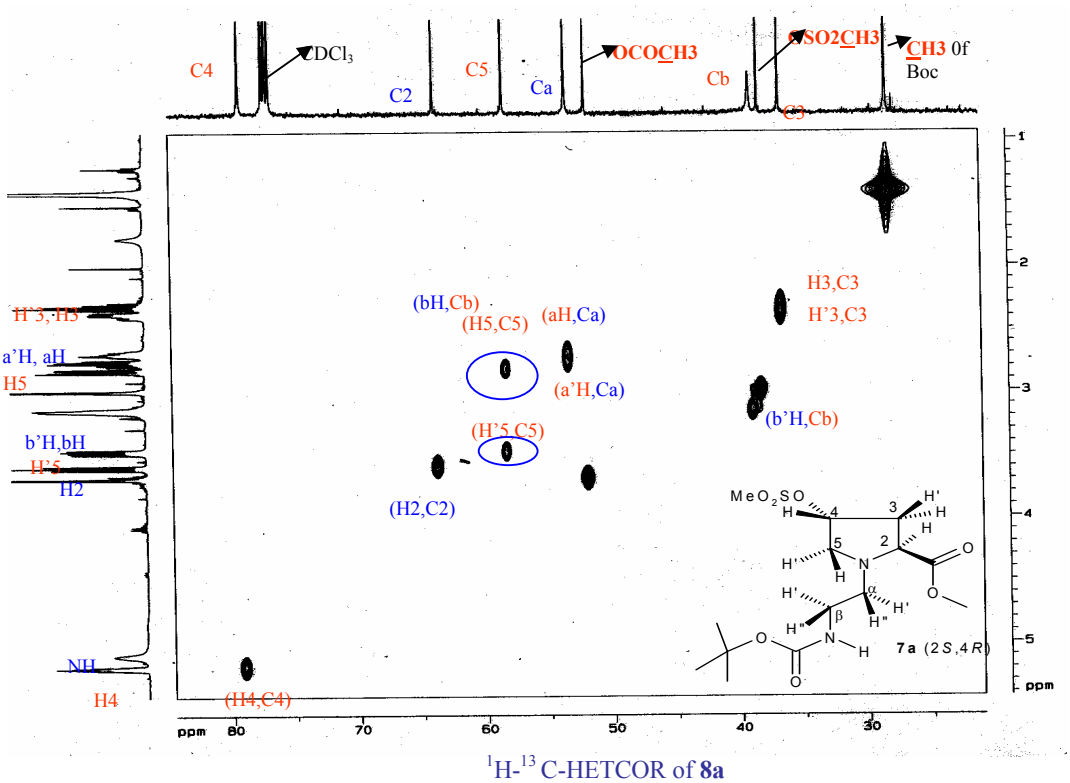

^{1}H-^{13} C-HETCOR of **8a**

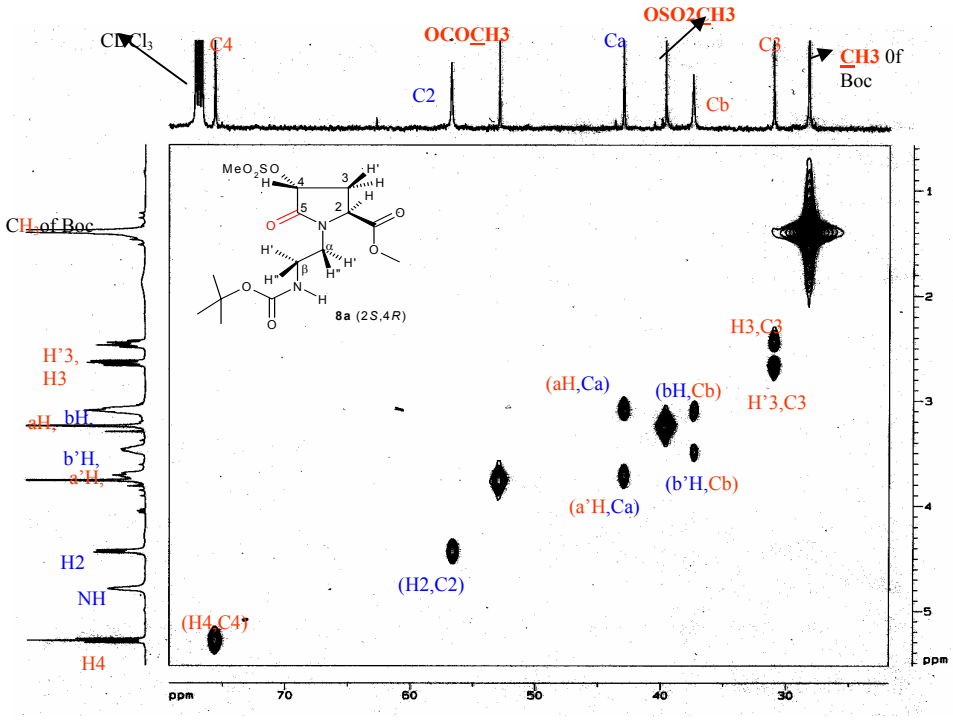

Figurer 12: ^{1}H-^{13} C-HETCOR of **7a** and **8a**

The oxidised products **8** exhibited characteristic commonalities in their ^{1}H and ^{13}C NMR data shown in Table 3. In ^{13}C NMR, the signal around 68.0 ppm due to C5 in substrates **7** disappeared after oxidation giving rise a new signal around 170.0 ppm characteristic of C=O. The C4 signal was upfield shifted by 3.4 ppm upon oxidation, while that of Cα was upfield shifted by 10-12 ppm. In contrast, chemical shift of Cβ was not affected much. In ^{1}H NMR of **7**, the multiplets arising from non equivalent H5'5" around 2.6 and 3.4 ppm disappeared in product **8**, while signals due to αH and βH were retained with a downfield shift of 0.3 ppm perhaps due to anisotropic effects of C5 carbonyl.

Interestingly, no significant changes were seen for H4, except for collapse of multiplet to a triplet. The spectral data shown in Table 3 are for **8a** whose crystal structure is known along with **8b** and **8h** whose crystal structures are not available. All three compounds showed similar patterns in NMR, strongly supporting the regiospecificity of the reaction. Similarlly, **8a, 8b** and **8h**

Thus, the endocyclic methylene group at C5 of pyrrolidine derivatives is more susceptible to oxidation with $RuCl_3/NaIO_4$ than the other two exocyclic methylene groups α to heteroatom-N. These derivatives could be useful for synthesis of *N*-alkylated pyrrolidinones and unnatural amino acids.

The side products of this oxidation reaction on compounds **8a**, **8e** and **8f** were also characterized by Mass and NMR. It was found that oxidation occurred at *β*-position in side chain of **7a**, **7e** and **7f**.

2.3.2 Synthesis of the protected nucleobases

To prevent the side reaction on other active sites of nucleobases during *N*-alkylation, these active site were selectively protected by a chemical reaction, which can

be easily deprotected in final steps (Scheme 5). Synthesis of the following protected nucleobases were completed by the reported procedure.

N3-benzoylthymine ***(11)***.[51] Thymine **9** was treated with benzoyl chloride in acetonitrile:pyridine (4:1) to obtain the N1, N3-dibenzoyl thymine derivative **10**. The N1-benzoyl group, being more labile than the imide N3-benzoyl group, was preferentially hydrolyzed using 0.25M K_2CO_3 in dioxane:water (1:1), to yield the N3-benzoyl thymine **11** (Scheme 5).

Scheme 5: Protection of exocyclic amino groups of the nucleobases

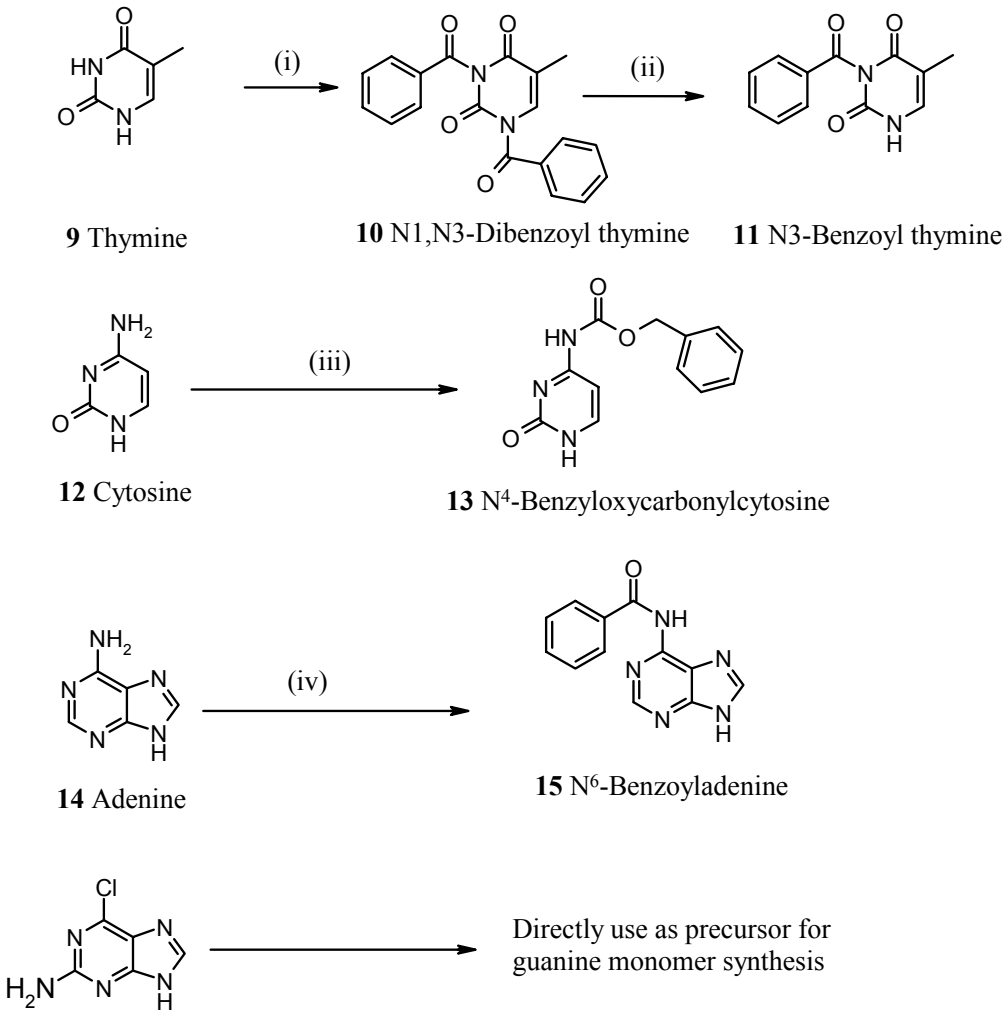

9 Thymine

10 N1,N3-Dibenzoyl thymine

11 N3-Benzoyl thymine

12 Cytosine

13 N^4-Benzyloxycarbonylcytosine

14 Adenine

15 N^6-Benzoyladenine

16 2-amino-6-chloro-purine

Reagent: (i) Benzoyl chloride, AcCN:Py, (ii) k_2CO_3, Dioxane:H_2O (iii) benzyloxycarbonyl chloride, dry pyridine. (iv) Benzoyl chloride, Py.

*N^4-benzyloxycarbonylcytosine (**13**)*.[52] Cytosine **12** was treated with benzyloxycarbonyl chloride in dry pyridine to get the desired product, N^4-benzyloxycarbonylcytosine (**13**).

*N^6-benzoyladenine (**15**)*.[53] Adenine **14**, upon treatment with benzoyl chloride in dry pyridine gave the N^6-benzoyl adenine **12** in good yield, which was obtained as white crystals.

*2-amino-6-chloro-purine (**16**)*: It was directly used for synthesis of guanine monomer of PNA.

2.3.3 Synthesis of L-*cis*-(2*S*,4*S*)-aminoethylpyrrolidinone PNA monomers

Synthesis of 1-*N*-(Boc-aminoethyl)-4(*S*)-(A/T/G/C)-2(*S*)-pyrrolidin-5-one (*cis*-*aepone*) PNA monomers was achieved by *N*-alkylation of nucleobases **9-16** at C4 of pyrrolidinone 1-*N*-(Boc-aminoethyl)-4*R*-(*O*-mesyl)-5-one-2*S*-proline methyl ester **8a** accompanied by S_N2 inversion (Scheme 6).[41]

1-*N*-(Boc-aminoethyl)-4*S*-(thymin-1-yl)-5-one-2*S*-proline methyl ester **(17):** The ester derivative of thymine monomer of L-*cis*-(2*S*,4*S*)-*aepone*-PNA **14** was prepared by N1-alkylation of thymine **9** nucleobase at C4 of compound **8a** in aprotic polar solvent DMF in presence of base K_2CO_3 and catalyst 18-crown-6. The N1 alkylated product **17** was characterized ^{1}H-NMR with disappearence of singlet at δ 3.0 due to CH_3 of mesylate residue in **8a** and appearance of a singlet at δ1.8 for three protons of CH_3 of thymine residue. This indicated the N1-alkylation of thymine. Further this compound was characterized by ^{13}C, IR and mass spectra (experimental section).

Scheme 6: Synthesis of L-*cis*-(2*S*,4*S*)-*aepone*-PNA Monomer

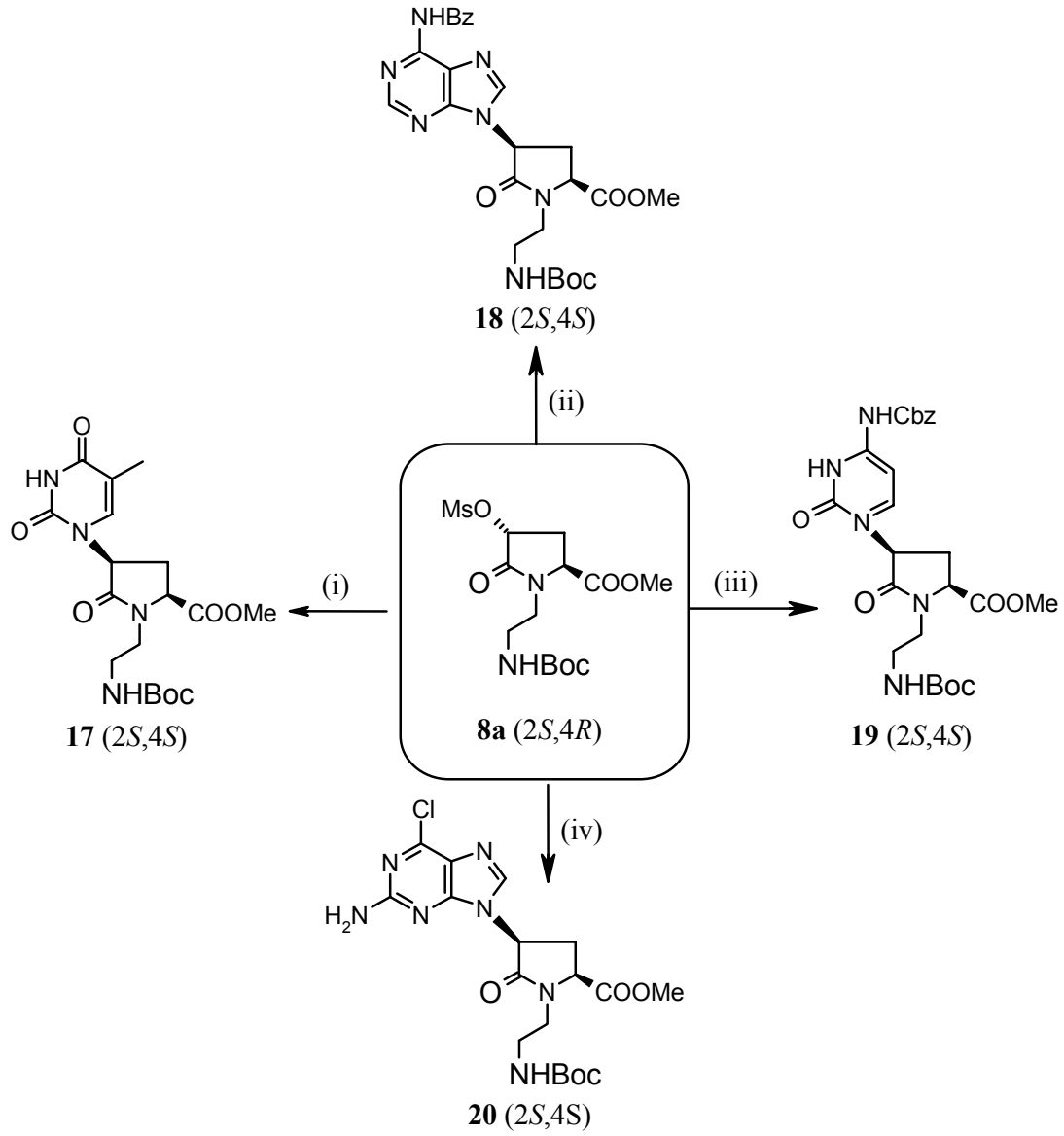

Reagents: (i)Thymine, K_2CO_3, 18-Crown-6 ether, DMF, 70 ^oC; (ii) N^6Bz-Adenine K_2CO_3, 18-Crown-6 ether, DMF, 70 ^oC; (iii) N4cbz-Cytosine, K_2CO_3, 18-Crown-6 ether, DMF, 70 ^oC; (iv) 2-Amino-6-chloro purine, K_2CO_3, 18-Crown-6 ether, DMF, 70 ^oC.

1-*N*-(Boc-aminoethyl)-4*S*-(N^6-benzoyladenin-9-yl)-5-one-2*S*-proline methyl ester (**18**): Condensation of L-*trans*-(2*S*,4*R*)-4-*O*-mesylate **8a** and the exocyclic-amine protected nucleobase N^6-benzoyladenine (**15**) under similar synthetic conditions of compound **17** yielded 1-*N*-(-Boc-aminoethyl)-4*S*-(N^6-benzoyladenin-9-yl)-5-one-2*S*-proline methyl ester

(**18**). The purified product **18** was characterized by ^{1}H-NMR, ^{13}C-NMR, IR and Mass spectral data. In ^{1}H-NMR spectra of **18,** the disappearance of singlet at δ 3.0 of CH_3 of mesylate residue of **8a** and appearance a singlet at δ 8.8, 8.2 due to H-2/8 of adenine residue and multiplet at δ 7.5 for 5H's of phenyl residue of N^{6Bz} adenine supported the structure.

1-*N*-(Boc-aminoethyl)-4*S*-(N^4-benzyloxycarbonylcytosin-1-yl)-5-one-2*S*-proline methyl ester **(19)**: The exocyclic-amine protected cytosine monomer of L-*cis*-(2*S*,4*S*)-*aepone*-PNA **19** was prepared from same intermediate as L-*trans*-(2*S*,4*R*)-4-*O*-mesylate **8a**, used in synthesis of thymine and adenine monomers. The protected nucleobase N^4-benzyloxycarbonylcytosine (**13**) was treated with mesylate derivative **8a** under similar reaction conditions. The reaction proceeded by S_N2 inversion to yield the carbamate protected cytosine monomer of L-*cis*-(2*S*,4*S*)-*aepone*-PNA **19**. The disappearance of singlet of mesylate and appearance of singlet at δ 7.6 due to H6 of cytosine and multiplet at δ 7.5 of phenyl group of benzyloxycarbonylcytosin supported the identity of product.

1-*N*-(Boc-aminoethyl)-4*S*-(2-amino-6-chloropurin-9-yl)-5-one-2*S*-proline methyl ester **(20)**: To complete the synthesis of all four monomers, L-*cis*-(2*S*,4*S*)-*aepone*-PNA and the 2-amino-6-chloropurine derivative **16** were reacted to obtain **20** the precursor of guanine monomer (Scheme 6). The product was characterized by ^{1}H-NMR, in which the singlet of mesylate group of starting material was absent and a singlet at 7.6 (ma) and 7.5 (mi) due to H8 suggested the formation of compound **20.** Detailed Characterization is shown in experimental section.

2.3.4 Synthesis of L-*trans*-(2*S*,4*R*)-aminoethylpyrrolidinone PNA monomers

In order to study the effects of streochemistry at C4 of pyrrolidinone ring in *aepone*-PNA, all four monomers of L-*trans*-(2*S*,4*R*)-*aepone* were synthesized (Scheme 7). To achieve the required 4*R* stereochemistry at C4 in pyrrolidinone ring, two inversions are necessary at C4 of L-*trans*-(2*S*,4*R*)-hydroxyproline derivative **6**. Compounds **8d**, **8e** and **8g** were synthesized with first inversion under Mitsunobu reaction conditions to get L-*cis*-(2*S*,4*S*)-pyrrolidinone derivatives (see in above section). These derivatives were used to prepare the L-*trans*-(2*S*,4*R*)-*aepone* monomers (**23**-**27**) with a second inversion by S_N2 at C4. For this purpose, the compound 1-(*N*-Boc-aminoethyl)–4*S*-hydroxyl-5-one-2*S*-proline methyl ester **21** was prepared by mild *base hydrolysis* of pyrrolidinone derivatives such as **8d**, **8e** and **8g** (Scheme 7) by using K_2CO_3 and MeOH. Further, compound **21** was converted into its L-*cis*-(2*S*,4*S*)-4-O-mesylate derivative **22**, which was used as for synthesis of all monomers of the 4*R* series.

The *4(S)-O*-mesylate derivative **22** was used as a common intermediate for synthesis of L-*trans-aepone*-PNA monomer as shown in Scheme 7. Compound **22** was derived from *1-(N-Boc-aminoethyl)–4S-hydroxyl-5-one-2S-proline methyl ester* **21** in Scheme 7.

Scheme 7: Synthesis of *trans*-(2*S*,4*S*)-*aepone*-PNA monomers

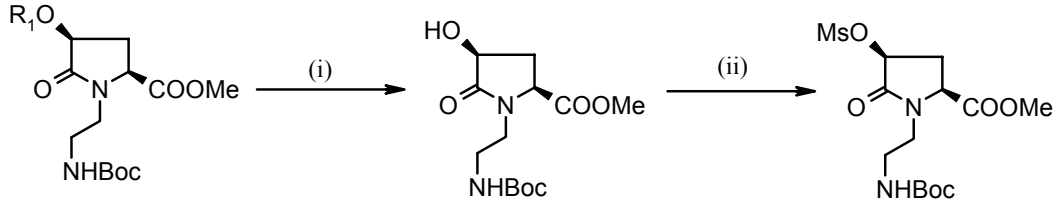

8 (2*S*,4*S*)

8d R1 = OAc
8e R1 = OBz
8g R1 = OPNB

21 (2*S*,4*S*)

22 (2*S*,4*S*)

Reagents: (i) K_2CO_3, dry MeOH, 30 min, 60%; (ii) $MeSO_2Cl$/ Et_3N/DCM, 1hr, 85%.

1-*N*-(Boc-aminoethyl)-4*R*-(thymin-1-yl)-5-one-2*S*-proline methyl ester **(23)**: The L-*cis*-(2*S*,4*S*)-4-*O*-mesylate **22** was coupled with thymine (**9**) to obtain L-*trans*-(2*S*,4*R*)-*aepone*-PNA thymine monomer **23** in presence of inorganic base K_2CO_3 and a catalytic amount of 18-crown-6 following the same procedure as for compound **17**. The appearance of singlet at δ 1.9 and absence of singlet from δ 3.0 in ^{1}H-NMR indicated the formation of desired

Scheme 8: Synthesis of *trans*-(2*S*,4*S*)-*aepone*-PNA monomers

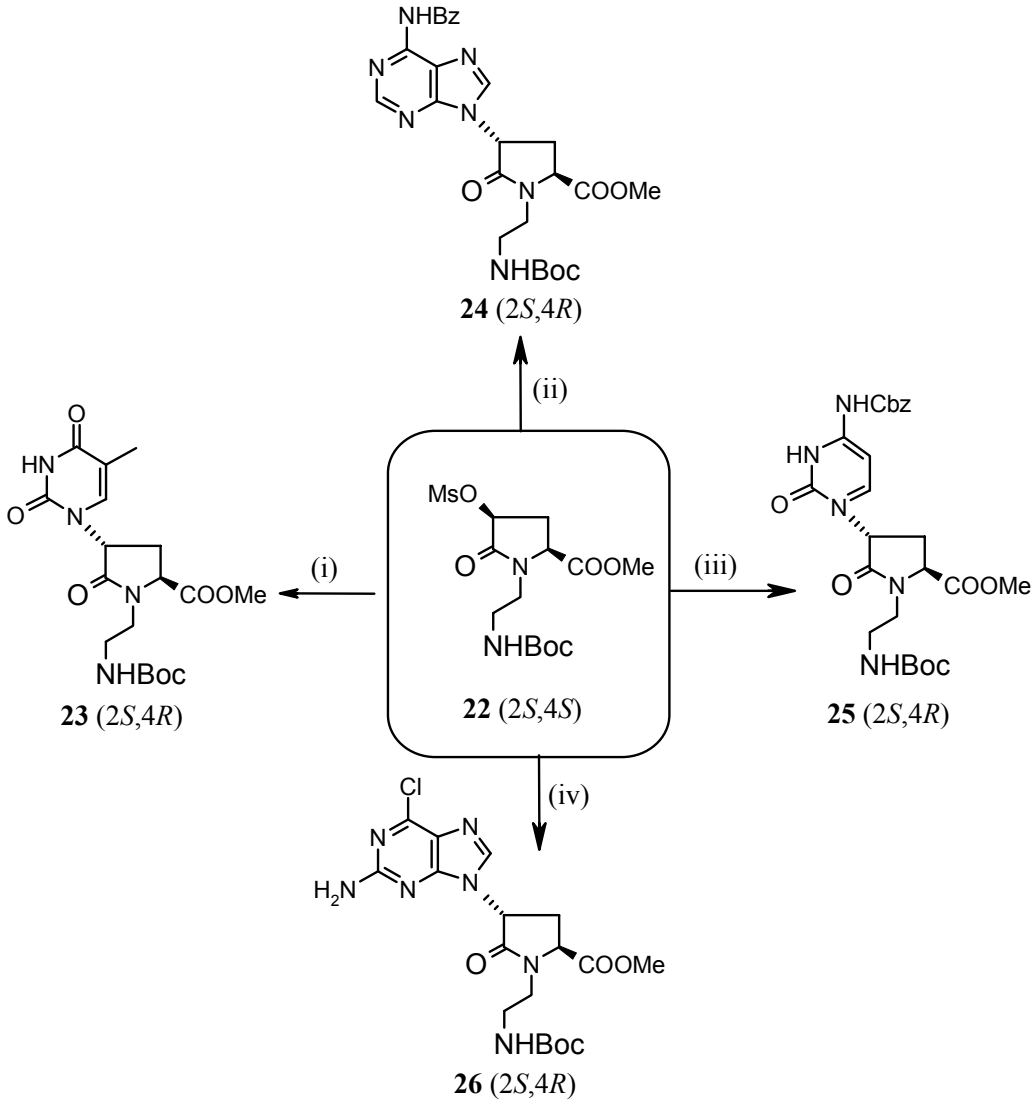

Reagents: (i)Thymine, K_2CO_3, 18-Crown-6 ether, DMF, 70 °C; (ii) N^6Bz-Adenine K_2CO_3, 18-Crown-6 ether, DMF, 70 °C; (iii) N4cbz-Cytosine, K_2CO_3, 18-Crown-6 ether, DMF, 70 °C; (iv) 2-Amino-6-chloro purine, K_2CO_3, 18-Crown-6 ether, DMF, 70 °C.

product **23** (Scheme 8).

1-*N*-(Boc-aminoethyl)-4*R*-(N^6-benzoyladenin-9-yl)-5-one-2*S*-proline methyls ester **(24)**: Compound **22** upon coupling with N-benzoyl protected adenine (**15**) using K_2CO_3 and catalyst 18-crown-6 in DMF gave the required L-*trans*-(2*S*,4*R*)-*aepone*-PNA monomer **24**. In ^{1}H-NMR spectra of **24,** absence of singlet at δ 3.0 of $C\underline{H}_3$ of mesylate and appearence singlets at δ 8.8, 8.2 due to H2/8 of adenine and a multiplet at δ 7.5 for 5H's phenyl residue of N^{6Bz}adeninme confirmed the identity of **24** (Scheme 8).

1-(N-boc-aminoethyl)-4*R*-(N^4-benzyloxycarbonylcytosin-1-yl)-5-one-2*S*-proline methyl ester **(25)**: The N-protected cytosine monomer L-*trans*-(2*S*,4*R*)-*aepone*-PNA was synthesized by a similar coupling of the 4-*O*-mesylate intermediate **22** with N^4-protected cytosine (**13**) in presence of K_2CO_3 and catalytic amount of 18-crown-6 in DMF. The absence of singlet due to CH_3 of mesylate at δ 3.0 and appearance of singlet at δ 7.6 of cytosine residue due to H6 and multiplet at δ 7.5 of phenyl group of benzyloxycarbonylcytosin supported the formation of product (Scheme 8).

1-*N*-(Boc-aminoethyl)-4*R*-(2-amino-6-chloropurin-9-yl)-5-one-2*S*-proline methyl ester **(26)**: The precursor for guanine nucleobase, 2-amino-6-chloropurine (**16**), was used to synthesize1-(N-boc-aminoethyl)-4*R*-(2-amino-6-chloropurin-9-yl)-5-one-2*S*-proline methyl ester **26** by coupling with **22** (Scheme 8). The newly prepared compound was characterized by ^{1}H-NMR, in which singlet due to CH_3 of mesylate was absent and the presence of singlets at 7.6 (ma) and 7.5 (mi) supported the formation of desired compound **26.**

2.3.5 Synthesis of L-*trans*-(2*S*,4*R*)-aminoethylprolyl (*aep*) PNA monomers

The synthesis of L-*trans*-(2*S*,4*R*)-*aep*-PNA (**25** and **27-29**) was carried out by starting L-*cis*-(2*S*,4*S*) C4 substituted prolyl derivatives **7d**, **7e** and **7g** (Scheme 9). To

achieve the synthesis of the four A/T/G/C monomers of L-*trans*-(2*S*,4*R*)-*aep*-PNA the hydrolysis of compound **7d**, **7e** and **7g** with mild K_2CO_3 or NaOH, then inversion at C4 from 4*R* to 4*S* in prolyl ring of their hydrolysed product **27** were needed (Scheme 9).

1-*N*-(Boc-aminoethyl)-4*R*-(N3-benzoylthymin-1-yl)-2*S*-proline methyl ester **(28)**:[45] The N3-benzoyl protected thymine *aep*PNA monomer **28** (Scheme 9) was synthesized under Mitsunobu condition by inversion at C4 of compound **27** in presence of Ph_3P and DIAD to obtain the desired product **28** in good yield. Compound **28** was characterized by ^{1}H-NMR and ^{13}C-NMR spectra (see in experimental section).

Scheme 9. Synthesis of L-trans (2*S*,4*R*)-*aep*-PNA Monomers

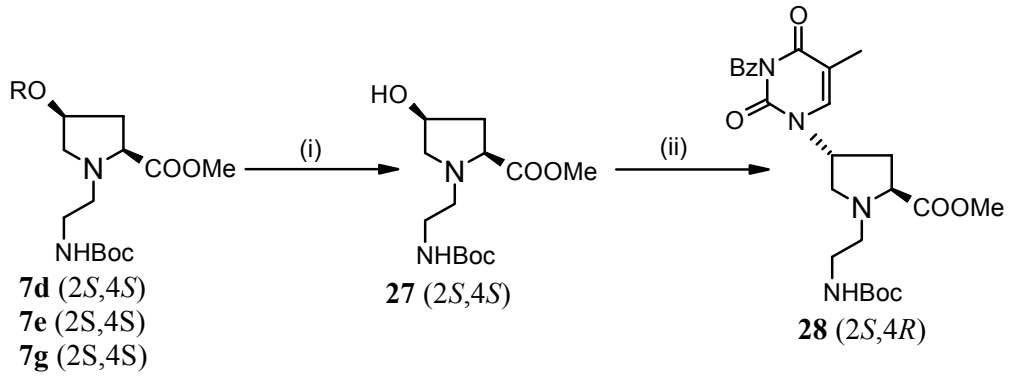

7d (2*S*,4*S*)
7e (2S,4S)
7g (2S,4S)

27 (2*S*,4*S*)

28 (2*S*,4*R*)

(i) NaOMe, dry MeOH; K_2CO_3, dry MeOH or 1% NaOH in MeOH, 50%; (ii) N^3BzPh_3P, DIAD, **27,** THF**,** 0 ^{o}C-rt, overnight, 65%

1-*N*-(Boc-aminoethyl)–4*R*-*O*-mesyl-2*S*-proline methyl ester **(29)**: L-*cis*-(2*S*,4*S*)-4-*O*-mesyl derivative **29** was prepared from **27** (Scheme 10) using mesyl chloride and Et_3N in DCM at The compound **29** was characterized by ^{1}H-NMR by appearance of singlet at δ 3.0. This intermediate was used for synthesis of adenine, cytosine and 2-amino-6-chloropurine (precursor of guanine monomer) monomer of L-*trans*-(2*S*,4*R*)-*aep*-PNA. The spectral data for characterization are given in experimental section.

1-*N*-(Boc-aminoethyl)-4*R*-(N^6-benzoyladenin-9-yl)-2*S*-proline methyl ester **(30)** was The prepared by N9-alkylation of protected adenine derivative **15** with L-*cis*-(2*S*,4*S*)-4-*O*-mesyl derivative **29** using K_2CO_3 and catalytic amount of 18-crown-6**.** The reaction proceeds by inversion at C4 from 4*S* into 4*R* (Scheme 10). The product **30** was characterized by spectral data as given in experimental section.

Scheme 10: Synthesis of L-trans (2*S*,4*R*)-*aep*-PNA Monomers

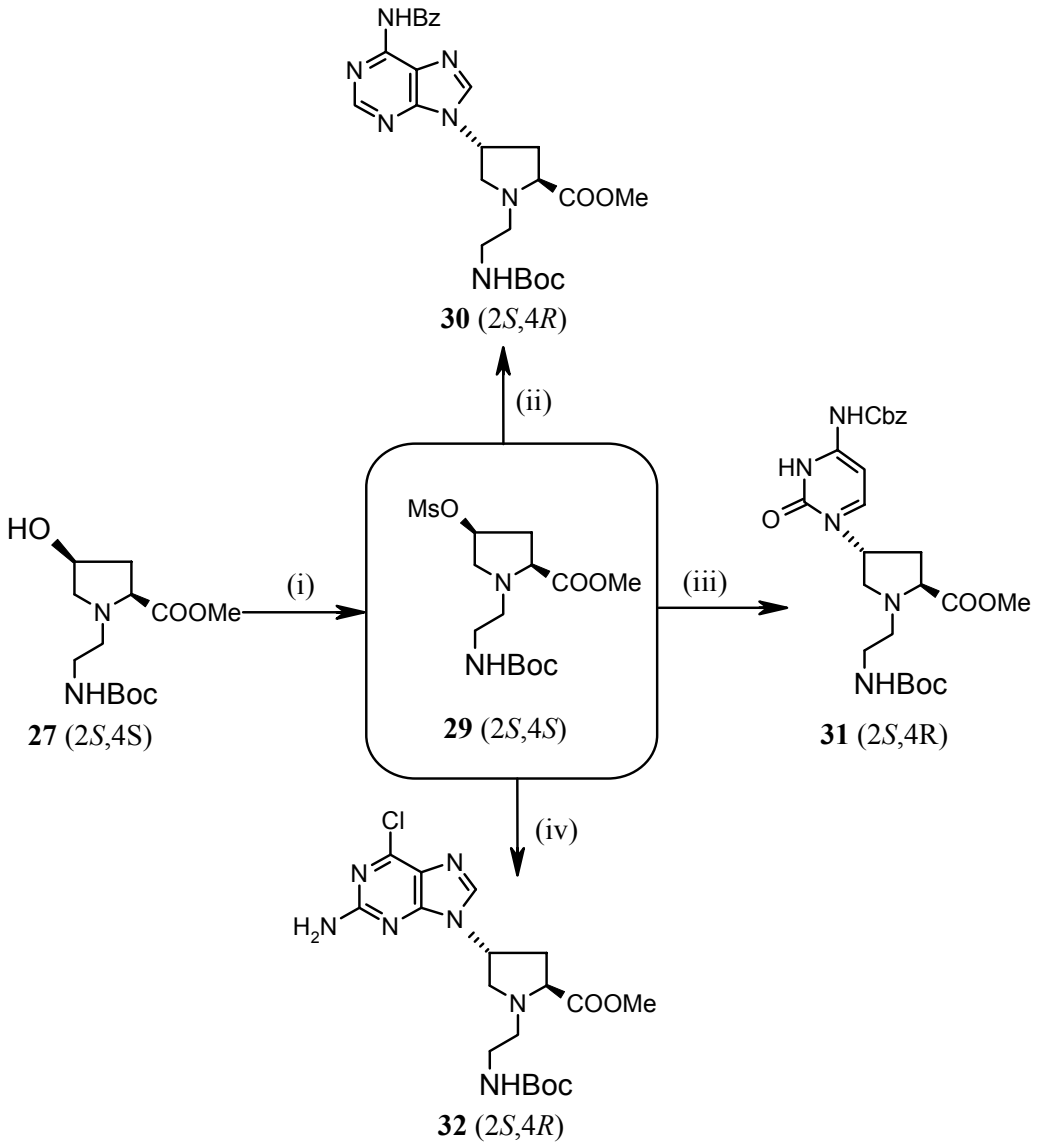

Reagents: (i) $MeSO_2Cl$/ Et_3N/DCM (ii) N^6Bz-Adenine K_2CO_3, 18-Crown-6 ether, DMF, 70 °C; (iii) N^4cbz-Cytosine, K_2CO_3, 18-Crown-6 ether, DMF, 70 °C; (iv) 2-Amino-6-chloro purine, K_2CO_3, 18-Crown-6 ether, DMF, 70 °C.

1-*N*-(Boc-aminoethyl)-4*R*-(N^4-benzyloxycarbonylcytosin-1-yl)-2*S*-proline methyl ester **(31)** was prepared from 4-*O*-mesylate intermediate **29** by coupling with N^4-carboxybenzylcytosine (**13**) in presence of anhydrous K_2CO_3 and a catalytic amount of 18-crown-6 in DMF. It was characterized by spectral data as given in experimental section (Scheme 10) .

1-*N*-(Boc-aminoethyl)-4*R*-(2-amino-6-chloropurin-9-yl)-2*S*-proline methyl ester **(32)**: The precursor of guanine nucleobase, L-*trans*-(2*S*,4*R*)-*aep*-2-amino-6-chloropurine PNA monomer was prepared with coupling between intermediate **29** and 2-amino-6-chloropurine (**16**) under similar synthesis condition **17**. Characterized spectral data of **32** are given in experimental section. (Scheme 10).

2.3.6 Synthesis of L-*cis*-(2*S*,4*S*)-aminoethylprolyl PNA monomers

The synthesis all four monomers of L-*cis*-(2*S*,4*S*)-*aep*-PNA were done for (i) use as control for biophysical study of *aepone*-PNA monomer and (ii) to find the ring conformation of prolyl ring in their monmer as these exhibited strong binding with DNA. Their synthetic outline is given Schemes 11 and 12.

Scheme 11: Synthesis of L-*cis*-(2*S*,4*S*)-*aep*-PNA Monomers

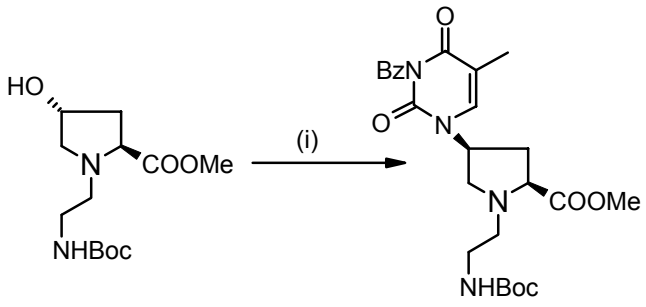

6 (2*S*,4*R*) **33** (2*S*,4*S*)

Reagents: (i) N3-benzoylthymine (**11**),Ph_3P, DIAD, THF**,** 0 ^oC-rt, overnight, 65%

1-*N*-(Boc-aminoethyl)-4*S*-(N3-benzoylthymin-1-yl)-2*S*-proline **(33)** was achieved starting from compound **6** (Scheme 11) by reported procedure,[25] starting from compound **6** which was subjected to Mitsunobu reaction conditions involvi,ng N3-benzoylthymine (**11**) as the incoming nucleophile. This reaction proceeds with inversion of stereochemistry at the C4 to yield the 4(*S*) product.

1-*N*-(Boc-aminoethyl)-4*S*-(N^6-benzoyladenin-9-yl)-2*S*-proline methyl ester **(34)** was prepared by coupling between 4-*O*-mesyl derivative (**7a**) and N^6-benzoyladenine **15** (Scheme 12) under reaction conditions similar to the compound **17**.

Scheme 12: Synthesis of L-*cis*-(2*S*,4*S*)-*aep*-PNA Monomers

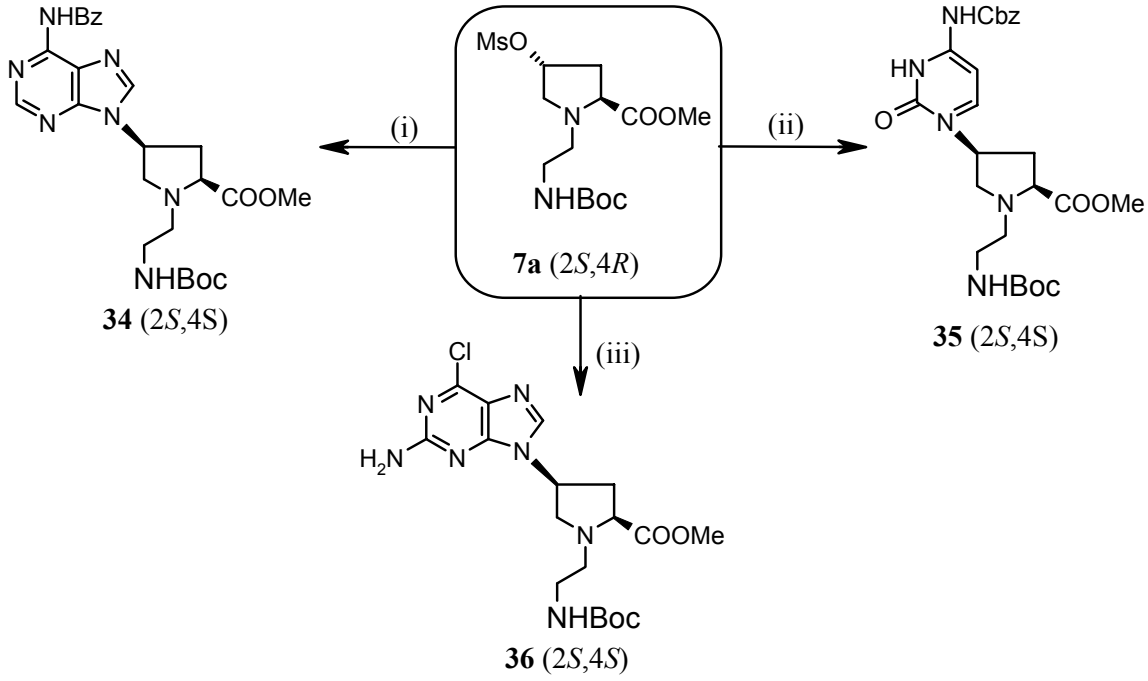

Reagents: (i) N^6Bz-Adenine K_2CO_3, 18-Crown-6 ether, DMF, 70 °C; (ii) N^4cbz-Cytosine, K_2CO_3, 18-Crown-6 ether, DMF, 70 °C; (iii) 2-Amino-6-chloro purine, K_2CO_3, 18-Crown-6 ether, DMF, 70 °C.

1-*N*-(Boc-aminoethyl)-4*S*-(N^4-benzyloxycarbonylcytosin-1-yl)-2*S*-proline methyl ester **(35)** synthesis was achieved in Scheme 12 in four steps. The compound (**7a**) was stirred with N^4-benzyloxycarbonyl cytosine, K_2CO_3 and a catalytic amount of 18-crown-6 in DMF to obtain (**35**).

1-*N*-(Boc-aminoethyl)-4*S*-(2-amino-6-chloropurin-9-yl)-2*S*-proline methyl ester **(36)** was synthesized from 4-*O*-mesylate intermediate **7a** by coupling with 2-amino-6-chloropurine (**16**) (Scheme 12).

2.3.7 Hydrolysis of methyl esters of *aep*/*aepone*-PNA monomers

2.3.7a Hydrolysis of aepone-PNA methyl esters

Solid phase synthesis of *aep/aepone*-PNA requires N-protected free carboxylic acids. To obtain these, the methyl ester groups of the *aep/aepone*-PNA monomers were subjected to saponification by sodium hydroxide in a water-methanol mixture to yield the corresponding carboxylic acids (Scheme 13).

Scheme 13: Hydrolysis of *aep*-PNA monomer

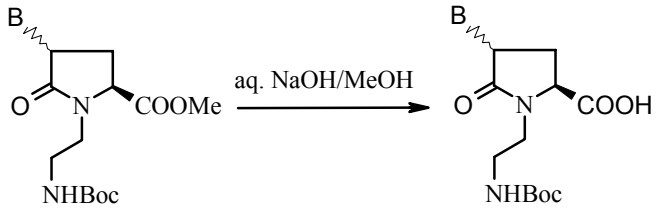

(2*S*,4*S*/*R*) (2*S*,4*S*/*R*)

(2*S*,4*S*)

20 B = Thymine(T)
21 B = N^{6Bz}Adenine(A^{Bz})
22 B = N^{4CBz}Cytosine(C^{CBz})
23 B = 2-amino-6-chloropurine

(2*S*,4*S*)

37 B = Thymine(T)
38 B = N^{6Bz}Adenine(A^{Bz})
39 B = N^{4CBz}Cytosine(C^{CBz})
40 B = Guanine (G)

(2S,4*R*)

26 B = Thymine(T)
27 B = N^{6Bz}Adenine(A^{Bz})
28 B = N^{4CBz}Cytosine(C^{CBz})
29 B = 2-amino-6-chloropurine

(2*S*,4*R*)

41 B = Thymine(T)
42 B = N^{6Bz}Adenine(A^{Bz})
43 B = N^{4CBz}Cytosine(C^{CBz})
44 B = Guanine (G)

1-*N*-(Boc-aminoethyl)-*4S/R*-(thymin-1-yl)-5-one-2*S*-proline carboxylic acid **(37,,41):** The hydrolysis of the methyl ester of thymine in 1-(*N*-Boc-aminoethyl)-4*S/R*-(thymin-1-yl)-5-one-2*S*-proline methyl ester (**17/23**) was achieved by treatment with 1N NaOH in methanol: water, (1:1) for 10 min. Neutralization of the excess alkali with Dowex 50 H^+ and work-up gave 1-(*N*-Boc-aminoethyl)-4*S/R*-(thymin-1-yl)-pyrrolidin-5-one-2*S*-carboxylic acids (**37, 41**) in quantitative yield.

Similarly, 1-(*N*-Boc-aminoethyl)-4*S/R*-(N^6-benzoyladenin-9-yl)-5-one-2*S*-proline methyl esters (1**8,24**) were hydrolyzed to obtain the their respective carboxylic acids **(35, 39)**. By following the same ester hydrolysis procedure, compounds1-(*N*-Boc-aminoethyl)-4*S/R*-(*N*^{4}-benzyloxycarbonylcytosin-1-yl)-5-one-2*S*-proline methyl esters (**19,25**) was hydrolyzed to give their acid compounds 1-*N*-(Boc-aminoethyl)-4*S*-(N^4-benzyloxycarbonylcytosin-1-yl)-5-one-2*S*-proline carboxylic acid **(39, 43).**

1-*N*-(Boc-aminoethyl)-4(*S/R*)-guanin-9-yl)-5-one-2*S*-proline carboxylic acid **(40, 44)**: 1-(*N*-Boc-aminoethyl)-4(*S*)-(2-amino-6-chloropurin-9-yl)-5-one 2(*S*/*R*)-proline methyl esters (**20,26**) upon treatment with NaOH in aqueous methanol, initially underwent ester hydrolysis within 10 min., followed by conversion of the 6-chloro function to the 6-oxo function. The oxidation reaction was complete after 24 h for the (2*R*,4*S*) isomer, while the (2*S*,4*S*) isomer required 72 h. The transformation of the nucleobase from 2-amino-6-chloropurine to guanine, i.e., 2-amino-6-oxopurine, was unambiguously confirmed by the UV spectra (Figure 11) in which the 2-amino-6-chloropurine derivative **20/26** exhibited a characteristic peak ~310nm, that was absent in the guanine derivative **40/44**. The guanine derivative **40**, on the other hand, sported a peak at ~280 nm, that was absent in the precursor, 2-amino-6-chloropurine derivative **20**. The conversion was also evident from the appearance of a carbonyl resonance at δ 167.8 in the ^{13}C NMR spectrum in the guanine monomer, which was absent in the 2-amino-6-chloropurine monomer.

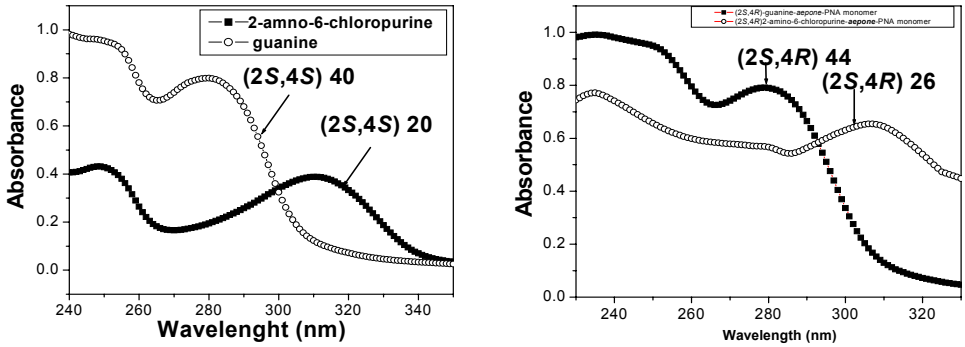

Figure 11: UV-spectra of L-*cis*-(2*S*,4*S*)-aminoethylpyrrolidine guanine monomer **17** and L-*cis*-(2*S*,4*R*)-aminoethylpyrrolidine guanine monomer **37**

2.3.7b Hydrolysis of aep-PNA methyl esters

1-*N*-(-Boc-aminoethyl)-4*S*-(thymin-1-yl)-2*R*-proline carboxylic acid (45, 49): The hydrolysis of the methyl ester and the N3-benzoyl group of thymine in 1-(*N*-Boc-aminoethyl)-4(*S*)-(thymin-1-yl)-2(*S*/*R*)-proline methyl esters (**28, 33**) were achieved similarly by treatment with 1N NaOH in methanol: water, (1:1) for 10 min. The cleavage of the N-benzoyl group was complete only after 9 h to give 1-(*N*-Boc-aminoethyl)-4(*S*)-(thymin-1-yl)-pyrrolidine-2*S*/*R*-carboxylic acid (**45, 49**) in quantitative yields (Scheme 14).

Scheme 14: Hydrolysis of *aep*-PNA monomer

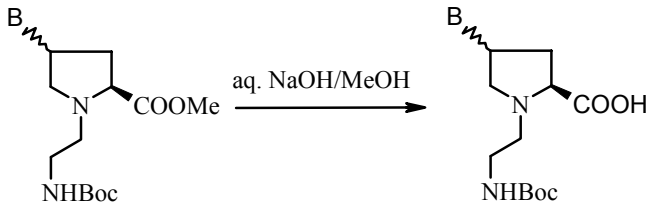

(2S,4S/R) (2S,4S/R)

(2S,4R)	(2S,4R)
28 B = N3-BzThymine(T)	45 B = Thymine(T)
30 B = N6BzAdenine(ABz)	46 B = N6BzAdenine(ABz)
31 B = N4CBzCytosine(CCbz)	47 B = N4CBzCytosine(CCBz)
32 B = 2-amino-6-chloropurine	48 B = Guanine (G)
(2S,4S)	**(2S,4S)**
33 B = N3-BzThymine(T)	49 B = Thymine(T)
34 B = N6BzAdenine(ABz)	50 B = N6BzAdenine(ABz)
35 B = N4CBzCytosine(CCbz)	51 B = N4CBzCytosine(CCBz)
36 B = 2-amino-6-chloropurine	52 B = Guanine (G)

The methyl ester of 1-*N*-(Boc-aminoethyl)-4(*S*)-(N^6-benzoyladenin-9-yl)-5-one 2(*S*/*R*)-proline methyl esters (**30, 34**) was hydrolyzed similarly to 1-*N*-(Boc-aminoethyl)-4*S/R*-(N^6-benzoyladenin-9-yl)-2*R/S*-proline carboxylic acid **(46, 50):**

The methyl ester in 1-(*N*-Boc-aminoethyl)-4(*S*)-(N^4-benzyloxycarbonylcytosin-1-yl)-5-one-2(*S*/*R*)-proline methyl ester (**31/35**) was also hydrolyzed by same procedure of to obtain acids 1-*N*-(Boc-aminoethyl)-4S/*R*-(N^4-benzyloxycarbonylcytosin-1-yl)-2*R*-proline carboxylic acid as **47, 51.**

1-*N*-(Boc-aminoethyl)-4*S*-(2-amino-6-chloropurin-9-yl)-2*R/S*-proline methyl ester **(45, 49)** was obtained from 1-(*N*-Boc-aminoethyl)-4*S*/R-(2-amino-6-chloropurin-9-yl)-5-one-2*S*-proline methyl ester (**32/36**) from a similar hydrolysis procedure.

2.3.8 Synthesis of aminoethylglycyl (*aeg*) PNA monomers

The sequential addition of *aep*PNA monomers into *aeg*PNA oligomers was carried to enable study of their effect on the binding properties of PNA. For this purpose, the synthesis of unmodified *aeg*PNA monomers is necessary and was carried out according to the literature procedures.[54]

The synthesis was carried out starting from the easily available 1,2-diaminoethane (**53**) (Scheme 15). This was treated with Boc-azide to give the mono-protected derivative **54**, using a large excess of 1,2-diaminoethane over the Boc-anhydride in high dilution conditions. The di-Boc derivative obtained in very small amounts (< 5%) being insoluble in water, could be removed by filtration. The *N*1-Boc-1,2-diaminoethane was then *N*-alkylated using ethylbromoacetate and KF-Celite in dry acetonitrile. The use of KF-Celite was found to be advantageous over K_2CO_3 both, in terms of the yield of the product, as well as the ease of work-up. Upon completion of the reaction, the KF-Celite was filtered off and the product isolated in the crude form after concentration of the filtrate. The

aminoethylglycine **55** obtained was further treated with chloroacetyl chloride[55] to yield the corresponding chloro derivative **56** in good yield, using Na_2CO_3 in aqueous dioxane as the base. The ethyl *N*-(Boc-aminoethyl)-*N*-(chloroacetyl)-glycinate (**56**) was used as a common intermediate in the preparation of all the PNA monomers.

Scheme 15: Synthesis of *aeg*-PNA Monomers

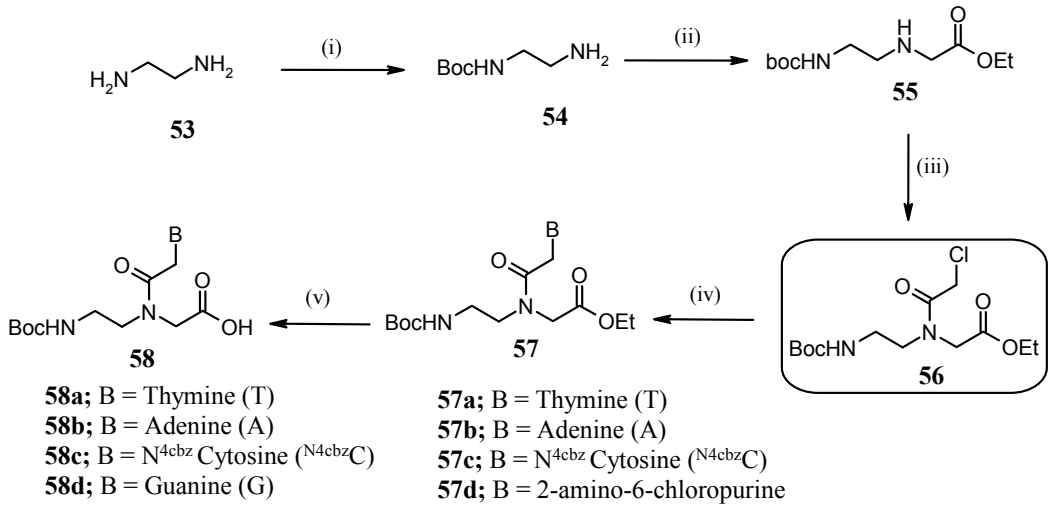

58a; B = Thymine (T)
58b; B = Adenine (A)
58c; B = N^{4cbz} Cytosine (^{N4cbz}C)
58d; B = Guanine (G)

57a; B = Thymine (T)
57b; B = Adenine (A)
57c; B = N^{4cbz} Cytosine (^{N4cbz}C)
57d; B = 2-amino-6-chloropurine

Reagents: (i) $(Boc)_2O$, THF, 0-25 ^oC, THF, 24 h, 85%; (ii) $BrCH_2COOEt$, KF-celite, CH_3CN, rt, 8 h, 80%; (iii) $ClCH_2COCl$, Na_2CO_3, Dioxane:Water (1:1), rt, 30min., 85%; (iv) a. Thymine, K_2CO_3, CH_3CN, rt, 12 h, 75%; b. Adenine, NaH, DMF, 75 ^0C, 10 h, 65%, c. Cytosine^{cbz}, NaH, DMF, 75 ^oC, O.N., 50%; c. 2-amino-6-chloropurine, NaH, DMF, 75 ^0C, 12 h, 70%.

The alkylation of ethyl *N*-(Boc-aminoethyl)-*N*-(chloroacetyl)-glycinate with thymine and cytosine is regiospecific. Thymine was reacted with ethyl *N*-(Boc-aminoethyl)-*N*-(chloroacetyl)-glycinate using K_2CO_3 as a base to obtain the *N*-(Boc-aminoethylglycyl)-thymine ethyl ester **(57a)** in high yield. Although adenine is known to undergo both N7- and N9-substitution, N7-alkylation was not observed when NaH was used as the base. It reacted with adenine forming sodium adenylide, which was then reacted with ethyl *N*-(Boc-aminoethyl)-*N*-(chloroacetyl)-glycinate to obtain *N*-(Boc-aminoethylglycyl)-adenine ethyl ester (**57b**) in moderate yield. In the case of cytosine, the N^4-amino group was protected as its benzyloxycarbonyl derivative, and used for alkylation

employing NaH as the base to provide the N1-substituted product (**57c**). The alkylation of 2-amino-6-chloropurine with ethyl *N*-(Boc-aminoethyl)-*N*-(chloroacetyl)-glycinate was facile with K_2CO_3 as the base and yielded the corresponding *N*-(Boc-aminoethylglycyl)-(2-amino-6-chloropurine)-ethyl ester (**57d**) in excellent yield. All compounds exhibited ^1H and ^{13}C NMR spectra consistent with the reported data. The ethyl esters were hydrolyzed in the presence of NaOH to give the corresponding acids (**58a-58d**), which were used for solid phase synthesis. The need for the exocyclic amino groups of adenine and guanine to be protected was eliminated, as these were found to be unreactive under the conditions used for peptide coupling.

2.4 CONCLUSIONS

In summary, this Chapter demonstrates that the endocyclic methylene group at C5 of pyrrolidine derivatives is more susceptible to oxidation with $RuCl_3/NaIO_4$ than the other two exocyclic methylene groups α to nitrogen heteroatom. These derivatives have been used for the synthesis of (2*S*,4*S/R*)-*aepone*-PNA T/A/G/C monomers as new PNA analogues and it useful for synthesis of *N*-alkylated pyrrolidinones and unnatural amino acids. The synthesis of other diastereomer (2*S*,4*R*) of *aep*-PNA T/A/G/C monomers are also demonstrated for comparison study of *aepone*-PNA:DNA binding.

The next Chapter describes the biophysical studies (UV, CD and gel retardation assays of *aepone/aep*-PNA:DNA hybrids.

2.5 EXPERIMENTAL

2.5.1 General

Analytical grade chemicals were used in all reactions. All solvents used were purified according to the literature procedure. All reactions were monitored for completion by TLC. Usual workup implies sequential washing of the organic extract with water and brine followed by drying over sodium sulphate and evaporation under high vacuum. Column chromatography was performed for purification of compounds on silica gel (100-200 mesh). TLC was carried out on pre-coated silica gel GF_{254} aluminium sheets (Merck 5554, Spectrochem/LOBA chemie) using in organic solvents ethyl acetate/petroleum ether or dichloromethane/MeOH. Free acids were chromatographed on TLC using solvent system isopropyl alcohol: acetic acid: water in proportion (9:1:1). The compounds were visualized with UV light and /or by spraying with ninhydrin reagent subsequent to Boc-deprotection (exposing to HCL vapors) and heating.

^{1}H (200/300/500 MHz) and ^{13}C (50/75/125 MHz) NMR spectra were recorded on a Bruker ACF 200 or MSL 300 spectrometers fitted with an aspect 3000 computer and all chemical shifts are referred in δ (ppm) scale. For compounds that bear a tertiary amide group, splitting of NMR signal was observed due to the presence of rotamers. In such cases the major isomer is designed as ‘maj’ and minor isomer, ‘min’. Optical rotations were measured on ADP-polarimeter and CD spectra were recorded on a JASCO J715 spectrometer. Mass spectra were recorded on Finnigan-Matt mass spectrometer (ABI), ESI- spectrometer while MALDI-TOF spectra were obtained from KRATOS PCK compact instrument.

2.5.2 Procedures and spectral data

***N*-Boc-2-aminoethanol (2)**: To a cooled, stirred solution of 2-aminoethanol **1** (6.6 mL, 98.0 mmol) and Et_3N (11.1 mL, 164.0 mmol) in water-dioxane (1:1), was added drop-wise *t*-Boc anhydride (12 mL, 0.54mol). The reaction was stirred at room temperature overnight. The dioxane was then removed under vacuum, and the water layer extracted several times with ethyl acetate. The organic layer was dried over sodium sulphate and then, evaporated to dryness under vacuum to get the product 2-*N*-Boc-aminoethanol **2** (8.0 g, 90.1% yield), which was used in further steps without purification.

Compound	Spectral Data
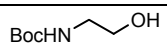 **2**	^{1}H NMR ($CDCl_3$): δ 4.93 (bs, 1H), 4.10(t, 2H), 3.36 (m, 2H), 1.47 (s, 9H)

2-*N*-Boc-1-*O*-mesylate aminoethanol (3): To an ice-cooled solution of 2-*N*-Boc-aminoethanol **2** (9 g, 55.9 mmol) and in dry DCM and Et_3N (11.3 mL, 111.8 mmol), was added dropwise methansulphonyl chloride (5.6 mL, 72.6 mmol) over 10-15 min. After 30 min. solvent was evaporated and the product immediately purified by silica gel column chromatography to get 2-*N*-Boc-aminoethymesylate **3.**

Compound	Spectral Data
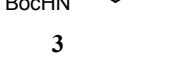 **3**	**^{1}H NMR ($CDCl_3$):** δ 5.0 (bs, 1H), 4.3 (t, 2H, J = 5.0 Hz), 3.45 (m, 2H), 3.0 (s, 3H), 1.43 (s, 9H)

1-*N*-(Boc-aminoethyl)-4*R*-hydroxy-2*S*-proline methyl ester (6): A mixture of 4-(*R*)-hydroxy-2-(*S*)-proline methyl ester hydrochloride **5** (3.24 g, 17.9 mmol), 2-(*N*-Boc)-aminoethy mesylate **3** (2.0 g, 8.9 mmol) and anhydrous potassium carbonate (3.69 g, 26.7 mmol) were stirred together in DMF: acetonitrile (1:1) at room temperature for 72 h under argon atmosphere. After completion of reaction as indicated by TLC, solvents were removed *in vacuo*. The residue was taken in water and extracted with ethyl acetate (4x 30

mL). The organic layer was dried over sodium sulphate and concentrated to get the crude product, which was purified by silica gel column chromatography. The pure product **3** was obtained in 56% yield.

Compound	Spectral Data
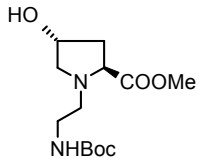 **6** (2*S*,4*R*)	**^{1}H NMR 200 MHz ($CDCl_3$)** δ: 5.30(br s, 1H, NH), 4.40 (m, 1H, H4), 3.70 (s, 3H, OC$\underline{H}_3$), 3.50 (t, 1H, H5), 3.38 (dd, 1H, H5'), 3.10 (dd, 2H, Boc-NH-C$\underline{H}_2$), 2.70 (br m, 4H, H2, Boc-NH-CH_2-C$\underline{H}_2$, OH), 2.50 (dd, 1H, H3), 2.10 (m, 1H, H3'), 1.40 (s, 9H, C(C$\underline{H}_3$)$_3$).

1-*N*-(Boc-aminoethyl)–4*R*-*O*-mesyl-proline methyl ester (7a): Compond **6** (1.7 g, 5.9 mmol) was dried by evaporation from CH_3CN/CH_2Cl_2 (1:1) and then redissolved in CH_2Cl_2. Et_3N (1.8 mL, 17.7 mmol) and methansulfonyl chloride (0.9 mL, 7.60 mmol) were added at 0 ^oC and stirred for 2 h. The reaction mixture was quenched by addition of half saturated aqueous $NaHCO_3$ (30 mL) and CH_2Cl_2. The aqueous phase was extracted with CH_2Cl_2 (3 x). The organic extract was dried over Na_2SO_4 and evaporated in vacuo to give 2.5 g of crude product which was purified by chromatography to obtain **7a** as clear oil. Yield: 1.7 g (68 %), Reported in *aep*-PNA.

Compound	Spectral Data
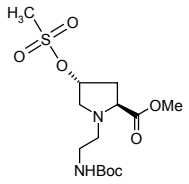 **7a**	**^{1}H NMR 200 MHz ($CDCl_3$)** δ 5.2 (m, 1H), 5.1 (bs, 1H), 3.7 (s, 3H), 3.6 (t, 1H), 3.5 (dd, 1H), 3.4 (m, 2H), 3.2 (m, 2H), 3.0 (s, 3H), 2.8 (dd, 1H), 2.8-2.6 (m, 2H), 2.4-2.2 (m, 2H). 1,4 (s, 9H). **^{13}C NMR 50 MHz:** δ 173.8, 156.9, 79.1, 58.4, 53.5, 51.9, 39.1, 38.4, 36.7, 28.4

1-*N*-(Boc-aminoethyl)–4*R*-*O*-mesyl-5-one-2*S*-proline methyl ester (8a): To a vigorous stirred solution of compound **7a** (380 mg, 0.95 mmol) in 10 mL of CH_3CN and CCl_4 (1:1) an aqueous solution (10 mL) of $NaIO_4$ (2.0 g, 9.08 mmole) and $RuCl_3.xH_2O$ (catalytic

amount, 0.02 mmol) was added. After 30 min, the reaction was quenched by addition of isopropyl alcohol or 20% of aqueous solution (10 mL) of $NaHSO_3$ and stirred for another 20 min and the reaction mixture was concentrated under vacuum. The residue was taken into ethyl acetate (20 mL) and washed with water, the organic extract dried over Na_2SO_4 and concentrated to dryness. The resultant product was purified by column chromatography to obtain **8a** as solid. Yield: 177 mg (45%). This reaction was also carried out in AcOEt and water (1:1) to obtain **8a** with almost same yield (45%). Compound **8a** was also synthesized oxidation of compound **7a** using same oxidizing agent and procedure but organic solvent was used EtOAc instead of CH_3CN and CCl_4. **8a** was crystallized in CH_2Cl_2 and MeOH. Yield (49%).

Compound	Molecular Chrecterization
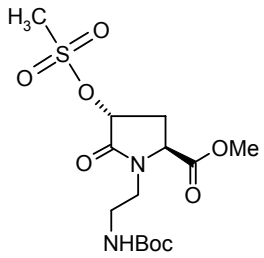 **8a**	**$[\alpha]^{30}_D$** +80.8 (c 0.47, $CHCl_3$) **IR ν_{max} (cm^{-1})**:1747.39, 1731.96, 1714.6, 1693.38, 1681.81. **^{1}H NMR $CDCl_3$**: δ 5.3 (dd, J = 5.6, J = 5.4, 1H), 4.8 (bs, 1H), 4.5 (m, 1H), 3.9 (s, 3H), 3.8 (m, 1H), 3.4 (s, 3H), 3.2 (m, 2H), 3.1 (m, 2H), 2.8 (m, 1H), 1.4 (s, 9H). **^{13}C NMR:** δ 170.8, 169.4, 155.8, 79.3, 75.5, 56.3, 52.6, 42.9, 39.3, 37.4, 30.0, 28.1. **Mass (m/z):** 380.42 (calculated); M^+ = 380 (observed) **Molecular formula:** $C_{14}H_{24}N_2O_8S$ **Analysis**: C 44.20%, H 6.36%, N 7.36%, O 33.65%, S 8.43%.(calculated) C 44.00%, H 6.56%, N 7.30%, O 33.71%, S 8.40%. (observed)

1-*N*-(Boc-aminoethyl)–4*R*-*O*-acetyl-2*S*-proline methyl ester (7b): To a stirred solution of **6** (150 mg, 0.52 mmol) in dry pyridine (5 mL) was added acetic anhydride (0.16 mL, 1.0 mmol) at room temperature. The reaction mixture was stirred for 5 h. The solvent was evaporated off and residue was redissolved in water (10 mL). The solution was extracted with AcOEt (3 x). The organic phase was washed with brine, dried (Na_2SO_4) and evaporated in vacuo to give the crude product as oil (2.5 g), which was purified by chromatography to obtain **7b**. Yield: 150 mg (88%).

Compound	Molecular Characterization
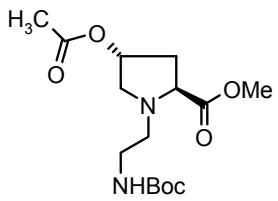 **7b**	**$[\alpha]^{30}_D$** -29.1 (c 0.24, $CHCl_3$). **IR ν_{max} (cm^{-1})**: 1737.7, 17.8.81. **^{1}H NMR $CDCl_3$**: δ 5.2 (m, 2H), 3.7 (s, 3H), 3.5 (m, 2H), 3.2 (q, J =5.9, J = 5.8, J = 5.4), 2.2 (m, 1H), 2.6 (m, 1H), 2.3 (m, 3H), 2.0 (m, 3H), 1.4 (s, 9H). **^{13}C NMR:** δ 173.2, 170.1, 155.6, 78.6, 72.57, 63.9, 58.1, 53.3, 51.5, 36.0, 28.0, 20.6. **Mass (m/z):** 330.38 (calculated); $(M+1)^+$ = 331 (observed) **Molecular formula:** $C_{15}H_{26}N_2O_6$

1-*N*-(-Boc-aminoethyl)–4*R*-*O*-acetyl-5-one-2*S*-proline methyl ester (8b):To a vigorous stirred solution of compound **7b** (750 mg, 2.3 mmol) in AcOEt (20 mL), an aqueous solution (20 mL) of $NaIO_4$ (2.0 g, 9.08 mmol) and $RuCl_3.xH_2O$ (catalytic amount, 0.02 mmol) was added. After 30 min, the reaction was quenched by addition of isopropyl alcohol and stirred for another 20 min and the reaction mixture was concentrated in vaccuo. The residue was taken into ethyl acetate (20 mL) and washed with water, the organic extract dried over Na_2SO_4 and concentrated to dryness. The crude product was purified by column chromatography to obtain **8b** as white foam. Yield: 300 mg (41%).

Compound	Molecular Charecterization
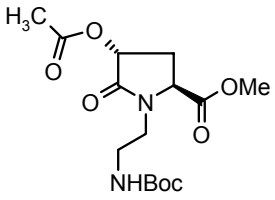 **8b**	**$[\alpha]^{30}_D$** +32 (c 0.28, $CHCl_3$), **IR ν_{max} (cm^{-1})**: 1743.5, 1710.7, 1236.3 **^{1}H NMR $CDCl_3$**: δ 5.4 (m, 1H), 4.9 (m, 1H), 4.4 (m, 1H), 3.8 (s, 4H), 3.5 (m, 1H), 3.1 (m, 2H), 2.7 (m, 1H), 2.2 (m, 1H), 2.1 (s, 3H), 1.5 (s, 9H). **^{13}C NMR:** δ 171.7, 171.2, 170.1, 156.2, 79.1, 72.7, 69.6, 60.3, 57.7, 56.7, 52.7, 42.7, 37.5, 30.7, 28.2, 20.6. **Mass (m/z):** 344.37 (calculated); $(M)^+$ = 344 (observed) **Molecular formula:** $C_{15}H_{24}N_2O_7$.

1-*N*-(-boc-aminoethyl)-4*R*-(t*ert*-butyldimethylsilyloxy)-2S-proline methylester (7c). Compound **6** (600 mg, 2.08 mmol), TBDMSCl (376 mg, 2.5 mmol) and imidazole (180 mg, 2.5 mmol) were stirred in dry DMF (5 mL) at room temprature overnight under N_2

atm. The solvent was evaporated off and the residue was purified by chromatography (15 % AcOEt in petroleum ether) to obtain compound **7c**. Yield: 700 mg (84%).

Compound	Molecular Characterization
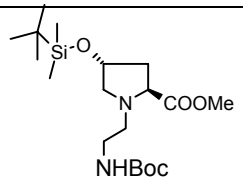 **7c** (2*S*,4*S*)	$[\alpha]^{25}_{D}$ +25.9 (c , $CHCl_3$). **^{1}H NMR $CDCl_3$**: ^{1}H NMR: δ 4.86 (bs, 1H), 4.4 (m, 1H), 3.75 (s, 4H), 3.6 (m,1H), 3.42 (m, 1H), 3.1 (m, 2H), 2.4 (m, 2H), 2.2 (m, 1H), 1.4 (s, 9H), 0.87 (s, 9H), 0.1 (s, 6H).

1-*N*-(Boc-aminoethyl)-4*R*-(t*ert*-butyldimethylsilyloxy)-5-one-2*S*-proline methylester (8c). To a vigorous stirred solution of **6** (380 mg, 0.95 mmol) in 10 mL of CH_3CN and CCl_4 (1:1) an aqueous solution (10 mL) of $NaIO_4$ (2.0 g, 9.08 mmol) and $RuCl_3$ (catalytic amount, 0.02 mmol) was added. After 60 min, the reaction was quenched by addition of isopropyl alcohol or 20% aqueous of $NaHSO_3$ and stirred for another 20 min and the reaction mixture was concentrated under vacuum. The residue was taken into ethyl acetate (20 mL) and washed with water, the organic extract dried over Na_2SO_4 and concentrated to dryness. The resultant product was purified by column chromatography to obtain **8c**. Yield: 300 mg (41%) of **2c** as foam. This reaction was also carried out in AcOEt and water (1:1) to obtain **8c** with almost same yield (45%).

Compound	Molecular Characterization
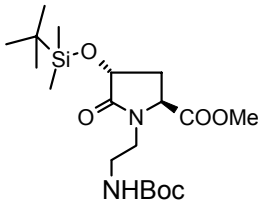 **8c** (2*S*,4*S*)	$[\alpha]^{25}_{D}$ +25.9 (c , $CHCl_3$). **^{1}H NMR $CDCl_3$**: ^{1}H NMR: δ 4.86 (bs, 1H), 4.4 (m, 1H), 4.3 (m,1H), 3.75 (s, 4H), 3.42 (m, 1H), 3.1 (m, 2H), 2.4 (m, 1H), 2.2 (m, 1H), 1.4 (s, 9H), 0.87 (s, 9H), 0.1 (s, 6H). **Mass (m/z):** 453 (M^+)

1-*N*-(Boc-aminoethyl)–4*S*-*O*-acetyl-2*S*-proline methyl ester (7d): Compound **6** (150 mg, 0.52 mmol) was dried by evaporation from CH_3CN (10 mL). Ph_3P (0.439 g, 1.67 mmol) and methyltosylate (0.4 g, 2.92 mmol) were successively added. The reaction mixture was dissolved in THF (20 mL) and stirred at 0 ^oC for 10 min before DIAD (0.29 mL, 1.67 mmol) was added dropwise. The clear yellow solution was allowed to warm to room temperature and stirred overnight. Solvent was evaporated off and residue was purified by column chromatography to obtain (**8d**) as white gum Yield: 150 mg (88%).

Compound	Molecular Characterization
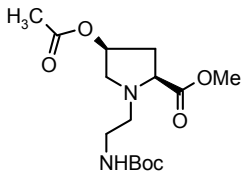 **7d**	$[\alpha]^{30}_D$ -29.1 (c 0.24, $CHCl_3$). **IR ν_{max} (cm^{-1})**: 1737.7, 17.8.81. **^{1}H NMR $CDCl_3$**: δ 5.2 (m, 2H), 3.7 (s, 3H), 3.5 (m, 2H), 3.2 (q, J =5.9, J = 5.8, J = 5.4), 2.2 (m, 1H), 2.6 (m, 1H), 2.3 (m, 3H), 2.0 (m, 3H), 1.4 (s, 9H). **^{13}C NMR:** δ 173.2, 170.1, 155.6, 78.6, 72.57, 63.9, 58.1, 53.3, 51.5, 36.0, 28.0, 20.6. **Mass (m/z):** 330.38 (calculated); $(M+1)^+$ = 331 (observed) **Molecular formula:** $C_{15}H_{26}N_2O_6$

1-*N*-(-Boc-aminoethyl)–4*S*-*O*-acetyl-5-one-2*S*-proline methyl ester (8d). Compound **7d** was used to obtain the compound **8d** by follow similar procedure of compound **8a:** Yield: 300 mg (41%).

Compound	Molecular Characterization
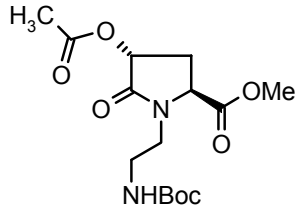 **8d**	$[\alpha]^{30}_D$ +32 (c 0.28, $CHCl_3$), **IR ν_{max} (cm^{-1})**: 1743.5, 1710.7, 1236.3 **^{1}H NMR $CDCl_3$**: δ 5.4 (m, 1H), 4.9 (m, 1H), 4.4 (m, 1H), 3.8 (s, 4H), 3.5 (m, 1H), 3.1 (m, 2H), 2.7 (m, 1H), 2.2 (m, 1H), 2.1 (s, 3H), 1.5 (s, 9H). **^{13}C NMR:** δ 171.7, 171.2, 170.1, 156.2, 79.1, 72.7, 69.6, 60.3, 57.7, 56.7, 52.7, 42.7, 37.5, 30.7, 28.2, 20.6. **Mass (m/z):** 344.37 (calculated); $(M)^+$ = 344 (observed) **Molecular formula:** $C_{15}H_{24}N_2O_7$.

1-*N*-(Boc-aminoethyl)–4S-*O*-benzoyl-2S-proline methyl ester (7e). Compound **6** was used to obtain as white gum as same procedure of **7d.** Yield (82.03%),

Compound	Molecular Characterization
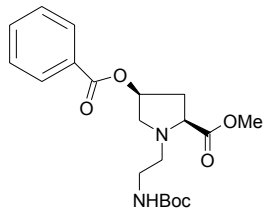 **7e** (2S, 4S)	$[\alpha]^{30}_{D}$ -10.8 (c 0.92, $CHCl_3$). **IR ν_{max} (cm^{-1})**: 1749, 1706, 1685 **^{1}H NMR $CDCl_3$**: 8-7.4 (m, 5H), 6.9 (bs, 1H), 5.4 (bs, 1H), 4.9 (m, 1H), 3.7 (s, 3H), 3.4 (m, 2H), 3.1 (t, 1H), 2.9 (m, 2H), 2.6 (m, 2H), 2.2 (m, 1H), 1.3 (s, 9H), **^{13}C NMR $CDCl_3$:** 173.2, 165.8, 154.5, 156.0, 132.6, 129.3, 128.0, 78.5, 73.0, 69.1, 64.0, 58.2, 53.1, 51.4, 36.0, 28.0. **Mass (m/z):** 453.89 (calculated); $(M)^+$ = 393 (observed).

1-*N*-(Boc-aminoethyl)–4S-*O*-benzoyl-5-one proline methyl ester (8e). 8e was obtained as foam from same procedure of **8a**. Yield: 2.0 g (43.3%).

Compound	Molecular Characterization
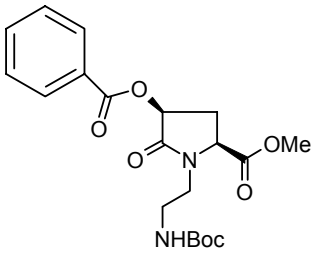 **8e**	$[\alpha]^{30}_{D}$ +20.0 (c 0.5, $CHCl_3$). **IR ν_{max} (cm^{-1})**: 1749, 1706, 1685 **^{1}H NMR $CDCl_3$**: δ 8.0 (d, 2H), 7.5-7.2 (m, 3H), 5.5 (m, 1H), 5.0 (bs, 1H), 4.5 (t, 1H), 3.8 (m, 1H), 3.7 (s, 3H), 3.5 (m, 1H), 3.2-3.0 (m, 2H), 2.9 (m, 1H)), 2.1 (m, 1H), 1.4 (s, 9H). **^{13}C NMR $CDCl_3$:** δ 171.5,165.7, 156.4, 133.5, 130.0, 128.5, 77.3, 70.0, 57.0, 52.6, 42.9, 37.8, 30.8, 28.4 **Mass (m/z):** (calculated); $(M)^+$ = 406 (observed).

1-*N*-(Boc-aminoethyl)–4S-*O*-tosyl-proline methyl ester (7f): Compound **6** was dried by evaporation from CH_3CN (10 mL). Ph_3P (4.39 g, 16.7 mmol) and methyltosylate (4.13 g, 29.2 mmol) were successively added. The reaction mixture was dissolved in THF (20 mL) and stirred at 0 ^oC for 10 min before DIAD (2.9 mL, 16.7 mmol) was added dropwise. The clear yellow solution was allowed to warm to room temperature and stirred overnight.

Solvent was evaporated off and residue was purified by column chromatography to obtain (**8d**) as white gum. Yield: 2.1 g (43.3%).

Compound	Molecular Characterization
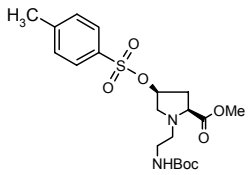 **7f** (2S,4S)	**^{1}H NMR $CDCl_3$**: 7.8 (d, 2H), 7.3 (d, 2H), 5.3 (bs, 1H0, 5.0 (m, 2H), 3.7 (s, 3H), 3.3 (m, 4H), 2.7 (m, 2H), 2.5 (m, 1H), 2.4 (s, 3H), 2.2 (m, 1H), 1.4 (s, 9H), 172.6, 155.6, 144.5, 133.6, 129.5, 127.3, 78.9, 69.0, 63.5.

1-*N*-(Boc-aminoethyl)–4*S*-*O*-tosyl-5-one-proline methyl ester (8f). 7f was used to obtain **8f** as white solid as procedure of **7a**. Yield: (43.3%).

Compound	Molecular Characterization
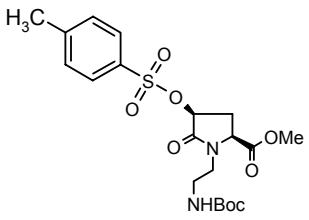 **8f** (2S,4S)	**$[\alpha]^{30}_D$** +5.0 (c 0.8 , $CHCl_3$), **IR ν_{max} (cm^{-1})**: 1749, 1706, 1685 **^{1}H NMR $CDCl_3$**: 7.5 (m, 1H), 7.5 (s, 5H), 6.5 (m,1H), 5.3 (s, 4H), 3.15 (bs, 5H), 2.0 (m, 1H), 1.48 (s, 9H), **^{13}C NMR $CDCl_3$:** 172.0, 170.0, 162.6, 159.4, 156.1, 152.4, 148.4, 134.9, 128.3, 99.5, 67.5, 57.7, 56.6, 52.4, 43.0, 37.7, 28.8, 28.1 **Mass (m/z):** (calculated); $(M)^+$ = 530.0 (observed).

1- 1-(*N*-Boc-aminoethyl)-4*S*-(thymin-1-yl)-5-one-2*S*-proline methyl ester (17): The compound **8a** (200 mg, 0.52 mmol), Thymine **9** (80 mg, 0.63 mmol), K_2CO_3 (86.9 mg, 0.63 mmol) and catalytic amount of 18-crown-6 (54 mg, 0.15 mmol) in dry DMF (5 mL) were stirred at 65 ^oC overnight under N_2 atmosphere. The solvent was evaporated off and

Compound	Molecular Characterization
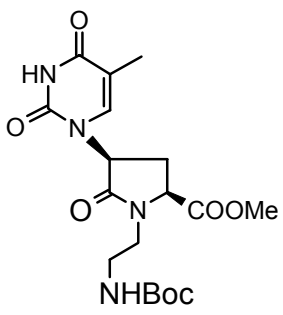 **17** (2*S*,4*S*)	**$[\alpha]^{30}_D$** -21.6 (c 0.6 , $CHCl_3$). **IR ν_{max} (cm^{-1})**: 1731, 1701, 1514. **^{1}H NMR $CDCl_3$**: δ 9.2 (bs, 1H), 7.2 (bs, 1H), 5.25 (bs, 1H), 5.0 (m, 1H), 4.5 (m, 1H), 3.9 (s, 3H), 3.5 (m, 2H), 3.25 (m, 2H), 2.5 (m, 1H), 2.0 (s, 3H), 1.9 (m, 1H), 1.49 (s, 9H). **^{13}C NMR $CDCl_3$:** δ 171.4, 170.0, 164.0, 156.2, 151.0, 139.3, 137.4, 111.6, 79.5, 56.6, 52.7, 43.1, 37.9, 29.1, 28.2, 12.1. **Mass (m/z):** 410.43 (calculated); $(M)^+$ = 410.0 (observed). **Molecular formula**: $C_{18}H_{26}N_4O_7$. **Analysis**: C 52.68%, H 6.39%, N 13.65%, O 7.29%.(Calculated), C 52.8%, H 6.31%, N 13.45%, O 7.33%(observed)

the residue was purified by chromatography (3% MeOH in CH_2Cl_2) to obtain **17** as white foam. Yield: (65 mg, 30.0%).

1-*N*-(boc-aminoethyl)-4*S*-(N^6-benzoyladenin-9-yl)-5-one-2*S*-proline methyl ester (18). Compound **8a** was used to obtain **18** as foam by same procedure as used for **17**. Yield (57%) of **18** as white foam.

Compound	Molecular Characterization
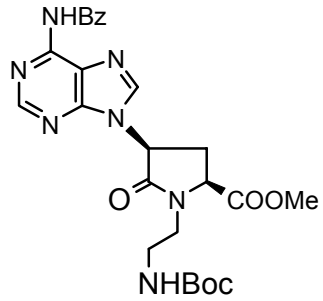 **18** (2*S*,4*S*)	$[\alpha]^{30}_D$ = -27.6 (c 0.8 , $CHCl_3$). **IR ν_{max} (cm^{-1})**: 1730-1708, 1610. **^{1}H NMR $CDCl_3$**: δ 8.8 (m, 1H), 8.2 (m, 1H), 8.0 (m, 1H), 7.5 (m, 3H), 5.5 (m, 1H), 5.0 (m, 1H), 3.9 (s, 3H), 3.7 (m, 1H), 3.4 (m, 2H), 3.2 (m, 2H), 2.8 (m, 2H), 1.49 (s, 9H). **^{13}C NMR $CDCl_3$:** δ 171.0, 169.0, 158.9, 155.8, 152.1, 149.6, 142.6, 141.6, 133.5, 132.9, 128.4, 127.7, 95.8, 79.3, 57.5, 54.3, 52.6, 43.1, 37.4, 30.1, 28.0. **Mass (m/z):** 532.55 (calculated); $(M)^+$ = 523 (observed). **Molecular formula**: $C_{25}H_{29}N_7O_6$ **Analysis**: C 52.8%, H 6.31%, N 13.45%, O 7.33% (Calculated), C 51.8%, H 6.41%, N 14.05%, O 7.33% (Observed)

***1-(N*-Boc-aminoethyl)-4*S*-(N^4-benzyloxycarbonylcytosin-1-yl)-5-one-2*S*-proline methyl ester (19).** Compound **8a** and nucleobase **13** was used to obtain **19** as foam by similar synthetic procedure of compound **17.** Yield: (36.0%).

Compound	Molecular Characterization
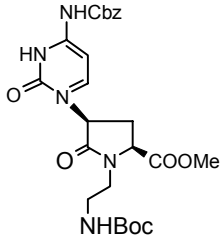 **19** (2*S*,4*S*)	$[\alpha]^{30}_D$ +5.0 (c 0.8 , $CHCl_3$). **IR ν_{max} (cm^{-1})**: 1749, 1706, 1685. **^{1}H NMR $CDCl_3$**: δ 7.5 (m, 1H), 7.5 (s, 5H), 6.5 (m, 1H), 5.3 (s, 4H), 3.15 (bs, 5H), 2.0 (m, 1H), 1.48 (s, 9H). **^{13}C NMR $CDCl_3$:** δ 172.0, 170.0, 162.6, 159.4, 156.1, 152.4, 148.4, 134.9, 128.3, 99.5, 67.5, 57.7, 56.6, 52.4, 43.0, 37.7, 28.8, 28.1. **Mass (m/z):** 531.57 (calculated); $(M)^+$ = 531.0 (observed). **Molecular formula**: $C_{25}H_{33}N_5O_8$ **CHN Analysis**: C 56.49%, H 6.26%, N 13.17% O 24.08% (Calculated). C 56.7%, H 6.26%, N 13.2% O 24.18% (observrd).

1-*N*-(Boc-aminoethyl)-4*S*-(2-amino-6-chloropurin-9-yl)-5-one-2*S*-proline methyl ester (20). The compound **8a** and precursor of nucleobase **16** was used to obtain **20** by using similar synthesis procedure of compound **17.** Yield: (45.0 %),

Compound	Molecular Characterization
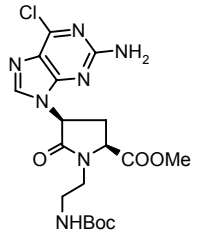 **20** (2*S*,4*S*)	$[\alpha]^{30}_{D}$ +10.0 (c 0.2, $CHCl_3$). **IR ν_{max} (cm^{-1})**:1714, 1706, 1610. **^{1}H NMR $CDCl_3$**: 7.6-7.9 (m, 1H), 5.4 (m, 1H), 5.2 (m, 2H), 4.5 (m, 1H), 3.8 (bs, 4H), 3.5 (m, 2H), 3.2 (m, 2H), 2.7 (m, 2H), 1.5 (s, 9H) **^{13}C NMR $CDCl_3$:** 171.0, 170.0, 158.9, 155.9, 142.4 141.6, 125.2, 95.9, 79.9,57.79, 52.71, 43.0, 73.4, 30.0, 29.2, 28.1. **Mass (m/z):** 453.89 (calculated); $(M)^+$ = 453 (observed). **Molecular formula**: $C_{18}H_{24}ClN_7O_5$ **CHN Analysis**: C 47.63%, H 5.33%, Cl 7.81%, N 21.60%, O 17.62% (Calculated). C 47.93%, H 5.43%, C l 7.71%, N 21.70%, O 17.64% (Observed).

1-*N*-(Boc-aminoethyl)–4*S*-hydroxy-5-one-2*S*-proline methyl ester (21). 8b (50 mg, 0.1 mmol) was dissolved in dry MeOH (5 mL) and cooled to 0 ^oC. NaOMe in methanol (1.05 M, 1.0 mL, 0.20 mmol) was added drop wise and the solution was stirred at 0 ^oC for 30 min. the reaction was quenched by addition of half saturated aqueous NH_4Cl (10 mL). The aqueous phasse was extracted with AcOEt (2 x). The organic extract was evaporated off and residue was purified by column chromatography (30 % AcOEt in petrolium ether) to obtain desired product **21** as white foam. Yield: 15 mg (48 %).

Compound	Molecular Characterization
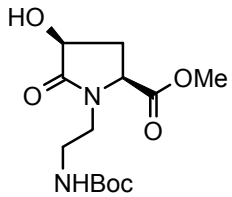 **21** (2*S*,2*S*)	**$[\alpha]^{30}_{D}$:** -18.7 (c 0.16 , $CHCl_3$). **IR ν_{max} (cm^{-1})**:1716, 1705, **^{1}H NMR $CDCl_3$**: 5.1 (bs, 1H), 4.4 (m, 1H), 4.2 (t, 1H), 3.8 (m, 1H), 3.7 (s, 3H), 3.4 (m, 2H), 3.1 (m, 2H), 2.7 (m, 1H), 2.0 (q, 1H), 1.4 (s, 9H), 1.2 (m, 1H). **^{13}C NMR $CDCl_3$:** 175.6, 171.7, 156.2, 79.6, 68.8, 56.8, 42.6, 38.1, 32.3, 28.3. **Mass (m/z):** 302.33 (calculated); $(M+1)^+$ = 303 (observed). **Molecular formula**: $C_{13}H_{22}N_2O_6$

1-*N*-(Boc-aminoethyl)–4*S*-*O*-mesyl-5-one-2*S*-proline methyl ester (22): Compound **21** (240 mg, 0.79 mmol) was dried by evaporation from CH_3CN/CH_2Cl_2 (1:1) and then stirred in dry pyridine (5 mL) at 0 ^oC for 20 min. Methasulfonyl chloride (0.79 mL, 1.0 mmol) were added to reaction mixture at 0 ^oC and stirred for 2 h. The solvent was evaporated off. The residue was dissolved in water (10 mL) and solution was extracted with AcOEt (3x). Organic extract was dried over $Na_2 SO_4$ and concentrated to give crude product, which was purified by column chromatography to obtain product **22** as yellow oil. Yield: 219.7 mg (73.0).

Compound	Molecular Characterization
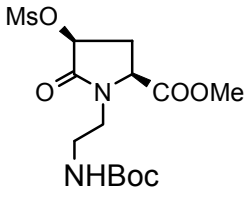 **22** (2*S*,4*S*)	**$[\alpha]^{30}_D$:** +13.3 (c 0.3 , $CHCl_3$) **IR ν_{max} (cm^{-1})**:1711, 1700, **^{1}H NMR $CDCl_3$**: 5.0 (dd, J = 5.4, J = 5.4, 1H), 4.8 (bs, H), 4.5 (dd, J = 5.9, J = 5.9, 1H), 3.7 (s, 3H), 3.4 (m, 1H), 3.2 (s, 3H), 3.1 (m, 1H), 2.9 (m, 1H), 2.3 (m, 1H), 1.4 (s, 9H). **^{13}C NMR $CDCl_3$:** 170.6, 169.3, 156.1, 79.3, 75.5, 56.3, 52.6, 42.6, 39.3, 37.4, 30.0, 28.1. **Mass (m/z):** 380.33 (calculated); $(M+1)^+$ = 381 (observed). **Molecular formula**: $C_{13}H_{22}N_2O_6$

1-*N*-(Boc-aminoethyl)-4*R*-(thymin-1-yl)-5-one-2*S*-proline methyl ester (23). Compound **8f** and nucleobase thymine **9** was used to obtain **23** as white foam by using similar synthesis procedure of **17**.Yield: (40.9%). This compound was also synthesized with tosylate compound **8f** and thymine **9** by similar procedure

Compound	Molecular Characterization
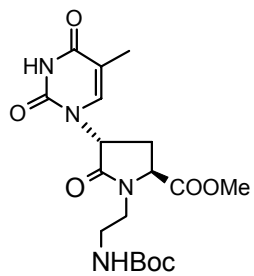 **23** (2*S*,4*R*)	**$[\alpha]^{30}_D$** 21.6 (c 0.6 , $CHCl_3$). **IR ν_{max} (cm^{-1})**: 1730, 1700, 1514. **^{1}H NMR $CDCl_3$**: 9.0 (bs, 1H), 7.0 (s, 1H), 4.9 (m, 1H), 4.5 (dd, J = 7.8, J = 9.7), 3.9 (m, 1H), 3.7 (m, 1H), 3.5 (m, 1H), 3.3 (m, 1H), 3.1 (m, 1H), 2.5 (m, 2H), 2.2 (m, 1H), 1.9 (s, 3H), 1.4 (s, 9H). **^{13}C NMR $CDCl_3$:** 171.5, 163.7, 156.3, 150.7, 139.2, 137.4, 11.6, 79.5, 77.2, 57.7, 52.9, 43.4, 37.9, 28.3, 12.3. **Mass (m/z):** 410.43 (calculated); $(M+1)^+$ = 411 (observed). **Molecular formula:** $C_{18}H_{26}N_4O_7$. **Analysis**: C 52.68%, H 6.39%, N 13.65%, O 7.29%. (Calculated) C 52.7%, H 6.4%, N 13.5%, O 7.5%. (Observed)

1-(*N*-boc-aminoethyl)-4*R*-(N^6-benzoyladenin-9-yl)-5-one-2S-proline methyl ester (24). **8f** or **22** was used to obtain **24** as white foam as same procedure of **17**. Yield:(43.3%).

Compound	Molecular Characterization
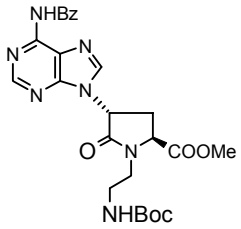 **24** (2*S*,4*R*)	**IR ν_{max} (cm^{-1})**: 1731-1705, 1611. **^{1}H NMR $CDCl_3$**: δ 9.2 (bs, 1H), 8.7 (s, 1H), 7.9 (d, 2H), 7.5 (m, 3H), 5.6 (bs, 1H), 5.4 (t, 1H), 4.5 (m, 1H), 3.9 (m, 1H), 3.8 (s, 3H), 3.4 (m, 2H), 3.1 (m, 1H), 2.8 (m, 2H), 1.4 (s, 9H). **^{13}C NMR $CDCl_3$:** δ 171.3, 169.3, 164.8, 156.2, 152.2, 151.5, 149.8, 142.8, 133.6, 132.7, 128.7, 127.9, 123.4, 79.7, 57.8, 54.7, 53.0, 43.4, 37.5, 30.7, 28.4. **Mass (m/z):** 523.55 (calculated); $(M+1)^+$ = 524 (observed). **Molecular formula**: $C_{25}H_{29}N_7O_6$ **Analysis**: (Calculated), C 52.8%, H 6.31%, N 13.45%, O 7.33% C 52.6%, H 6.41%, N 13.75%, O 7.53% (Observed)

1-*N*-(Boc-aminoethyl)-4*R*-(N^4-benzyloxycarbonylcytocin-1-yl)-5-one-2S-proline methyl ester (25). Compound **22** and thymine **9** was used to obtain **25** as white foam as same procedure of **17**. Yield: (43.0%).

Compound	Molecular Characterization
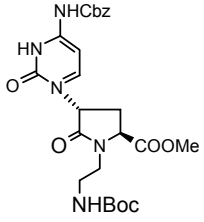 **25** (2*S*,4*R*)	**$[\alpha]^{30}_D$** +70.4 (c 0.31 , $CHCl_3$). **IR ν_{max} (cm^{-1})**: 1750, 1703, 1690. **^{1}H NMR $CDCl_3$**: δ 7.6 (m, 1H), 7.5 (s, 5H), 7.3 (s, 1H), 5.4 (bs, 1H), 5.0(s, 2H), 4.9 (m, 1H), 4.5 (m, 1H), 3.7 (s, 3H), 3.3 (m, 2H), 3.1-2.8 (m, 1H), 2.6 (m, 1H), 2.0 (m, 2H), 1.4 (s, 9H), 1.2 (m, 1H) **^{13}C NMR $CDCl_3$:** δ 171.7, 1760, 162.9, 159.6, 154.9, 152.5, 150.0, 148.0, 135.0, 128.5, 96.5, 79.2, 67.7, 60.2, 58.2, 52.7, 43.2, 37.7, 29.0, 28.3. **Mass (m/z):** 531.57 (calculated); $(M)^+$ = 530.0 (observed). **Molecular formula**: $C_{25}H_{33}N_5O_8$ **Analysis**: C 56.49%, H 6.26%, N 13.17% O 24.08% (Calculated).

1-*N*-(Boc-aminoethyl)-4*R*-(2-amino-6-chloropurin-9-yl)-5-one-2*S*-proline methyl ester (26): Compound **22** or **8f** were used to obtain **26** as white foam as same procedure of **17.** Yield: 2.1 g (47.0%).

Compound	Molecular Characterization
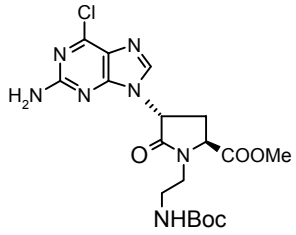 **26** (2*S*,4*R*)	**IR ν_{max} (cm^{-1})**:1712, 1703, 1608. **^{1}H NMR $CDCl_3$**: 7.8 (s, 1H), 5.4 (bs, 2H), 5.2 (dd, J = 9.2, J = 2.4, 1H), 5.0 (bs, 1H), 4.5 (dd, J = 8.7, J = 6.9, 1H), 3.8 (s, 3H), 3.4 (m, 2H), 3.1 (m, 2H), 2.8 (m, 2H), 1.4 (s, 9H), **^{13}C NMR $CDCl_3$:** 171.4, 169.2, 159.0,156.0, 151.9, 142.0, 125.5, 58.1, 54.5, 53.0, 43.3, 37.6, 30.1, 28.4. **Mass (m/z):** 453.89 (calculated); $(M+1)^+$ = 454 (observed). **Molecular formula**: $C_{18}H_{24}ClN_7O_5$ **Analyis**: C 47.63%, H 5.33%, Cl 7.81%, N 21.60%, O 17.62% (Calculated).

1-*N* -(Boc-aminoethyl)-4*S*-hydroxy-2*S*-proline methyl ester 27: This compound **27** was synthesized by hydrolysis of compounds **7d, 7e** and **7g** in presence of 2% of aqueous solution of NaOH by followed similar synthesis procedure of compound **21.**

Compound	Spectral Data
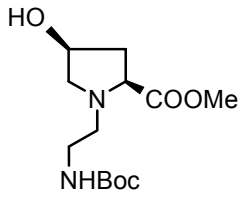 **27** (2*S*,4*S*)	**^{1}H NMR $CDCl_3$**: 5.0 (bs, 1H), 4.5-4.1(m, 2H), 3.7(m, 3H), 4.0 (m, 1H), 3.2-3.0 (m, 2H), 2.8-2.5 (m, 1H), 2.0-1.9 (m,1H), 1.4 (s, 9H). **^{13}C NMR $CDCl_3$:** 175.5, 156.0, 79.0, 70.0, 64.1, 61.9, 53.7, 52.1, 39.0, 28.37. **Mass (m/z):** 288.35 (calculated); $(M)^+$ = 288 (observed). **Molecular formula**: $C_{13}H_{24}N_2O_5$ **Analysis:** C 54.15%, H 8.39%, N 9.72%, O 27.74% (Calculated) C 54.45%, H 8.40%, N 9.62%, O 27.84% (Observed)

1-*N*-(Boc-aminoethyl)-4*R*-(N3-benzoylthymine-1yl)-2*S*-proline methyl ester (28). To a stirred solution of 1-(*N*-Boc-aminoethyl)-4-(*S*)-hydroxy-2-(*S*)-proline methyl ester **27** (2.0 g, 7.1 mmol), N3-benzoyl thymine **10** (1.6 g, 7.1 mmol) and triphenylphosphine (1.9 g, 7.5 mmol) in anhydrous THF (20 mL) at room temperature, was added dropwise diisopropylaxodicarboxylate (DIAD, 1.5 mL, 7.5 mmol). After completion of the reaction as indicated by TLC (overnight), the solvent was removed *in vacua* and residue purified by silica gel column chromatography to get the pure product **28** as yield 50%.

Compound	Spectral Data
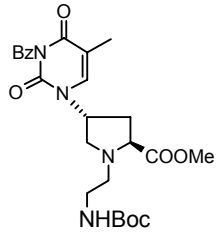 **28** (2*S*,4*R*)	**^{1}H-NMR CDCl$_3$** δ ^{1}H NMR δ 7.9 (s, 1H), 7.7-7.4 (m, 5H), 5.2 (m, 1H), 4.8 (bs, 1H), 3.8 (t, 1H), 3.7 (s, 3H), 3.4 (dd, 1H), 3.3-3.3.0 (m, 2H), 2.9-2.6 (dd, 1H), 2.8 (t, 2H), 2.6-2.4 (m, 1H), 2.2-2.1 (m, 1H), 1.9 (s, 3H), 1.4 (s, 9H), ^{13}C **^{13}C-NMR CDCl$_3$**: δ 172.2, 169.0, 162.5, 155.8, 149.5, 137.5, 134.8, 131.3, 130.0, 128.9, 111.1, 78.8, 63.1, 55.5, 53.7, 51.4, 50.6, 38.7, 35.1, 28.1, 12.3

1-*N*-(Boc-aminoethyl)-4*S*-*O*-mesyl-2*S*-proline methyl ester (29): To a stirred ice cold solution of 1-(*N*-Boc-aminoethyl)-4-(*S*)-hydroxy-2-(*S*)-proline methyl ester **27** (3.4 g, 11.8 mmol) and triethylamine (5 mL, mmol) in dry DCM, was added dropwise methane sulphonyl chloride (3.6 g , 35.4 mmol) After 2 h, upon completion of reaction, the DCM was removed under vacuum and the residue was taken in water and extracted with DCM (4x20mL). The organic layer was dried over sodium sulphate and concentrated to get the crude product of **29**, which was purified by silica gel column chromatography as yield: 3.4 g, 80%.

Compound	Spectral Data
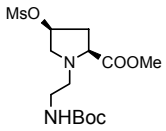 **29** (2*S*,4*S*)	**^{1}H NMR CDCl$_3$**: 5.3 (m, 1H), 5.2 (m, 1H), 3.75 (s, 3H), 3.42 (m, 2H), 3.20 (m, 2H), 3.0 (s, 3H), 2.85 (m, 2H), 2.6 (m, 2H), 2.35 (m, 1H), 1.45 (s, 9H). **^{13}C NMR CDCl$_3$:** 172.4, 155.6, 79.0, 78.4, 63.6, 58.3, 53.1, 51.7, 38.6, 38.2, 36.1, 28.2.

1-*N*-(Boc-aminoethyl)-4*R*-(N^6-benzoyladenin-9-yl)-2*S*-proline methyl ester (30). A mixture of 1-(N)-(Boc-aminoethyl)-4-(S)-*O*-mesyl-2-(*S*)-proline methyl ester **29** (1.2 g, 3.2 mmol), N^6-benzoyladenine (**15**) (2 g, 8.1 mmol), anhydrous potassium carbonate (2.2 g, 16.4 mmol) and 18-crown-6 (0.34 g, 1 mmol) in anhydrous DMF (10 mL) was stirred under nitrogen atmosphere at 75 ^{0}C for overnight by similar synthesis procedure of compound **17**. The residue purified twice by silica gel column chromatography to get the pure product 27 (50%). This product **30** was also synthesized with other bases as cesium carbonate ($CsCO_3$) and sodium hydride (NaH) in different solvent as acetonitrile or DMF under anhydrous condition at 70 ^{0}C condition, but yield was poor.

Compound	Spectral Data
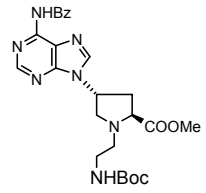 **30** (2*S*,4*R*)	**NMR $CDCl_3$**: δ 8.7 (s,1H), 8.3 (s,1H), 8.0-7.4 (m, 5H), 5.3 (m, 2H), 3.9 (t, 1H), 3.6 (s, 3H), 3.2 (m, 3H), 2.8 (m, 2H), 2.5 (m, 2H), 2.0 (m, 1H), 1.4 (s, 9H). **^{13}C-NMR $CDCl_3$:** 172.9, 164.9, 155.9, 152.0, 151.6, 149.6, 141.7, 133.6, 132.3, 128.4, 127.8, 126.0, 79.0, 70.4, 63.4, 56.7, 53.2, 51.8, 39.0, 35.6

1-*N*-(Boc-aminoethyl)-4*R*-(N^4-benzyloxycarbonyl-cytosin-9-yl)-2*S*-proline methyl ester (31). A mixture of 1-(N)-(Boc-aminoethyl)-4-(S)-*O*-mesyl-2- (*S*)-proline methyl ester **29** (1.2 g, 3.2 mmol), N^4-benzyloxycarobyl-cytosine (2g, 8.1 mmol), anhydrous potassium carbonate (2.2 g, 16.4 mmol) and 18-crown-6 (0.34 g, 1 mmol) in anhydrous DMF (10 mL) by using similar synthesis procedure of compound **17**. yield (50%).

Compound	Spectral Data
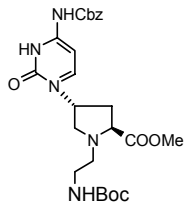 **31** (2S,4*R*)	**NMR $CDCl_3$** : δ 7.85 (s, 1H), 7.36 (s, 6H), 5.29 (m, 2H), 3.9 (t, 1H), 3.7 (s, 3H), 3.5-3.0 (m, 4H), 2.9-2.7 (m, 2H), 2.6-2.4 (m, 2H), 1.45 (s, 9H). **^{13}C-NMR $CDCl_3$:** δ 17.2, 163.2, 159.2, 148.0, 137.2, 130, 128, 95, 79.0, 65.1, 63.1, 59.0, 52.0, 50.1, 39.1, 37.2, 27.2, 25.2.

1-*N*-(Boc-aminoethyl)-4*R*-(2-amino-6-chloropurin-9-yl)-2*S*-proline methyl ester (32): A mixture of 1-(N)-(Boc-aminoethyl)-4-(S)-*O*-mesyl-2- (*S*)-proline methyl ester **29** (1.2 g, 3.2 mmol), 2-amino-6-chloropurine **32** (2 g, 8.1 mmol), anhydrous potassium carbonate (2.2 g, 16.4 mmol) and 18-crown-6 (0.34 g, 1 mmol) in anhydrous DMF (10 mL) was stirred under nitrogen atmosphere at 75 ^{0}C for overnight.

Compound	Spectral Data
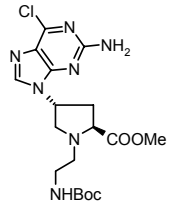 **32** (2S,4*R*)	**NMR $CDCl_3$:** δ 7.8 (s, 1H), 5.4 (bs, 2H), 5.2 (m, 1H), 3.5 (t,1H), 3.7 (s, 3H), 3.4 (m, 1H), 3.3-3.3.0 (m, 3H), 2.9-2.6 (m, 2H), 2.49 (t, 2H), 1.4 (s, 9H), ^{13}C NMR $CDCl_3$ **^{13}C-NMR $CDCl_3$:** δ 173.2, 158.9, 155.9, 153.2, 150.8, 141.5, 124.7, 79.2, 64.4, 58.9, 53.4, 52.2, 51.6, 38.9, 36.7, 23.8

1-(N)-(Boc-aminoethyl)-4S-(N3-benzoylthymine-1yl)-2*S*-proline methyl ester (33). Compound **33** was synthesized by reported procedure.[30]

Compound	Spectral Data
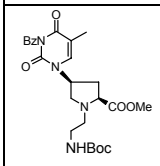 **34** (2*S*,4*R*)	**^{1}H-NMR $CDCl_3$** δ 7.6 (s, 1H), 7.7-7.4 (m, 5H), 5.2 (m, 1H), 4.8 (bs, 1H), 3.7 (s, 3H), 3.8 (m, 1H), 3.4 (dd, 1H), 3.3-3.3.0 (m, 2H), 2.9-2.6 (dd, 1H), 2.8 (t, 2H), 2.6-2.4 (m, 1H), 2.2-2.1 (m, 1H), 1.9 (s, 4H), 1.4 (s, 9H).

1-(*N*)-(Boc-aminoethyl)-4*S*-(N^6-benzoyladenin-9-yl)-2S-proline methyl ester (34). Compound **34** was synthesized by reported procedure.[30]

Compound	Spectral Data
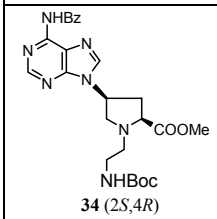 **34** (2*S*,4*R*)	**NMR $CDCl_3$**: δ 8.0 (s, mi, 1H), 8.7(s, ma, 1H), 8.0 (s, ma/mi, 1H), 7.6-7.4 (m, 5H), 5.4 (m, 1H), 5.1 (bs, 1H), 3.7 (s, 3H), 3.5 (dd, 1H), 3.2 (m, 2H), 3.0-2.8 (m, 2H), 2.7 (m, 1H), 2.4 (m, 1H), 2.2 (m, 1H), 1.4 (s, 9H).

1-(N)-(Boc-aminoethyl)-4S-(N^4-benzyloxycarbonyl-cytosin-9-yl)-2*S*-proline methyl ester (35). Compound **35** was synthesized by reported procedure.[30]

Compound	Spectral Data
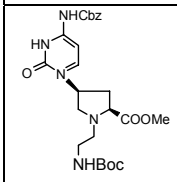 **35** (2*S*,4S)	**NMR $CDCl_3$** : δ 8.4 (s, 1H), 7.4 (s, 5H), 7.29 (m, 1H), 5.4 (bs, 1H), 5.2 (s, 2H), 5.1 (m, 1H), 3.7 (s, 3H), 3.4-3.1 (m, 4H), 2.8 (m, 3H), 2.6 (m, 1H), 1.9 (dd, 2H), 1.4 (s, 9H).

1-(N)-(Boc-aminoethyl)-*4S*-(2-amino-6-chloropurin-9-yl)-2-(S)-proline methyl ester (36). Compound **36** was synthesized by reported procedure.[30]

Compound	Spectral Data
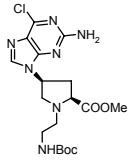 **36** (2S,4S)	**NMR $CDCl_3$** δ 8.4 (s, 1H), 5.4 -5.0 (m, 3H), 3.8 (s, 3H), 3.4 (dd, 1H), 3.4 (d, 1H), 3.3 (d, 1H), 3.2 (m, 2H), 2.9-2.6 (m, 4H), 2.2 -2.1 (m, 1H), 1.4 (s, 9H).

Synthesis of Aminoethylglycyl PNA Monomers (A/ T/ G/ C)[55]

1-*N*-(Boc)-1,2-diaminoethane (54): 1,2-diaminoethane **53** (20 g, 0.33 mol) was taken in dioxane: water (1:1, 500 mL) and cooled in an ice-bath. Boc-azide (5 g, 35 mmol) in dioxane (50 mL) was slowly added with stirring and the pH was maintained at 10.0 by continuous addition of 4N NaOH. The mixture was stirred for 8h and the resulting solution was concentrated to 100 mL. The N1, N2-di-Boc derivative not being soluble in water, precipitated, and it was removed by filtration. The corresponding N1-mono-Boc derivative was obtained by repeated extraction from the filtrate in ethyl acetate. Removal of solvents yielded the mono-Boc-diaminoethane **54** (3.45 g, 63%).

Compound	Spectral Data
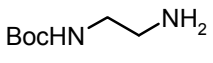 **54**	^{1}H NMR ($CDCl_3$) δ: 5.21 (br s, 1H, N*H*), 3.32 (t, 2H, J=8 Hz), 2.54 (t, 2H, J=8 Hz), 1.42 (s, 9H).

Ethyl N-(2-Boc-aminoethyl)-glycinate (55): The *N1*-(Boc)-1,2-diaminoethane **54** (3.2 g, 20 mmol) was treated with ethylbromoacetate (2.25 mL, 20 mmol) in acetonitrile (100 mL) in the presence of K_2CO_3 (2.4 g, 20 mmol) and the mixture was stirred at ambient temperature for 5 h. The solid that separated was removed by filtration and the filtrate was evaporated to obtain the ethyl *N*-(2-Boc-aminoethyl)-glycinate **55** (4.3 g, 83%) as a colourless oil.

Compound	Spectral Data
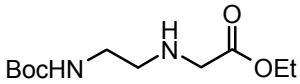 **55**	^{1}H NMR ($CDCl_3$) δ 5.02 (br s, 1H, N*H*), 4.22 (q, 2H, J=8Hz), 3.35 (s, 2H), 3.20 (t, 2H, J=6Hz), 2.76 (t, 2H, J=6Hz), 1.46 (s, 9H), 1.28 (t, 3H, J=8Hz).

Ethyl N-(Boc-aminoethyl)-N-(chloroacetyl)-glycinate (56): The ethyl *N*-(2-Boc-aminoethyl)-glycinate **55** (4.0 g, 14 mmol) was taken in 10% aqueous Na_2CO_3 (75 mL) and dioxane (60 mL). Chloroacetyl chloride (6.5 mL, 0.75 mmol) was added in two portions with vigorous stirring. The reaction was complete within 5 min. The reaction mixture was brought to pH 8.0 by addition of 10% aqueous Na_2CO_3 and concentrated to remove the dioxane. The product was extracted from the aqueous layer with dichloromethane and was purified by column chromatography to obtain the ethyl *N*-(Boc-aminoethyl)-*N*-(chloroacetyl)-glycinate **56** as a colourless oil in good yield (4.2 g, 80%).

Compound	Spectral Data
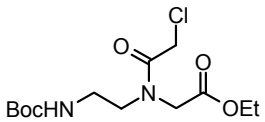 **56**	^{1}H NMR ($CDCl_3$): δ 5.45 (br s, 1H), 4.14 9S, 2H), 4.00 (s, 2H), 3.53 (t, 2H), 3.28 (q, 2H), 1.46 (s, 9H), 1.23 (t, 3H, J=8Hz).

***N*-(Boc-aminoethylglycyl)-thymine ethyl ester (57a):** Ethyl *N*-(Boc-aminoethyl)-*N*-(chloroacetyl)-glycinate **56** (4.0 g, 11.6 mmol) was stirred with anhydrous K_2CO_3 (1.56 g, 11.8 mmol) in DMF with thymine (1.4 g, 11.2 mmol) to obtain the desired compound **57a** in good yield. DMF was removed under reduced pressure and the oil obtained was purified by column chromatography.

Compound	Spectral Data
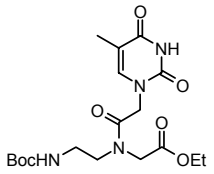 **57a**	**^{1}H NMR ($CDCl_3$)** δ: 9.00 (br s, 1H, *T*-N*H*), 7.05 (min) & 6.98 (maj) (s, 1H, *T*-*H*6), 5.65 (maj) & 5.05 (min) (br s, 1H, N*H*), 4.58 (maj) & 4.44 (min) (s, 1H, *T*-CH_2), 4.25 (m, 2H, OCH_2), 3.55 (m, 2H), 3.36 (m, 2H), 1.95 (s, 3H, *T*-CH_3), 1.48 (s, 9H), 1.28 (m, 3H).

***N*-(Boc-aminoethylglycyl)-adenine ethyl ester (57b)**: NaH (0.25 g, 6.1 mmol) was taken in DMF (15mL) and adenine (0.8 g, 6.1 mmol) was added. The mixture was stirred at 75 ^oC till the effervescence ceased and the mixture was cooled before adding ethyl *N*-(Boc-aminoethyl)-*N*-(chloroacetyl)-glycinate **56** (2.0 g, 6.1 mmol). The reaction mixture was heated once again to 75 ^oC for 1 h, when TLC analysis indicated the disappearance of the starting ethyl *N*-(Boc-aminoethyl)-*N*-(chloroacetyl)-glycinate. The DMF was removed under vacuum and the resulting thick oil was taken in water and the product, extracted in ethyl acetate. The organic layer was then concentrated to obtain the crude product, which was purified by column chromatography to obtain the pure *N*-(Boc-aminoethylglycyl)-adenine ethyl ester **57b**.

Compound	Spectral Data
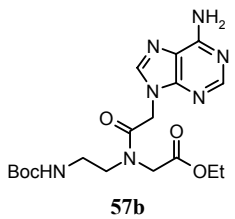 **57b**	^{1}H NMR ($CDCl_3$) δ: 8.32 (s, 1H), 7.95 (min) & 7.90 (maj) (s, 1H), 5.93 (maj) & 5.80 (min) (br s, 2H), 5.13 (maj) & 4.95 (min), 4.22 (min) & 4.05 (maj) (s, 2H), 4.20 (m, 2H), 3.65 (maj) & 3.55 (min) (m, 2H), 3.40 (maj) & 3.50 (min) (m, 2H), 1.42 (s, 9H), 1.25 (m, 3H).

***N*-(Boc-aminoethylglycyl)-(N^4-benzyloxycarbonyl cytosine)-ethyl ester (57c):** A mixture of NaH (0.25 g, 6.2 mmol) and N^4-benzyloxycarbonyl cytosine **3** (1.24 g, 6.2 mmol) was taken in DMF and stirred at 75 ^oC till the effervescence ceased. The mixture was cooled and ethyl *N*-(Boc-aminoethyl)-*N*-(chloroacetyl)-glycinate **56** (2.0 g, 6.2 mmol) was added. Stirring was then continued at 75 ^oC to obtain the cytosine monomer, *N*-(Boc-aminoethylglycyl)-(N^4-benzyloxycarbonyl cytosine)ethyl ester **57c**, in moderate yield (1.62 g, 50%).

Compound	Spectral Data
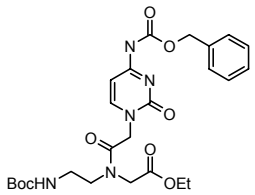 **57c**	^{1}H NMR ($CDCl_3$): δ 7.65 (d, 1H, *C-H6*, J=8Hz), 7.35 (s, 5H, Ar), 7.25 (d, 1H, *C-H*5, J=8Hz), 5.70 (br s, 1H, N*H*), 5.20 (s, 2H, Ar-CH_2), 4.71 (maj) & 4.22 (min) (br s, 2H), 4.15 (q, 2H), 4.05 (s, 2H), 3.56 (m, 2H), 3.32 (m, 2H), 1.48 (s, 9H), 1.25 (t, 3H).

***N*-(Boc-aminoethylglycyl)-2-amino-6-chloropurine ethyl ester (57d):** A mixture of 2-amino-6-chloropurine (1.14 g, 6.8 mmol), K_2CO_3 (0.93 g, 7.0 mmol) and ethyl *N*-(Boc-aminoethyl)-*N*-(chloroacetyl)-glycinate **53** (2.4 g, 7.0 mmol) were taken in dry DMF (20 mL) and stirred at room temperature for 4 h. K_2CO_3 was removed by filtration, and the DMF, by evaporation under reduced pressure. The resulting residue was purified by column chromatography to obtain the *N*-(Boc-aminoethylglycyl)-2-amino-6-chloropurine ethyl ester (**57d**) in excellent yield (2.65 g, 98%).

Compound	Spectral Data
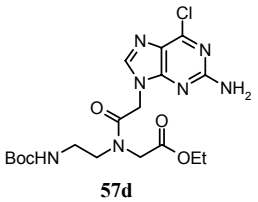 **57d**	**^{1}H NMR ($CDCl_3$):** δ 7.89 (min) & 7.85 (maj) (s, 1H), 7.30 (s, 1H), 5.80 (br s, 1H, N*H*), 5.18 (br, 2H), 5.02 (maj) & 4.85 (min) (s, 2H), 4.18 (min) & 4.05 (maj) (s, 2H), 3.65 (maj) & 3.16 (min) (m, 2H), 3.42 (maj) and 3.28 (min) (m, 2H), 1.50 (s, 9H), 1.26 (m, 3H).

2.6 REFERENCES

1. Uhlmann, E.; Peyman, A. Antisense oligonucleotides: A new therapeutic principle. *Chem. Rev.* **1990,** *90*, 543-584
2. Noble, S. A.; Bonham, M. A.; Bisi, J. E.; Bruckenstein, D. A.; Brown P. H.; Brown, S. C. Impact of biophysical parameters on the biological assessment of peptide nucleic acids, antisense inhibitors of gene expression. *Drug Dev*. *Res*. **1995**, *34*, 184-195.
3. *Antisense Research and Applications* (Eds.: Crooke, S. T.; Lebleu, B.), CRC Press, Boca Raton, FL, **1993**.
4. Zamecnik, P. C. Stephenson, M. L. Inhibition of Rous sarcoma virus replication and cell transformation by a specific oligodeoxynucleotide. *Proc. Natl. Acad. Sci.* **1978**, *75*, 280-284.
5. Uhlmann, E.; Peyman, A. Encyclopaedia of Molecualr Biology and Antisense Oligonucleotides-Chemical Modifications. *Biotechnology* (Ed.: Meyer, E.), New York, **1995**.
6. Agrawal, S. Methods in Molecular Biology: Protocols for Oligonucleotides and Analogs (Chapter 16). Humana Press, New Jersey, Totowa, **1993**, *20*, 355-389.
7. Mesmaekar, A. D.; Haner, R.; Martin, P.; Moser, E. H. Antisense oligonucleotides. *Acc. Chem. Res.* **1995**, *28*, 366-374.
8. Crooke, S. T.; Lemonidis, K. M.; Neeilson, L.; Griffey, R.; Lesnik, E. A.; Monia, B. P. Kinetic characteristics of Escherichia colli Rnase H1: cleavage of various antisense oligonucleotide-RNA duplexes. *Biochem. J.* **1995**, *312*, 599-607
9. Marwick, C. First "antisense'' drug will treat CMV retinitis. *J. Am. Med. Assoc*. **1998**, *280*, 871.
10. Summerton, J. D.; Weller. D. Morpholino antisense oligomers: design, preparation and properties. *Antisense Nucleic Acid Druug Dev.* **1997,** *7*, 187-195.
11. Milligan, J.; Matteucci, M. D.; Martin, J. C. Current concepts in antisense drug design *J. Med. Chem.* **1993**, *36*, 1921-1937.
12. Walder, R. Y. & Walder, J. A. Role of R-NaseH in hybrid arrested translation by antisense oligonucleotides. *Proc. Natl. Acad. Sci.U.S.A,* **1988**, *85*, 5011-5015.
13. Herdewijn, P. Heterocyclic modifications of oligonucleotides and antisense technology. *Antisense Nucleic Acid Drug Dev.* **2000**, *10*, 297-310.
14. Woolf, T. M.; Melton, D. A.; Jennings, C. Specificity of antisense oligonucleotides *in vivo*. *Proc. Natl. Acad. Sci. USA*. **1992**, *89,* 7305-7309.
15. Giles, R.V.; Spiller, D. G.; Clark, R. E.; Tidd, D. M. Antisense morpholino analog induces missplicing of C-myc m-RNA. *Antisense Nucleic Acid Drug Dev*. **1999**, *9*, 213-220.
16. Skorski, T.; Perrotti, D.; Nieborowska-Skorska, M.; Gryaznov, S. M.; Calabretta, B. Antileukemia effect of C-myc N3'-P5' phosphoramidate antisense oligonucleotide *in vivo. Proc. Natl. Acad. Sci.* USA **1997**, *94*, 3966-3971.
17. Kurreck, J.; Wyszko, E.; Gillen, C.; Erdmann, V. A. Design of antisense oligonucleotides by locked nucleic acids. *Nucleic Acid Res*. **2002**, *30*, 1911-1918.

18. Sazani, P.; Shin-Hong Kong, Maier, M.; Weic, D.; Summerton, J.; Manoharan, M.; Kole, R. Nuclear antisense effects of neutral, anionic and cationic oligonucleotide analogues. *Nucleic Acid Res*. **2001**, *29*, 3965-3974.
19. Nielsen P. E.; Egholm, O.; Berg R. H. & Buchardt, O. Sequence selective recognition of DNA by strand displacement with a thymine substituted polyamide. *Science* **1991**, *254*, 1497-1500.
20. Hanvey, J. C.; Peffer, N. J.; Bissi, J. E.; Thomson, S. A.; Cadilla, R.; Josey, J. A.; Ricca, D. J.; Hassman, C. F.; Bonham, M. A.; Au, K. G. Antisense and antigene properties of peptide nucleic acids. *Science* **1992**, *258*, 1481-1485.
21. Egholm, M.; Buchardt, O.; Christensen, L.; Beherns, C.; Freier, S. M.; Driver, D. A.; Berg, R. H.; Kim, S. K.; Norden, B.; Nielsen, P. E. PNA hybridizes to complementary oligonucleotides obeying the Watson-Crick hydrogen bonding rules. *Nature* **1993**, *365*, 566-568.
22. Nielsen, P. E.; Egholm, M.; Buchardt, O. Peptide nucleic acid(PNA). A DNA mimic with a peptide backbone. *Bioconjugate Chem*. **1994**, *5*, 3-7.
23. Demidov, V. V.; Potaman, V. N.; Kamenetskii, M. D. F.; Egholm, M.;Buchart, O.; Sonnischsen, S. H. and Nielsen, P. E. *Biochem. Pharmacol.***1994**, *48*, 1310–1313.
24. Hamilton, S.; Iyer, M.; Norton, J.; Corey, D. Specific and nonspecific inhibition of transcription by DNA, PNA and phosphorothioate promoter analog complexes. *Bioorg. Med. Chem. Lett*. **1996**, *6*, 2897-2900.
25. Smulevitch, S. V.; Simmons, C. G.; Norton, J. C.; Wise, J. W.; Corey, D. R. Enhanced strand invasion by oligonucleotides through manipulation of backbone charges. *Nat. Biotech*. **1996**, *14*, 1700-1704.
26. Corey, D. R. Peptide nucleic acids: expanding the scope of nucleic acid recognition. *Trends Biotechnol.* **1997**, *15*, 224–229. (d) Eriksson, M.; Nielsen, P. E. PNA-nucleic acid complexes: Structure, stability and dynamics. *Q. Rev. Biophys.* **1996**, *29,* 369–394
27. Tomac, S.; Sarkar, M.; Ratilainen, T.; Wittung, P.; Nielsen, P. E.; Nordén, B.; Gräslund, A. Ionic effects on the stability and conformation of PNA complexes. *J. Am. Chem. Soc.* **1996,** *118*, 5544-5552.
28. Knudsen, H. & Nielsen, P. E. Antisense properties of duplex and triplex forming Peptide nucleic Acids. *Nucleic Acid Res*. **1996,** *24*, 494-500.
29. Good, L.; Awasthi, S. K.; Dryselius, R.; Larsson, O.; Nielsen, P. E. Bacterisidal antisense effects of peptide –PNA conjugates. *Nature biotech.* **2001**, *19*, 360-364.
30. (a) Nielsen, P. E. DNA analogs with nonphosphodiester backbones. *Annu. Rev. Biophys. Biomol. Struct*. **1995**, 167-183. (b) Nielsen, P. E. Applications of PNA. *Current Opinion in Biotechnology* **1999**, *10,* 71-75.
31. (a) Orum, H.; Nielsen, P. E.; Jorgensen, M.; Larsson, C.; Stanley, C.; Koch, T.; Sequence-specific pification of nucleic acids by PNA-controlled hybrid selection. *Biotechniques* **1995**, *19*, 472-80. (b) Kuhn, H.; Demidov, V. V.; Nielsen, P. E.; Frank-Kamenetskii, M. D. An experimental study of mechanism and specificity of peptide nucleic acid (PNA) binding to duplex DNA. *J Mol. Biol*. **1999**, *286*, 1337-13345. Ishihara, T.; Corey, D. R. Rules for Strand Invasion by Chemically Modified Oligonucleotides. *J. Am. Chem. Soc.* **1999**, *121*, 2012-2020.

32. Savithri, D.; Leumann, C.; Scheffold, R. Synthesis of a building block for a nucleic-acid analog with a chiral, flexible peptide backbone. *Helvetica Chimica Acta* **1996**, *79*, 288-294.
33. (a) Efimov, V. A.; Choob, M. V.; Buryakova, A. A.; Kalinkina, A. L.; Chakhmakhcheva, O. G. Synthesis and evaluation of some properties of chimeric oligomers containing PNA and phosphono-PNA residues. *Nucleic Acids Res*. **1998**, *26*, 566-575. (a) Hyrup, B.; Egholm, M.; Nielsen, P. E.; Wittung, P.; Norden, B.; Buchardt, O. Structure activity studies of the binding of modified peptide nucleic acids to DNA. *J. Am. Chem. Soc.* **1994**, *116*, 7964-7970. (b) Hyrup, B.; Egholm, M.; Rolland, M.; Nielsen, P. E.; Berg, R. H.; Buchardt, O. Modification of the binding affinity of peptide nucleic acids (PNA). PNA with extended backbones consisting of 2-aminoethyl-.beta.-alanine or 3-aminopropylglycine units. *J. Chem. Soc., Chem. Commun.* **1993**, 518-519. (c) Hyrup, B.; Egholm, M.; Rolland, M.; Nielsen, P. E.; Berg, R. H.; Buchardt, O. Modification of the binding affinity of peptide nucleic acids (PNA). PNA with extended backbones consisting of 2-aminoethyl-.beta.-alanine or 3-aminopropylglycine units. *J Chem. Soc. , Chem. Commun.* **1993**, 518-519.
34. (a) Gangamani, B. P.; Kumar, V. A.; Ganesh, K. N. Spermine conjugated peptide nucleic acids (spPNA): UV and fluorescence studies of PNA-DNA hybrids with improved stability. *Biochem Biophys. Res. Commun*. **1997**, *240*, 778-782. (b) Kumar VA: Structural pre-organization of peptide nucleic acids: chiral cationic analogues with five- or six-membered ring structures. *Eur. J. Org. Chem*. **2002**, 2021-2032.
35. Brown, S. C.; Thomson, S. A.; Veal, J. M.; Davis, D. G. NMR Solution structure of a Peptide nucleic acid complexed with RNA. *Science* **1994**, *265*, 777-780.
36. (a) Lowe, G.; Vilaivan, T. Amino acids bearing nucleobases for the synthesis of novel peptide nucleic acids. *J. Chem. Soc., Perkin Trans. 1*, **1997**, 539-547. (b) Lowe, G.; Vilaivan, T. Dipeptides bearing nucleobases for the synthesis of novel peptide nucleic acids. *J. Chem. Soc., Perkin Trans. 1* **1997**, 547-555. (c) Lowe, G.; Vilaivan, T.; Westwell, M. S. Hybridization studies with chiral peptide nucleic acids. *Bioorg. Chem*. **1997,** *25*, 321-329. (d) Lowe, G.; Vilaivan, T. A novel pyrrolidinyl PNA showing high sequence specificity and preferential binding to DNA over RNA. *J. Am. Chem. Soc*. **2002**, *124*, 9326-9327. (e) Lowe, G.; Vilaivan, T. Solid phase synthesis of novel peptide nucleic acids. *J. Chem. Soc., Perkin Trans I* **1997**, 555-560. (f) Vilaivan, T.; Khongdeesameor, C.; Harnyuttanokam, P.; Lowe, G. Synthesis and properties of novel pyrrolidinyl PNA carrying β amino acid spacers. *Tetrahedron Lett.* **2001**, *42*, 5533-5536..
37. Hyrup, B.; Egholm, M.; Buchardt, O.; Nielsen, P. E. A flexible and positively charged PNA analogue with an ethylene-linker to the nucleobase: synthesis and hybridization properties. *Bioorg. Med. Chem. Lett.* **1996**, *6,* 1083-1088.
38. (a) Tan, T. H.; Hickman, D. T.; Morral, J.; Beadham, I. G.; Micklefield J. Nucleic acid binding properties of thyminyl and adeninyl pyrrolidine-amide oligonucleotide mimics (POM). *Chem. Commun*. (Camb). **2004**, *5*, 516-517. (b) Hickman, D.T.; Tan, T. H.; Morral, J.; King, P. M.; Cooper, M. A.; Micklefield, J. Design, synthesis, conformational analysis and nucleic acid hybridization properties of thymidyl pyrrolidine-amide oligonucleotide mimics (POM). *Org. Biomol. Chem*. **2003**, *1*, 3277-3292.

39. Püschl, A.; Tedeschi, T.; Nielsen, P. E.; Pyrrolidine PNA: a novel conformationally restricted PNA analogue. *Org*. *Lett*. **2000**, *2*, 4161-4163.
40. (a) D'Costa, M.; Kumar, V. A.; Ganesh, K. N. Aminoethylprolyl peptide nucleic acids(*aep*PNA) : chiral PNA analogues that forms highly stable DNA:aepPNA$_2$ triplexes. *Org. Lett*. **1999**, *1*, 1513-1516. (b) D'Costa, M..; Kumar, V. A.; Ganesh, K. N. Aminoethylprolyl (*aep*PNA): mixed purine, pyrimidine oligomers and binding orientation preferences for PNA:DNA duplex formation. *Org. Lett*. **2001**, *3*, 1281-1284. (c) Gangamani, B. P.; Kumar, V. A.; Ganesh, K.N. Synthesis of Na-(purinyl/pyrimidylacetyl)-4-aminoproline diastereomers with potential use in PNA synthesis. *Tetrahedron* **1996**, *52*, 15017-15030. (d) Gangamani, B. P.; Kumar, V. A.; Ganesh, K. N. Chiral analogues of peptide nucleic acids:synthessi of 4-aminoprolyl nucleic acids and DNA complementation studies using UV-CD spectroscopy. *Tetrahedron* **1999**, *55*, 177-192
41. Püsch,l A.; Boesen, T.; Zuccarello, G.; Dahl, O.; Pitsch, S.; Nielsen, P. E. Synthesis of pyrrolidinone PNA: a novel conformationally restricted PNA analogue. *J. Org. Chem*. **2001**, *66*, 707-712.
42. Vilaivan, T.; Khongdeesameor, C.; Harnyuttanokam, P.; Lowe, G. J. A novel pyrrolidinyl PNA showing high sequence specificity and preferential binding to DNA over RNA. *J. Am. Chem. Soc.* **2002,** *124,* 9326-9327
43. Schultz, R.; Cantin, M.; Roberts, C.; Greiner, B.; Uhlmann, E.; Leumann, C. Olefinic Peptide Nucleic Acids (OPAs): New Aspects of the Molecular Recognition of DNA by PNA The team at the University of Bern thanks the Swiss National Science Foundation and Novartis Pharma AG, Basel, for generous financial support. *Angew*. *Chem*. *Int*. *Ed*. **2000**, *39*, 1250-1253.
44. (a) Ganesh, K. N.; Nielsen, P. E. Peptide nucleic acids: analogs and derivatives. *Current Org. Chem.* **2000**, 931-943. (b) Kumar, V. A.; Ganesh, K. N. Conformationally constrained PNA analogues: structural evolution toward DNA/RNA binding selectivity. *Acc. Chem. Res*. **2005,** *38*, 404-412.
45. Almarison, O.; Bruice, T. C. Peptide Nucleic Acids (PNA) conformation and polymorphism in PNA-DNA and PNA-RNA hybrids. *Proc. Natl. Acad. Sci*. USA **1993**, *90*, 9542-9546. Buchardt, O.; Egholm, M.; Nielsen, P. E.; Berg, R.H. *Int. PCT Appl*. Wo 92/20702, **1992**.
46. Merino, P.; Revuelta, J.; Tejero, T.; Chiacchio, U.; Rescifina, A.; Piperno, A.; Romeo, G. Enantioselective synthesis of 4-hydroxy-D-pyroglutamic acid derivatives by an asymmetric 1,3-dipolar cycloaddition. *Tetrahedron: Asymmetry* **2002**, *13*, 167–172.
47. (a) Zhang, X.; Schmitt, A. C.; Jiang, W. A convenient and high yield method to prepare 4-hydroxypyroglutamic acids. *Tetrahedron Lett*. **2001**, *42*, 5335–5338. (b) Qiu, X. L.; Qing, F. L. Synthesis of *cis*-4-Trifluoromethyl- and *cis*-4-Difluoromethyl-L-pyroglutamic Acids. *J. Org. Chem.* **2003**, *68*, 3614–3617.
48. Sheehan, J. C.; Tulis, R. W. Oxidation of cyclic amines with ruthenium tetroxide. *J. Org. Chem*. **1974**, *39*, 2264-2267.
49. Konas, D. W.; Coward, J. K. Electrophilic Fluorination of pyroglutamic acid derivatives: application of aubstrate-dependent reactivity and diastereoselectivity to the synthesis of optically active 4-Fluoroglutamic Acids. *J. Org. Chem*. **2001**, *66*, 8831-8842.

50. (a) Ezquerra, J.; Pedregal, C.; Rubio, A.; Yruretagoyena, B.; Escribano, A.; Ferrando, S. S. Stereoselective reactions of lithium enolates derived from *N*-BOC protected pyroglutamic esters. *Tetrahedron* **1993,** *49*, 8665–8678; (b) Ezquerra, J.; Pedregal, C.; Rubio, A. Stereoselective double alkylation of ethyl *N*-Boc-pyroglutamate. *J. Org. Chem*. **1994**, *59*, 4327–4331. (c) Dikshit, D. K.; Panday, S. K. Aldol reactions of pyroglutamates: chiral synthesis of 4.alpha.(S)- and 4.beta.(R) (arylmethyl)pyroglutamates. *J. Org. Chem.* **1992**, *57*, 1920–1924.
51. O. Mitsunobu, Mitsunobu reaction. *Synthesis* **1981**, 1-28
52. Cruickshank, K. A.; Jiricny, J.; Colin, B.; Reese, C. B. The benzoylation of uracil and thymine. *Tetrahedron Lett*. **1984**, *25*, 681-684.
53. Bulloc, M. W.; Hand, J. J.; Stokstad, E. L. R. Notes-reduction of 6-aroylaminopurines with lithium aluminum H\hydride. *J. Org*. *Chem*. **1957**, *22*, 568.
54. Brown, D, M.; Varadarjan, S. *J. Chem*. *Soc*. **1956**, 2384.
55. Dueholm, K. L.; Egholm, M.; Beherns, C.; Christensen, L.; Hansen, H. F.; Vulpius, T.; Petersen, K. H.; Berg. R. H.; Nielsen, P. E.; Buchardt, O. Synthesis of peptide nucleic acid monomers containing the four natural nucleobases: thymine, cytosine, adenine, and guanine and their oligomerization. *J. Org. Chem*. **1994**, *59*, 5767-5773.

2.7 APPENDIX

1. Compound Crystal data and structure refinement for compound **8a**

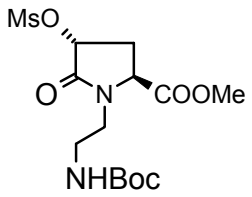

8a (2*S*,4*S*)

Crystal data and structure refinement for 8a

Identification code	**8a**
Empirical formula	$C_{14}H_{24}N_2O_8S$
Formula weight	380.41
Temperature	293(2) K
Wavelength	0.71073 A
Crystal system, space group	Monoclinic, P21
Unit cell dimensions	a = 12.739(5) A alpha = 90 deg.
b = 9.294(4) A beta = 103.419(8) deg.	
c = 15.994(6) A gamma = 90 deg.	
Volume	1841.9(13) A^3
Z, Calculated density	4, 1.372 Mg/m^3
Absorption coefficient	0.219 mm^-1
F(000)	808
Crystal size	0.61 x 0.09 x 0.05 mm
Theta range for data collection	1.64 to 25.00 deg.
Limiting indices	-10<=h<=15, -10<=k<=11, -19<=l<=17
Reflections collected / unique	9094 / 6134 [R(int) = 0.0354]
Completeness to theta = 25.00	99.4 %
Max. and min. transmission	0.9885 and 0.8780
Refinement method	Full-matrix least-squares on F^2
Data / restraints / parameters	6134 / 1 / 470
Goodness-of-fit on F^2	1.103
Final R indices [I>2sigma(I)]	R1 = 0.0655, wR2 = 0.1219
R indices (all data)	R1 = 0.0819, wR2 = 0.1290
Absolute structure parameter	0.02(9)
Extinction coefficient	0.0000(6)
Largest diff. peak and hole	0.243 and -0.168 e.A^-3

Table 2. Atomic coordinates (x 10^4) and equivalent isotropic displacement parameters (A^2 x 10^3) for nag3.
U(eq) is defined as one third of the trace of the orthogonalized Uij tensor.

x	y	z	U(eq)	
S(1')	3171(1)	10092(1)	11719(1)	43(1)
S(2)	-1918(1)	9794(2)	6742(1)	58(1)
N(1)	-993(2)	9720(4)	3955(2)	36(1)
N(1')	4204(3)	10375(3)	9037(2)	34(1)
N(2')	6349(3)	9160(4)	8993(3)	46(1)
N(2)	1212(3)	8539(5)	4084(2)	47(1)
O(1)	-315(2)	11272(3)	5062(2)	56(1)
O(1')	4735(2)	11808(3)	10227(2)	54(1)
O(3)	-1196(5)	10622(5)	7345(3)	121(2)
O(8)	-2937(3)	10347(6)	6353(3)	106(2)
O(3')	3848(3)	11193(4)	12150(2)	76(1)
O(8')	2067(3)	10413(4)	11405(2)	68(1)
O(4')	2339(3)	11051(4)	7793(2)	65(1)
O(5')	2115(3)	8743(4)	7449(2)	66(1)
O(2')	3653(2)	9527(3)	10948(2)	51(1)
O(2)	-1304(3)	9391(5)	6029(2)	74(1)
O(6)	2585(2)	10075(4)	4063(2)	60(1)
O(7)	2722(2)	8302(3)	5063(2)	50(1)
O(7')	7835(2)	8856(3)	9995(2)	50(1)
O(6')	7630(3)	10862(4)	9153(2)	69(1)
O(5)	-2609(2)	9664(4)	2455(2)	57(1)
O(4)	-3678(3)	8502(4)	3138(2)	70(1)
C(5')	4161(3)	10874(5)	9808(2)	38(1)
C(8')	7314(4)	9729(5)	9362(3)	43(1)
C(8)	2205(4)	9072(5)	4372(3)	42(1)
C(13)	-2794(4)	8919(5)	3102(3)	45(1)
C(6)	-285(3)	10158(5)	3413(2)	41(1)
C(5)	-926(3)	10310(4)	4727(2)	37(1)
C(9')	8991(3)	9091(6)	10386(3)	52(1)
C(2)	-1779(3)	8541(4)	3765(3)	40(1)
C(2')	3408(3)	9275(5)	8696(3)	40(1)
C(6')	4906(3)	10971(5)	8524(3)	40(1)
C(4')	3254(3)	10094(5)	10094(2)	45(1)
C(15')	3362(4)	8546(6)	12340(3)	64(1)
C(7')	5637(3)	9848(5)	8268(2)	42(1)
C(9)	3874(3)	8538(5)	5470(3)	51(1)
C(13')	2570(3)	9814(5)	7938(3)	43(1)
C(7)	507(3)	9009(6)	3286(3)	51(1)
C(11)	4017(4)	10009(6)	5887(3)	64(1)
C(11')	9154(4)	10479(6)	10883(3)	66(2)
C(4)	-1769(3)	9593(5)	5123(2)	44(1)
C(3)	-2007(4)	8188(5)	4641(3)	51(1)
C(3')	2930(4)	8878(5)	9462(3)	56(1)

C(10')	9629(4)	9040(7)	9691(3)	79(2)
C(10)	4559(4)	8387(7)	4815(3)	82(2)
C(14')	1258(5)	9119(7)	6712(3)	93(2)
C(14)	-3528(4)	9985(7)	1751(3)	69(2)
C(15)	-2010(6)	8114(7)	7197(4)	102(2)
C(12')	9260(4)	7816(7)	10982(4)	83(2)
C(12)	4104(4)	7355(6)	6144(4)	82(2)

Table 3. Bond lengths [A] and angles [deg] for **8a**.

S(1')-O(3')	1.411(4)
S(1')-O(8')	1.411(3)
S(1')-O(2')	1.589(3)
S(1')-C(15')	1.732(5)
S(2)-O(3)	1.399(5)
S(2)-O(8)	1.401(4)
S(2)-O(2)	1.571(3)
S(2)-C(15)	1.738(6)
N(1)-C(5)	1.336(5)
N(1)-C(6)	1.448(5)
N(1)-C(2)	1.467(5)
N(1')-C(5')	1.331(5)
N(1')-C(2')	1.453(5)
N(1')-C(6')	1.456(5)
N(2')-C(8')	1.342(6)
N(2')-C(7')	1.446(5)
N(2)-C(8)	1.336(6)
N(2)-C(7)	1.447(5)
O(1)-C(5)	1.223(5)
O(1')-C(5')	1.228(5)
O(4')-C(13')	1.196(5)
O(5')-C(13')	1.314(5)
O(5')-C(14')	1.451(6)
O(2')-C(4')	1.441(5)
O(2)-C(4)	1.444(5)
O(6)-C(8)	1.208(5)
O(7)-C(8)	1.353(5)
O(7)-C(9)	1.478(5)
O(7')-C(8')	1.346(5)
O(7')-C(9')	1.476(5)
O(6')-C(8')	1.202(5)
O(5)-C(13)	1.312(5)
O(5)-C(14)	1.454(5)
O(4)-C(13)	1.205(5)
C(5')-C(4')	1.521(6)
C(13)-C(2)	1.511(6)
C(6)-C(7)	1.514(6)
C(5)-C(4)	1.522(6)
C(9')-C(11')	1.505(7)
C(9')-C(12')	1.509(7)
C(9')-C(10')	1.522(6)
C(2)-C(3)	1.531(5)
C(2')-C(13')	1.503(6)
C(2')-C(3')	1.534(6)
C(6')-C(7')	1.517(6)
C(4')-C(3')	1.510(6)
C(9)-C(11)	1.514(7)
C(9)-C(10)	1.519(6)
C(9)-C(12)	1.519(7)
C(4)-C(3)	1.511(6)

O(3')-S(1')-O(8')	117.8(2)
O(3')-S(1')-O(2')	108.5(2)
O(8')-S(1')-O(2')	109.08(18)
O(3')-S(1')-C(15')	109.4(2)
O(8')-S(1')-C(15')	112.0(3)
O(2')-S(1')-C(15')	98.2(2)
O(3)-S(2)-O(8)	119.8(3)
O(3)-S(2)-O(2)	105.8(3)
O(8)-S(2)-O(2)	109.4(2)
O(3)-S(2)-C(15)	107.7(3)
O(8)-S(2)-C(15)	111.7(3)
O(2)-S(2)-C(15)	100.6(3)
C(5)-N(1)-C(6)	121.5(3)
C(5)-N(1)-C(2)	113.1(3)
C(6)-N(1)-C(2)	125.2(3)
C(5')-N(1')-C(2')	114.7(3)
C(5')-N(1')-C(6')	123.5(3)
C(2')-N(1')-C(6')	121.5(3)
C(8')-N(2')-C(7')	121.2(4)
C(8)-N(2)-C(7)	122.4(4)
C(13')-O(5')-C(14')	116.5(4)
C(4')-O(2')-S(1')	120.0(3)
C(4)-O(2)-S(2)	122.7(3)
C(8)-O(7)-C(9)	121.8(4)
C(8')-O(7')-C(9')	119.9(3)
C(13)-O(5)-C(14)	117.4(4)
O(1')-C(5')-N(1')	127.2(4)
O(1')-C(5')-C(4')	124.7(4)
N(1')-C(5')-C(4')	108.1(4)
O(6')-C(8')-N(2')	123.8(4)
O(6')-C(8')-O(7')	126.7(4)
N(2')-C(8')-O(7')	109.5(4)
O(6)-C(8)-N(2)	125.6(4)
O(6)-C(8)-O(7)	125.2(4)
N(2)-C(8)-O(7)	109.2(4)
O(4)-C(13)-O(5)	123.2(4)
O(4)-C(13)-C(2)	123.3(4)
O(5)-C(13)-C(2)	113.3(4)
N(1)-C(6)-C(7)	114.1(4)

O(1)-C(5)-N(1)	127.0(4)
O(1)-C(5)-C(4)	125.2(4)
N(1)-C(5)-C(4)	107.7(4)
O(7')-C(9')-C(11')	110.6(4)
O(7')-C(9')-C(12')	102.1(4)
C(11')-C(9')-C(12')	110.9(4)
O(7')-C(9')-C(10')	109.6(4)
C(11')-C(9')-C(10')	112.4(4)
C(12')-C(9')-C(10')	110.8(4)
N(1)-C(2)-C(13)	113.8(3)
N(1)-C(2)-C(3)	103.7(3)
C(13)-C(2)-C(3)	112.3(4)
N(1')-C(2')-C(13')	111.8(4)
N(1')-C(2')-C(3')	104.0(3)
C(13')-C(2')-C(3')	112.6(4)
N(1')-C(6')-C(7')	112.7(3)
O(2')-C(4')-C(3')	110.0(4)
O(2')-C(4')-C(5')	109.5(3)
C(3')-C(4')-C(5')	105.3(3)
N(2')-C(7')-C(6')	113.4(3)
O(7)-C(9)-C(11)	109.5(4)
O(7)-C(9)-C(10)	110.7(3)
C(11)-C(9)-C(10)	110.9(5)
O(7)-C(9)-C(12)	102.3(4)
C(11)-C(9)-C(12)	111.0(4)
C(10)-C(9)-C(12)	112.1(5)
O(4')-C(13')-O(5')	123.9(4)
O(4')-C(13')-C(2')	125.0(4)
O(5')-C(13')-C(2')	111.2(4)
N(2)-C(7)-C(6)	113.0(3)
O(2)-C(4)-C(3)	112.7(4)
O(2)-C(4)-C(5)	108.0(3)
C(3)-C(4)-C(5)	104.1(3)
C(4)-C(3)-C(2)	102.9(3)
C(4')-C(3')-C(2')	104.9(3)

Symmetry transformations used to generate equivalent atoms:

Table 4. Anisotropic displacement parameters (A^2 x 10^3) for **8a**
The anisotropic displacement factor exponent takes the form:
-2 pi^2 [h^2 a*^2 U11 + ... + 2 h k a* b* U12]

U11	U22	U33	U23	U13	U12
S(1')	45(1)	45(1)	40(1)	-4(1)	13(1)	7(1)
S(2)	77(1)	60(1)	48(1)	3(1)	33(1)	0(1)
N(1)	33(2)	44(2)	31(2)	-1(2)	7(1)	3(2)
N(1')	36(2)	27(2)	37(2)	0(2)	6(2)	-1(1)
N(2')	45(2)	36(2)	53(2)	9(2)	3(2)	-5(2)
N(2)	35(2)	59(3)	45(2)	13(2)	9(2)	1(2)
O(1)	51(2)	61(2)	55(2)	-23(2)	9(2)	-14(2)
O(1')	55(2)	57(2)	48(2)	-21(2)	11(2)	-15(2)
O(3)	184(5)	98(4)	83(3)	-37(3)	37(3)	-56(3)
O(8)	97(3)	147(5)	89(3)	33(3)	54(3)	61(3)
O(3')	92(3)	56(2)	77(2)	-26(2)	16(2)	-9(2)
O(8')	50(2)	88(3)	68(2)	-4(2)	20(2)	22(2)
O(4')	70(2)	45(2)	67(2)	6(2)	-10(2)	4(2)
O(5')	64(2)	56(2)	63(2)	-11(2)	-15(2)	-14(2)
O(2')	56(2)	65(2)	34(2)	10(1)	12(1)	18(2)
O(2)	45(2)	138(4)	40(2)	10(2)	9(2)	17(2)
O(6)	62(2)	65(2)	50(2)	21(2)	12(2)	-10(2)
O(7)	45(2)	52(2)	46(2)	11(2)	-1(2)	2(2)
O(7')	41(2)	49(2)	54(2)	17(2)	-3(2)	-3(2)
O(6')	64(2)	61(2)	72(2)	32(2)	-6(2)	-18(2)
O(5)	40(2)	68(2)	57(2)	22(2)	-4(2)	-1(2)
O(4)	40(2)	98(3)	67(2)	10(2)	2(2)	-12(2)
C(5')	36(2)	43(3)	32(2)	2(2)	1(2)	12(2)
C(8')	47(3)	41(3)	41(2)	-1(2)	10(2)	4(2)
C(8)	48(3)	48(3)	34(2)	1(2)	16(2)	13(2)
C(13)	46(3)	41(3)	47(3)	-11(2)	10(2)	-4(2)
C(6)	37(2)	51(3)	33(2)	3(2)	6(2)	-8(2)
C(5)	32(2)	38(3)	39(2)	-5(2)	3(2)	7(2)
C(9')	36(3)	64(3)	51(3)	4(3)	2(2)	1(2)
C(2)	43(2)	30(2)	47(2)	0(2)	10(2)	-2(2)
C(2')	41(2)	33(2)	44(2)	-4(2)	7(2)	-3(2)
C(6')	40(2)	40(3)	39(2)	5(2)	9(2)	0(2)
C(4')	42(2)	56(3)	36(2)	7(2)	4(2)	5(2)
C(15')	79(4)	66(4)	54(3)	3(3)	28(3)	6(3)
C(7')	41(2)	49(3)	34(2)	7(2)	4(2)	-1(2)
C(9)	40(3)	54(3)	51(3)	-2(2)	-4(2)	4(2)
C(13')	44(2)	44(3)	39(2)	-1(2)	9(2)	-3(2)
C(7)	44(3)	72(4)	36(2)	2(2)	8(2)	4(2)
C(11)	69(3)	59(3)	59(3)	-12(3)	3(3)	5(3)
C(11')	59(3)	70(4)	64(3)	-10(3)	4(3)	-3(3)
C(4)	32(2)	62(3)	35(2)	6(2)	5(2)	7(2)
C(3)	52(3)	46(3)	51(3)	15(2)	6(2)	-9(2)
C(3')	62(3)	66(3)	39(2)	0(2)	6(2)	-22(3)
C(10')	64(4)	100(5)	75(4)	-2(3)	22(3)	9(3)
C(10)	45(3)	110(5)	87(4)	-29(4)	8(3)	9(3)
C(14')	81(4)	106(5)	71(4)	-7(4)	-26(3)	-23(4)
C(14)	56(3)	86(4)	55(3)	13(3)	-6(2)	-5(3)
C(15)	151(6)	72(4)	110(5)	11(4)	85(5)	-11(4)
C(12')	53(3)	85(4)	92(4)	30(4)	-18(3)	6(3)
C(12)	72(4)	66(4)	87(4)	14(3)	-23(3)	8(3)

Table 5. Hydrogen coordinates (x 10^4) and isotropic
displacement parameters (A^2 x 10^3) for **8a**.

x	y	z	U(eq)

H(6A)	117	11000	3665	49
H(6B)	-721	10435	2855	49
H(2)	-1437	7707	3563	48
H(2')	3772	8434	8524	48
H(6'A)	5347	11724	8850	48
H(6'B)	4466	11405	8009	48
H(4')	2644	10743	10079	55
H(15D)	4113	8292	12475	96
H(15E)	2947	7774	12027	96
H(15F)	3132	8715	12862	96
H(7'A)	5194	9119	7920	50
H(7'B)	6068	10302	7916	50
H(7A)	107	8187	3002	61
H(7B)	942	9381	2911	61
H(11A)	3872	10738	5450	97
H(11B)	4745	10108	6220	97
H(11C)	3526	10114	6256	97
H(13D)	9006	11275	10490	99
H(13E)	9886	10536	11211	99
H(13F)	8673	10513	11265	99
H(4)	-2421	10187	5037	52
H(3A)	-2752	7902	4583	61
H(3B)	-1538	7426	4927	61
H(3'A)	2150	8799	9285	68
H(3'B)	3221	7970	9712	68
H(10F)	9489	8146	9384	118
H(10D)	10385	9115	9952	118
H(10E)	9414	9826	9299	118
H(10A)	4358	7526	4485	123
H(10B)	5307	8335	5107	123
H(10C)	4446	9205	4438	123
H(14F)	643	9458	6905	140
H(14E)	1059	8286	6355	140
H(14D)	1505	9862	6387	140
H(14A)	-3837	9103	1494	103
H(14B)	-3294	10556	1328	103
H(14C)	-4059	10508	1967	103
H(15A)	-1304	7696	7368	153
H(15B)	-2465	7501	6782	153
H(15C)	-2312	8217	7690	153
H(12E)	8855	7874	11418	124
H(12F)	10018	7821	11247	124
H(12D)	9079	6943	10660	124
H(12A)	3586	7404	6493	122
H(12B)	4817	7479	6499	122
H(12C)	4055	6435	5864	122
H(3)	940(30)	7870(50)	4350(20)	43(13)
H(3')	6170(30)	8420(50)	9200(30)	44(14)

Table 6. Torsion angles [deg] for **8a**.

O(3')-S(1')-O(2')-C(4')	-95.7(4)
O(8')-S(1')-O(2')-C(4')	33.8(4)
C(15')-S(1')-O(2')-C(4')	150.6(4)
O(3)-S(2)-O(2)-C(4)	-130.2(4)
O(8)-S(2)-O(2)-C(4)	0.1(5)
C(15)-S(2)-O(2)-C(4)	117.8(5)
C(2')-N(1')-C(5')-O(1')	-179.3(4)
C(6')-N(1')-C(5')-O(1')	-5.6(6)
C(2')-N(1')-C(5')-C(4')	0.1(5)
C(6')-N(1')-C(5')-C(4')	173.8(3)
C(7')-N(2')-C(8')-O(6')	3.9(7)
C(7')-N(2')-C(8')-O(7')	-177.4(4)
C(9')-O(7')-C(8')-O(6')	-13.4(7)
C(9')-O(7')-C(8')-N(2')	168.0(4)
C(7)-N(2)-C(8)-O(6)	7.7(7)
C(7)-N(2)-C(8)-O(7)	-171.8(4)
C(9)-O(7)-C(8)-O(6)	-6.0(6)
C(9)-O(7)-C(8)-N(2)	173.6(3)
C(14)-O(5)-C(13)-O(4)	-0.3(7)
C(14)-O(5)-C(13)-C(2)	175.4(4)
C(5)-N(1)-C(6)-C(7)	112.5(4)
C(2)-N(1)-C(6)-C(7)	-62.3(5)
C(6)-N(1)-C(5)-O(1)	1.9(6)
C(2)-N(1)-C(5)-O(1)	177.3(4)
C(6)-N(1)-C(5)-C(4)	-179.3(3)
C(2)-N(1)-C(5)-C(4)	-3.8(5)
C(8')-O(7')-C(9')-C(11')	67.5(5)
C(8')-O(7')-C(9')-C(12')	-174.5(4)
C(8')-O(7')-C(9')-C(10')	-57.0(5)
C(5)-N(1)-C(2)-C(13)	107.7(4)
C(6)-N(1)-C(2)-C(13)	-77.1(5)
C(5)-N(1)-C(2)-C(3)	-14.5(4)
C(6)-N(1)-C(2)-C(3)	160.7(4)
O(4)-C(13)-C(2)-N(1)	-142.8(4)
O(5)-C(13)-C(2)-N(1)	41.5(5)
O(4)-C(13)-C(2)-C(3)	-25.4(6)
O(5)-C(13)-C(2)-C(3)	158.8(4)
C(5')-N(1')-C(2')-C(13')	110.9(4)
C(6')-N(1')-C(2')-C(13')	-62.9(5)
C(5')-N(1')-C(2')-C(3')	-10.8(5)
C(6')-N(1')-C(2')-C(3')	175.4(4)
C(5')-N(1')-C(6')-C(7')	124.7(4)
C(2')-N(1')-C(6')-C(7')	-62.1(5)
S(1')-O(2')-C(4')-C(3')	-128.0(3)
S(1')-O(2')-C(4')-C(5')	116.7(3)
O(1')-C(5')-C(4')-O(2')	-51.4(6)
N(1')-C(5')-C(4')-O(2')	129.1(4)
O(1')-C(5')-C(4')-C(3')	-169.7(4)
N(1')-C(5')-C(4')-C(3')	10.8(5)
C(8')-N(2')-C(7')-C(6')	-87.1(5)

N(1')-C(6')-C(7')-N(2')	-60.2(5)
C(8)-O(7)-C(9)-C(11)	67.4(5)
C(8)-O(7)-C(9)-C(10)	-55.3(6)
C(8)-O(7)-C(9)-C(12)	-174.8(4)
C(14')-O(5')-C(13')-O(4')	-2.4(7)
C(14')-O(5')-C(13')-C(2')	177.6(4)
N(1')-C(2')-C(13')-O(4')	-23.5(6)
C(3')-C(2')-C(13')-O(4')	93.2(5)
N(1')-C(2')-C(13')-O(5')	156.5(4)
C(3')-C(2')-C(13')-O(5')	-86.8(4)
C(8)-N(2)-C(7)-C(6)	-96.5(5)
N(1)-C(6)-C(7)-N(2)	-59.4(5)
S(2)-O(2)-C(4)-C(3)	-112.2(4)
S(2)-O(2)-C(4)-C(5)	133.4(4)
O(1)-C(5)-C(4)-O(2)	-40.2(6)
N(1)-C(5)-C(4)-O(2)	140.9(4)
O(1)-C(5)-C(4)-C(3)	-160.3(4)
N(1)-C(5)-C(4)-C(3)	20.9(4)
O(2)-C(4)-C(3)-C(2)	-145.2(3)
C(5)-C(4)-C(3)-C(2)	-28.4(4)
N(1)-C(2)-C(3)-C(4)	26.2(4)
C(13)-C(2)-C(3)-C(4)	-97.0(4)
O(2')-C(4')-C(3')-C(2')	-134.6(4)
C(5')-C(4')-C(3')-C(2')	-16.7(5)
N(1')-C(2')-C(3')-C(4')	16.6(4)
C(13')-C(2')-C(3')-C(4')	-104.6(4)

Symmetry transformations used to generate equivalent atoms:

Table 7. Hydrogen bonds for **8a** [A and deg.].

Nr	Typ	Res	Donor	---	H	....Acceptor	[ARU]	D - H	H...A	D...A	D - H...A
1		2	N2	--	H3	.. O1	[2546.02]	0.8755	2.0130	2.8882	178.14
2		1	N2'	--	H3'	.. O1'	[2645.01]	0.8200	2.2111	3.0063	163.47
3	Intra	1	C6'	--	H6'A	.. O1'	[ ]	0.9700	2.5028	2.8896	103.64
4	Intra	2	C3	--	H3A	.. O4	[ ]	0.9700	2.4046	2.8325	106.18
5		2	C3	--	H3B	.. O1	[2546.02]	0.9700	2.5887	3.3900	140.05
6	Intra	2	C4	--	H4	.. O8	[ ]	0.9800	2.3522	2.8172	108.25
7	Intra	1	C4'	--	H4'	.. O8'	[ ]	0.9800	2.4194	2.8704	107.49
8	Intra	2	C6	--	H6A	.. O1	[ ]	0.9700	2.4355	2.8415	104.73
9	Intra	2	C6	--	H6B	.. O5	[ ]	0.9700	2.4474	3.0366	118.83
10	Intra	2	C10	--	H10C	.. O6	[ ]	0.9600	2.4438	2.9712	114.35
11	Intra	1	C10'	--	H10E	.. O6'	[ ]	0.9600	2.4283	3.0118	118.90
12	Intra	2	C11	--	H11A	.. O6	[ ]	0.9600	2.5106	3.0621	116.51
13	Intra	1	C11'	--	H13D	.. O6'	[ ]	0.9600	2.4597	3.0086	116.13
14		1	C14'	--	H14F	.. O2	[2646.02]	0.9600	2.5508	3.2023	125.25
15		1	C15'	--	H15E	.. O6'	[2645.01]	0.9600	2.5730	3.4820	158.07
16		1	C15'	--	H15F	.. O6	[2645.02]	0.9600	2.5282	3.4433	159.39

Translation of ARU-code to Equivalent Position Code

[2645.] = 1-x,-1/2+y,-z
[2646.] = 1-x,-1/2+y,1-z
[2546.] = -x,-1/2+y,1-z

2. Compound **8e**; Crystal data and structure refinement

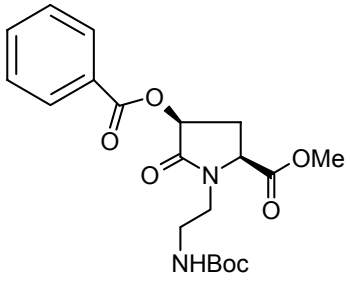

8e

Crystal data and structure refinement for 8e

Identification code	**8e**
Empirical formula	$C_{20}H_{25}N_2O_7$
Formula weight	405.42 Temperature 293(2) K Wavelength 0.71073 A
Crystal system, space group	Monoclinic, P21
Unit cell dimensions	a = 9.2779(15) A alpha = 90 deg. b = 8.9289(14) A beta = 96.512(3) deg. c = 13.239(2) A gamma = 90 deg.
Volume	1089.7(3) A^3
	Z, Calculated density 2, 1.236 Mg/m^3
Absorption coefficient	0.094 mm^-1
F(000)	430
Crystal size	0.61 x 0.59 x 0.14 mm
Theta range for data collection	1.55 to 25.00 deg.
Limiting indices	-9<=h<=11, -10<=k<=9, - 15<=1<=11
Reflections collected / unique	5493 / 3634 [R(int) = 0.0188]
Completeness to theta = 25.00	98.9 %
Max. and min. transmission	0.9873 and 0.9452
Refinement method	Full-matrix least-squares on F^2
Data / restraints / parameters	3634 / 1 / 267
Goodness-of-fit on F^2	1.046
Final R indices [I>2sigma(I)]	R1 = 0.0415, wR2 = 0.1177
R indices (all data)	R1 = 0.0439, wR2 = 0.1199
Absolute structure parameter	-0.4(9)
Extinction coefficient	0.012(4)
Largest diff. peak and hole	0.249 and -0.173 e.A^-3

Table 2. Atomic coordinates (x 10^4) and equivalent isotropic displacement parameters (A^2 x 10^3) for **8e**. U(eq) is defined as one third of the trace of the orthogonalized Uij tensor.

	x	y	z	U(eq)
O(2)	7190(2)	4552(2)	5979(1)	59(1)
O(7)	10325(2)	4215(2)	1593(1)	64(1)
O(3)	8229(2)	2848(2)	7067(1)	76(1)
O(6)	7877(2)	4048(2)	1582(1)	68(1)
O(5)	4165(2)	4162(2)	3769(1)	72(1)
C(20)	5127(2)	5225(2)	3995(1)	52(1)
N(1)	7687(2)	5924(2)	3939(1)	53(1)
C(8)	9009(2)	4738(2)	1745(1)	51(1)
N(2)	9146(2)	6150(2)	2099(1)	59(1)
C(14)	6249(2)	4283(2)	7537(1)	53(1)
O(1)	9545(2)	6479(2)	5179(1)	80(1)
O(4)	4882(2)	6392(2)	4386(1)	78(1)
C(5)	8575(2)	5662(3)	4789(2)	57(1)
C(19)	5297(2)	5450(3)	7290(2)	60(1)
C(7)	7890(2)	7055(2)	2252(2)	60(1)
C(13)	7326(2)	3788(2)	6851(2)	53(1)
C(2)	6603(2)	4761(2)	3702(1)	53(1)
C(15)	6235(3)	3565(3)	8465(2)	70(1)
C(4)	8126(2)	4147(3)	5212(2)	59(1)
C(6)	7721(2)	7313(2)	3363(2)	59(1)
C(3)	7257(2)	3429(2)	4325(2)	61(1)
C(18)	4371(3)	5912(3)	7978(2)	72(1)
C(17)	4390(3)	5214(4)	8899(2)	80(1)
C(21)	2732(3)	4390(4)	4081(3)	90(1)
C(11)	9558(4)	2512(4)	179(2)	100(1)
C(16)	5318(3)	4034(4)	9138(2)	85(1)
C(10)	10154(4)	1545(3)	1952(2)	87(1)
C(9)	10508(3)	2703(3)	1187(2)	70(1)
C(12)	12112(4)	2685(5)	1049(3)	114(1)

Table 3. Bond lengths [A] and angles [deg] for **8e**.

O(2)-C(13)	1.335(2)
O(2)-C(4)	1.454(2)
O(7)-C(8)	1.344(3)

O(7)-C(9)	1.471(3)
O(3)-C(13)	1.198(3)
O(6)-C(8)	1.216(3)
O(5)-C(20)	1.315(3)
O(5)-C(21)	1.450(3)
C(20)-O(4)	1.197(3)
C(20)-C(2)	1.522(3)
N(1)-C(5)	1.338(3)
N(1)-C(2)	1.455(3)
N(1)-C(6)	1.458(3)
C(8)-N(2)	1.346(3)
N(2)-C(7)	1.450(3)
C(14)-C(19)	1.381(3)
C(14)-C(15)	1.388(3)
C(14)-C(13)	1.491(3)
O(1)-C(5)	1.226(3)
C(5)-C(4)	1.540(3)
C(19)-C(18)	1.384(3)
C(7)-C(6)	1.514(3)
C(2)-C(3)	1.533(3)
C(15)-C(16)	1.365(4)
C(4)-C(3)	1.492(3)
C(18)-C(17)	1.368(4)
C(17)-C(16)	1.375(4)
C(11)-C(9)	1.523(4)
C(10)-C(9)	1.509(4)
C(9)-C(12)	1.520(4)
C(13)-O(2)-C(4)	118.14(16)
C(8)-O(7)-C(9)	121.20(18)
C(20)-O(5)-C(21)	117.0(2)
O(4)-C(20)-O(5)	124.7(2)
O(4)-C(20)-C(2)	124.62(19)
O(5)-C(20)-C(2)	110.64(18)
C(5)-N(1)-C(2)	113.66(16)
C(5)-N(1)-C(6)	122.75(18)
C(2)-N(1)-C(6)	123.35(16)
O(6)-C(8)-O(7)	125.4(2)
O(6)-C(8)-N(2)	125.58(19)
O(7)-C(8)-N(2)	109.02(17)
C(8)-N(2)-C(7)	121.66(17)
C(19)-C(14)-C(15)	119.2(2)
C(19)-C(14)-C(13)	122.34(18)
C(15)-C(14)-C(13)	118.4(2)
O(1)-C(5)-N(1)	127.1(2)
O(1)-C(5)-C(4)	125.8(2)
N(1)-C(5)-C(4)	107.05(18)
C(14)-C(19)-C(18)	119.9(2)
N(2)-C(7)-C(6)	113.19(18)
O(3)-C(13)-O(2)	124.0(2)
O(3)-C(13)-C(14)	124.19(19)
O(2)-C(13)-C(14)	111.78(16)
N(1)-C(2)-C(20)	111.74(16)
N(1)-C(2)-C(3)	102.50(16)
C(20)-C(2)-C(3)	112.74(16)
C(16)-C(15)-C(14)	120.4(3)
O(2)-C(4)-C(3)	110.12(17)
O(2)-C(4)-C(5)	104.04(17)
C(3)-C(4)-C(5)	103.65(17)
N(1)-C(6)-C(7)	112.91(17)
C(4)-C(3)-C(2)	103.62(17)
C(17)-C(18)-C(19)	120.3(2)
C(18)-C(17)-C(16)	119.9(3)
C(15)-C(16)-C(17)	120.3(2)
O(7)-C(9)-C(10)	109.88(19)
O(7)-C(9)-C(12)	102.0(3)
C(10)-C(9)-C(12)	111.3(3)
O(7)-C(9)-C(11)	110.2(2)
C(10)-C(9)-C(11)	111.3(3)
C(12)-C(9)-C(11)	111.8(2)

Symmetry transformations used to generate equivalent atoms:

Table 4. Torsion angles [deg] for **8e**.

C(21)-O(5)-C(20)-O(4)	-4.4(3)
C(21)-O(5)-C(20)-C(2)	175.01(19)
C(9)-O(7)-C(8)-O(6)	0.7(3)
C(9)-O(7)-C(8)-N(2)	-178.71(16)
O(6)-C(8)-N(2)-C(7)	-4.8(3)
O(7)-C(8)-N(2)-C(7)	174.60(17)
C(2)-N(1)-C(5)-O(1)	-177.3(2)
C(6)-N(1)-C(5)-O(1)	-2.8(3)
C(2)-N(1)-C(5)-C(4)	1.2(2)
C(6)-N(1)-C(5)-C(4)	175.64(16)
C(15)-C(14)-C(19)-C(18)	1.6(3)
C(13)-C(14)-C(19)-C(18)	-176.7(2)
C(8)-N(2)-C(7)-C(6)	109.2(2)
C(4)-O(2)-C(13)-O(3)	4.6(3)
C(4)-O(2)-C(13)-C(14)	-177.26(17)
C(19)-C(14)-C(13)-O(3)	174.9(2)
C(15)-C(14)-C(13)-O(3)	-3.4(3)
C(19)-C(14)-C(13)-O(2)	-3.2(3)
C(15)-C(14)-C(13)-O(2)	178.5(2)
C(5)-N(1)-C(2)-C(20)	101.54(19)
C(6)-N(1)-C(2)-C(20)	-72.9(2)
C(5)-N(1)-C(2)-C(3)	-19.4(2)
C(6)-N(1)-C(2)-C(3)	166.15(16)
O(4)-C(20)-C(2)-N(1)	-1.0(3)
O(5)-C(20)-C(2)-N(1)	179.59(16)
O(4)-C(20)-C(2)-C(3)	113.9(2)
O(5)-C(20)-C(2)-C(3)	-65.6(2)
C(19)-C(14)-C(15)-C(16)	-1.8(4)

```
          C(13)-C(14)-C(15)-C(16)                          176.6(2)
          C(13)-O(2)-C(4)-C(3)                             110.4(2)
          C(13)-O(2)-C(4)-C(5)                            -139.07(18)
          O(1)-C(5)-C(4)-O(2)                               81.5(2)
          N(1)-C(5)-C(4)-O(2)                              -97.02(18)
          O(1)-C(5)-C(4)-C(3)                             -163.3(2)
          N(1)-C(5)-C(4)-C(3)                               18.2(2)
          C(5)-N(1)-C(6)-C(7)                              126.2(2)
          C(2)-N(1)-C(6)-C(7)                              -59.8(2)
          N(2)-C(7)-C(6)-N(1)                              -54.8(2)
          O(2)-C(4)-C(3)-C(2)                               81.8(2)
          C(5)-C(4)-C(3)-C(2)                              -29.0(2)
          N(1)-C(2)-C(3)-C(4)                               29.46(19)
          C(20)-C(2)-C(3)-C(4)                             -90.83(19)
          C(14)-C(19)-C(18)-C(17)                           -0.3(4)
          C(19)-C(18)-C(17)-C(16)                           -0.9(4)
          C(14)-C(15)-C(16)-C(17)                            0.6(4)
          C(18)-C(17)-C(16)-C(15)                            0.8(5)
          C(8)-O(7)-C(9)-C(10)                             -67.4(3)
          C(8)-O(7)-C(9)-C(12)                             174.4(2)
          C(8)-O(7)-C(9)-C(11)                                                    55.6(3)
_____________________________________________________
         Symmetry transformations used to generate equivalent atoms:
=========================================================
Analysis of Potential Hydrogen Bonds
=========================================================
 Nr Typ  Donor --- H....Acceptor   H...A      D...A  D - H...A
---------------------------------------------------------------------
 1 Intra  C(2)  -- H(2)  .. O(6)  2.3845     3.2305     144.18
 2 Intra  C(3)  -- H(3A) .. O(5)  2.5967     2.9532     101.88
 3 Inter  C(3)  -- H(3A) .. O(4)  2.3734     3.3048     160.76'
 4 Intra  C(4)  -- H(4)  .. O(3)  2.3538     2.7081     100.40
 5 Inter  C(4)  -- H(4)  .. O(1)  2.5228     3.2966     135.77'
 6 Intra  C(6)  -- H(6A) .. O(1)  2.4830     2.8770     104.07
 7 Intra  C(7)  -- H(7A) .. O(6)  2.4426     2.8272     103.24
 8 Intra  C(10) -- H(10C).. O(6)  2.5297     3.0765     116.20
 9 Intra  C(11) -- H(11A).. O(6)  2.3754     2.9021     114.04

:: No Classic Hydrogen Bonds Found
```

3. Compound **8a**; ^{1}H ,^{13}C and ^{13}C-DEPT NMR spectra

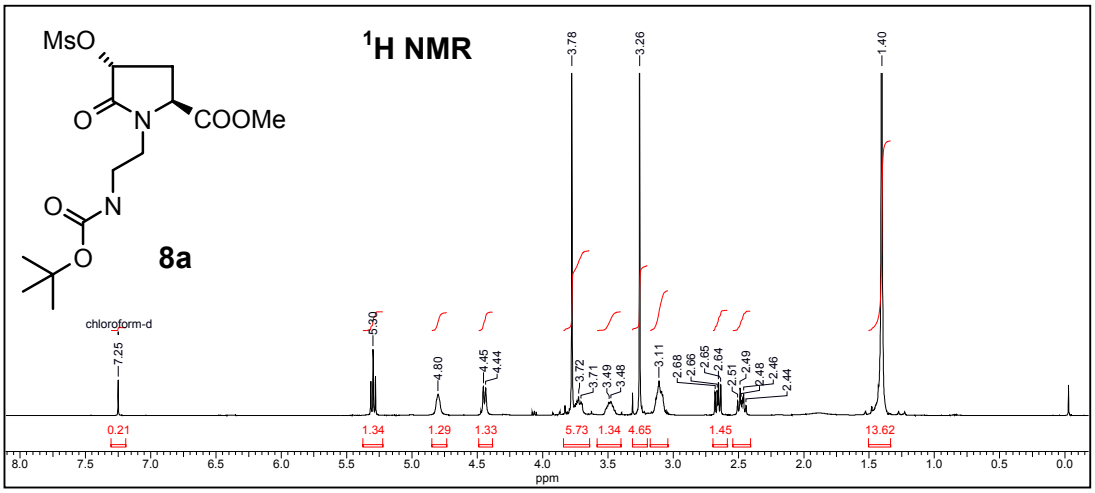

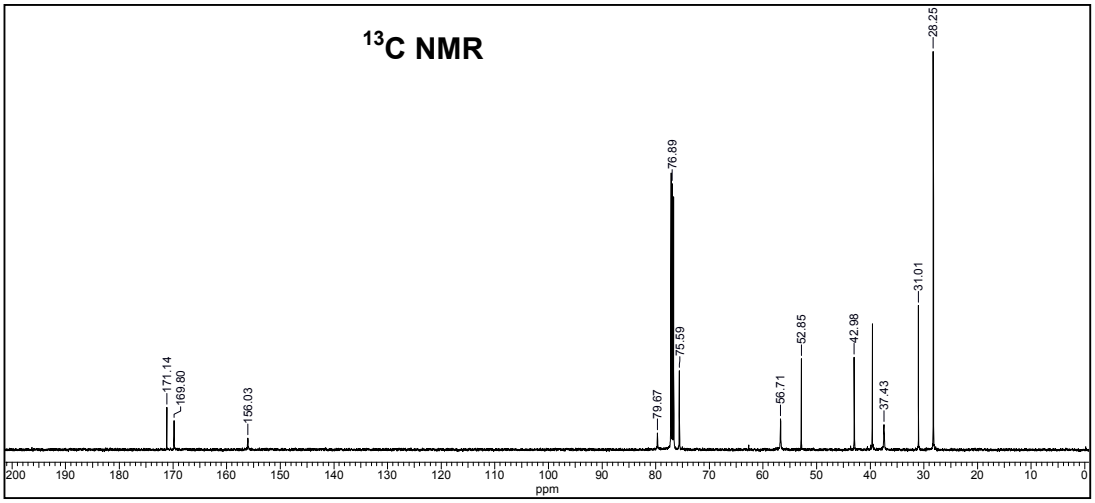

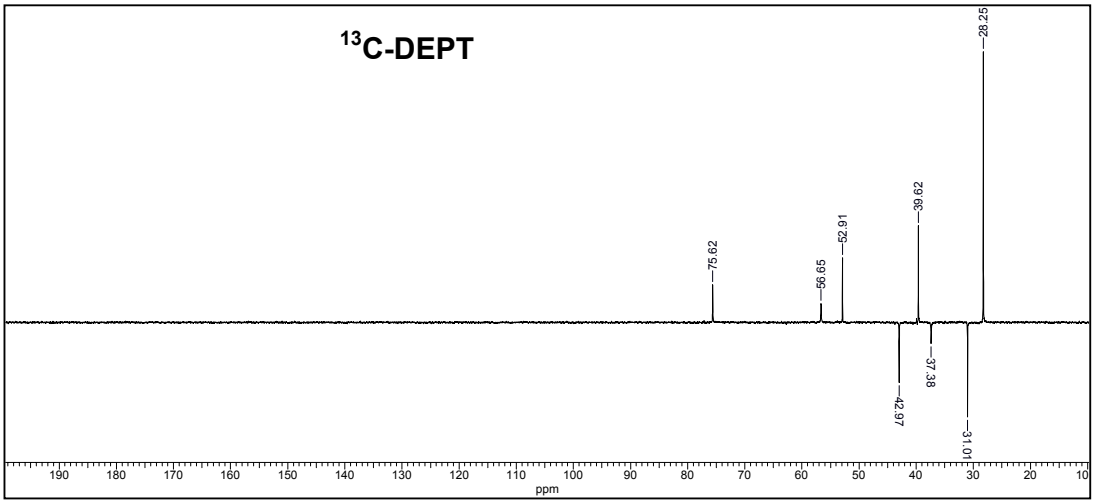

4. Compound **8b**; ^{1}H ,^{13}C and ^{13}C-DEPT NMR

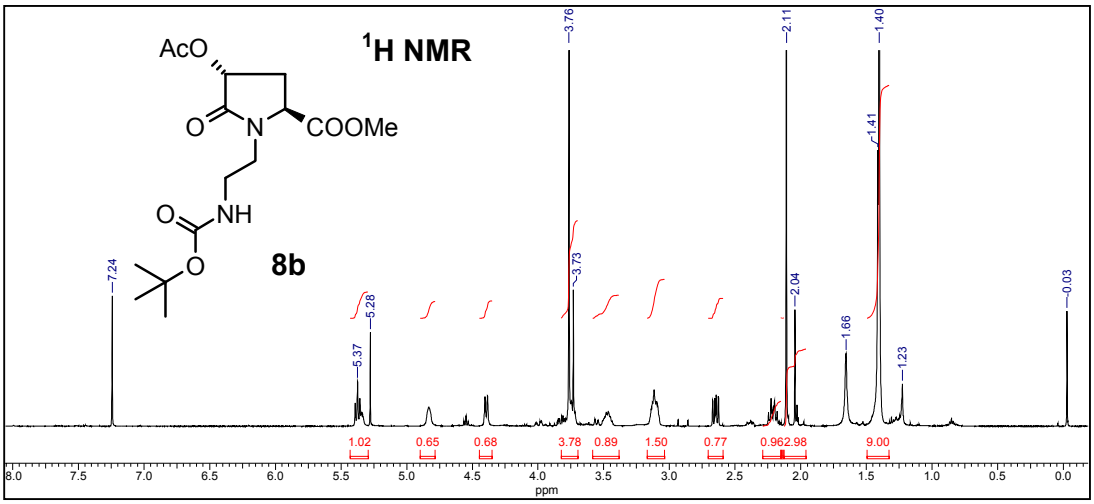

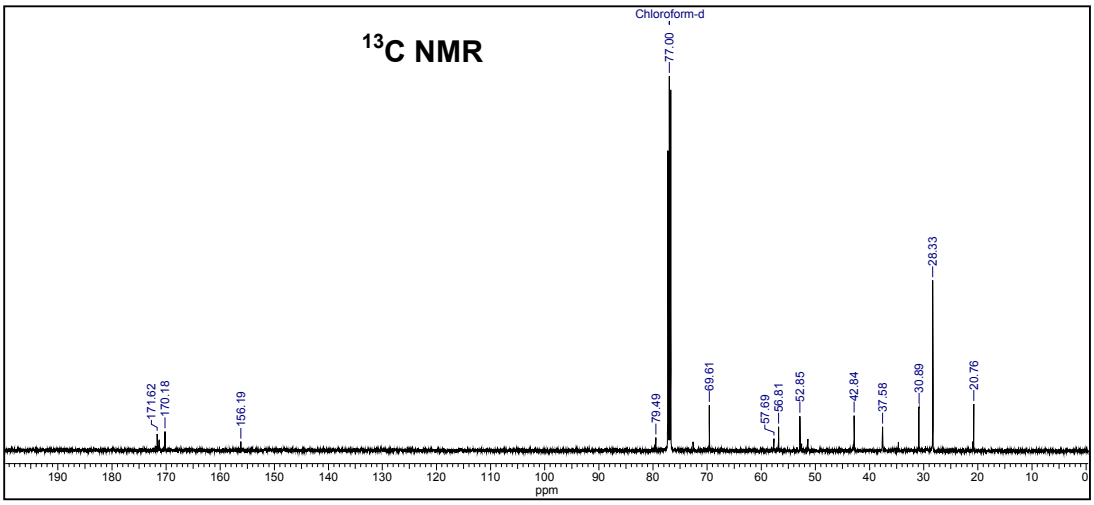

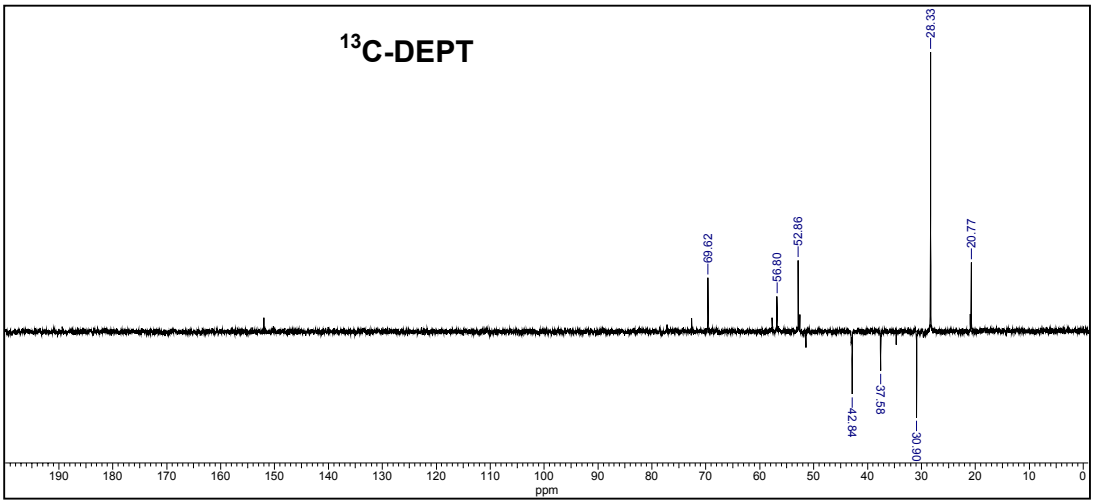

5. Compound **8e**; ^{1}H ,^{13}C and ^{13}C-DEPT NMR

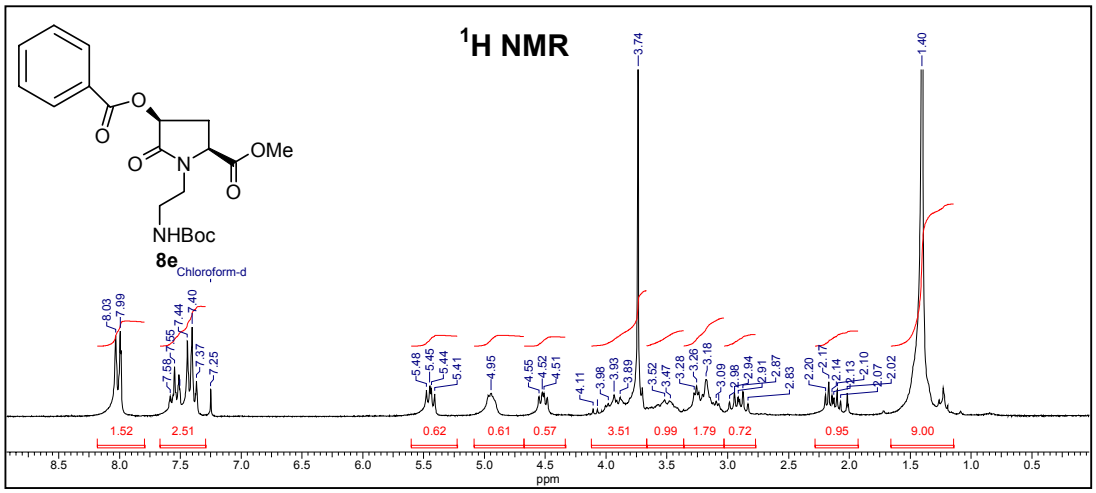

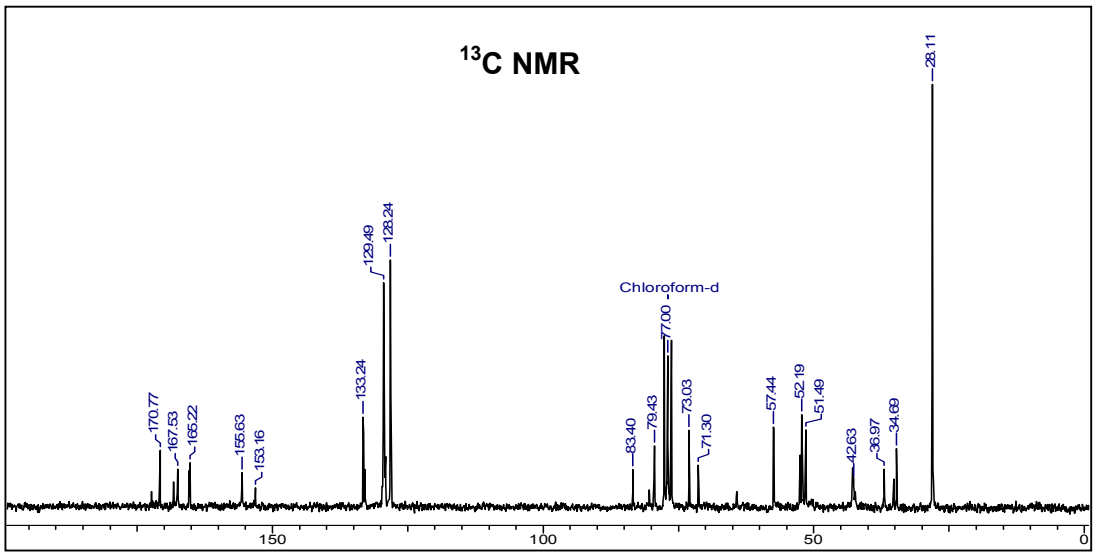

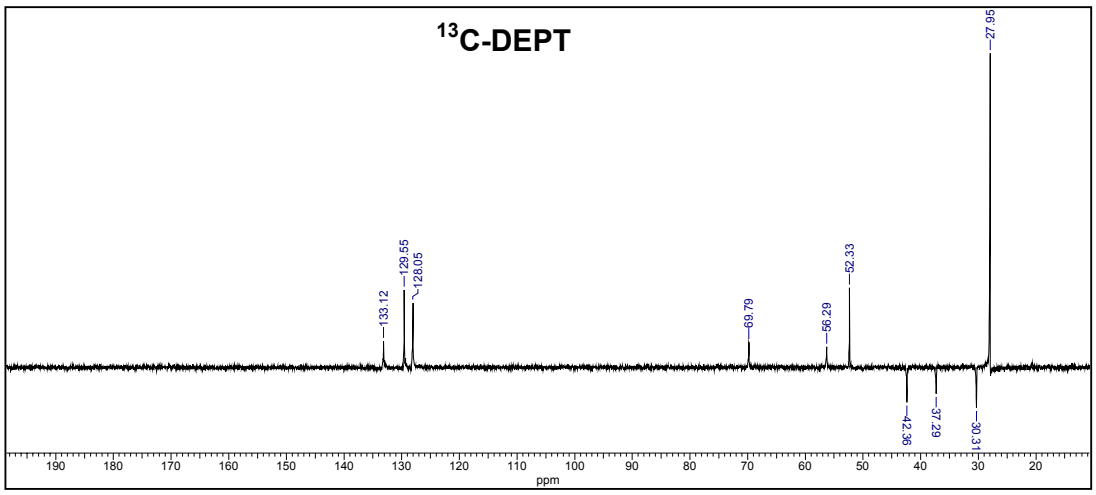

6. Compound **7f**; ^{1}H ,^{13}C and ^{13}C-DEPT NMR

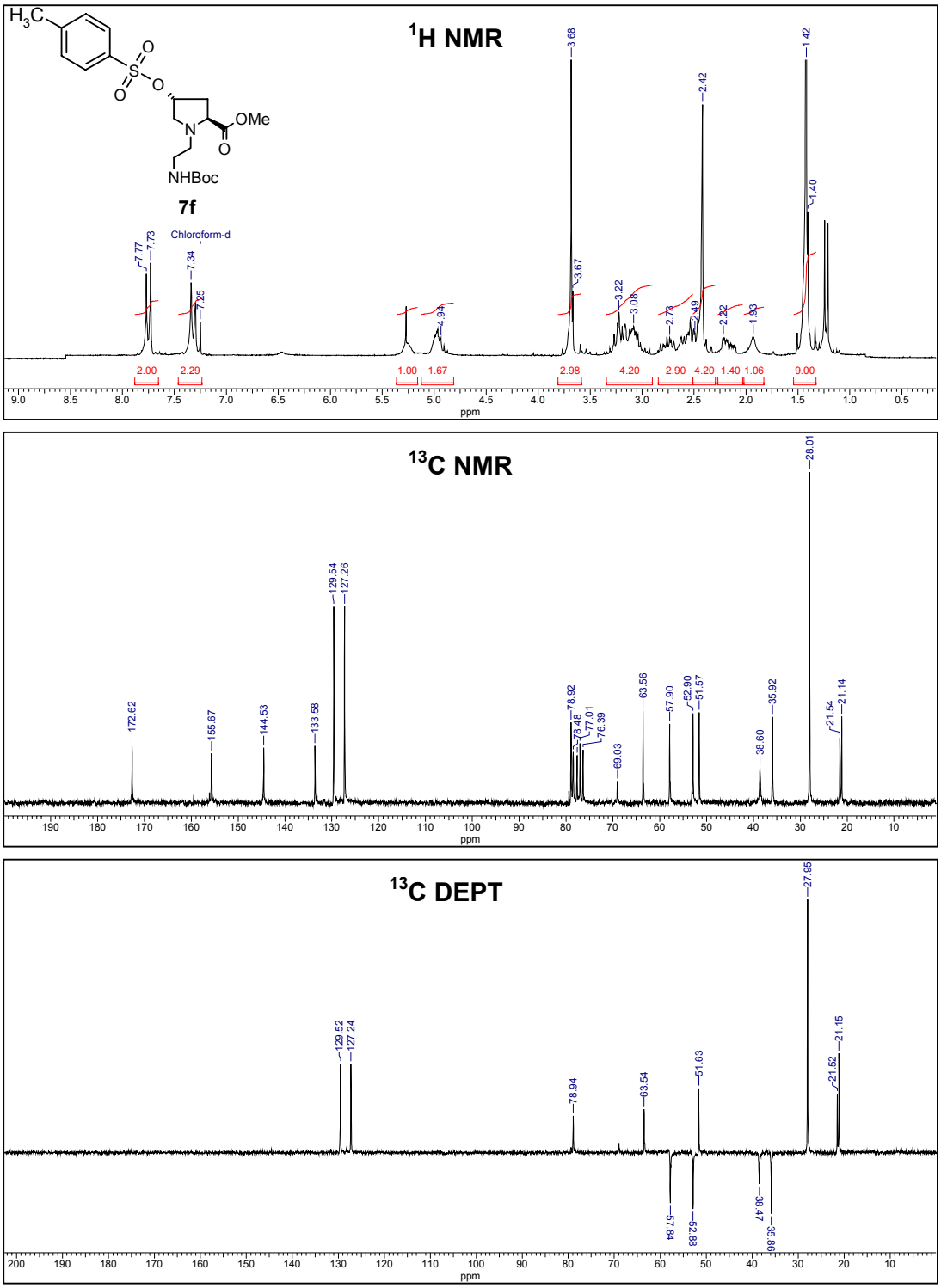

7. Compound **8f**; ^{1}H ,^{13}C and ^{13}C-DEPT NMR

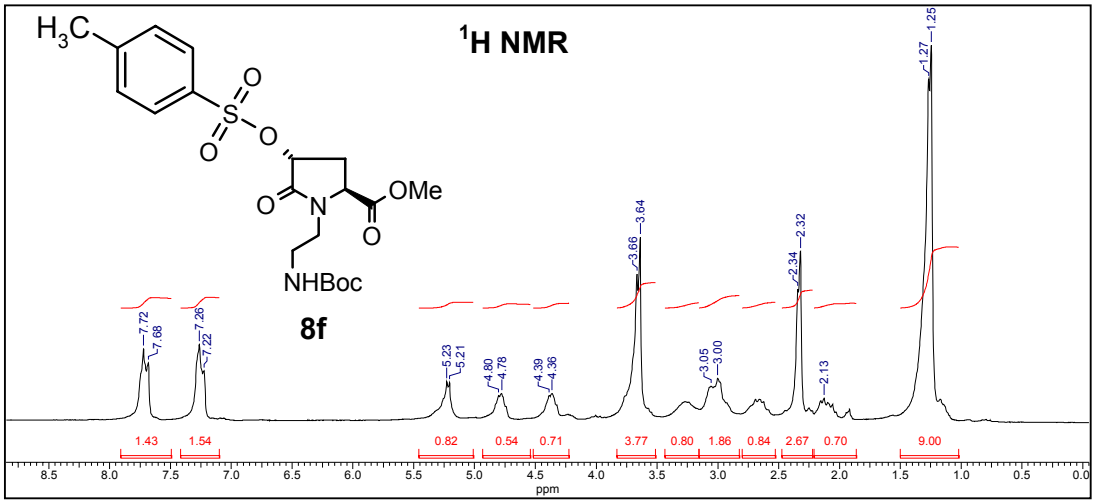

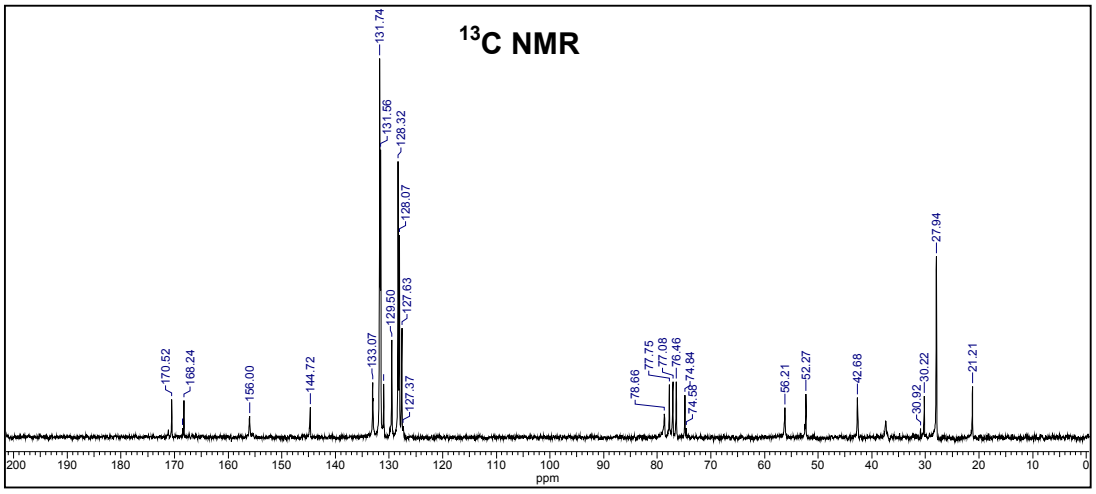

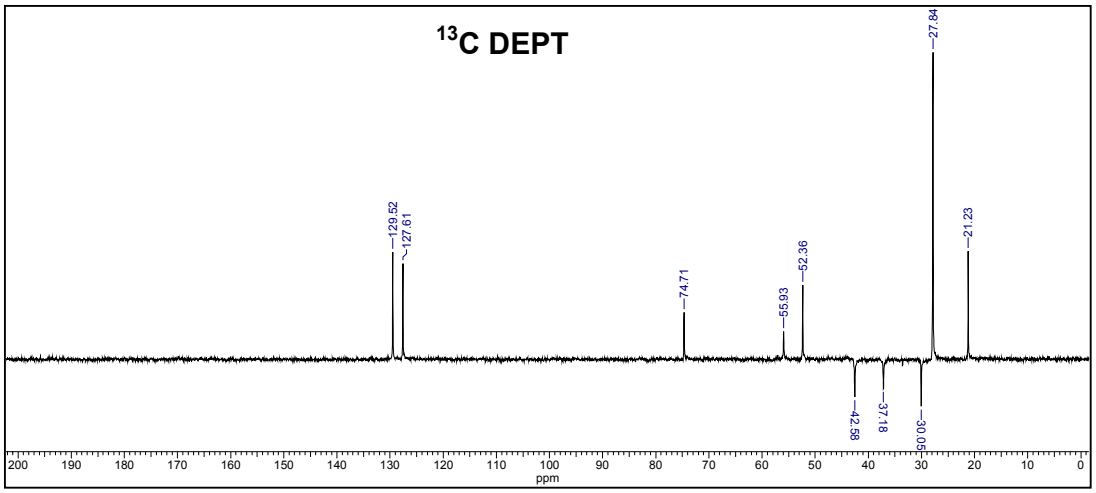

8. Compound **8h**; ^{1}H ,^{13}C and ^{13}C-DEPT NMR spectra

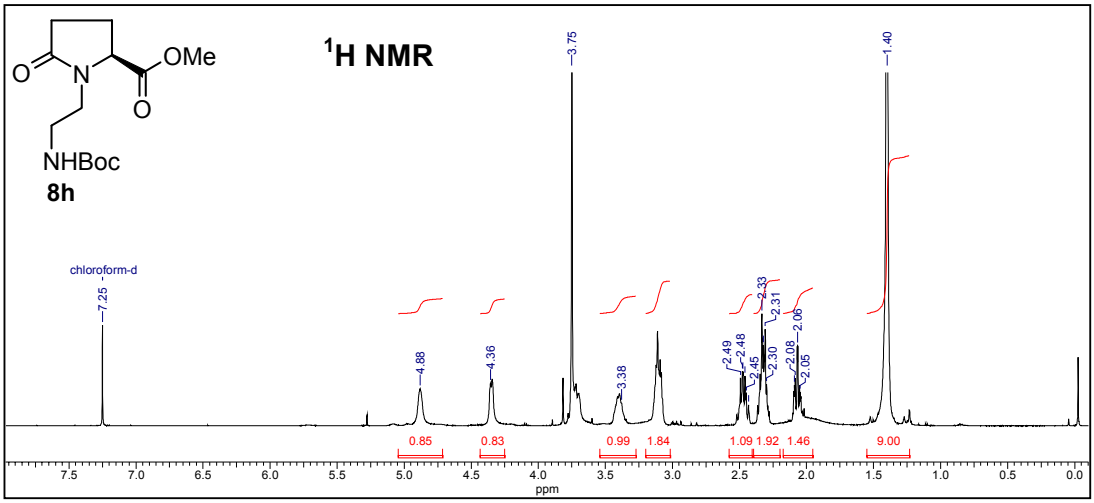

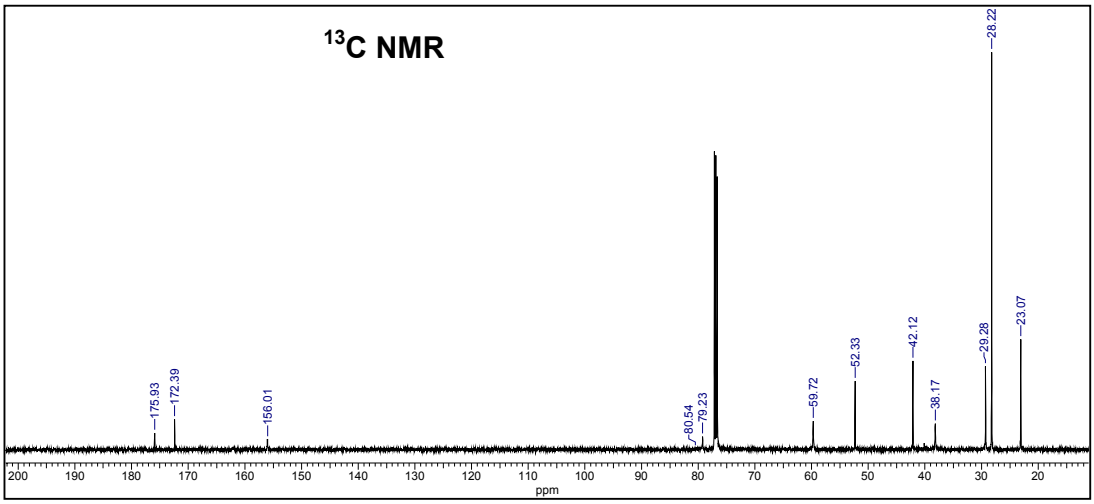

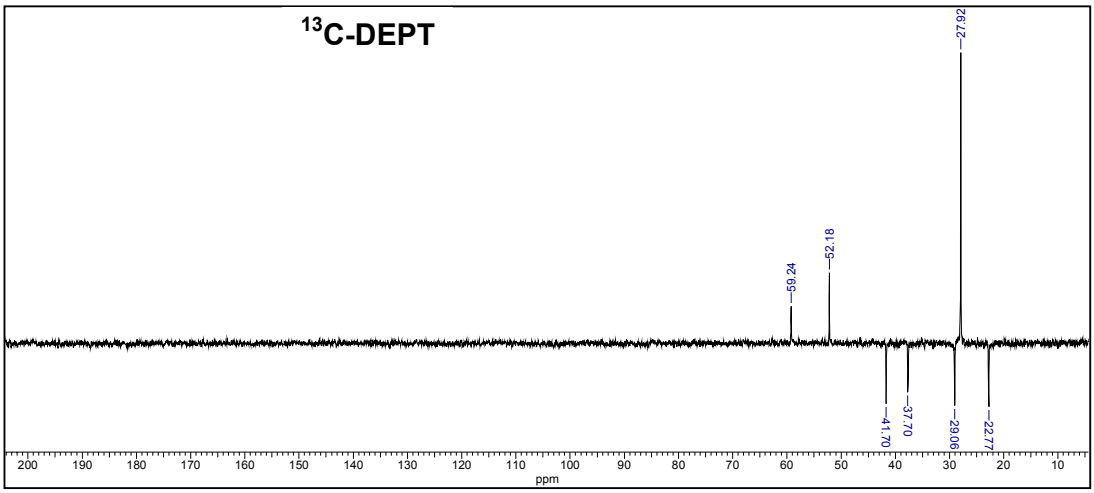

9. Compound **17**; ^{1}H , ^{13}C and ^{13}C-DEPT NMR spectra

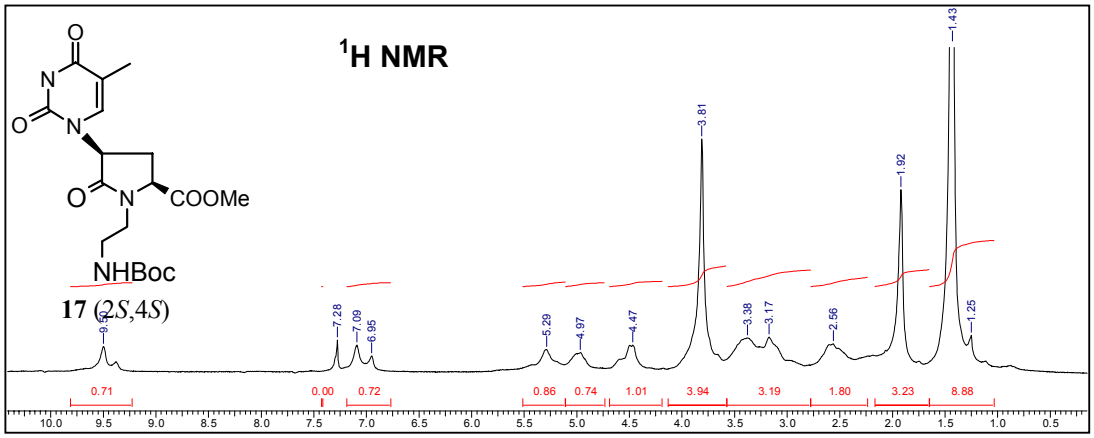

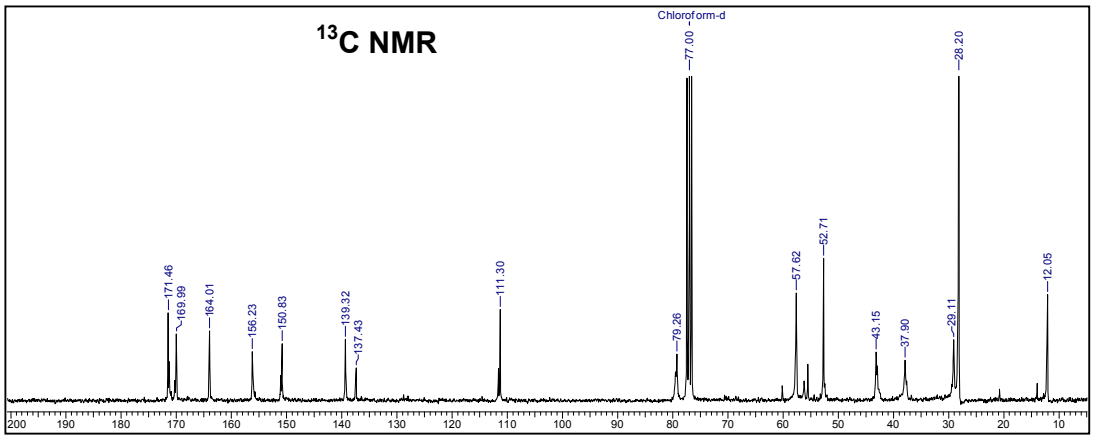

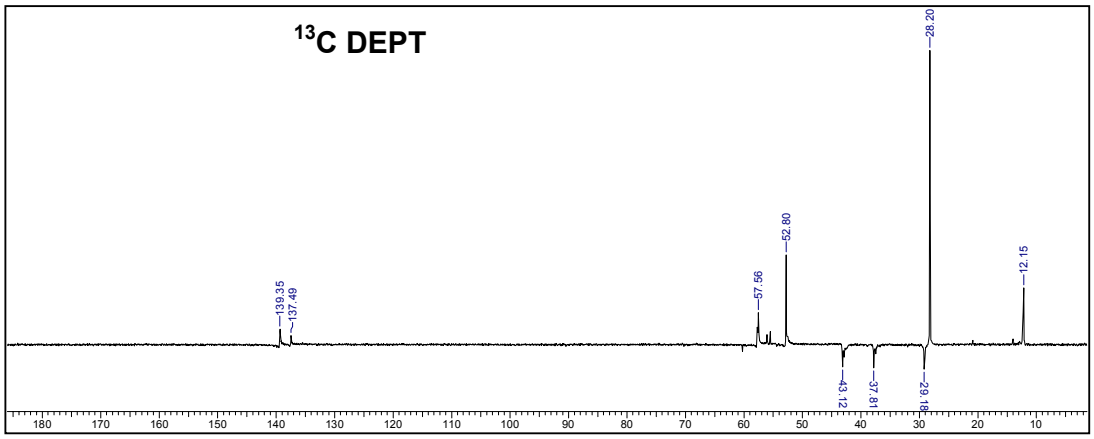

10. Compound **18**; ^{1}H and ^{13}C NMR spectra

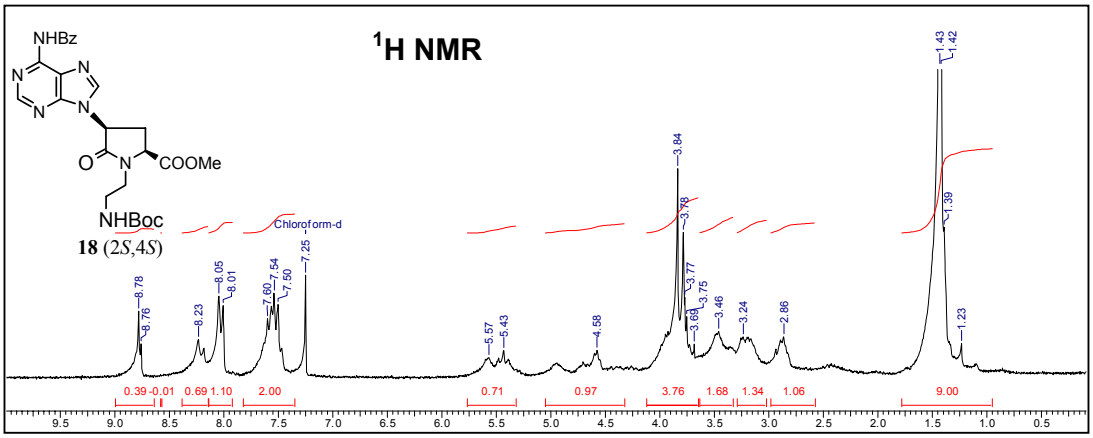

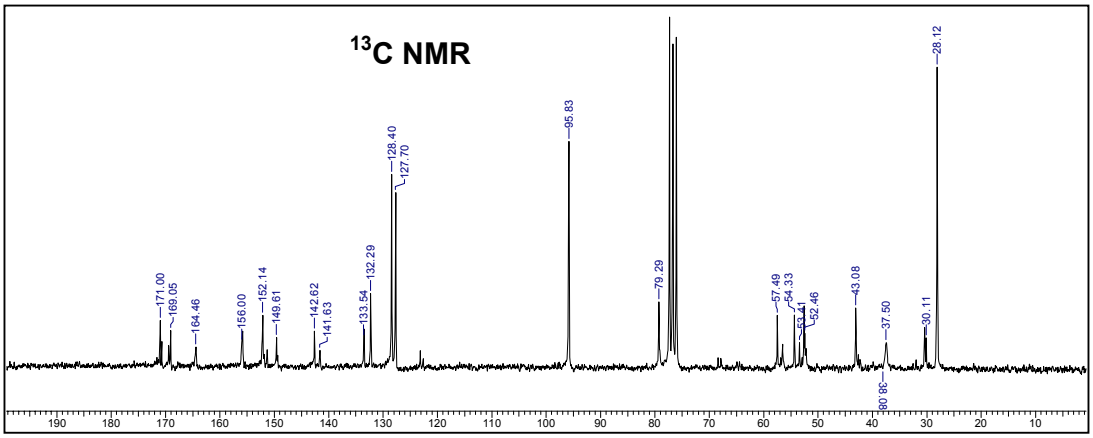

11. Compound **19**; ^{1}H ,^{13}C and ^{13}C-DEPT NMR spectra

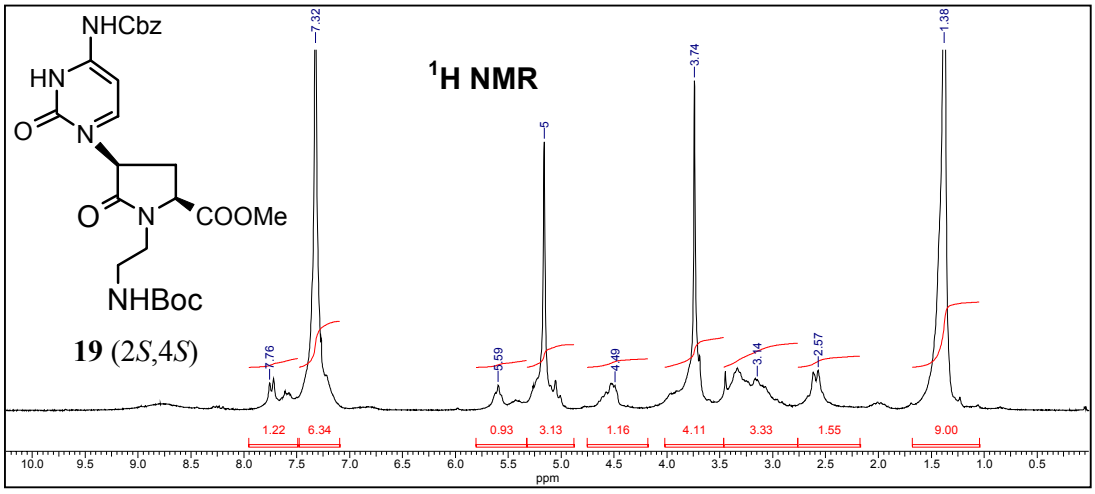

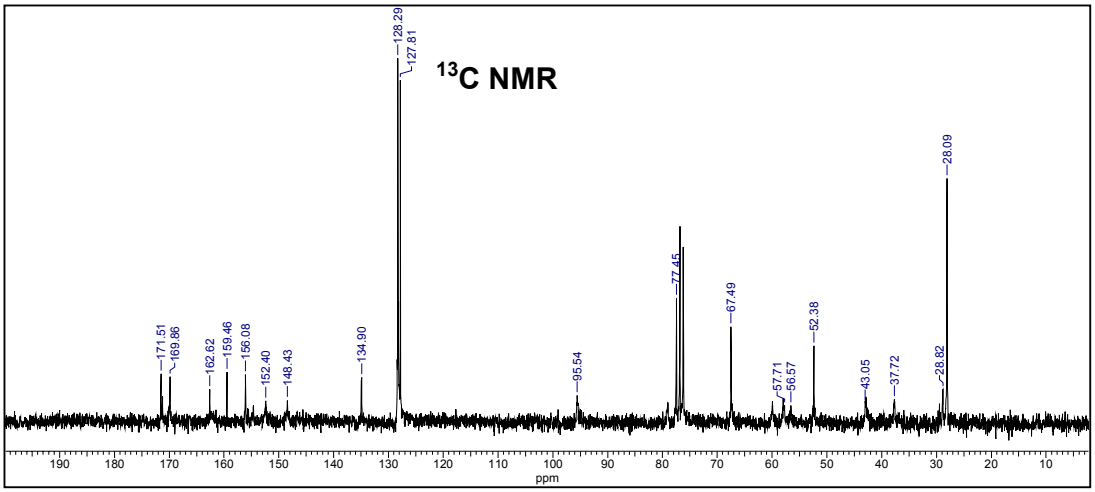

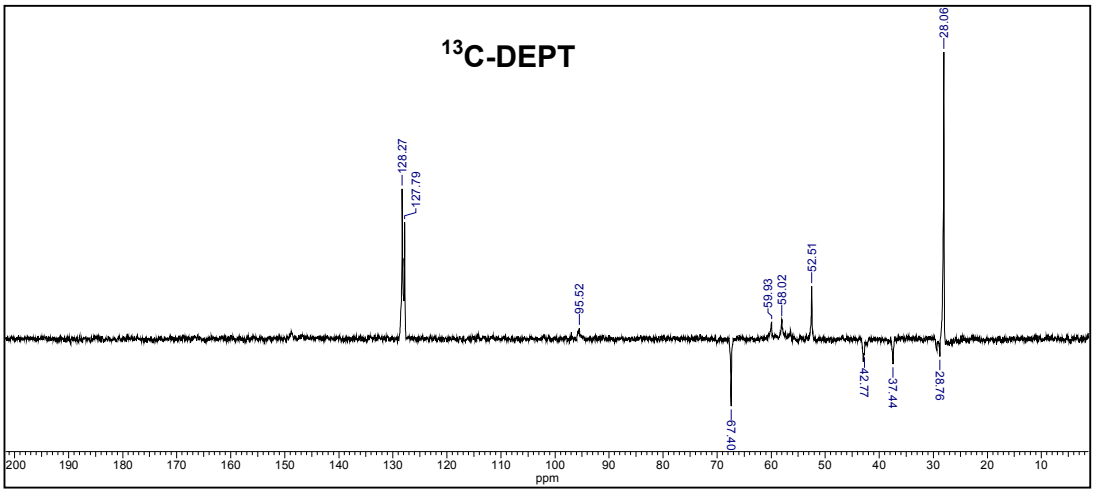

12. Compound **20**; ^{1}H ,^{13}C and ^{13}C-DEPT NMR spectra

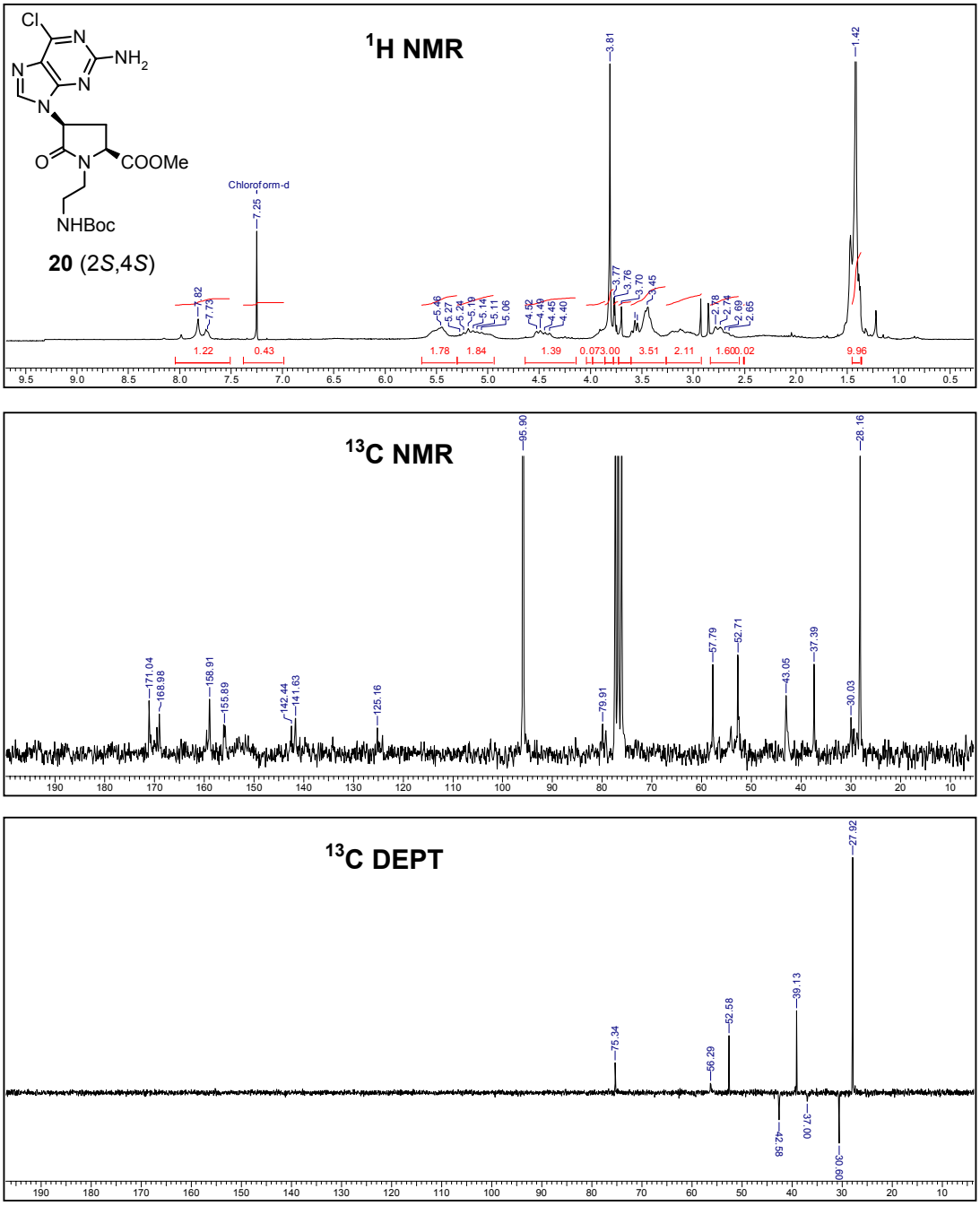

13. Compound **21**; ^{1}H ,^{13}C and ^{13}C-DEPT NMR

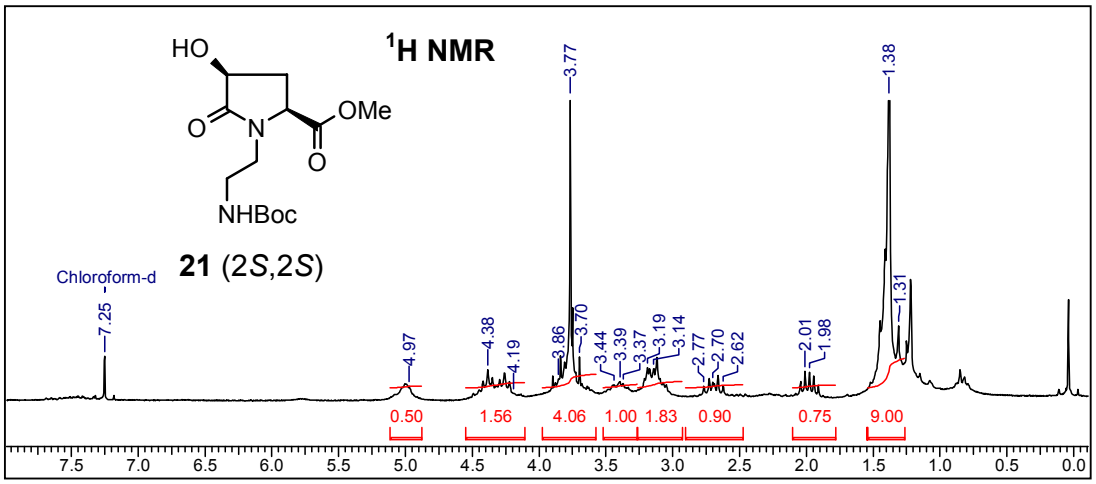

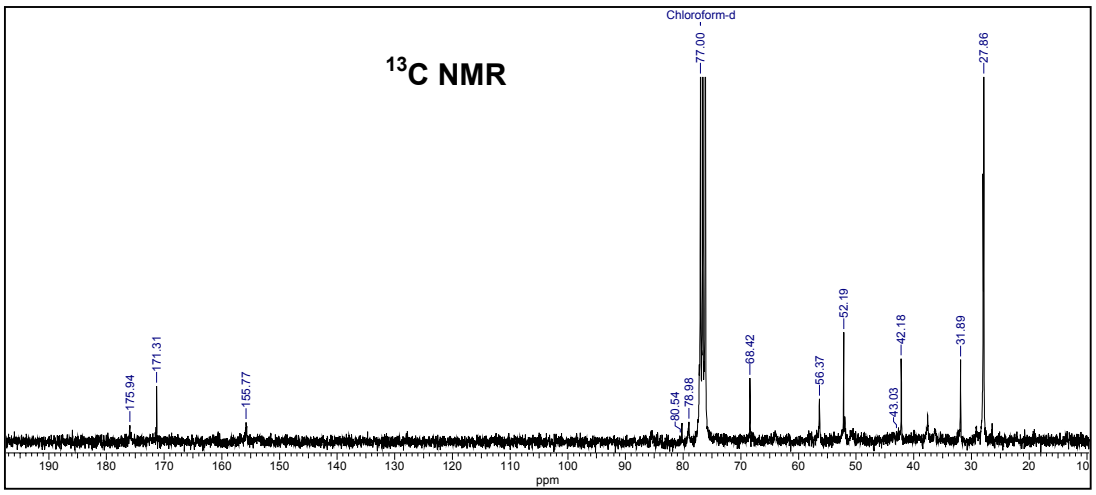

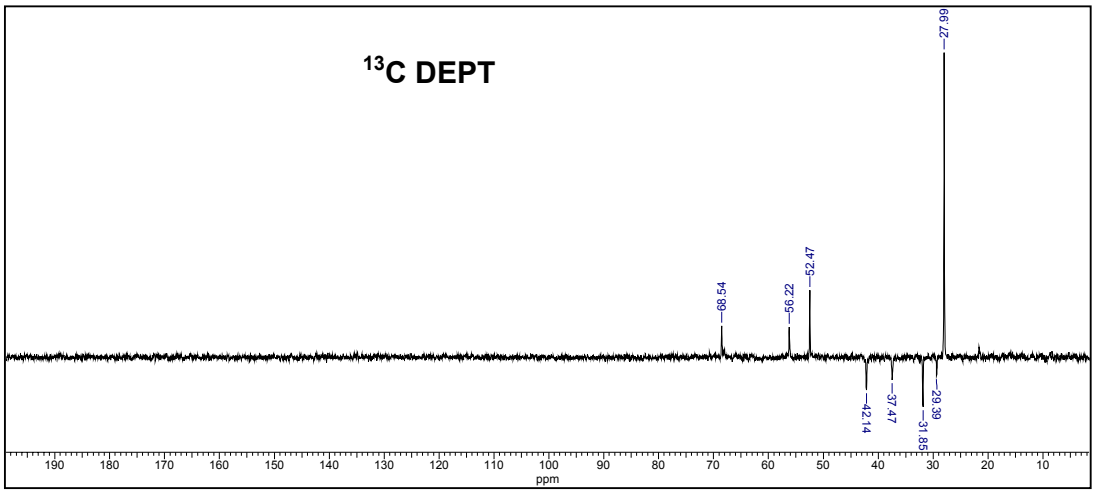

14. Compound **22**; ^{1}H ,^{13}C and ^{13}C-DEPT NMR spectra

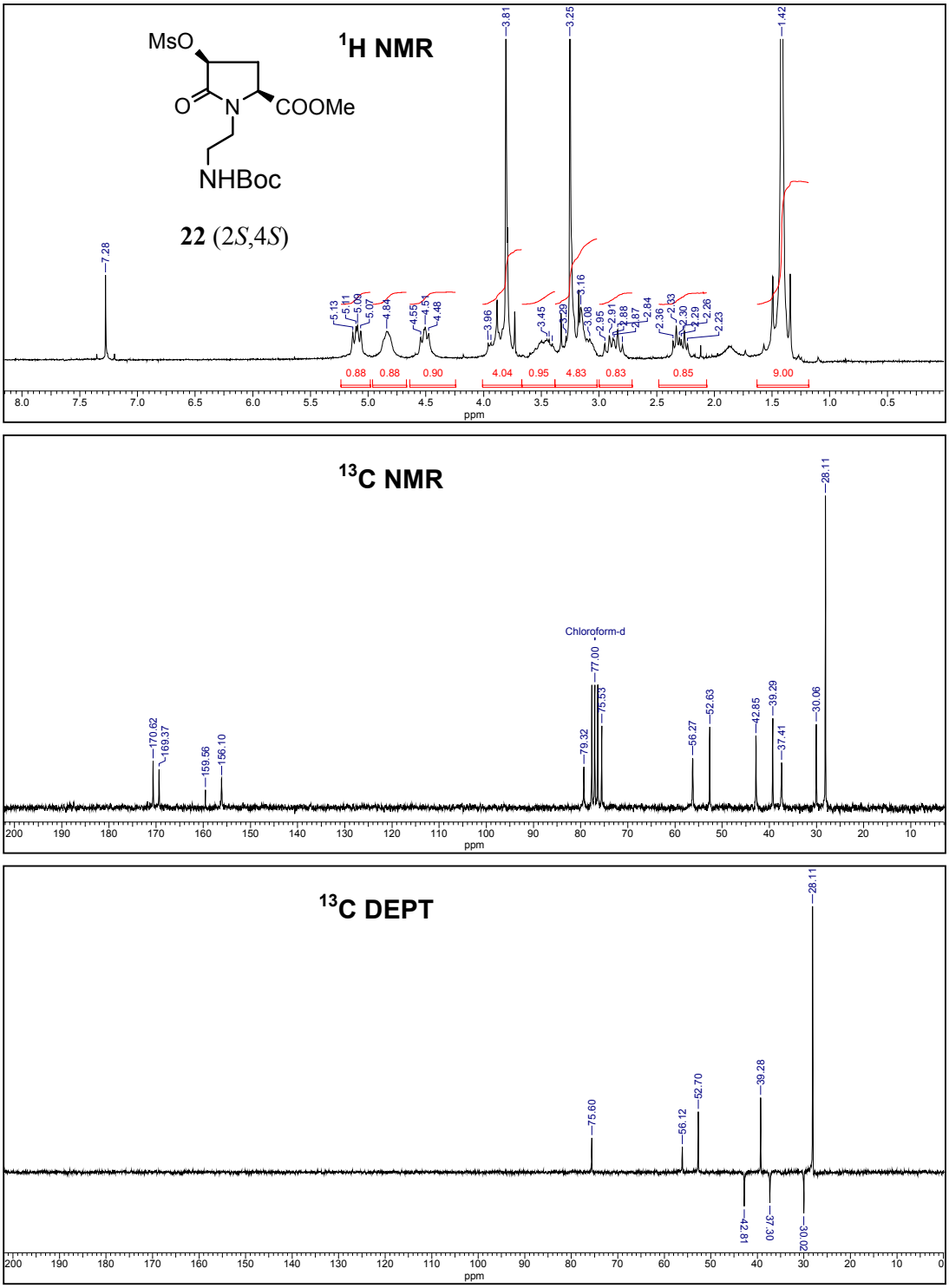

15. Compound **23**; ^{1}H ,^{13}C and ^{13}C-DEPT NMR spectra

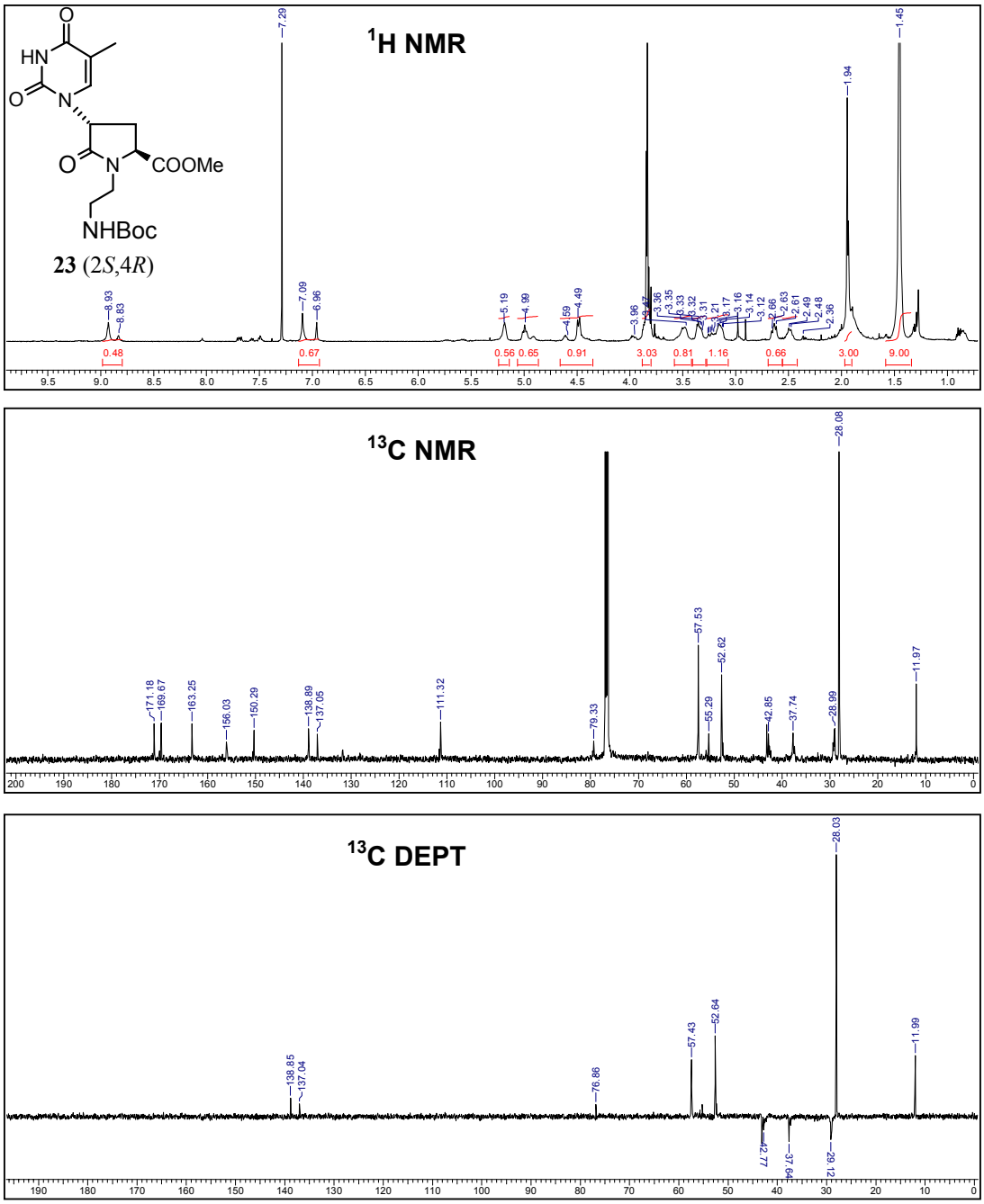

16. Compound **24**; ^{1}H ,^{13}C and ^{13}C-DEPT NMR spectra

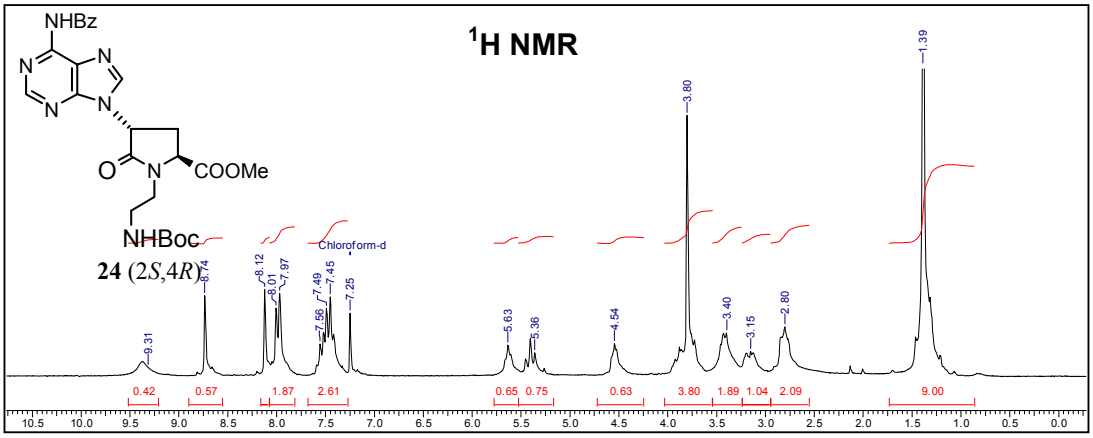

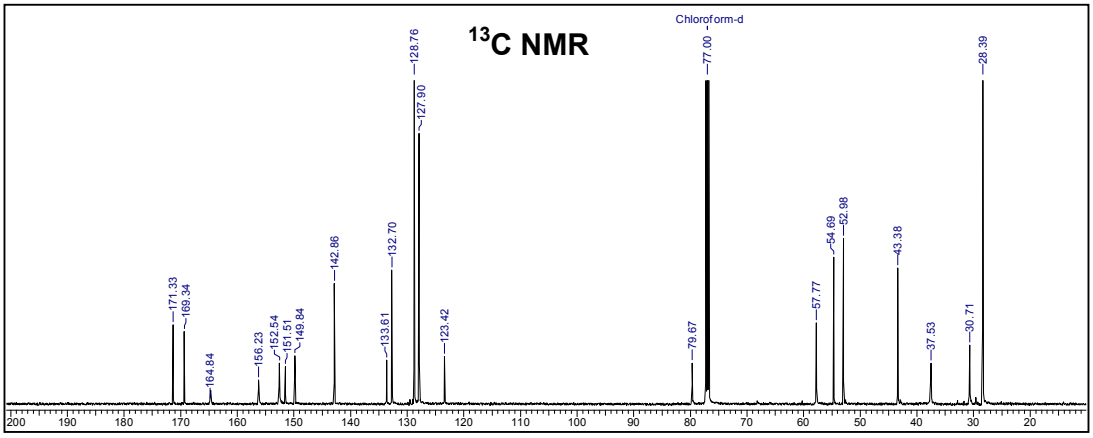

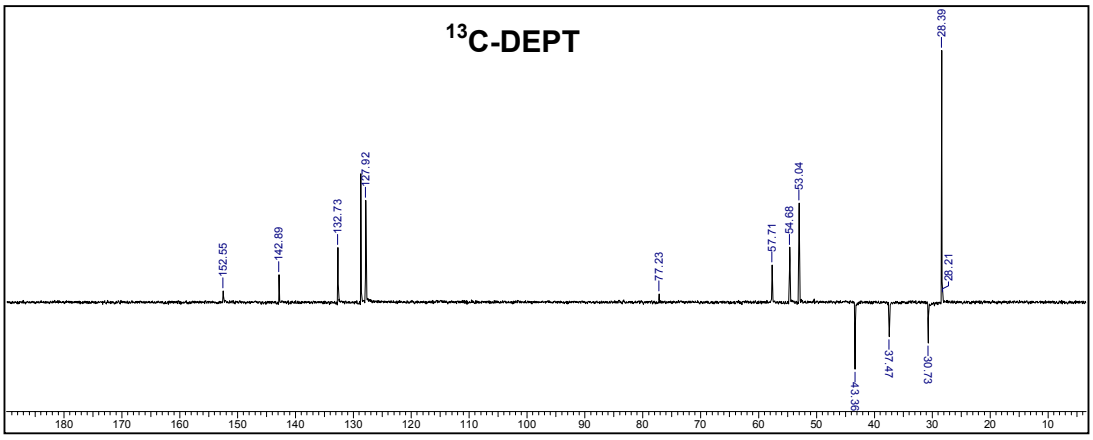

17. Compound **25**; ^{1}H ,^{13}C and ^{13}C-DEPT NMR spectra

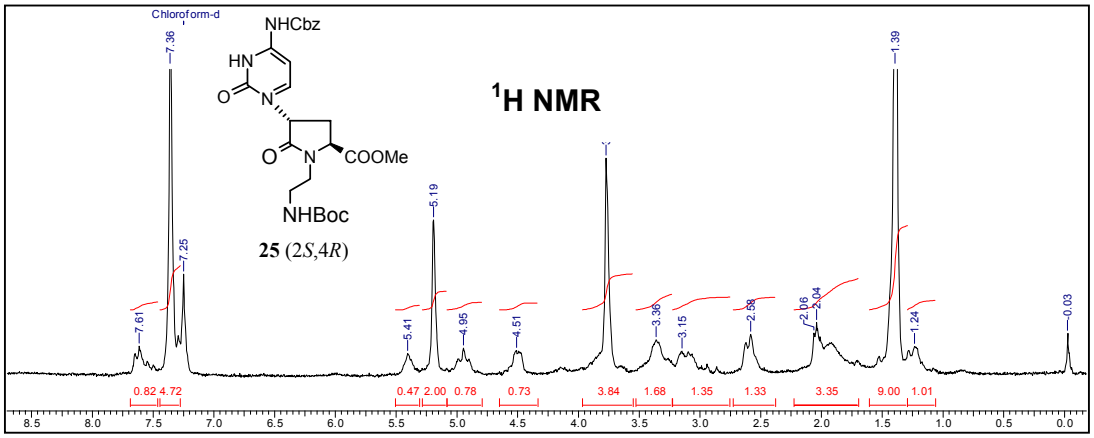

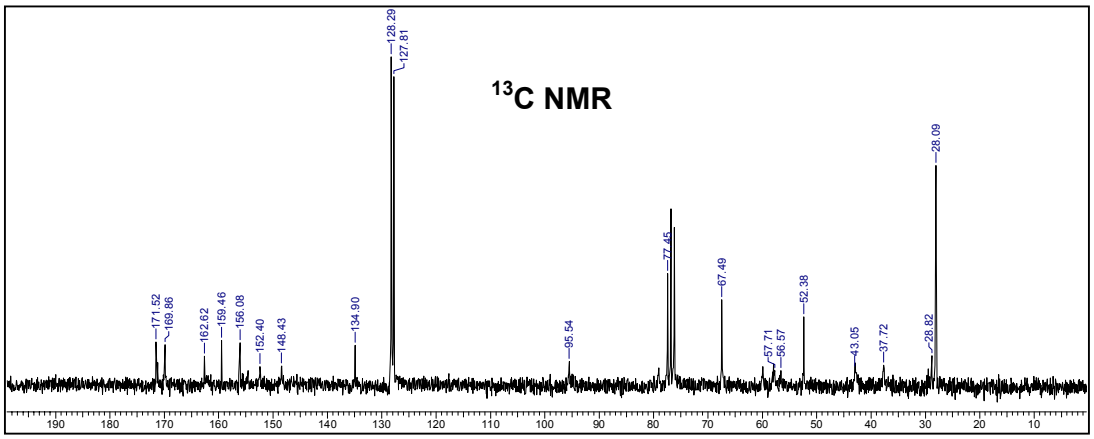

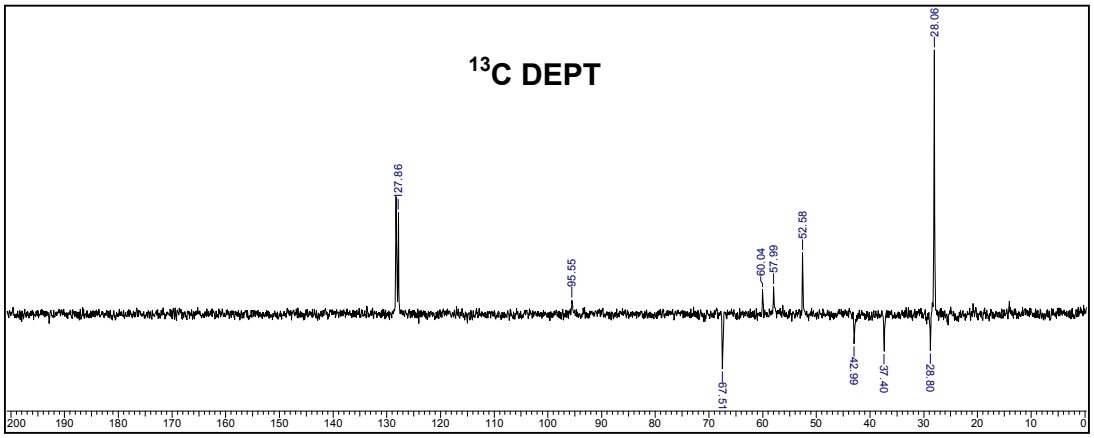

18. Compound **26**; ^{1}H ^{13}C NMR and ^{13}C-DEPT

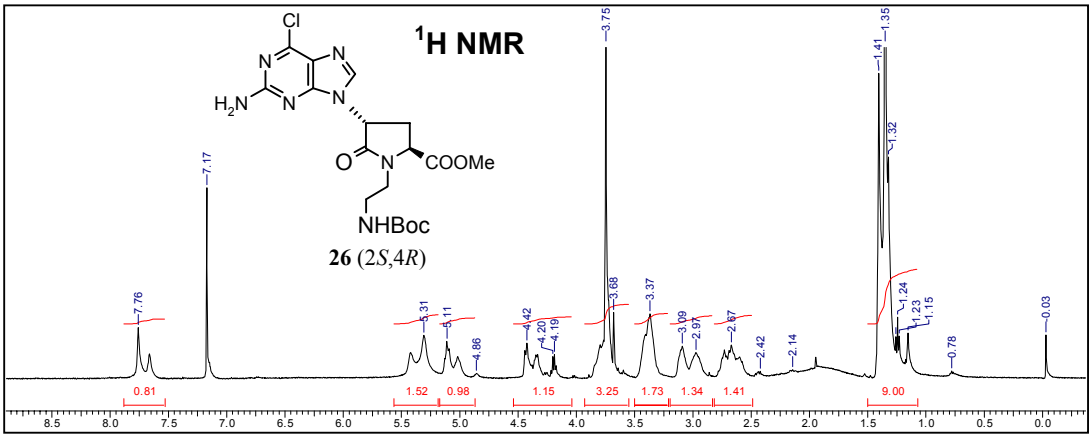

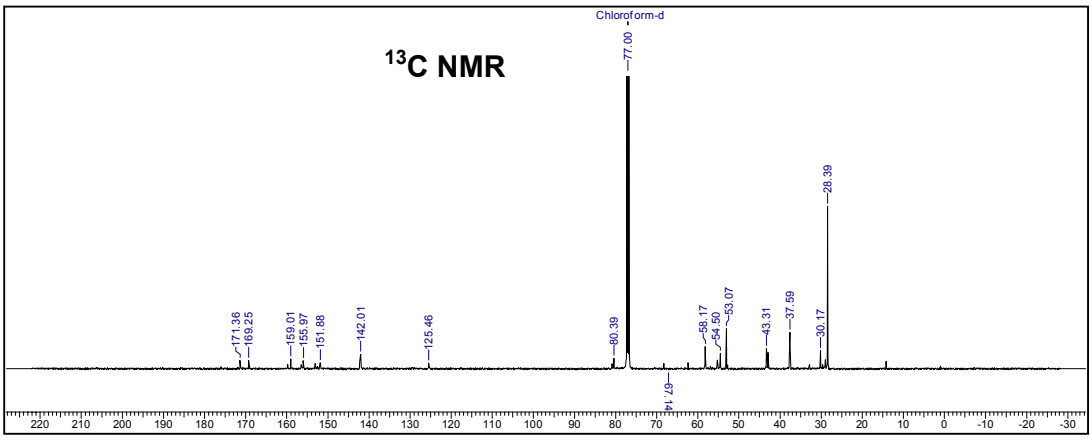

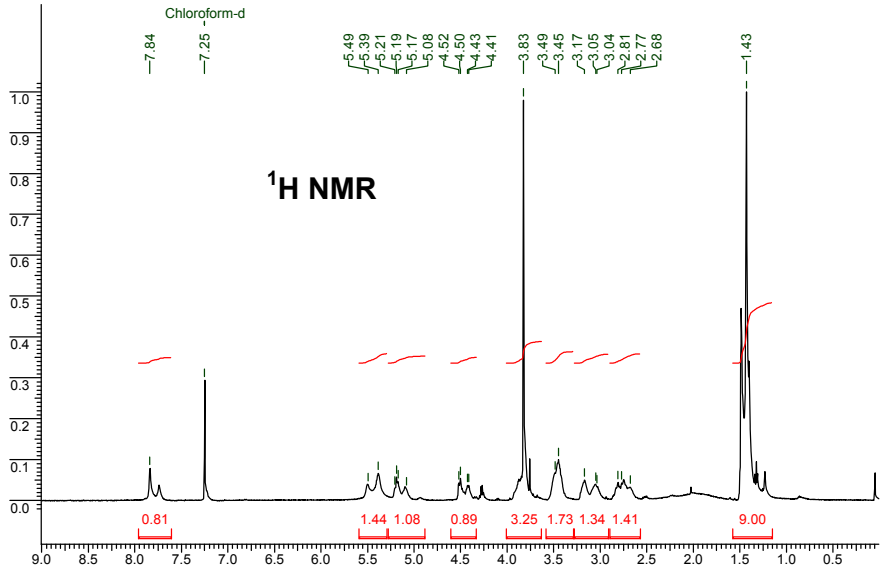

19. Compound **27**; ^{1}H ,^{13}C and ^{13}C-DEPT NMR spectra

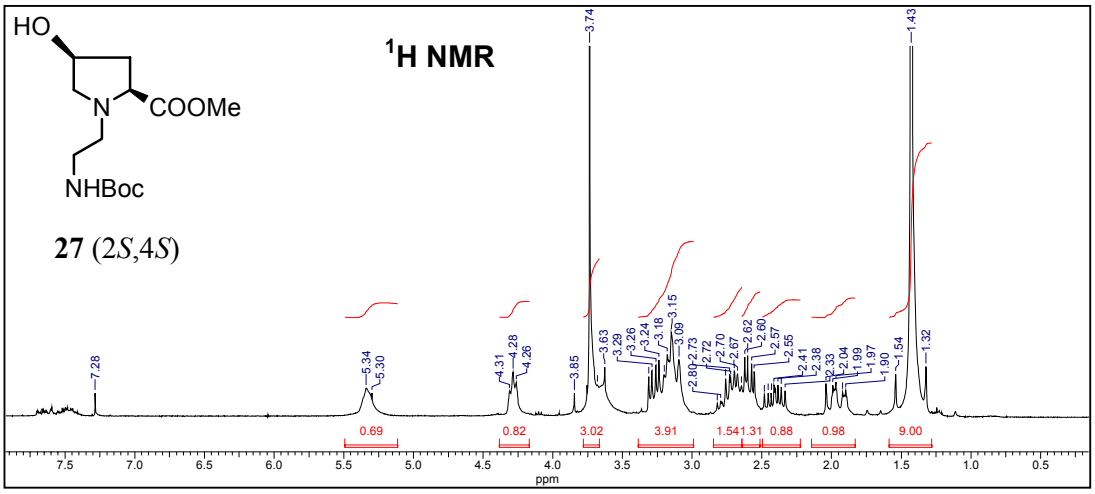

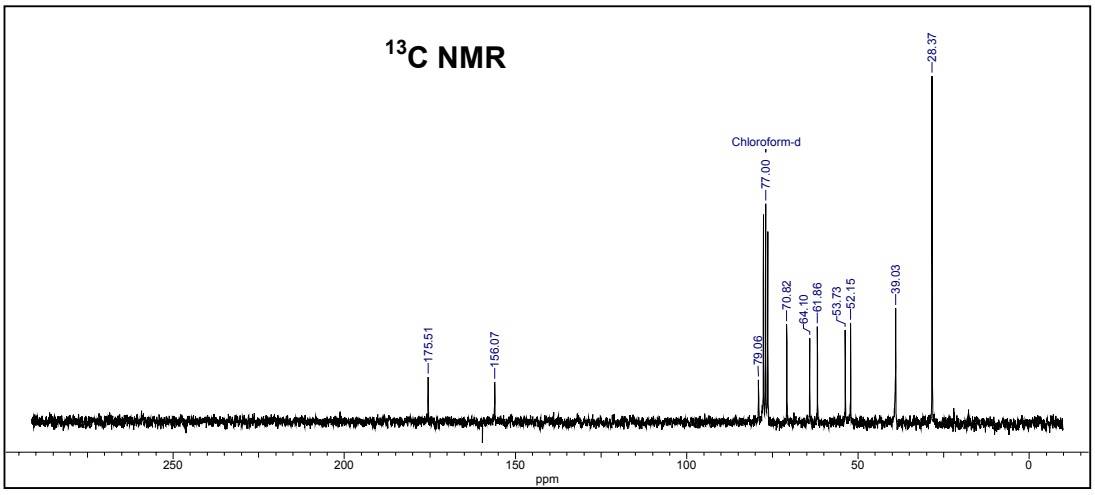

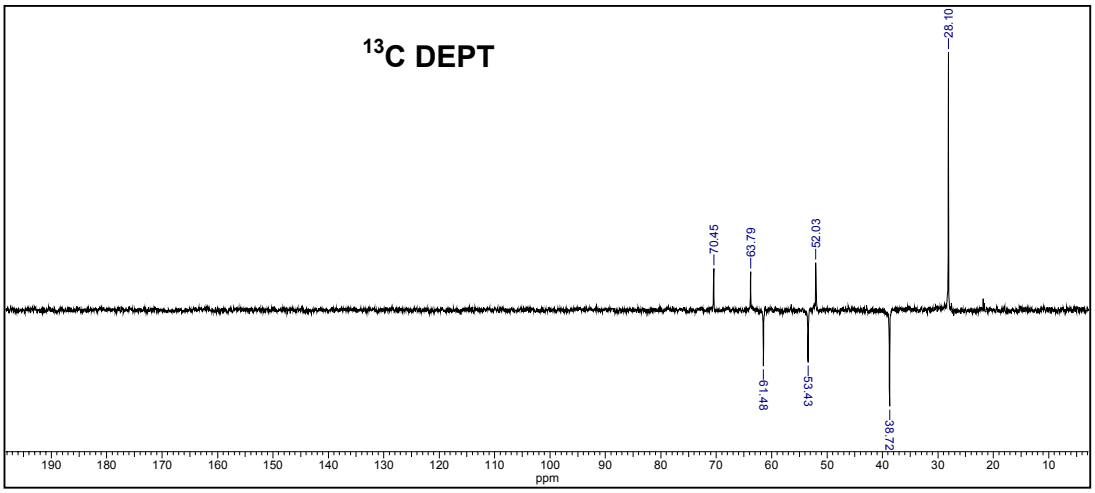

20. Compound **7h-7g**; ^{1}H-^{1}H COSY and ^{1}H-^{13}C HETCOR (500MHz)

^{1}H-^{1}H COSY **7h**

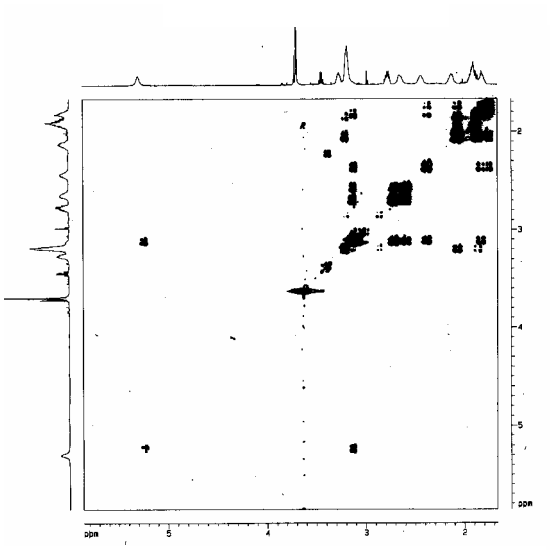

^{1}H-^{13}C HETCOR **7h**

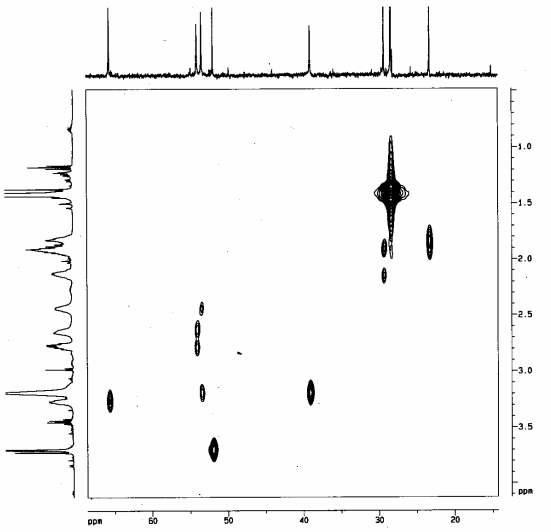

^{1}H-^{1}H COSY **8h**

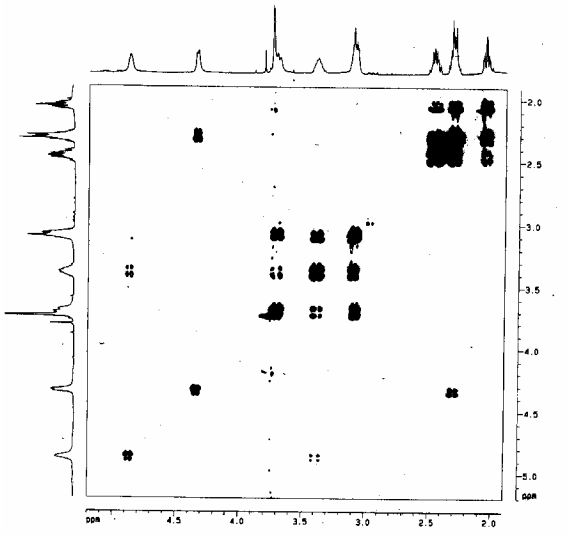

^{1}H-^{13}C HETCOR **8h**

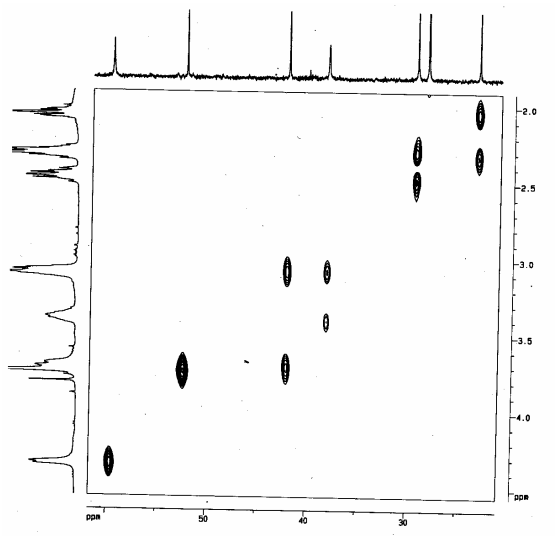

21. Compound **7h-7g**; ^{1}H-^{1}H COSY and ^{1}H-^{13}C HETCOR 2D NMR,

^{1}H-^{1}H COSY **8b**

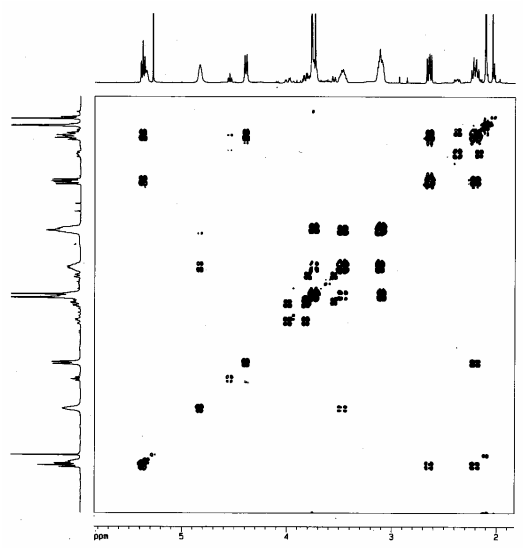

^{1}H-^{1}H COSY **8b**

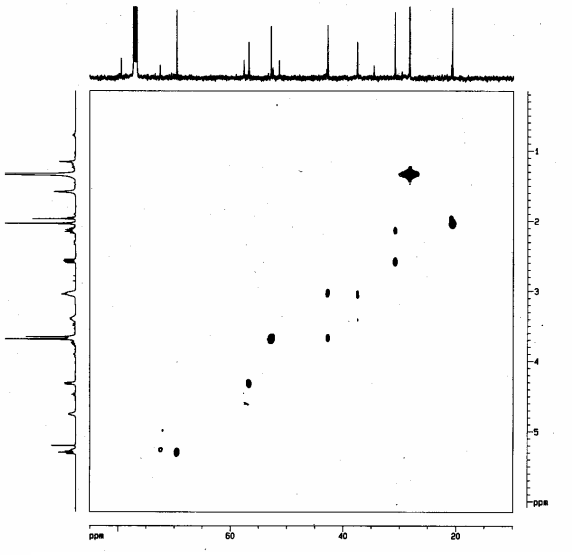

^{1}H-^{1}H COSY **7b**

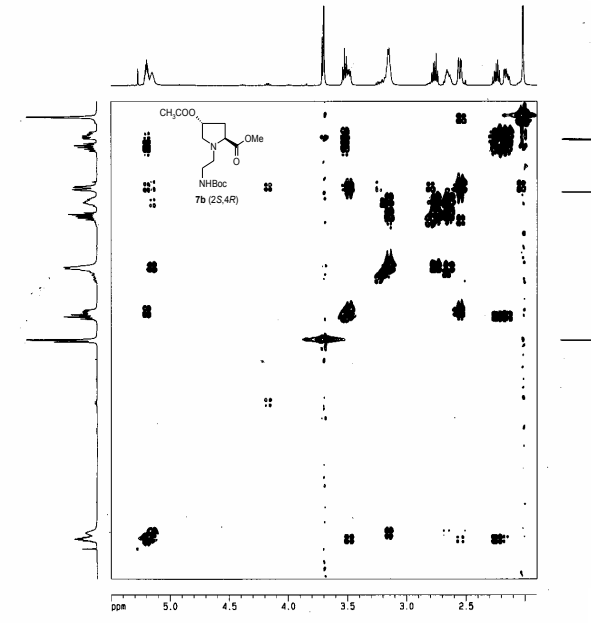

^{1}H-^{13}C HETCOR **7b**

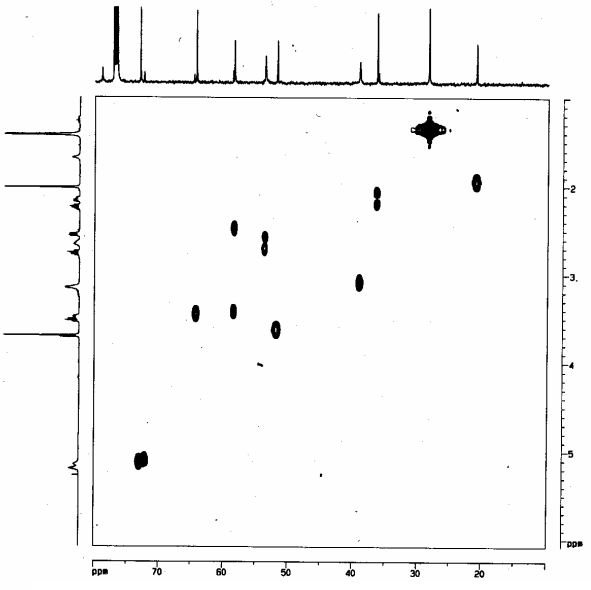

22. ^{1}H-^{1}H NOESY 2D NMR spectra of **a/8a/7b/8b/7h/8h**

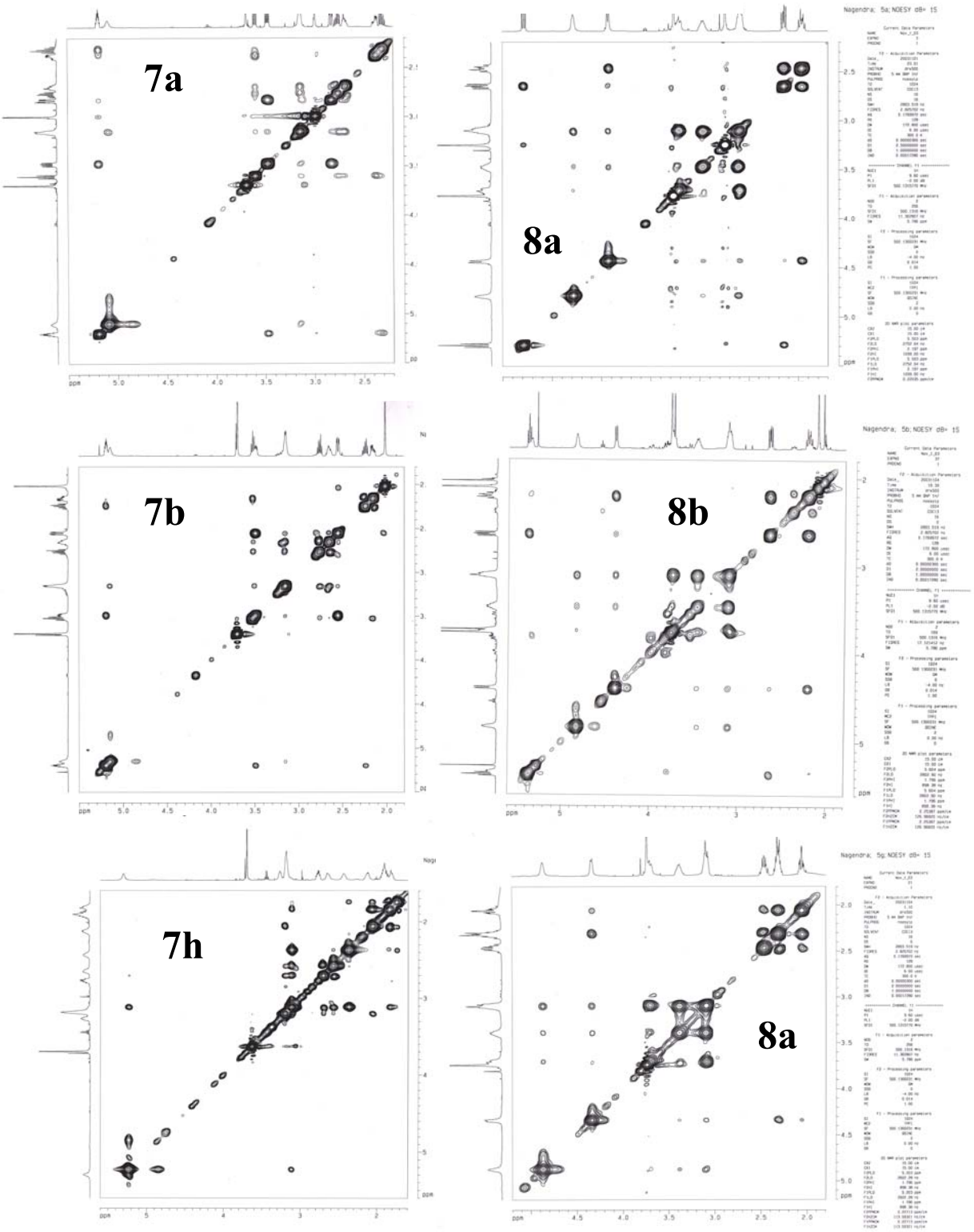

23. Compound **23**; ^{1}H-^{1}H COSY 2D NMR spectra

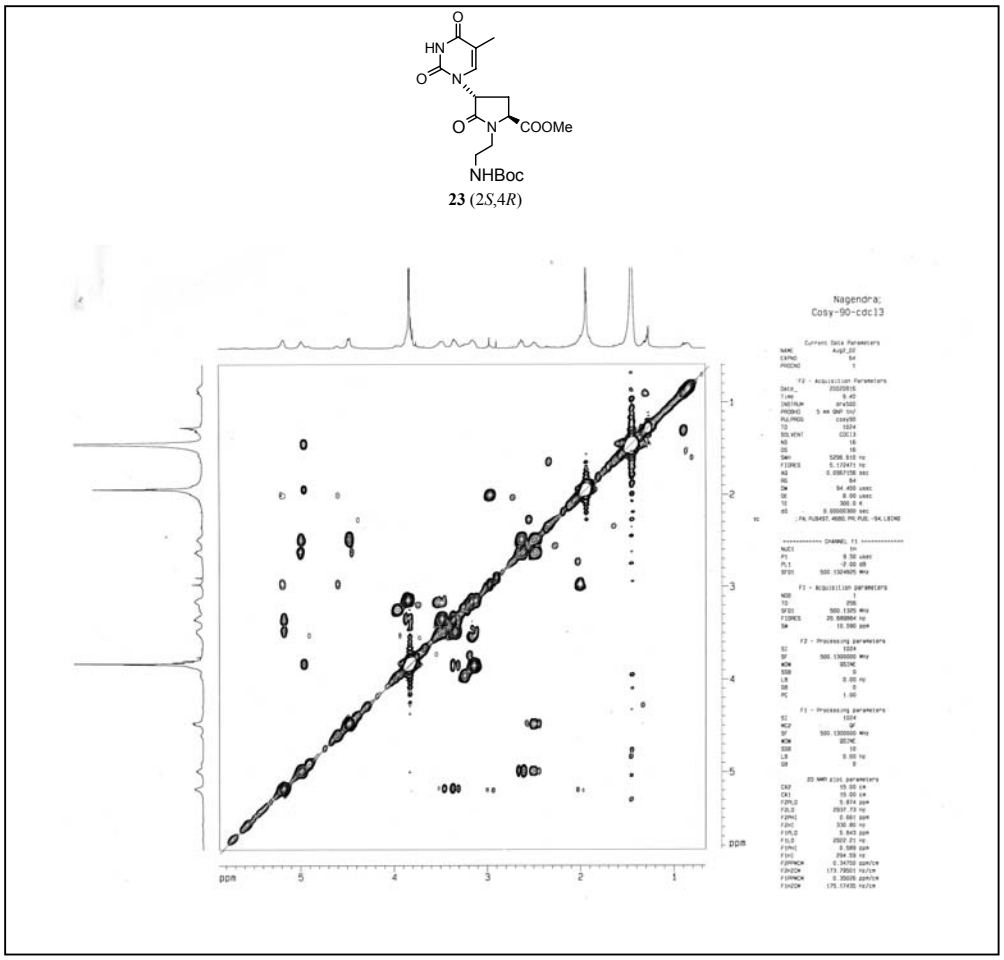

24. Compound **27**, ^{1}H-^{1}H COSY 2D NMR spectra

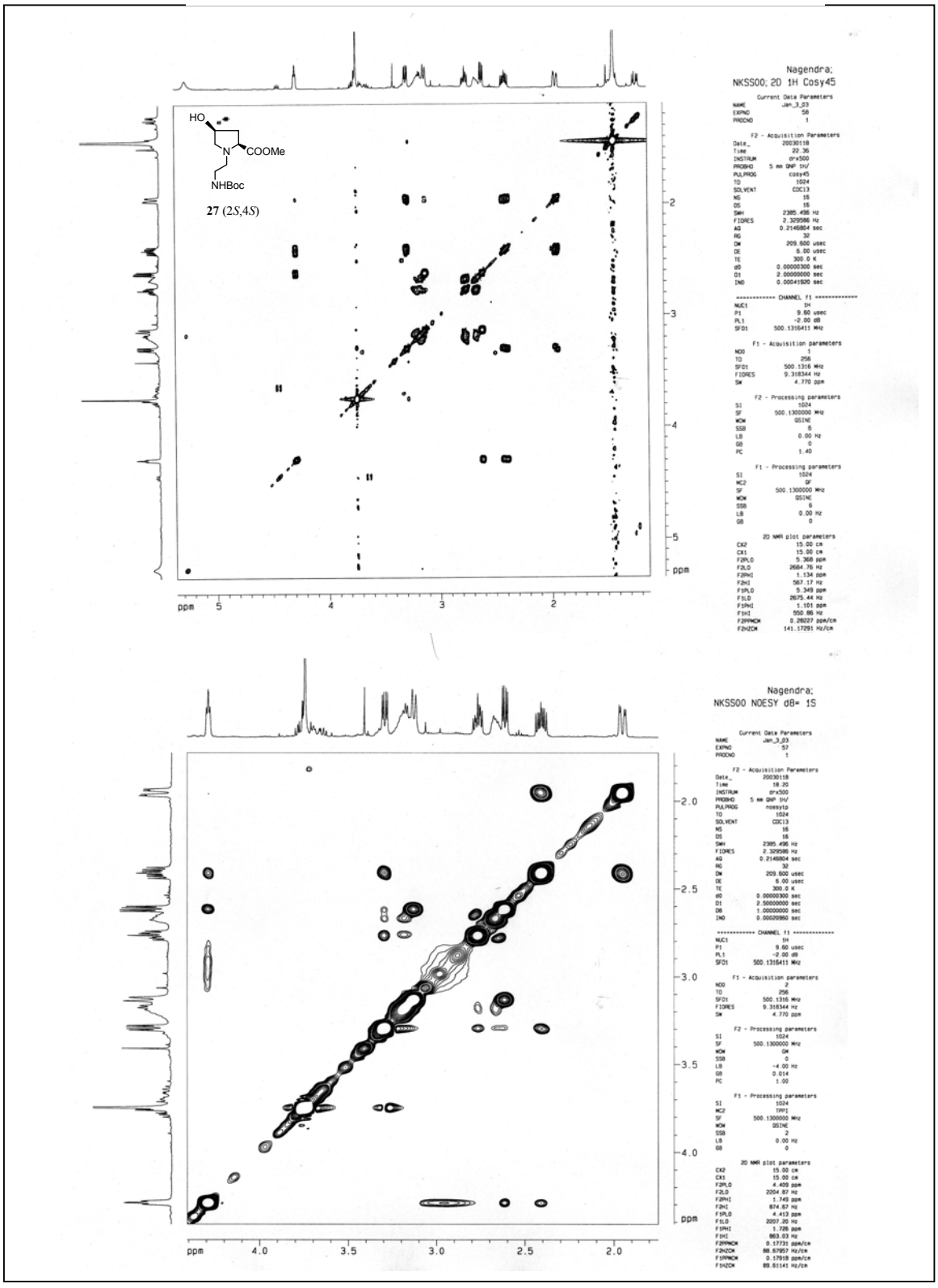

25. Compound **27**, ^{1}H-^{13}C HETCOR 2DNMR spectra (500MHz)

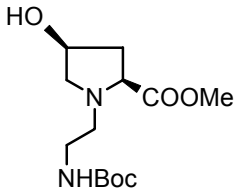

27 (2*S*,4*S*)

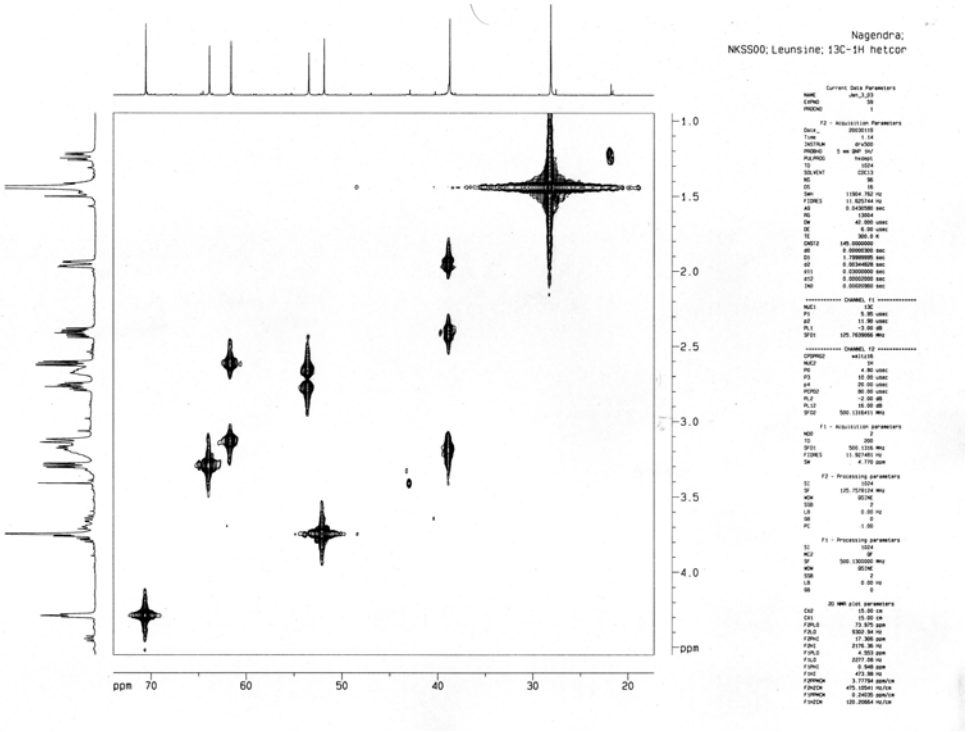

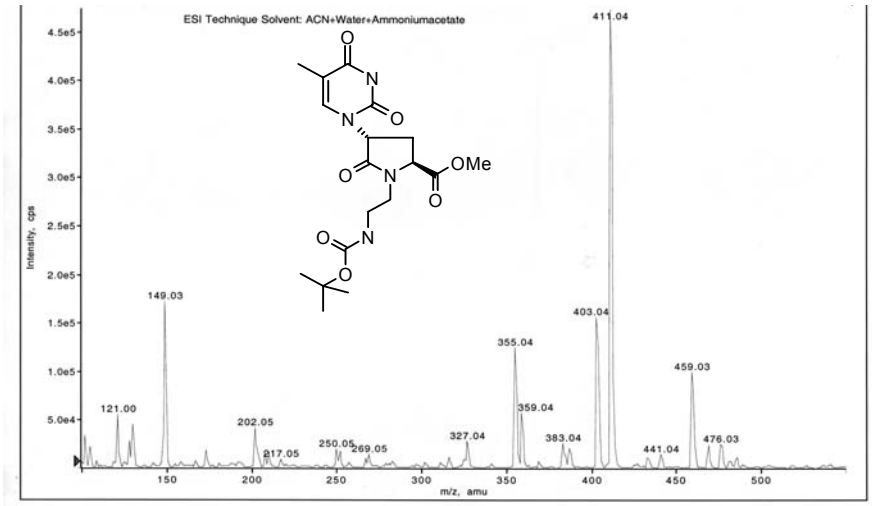
ESI Technique Solvent: ACN+Water+Ammoniumacetate
Intensity, cps
m/z, amu
411.04
149.03
403.04
355.04
459.03
359.04
121.00
202.05
383.04
327.04
476.03
441.04
250.05
269.05
217.05

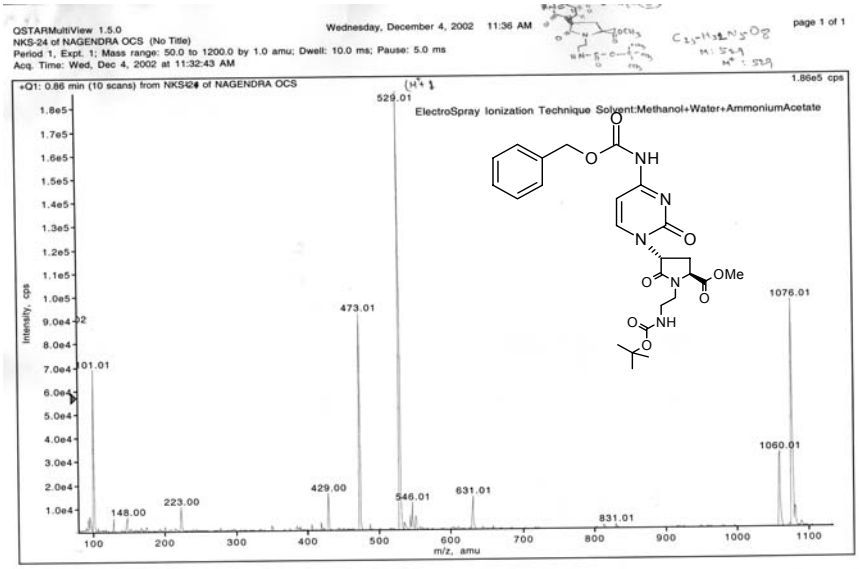
QSTARMultiView 1.5.0
Wednesday, December 4, 2002 11:36 AM
page 1 of 1
NKS-24 of NAGENDRA OCS (No Title)
Period 1, Expt. 1; Mass range: 50.0 to 1200.0 by 1.0 amu; Dwell: 10.0 ms; Pause: 5.0 ms
Acq. Time: Wed, Dec 4, 2002 at 11:32:43 AM
+Q1: 0.86 min (10 scans) from NKS-24 of NAGENDRA OCS
1.86e5 cps
ElectroSpray Ionization Technique Solvent:Methanol+Water+AmmoniumAcetate
Intensity, cps
m/z, amu
529.01
473.01
1076.01
1060.01
101.01
429.00
546.01
631.01
223.00
148.00
831.01

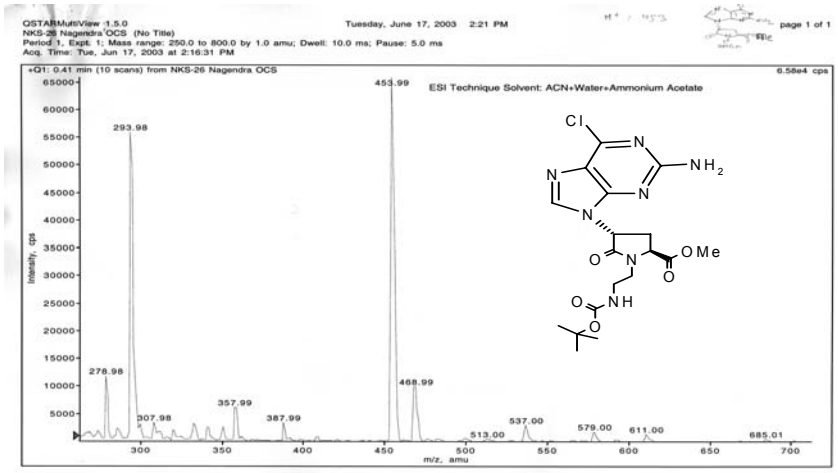
QSTARMultiView 1.5.0
Tuesday, June 17, 2003 2:21 PM
page 1 of 1
NKS-26 Nagendra OCS (No Title)
Period 1, Expt. 1; Mass range: 250.0 to 800.0 by 1.0 amu; Dwell: 10.0 ms; Pause: 5.0 ms
Acq. Time: Tue, Jun 17, 2003 at 2:16:31 PM
+Q1: 0.41 min (10 scans) from NKS-26 Nagendra OCS
6.58e4 cps
ESI Technique Solvent: ACN+Water+Ammonium Acetate
Intensity, cps
m/z, amu
453.99
293.98
468.99
278.98
357.99
307.98
387.99
537.00
579.00
611.00
685.01
513.00

27. Mass spectra of compound **17** and **18**

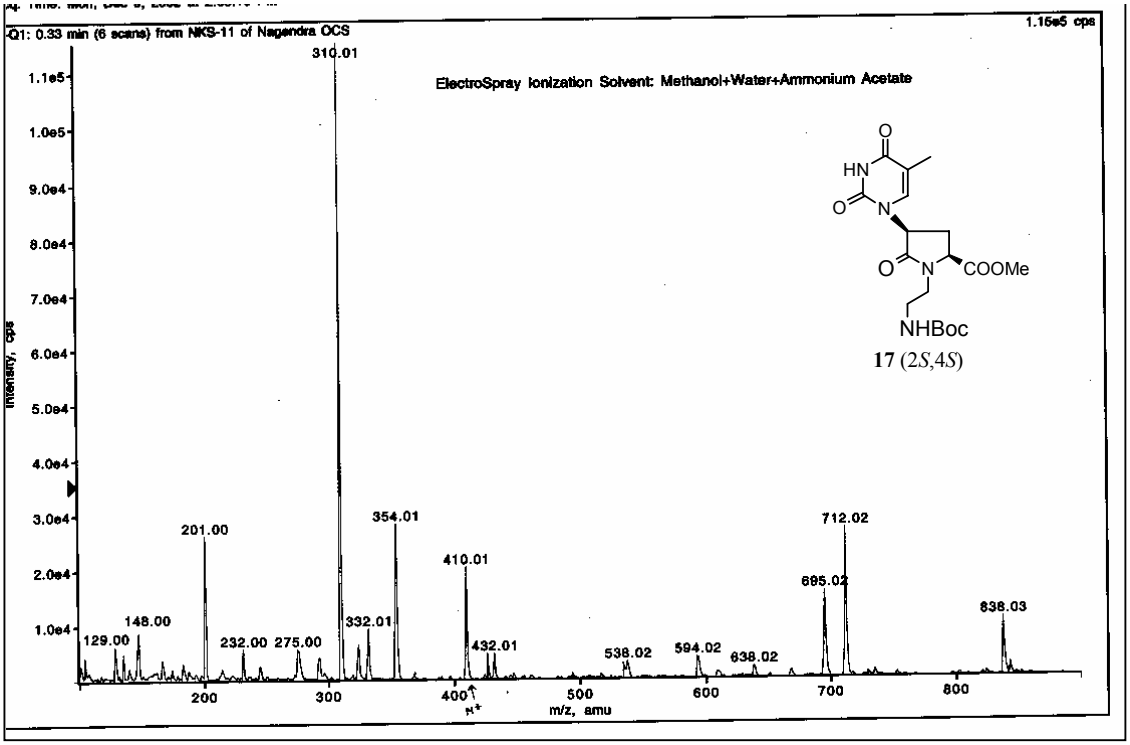

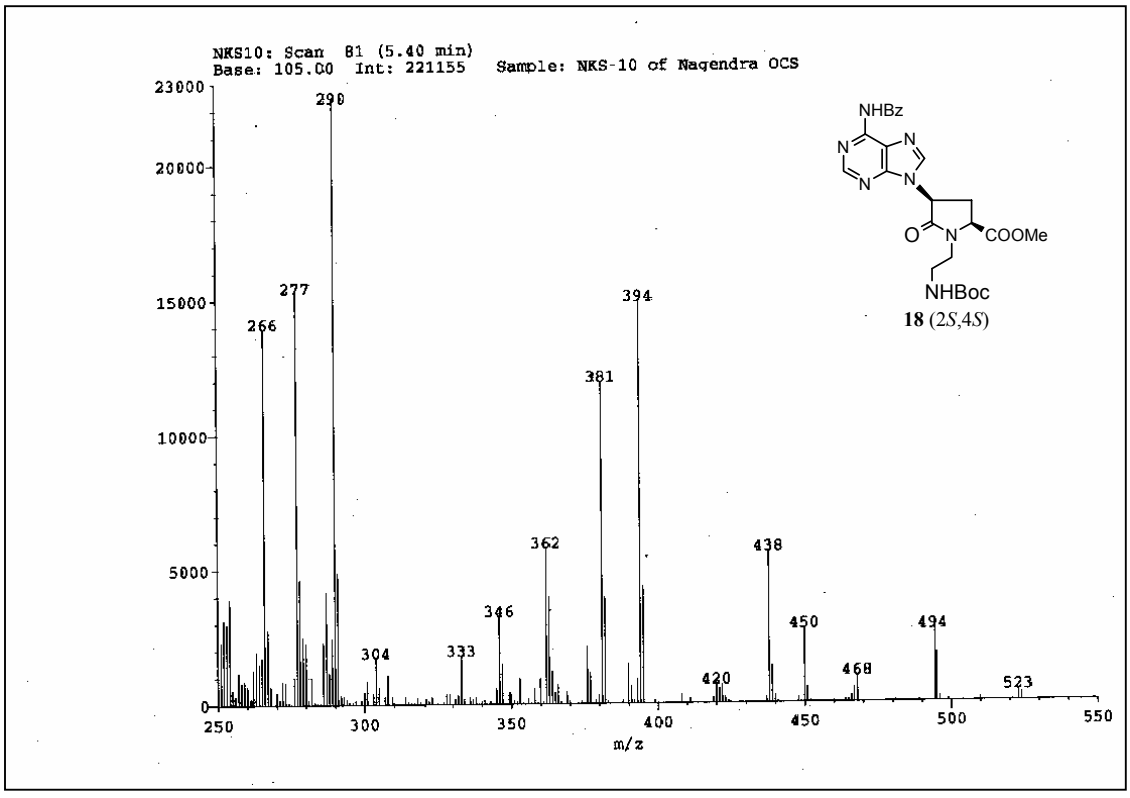

28. Mass spectra of compound **19** and **20**

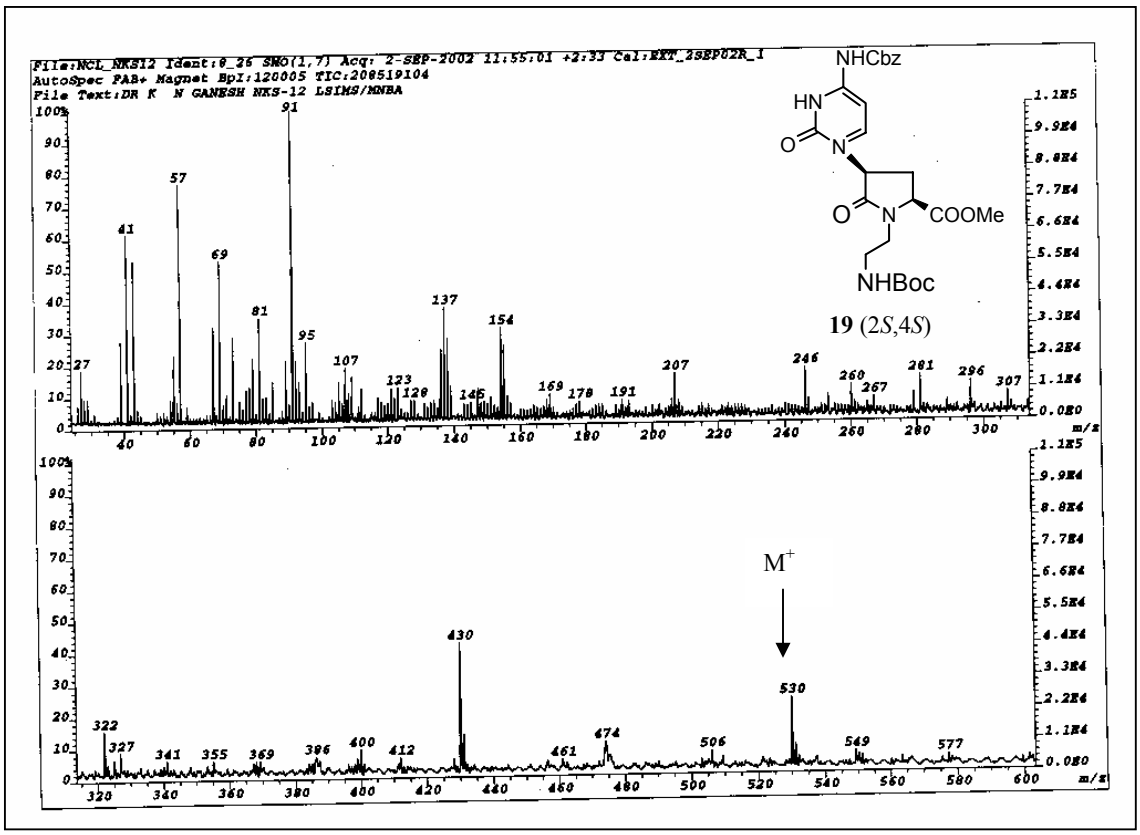

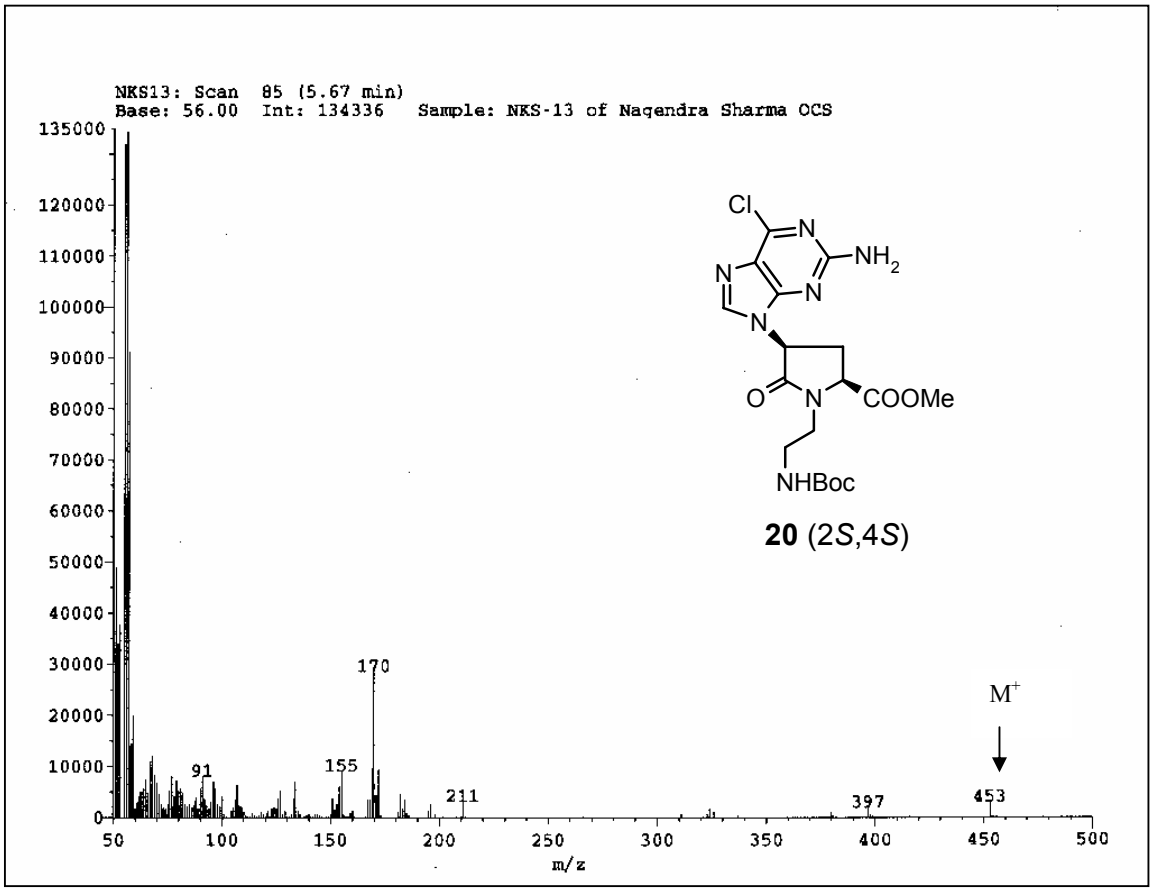

CHAPTER 3

CONFORMATIONAL STUDIES OF PYRROLIDINE RING IN PYRROLIDINE PNA MONOMERS

CHAPTER 3: CONFORMATIONAL STUDIES OF PYRROLIDINE RING IN PYRROLIDINE PNA MONOMERS

3.1 INTRODUCTION

The relation between structure and function of bio-molecules is an ever-important central theme in chemistry and biology. The role of conformation in determining molecular structure-function relationship is a critical factor. A conformer is not an isolable form of a compound and therefore cannot be analyzed exclusively for biological activity.[1] Different conformers are not isomers, although they are equivalent in structure and interconvertable. These forms arise from the rotation of carbon-carbon sigma bonds. Usually at room temperature, different conformers are many times indistinguishable because small molecules have enough thermal energy to effect rotation about single bonds,[2] thereby interconverting different conformers very rapidly. The identification and characterization of conformers depends on the rate of interconversion and the technique that can detect them on that time scale.[3] The resolution of conformers is favoured by lowering of temperature. For study conformational analysis of molecule, X-ray crystallography[4] and NMR[2,5] have emerged as powerful techniques. X-ray diffraction study can provide the structure of only stable form while NMR has the potential to provide information on kinetics and thermodynamics of the interacting systems.

One of the prime reasons for the success of NMR spectroscopy as a structural tool has been the widespread application of vicinal proton-proton coupling constants to determine stereochemistry.[6,7] Spin-spin coupling constants ($^{n}J_{x\text{-}y}$) in NMR are sensitive to the geometrical features of a molecule. The magnitude of ^{1}H-^{1}H coupling constants ($^{n}J_{x\text{-}y}$) provides a direct insight into the geometry such as dihedral angle (θ) around C-C bonds (Figure 1).[7]

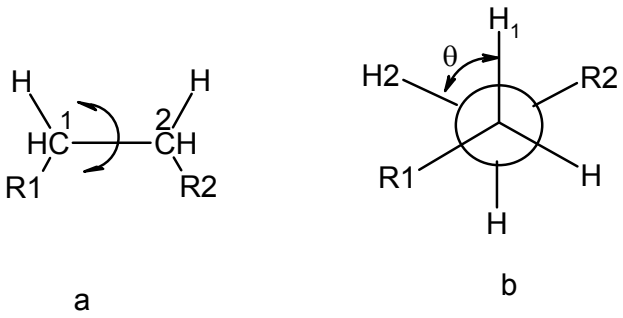

Figure: (a) Vicinal protons (b) Dihedral angle of vicinal protons

Karplus-equation[8] relates the vicinal coupling constants to the torsion angle between the coupling protons and was originally derived from valence bond calculations for the unperturbed ethane molecule spin-spin coupling constant, was shown to depend also on a variety of other molecular parameters, such as electronegativity of the substitutent, bond-angles, bond-lengths etc.

$$^{3}J_{H\text{-}H} = A\cos^2\theta + B\cos\theta + C \quad \text{---------- (1)}$$

where A, B and C are constants called as Karplus parameters.

Changes in bond-lengths and bond-angles due to the effects of molecular vibrations is small compared to the effect of electronegativity and the relative position of substituents, attached to the H-C-C-H fragment.[9] In fact, ample experimental proof is now available to demonstrate that the latter effect is the second important factor, next to the dihedral angle dependence, in determining the magnitude of vicinal coupling constants.[10] In order to account for this influence of substituents and several approximating approaches have been advocated in the past.[11] The most disseminated method is the parameterization of the Karplus equation to the H-C-C-H fragment of interest, yielding Karplus-type relations for highly specific compounds such as nucleotides, peptides and so forth.[12] The drawback of this method is the need for more or less rigid model compounds appropriate for the H-C-C-H fragment under study, to provide the necessary Karplus parameters.[13]

A second approach is the "generalization" of the Karplus-relation by superimposing the angle dependency of the vicinal coupling constant and a linear dependency of the electronegativity of the substituents attached to the H-C-C-H fragment under study. This method is based upon the well-documented linear decrease of the averaged coupling constants in substituted ethanes.[14] A genera1 relation for these molecules was formulated by Abraham and Pachler.[15a]

$$^{3}J_i = 8.0 - 1.0 * \Sigma\Delta\chi_i \text{ ----------(2)}$$

$$^{3}J_{H\text{-}H} = (7.8 - 1.0 \cos\theta + 5.6 \cos 2\theta)(1 - 0.1 \Sigma\Delta\chi_i) \text{---------- (3)}$$

where $\Sigma\Delta\chi_i$, is the sum of the electronegativity differences between the substituents attached to the ethane fragment and hydrogen and θ is the proton-proton torsion angle Durette and Horton'[15b] e.g. combined this dependency on electronegative substituents with the Karplus-equation and parameterized the formula by means of coupling constants found in carbohydrate compounds,

3.1.1 Conformational analysis of five membered rings by NMR

In general, for all types of molecules, the relation between the 3-bond vicinal coupling constant ^{3}J (H-C-C-H) to the intervening dihedral angle θ (H-C-C-H) is by a simple trigonometric equation 3.[16]

The values of the Karplus parameters A, B, and C depend on the *electronegativities* of the functional groups to which the nuclei are linked.[13] This relation plays an important role in searching the approximate molecular conformation of cyclic molecules by NMR spectroscopy.[17] Because of the closed structure of the five-membered rings, the geometrically possible disordered puckered states depend on the number of atoms that are invariant.[13] There are two main cases of disorder in five membered ring containing cyclic compounds (Figure 2). In case I disorder (left), one bond angle is

assumed constant and three consecutive atoms of the ring do not show residual difference in electron densities. In case II disorder (right), one torsion angle is assumed constant and four consecutive atoms of the five-membered ring are anchored which is also observed in the crystal structure.[4b]

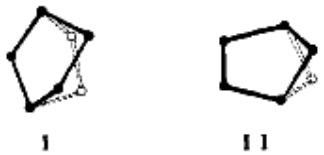

Figure 2: disordered puckered in five membered ring

In the all planar conformation, the five atoms in a cyclopentose ring induces unfavourable steric interactions among the vicinal substituents due to their eclipsed forms.[18a] This is relieved by out of plane puckering of one of the atoms leading to gauche relation among the vicinal substituents (Figure 3).[18b]

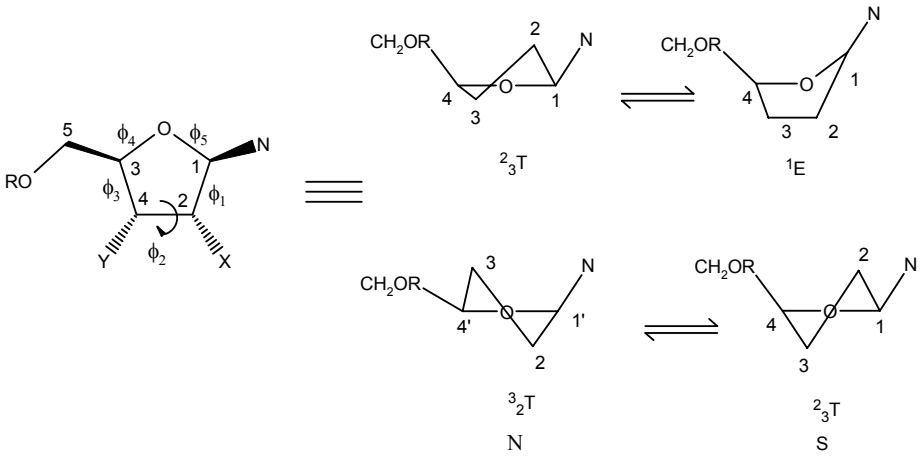

Figure 3: Puckering of furanose ring

From the early reviews and available crystal structures of proline derivatives, it was found that the five-membered ring in this imino acid prefers to adopt either of the two conformations in the solid-state.[4b] The atoms C^{δ}-N-C^{α}-C^{β} (Figure 4) are nearly coplanar and C^{γ} is displaced from this plane, either *up* (C^{γ}-*exo*) with respect to the α-COR group or *down* (C^{γ}-*endo*). Thus, the conformational analysis of prolines appears to be limited into two "envelope" forms: ^{2}E and $_{2}$E or γ^{+} and γ^{-}.

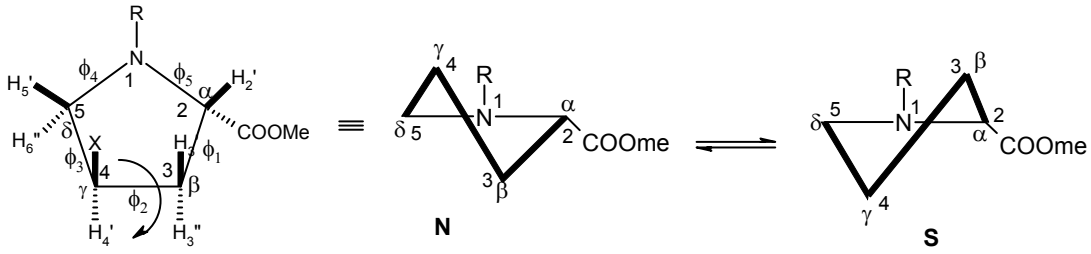

Figure 4: Pseudorotational disorder of a pyrrolidine ring with two different sugar conformations

3.1.2 Pseudorotation

The pseudorotation concept originated to describe the continuous interconversions of puckered forms of the cyclopentane ring.[19] The furanose geometry is conveniently described using the puckering parameters based on the endocyclic torsion angles. Altona and Sundaralingam,[20] developed the formalism for applying Karplus equation (1) to determine the conformation of the furanoid ring in sugar unit of DNA/RNA using the pseudorotation concept. This concept was introduced by Kalpatrick, *et. al*.[21] to determine the exact conformation of furanoid ring in sugar in terms of two parameters: (i) the phase angle of pseudorotaion (P) and (ii) the degree of pucker (ϕ). The angle of maximum puckering in the cyclopentane ring is achieved with minimal change in the potential energy. However, in the presence of one or more endocyclic or exocyclic substituents, this

will give rise to an *induced* potential energy barrier that opposes the free carbon-carbon sigma bond rotation.[22]

The generalized Karplus equation has been applied to delineate the conformational properties of five-membered sugar rings in nucleosides and nucleic acids.[22] In order to maintain the correspondence with the conformational nomenclature of ribose moiety, the notation for prolines shown in Figure 5 is used.[23] The conformation characterized by positive value of torsion angle H3'-C3-C4-H4 (ϕ_2) is denoted by *N*-type while the conformation having a negative angle ϕ_2 denoted by *S*-type. The transition points between *N* and *S* conformation ranges at $\phi_2 = 0$ are defined by ^{N}E and $_{N}E$, which represent maximum-energy regions in the conformational space. Thus, N/S classification is directly related to the sign sequence of the endocyclic torsion angles and not on the manner by which way the molecule is drawn. The conformational nomenclature of proline and hydroxyl proline moieties is briefed in Figure 5.[23]

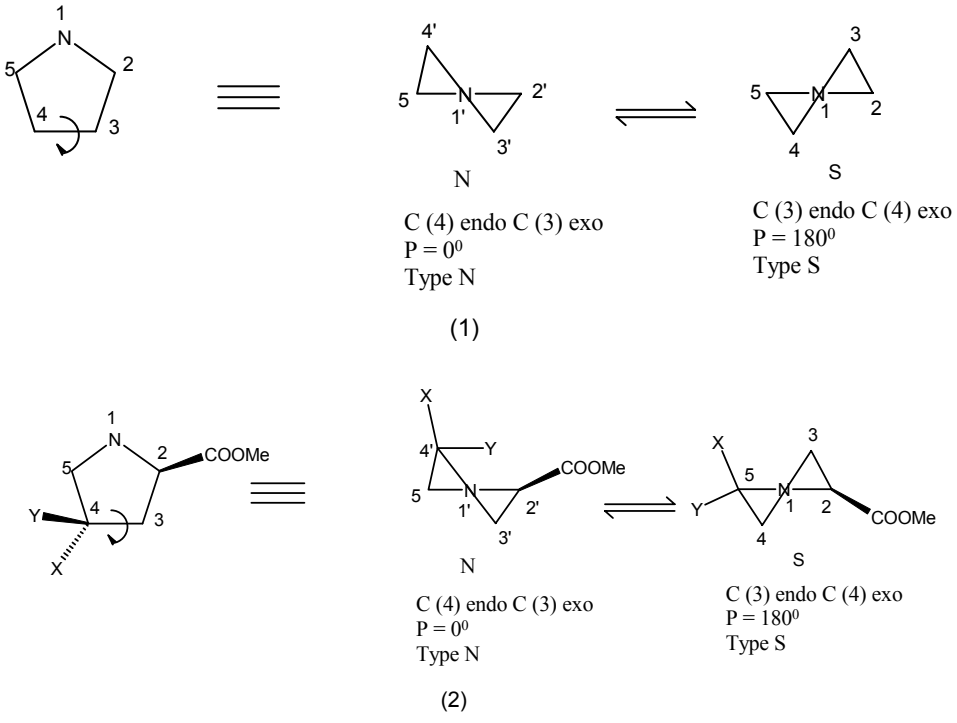

Figure 5: Diagrammatic projections of (1) proline ring in two Idealized twist conformations and (2) 4-hydroxyproline ring

The pseudorotation equation (4)[25,13] is the simplest modification of Karplus relationship between the endocyclic torsion angle (ϕ) and phase angle (P).

$$\phi_j = \phi_m \cos(P + 4\pi j / 5), \text{ in which } j = 0.\ 1.\ 2,\ 3,\ 4 \text{ ---------- (4)}$$

where P is defined as

$$\text{Tan } P = \frac{(\phi_2+\phi_4) - (\phi_1+\phi_3)}{2\phi_0 (\text{Sin } 36 + \text{sin } 72)}$$

The endocyclic torsion angles ϕ_j in saturated five-membered ring (Figure 6) in an arbitrary low energy conformational state are interrelated via the pseudorotation equation.

P represents the phase angle that maps the specific location of a given conformation on pseudorotation circle. The radius of the circle is given by ϕ_m, the puckering amplitude or the maximum value attainable by ϕ_j upon pseudorotation.

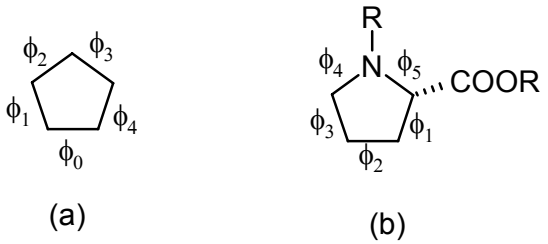

Figure 6: (a) The notation of endocyclic torsion angles for use in equation (2).
(b) Conventional ϕ notation of endocyclic torsion angles in the proline residue.

The correspondence between *P*, on the one hand, and the usual envelop (E) and twist (T) conformational notation, on the other, is given in Table 1 and the diagrammatic projection (pseudorotation cycle of furanose ring) is shown in Figure 8.[25] The furanose ring is shown in in two idealized twist conformations, looking toward the oxygen atom from the center of the C (3')-C(4') bond. Type N at $P = 0^o$ represents the chosen standard ${}^3_2T$ corresponding to type *S* at $P = 180^o$ and represents its mirror image ${}^2_3T$ (Figure 7).

Table 1: The correspondence between *P* and the usual envelop (E) and twist (T) conformational notation[28]

P_N	-72^0	-54^0	-36^0	-18^0	0^0	18^0	36^0	54^0	72^0
	T	$^{\alpha}$E	T	$_{\beta}$E	T	$^{\gamma}$E	T	$^{\delta}$E	$^{N}{}_{\delta}$T
P_S	108^0	126^0	144^0	162^0	180^0	198^0	216^0	234^0	252^0
	T	$_{\alpha}$E	T	$^{\beta}$E	T	$_{\gamma}$E	T	$_{\delta}$E	$_{N}{}^{\delta}$T

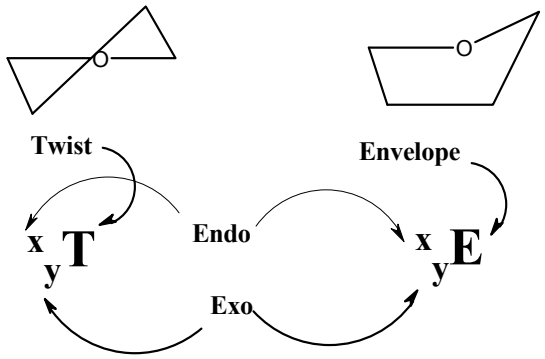

x and y are displaced atoms from plane of furanose sugar ring

Figure 7: Notation of twist and envelope for five membered ring

In Figure 8, pseudorotational pathway of the furanose ring is given.[25] Each point on the circle represents a specific value of the phase angle of pseudorotation *P*. Heavy radial lines represent *T* conformations, dotted radials represent *E* forms; the corresponding signs of the ring torsion angles are also shown. Heavy arrows indicate the preferred pseudorotational regions. For details of abbreviated nomenclature, see ref 15b.

Altona and Sundaralingam[25] have defined two parameters: the phase angle of pseudorotation (*P*), which defines the part of the ring that is most puckered and puckering amplitude (ϕm), which is the extent of puckering. In pseudorotation cycle, *P* varies from 0' to 360' through a set of 20 distinct twist and envelope conformations and can be subdivided into North (*P* = O'), East (*P* = 90°), South (*P* = 1 80°), and West (*P* = 270') regions (Scheme I). A survey of 178 X-ray crystal structures of nucleosides and nucleotides found the nucleosides to be in both North (N) and South (S) conformations

(Figure 8).[4b] The North range is centred around P = 18' (C3'-*endo*), whereas the South range is centred around *P* = 162' (C2'-*endo*). However, there are a few examples of both X-ray and solution structures which have sugar conformations with *P* = 90°. The relevance of East (E) structures support the hypothesis that N→S interconversion proceeds through the East (E) structure rather than the West (W) conformation. The values of ϕm were found in a range from 30' to 46', and most of them fall within 38.6±3.0°.4. For 178 β-D-furanoside moieties, the ratio between *N* and *S* states in ribonucleosides is approximately 1: 1, and for 2'-deoxyribonucleosides**,** it is 1:3.[20]

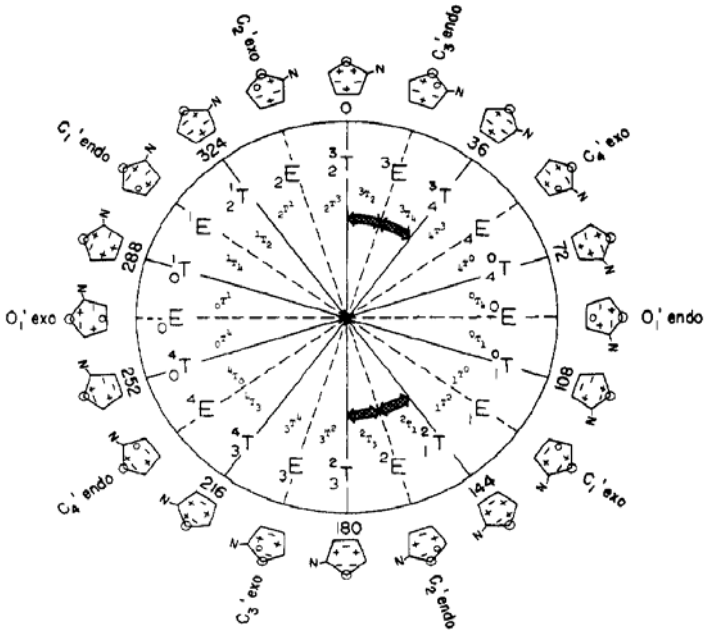

Figure 8: Pseudorotational pathway of the furanose ring.[25].

3.1.3 Conformational geometry of five membered ring

3.1.3a Furanose rings

The geometry of furanose rings and derivatives have been determined from vicinal proton-proton coupling constants using the concept of pseudorotation[27] in which the conformation of a puckered five-membered ring is fully described by two parameters: a

phase angle of pseudorotation *P* and puckering amplitude (ϕ_m). From a survey of x-ray crystallography studies on nucleoside and nucleotide,[4b] it is known that ϕ_m ranges from 35° to 45° with an average range of 39°. Two narrow ranges of P are found. First range is centered on P = 18° (C3'-*endo*, N) and second range is centered on P =162° (C2'-*endo*, S) (Figure 8). The puckering amplitude is flattened as indicated by ϕ_m value between 22° and 36°. The pseudorotational parameters were obtained experimentally from the measured *J*-couplings using the computer program PSEUROT which has been developed by Altona and co-workers.[28]

In solution, the furanose ring exists as equilibrium mixture of the two rapidly inconverting conformers N and S and described four conformational parameters P_N, Ps, ϕ_N, ϕ_S as well as the mole fraction of each conformer. The position of the conformational equilibrium is mainly determined by two factors: the *gauche* effect and the *anomeric* effect. The *gauche* effect defined is as the tendency to adopt the structure in which the O4' of sugar and 3'- and/or 2' substituents are in *gauche* rather than *trans* orientation.[29] The anomeric effect is described as the tendency of the lone pair of the furanose oxygen to be *antiperiplanar* to the nitrogen of the nucleobase.

3.1.3b Pyrrolidine rings

The conformations of the five-membererd pyrrolidine rings in proline and 4-hydroxy-proline are important in controlling the stability and physiological functions of collagen fibrils.[30] L-proline (pro) is a cyclic α-imino acid that occurs in protein structures and enhances the probability of β-turn formation in polypeptides and proteins. The 4-hydroxy-L-proline (Hyp) occurs in certain structural proteins such as collagen which exist in a coiled triple helix and the conformational properties of this class of compounds are therefore interesting.[31]

The proline ring is a substituted pyrrolidine ring. It has been shown that in solution, proline ring like furanose also occurs in equilibrium between the *N* and *S* conformation. The relationship between the vicinal proton-proton coupling constant and the pseudorotation properties of the pyrrolidine ring in 4-hydroxy-L-proline derivatives has been investigated,[32] which allows (1) valid correction taking into the account the effects of electronegativity and orientation of substituents on $^3J_{H\text{-}H}$, (2) an empirical correlation between proton-proton torsion angles and the pseudorotational parameters *P* and ϕ_m and (3) the best fit of the conformational parameters to the experimental coupling constants obtained by means of a computerized iterative least–squares procedures.[33]

3.1.4 Application of Karplus equation

Empirical generalization of the Karplus equation for proton-proton coupling[37] was utilized to describe the conformation of the substituted ribose ring in nucleosides and nucleotides. In 4-substituted prolines, each H-C-C-H fragment carries three substituents, and the generalized equation 4 takes the form.[34]

$$^3J_{H\text{-}H} = 13.22 \cos^2 \phi - 0.99 \cos \phi + \Sigma \Delta\chi_I \{0.87 - 2.46 \cos^2 (\xi_i \bullet \phi + 19.9 \mid \Delta\chi_i \mid)\} \text{ ------ (5)}$$

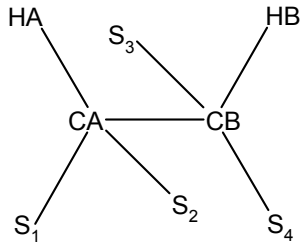

S_i (S_1, S_2, S_3 and S_4) are substituents

where ϕ is the Klyne-Prelog[34] sign for the proton-proton torsion angle and $\Delta\chi_I$ denotes the difference in electronegativity between the substituent S_i and hydrogen on the Huggien's scale[13]; ξ_I stand for +1 or –1 according to the orientation of the substituent S_i located on the fragment $S_1S_2H_AC_AC_BH_BS_3S_4$. The summation is taken over the three non-

hydrogen substituents, including of the ring carbon and /or nitrogen.

A complicating factor in the pseudorotation analysis lies in the fact that the proline under investigation may be engaged in a conformational equilibrium:

$$N \rightleftharpoons S$$

and, the observed coupling constants represent a time average value (Equation 6):

$$J_{exp} = X_n J_N + X_S J_N \text{----------6}$$

Where X_N and X_S are mole fractions $X_N + X_S = 1$ and J_N and J_S the coupling constants for the pure conformers

The complete conformational analysis thus entails the determination of five independent parameters, P_N, ϕ_N, P_S, ϕ_S, and K from the six observed coupling costants in hydroxyl proline or from 10 couplings constants in proline.

3.2 RATIONAL OF PRESENT WORK AND OBJECTIVES

In this chapter the aim is to study the prolyl ring conformation in aminoethyl prolyl (*aep*) PNA monomers.[35] The aminoethyl prolyl (*aep*) PNA **3** (Figure 9) was found to be a promising analogue due to its higher affinity and selectivity in binding to complementary DNA sequences. *aep*-PNA is chiral, constrained and cationic in comparison with the *aeg*-PNA that is achiral, relatively flexible and neutral in nature (Figure 9). The PNA oligomer containing the *aep*-A/T/G/C monomers upon complexation with DNA exhibit stabilization depending upon the nucleobase, stereochemistry and the binding orientation. This may arise from the fact that the nature of the 4-substituent plays an important role in defining the pucker of the pyrrolidine ring in 4-substituted prolines.[36] The individual purines or pyrmidines differ in their group electronegativities and when present at the 4-position of the pyrrolidine ring may cause differential ring pucker effects. This would consequently lead to backbone conformational changes causing sequence specific effects.

Thus it is important to determine the conformational preferences of pyrrolidine ring in *aep*-PNA monomers[41] and the effects of 4-substitution on conformational preferences.

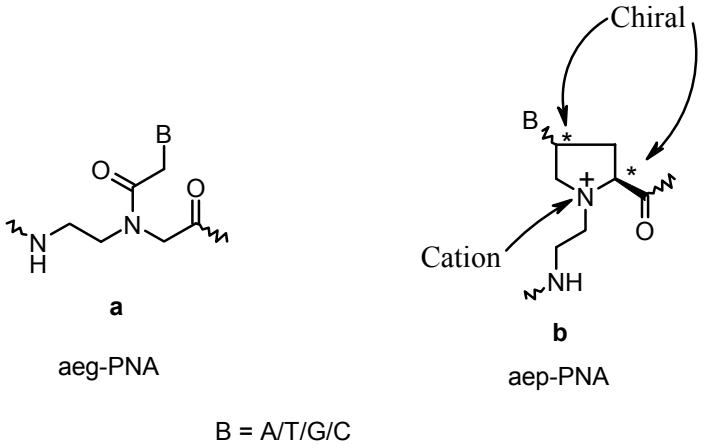

Figure 9: Chemical structure of *aeg*-PNA and *aep*-PNA.

Specific objectives of this chapter are the following

(i) NMR assignment of ring protons of pyrrolidine ring of *aep*-PNA derivatives including four monomers of *aep*-PNA (Figure 10) by a combination of 1D-proton decoupling and 2D-NMR experiments such as COSY and NOESY.

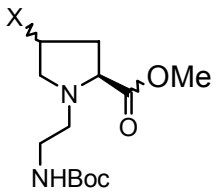

X = OH, OMs, OTs, OBz, N3BzT,
A, C, 2-amino-6-chloropurine prolyl derivative

Figure 10: Chemical structure of prolyl derivatives

(ii) HETCOR assignments and 2D-J resolved experiments, followed by determination of ^{3}J value of ring protons.

(iii) Determination of the conformation of pyrrolidine ring of 4-substituted proline derivatives by comparative *J* values obtained from pseurot (PSEUROT 5.4.1) program.

3.3 PRESENT WORK

3.3.1 Assignment of pyrrolidine ring protons in *aep*

To see the effect of 4-substitution on prolyl ring conformation by ^{1}H-NMR, chemical shift assignment of all ring protons is essential to obtain the respective coupling constants. The synthesis and chemical characterization of compounds (**1-10**) (Scheme 1) used here are described in Chapter 2. All compounds were synthesized starting from the hydroxyl intermediate **1**, from which other 4-substituted prolyl compounds **2-10** were obtained**.** L-*trans-and cis*-(2*S*,4*R/S*)-*aep*-thymine **(5/7/8),** L-*trans/cis*-(2*S*,4*R/S*)-*aep*-adenine **6/9**.[35] L-*cis* -(2*S*,4*S*)-cytosine *aep* **10** and L-*cis*-(2*S*,4*S*)-*aep*-2-amino-6-chloropurine (**11)** were chosen for conformational study by NMR.

Scheme 1: Synthesis of pyrrolidine derivatives

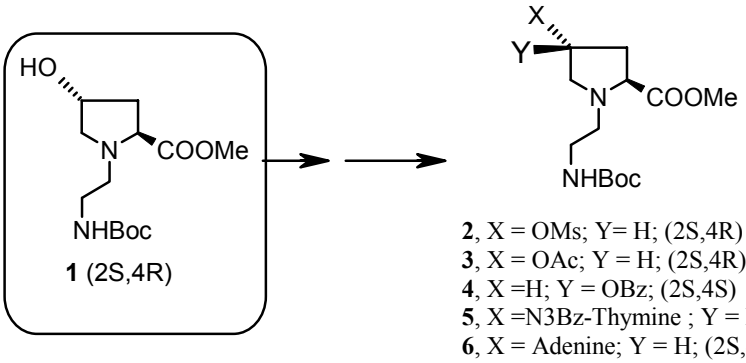

2, X = OMs; Y= H; (2S,4R)
3, X = OAc; Y = H; (2S,4R)
4, X =H; Y = OBz; (2S,4S)
5, X =N3Bz-Thymine ; Y = H; (2S,4R)
6, X = Adenine; Y = H; (2S,4R)
7, X = H; Y=N3Bz-Thymine; (2S,4S)
8, X = H; Y=Thymine; COOMe = COOH; (2S,4S)
9, X =H; Y = N^{6Bz}Adenine; (2S,4S)
10, X = H; Y= N^{4Cbz}Cytosine; (2S,4S)
11, X = H; Y = 2-amino-6-chloropurine; (2S,4S)

3.3.2 Assignment strategies

Evaluation of coupling constant requires unambiguous assignments of chemical shift of the all protons. This was done by a combination of ^{1}H-NMR 2D COSY (^{1}H-^{1}H) and 2D NOESY experiments. [36,37]

3.3.2a *^{1}H-Decoupling NMR (1D) experiment*: A typical assignment procedure is demonstrated for the compound **1**. The assignment of each protons of compound **1** was done by use of ^{1}H-Decoupling NMR (1D) experiment and results are shown in Figure 11-13.

Spectra 1: In the ^{1}H-proton NMR of scanned at 200 MHz in $CDCl_3$, the methyl group (δ 3.7, s, 3H) of methyl ester and Boc group (δ 1.4, s, 9H) of compound **1** is assigned by their characteristic chemical shift (ppm) and the assignment of other protons was done by decoupling experiments of desired protons (Figure 11). The composition of the region δ 1.5-4.0 is shown below.

Spectra 2: The NH group of compound **1** was assigned by scanning the same compound in $CDCl_3$ and D_2O (8:2, v/v). In this spectrum, the broad singlet at δ 5.4 (bs, 1H) due to NH protons disappears after exchange with D_2O.

Spectra 3: Expanded proton spectra (δ1.5-5.5) of compound **1** exchanged with D_2O.

Spectra 4: Decoupling of the most down field proton (δ 4.5, m, 1H) changes the signal at δ 3.48 (dd becomes d, 1H), δ 2.5 (dd becomes d, 1H) and δ 2.2 (m becomes d, 2H). From chemical of structure compound **1**, it is seen that H4 has four adjacent protons H5', H5", H3' and H3"and this signal at 4.5 is due to H4.

Spectra 5: Decoupling of the proton signal at δ 3.6 (t, 1H), causes change only in the proton signal at δ 2.2 (m becomes d, 2H), indicating that the proton signal at δ 3.6 has

only two adjacent protons. Hence, signal at δ 3.6 represents H2, which has two adjacent protons H3'/H3" and assignable to signal at δ 2.2 (m, 2H) and not at δ 3.48 (dd, 1H), δ 2.5 (dd, 1H).

Spectra 6: Decoupling of proton signal at δ 2.5 (dd, 1H) shows a collapse of proton signal at δ 3.48 (dd becomes d, 1H) and simplification in multiplet at most down field proton δ 4.5 (multiple, 1H) assigned to H4. This indicates that signals at δ 3.48 and δ 2.5 correspond to represent H5', H5".

Spectra 7: The decoupling of proton signal δ 2.1 (m, 2H), leads to changes at δ 4.5 (multiplet becomes t, 1H, H4) and δ 3.6 (t becomes s, 1H, H2) suggesting this signal to be due to H3"/H3'.

Spectra 8: Decoupling of proton signal at δ 3.2 (m, 2H) result in only one change at δ 2.7 (multiplet becomes quartet, 2H) and thus signals at δ 3.2 and δ 2.7 are the vicinal protons αH'αH", βH'βH" in *N*-ethyl substituent of compound **1**.

Thus all protons of ring and *N*-alkyl side chain are assigned systematically by 1D-decoupling spectra and this aids in determination of accurate coupling constants from further experiment.

^{1}H-NMR spectra (200 MHz) of compound **1**

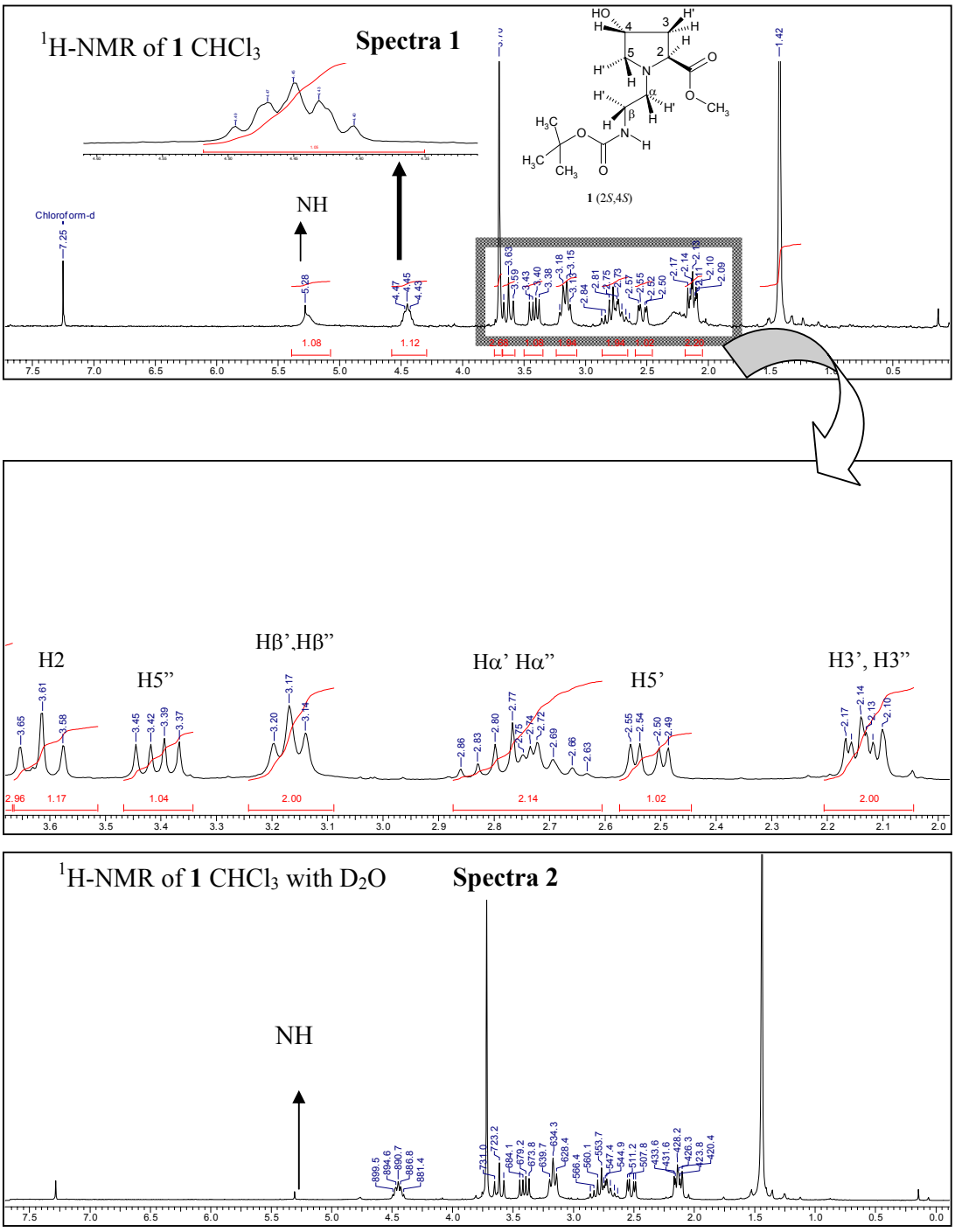

Figure 11: 1D ^{1}H decoupled NMR spectra of **1** (200 MHz NMR)

^{1}H-NMR spectra (200 MHz) of compound **1**

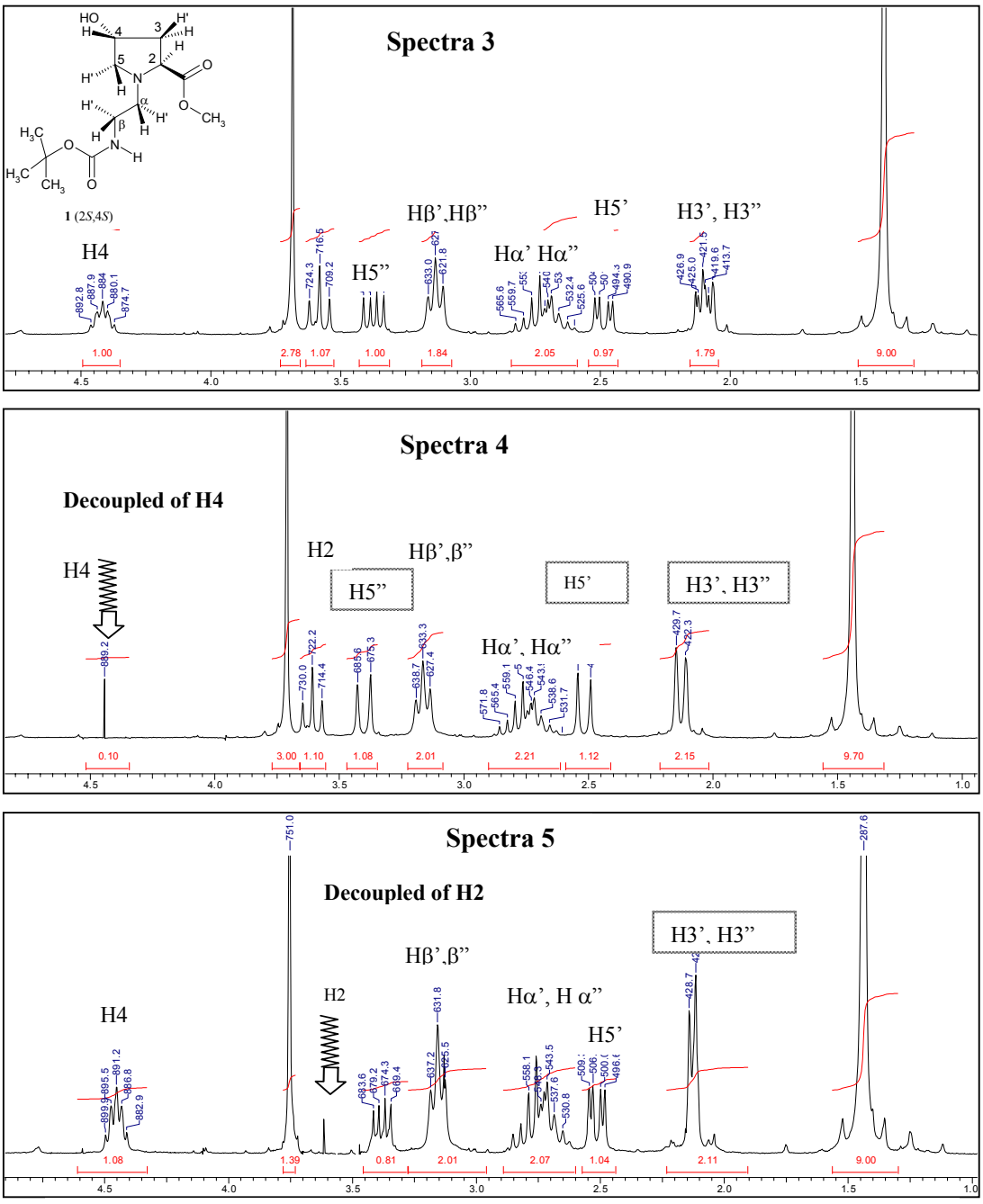

Figure 12: 1D ^{1}H decoupled NMR spectra of **1** (200 MHz NMR)

^{1}H-NMR decoupled spectra (200 MHz) of compound **1**

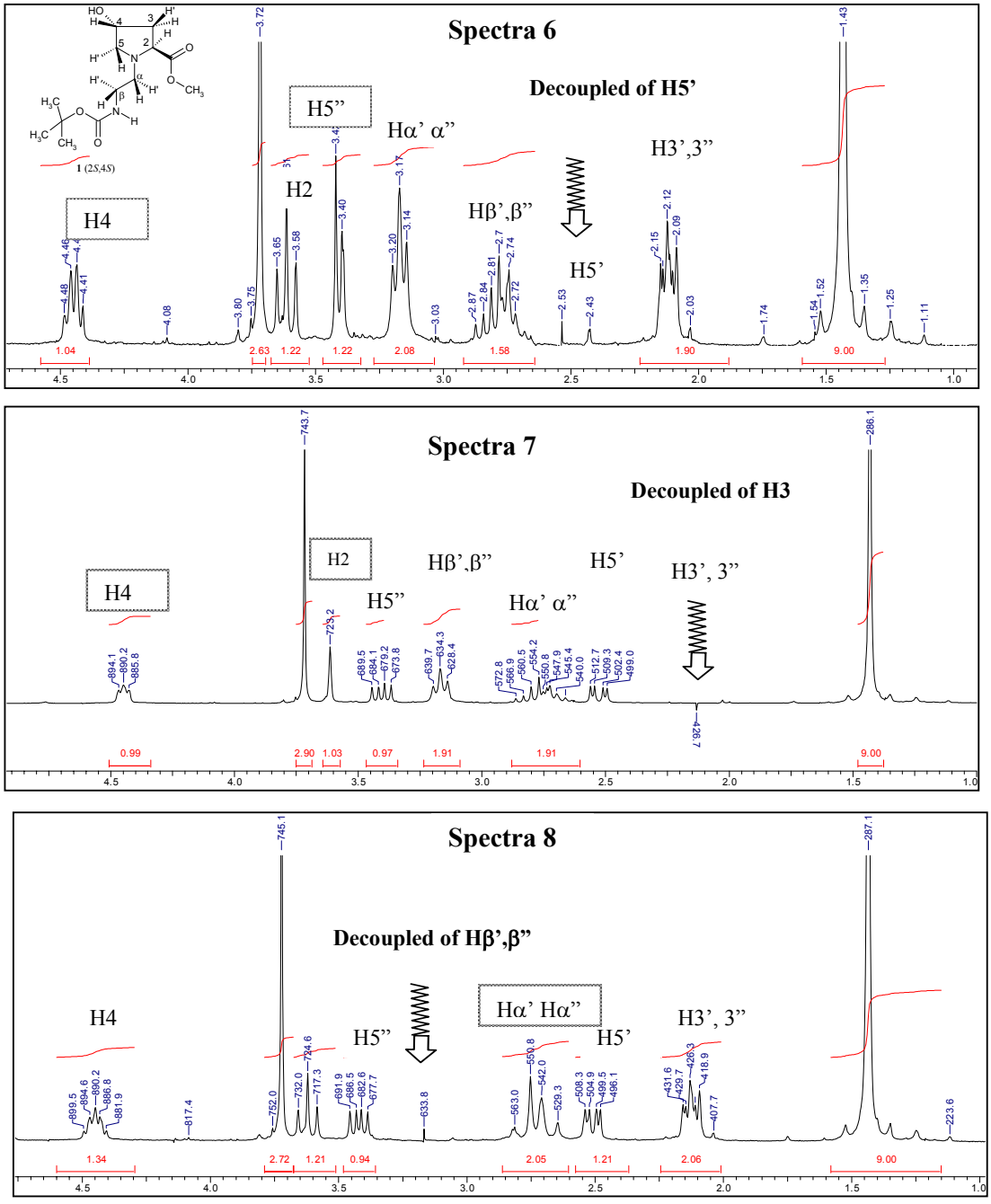

Figure 13: 1D ^{1}H decoupled NMR spectra of **1** (200 MHz NMR)

3.3.2b 2D J-Resolved spectroscopy: coupling constants

2D J-resolved NMR[37] spectra of compound **1** (Figure 14-16) was recorded at 500 (MHz) in $CHCl_3$ and was used to obtain the accurate coupling constants of prolyl ring protons in compound **1** (Table 2). The assignment done by ^1H 1D decoupling experiments[37] were used for identification of different protons. The coupling constants extended from there spectra are shown in Table 2

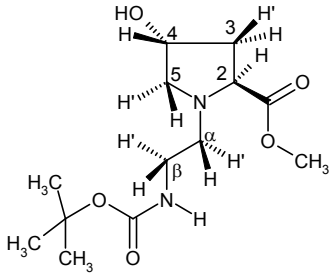

1 (2*S*,4*S*)

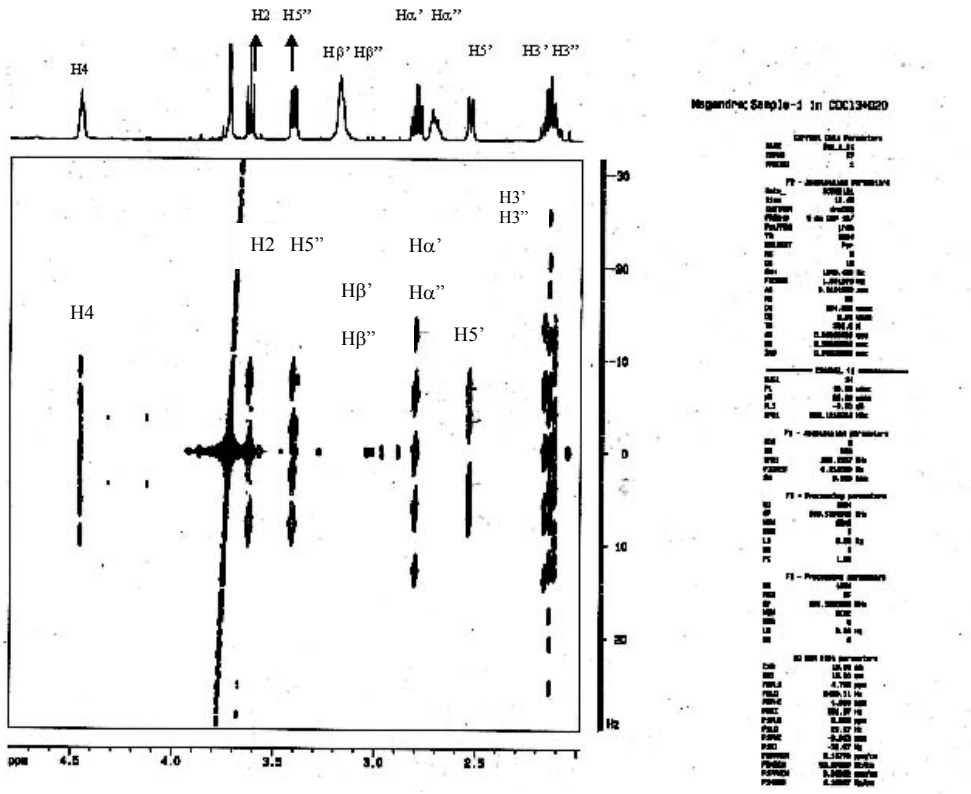

Figure 14: 2D J-resolved spectra of **1** (500 MHz NMR) where the x axis is chemical shift (δ) and the y axis is coupling constant (Hz)

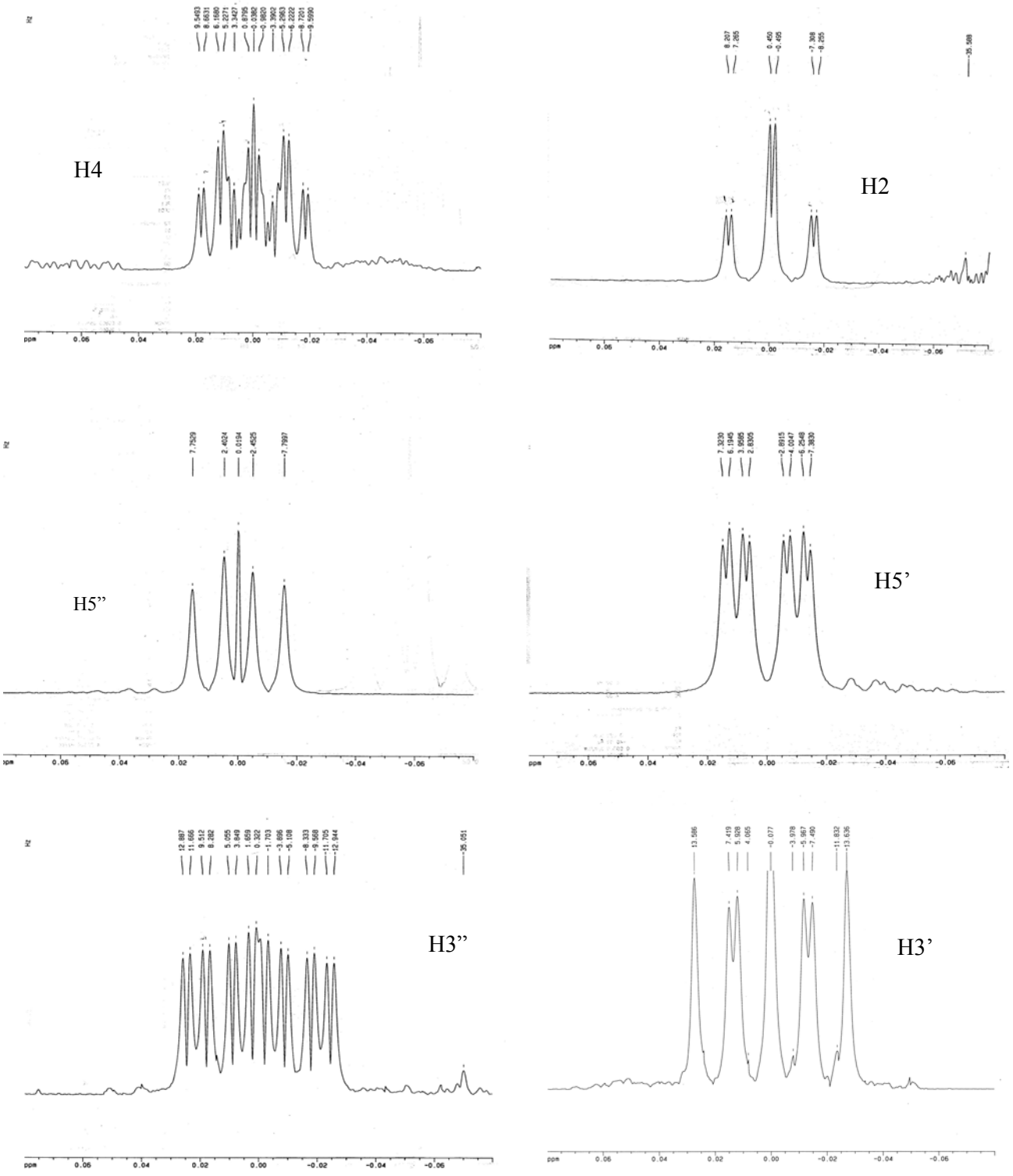

Figure 15: 2D J-resolved spectra of **1** (500 MHz NMR)

Side Chain protons of compound **1**

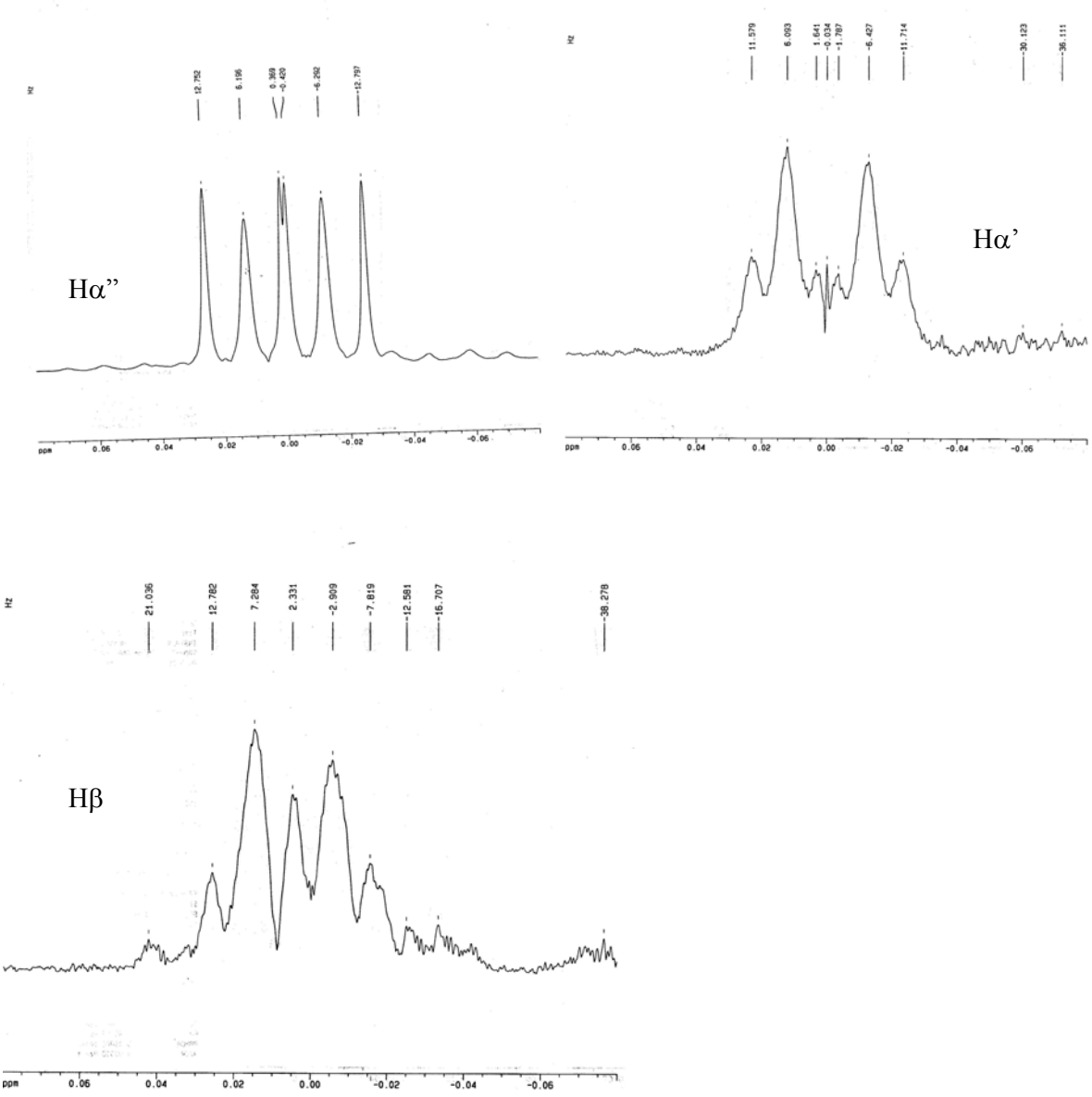

Figure 16: 2D J-resolved spectra of **1** (500 MHz NMR)

2D ^{1}H-^{1}H COSY:

The application of ^{1}H-^{1}H COSY for structural determination assignment is illustrated with compound **2** as an example. The 1D ^{1}H NMR and the expanded δ 3.7-2.2 region are shown in Figure 17 and some of these could be tentatively assigned in comparison with that of compound **1**. The H4 is downfield shifted to δ 5.2 due to mesyalation of 4-hydroxy group. Further assignment of chemical shift of the corresponding protons in compound **2** was done by 2D NMR ^{1}H-^{1}H COSY and that of the corresponding carbons by 2D ^{1}H-^{13}C HETCOR spectral analysis.

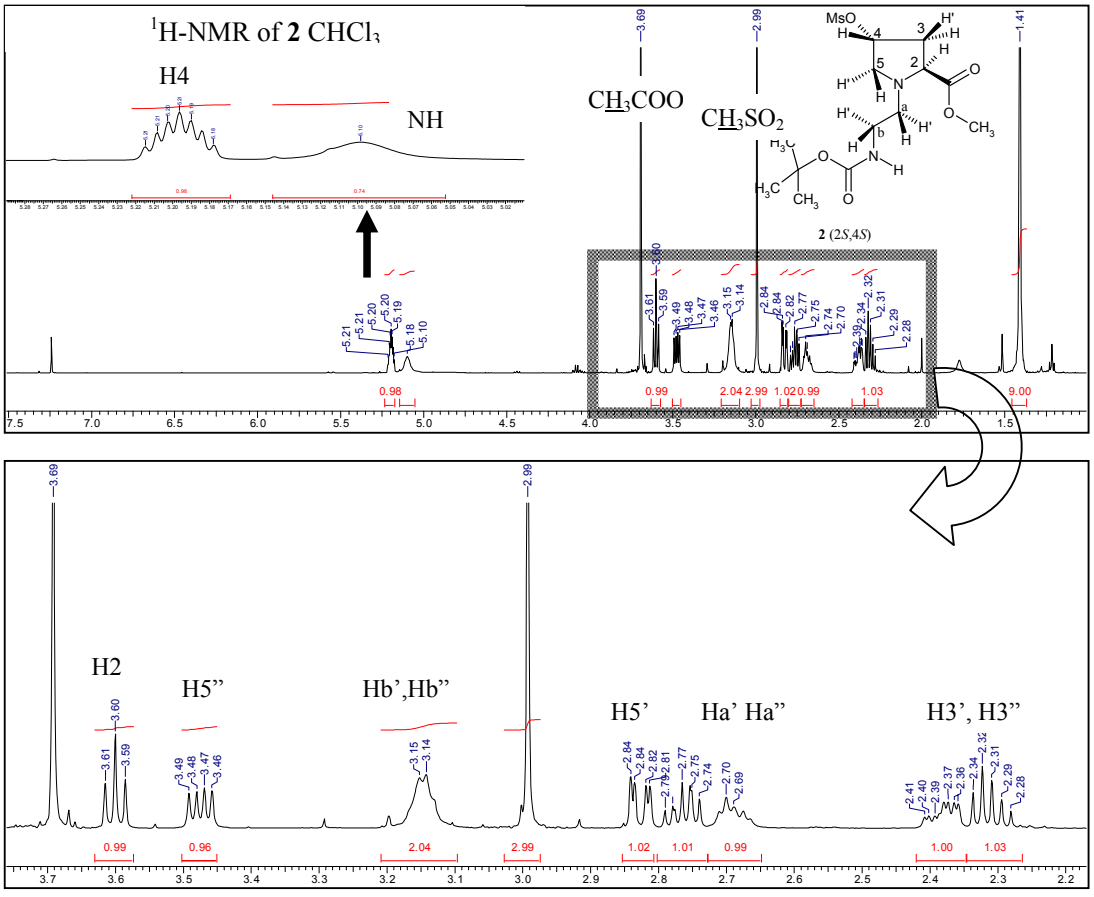

Figure 17: 1D ^{1}H-NMR spectra of **2** (500 MHz)

In the ^{1}H-^{1}H COSY spectra of compound **2** (Figure 18, top), the diagonal and cross peaks and their assignments by correlations are shown. The diagonal peaks show the

chemical shift of corresponding protons while the cross peaks (1 to 8) represent the connectivity (H1-C1-C2-H2) between protons bonded to adjacent carbons (vicinal coupling).

2D The assignment starts by identifying easily assignable protons. The chemical shift of the most downfield proton is that of H4 which shows four cross peaks (1, 2, 3 and 4). H4 is copiled to two neighbours H5 and H3, and each set H5'H5" and H3'H3" has 2 non-equivalent protons leading to expected 4 cross peaks as shown. From chemical shift assignment by comparison with that done on compound **1**, the four cross peaks are assigned as follows 1 (H4, H5"), 2 (H4, H5'), 3 (H4, H3"), 4 (H4, H3") and this assignment confirms the chemical shift of H3'H3" and H5'H5". Assignment of H3'H" thus paves way for identifying H2 at δ 3.6 which shows H2-H3' and H2-H3" (cross peak 5).

The assignment of N-ethylamino side chain protons Ha", Ha', Hb" and Hb' starts from assignment of NH δ 5.1 which shows cross peaks to Hb',b" at δ 3.1 (cross peaks 5). This is coupled to Ha'a" shown by cross peak at δ 2.7 (cross peaks 8-9).

After assignment of ^{1}H-NMR, corresponding ^{13}C peak are assigned by 2D-HETCOR spectra (Figure 18, below). The cross peaks represent correlation of ^{13}C to the attached protons and with assignment of specific ^{1}H by 2D COSY, the assignment of ^{13}C becomes straight forward. The ^{1}H and ^{13}C chemical shifts derived by NMR for different compounds are shown in Table 2.

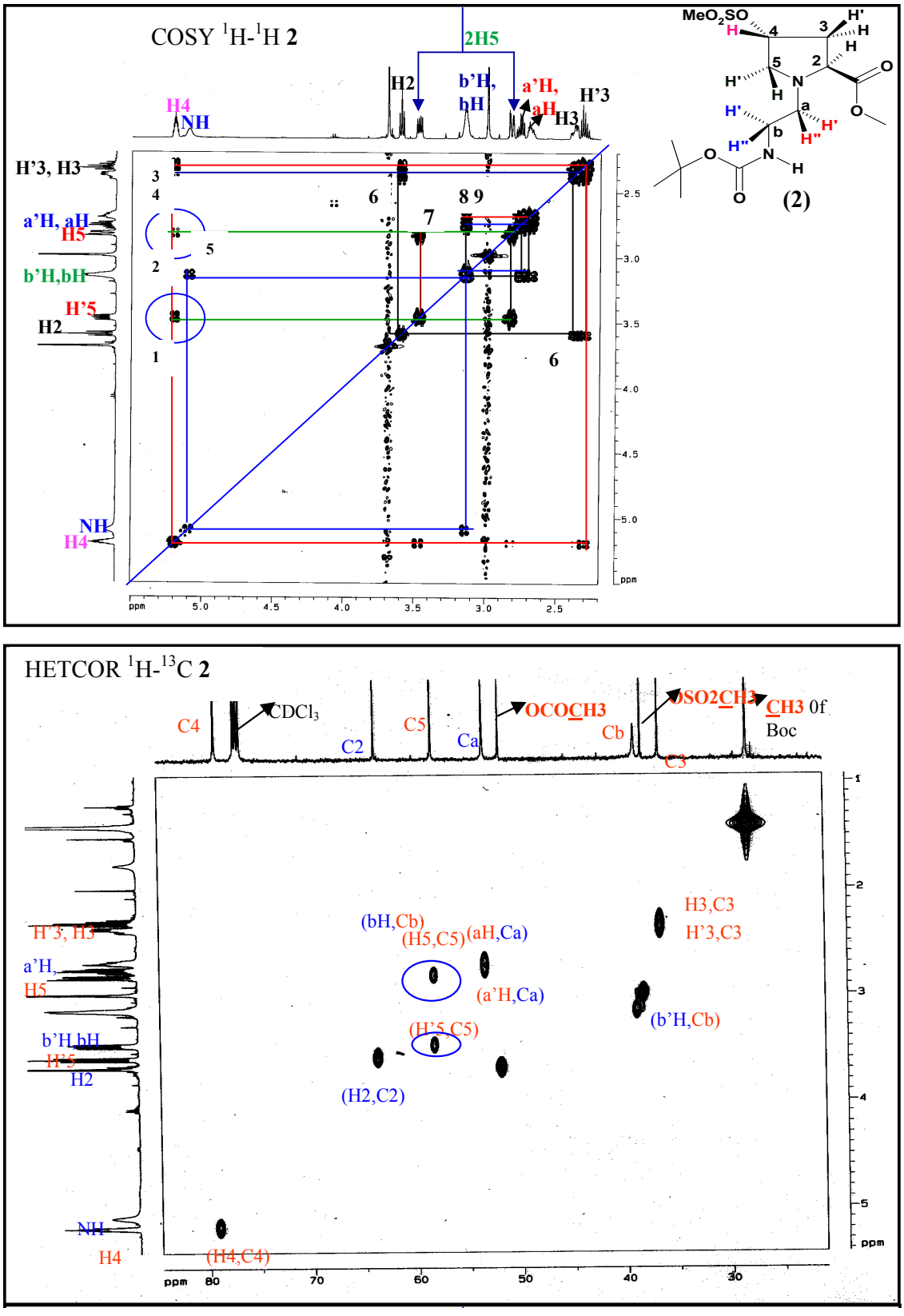

Figure 18: 2D-^{1}H-^{1}H COSY and HETCOR NMR spectra of **2** (500 MHz)

Similarly, the protons of *aep*-monomers (**5-11**) were also assigned by 2D ^{1}H-^{1}H-COSY (see in Figure 19-22) and other derivative. The chemical shifts of assigned protons for compounds **1-11** are given in Table 2.

Table 2: Chemical Shift of pyrrolidine ring protons (determined 2D COSY /HETCOR NMR)*

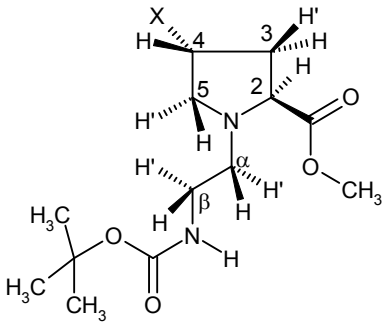

I

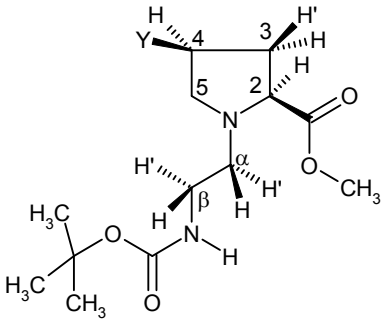

II

Compound	H2	H3	H3'	H4	H5	H5'	αH	α H'	βH	β H'	NH	Base Protons
1 (X = OH)	3.4	2.2	2.3	4.4	3.4	2.5	2.8	2.8	3.4	3.4	5.3	-
2 (X = OMs)	3.6	2.2	2.3	5.3	2.8	3.4	2.6	2.7	3.1	3.1	5.1	-
3 (X = OAc)	3.5	2.1	3.3	5.3	2.6	3.5	2.6	2.7	3.1	3.2	5.2	-
4 (X = OBz)	3.4	2.2	3.2	4.8	2.7	3.3	2.8	2.8	3.1	3.1	5.4	-
5 (X = N3BzT)	3.4	2.2	2.9	4.8	3.8	3.2	2.8	2.8	3.2	3.2	5.2	-
6 (X = A)	3.5	2.5	2.3	5.2	3.8	3.3	2.6	2.6	3.0	3.2	5.4	AH8 8.8, AH2 8.7
7 (Y =N3BzT)	3.4	2.0	2.9	5.2	2.8	3.3	2.7	2.9	2.7	2..8	5.2	TH6 8.1
8 (Y = T)	3.3	2.0	2.8	5.2	2.8	3.2	2.7	2.9	2.7	2..6	-	TH6 8.1
9 (Y = N^{6bz}A)	3.4	2.2	3.0	5.4	3.1	3.4	2.8	2.9	3.2	3..3	5.2	AH8 8.8, AH2 8.7
10 (Y = N^{4Cbz}C)	3.4	2.0	2.8	5.3	2.8	3.2	2.6	2.9	3.2	3..3	5.2	CH5 7.5, CH6 8.5
11 (Y =ACP)[a]	3.5	2.2	2.9	5.2	3.0	3.3	2.7	2.9	2.9	3..2	5.3	$_{ACP}$H 8 8.3

[a]ACP = 2-amino-6-chloropurine ; *NMR of all compounds have scanned at 500 Mz MNR

3.3.2c 2D NOESY correlation of *aep*-PNA monomers

Pyrimidines: 2D NOESY spectroscopy correlates spatially close-by (< 5Å) protons which are not directly connected through bonds. Figure 19B shows the 2D ^{1}H-^{1}H NOESY spectra of N3-benzoyl *aep*-PNA-T monomer **7**. In addition to the spatially correlated spins, 2D NOESY spectra also contain cross peaks due to J coupled ^{1}H-^{1}H spins. The presence of these peaks helps to confirm the assignments, but needs to be

eliminated from NOESY analysis. Cross peaks due to J-coupled ^{1}H-^{1}H systems are identified by 2D COSY spectrum (Figure 19A). In 2D NOESY spectra (Figure 19B) the cross peaks not arising purely from spin-spin spatial correlation are marked and. these correspond to correlation of the base protons with the pyrrolidine ring protons. Cross peaks are seen due to spatial proximity (dipolar coupled) of H6 of T at δ 8.3 with (i) H3' (upfield component of H3'/H3") at δ1.9, (ii) H5" (upfield component of H5'/H5") at δ 3.2 and (iii) with H4. This suggests that the pyrrolidine ring system has a pucker with H5', H3' and H4 on the same face of the ring.

In case of *aep*-PNA-C(N^{4Cbz}) **10**, the NOESY spectra H6 of C showed NOE cross peaks to H3' and H5' of the pyrrolidine ring. However, under the conditions of experiment H6-H4 cross peak, which is normally weak, was not seen. This suggests a similar conformation of pyrrolidine ring of **10** in which H6 is on the same face as H5" and H3'.

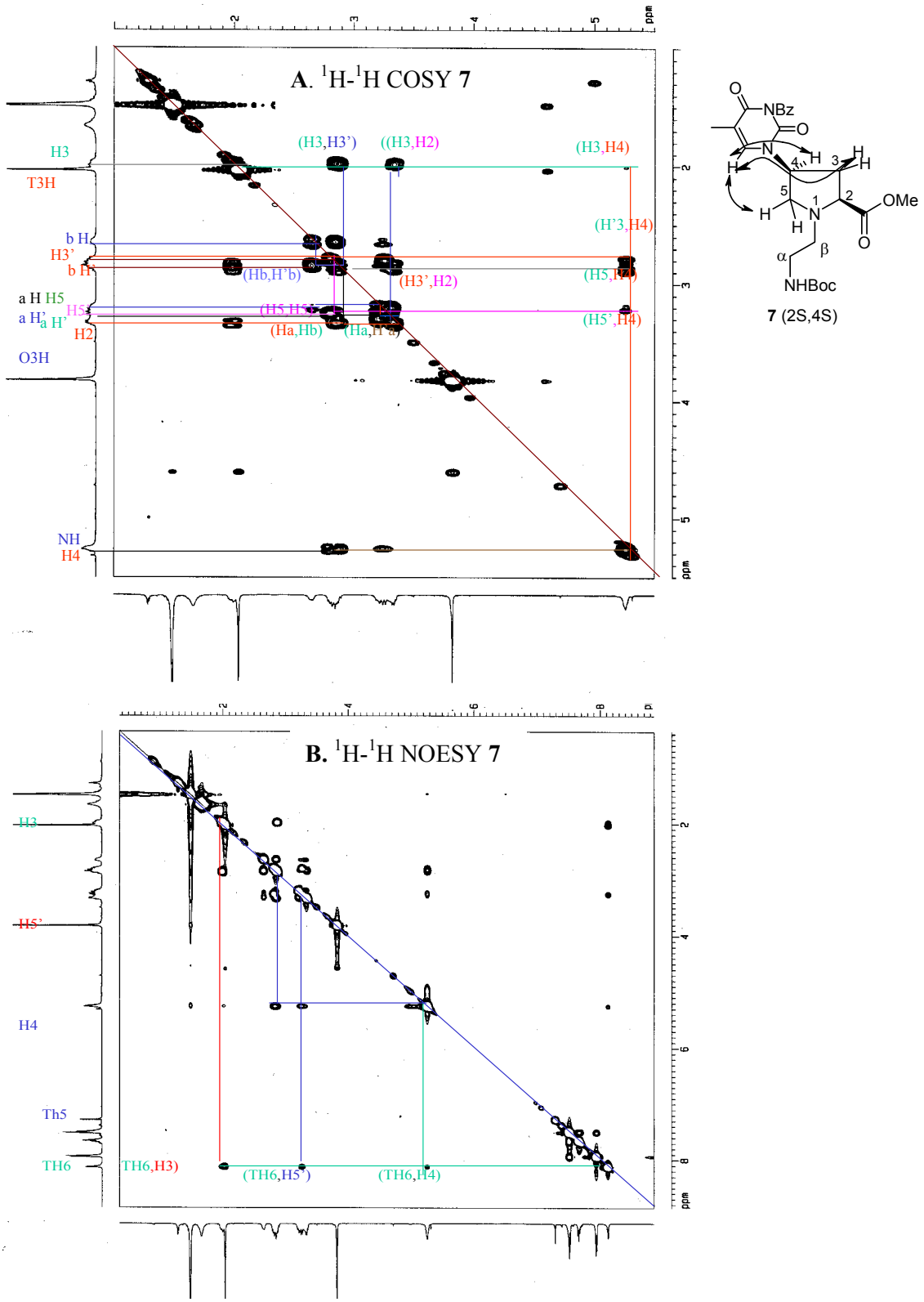

Figure 19: 2D-^{1}H-^{1}H COSY and NOESY NMR spectra of **7** (500 MHz)

Purines: In the case of N^{6Bz}-adenine *aep*-PNA monomer **9** and 2-amino-6-chloro-purine *aep*-PNA monomer (**10**), the NOESY spectra (Figure 20 B) shows NOE cross peaks from H8 of A to H3' and H5" of pyrrolidine ring. However, under conditions of experiment H8-H4 cross peak, which is normally weak, was not seen. This suggested a conformation of pyrrolidine ring in adenine and 2-amino-6-chloro-purine monomer in which H8 is on the same face as H5' and H3'. The data suggests that compounds **7**, **9** **10** and **11** have a relative conformation of Pu/Py and pyrrolidine rings in such a way that pyrrolidine ring has a pucker with H5', H3' on the same side as the H6 of pyrimidines and H8 of purines.

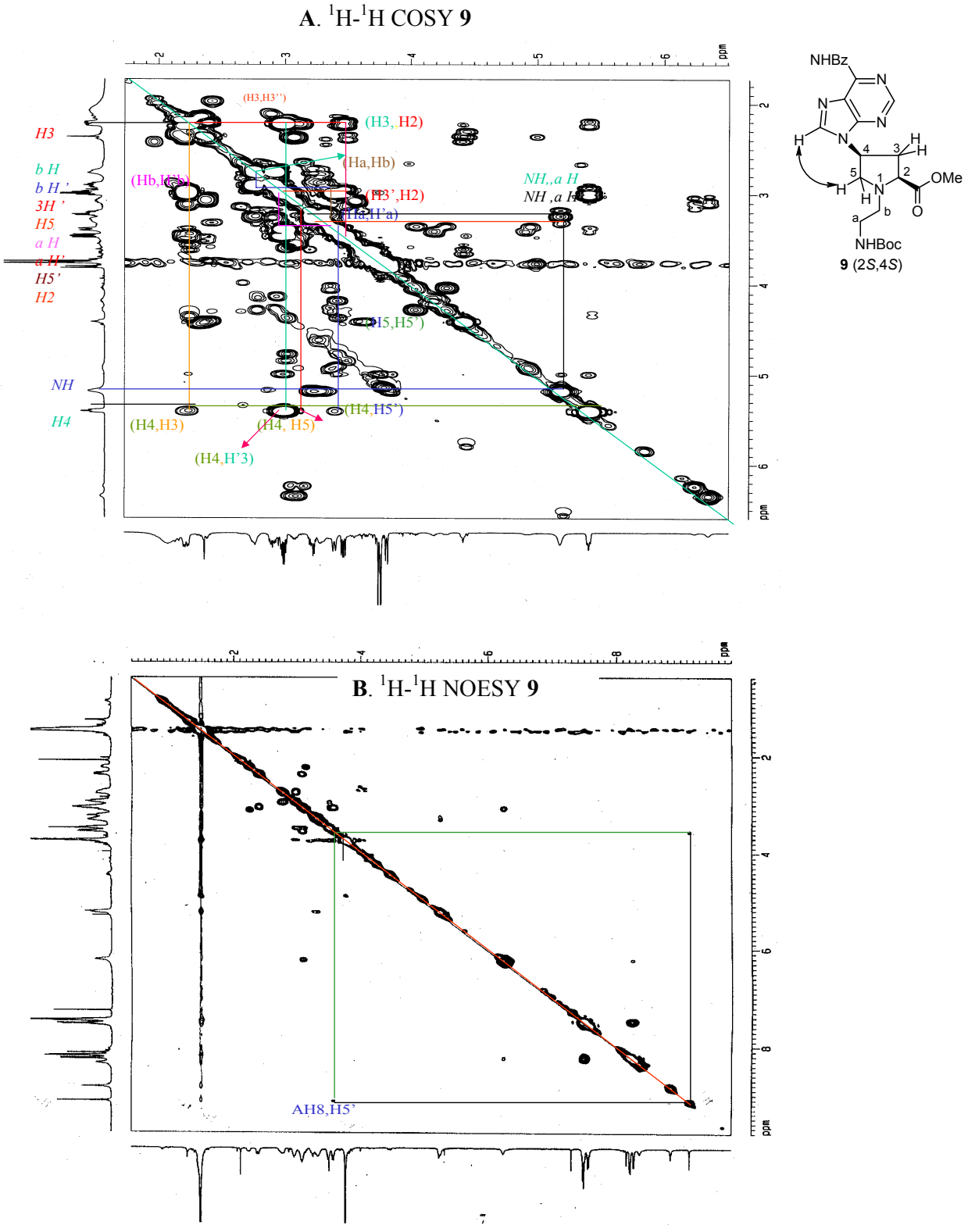

Figure 20: 2D-^{1}H-^{1}H COSY and NOESY NMR spectra of **9** (500 MHz)

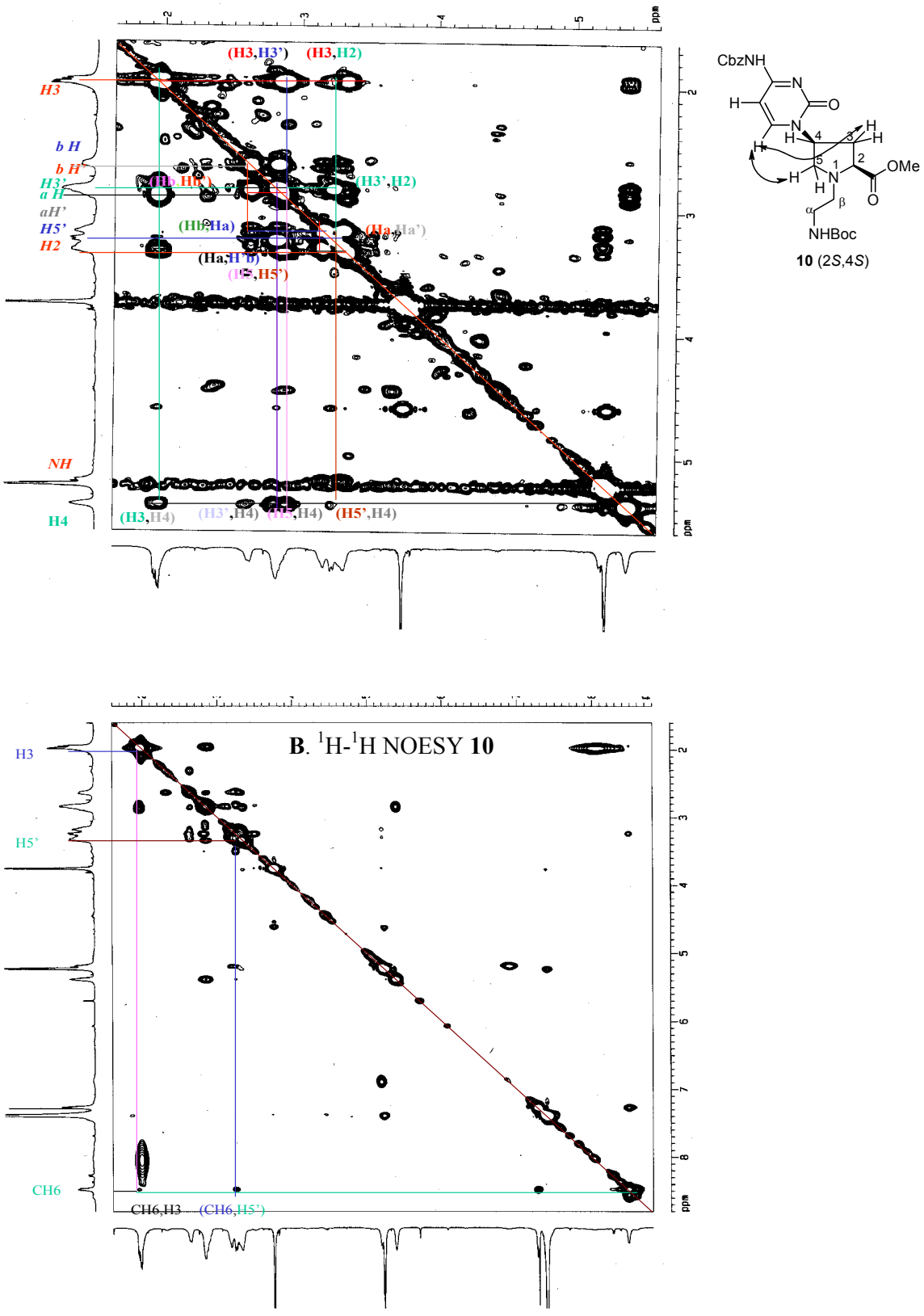

Figure 21: 2D-^{1}H-^{1}H COSY and NOESY NMR spectra of **10** (500 MHz)

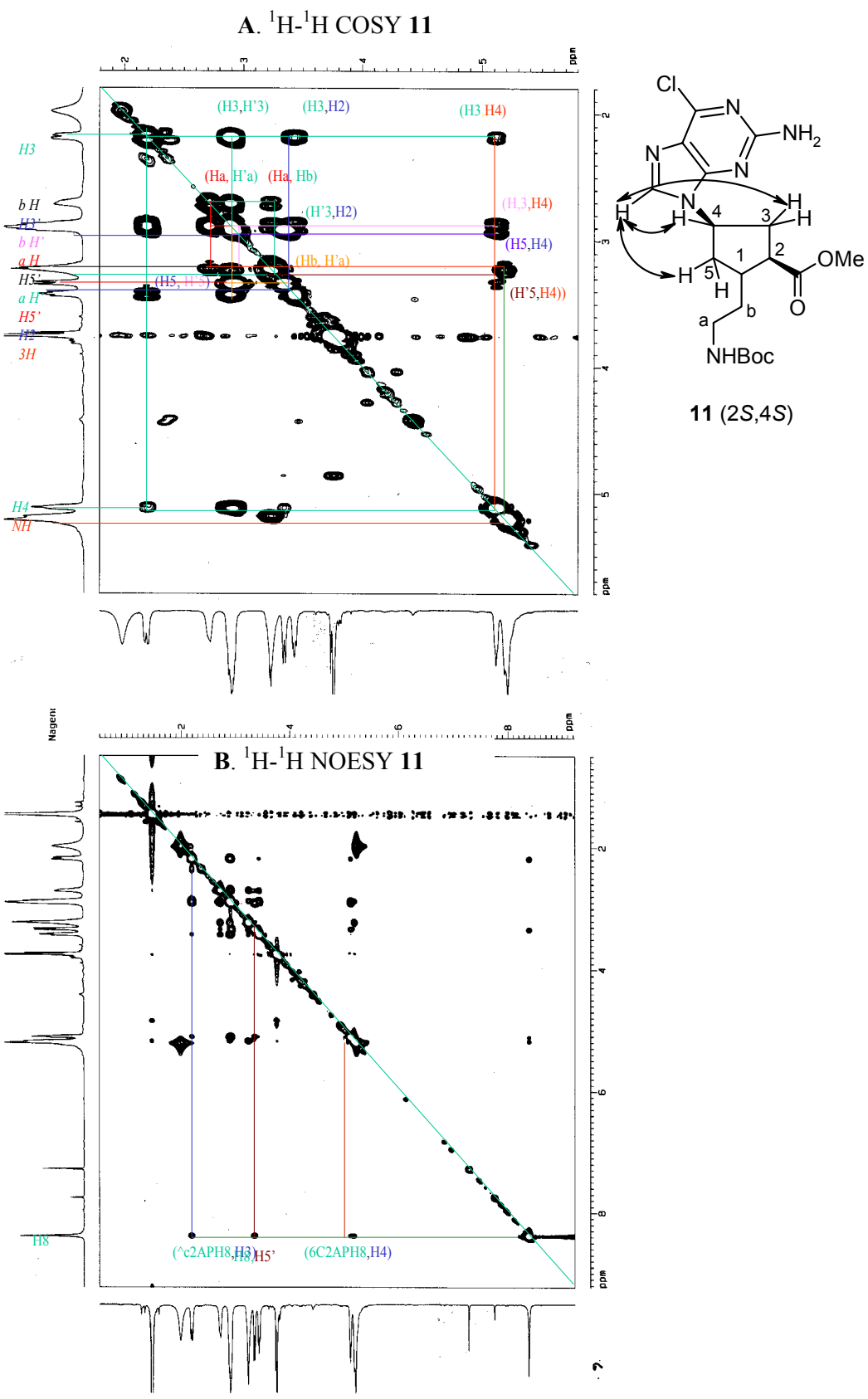

Figure 22: 2D-^{1}H-^{1}H COSY and NOESY NMR spectra of **11** (500 MHz)

3.3.2d Calculation of the vicinal coupling constants

The vicinal coupling constants ($^3J_{x-y}$) of 4-substituted pyrrolidine rings were obtained from ^{1}H-spectra of the pyrrolidine derivatives **1-4** (4*R*-OH, **1**, 4*R*-OMs **2**, 4*R*-OAc **3** and 4*S*-OBz **4),** *aep*-PNA monomers **5**,**6**,**8-10** (L-*trans*-(2*S*,4*R*)-*aep*-PNA-T(N3Bz) **5**, L-*trans*-(2*S*,4*R*)-*aep*-PNA-A **6** and L-*cis*-(2*S*,4*S*)-*aep*-PNA-T **8,** L-*cis*-(2*S*,4*S*)-*aep*-PNA-A **9,** L-*cis*-(2*S*,4*S*)-*aep*-PNA-C **10** and L-*cis*-(2*S*,4*S*)-*aep*-PNA-(6-Cl-2-aminopurine) **11** (precursor of *aep*-G-PNA monomer) (Table 3). The splitting pattern of pyrrolidine ring protons peaks was not resolved in some cases and hence the coupling constants data such monomers were unavailable for conformational study of their pyrrolidine ring.

Table 3: Vicinal proton-proton coupling ($^3J_{H-H}$ / Hz) constants of pyrrolidine ring

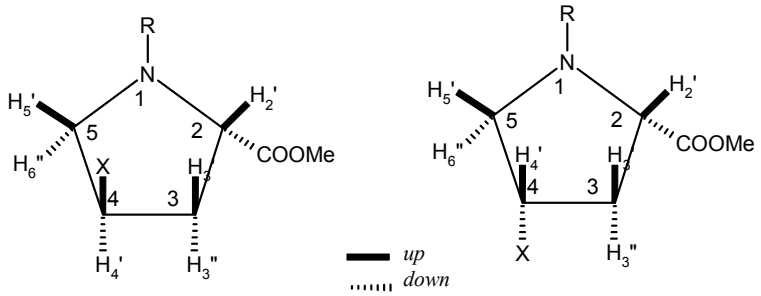

R = $BocNHCH_2CH_2$-

I (*cis*)
1; X = OH
2; X = OMs
3; X = OAc
5; X = N3Bz Thymine
6; X = Adenine

II (*trans*)
4; X = OBz
8; X = Thymine; COOMe = COOH

Compound	H'$_2$-H'$_3$	H'$_2$-H"$_3$	H'$_3$-H'$_4$	H"$_3$-H'$_4$	H'$_4$-H'$_5$	H'$_4$-H"$_5$	Solvent
1	7.80	7.80	5.40	5.40	3.40	4.90	$CDCl_3$
2	7.30	7.40	6.80	3.20	2.80	5.50	
3	7.30	8.30	3.20	5.90	3.20	6.00	
4	6.40	5.80	3.90	4.90	2.00	4.90	
5	8.10	7.90	2.90	4.20	3.70	2.90	
6	6.30	6.50	7.10	5.80	5.90	5.30	
8	8.10	7.30	5.80	5.90	8.80	3.75	D_2O

3.3.3 Calculation of pyrrolidine ring conformation using *Pseurot 5.4.1*

The vicinal coupling constant ($^3J_{x-y}$) was used to derive the pseudorotation phase angle (P) and puckering amplitude (ϕ_m) of pyrrolidine rings in different compounds by using PSEUROT programming version (5.4.1),[38] based on the relation between ϕ (H-H) and P as equation 6.

$$\phi\ (H\text{-}H) = A * \phi_{Max} * \cos (P + \text{phase}) + B \text{----------(6)}$$

where ϕ(H-H) = torsional angle between two adjacent hydrogens, P = pseudorotation angle, ϕ_{Max} = puckering amplitude and A and B are constants. For the 4-substiuted prolines the parameters phase angle P and B value of corresponding vicinal proton pairs were used as in the software (PSEUROT 5.1.4). The role of electronegativities of substituents in 5-membered rings (furanose and pyrolidine) are also important in determining the puckering of rings. The electronegativity values of different substituents in pyrrolidine ring shown in Table 4 and 5 were used in PSEUROT 5.4.1 program to find the conformation of 4-substituted pyrrolidine ring.

Table 4: Group electronegativities (L value) for L-4-hydroxyl proline[38]

Substituent or ring carbon Proline in H_2O or D_2O	**L Value**
H	0.0
C1	0.60
C2	0.74
C3	0.74
C4	0.68
COOH(R)/COO-	0.39/0.41
NHR	1.02
NRC(=O)R	0.53
NH_3^+	0.82
C3	0.62 (4-Hypro)
OH	1.25 (Idem)

Table 5: Group electronegativities (L value) for Proline*

Substituent on pyrolidine ring	Solvent-Dependent L(D_2O)	L($CDCl_3$)	L(DMSO)
OH	1.25	1.34	1.42
OR)	1.26	1.40	1.42
(but OR/OR	1.41	1.41	1.42)
OAr	1.34	1.42	1.47
OPO2(OR)	1.25	--	--
OC(=O)R	1.17	1.17	1.22
NR2	1.01	1.12	1.20
NHR	1.02	1.16	1.22
NHAr	1.12	1.16	1.20
NH2	1.10	1.19	1.27
NHC(=O)R	0.81	0.86	--
NRC(=O)H	0.53	0.54	--
A, G, C, T, U	0.56	0.56	0.56

*Accuracy of L values ca 0.05, hence in practice one may set most oxygen in H_2O/D_2O at 1.3, all ring carbons at 0.65

The NMR measured (experimental) values of $^3J_{H-H}$ of all protons in proline ring in all compounds were used as input values of PSEUROT 5.1.4 programme. The input parameters PSEUROT 5.4.1 are $^3J_{H-H}$ (experimental), phase angle, A and B along with electronegativities values of substituents as $\chi1$, $\chi2$, $\chi3$ and $\chi4$ in pyrolidine ring and are shown in Table 6.

Table 6: General pattern of Input values of PSEUROT 5.4.1*

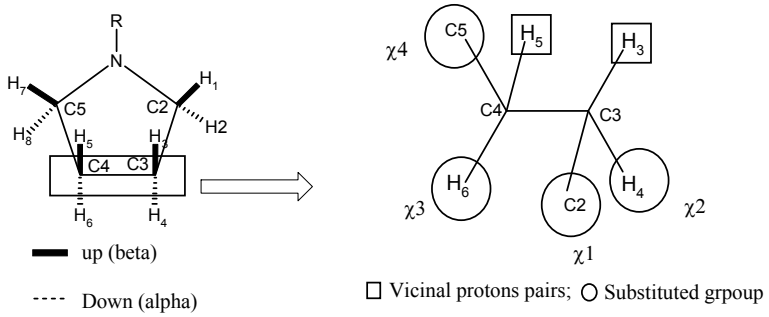

Coupling	Phase (^{o})	A	B (^{o})	Substitution patternof Eectronegativities $\chi1$	$\chi2$	$\chi3$	$\chi4$
H1 -H3	-144	1	0	N	H2	H4	C3'
H1 -H4	-144	1	-120	N	H2	C4'	H3
H2 - H3	-144	1	+120	H1	N	H4	C4'
H2 - H4	-144	1	0	H1	N	C3'	H3
H3 - H5 (2'-3')	0	1	0	C2	H4	H6	C5'
H3 -H 6	0	1	-120	C2'	H4	C5'	H5
H4 - H5 (2"-3')	0	1	+120	H3	C5'	H6	C4'
H 4 -H6	0	1	0	H3	C5'	C5'	H5
H5 - H7	+144	1	0	C3'	H 6	H8	N
H5 -H 8 (3'-4')	+144	1	-120	C3'	H6	N	H7
H6 - H7	+144	1	+120	H5	C3	H8	N
H6 - H8	+144	1	0	H5	C3'	N	H7

*Values of Phase, A and B taken from recent publication.

The phase angle, A and B along with electronegativities from Table 5 and J_{exp}, were used as the input in PSEUROT programme to obtain the output values as $^{3}J_{x-y}$ (calculated), P_N, ϕ_N, P_S, ϕ_s, MF (mole fraction) and dihedral angle (ϕ_{1-3}) of all vicinal pairs of pyrrolidine ring for two most probable conformers. A typical format of PSEUROT 5.4.1 is given in the text box, as five steps:

Step1: Parametrs in pseudorotation relation as vicinal coupling pairs, phase angle of equation karplus equation, A, B, electronegativities of substitution and no of substitution.

Step 2: Input data

J --> 2'-3' 2'-3" 3'-4' 3"-4" 4'-5' 4'-5"

Step 3: First estimates

Conformer 1: P_N and ϕ_N

Conformer 2: P_S and ϕ_S

Mole fraction of conformer 2 (MF2) = .500

Step 4: Final outputs

2'-3' J_{exp}; J_{cal}; ΔJdiff
2'-3" J_{exp}; J_{cal}; ΔJdiff
3'-4' J_{exp}; J_{cal}; ΔJdiff
3"-4" J_{exp}; J_{cal}; ΔJdiff
4'-5' J_{exp}; J_{cal}; ΔJdiff
4'-5" J_{exp}; J_{cal}; ΔJdiff

MF1 MF2 RMS

Conformer 1(*N*):		Conformer 2 (*S*):	
P =		P =	
ϕ		ϕ	
ϕ2'-3'	; J2'-3'	ϕ2'-3'	; J2'-3'
ϕ2'-3"	; 2'-3"	ϕ2'-3"	; J2'-3"
ϕ3'-4'	; J3'-4'	ϕ3'-4'	; J3'-4'
ϕ3"-4"	; J3"-4"	ϕ3"-4"	J3"-4"
ϕ4'-5'	; J4'-5'	ϕ4'-5'	; J4'-5'
ϕ4'-5"	; J4'-5"	ϕ4'-5"	J4'-5"

Step 5: Error analysis

Overall RMS

Standard deviation on parameters

Correlation matrix of parameters

AR. 1 2 3 4 5

End of program PSEUROT

3.3.4 PSEUROT Results

The validity of PSEUROT is reflected in the difference between J_{exp} and J_{calcd} (ΔJ, Hz), which should be in 0.0 ± 0.8 Hz and the least root mean square (rms) in range of 0.0-0.5. In this program, the mole fraction (MF) of the two probable conformers of pyrolidine ring of compounds **1-6** and **8** are denoted as MF1 (*N* conformer; P = 0^o) and MF2 (*S* conformer, P = 180^o), which are in equilibrium with the fractional ratio of conformers being 1:1.

The dihedral angles $\phi_{Hx\text{-}Hy}$ of 4-substituted pyrrolidine ring in compounds **1-6** and **8** as obtained from PSEUROT analysis are given in Table 7-8.

3.3.4a aep-derivatives

In Table 7, the outputs of PSEUROT computational experiment (see in appendix) for all 4-substituted pyrrolidine ring containing compounds **1-6** are summarized. These show enough indication of validity of the output results in term of ΔJ (Hz) for all six vicinal proton pair of 4-subsituted pyrolidine ring and least rms values.

For compound **1** (Table 7, entry 1), $\Delta J \sim 0.0\text{-}0.01$ for all six vicinal protons pair of 4-*R*-hydroxy substituted pyrolidine ring, the rms value is 0.008, MF1 is 0.548 and ϕ_N = 44.0 for N-conformer at $P_N = 15.2^o$.

For compound **2** (Table 7, entry 2),, $\Delta J \sim 0.0 \pm 0.29$ Hz for all six vicinal protons pair of 4*R*-O-mesylate substituted pyrolidine ring, the rms value is 0.216, MF1 is 0.503 and $\phi_N = 59.70^o$ (maximum deviation of torsional angle of C3-C4 or dihedral angle H3-H4) for N-conformer at $P_N = 7.7^o$.

Table 7: Summary of input and output data of *aep*-derivatives*

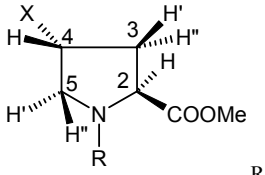

L-trans-(2*S*,4*R*)

R = CH_2CH_2NHBoc

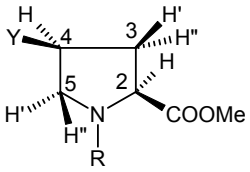

L-cis-(2*S*,4*S*)

Entry	Compound	Vicinal Proton-Pair[a]	ϕ_{H-H}[b]	J_{calcd}[c]	J_{exp}[d]	ΔJ[e]	MF[f]	P_N[g]	ϕ_N[h]	rms[i]
1	**1**	$H_{2'}$-$H_{3'}$	-29.2	7.79	7.80	0.01				
	X = OH	$H_{2'}$-$H_{3''}$	-150.4	7.79	7.80	0.01				
	Y = H	$H_{3''}$-H_4	-79.7	5.40	5.40	0.00				
		$H_{3''}$-H_4	41.4	5.40	5.40	0.00				
		$H_{4'}$-$H_{5'}$	81.6	4.90	4.90	0.00				
		$H_{4'}$-$H_{5''}$	-40.0	3.39	3.40	0.01				
							0.548	15.2	44.0	0.008
2	**2**	$H_{2'}$-$H_{3'}$	-44.9	7.02	7.30	0.28				
	X = OMs;	$H_{2'}$-$H_{3''}$	-166.1	7.25	7.40	0.15				
	Y = H	$H_{3''}$-H_4	-62.9	6.75	6.80	0.05				
		$H_{3''}$-H_4	58.2	3.39	3.20	-0.29				
		$H_{4'}$-$H_{5'}$	70.1	5.47	5.50	0.03				
		$H_{4'}$-$H_{5''}$	-51.5	2.51	2.80	0.29				
							0.503	7.7	59.7	0.216
3	**3**	$H_{2'}$-$H_{3'}$	-35.9	7.04	7.30	0.26				
	X = OAc	$H_{2'}$-$H_{3''}$	-157.7	8.21	8.30	0.09				
	Y = H	$H_{3''}$-H_4	-77.7	3.19	3.20	0.01				
		$H_{3''}$-H_4	43.4	6.15	5.90	-025				
		$H_{4'}$-$H_{5'}$	85.0	3.19	3.20	0.01				
		$H_{4'}$-$H_{5''}$	-36.6	5.82	6.00	0.18				
							0.714	3.9	44.5	0.169
4	**4**	$H_{2'}$-$H_{3'}$	-14.8	6.74	6.40	-0.34				
	Y= OBz	$H_{2'}$-$H_{3''}$	-136.0	6.16	5.80	-0.36				
	X = H	$H_{3''}$-H_4	-80.0	3.40	2.90	-0.50				
		$H_{3''}$-H_4	41.1	5.69	4.90	-0.79				
		$H_{4'}$-$H_{5'}$	67.6	2.24	2.00	-0.24				
		$H_{4'}$-$H_{5''}$	-54.0	4.74	4.90	0.16				
							0.756	40.3	55.2	0.448

*Proton Pair[a]: Vicinal protons pair; ϕ_{H-H}[b] Torsional angle; J_{calcd}[c] : Calculated coupling constants from pseurot program; J_{exp}[d] : Experimentally observed coupling constants; ΔJ^e : J_{exp}-J_{calcd} (in Hz); MF[f] : Mole fraction of one of the conformer (N conformer; P = 0); P_N[g]: Psuedorotaion angle for N conformer; ϕ_N[h] : Puckering amplitude for N conformer(P = 0); rms[i] : Root mean square

For compound **3** (Table 7, entry 3), $\Delta J \sim 0.0 \pm 0.25$ Hz for all six vicinal protons pair of 4*R*-O-acetyl substituted pyrolidine ring, the rms value is 0.169, MF1 is 0.714 and $\phi_N = 44.5$ for N-conformer at $P_N = 3.9^o$.

For compound **4** (Table 7, entry 4), ΔJ = -0.79-0.16 Hz for all six vicinal protons pair of 4*S*-O-benzoyl substituted pyrolidine ring, the rms value is 0.448, MF1 is 0.756 and $\phi_N = 55.2$ for N-conformer at $P_N = 44.3^o$

3.3.4b aep-PNA monomers

After getting satisfactory results of PSEUROT program in terms of approximate conformation of pyrrolidine ring in 4-substituted pyrrolidine compounds **1-4,** the effects in the ring puckering extent caused by 4- nucleobases substituted *aep*-PNA monomers (**5,6,8**,) were examined and the results are shown in Table 8.

For compound **5** (Table 8, entry 1), $\Delta J \sim 0.0 \pm 0.24$ Hz for all six pairs of vicinal protons of 4*R*-N3-benzoylthymine substituted pyrrolidine ring, the rms value is 0.112, MF1 is 0.934 major conformer and $\phi_N = 68.9$ for N-conformer at $P_N = 36.2^o$.

For compound **8** (Table 8, entry 2), $\Delta J \sim 0.0 \pm 0.32$ Hz for all six pairs of vicinal protons of 4*S*-thymine substituted pyrrolidine ring, the rms value is 0.180, MF1 is 0.857 and $\phi_N = 68.9$ for N-conformer at $P_N = 41.9^o$.

For purine derivative **6** (Table 8, entry 7), $\Delta J \sim 0.0 \pm 0.26$ Hz for all six pair of vicinal protons of 4*R*-adenine-9-yl substituted pyrrolidine ring, the rms value is 0.112, MF2 is 0.551 MF2 is major and $\phi_S = 28.9$ (maximum deviation of torsional angle of C3-C4 or dihedral angle H3-H4) for S-conformer at $P_S = 203.2^o$ which is unlike the results of other 4*R*-substituted pyrrolidine compounds **1-5**.

Table 8: Summary of input and output data of *aep*-derivatives

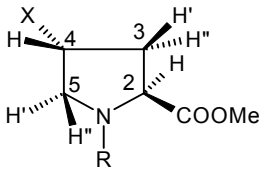

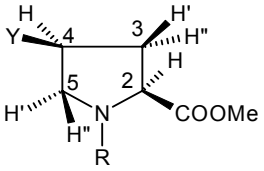

R = CH_2CH_2NHBoc

L-trans-(2*S*,4*R*) *L-cis*-(2*S*,4*S*)

Entry	Compound	Vicinal Proton-Pair[a]	ϕ_{H-H}[b]	J_{calcd}[c]	J_{exp}[d]	ΔJ[e]	MF[f]	P_N[g]	ϕ_N[h]	rms[i]
1	**5**	$H_{2'}$-$H_{3'}$	-22.7	7.86	8.10	0.24				
		$H_{2'}$-$H_{3''}$	-143.9	7.83	7.90	0.07				
	X = N3Bz-T	$H_{3''}$-H_4	-66.6	2.89	2.90	0.01				
	Y = H	$H_{3''}$-H_4	54.5	4.29	4.20	-0.09				
		$H_{4'}$-$H_{5'}$	53.8	3.69	3.70	0.01				
		$H_{4'}$-$H_{5''}$	-67.8	2.82	2.90	0.08				
							0.934	36.2	68.9	0.112
2	**8**	$H_{2'}$-$H_{3'}$	-108.4	8.03	8.10	0.07				
		$H_{2'}$-$H_{3''}$	-148.0	5.96	5.90	-0.06				
	Y= T	$H_{3''}$-H_4	-26.9	3.06	2.90	-0.16				
	X = H	$H_{3''}$-H_4	150.1	4.52	4.20	-0.32				
		$H_{4'}$-$H_{5'}$	28.5	3.84	3.80	-0.04				
		$H_{4'}$-$H_{5''}$	12.8	2.90	2.66	0.24				
							0.857	41.9	68.4	0.180
3	**6**	$H_{2'}$-$H_{3'}$	-54.9	6.42	6.30	-0.12	MF_{Sj}	P_S[g]	ϕ_S[h]	
		$H_{2'}$-$H_{3''}$	-176.1	6.45	6.50	0.05				
	X = A	$H_{3''}$-H_4	-55.1	6.83	7.10	0.27				
	Y = H	$H_{3''}$-H_4	66.1	5.34	5.80	0.46				
		$H_{4'}$-$H_{5'}$	67.4	6.16	5.90	-0.26				
		$H_{4'}$-$H_{5''}$	-53.0	5.61	5.30	-0.26				
							0.551	203.0	28.1	0.279

3.3.4c Pseudorotation cycle of 4-substituted pyrrolidine derivatives

The pseudorotation cycle of *N*-substituted pyrrolidine derivatives (Figure 20) is sketched by using the Pseudorotation angle for P_N and P_S (Table 9) in way similar to that of furanose ring.[30] This cycle is used to determine the conformation of compounds **1-6** and **8 (**see in Table 11) as well as for L-4-hydroxyproline and of L-4-fluoroproline (Table 10).

Table 9: Pseudorotation cycle of *N*-substituted pyrrolidine derivative[30]

P_N	-72^0	-54^0	-36^0	-18^0	0^0	18^0	36^0	54^0	72^0
Geometry	T	^{2}E	T	$_3$E	T	^{4}E	T	^{5}E	$^N_5$T
P_S	108^0	126^0	144^0	162^0	180^0	198^0	216^0	234^0	252^0
Geometry	T	$_2$E	T	^{3}E	T	$_4$E	T	$_5$E	$_N^5$T

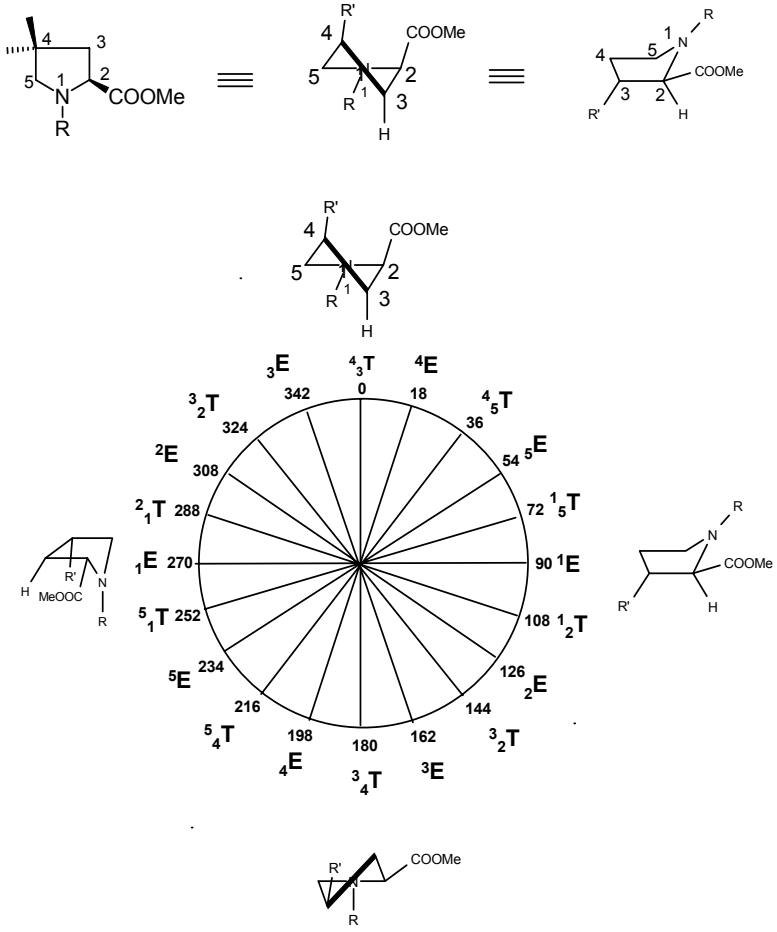

Figure 23: Pseudorotation cycle of *N*-substituted pyrrolidine derivative

3.3.4d L-4-Hydroxyproline and of L-4-Fluoroproline

Geometry of L-4-substituted pyrrolidine ring of *aep*-PNA derivatives in solution**:** Altona *et. al.*[38] used PSEROT program for conformational studies of pyrrolidine ring in L-4-Hydroxyproline and of L-4-Fluoroproline and the outcome are summarized in Table 10. For L-4-Hydroxyproline (Table 10) $\Delta J \sim -0.24$-0.43 Hz for all six pairs vicinal protons of pyrrolidine ring, the rms value is 0.31, and $\phi_N = 43.6.9$ for N-conformer at $P_N = 12.8.9^o$,

while for L-4-Fluoroproline (Table 10) $\Delta J \sim$ -0.31-0.63 Hz for all six pairs vicinal protons of pyrrolidine ring, the rms value is 0.31, and ϕ_N = 41.9 for N-conformer at P_N = 14.3°. Hence, from the pseudorotational cycle of pyrolidine ring (Figure 23), is observed that the geometry of pyrolidine ring of both 4-substituted compounds is C4-*endo*/C3-*exo* ($^4{}_3$T).

The geometry of pyrrolidine ring of compounds **1-6** and **8** (Table 11) is derived

Table 10: Geometry of L-4-Hydroxyproline and of L-4-Fluoroproline (Fpro) in solution*

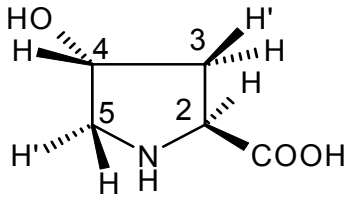

L-4-Hydroxy proline

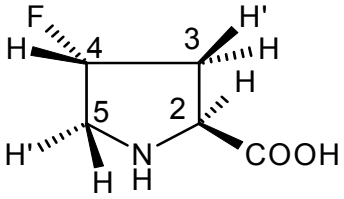

L-4-Fluoroprolines

Compound	Proton Pair	ϕ_{H-H}	J_{calcd}	J_{exp}	ΔJ	P_N	ϕ_N	Rms	Geometry
Hyp	$H_{2'}$-$H_{3'}$	-30.4	7.23	7.66	0.43				
	$H_{2'}$-$H_{3''}$	-151.6	9.99	10.44	0.45				
	$H_{3'}$-H_4	-79.6	1.65	1.41	-0.24				
	$H_{3''}$-H_4	41.5	4.44	4.31	-0.13				
	H_4-$H_{5'}$	82.7	1.56	1.21	-0.34				
	H_4-$H_{5''}$	-38.9	4.15	4.09	-0.07				
						12.8	43.6	0.31	$^4{}_3$T
FPro	$H_{2'}$-$H_{3'}$	-28.5	7.50	8.10	0.60				
	$H_{2'}$-$H_{3''}$	-149.7	9.73	10.36	0.63				
	$H_{3'}$-H_4	81.5	1.39	0.93	-0.44				
	$H_{3''}$-H_4	39.6	3.96	3.82	-0.14				
	H_4-$H_{5'}$	83.8	1.34	0.62	-0.72				
	H_4-$H_{5''}$	-37.8	3.57	3.26	-0.31				
						14.3	41.9	0.52	$^4{}_3$T

from pseudorotational angle (P) obtained from PSEUROT output (Table 12) as P_N = 15.2° for 4*R*-hydroxy pyrrolidine **1** (Table 12, entry 1), P_N = 7.7° for 4*R*-O-mesyl pyrrolidine **2** (Table 11, entry 2) and P_N = 3.2° for 4*R*-O-acetyl pyrrolidine **3** (Table 11, entry 3). These are fitted into the pseudorotational cycle (Figure 23) to obtain the geometry of pyrrolidine ring as C4-*endo*/C3-*exo* ($^4{}_3$T) which is similar to that observed for 4-OH and 4-F-prolines. The pyrrolidine ring in 4*S*-O-benzoyl pyrolidine **4** (Table 11, entry 4) with P_N = 36.2° and 4*R*-N3Bz-T pyrolidine **5** with P_N = 40.3° (Table 11, entry 5) and 4*S*-thymine-pyrrolidine **8**

with P_N = 41.9° (Table 11, entry 6) correspond to C4-*endo*/C5-*exo* ($^4_5$T) geometry. The probable geometry of compound **8** is shown in Figure 24. The envelop form of 4-adenine substituted pyrrolidine ring as C4-exo ($_4$E) geometry is observed with P_S = 28.1° for 4*R*-adenine pyrrolidine **6** (Table 11, entry 7).

Table 11: Geometry of pyrrolidine derivatives

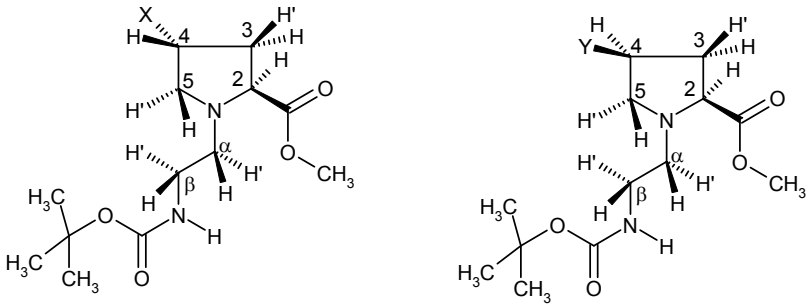

L-cis/trans-(2*S*,4*S*/*R*)

Entry	Compound	MF_N	P_N	ϕ_N	rms	geometry
1	**1**. X = OH; Y = H	0.548	15.2	44.0	0.008	$^4_3$T
2	**2**. X = OMs; Y = H	0.503	7.7	59.7	0.216	$^4_3$T
3	**3**. X = OAc; Y = H	0.714	3.9	44.5	0.169	$^4_3$T
4	**4** Y= Obz; X = H	0.756	40.3	55.2	0.448	$^4_5$T
5	**5**. X = N3bzThymine; Y = H	0.934	36.2	68.9	0.112	$^4_5$T
6	**8**. X= H; Y = = Thymine	0.857	41.9	68.4	0.180	$^4_5$T
7		0.449 (minor)	2.2	68.5	0.279	$^4_3$T
	6. X = A; Y = H	**MF_S**	**P_S**	**ϕ_S**		
		0.551 (major)	203.0	28.1	0.279	$_4$E

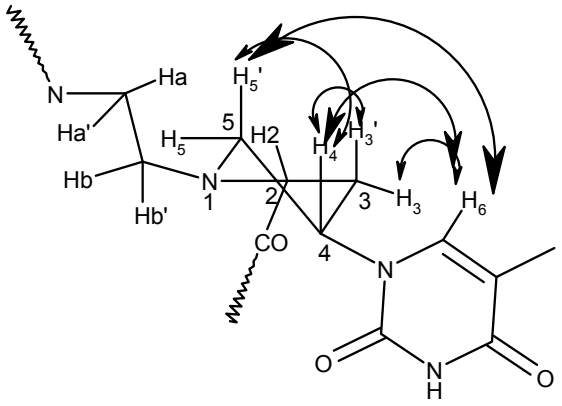

Figure 24: $^4_5$T conformation for compound **8**

3.3.5 Discussion

In this Chapter, the conformation of pyrrolidine ring in 4-substituted pyrrolidine compounds **1-4** and *aep* monomers (T/A) have been analysed by using PSEUROT software. The ^{1}H NMR spectra were completely assigned by a combination of 1D ^{1}H-^{1}H decoupling, 2D-COSY and 2D NOESY ^{1}H –NMR spectroscopic techniques and the six pairs of vicinal coupling constants of the pyrrolidine ring were determined from 2D J-spectroscopy. These experimentally measured coupling constants were used as inputs into the PSEUROT programme of Altona *et. al*.[43] to analyse the conformations adopted by 5-membered pyrrolidine rings. From such an analysis, it is seen that the *N*-conformer was preferred in solution by 4-O-substituted pyrrolidines and this is similar to the conformation adopted by pyrrolidine ring in L-4-Hydroxy and L-4-Fluoro prolines. It was observed that when pyrimidine is substituted at C4 in pyrrolidine ring as in 4*R*-*aep*-PNA-thymine (N3Bz) **5** and 4*S*-*aep*-PNA-T **8**, the conformation in pyrrolidine ring is remarkably biased to N-type (93.4 %) for compound **5** and 85.7% for compound **8** (Figure 24). When purine is substituted into pyrrolidine ring as 4*R*-*aep*-PNA-A **6,** the equilibrium is shifted to a slight preference for *S*-conformer in pyrrolidine ring (55.1%).

Table 12: Conformation of riboside and deoxyribonucleosides[25]*

Ribosides	**MF_N**	**Deoxyribosides**	**MF_N**
Adenosine	0.40	Adenosine	-
Adenosine-5'-phosphate	0.48	Adenosine-5'-phosphate	0.30
Adenosine-3'-phosphate	0.43	Adenosine-3'-phosphate	0.22
Cytidine	0.60	Cytidine	-
Uridine	0.52	D(Uridine)	0.30

*MF_N: Mole fraction of N-conformer

Altona and Sunderlingam[25] have reported the conformational analysis of deoxyribose and ribose ring in nucleotides (Table 12) and observed that the purine ribosides show a small conformational preference for *S*-type conformation, whereas the pyrimidine derivatives slightly favour the *N*-type conformer. The deoxyribose ring in both

purine/pyrimidine deoxyribonucleosides show equilibrium compositions, which are substantially biased toward the *S*-type conformer. In analogy and agreement with these results, the present analysis of the purine substituted pyrrolidines in 4*R*-*aep*-PNA-A indicated almost a similar conformation in solution for pyrrolidine ring as for the ribose in ribosides and the pyrimidine substituted pyrrolidines in 4-*R/S*-*aep*-PNA-T monomer showing major *N*-type conformation as in ribose ring. An equivalent analysis for pyrrolidinone-PNA remains to be done; since the validity of PSEUROT is not established for these analogues, such an analysis is not reported here.

3.4 CONCLUSIONS

The complete assignment of all pyrrolidine ring containing *aep* compounds (**1-6** and **7**) have been achieved by 1D decoupling and 2D-NMR (^{1}H-^{1}H-COSY, NOESY and 2D-J-resolved) experiments. The vicinal coupling constants ($^{3}J_{x\text{-}y}$/Hz) of all ring protons in pyrrolidine ring are measured and used as input into computer based PSEUROT 5.1.4 to obtain the most stable conformation of *aep* pyrrolidine ring. It is demonstrated that for L-*cis*-*aep*-PNA-T **8** and L-*trans*-*aep*-PNA-T **5** the preferred conformation is $^{4}_{5}$T while for *trans*-*aep*-PNA-A monomer **6** the preferred conformation is $_{4}$E. Similarly, the proline ring conformation in *aep*-PNA intermediates was established as **1** ($^{4}_{3}$T), **2** ($^{4}_{3}$T), **3** ($^{4}_{3}$T) and **4** ($^{4}_{5}$T). Such base type (C, T/A, G) dependent pyrrolidine pucker in *aep*-PNA is of importance in determining the final hybridization properties of derived *aep*-PNA oligomers.

3.5 REFERENCES

1. Franchetti, P.; Marchetti, S.; Cappellacci, L.; Jayaram, H. N.; Yalowitz, J. A.; Goldstein, B. M.; Barascut, J. L.; Dukhan, D.; Imbach, J. L.; Grifantini, M. Synthesis, conformational analysis, and biological activity of C-thioribonucleosides related to tiazofurin. *J. Med. Chem*. **2000**, *43*, 1264-1270
2. Cardenas, F.; Caba, J. M.; Feliz, M.; Lloyd-Williams, P.; Giralt, E. Analysis of conformational equilibria in aplidine using selective excitation 2D NMR spectroscopy and molecular mechanics/dynamics calculations. *J. Org. Chem*. **2003**, *68*, 9554-9562.
3. Podkorytov, I. S.; Skrynnikov, N. R. Microsecond time-scale dynamics from relaxation in the rotating frame: experiments using spin lock with alternating phase. *J. Magn. Reson*. **2004**, *169*, 164-173.
4. (a) David, W. I. F.; Ibberson, R. M. A reinvestigation of the structure of tetrahydrofuran by high-resolution neutron powder diffraction. *Acta Crystallogr., Sect. C* **1992**, *48*, 301-303. (b) Luger, P.; Buschmann, J. Twist Conformation of Tetrahydrofuran in the Crystal Form. *Angew. Chem.* **1983**, *95*, 423-424. (c) Sychrovsky, V.; GrÄafenstein, J.; Cremer, D. Nuclear magnetic resonance Spin-Spin Coupling constants from coupled Perturbed Density Functional Theory. *J. Chem. Phys.* **2000**, *113*, 3530-3547.
5. Mac Arthur, M. W.; Thornton, J. M. Conformational analysis of protein structures derived from NMR data. *Protein* **1993**, *17*, 232-251.
6. Auer, A. A.; Gauss, J. Triple Excitation Effects in Coupled-Cluster Calculations of Indirect Spin-Spin Coupling Constants. *J. Chem. Phys.* **2001**, *115,* 1619-1622.
7. (a) Kowalewski, J. Calculations of Nuclear Spin-Spin Coupling Constants. *Prog. NMR Spectrosc.* **1977**, *11*, 1-78. (b) Kowalewski, J. Calculations of Nuclear Spin-Spin Couplings. *Ann. Rep. NMR Spectrosc*. **1982**, *12*, 81-176. (c) Contreras, R. H.; Peralta, J. E. Angular dependence of spin-spin coupling constabts. *Prog. NMR Spectrosc.* **2000**, *37*, 321-425
8. (a) Karplus, M.; Anderson, D. H. Valence-bond interpretation of electron-coupled nuclear spin interactions; application to methane. *J. Chem. Phys.* **1959**, *30*, 6-10. (b) Karplus, M. Contact electron-spin interactions of nuclear magnetic moments. *J. Chem. Phys*. **1959**, *30*, 11-15. Ludvigsen, S.; Andersen, K. V.; Poulsen, F. M. Accurate measurements of coupling constants from two-dimensional nuclear magnetic resonance spectra of proteins and determination of phi-angles. *J. Mol. Biol*. **1991**, *217*, 731-6
9. Haasnoot, *C.* A. G.; De Leeuw, F. A. A. M.; Altona. C. The relationship between proton-proton NMR coupling constants and substituents electronegativities-I. *Tetrahedron* **1980**, *36*, 2783-2792. (b) Pachler, K. G. R. *J. Chem. Soc., Perkin Trans. II* **1936,** 1972. (c) Pachler, K. G. R *Tetrahedron* **1971**, *27*, 187.
10. (a) Helgaker, T.; Watson, M.; Handy, N.C. Analytical Calculation of Nuclear Magnetic Resonance Indirect Spin-Spin Coupling Constants at the Generalized Gradient Approximation and Hybrid Levels of Density-Functional Theory. *J. Chem. Phys.* **2000**, *113*, 9402-9409.
11. Diez, E.; Palma, J.; San-Fabian, J.; Guilleme, J. Effect of the Substituents on the Conformational Behavior of Five-Membered Rings: Application to *cis*- and *trans*-2,5- Dimethoxytetrahydrofuran. *J. Comp. Chem.* **1988**, *9*, 189-199.

12. Haasnoot, C. A. G.; de Leeuw, F. A. A. M.; de Leeuw, H. P. M.; Altona, C. *Biopolymers* **1981**, *20*, 1211.
13. Oppenheimer, N. J.; Kaplan, N. O. Proton magnetic resonance study of the intramolecular association and conformation of the alpha and beta pyridine mononucleotides and nucleosides. *Biochemistry* **1976**, *15*, 3981-3988. (b) Kutzelnigg, W.; Fleischer, U.; Schindler, M. in *NMR-Basic Principles and Progress*; Springer: Heidelberg, **1990**, *23*, 165.
14. (a) Ludvigsen, S.; Andersen, K. V.; Poulsen, F. M. Accurate measurements of coupling constants from two-dimensional nuclear magnetic resonance spectra of proteins and determination of phi-angles. *J. Mol. Biol*. **1991**, *217*, 731-6. (b) Silverstein, R. M.; Webster, F. F. Spectrometric identification of organic compounds. Sixth edition, *John Wiley & sons, Inc*, **1998**, 144-163.
15. .(a) Kutzelnigg, W.; Fleischer, U.; Schindler, M. *In NMR-Basic Principles and Progress*; Springer: Heidelberg, **1990**, *23*, 165.
16. Saenger, W. *Principles of Nucleic Acid Structure*. Springer-Verlag New York Inc.: New York, **1984**.
17. Guschlbauer, W. Conformational analysis of ribonucleosides from proton-proton coupling constants. *Biochim*. *Biophys*. *Acta*. **1980**, *610*, 47-55
18. (a) Lambert, J. B.; Papay, J. J.; Khan, S. A.; Kappauf, K. A.; Magyar, E. S. Conformational analysis of five-membered rings. *J. Am. Chem. Soc.* **1974**, *96*, 6112-6118. Cremer, D.; Pople, J. A. General definition of ring puckering coordinates. *J. Am. Chem. Soc.* **1975**, *97*, 1354-1358. (b) Cremer, D. A general definition of ring Substituent positions. *Isr. J. Chem.* **1980**, *20*, 12-19. (c) Cremer, D. A general definition of ring Substituent positions *Int. J. Mol. Sci.* **2003**, *4,* 190. (c) Cremer, D. Calculation of Puckered Rings with Analytical Gradients. *J. Phys. Chem.* **1990**, *94*, 5502-5509. (d) Cremer, D.; Szabo, K. J. Methods in Stereochemical Analysis, Conformational Behavior of Six-Membered Rings, Analysis, Dynamics, and Stereoelectronic Effects, E. Juaristi, Edt., VCH Publishers, 1995, 59-135. (e) Cremer, D. Theoretical Determination of Molecular Structure and Conformation. *J. Chem. Phys.* **1979**, *70*, 1898-1910; 1911-1927; 1928-1938.
19. (a) Davidson, R.; Warsop, P. A. Energy Levels for Pseudorotation and Their Application to Cyclopentane, Tetrahydrofuran, and 1,3-Dioxolane. *J. Chem. Soc., Faraday Trans II* **1972**, *68*, 1875-1889. (b) Deleeuw, F.; Altona, C. Computer-assisted pseudorotation analysis of five-membered rings by means of proton spin-spin coupling-constants-program pseurot. *J. Comput. Chem.* **1983**, *4*, 428-437.
20. Deleeuw, H. P. M.; Haasnoot, C. A. G.; Altona, C. Nucleic-Acid Constituents 0.13. Empirical correlations between conformational Parameters in beta-D-furanoside fragments derived from a statistical-survey of crystal-structures of nucleic-acid constituents–full description of nucleoside molecular geometries in terms of parameters. *Isr. J. Chem.* **1980**, *20*, 108-126.
21. Kilpatrick, J. E.; Pitzer, K. S.; Spitzer, R. *J. Am. Chem. Soc*. **1947**, *69*, 2483.
22. Wu, A.A.; Cremer, D.; Auer, A.A.; Gauss, J. Extension of the Karplus relationship for NMR spin-spin coupling constants to nonplanar ring systems: pseudorotation of cyclopentane. *J. Phys. Chem. A* **2002**, *106*, 657-667.
23. Han, S. J.; Kang, Y. K. Pseudorotation in Heterocyclic Five-Membered Rings: Tetrahydrofuran and Pyrrolidine. *J. Mol. Struc. (Theochem)* **1996**, *369*, 157-165.

24. Altona, C.; Sundaralingam, M. Conformational Analysis of the Sugar Ring in Nucleosidesand Nucleotides. Improved Method for the Interpretation of Proton Magnetic Resonance Coupling Constants. *J. Am. Chem. Soc.* **1973**, *95*, 2333-2344.
25. Altona, C.; Franke, R.; De Haan, R.; Ippel, J. H; Daalmans, G. J.; Hoekzema, W. A.; VanWijk, J. *J. Magn. Reson. Chem*. **1994**, *32*, 670-678.
26. (a) Jaworski, A.; Ekiel, I. Calculations of proton NMR coupling constants for conformational studies of isomeric pentofuranosyl nucleosides. *Int. J. Quant. Chem.* **1979**, *16*, 615-622. (b) Haasnoot, C. A. G. Conformational Analysis of Six-Membered Rings in Solution: Ring Puckering Coordinates Derived from Vicinal NMR Proton-Proton Coupling Constants. *J. Am.Chem. Soc.* **1993**, *115*, 1460-1468.
27. De Leeuw, F. A. A. M.; Altona, C. *J. Comp. Chem.* **1983**, *4*, 438. (b) Haasnoot, C. A. G. conformational analysis of six-membered rings in solution: ring puckering coordinates derived from vicinal NMR proton-proton coupling constants. *J. Am. Chem. Soc*. **1993**, *115*, 1460-1468.
28. van Wijk, J.; Haasnoot, C. A. G.; de Leeuw, F. A. A. M.; Huckriede, B. D.; Westra Hoekzema, A.; Altona, C. *Pseurot 6.3* Ver. 6.3; Leiden Institute of Chemistry: Leiden University, **1999**.
29. Kirby, A. J. The Anomeric effect and related Stereoelectronic Effects at Oxygen, Springer Verlag: New York, 1983.
30. Haasnoot, C. A. G. Conformational Analysis of Six-Membered Rings in Solution: Ring Puckering Coordinates Derived from Vicinal NMR Proton-Proton Coupling Constants. *J. Am. Chem. Soc.* **1993**, *115*, 1460-1468.
31. (a) Umashankara, M.; Babu, I. R.; Ganesh, K. N. Two prolines with a difference: contrasting stereoelectronic effects of 4R/S-aminoproline on triplex stability in collagen peptides [pro(X)-pro(Y)-Gly]n. *Chem Commun (Camb)*. **2003**, 2606-2607. (b) Babu, I. R. Ganesh, K. N. Enhanced triple helix stability of collagen peptides with 4R-aminoprolyl (Amp) residues: relative roles of electrostatic and hydrogen bonding effects. *J. Am. Chem. Soc*. **2001**, *123*, 2079-2080.
32. Altona, C.; Sundaralingam, M. Conformational Analysis of the Sugar Ring in Nucleosides and Nucleotides. A New Description Using the Concept of Pseudorotation. *J. Am. Chem. Soc.* **1972**, *94*, 8205-8212.
33. Haasnoot, C. A. G.; De Leeuw, F. A. A. M.; Altona, C. The relationship between proton-proton NMR coupling constants and substituents electronegativities-I. *Tetrahedron,* 1980, *36*, 2783-2792. (b) Pachler, K. G. R. *J. Chem Soc., Perkin Trans II* **1972**, 1936. (c) Pachler, K. G. R. *Tetrahedron Lett.* **1970***,* 1955. (d) Pachler, K. G. R. *Tetrahedron.* **1971**, *27*, 187.
34. Džakula, Z.; DeRider, M. L.; John L.; Markley, J. L Conformational Analysis of Molecules with Five-Membered Rings through NMR Determination of the Continuous Probability Distribution (CUPID) for Pseudorotation. *J. Am. Chem. Soc.* **1996**, *118,* 12796-12803.
35. Michl, J.; West, R. Conformations of linear chains. systematics and suggestions for nomenclature. *Acc. Chem. Res*. **2000**, *33*, 821-3.
36. D'Costa, M.; Kumar, V. A.; Ganesh, K. N. Aminoethylprolyl (*aep*PNA): mixed purine, pyrimidine oligomers and binding orientation preferences for PNA:DNA duplex formation. *Org. Lett*. **2001**, *3*, 1281-1284.

3.6 APPENDIX

1. Typical format of PSEUROT

Typical format of PSEUROT*

(1) P A R A M E T E R S I N P S E U D O R O T A T I O N R E L A T I O N S

NAME: Vicinal coupling pair
FASE : phase angle of equation karplus equation
A : constant
B : constant
ELECTRONEGATIVITIES: Electro negativity of substituents
No OF SUBSTITUENTS: no of substituent

(2) I N P U T D A T A

J --> 2'-3' 2'-3" 3'-4' 3"-4" 4'-5' 4'-5"

(3) F I R S T E S T I M A T E S

==========

CONFORMER 1: P = 10.1 DEGREES ---> TO BE REFINED
PHI = 34.0 DEGREES ---> TO BE REFINED

CONFORMER 2: P = 147.5 DEGREES ---> TO BE REFINED
PHI = 35.0 DEGREES = .611 RAD ---> TO BE REFINED

AB : MF2 = .500 ---> TO BE REFINED

(4) F I N A L O U T P U T

2'-3' JEXP; JCAL; DIFF
2'-3" JEXP; JCAL; DIFF
3'-4' JEXP; JCAL; DIFF
3"-4" JEXP; JCAL; DIFF
4'-5' JEXP; JCAL; DIFF
4'-5" JEXP; JCAL; DIFF
MF1 MF2 RMS

CONFORMER 1:	**CONFORMER 2:**
P DEGREES =	P =
PHI	PHI
PHI2'-3' ; J2'-3'	PHI2'-3' ; J2'-3'
PHI2'-3" ; 2'-3"	PHI2'-3" ; J2'-3"
PHI3'-4' ; J3'-4'	PHI3'-4' ; J3'-4'
PHI3"-4" ; J3"-4"	PHI3"-4" J3"-4"
PHI4'-5' J4'-5'	PHI4'-5' ; J4'-5'
PHI4'-5" ; J4'-5"	PHI4'-5" J4'-5"

1CASE NR: 1

(5) E R R O R A N A L Y S I S

==========

OVERALL RMS
STANDARD DEVIATIONS IN PARAMETERS:

CORRELATION MATRIX OF PARAMETERS
PAR. 1 2 3 4 5
*** END OF PGM PSEUROT ***

*Fase: Phase angle; A and B Karplus parameters; ϕ = Dihedral angle; p = Pseudorotaion angle; rms = Root mean square; MF_1= Mole fraction of conformer 1; MF_2= Mole fraction of conformer 2; J_{cal} = Calculated coupling constant; J_{exp} = Experimental observed coupling constant $J_{diff} = J_{cal}-J_{diff}$

2. 1-*N*-(Boc-aminoethyl)-4*R*-hydroxyl-2*S*-proline methyl ester (**1**)

```
Input


1: 6 J's
    1  25    0.1       0.5       0.0        1
2'-3'   0  -144.0      1.000    -1.7       1.02      0.39      0.00      0.74
2'-3"   0  -144.0      1.000  -122.9       1.02      0.39      0.00      0.74
3'-4'   0     0.0      1.000  -122.1        0.64     0.00     1.25       0.68
3"-4"   0     0.0      1.000    -1.0       0.64      0.00      1.25      0.68
4'-5'   0   144.0      1.000   122.7       1.25      0.74      0.00      1.02
4'-5"   0   144.0      1.000     1.1       1.25      0.74      0.00      1.02

AB        7.80 7.80 5.40 5.40 4.90 3.40

   10.1      34.0     147.5      35.0
.5
11111

Output

1CASE NR:    1
 TITLE  :1 : 6 J's                                                                                                    PSEUROT-5.4
0=============================================================================================================================
 P A R A M E T E R S   I N   P S E U D O R O T A T I O N   R E L A T I O N S
 ============================================================================================================================
0COUPLING CONSTANTS DEFINED BY:

 NAME           FASE         A            B                  ELECTRONEGATIVITIES             no OF SUBSTITUENTS

 2'-3'         -144.0       1.000        -1.7       1.020        .390        .000        .740          3
 2'-3"         -144.0       1.000      -122.9       1.020        .390        .000        .740          3
 3'-4'             .0       1.000      -122.1        .640        .000       1.250        .680          3
 3"-4"             .0       1.000        -1.0        .640        .000       1.250        .680          3
 4'-5'          144.0       1.000       122.7       1.250        .740        .000       1.020          3
 4'-5"          144.0       1.000         1.1       1.250        .740        .000       1.020          3


0=============================================================================================================================
 I N P U T   D A T A
 ============================================================================================================================


      J -->   2'-3'     2'-3"     3'-4'     3"-4"     4'-5'     4'-5"
 AB            7.80      7.80      5.40      5.40      4.90      3.40
0CASE     1 HAS   1 SETS ->   6 OBSERVATIONS
0MAX STEPSIZE                =    .100
 CONVERGENCE CRITERIUM       =   5.000E-04
 MAXIMUM NUMBER OF ITERATIONS =  25
1CASE NR:    1
 TITLE  :1 : 6 J's                                                                                                    PSEUROT-5.4
0=============================================================================================================================
 F I R S T   E S T I M A T E S
 ============================================================================================================================


 CONFORMER 1:       P =  10.1 DEGREES =   .176 RAD  ---> TO BE REFINED
                  PHI =  34.0 DEGREES =   .593 RAD  ---> TO BE REFINED

 CONFORMER 2:       P = 147.5 DEGREES =  2.574 RAD  ---> TO BE REFINED
                  PHI =  35.0 DEGREES =   .611 RAD  ---> TO BE REFINED

                      AB       : MF2 =   .500      ---> TO BE REFINED
1CASE NR:    1
 TITLE  :1 : 6 J's                                                                                                    PSEUROT-5.4
0=============================================================================================================================
 F I N A L   O U T P U T
 ============================================================================================================================

0               2'-3'                  2'-3"                  3'-4'                  3"-4"                  4'-5'
     JEXP JCAL DIFF  JEXP JCAL  DIFF  JEXP JCAL DIFF JEXP JCAL DIFF JEXP JCAL DIFF
AB! 7.80 7.79 .01 ! 7.80  7.79 .01 ! 5.40  5.40 .00 !  5.40    5.40     .00 !  4.90    4.90     .00   !
0               4'-5"
            JEXP    JCAL    DIFF
 AB       !  3.40    3.39     .01 !
0             MF1       MF2       RMS
 AB             .548      .452      .008
0CONFORMER 1:                              CONFORMER 2:
        P =   15.2   DEGREES   =   .265 RAD            P =  240.9   DEGREES   =  4.204 RAD
      PHI =   44.0   DEGREES   =   .767 RAD          PHI =   84.4   DEGREES   =  1.472 RAD
  PHI2'-3' =  -29.2 ---> J2'-3' =  7.08          PHI2'-3' =  -11.8 ---> J2'-3' =  8.64
  PHI2'-3" = -150.4 ---> J2'-3" =  9.35          PHI2'-3" = -133.0 ---> J2'-3" =  5.90
  PHI3'-4' =  -79.7 ---> J3'-4' =   .78          PHI3'-4' = -163.2 ---> J3'-4' = 10.99
  PHI3"-4" =   41.4 ---> J3"-4" =  6.36          PHI3"-4" =  -42.1 ---> J3"-4" =  4.24
  PHI4'-5' =   81.6 ---> J4'-5' =   .95          PHI4'-5' =  199.2 ---> J4'-5' =  9.70
  PHI4'-5" =  -40.0 ---> J4'-5" =  5.23          PHI4'-5" =   77.6 ---> J4'-5" =  1.17
1CASE NR:    1
 TITLE  :1 : 6 J's                                                                                                    PSEUROT-5.4
0=============================================================================================================================
 E R R O R   A N A L Y S I S
 ============================================================================================================================
0OVERALL RMS  =   .779E-02
0STANDARD DEVIATIONS IN PARAMETERS:


     0      .005      .003      .002      .005      .002
0CORRELATION MATRIX OF PARAMETERS
0PAR.       1          2          3          4          5
  1      1.000
  2       .409      1.000
  3       .511      -.079      1.000
  4       .214      -.337       .252      1.000
  5      -.151      -.446       .267       .287      1.000
0*** END OF PGM PSEUROT ***
```

3. 1-*N*-(Boc-aminoethyl)-4*R*-*O*-meysl-2*S*-proline methyl ester (**2**)

```
Input

2 : 6 J's
    1  25    0.1       0.5       0.0        1
2'-3'   0  -144.0      1.000    -1.7       1.02      0.39      0.00      0.74
2'-3"   0  -144.0      1.000  -122.9       1.02      0.39      0.00      0.74
3'-4'   0     0.0      1.000  -122.1       0.64      0.00      1.17      0.68
3"-4"   0     0.0      1.000    -1.0       0.64      0.00      1.17      0.68
4'-5'   0   144.0      1.000   122.7       1.17      0.74      0.00      1.02
4'-5"   0   144.0      1.000    1.10       1.17      0.74      0.00      1.02

AB        7.30 7.40 6.80 3.20 5.50 2.80

   10.0      34.0     147.5      35.0
.5
11111

Out Put
1CASE NR:    1
 TITLE  :2 : 6 J's                                                                                                    PSEUROT-5.4
0=============================================================================================================================
 P A R A M E T E R S   I N   P S E U D O R O T A T I O N   R E L A T I O N S
 ============================================================================================================================


0COUPLING CONSTANTS DEFINED BY:

 NAME           FASE         A             B                 ELECTRONEGATIVITIES             # OF SUBSTITUENTS

 2'-3'         -144.0       1.000        -1.7       1.020        .390        .000        .740          3
 2'-3"         -144.0       1.000      -122.9       1.020        .390        .000        .740          3
 3'-4'            .0        1.000      -122.1        .640        .000       1.170        .680          3
 3"-4"            .0        1.000        -1.0        .640        .000       1.170        .680          3
 4'-5'          144.0       1.000       122.7       1.170        .740        .000       1.020          3
 4'-5"          144.0       1.000         1.1       1.170        .740        .000       1.020          3


0PARAMETERS USED IN GENERALIZED KARPLUS EQUATION: similar of compound 2

0=============================================================================================================================
 I N P U T   D A T A
 ============================================================================================================================


      J -->   2'-3'     2'-3"     3'-4'     3"-4"     4'-5'     4'-5"
 AB            7.30      7.40      6.80      3.20      5.50      2.80
0CASE     1 HAS   1 SETS ->   6 OBSERVATIONS
0MAX STEPSIZE                =    .100
 CONVERGENCE CRITERIUM       =   5.000E-04
 MAXIMUM NUMBER OF ITERATIONS =  25
1CASE NR:    1
 TITLE  :2 : 6 J's                                                                                                    PSEUROT-5.4
0=============================================================================================================================
 F I R S T   E S T I M A T E S
 ============================================================================================================================

 CONFORMER 1:       P =  10.0 DEGREES =   .175 RAD  ---> TO BE REFINED
                  PHI =  34.0 DEGREES =   .593 RAD  ---> TO BE REFINED

 CONFORMER 2:       P = 147.5 DEGREES =  2.574 RAD  ---> TO BE REFINED
                  PHI =  35.0 DEGREES =   .611 RAD  ---> TO BE REFINED

                     AB       : MF2 =   .500      ---> TO BE REFINED
1CASE NR:    1
 TITLE  :2 : 6 J's                                                                                                    PSEUROT-5.4
0=============================================================================================================================
 F I N A L   O U T P U T
 ============================================================================================================================


0               2'-3'                   2'-3"                   3'-4'                   3"-4"                   4'-5'
             JEXP    JCAL    DIFF    JEXP    JCAL    DIFF    JEXP    JCAL    DIFF    JEXP    JCAL    DIFF    JEXP    JCAL    DIFF
 AB       !  7.30    7.02     .28 !  7.40    7.25     .15 !  6.80    6.75     .05 !  3.20    3.49    -.29 !  5.50    5.47     .03   !
0               4'-5"
             JEXP    JCAL    DIFF
 AB       !  2.80    2.51     .29 !
0             MF1       MF2       RMS
 AB            .503      .497      .216
0CONFORMER 1:                                  CONFORMER 2:
         P =    7.7   DEGREES   =   .134 RAD            P =  229.6   DEGREES   =  4.008 RAD
       PHI =   59.7   DEGREES   =  1.042 RAD          PHI =   82.1   DEGREES   =  1.432 RAD
  PHI2'-3' =  -44.9 ---> J2'-3' =  5.04          PHI2'-3' =    4.5 ---> J2'-3' =  9.02
  PHI2'-3" = -166.1 ---> J2'-3" = 11.55          PHI2'-3" = -116.7 ---> J2'-3" =  2.91
  PHI3'-4' =  -62.9 ---> J3'-4' =  1.96          PHI3'-4' = -175.3 ---> J3'-4' = 11.60
  PHI3"-4" =   58.2 ---> J3"-4" =  4.06          PHI3"-4" =  -54.2 ---> J3"-4" =  2.92
  PHI4'-5' =   70.1 ---> J4'-5' =  1.70          PHI4'-5' =  202.5 ---> J4'-5' =  9.28
  PHI4'-5" =  -51.5 ---> J4'-5" =  4.04          PHI4'-5" =   80.9 ---> J4'-5" =   .95
1CASE NR:    1
 TITLE  :2 : 6 J's                                                                                                    PSEUROT-5.4
0=============================================================================================================================
 E R R O R   A N A L Y S I S
 ============================================================================================================================


0OVERALL RMS  =   .216E+00
0STANDARD DEVIATIONS IN PARAMETERS:

     0      .123      .076      .078      .117      .042
0CORRELATION MATRIX OF PARAMETERS
0PAR.       1         2         3         4         5
  1      1.000
  2       .239      1.000
  3       .292      .066      1.000
  4       .168     -.058      .447      1.000
  5      -.357     -.315      .356      .323      1.000
0*** END OF PGM PSEUROT ***
```

4. 1-*N*-(Boc-aminoethyl)-4*R*-*O*-acetyl-2*S*-proline methyl ester (**3**)

```
Input

2: 6 J's
    1  25    0.1       0.5       0.0        1
2'-3'   0  -144.0      1.000    -1.7       1.02      0.39      0.00      0.74
2'-3"   0  -144.0      1.000  -122.9       1.02      0.39      0.00      0.74
3'-4'   0     0.0      1.000  -122.1       0.64      0.00      1.17      0.68
3"-4"   0     0.0      1.000    -1.0       0.64      0.00      1.17      0.68
4'-5'   0   144.0      1.000   122.7       1.17      0.74      0.00      1.02
4'-5"   0   144.0      1.000    1.10       1.17      0.74      0.00      1.02

AB        7.30 8.30 3.20 5.90 3.20 6.00

   10.0      34.0     147.5      35.0
.5
11111

output

1CASE NR:    1
 TITLE  :3 : 6 J's                                                                                                    PSEUROT-5.4
0=============================================================================================================================
 P A R A M E T E R S   I N   P S E U D O R O T A T I O N   R E L A T I O N S
 =============================================================================================================================


0COUPLING CONSTANTS DEFINED BY:

 NAME           FlASE         A             B             ELECTRONEGATIVITIES             # OF SUBSTITUENTS

 2'-3'         -144.0       1.000        -1.7       1.020        .390        .000        .740          3
 2'-3"         -144.0       1.000      -122.9        1.020        .390        .000        .740          3
 3'-4'             .0       1.000      -122.1         .640        .000       1.170        .680          3
 3"-4"             .0       1.000        -1.0         .640        .000       1.170        .680          3
 4'-5'          144.0       1.000       122.7       1.170        .740        .000       1.020          3
 4'-5"          144.0       1.000         1.1       1.170        .740        .000       1.020          3

0PARAMETERS USED IN GENERALIZED KARPLUS EQUATION:

0=============================================================================================================================
 I N P U T   D A T A
 =============================================================================================================================

      J -->   2'-3'     2'-3"     3'-4'     3"-4"     4'-5'     4'-5"
 AB            7.30      8.30      3.20      5.90      3.20      6.00
0CASE     1 HAS   1 SETS ->   6 OBSERVATIONS
0MAX STEPSIZE                =    .100
 CONVERGENCE CRITERIUM       =   5.000E-04
 MAXIMUM NUMBER OF ITERATIONS =  25
1CASE NR:    1
 TITLE  :3 : 6 J's                                                                                                    PSEUROT-5.4
0=============================================================================================================================
 F I R S T   E S T I M A T E S
 =============================================================================================================================


 CONFORMER 1:       P =  10.0 DEGREES =   .175 RAD  ---> TO BE REFINED
                  PHI =  34.0 DEGREES =   .593 RAD  ---> TO BE REFINED

 CONFORMER 2:       P = 147.5 DEGREES =  2.574 RAD  ---> TO BE REFINED
                  PHI =  35.0 DEGREES =   .611 RAD  ---> TO BE REFINED

                    AB       : MF2 =   .500      ---> TO BE REFINED
0***** ITERATION CONVERGED *****
1CASE NR:    1
 TITLE  :3 : 6 J's                                                                                                    PSEUROT-5.4
0=============================================================================================================================
 F I N A L   O U T P U T
 =============================================================================================================================


0              2'-3'                  2'-3"                  3'-4'                  3"-4"                  4'-5'
            JEXP    JCAL    DIFF    JEXP    JCAL    DIFF    JEXP    JCAL    DIFF    JEXP    JCAL    DIFF    JEXP    JCAL    DIFF
 AB       !  7.30    7.04     .26 !  8.30    8.21     .09 !  3.20    3.19     .01 !  5.90    6.15    -.25 !  3.20    3.19     .01   !
0              4'-5"
            JEXP    JCAL    DIFF
 AB       !  6.00    5.82     .18 !
0             MF1       MF2       RMS
 AB             .714      .286      .169
0CONFORMER 1:                                  CONFORMER 2:
        P =    3.9   DEGREES   =   .068 RAD            P =  219.6   DEGREES   =  3.834 RAD
      PHI =   44.5   DEGREES   =   .777 RAD          PHI =   32.7   DEGREES   =   .571 RAD
  PHI2'-3' =  -35.9 ---> J2'-3' =  6.27          PHI2'-3' =    6.4 ---> J2'-3' =  8.99
  PHI2'-3" = -157.1 ---> J2'-3" = 10.43          PHI2'-3" = -114.8 ---> J2'-3" =  2.63
  PHI3'-4' =  -77.7 ---> J3'-4' =   .90          PHI3'-4' = -147.3 ---> J3'-4' =  8.93
  PHI3"-4" =   43.4 ---> J3"-4" =  6.05          PHI3"-4" =  -26.2 ---> J3"-4" =  6.40
  PHI4'-5' =   85.0 ---> J4'-5' =   .80          PHI4'-5' =  155.3 ---> J4'-5' =  9.18
  PHI4'-5" =  -36.6 ---> J4'-5" =  5.81          PHI4'-5" =   33.7 ---> J4'-5" =  5.84
1CASE NR:    1
 TITLE  :3 : 6 J's                                                                                                    PSEUROT-5.4
0=============================================================================================================================
 E R R O R   A N A L Y S I S
 =============================================================================================================================

0OVERALL RMS  =   .169E+00
0STANDARD DEVIATIONS IN PARAMETERS:

     0      .099      .056      .226      .121      .040
0CORRELATION MATRIX OF PARAMETERS
0PAR.       1          2          3          4          5
  1      1.000
  2       .440      1.000
  3       .378      -.003      1.000
  4      -.049      -.337       .497      1.000
  5      -.110       .207       .092      -.399      1.000
0*** END OF PGM PSEUROT ***
```

5. 1-*N*-(Boc-aminoethyl)-4*S*-*O*-benzoyl-2*S*-proline methyl ester (**4**)

```
Input
4 : 6 J's
    1  25    0.1       0.5       0.0        1
2'-3'   0  -144.0      1.000    -1.7       1.02      0.39      0.00      0.74
2'-3"   0  -144.0      1.000  -122.9       1.02      0.39      0.00      0.74
3'-4'   0     0.0      1.000  -122.1       0.64      0.00      1.17      0.68
3"-4"   0     0.0      1.000    -1.0       0.64      0.00      1.17      0.68
4'-5'   0   144.0      1.000   122.7       1.17      0.74      0.00      1.02
4'-5"   0   144.0      1.000    1.10       1.17      0.74      0.00      1.02

AB        6.40 5.80 2.90 4.90 2.00 4.90

   10.0      34.0     147.5      35.0
.5
11111

output
1CASE NR:    1
 TITLE  : 4 : 6 J's                                                                                                    PSEUROT-5.4
0=============================================================================================================================
 P A R A M E T E R S   I N   P S E U D O R O T A T I O N   R E L A T I O N S
 =============================================================================================================================


0COUPLING CONSTANTS DEFINED BY:

 NAME           FASE         A             B                 ELECTRONEGATIVITIES             # OF SUBSTITUENTS

 2'-3'        -144.0       1.000         -1.7       1.020        .390        .000        .740          3
 2'-3"        -144.0       1.000       -122.9       1.020        .390        .000        .740          3
 3'-4'           .0        1.000       -122.1        .640        .000       1.170        .680          3
 3"-4"           .0        1.000         -1.0        .640        .000       1.170        .680          3
 4'-5'         144.0       1.000        122.7       1.170        .740        .000       1.020          3
 4'-5"         144.0       1.000          1.1       1.170        .740        .000       1.020          3


0PARAMETERS USED IN GENERALIZED KARPLUS EQUATION:


0=============================================================================================================================
 I N P U T   D A T A
 =============================================================================================================================


      J -->   2'-3'     2'-3"     3'-4'     3"-4"     4'-5'     4'-5"
 AB            6.40      5.80      2.90      4.90      2.00      4.90
0CASE     1 HAS   1 SETS ->   6 OBSERVATIONS
0MAX STEPSIZE                =    .100
 CONVERGENCE CRITERIUM       =   5.000E-04
 MAXIMUM NUMBER OF ITERATIONS =  25
1CASE NR:    1
 TITLE  :4 : 6 J's                                                                                                     PSEUROT-5.4
0=============================================================================================================================
 F I R S T   E S T I M A T E S
 =============================================================================================================================


 CONFORMER 1:       P =  10.0 DEGREES =   .175 RAD  ---> TO BE REFINED
                  PHI =  34.0 DEGREES =   .593 RAD  ---> TO BE REFINED

 CONFORMER 2:       P = 147.5 DEGREES =  2.574 RAD  ---> TO BE REFINED
                  PHI =  35.0 DEGREES =   .611 RAD  ---> TO BE REFINED

                     AB       : MF2 =   .500      ---> TO BE REFINED
1CASE NR:    1
 TITLE  :4 : 6 J's                                                                                                     PSEUROT-5.4
0=============================================================================================================================
 F I N A L   O U T P U T
 =============================================================================================================================


0              2'-3'                  2'-3"                  3'-4'                  3"-4"                  4'-5'
            JEXP    JCAL    DIFF    JEXP    JCAL    DIFF   JEXP    JCAL    DIFF   JEXP    JCAL    DIFF   JEXP    JCAL    DIFF
 AB       !  6.40    6.74    -.34 !  5.80    6.16    -.36 !  2.90    3.40    -.50 !  4.90    5.69    -.79 !  2.00    2.24    -.24   !
0                4'-5"
            JEXP    JCAL    DIFF
 AB       !  4.90    4.74     .16 !
0             MF1       MF2       RMS
 AB             .756      .244      .448
0CONFORMER 1:                                  CONFORMER 2:
        P =   40.3   DEGREES   =   .703 RAD            P =  124.6   DEGREES   =  2.174 RAD
      PHI =   55.2   DEGREES   =   .964 RAD          PHI =   82.7   DEGREES   =  1.443 RAD
  PHI2'-3' =  -14.8 ---> J2'-3' =  8.44          PHI2'-3' =   76.3 ---> J2'-3' =  1.47
  PHI2'-3" = -136.0 ---> J2'-3" =  6.52          PHI2'-3" =  -44.9 ---> J2'-3" =  5.03
  PHI3'-4' =  -80.0 ---> J3'-4' =   .82          PHI3'-4' = -169.0 ---> J3'-4' = 11.43
  PHI3"-4" =   41.1 ---> J3"-4" =  6.33          PHI3"-4" =  -47.9 ---> J3"-4" =  3.69
  PHI4'-5' =   67.6 ---> J4'-5' =  1.93          PHI4'-5' =  120.6 ---> J4'-5' =  3.19
  PHI4'-5" =  -54.0 ---> J4'-5" =  3.73          PHI4'-5" =   -1.0 ---> J4'-5" =  7.91
1CASE NR:    1
 TITLE  :4 : 6 J's                                                                                                     PSEUROT-5.4
0=============================================================================================================================
 E R R O R   A N A L Y S I S
 =============================================================================================================================

0OVERALL RMS  =   .448E+00
0STANDARD DEVIATIONS IN PARAMETERS:

     0      .166      .167      .293      .444      .085
0CORRELATION MATRIX OF PARAMETERS
0PAR.       1          2          3          4          5
  1      1.000
  2      -.035      1.000
  3       .110      -.446      1.000
  4       .685      -.335      -.318      1.000
  5       .004      .196       -.236      -.050      1.000
0*** END OF PGM PSEUROT ***
```

6. 1-*N*-(Boc-aminoethyl)-4*R*-N3benzoyl-thymin-1yl-2*S*-proline (**5**)

```
Input
  25 : 6 J's
    1  25    0.1       0.5       0.0       1
2'-3'   0  -144.0      1.000    -1.7       1.02      0.39      0.00      0.74
2'-3"   0  -144.0      1.000  -122.9       1.02      0.39      0.00      0.74
3'-4'   0     0.0      1.000  -122.1       0.64      0.00       0.50     0.68
3"-4"   0     0.0      1.000    -1.0       0.64      0.00      0.50      0.68
4'-5'   0   144.0      1.000   122.7       0.50      0.74      0.00      1.02
4'-5"   0   144.0      1.000     1.1       0.50      0.74      0.00      1.02

AB        8.10 7.90 2.90 4.20 3.70 2.90

   10.0      34.0     147.5      35.0
.5
11111
Input
1CASE NR:    1
 TITLE  :5 : 6 J's                                                                                                    PSEUROT-5.4
0=============================================================================================================================
 P A R A M E T E R S   I N   P S E U D O R O T A T I O N   R E L A T I O N S
 ============================================================================================================================


0COUPLING CONSTANTS DEFINED BY:

 NAME           FASE         A             B                  ELECTRONEGATIVITIES             # OF SUBSTITUENTS

 2'-3'         -144.0       1.000         -1.7       1.020        .390        .000        .740          3
 2'-3"         -144.0       1.000       -122.9       1.020        .390        .000        .740          3
 3'-4'            .0        1.000       -122.1        .640        .000        .500        .680          3
 3"-4"            .0        1.000         -1.0        .640        .000        .500        .680          3
 4'-5'          144.0       1.000        122.7        .500        .740        .000       1.020          3
 4'-5"          144.0       1.000          1.1        .500        .740        .000       1.020          3


0PARAMETERS USED IN GENERALIZED KARPLUS EQUATION:

0=============================================================================================================================
 I N P U T   D A T A
 ============================================================================================================================


      J -->   2'-3'     2'-3"     3'-4'     3"-4"     4'-5'     4'-5"
 AB            8.10      7.90      2.90      4.20      3.70      2.90
0CASE     1 HAS   1 SETS ->   6 OBSERVATIONS
0MAX STEPSIZE                =    .100
 CONVERGENCE CRITERIUM       =   5.000E-04
 MAXIMUM NUMBER OF ITERATIONS =  25
1CASE NR:    1
 TITLE  :5 : 6 J's                                                                                                    PSEUROT-5.4
0=============================================================================================================================
 F I R S T   E S T I M A T E S
 ============================================================================================================================


 CONFORMER 1:       P =  10.0 DEGREES =   .175 RAD  ---> TO BE REFINED
                  PHI =  34.0 DEGREES =   .593 RAD  ---> TO BE REFINED

 CONFORMER 2:       P = 147.5 DEGREES =  2.574 RAD  ---> TO BE REFINED
                  PHI =  35.0 DEGREES =   .611 RAD  ---> TO BE REFINED

                    AB       : MF2 =   .500      ---> TO BE REFINED
0***** ITERATION CONVERGED *****
1CASE NR:    1
 TITLE  :5 : 6 J's                                                                                                    PSEUROT-5.4
0=============================================================================================================================
 F I N A L   O U T P U T
 ============================================================================================================================


0              2'-3'                 2'-3"                 3'-4'                 3"-4"                 4'-5'
            JEXP    JCAL    DIFF    JEXP    JCAL    DIFF    JEXP    JCAL    DIFF    JEXP    JCAL    DIFF    JEXP    JCAL    DIFF
 AB       !  8.10    7.86     .24 !  7.90    7.83     .07 !  2.90    2.89     .01 !  4.20    4.29    -.09 !  3.70    3.69     .01   !
0              4'-5"
            JEXP    JCAL    DIFF
 AB       !  2.90    2.82     .08 !
0             MF1       MF2       RMS
 AB            .934      .066      .112
0CONFORMER 1:                                CONFORMER 2:
         P =   36.2   DEGREES   =   .632 RAD            P =  233.4   DEGREES   =  4.073 RAD
       PHI =   68.9   DEGREES   =  1.202 RAD          PHI =   64.7   DEGREES   =  1.130 RAD
  PHI2'-3' =  -22.7 ---> J2'-3' =  7.78          PHI2'-3' =   -1.0 ---> J2'-3' =  9.02
  PHI2'-3" = -143.9 ---> J2'-3" =  8.11          PHI2'-3" = -122.2 ---> J2'-3" =  3.83
  PHI3'-4' =  -66.6 ---> J3'-4' =  2.30          PHI3'-4' = -160.7 ---> J3'-4' = 11.25
  PHI3"-4" =   54.5 ---> J3"-4" =  4.17          PHI3"-4" =  -39.6 ---> J3"-4" =  6.10
  PHI4'-5' =   53.8 ---> J4'-5' =  3.12          PHI4'-5' =  184.5 ---> J4'-5' = 11.75
  PHI4'-5" =  -67.8 ---> J4'-5" =  2.87          PHI4'-5" =   62.9 ---> J4'-5" =  2.06
1CASE NR:    1
 TITLE  :25 : 6 J's                                                                                                   PSEUROT-5.4
0=============================================================================================================================
 E R R O R   A N A L Y S I S
 ============================================================================================================================


0OVERALL RMS  =   .112E+00
0STANDARD DEVIATIONS IN PARAMETERS:

     0      .022      .024      .278      .458      .023
0CORRELATION MATRIX OF PARAMETERS
0PAR.      1         2         3         4         5
  1      1.000
  2       .311     1.000
  3       .322     -.067     1.000
  4       .276     -.511      .472     1.000
  5      -.133     -.467      .377      .326     1.000
0*** END OF PGM PSEUROT ***
```

7. 1-*N*-(Boc-aminoethyl)-4*R*-adenin-9-yl-2*S*-proline methyl ester (**6**)

```
6 : 6 J's
    1  25    0.1       0.5       0.0       1
2'-3'   0  -144.0      1.000    -1.7       1.02      0.39      0.00      0.74
2'-3"   0  -144.0      1.000  -122.9       1.02      0.39      0.00      0.74
3'-4'   0     0.0      1.000  -122.1       0.64      0.00      0.50      0.68
3"-4"   0     0.0      1.000    -1.0       0.64      0.00      0.50      0.68
4'-5'   0   144.0      1.000   122.7       0.50      0.74      0.00      1.02
4'-5"   0   144.0      1.000    1.10       0.50      0.74      0.00      1.02

AB        6.30 6.50 7.10 5.80 5.90 5.30

   0.0      34.0     147.5      36.0
.5
11111
1CASE NR:    1
 TITLE  : 6 : 6 J's                                                                                                    PSEUROT-5.4
0=============================================================================================================================
 P A R A M E T E R S   I N   P S E U D O R O T A T I O N   R E L A T I O N S
 ============================================================================================================================


0COUPLING CONSTANTS DEFINED BY:

 NAME           FASE         A             B                 ELECTRONEGATIVITIES             # OF SUBSTITUENTS

 2'-3'         -144.0       1.000         -1.7       1.020        .390        .000        .740          3
 2'-3"         -144.0       1.000       -122.9       1.020        .390        .000        .740          3
 3'-4'             .0       1.000       -122.1        .640        .000        .500        .680          3
 3"-4"             .0       1.000         -1.0        .640        .000        .500        .680          3
 4'-5'          144.0       1.000        122.7        .500        .740        .000       1.020          3
 4'-5"          144.0       1.000          1.1        .500        .740        .000       1.020          3


0PARAMETERS USED IN GENERALIZED KARPLUS EQUATION:


0=============================================================================================================================
 I N P U T   D A T A
 ============================================================================================================================


      J -->   2'-3'     2'-3"     3'-4'     3"-4"     4'-5'     4'-5"
 AB            6.30      6.50      7.10      5.80      5.90      5.30
0CASE     1 HAS   1 SETS ->    6 OBSERVATIONS
0MAX STEPSIZE                =    .100
 CONVERGENCE CRITERIUM       =   5.000E-04
 MAXIMUM NUMBER OF ITERATIONS =  25
1CASE NR:    1
 TITLE  : 6 : 6 J's                                                                                                    PSEUROT-5.4
0=============================================================================================================================
 F I R S T   E S T I M A T E S
 ============================================================================================================================


 CONFORMER 1:       P =    .0 DEGREES =   .000 RAD  ---> TO BE REFINED
                  PHI =  34.0 DEGREES =   .593 RAD  ---> TO BE REFINED

 CONFORMER 2:       P = 147.5 DEGREES =  2.574 RAD  ---> TO BE REFINED
                  PHI =  36.0 DEGREES =   .628 RAD  ---> TO BE REFINED

                     AB       : MF2 =   .500      ---> TO BE REFINED
1CASE NR:    1
 TITLE  : 6 : 6 J's                                                                                                    PSEUROT-5.4
0=============================================================================================================================
 F I N A L   O U T P U T
 ============================================================================================================================


0               2'-3'                   2'-3"                   3'-4'                   3"-4"                   4'-5'
             JEXP    JCAL    DIFF    JEXP    JCAL    DIFF    JEXP    JCAL    DIFF    JEXP    JCAL    DIFF    JEXP    JCAL    DIFF
 AB       !  6.30    6.42    -.12 !  6.50    6.45     .05 !  7.10    6.83     .27 !  5.80    5.34     .46 !  5.90    6.16    -.26   !
0               4'-5"
             JEXP    JCAL    DIFF
 AB       !  5.30    5.61    -.31 !
0             MF1       MF2       RMS
 AB            .449      .551      .279
0CONFORMER 1:                                  CONFORMER 2:
        P =    2.2   DEGREES   =   .038 RAD            P =  203.0   DEGREES   =  3.543 RAD
      PHI =   68.5   DEGREES   =  1.196 RAD          PHI =   28.1   DEGREES   =   .490 RAD
  PHI2'-3' =  -55.6 ---> J2'-3' =  3.54          PHI2'-3' =   12.8 ---> J2'-3' =  8.78
  PHI2'-3" = -176.8 ---> J2'-3" = 12.15          PHI2'-3" = -108.4 ---> J2'-3" =  1.80
  PHI3'-4' =  -53.6 ---> J3'-4' =  4.04          PHI3'-4' = -148.0 ---> J3'-4' =  9.10
  PHI3"-4" =   67.5 ---> J3"-4" =  2.38          PHI3"-4" =  -26.9 ---> J3"-4" =  7.76
  PHI4'-5' =   65.8 ---> J4'-5' =  1.78          PHI4'-5' =  150.1 ---> J4'-5' =  9.74
  PHI4'-5" =  -55.8 ---> J4'-5" =  4.56          PHI4'-5" =   28.5 ---> J4'-5" =  6.47
1CASE NR:    1
 TITLE  :6 : 6 J's                                                                                                     PSEUROT-5.4
0=============================================================================================================================
 E R R O R   A N A L Y S I S
 ============================================================================================================================


0OVERALL RMS  =   .279E+00
0STANDARD DEVIATIONS IN PARAMETERS:

     0      .176      .110      .312      .103      .050
0CORRELATION MATRIX OF PARAMETERS
0PAR.       1         2         3         4         5
  1      1.000
  2      -.231      1.000
  3      -.353       .337     1.000
  4      -.237      -.519       .137     1.000
  5      -.330       .447       .330     -.293     1.000
0*** END OF PGM PSEUROT ***
```

8. 1-*N*-(Boc-aminoethyl)-4*S*-thymin-1-yl-2*S*-proline methyl ester (**8**)

```
Input
Compound 8: 6 J's

Default:  1  25    0.1       0.5       0.0       1

Couplling    phase     A          B             Group  Eectronegativities (L)

     default                                  L1                  L2                  L3                  L4
2'-3'   0  -144.0      1.000    -1.7       1.02      0.39      0.00      0.74
2'-3"   0  -144.0      1.000  -122.9       1.02      0.39      0.00      0.74
3'-4'   0     0.0      1.000  -122.1       0.64      0.00      0.50      0.50
3"-4"   0     0.0      1.000    -1.0       0.64      0.00      0.50      0.50
4'-5'   0   144.0      1.000   122.7       0.50      0.74      0.00      1.02
4'-5"   0   144.0      1.000     1.1       0.50      0.74      0.00      1.02

JA-B        8.10 5.90 2.90 4.20 3.80 2.90

PH = 10.0      (N = 34.0     PS= 147.5      (S= 35.0
MFN = 0.5
11111

Output
1CASE NR:    1
 TITLE  :54 : 6 J's                                                                                                    PSEUROT-5.4
0=============================================================================================================================
 P A R A M E T E R S   I N   P S E U D O R O T A T I O N   R E L A T I O N S
 ============================================================================================================================
0COUPLING CONSTANTS DEFINED
 NAME         FASE     A         B              ELECTRONEGATIVITIES            N0 SUBSTITUENT
 2'-3'       -144.0   1.000     -1.7      1.020        .390        .000        .740          3
 2'-3"      -144.0   1.000    -122.9      1.020        .390        .000        .740          3
 3'-4'        0.0     1.000     -122.1     .640        .000        .500        .500          3
 3"-4"        0.0     1.000       -1.0     .640        .000        .500        .500          3
 4'-5'       144.0    1.000      122.7     .500        .740        .000       1.020          3
 4'-5"         144.0       1.000 1.1       .500        .740        .000       1.020          3


0PARAMETERS USED IN GENERALIZED KARPLUS EQUATION:
0=============================================================================================================================
 I N P U T   D A T A
 ============================================================================================================================


      J -->   2'-3'     2'-3"     3'-4'     3"-4"     4'-5'     4'-5"
 AB            8.10      5.90      2.90      4.20      3.80      2.90
0CASE     1 HAS   1 SETS ->   6 OBSERVATIONS
0MAX STEPSIZE                =    .100
 CONVERGENCE CRITERIUM       =   5.000E-04
 MAXIMUM NUMBER OF ITERATIONS =  25
1CASE NR:    1
 TITLE  :33a : 6 J's                                                                                                   PSEUROT-5.4
0=============================================================================================================================
 F I R S T   E S T I M A T E S
 ============================================================================================================================


 CONFORMER 1:       P =  10.0 DEGREES =   .175 RAD  ---> TO BE REFINED
                  PHI =  34.0 DEGREES =   .593 RAD  ---> TO BE REFINED

 CONFORMER 2:       P = 147.5 DEGREES =  2.574 RAD  ---> TO BE REFINED
                  PHI =  35.0 DEGREES =   .611 RAD  ---> TO BE REFINED

                     AB       : MF2 =   .500      ---> TO BE REFINED
0***** ITERATION CONVERGED *****
1CASE NR:    1
 TITLE  :54 : 6 J's                                                                                                    PSEUROT-5.4
0=============================================================================================================================
 F I N A L   O U T P U T
 ============================================================================================================================

0               2'-3'                   2'-3"                   3'-4'                   3"-4"                   4'-5'
            JEXP    JCAL    DIFF    JEXP    JCAL    DIFF    JEXP    JCAL    DIFF    JEXP    JCAL    DIFF    JEXP    JCAL    DIFF
 AB       !  8.10    8.03     .07 !  5.90    5.96    -.06 !  2.90    3.06    -.16 !  4.20    4.52    -.32 !  3.80    3.84    -.04   !
0               4'-5"
            JEXP    JCAL    DIFF
 AB       !  2.90    2.66     .24 !
0             MF1       MF2       RMS
 AB            .857      .143      .180
0CONFORMER 1:                          CONFORMER 2:
         P =   41.9   DEGREES   =   .731 RAD            P =  204.4   DEGREES   =  3.568 RAD
       PHI =   68.4   DEGREES   =  1.195 RAD          PHI =   85.9   DEGREES   =  1.500 RAD
  PHI2'-3' =  -16.1 ---> J2'-3' =  8.35          PHI2'-3' =   40.7 ---> J2'-3' =  6.07
  PHI2'-3" = -137.3 ---> J2'-3" =  6.79          PHI2'-3" =  -80.5 ---> J2'-3" =   .99
  PHI3'-4' =  -71.1 ---> J3'-4' =  1.73          PHI3'-4' = -200.4 ---> J3'-4' = 11.05

  PHI3"-4" =   50.0 ---> J3"-4" =  5.09          PHI3"-4" =  -79.3 ---> J3"-4" =  1.06
  PHI4'-5' =   54.6 ---> J4'-5' =  3.02          PHI4'-5' =  206.9 ---> J4'-5' =  8.75
  PHI4'-5" =  -67.0 ---> J4'-5" =  2.97          PHI4'-5" =   85.3 ---> J4'-5" =   .77
1CASE NR:    1
 TITLE : 33a : 6 J's                                                                                                   PSEUROT-5.4
0=============================================================================================================================
 E R R O R   A N A L Y S I S
 ============================================================================================================================


0OVERALL RMS  =   .180E+00
0STANDARD DEVIATIONS IN PARAMETERS:

     0      .036      .043      .234      .224      .043
0CORRELATION MATRIX OF PARAMETERS
0PAR.       1         2         3         4         5
  1      1.000
  2       .376     1.000
  3      -.283      .293     1.000
  4       .055      .393      .401     1.000
  5      -.103     -.342     -.058      .285     1.000
0*** END OF PGM PSEUROT ***
```

9. ^{1}H NMR spectra of **3** (500 MHz)

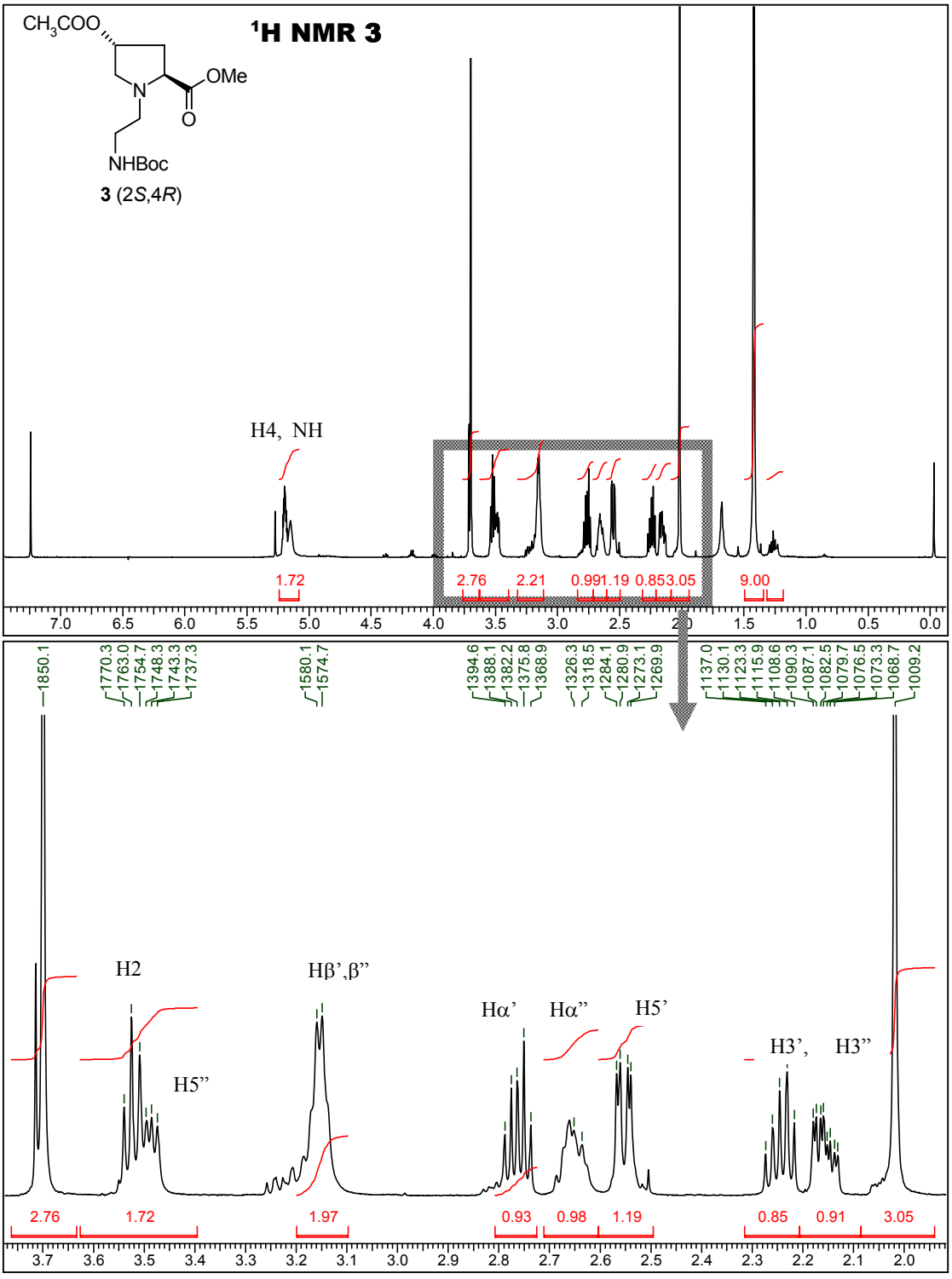

10. ^{1}H-NMR of compound **4**

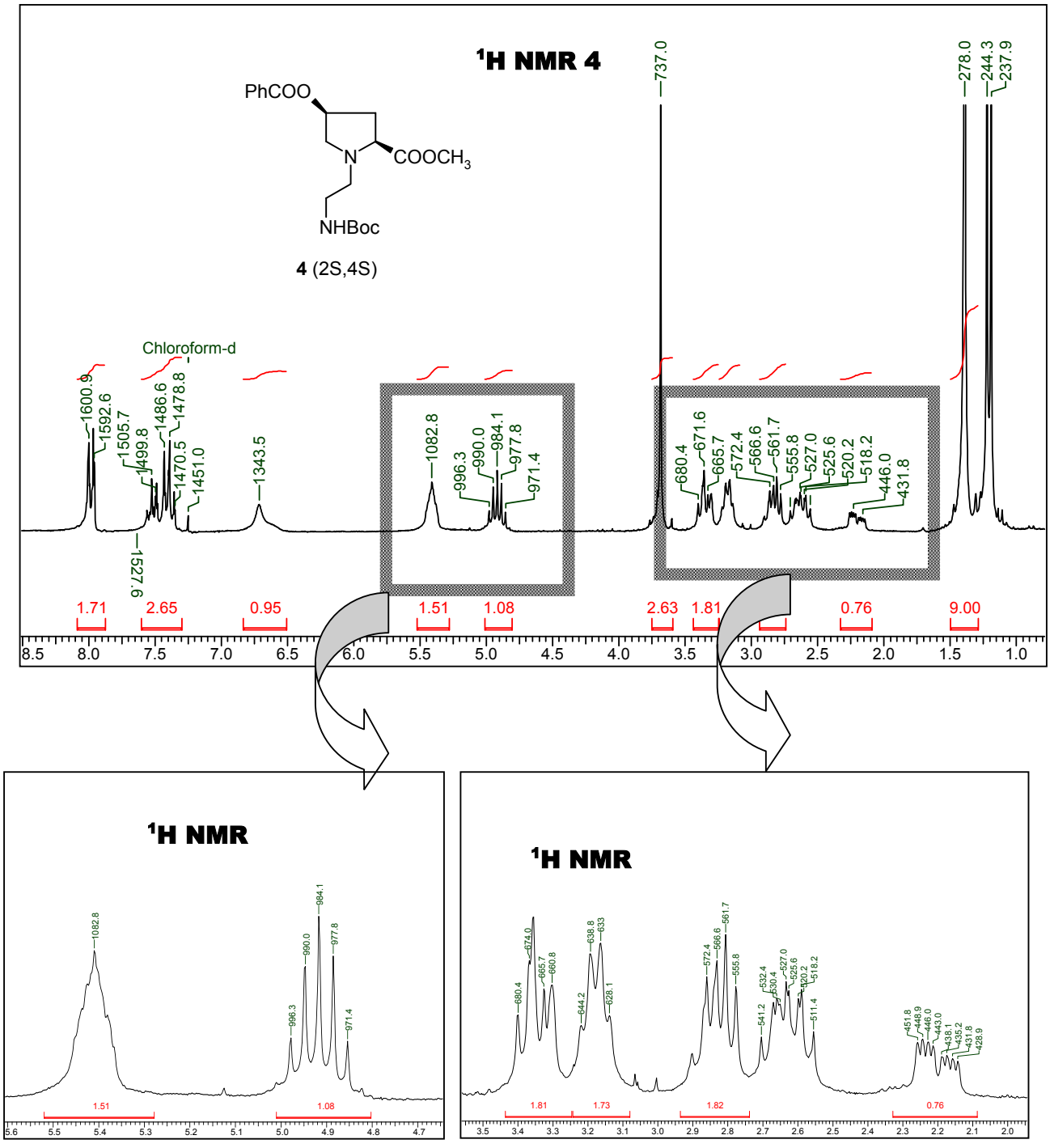

11. ^{1}H-NMR of compound **5**

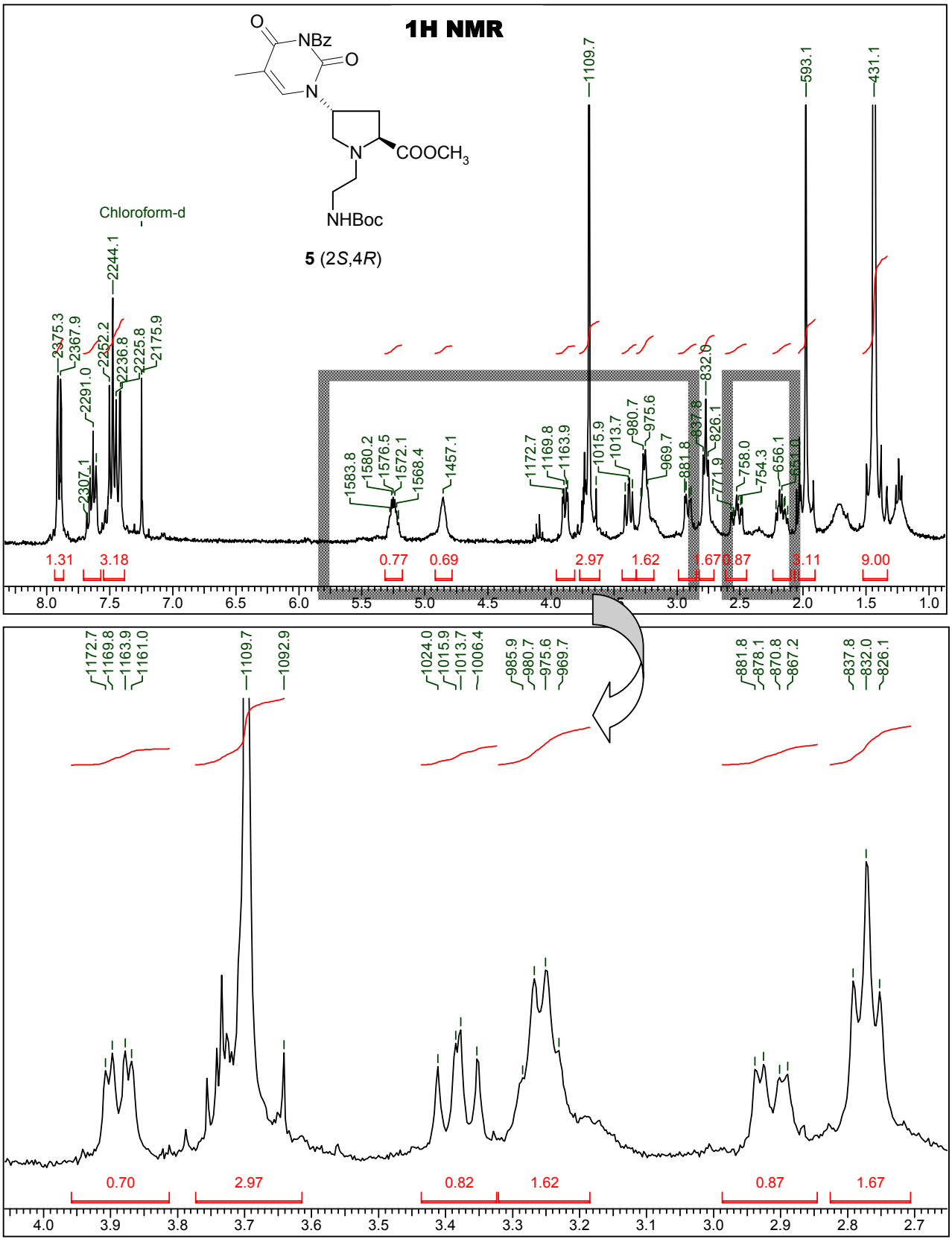

12. ^{1}H-NMR of Compound (**5**) and (**6**)

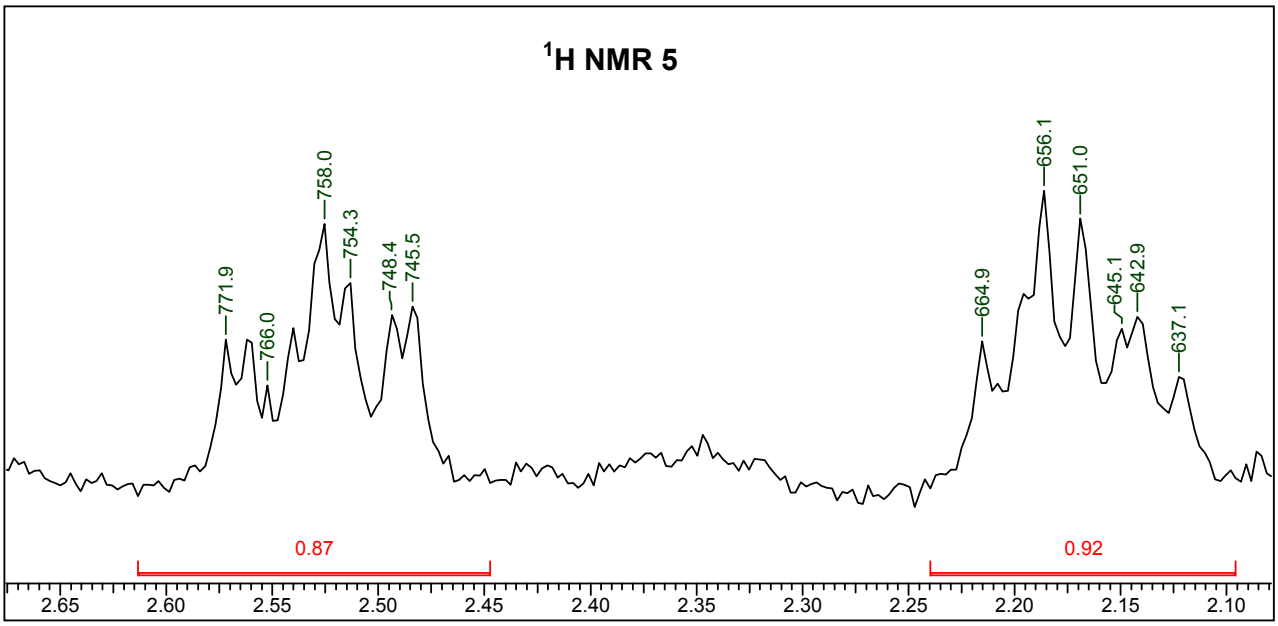

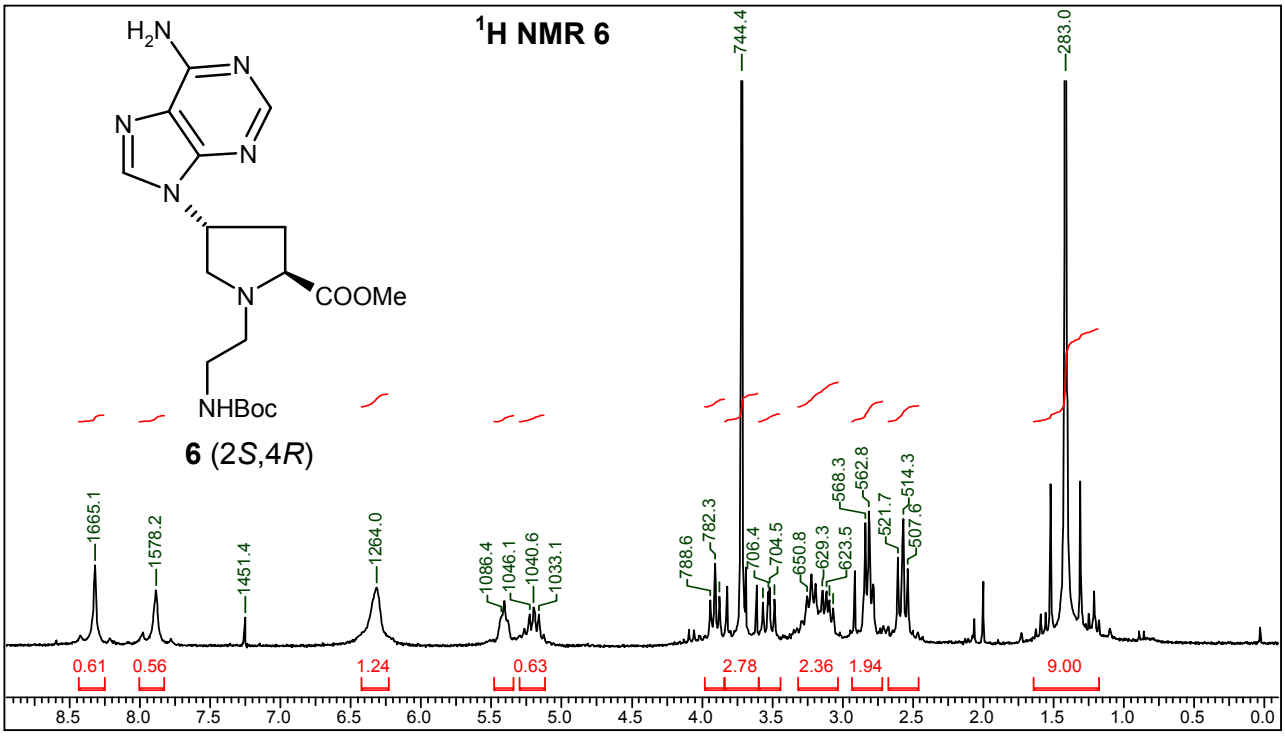

13. ^{1}H and 2D J-resolved NMR spectra of compound (**7**)

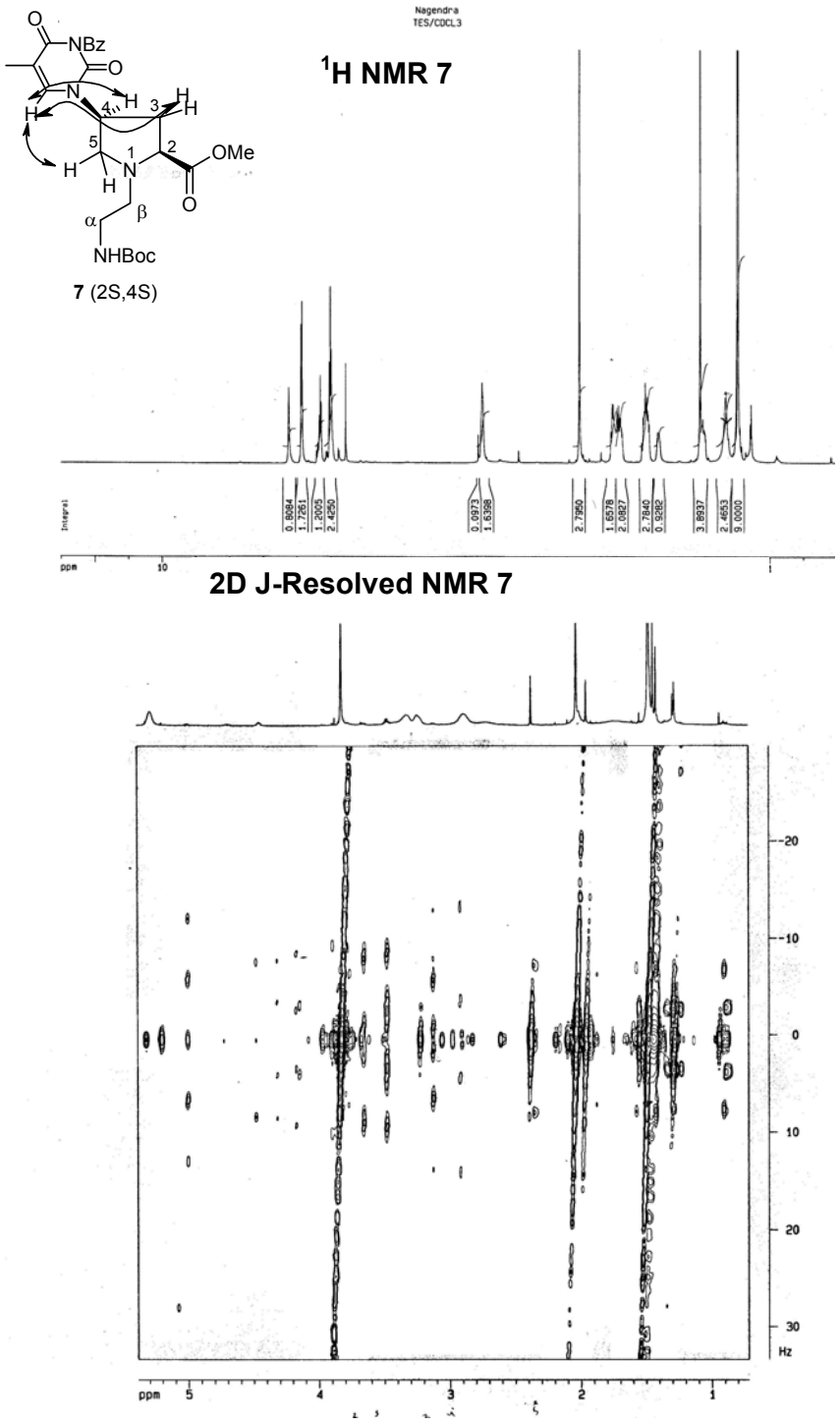

7 (2S,4S)

14. 2D-^{1}H-^{1}H NOESY **3** NMR spectra compound **2** and **3**

^{1}H-^{1}H NOESY **3**

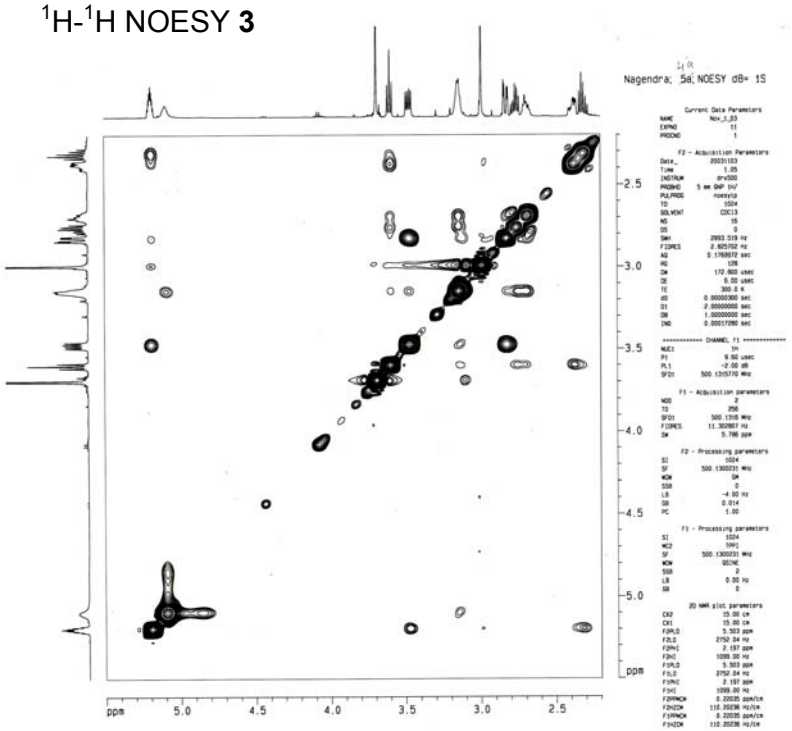

^{1}H-^{1}H NOESY 3

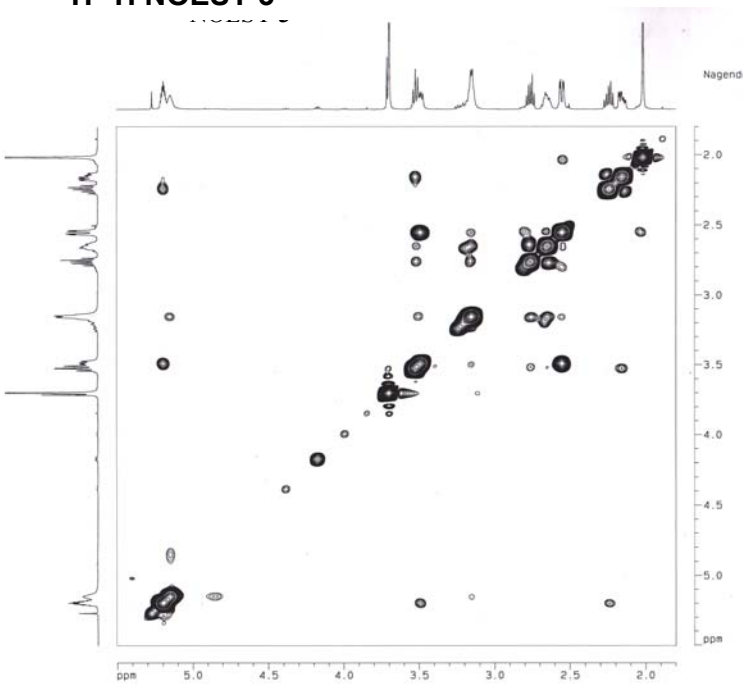

15. 2D-^{1}H-^{1}H COSY NMR spectra compound **3**

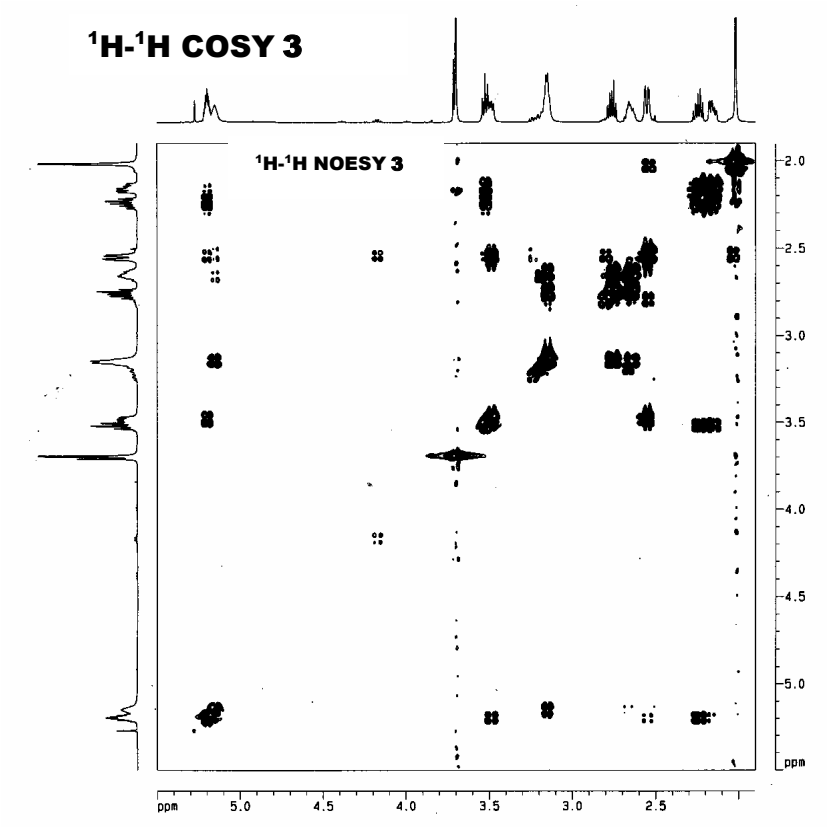

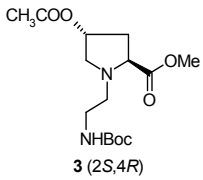

3 (2*S*,4*R*)

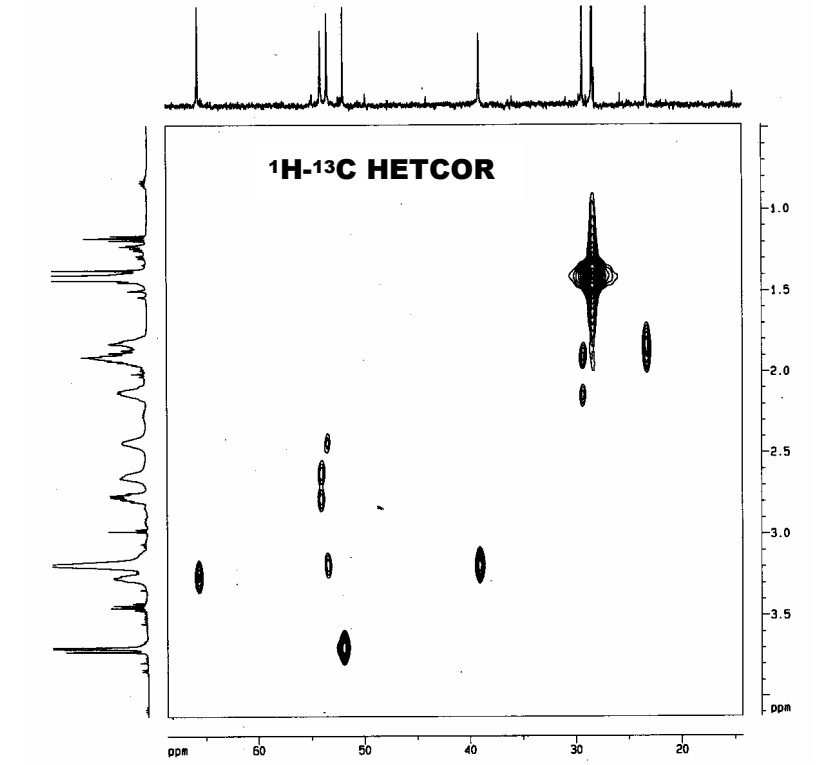

CHAPTER 4

SYNTHESIS OF PYRROLIDINE AND PYRROLIDINONE PNA OLIGOMERS AND THEIR HYBRIDIZATION STUDIES WITH COMPLEMENTARY

CHAPTER 4: SYNTHESIS OF PYRROLIDINE AND PYRROLIDINONE PNA OLIGOMERS AND THEIR HYBRIDIZATION STUDIES WITH COMPLEMENTARY DNA/RNA

4.1 INTRODUCTION

The main goals of designing antisense/antigene molecules is to achieve high binding affinity/specificity to the target nucleic acid and make them stable to cellular enzymes with a long enough half-life within the system to allow manifestation of its effect. Non-toxicity to the cell in which its activity is required is also desired.[1-2] All DNA analogues designed and synthesized are subjected to various biophysical studies to examine the affinity and specificity to the target and biochemical studies to evaluate their cellular stability and toxicity in order to evaluate their potential on antisense agents.[3-6]

The chemical approaches to improve the properties of oligonucleotides are mainly concentrated on the increase of nuclease resistance without affecting RNA binding affinity.[7] The latter is of importance for the antisense strategy and is usually reflected by alteration in "melt temperatures" (Tm's) PNA:RNA hybrids which are determined by temperature dependence of UV/CD absorption.[8]

4.2 BIOPHYSICAL TECHNIQUES: UV AND CD

4.2.1 UV-Studies

4.2.1a UV-Melting

UV absorption at 260 nm monitored as a function of temperature is used to determine the thermal stability of PNA:DNA hybrids. Increasing the temperature induces structural transition of complexes to single strands by loss of secondary and tertiary structure, leading to an increase in the UV absorption at 260 nm. This is termed as 'hyperchromicity' which is a measure of the extent of the secondary structure and base stacking present in nucleic acids.[9] The process is co-operative and the plot of the absorbance at 260 nm against temperature is sigmoidal (Figure 1a). A non-sigmoidal (e.g., linear) transition with negligible hyperchromicity is an evidence of non-duplexation (non-

complementation). In many cases, the transitions may be broad and the exact Tms are obtained from the peak in the first derivative plots.[10] An empirical formula for prediction of thermal stability (Tm) of PNA/DNA duplexes has been derived based on the model used for calculating Tm of the corresponding DNA/DNA duplex. This employs the nearest neighbour approach, by including the terms for pyrimidine content, length of PNA and takes into account the increased thermal stability of PNA/DNA hybrids and the asymmetry of the PNA-DNA heteroduplex.

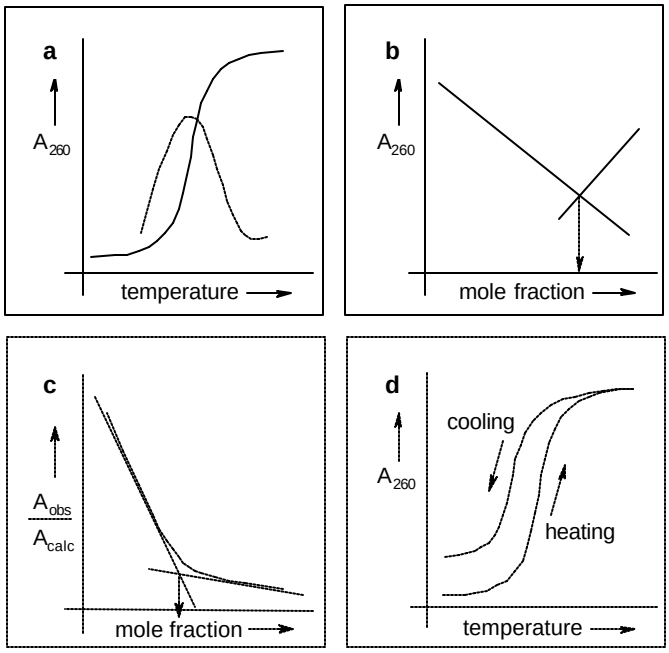

Figure 1: Schematic representation of **a**. UV-melting (thermal stability), **b**. UV-mixing, **c**. UV-titration (stoichiometry) and **d**. Hysteresis (rate of hybridization)

The linear model for melting temperature prediction of PNA/DNA duplexes[11a] is

$$Tm_{pred} = c_0 + c_1 * Tm_{nnDNA} + c_2 * f_{pyr} + c_3 * length$$

where Tm_{pred} is the melting temperature calculated using nearest neighbour model for the corresponding DNA/DNA duplex applying ΔH^0 and ΔS^0 values as described by Santa Lucia *et. al.*[11b] f_{pyr} denotes the fractional pyrimidine content and "length" is the PNA sequence length in bases and constants $c_0 = 20.79$, $c_1 = 0.83$, $c_2 = -26.13$ and $c_3 = 0.44$.

A basic requirement for performing any type of biophysical experiment is that the solubility of PNA should be enough in order to avoid aggregation. For thermal melting studies using temperature dependent absorbance technique, the minimum concentrations needed are usually in the μM range. Though this is not a problem for oligomers of DNA and RNA, certain sequences of PNA, especially those having large quantities of guanine content, have low solubility. A terminal lysine amide, which is doubly charged at neutral pH, improves the solubility significantly. The concentrations of PNAs were determined by UV-absorbance using from Beer-Lambert law,[12] $A = \varepsilon cl$, where A is the absorbance, ε is the extinction coefficient in units of $M^{-1}cm^{-1}$, C is the molar concentration and l is the path length in cm.

The sample was prepared from mixing the appropriate single and / or double strands and heating to 80-90 ^{o}C and kept for 5 min, then allowed slowly to reach the room temperature. Before starting UV experiment, this is kept for 5-6 hr at 4 ^{o}C and the sample is transferred to a suitable quartz cell followed by degassing with N_2/Ar in order to avoid the oxygen bubble formation at the elevated temperature.

4.2.1b Stoichiometry determination

The binding stoichiometry of nucleic acids is determined from UV-mixing or UV-titration experiments. The UV-mixing experiment is carried out by mixing the appropriate oligomers in different mole ratios, keeping the total concentration constant. The UV-absorbances of these samples are plotted against the mole fraction of one of the components, in what is termed as a Jobs plot[13] (Figure 1b). The absorbance steadily decreases until all the strands present are involved in complex formation as a result of the hypochromic effect and then rises afterwards when one strand is present in excess. The stoichiometry of the complexation is derived from the minimum in such a plot.

The stoichiometry of complexation can also be determined by UV-titration (Figure 1c). In this method, one of the strands involved in complexation is sequentially added in aliquots to a fixed amount of the complementary component and the UV-absorbance is recorded at each addition. Upon successive additions of the complementary strand, complex formation results in hypochromicity, which leads to a progressive decrease in the ratio of the observed to the calculated absorbance. After the first strand present in the buffer is exhausted, the absorbance reaches a plateau in the normalized plot of absorbance against the nucleic acid mole fraction; the point at which the plateau is reached indicates the stoichiometry of complexation.

4.2.1c Hysterisis

PNA/DNA strands bearing charged groups can be tested for hysteresis by thermal dissociation vs re-association plots. The experiment consists of recording the UV absorbance by first heating the duplexes/triplexes (UV-melting) followed by cooling the sample while recording the absorbance (re-association, cooling curve).[14] In DNA:PNA complexes, the cooling curve does not follow the melting curve and exhibits a hysteresis (Figure 1d). This is due to the fact that the re-association of duplexes or triplexes is much slower because of the inter-strand repulsion on account of the negative phosphate groups. When one of the strands bears cationic charges, the net repulsion between the two strands is reduced, leading to a lower hysterisis in the heating-cooling plots.

4.2.1d Mismatch studies

The fidelity of base-pairing in the PNA:DNA complexes can be examined by challenging the PNA oligomer with a DNA strand bearing a mismatch at a desired site,[15] preferably opposite to the site of modification. The base mismatch leads to the absence of or incorrect hydrogen bonding between the bases and causes a drop in the measured

melting temperature. A modification of the PNA structure is considered good if it gives a significantly lower Tm with DNA sequences containing mismatches as compared to that with unmodified PNA. It is to be pointed out that in all biophysical experiments described herein, the modified PNAs are always evaluated against the unmodified control PNA.

4.2.1e Parallel and antiparallel duplexes

Homopyrimidine thymine PNA sequences bind to the complementary homopurine DNA sequence forming PNA_2:DNA triplexes in which the central DNA strand binds by WC hydrogen bonding to one PNA strand and to the other by HG hydrogen bonding. Mixed base sequences form duplexes of antiparallel or parallel orientations that can be selected by proper design of the complementary DNA sequences.[16] By convention, antiparallel PNA:DNA complexes are defined as those in which the 'N' terminal of the PNA faces the 3′-end of the DNA with the 'C' terminal facing the 5′-end; parallel PNA:DNA complexes are those in which the 'C' terminal of PNA faces the 3′-end of DNA with the 'N' terminal towards the 5′-end of the DNA (Figure 2).[17]

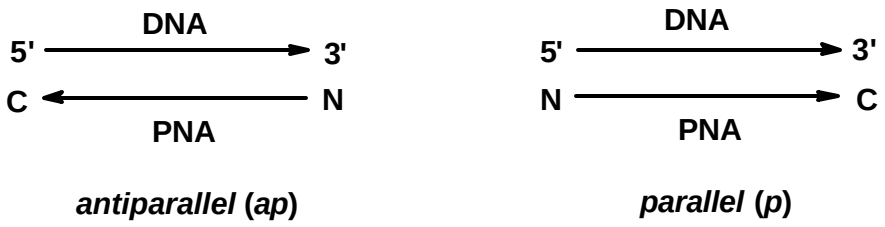

Figure 2: Schematic representation of the antiparallel and parallel modes of complexation of PNA with complementary DNA

4.3.2 Circular dichroism

Circular Dichroism (CD) is a well-established tool used to study the conformational aspects of nucleic acids.[18] Upon comparison with reference samples, CD spectra can provide reliable and useful data concerning the conformational states of the

system under study. However, CD does not give detailed structural data as obtained from X-ray crystallography or NMR, but it can be used as a complementary tool to UV spectroscopy to evaluate the overall base-stacking patterns. The differences in secondary structure and handedness of helices can be conformationally differentiated by changes in CD profiles.

CD of nucleic acids arises predominantly as an effect of coupling between the transition moments of adjacent nucleobases due to continuous stacking. The PNA backbone is inherently achiral. However, PNA, a polyamide, can be expected to form helices *via* intramolecular hydrogen bonding leading to a racemic mixture of right- and left-handed helices and no net CD is observed.[19] Upon complexation with DNA/RNA, which is a chiral molecule, PNA:DNA/RNA duplexes/triplexes exhibit strong CD signals.[19] Thus, the complex formed as a consequence of the binding of achiral PNA and chiral DNA leads to the formation of a chiral complex. CD thus assumes importance in the characterization of such complexes.

4.3 RATIONALE AND OBJECTIVES OF PRESENT WORK

The preceding Chapter 2 reports the synthesis of chiral and conformationally ring constrained *aep*- and *aepone*-PNA monomers. The aminoethylpyrrolidinone (*aepone*) PNA and aminoethylpyrrolidine (*aep*) PNA[20] units were introduced into achiral aminoethylglycyl (*aeg*) PNA[21] at various positions to study the effect of structural constraint and chirality in influencing the binding properties to target nucleic acids in terms of strength, specificity and directionality of binding. In order to investigate the complex forming potential of above modified PNAs, polypyrimidine PNA sequences for triplexes and mixed purine-pyrimidine sequences for duplexes were constructed. This

chapter reports biophysical studies on the stability of duplexes and triplexes comprised of mixed *aeg*/*aepone and aeg/aep* backbones.

Objectives

The following are the specific objectives of this Chapter:

(i) The synthesis, purification and characterization of various PNA oligomers by *solid phase synthesis method*, using *N*-Boc protected monomers of *aepone*-PNA, *aep*-PNA and *aeg*-PNA monomers (Figure 3).

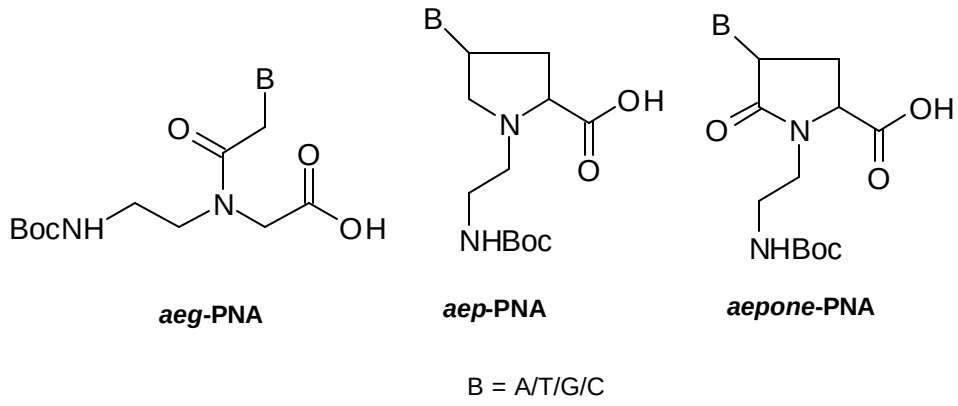

Figure 3: Chemical structure of *N*-Boc protected free acid of *aeg*-, *aep*- and *aepone*-PNA monomers

(ii) The systematic biophysical studies by using temperature dependent UV- and CD-spectroscopy of chiral PNAs L-*cis/trans*-(2*S*,4*R*)-*aepone*-PNA and L-*trans*-(2*S*,4*R*)-*aep*-PNA with target complementary oligo deoxyribonucleic acids (both, duplexes and triplexes).

4.4 PRESENT WORK

4.4.1 Solid phase synthesis of *aepone*-PNA oligomers

The PNA monomers L-*cis*-(2*S*,4*S*)-, L-*trans*-(2*S*,4*R*)-pyrrolidinone and L-*trans*-(2*S*,4*R*)-pyrrolidine PNA (Figure 4) were used to assemble PNA oligomers by well established solid phase peptide synthesis (SPPS) protocols.[22] The synthesized PNA oligomers were used for hybridization study with complementary DNA as triplexes and duplexes.

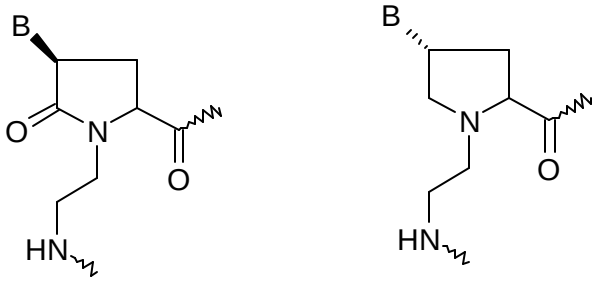

L-*cis*-(2S,4S) L-*trans*-(2S,4*R*)

a. L-*cis*-*aepone*-PNA

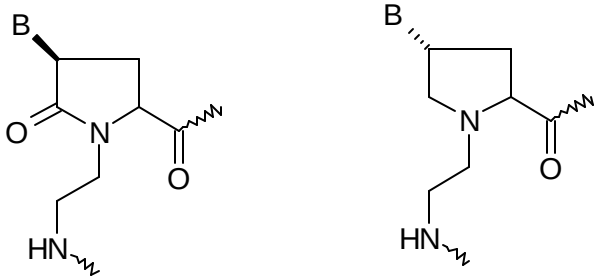

L-*cis*-(2S,4S) L-*trans*-(2S,4*R*)

b. L-*cis*-*aep*-PNA

B = A/T/G/C

Figure 4: a. *aepone*-PNA; b. *aep*-PNA

4.4.2 General protocols for PNA synthesis

As is the case with solid phase peptide synthesis, PNA synthesis is also done conveniently from the 'C' terminus to the 'N' terminus. For this, the monomeric units must have their amino functions suitably protected, with their carboxylic acid functions free. The most commonly used *N*-protecting groups for solid phase peptide synthesis are the *t*-butyloxycarbonyl (Boc)[23] and the 9-flurorenylmethoxycarbonyl (Fmoc)[24] groups. Fmoc protection strategy is associated with acyl migration from the tertiary amide to the free amine formed during deprotection under basic (piperidine) conditions. Hence, the Boc-protection strategy was selected for the present work. The amino function of the monomers was protected as the corresponding Boc-derivative and the carboxylic acid function was free to enable coupling with the resin-linked monomer. The diisopropylcarbodiimide (DIPCDI)/1-hydroxybenzotriazole (HOBt) activation was employed for the coupling reaction.[25] Merrifield resin was used as the solid polymeric matrix for assembly of oligomers. The first amino acid was linked to this matrix *via* benzyl ester linkage that can be cleaved either with a strong acid to yield the C-terminal free carboxylic acid, or with an amine to afford the C-terminal amide.

b-Alanine was used as the linker amino acid.[20] Being achiral, it would not interfere with the chirality-induced thermal and physical properties of the chiral pyrrolidyl units. Its contribution to the overall hydrophobicity of PNA is also minimal. *N*-Boc-*b*-alanine was first coupled to the resin through benzyl ester formation from its cesium salt.[26] The loading value of *b*-alanine on the resin (0.6 mmole/g) was determined by the picrate assay.[28] The resin loading was suitably lowered (0.2 mmol/m) by partial capping of the free amino groups after Boc-deprotection by *N*-acetylation. The free uncapped amino groups on the resin were estimated once again by the picrate assay prior to commencing solid phase synthesis.

The PNA oligomers were assembled using repetitive cycles, each comprising of the following steps:

Step 1: Deprotection of the *N*-Boc-group using 50% TFA in DCM (CH_2Cl_2).

Step 2: Neutralization of the TFA salt formed with diisopropylethyl amine (DIPEA) (5% DIPEA in DCM) to liberate the free amine.

Step 3: Coupling of the free amine of the resin with the free carboxylic acid group of the added monomer. The coupling reaction was carried out in DMF or NMP as the solvent in the presence of diisopropylcarbodiimide (DIPCDI) and 1-hydroxybenzotriazole (HOBt). These reagents are used for suppressing the racemization during coupling reaction. The deprotection of the *N*-Boc protecting group and the coupling reaction were monitored by Kaiser's test.[29]

Step 4: Capping of the unreacted amino groups by using acetic anhydride in pyridine:DCM. A typical synthesis cycle is depicted in Scheme 1.

Scheme 1: Protocol of solid phase synthesis

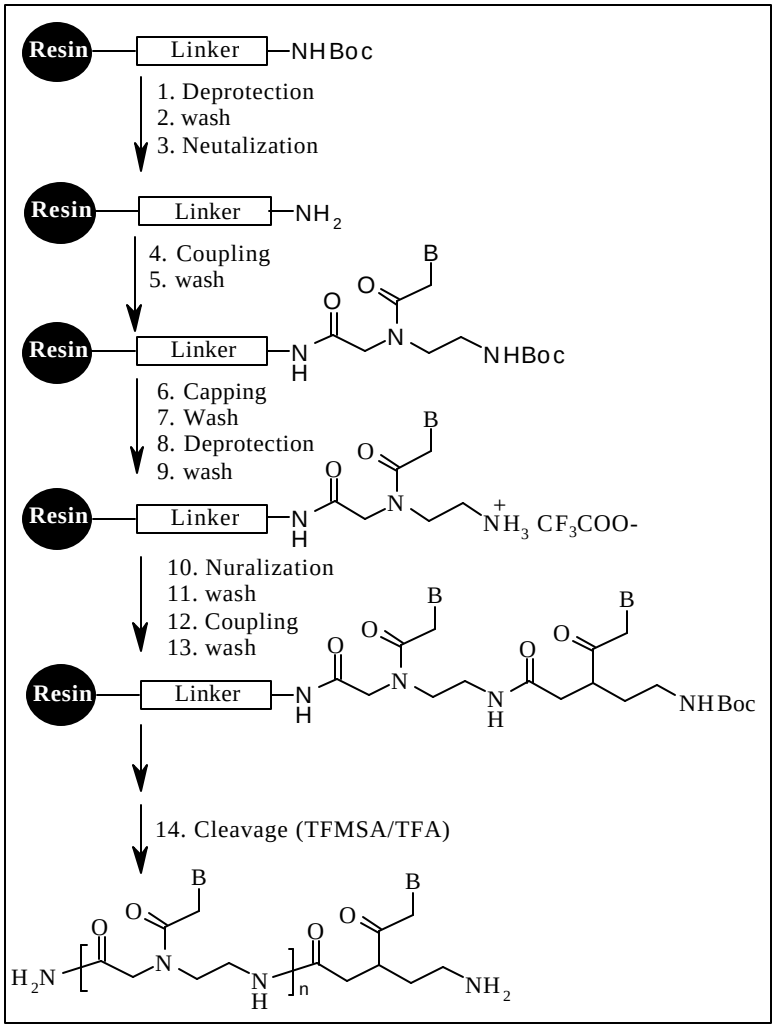

The solid phase synthesis is an efficient method although some problems arise due to side reactions occurring in peptide synthesis during the neutralization, leading to self-capping of the growing PNA chain. Mainly, two types of self-capping occur during synthesis: (i) transamidation derived from the primary amine i.e. acyl migration of the base acetyl segment (Figure 5a) and (ii) N-terminal detachment of the monomer during *N*-capping by uronium salt (Figure 5b).

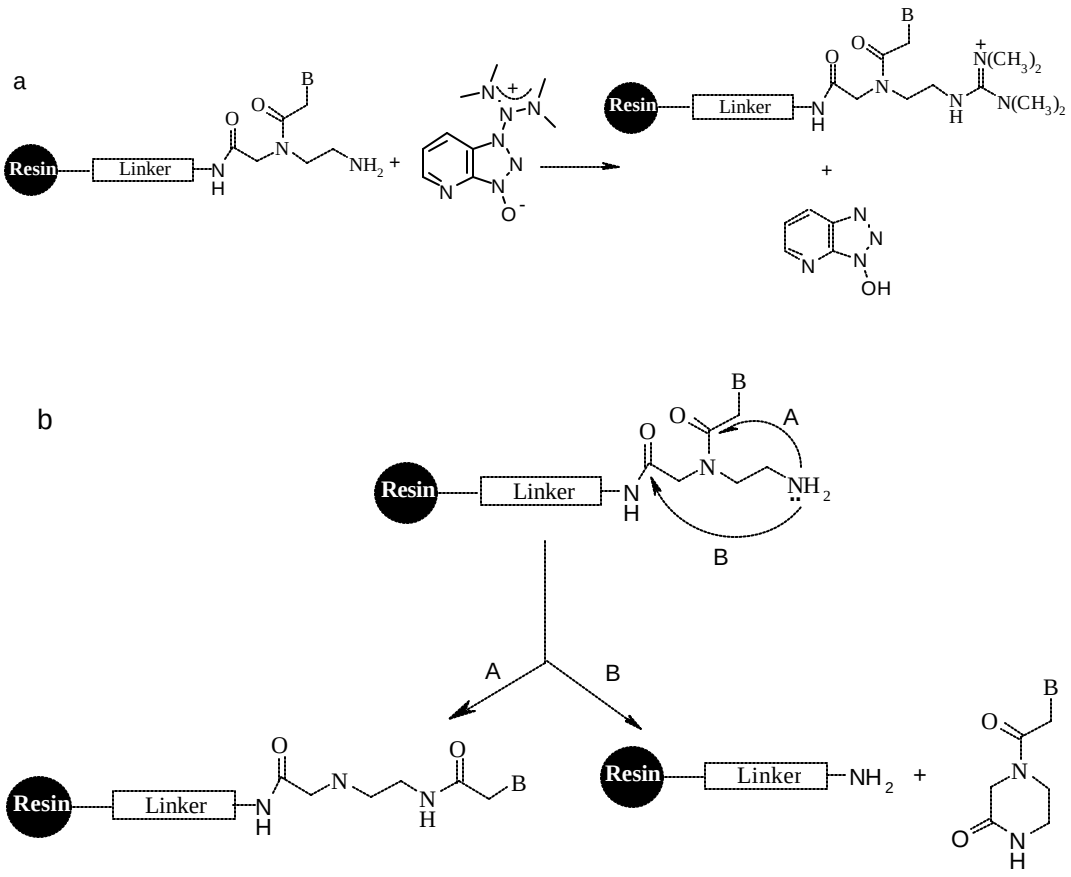

Figure 5: Side Reactions in PNA synthesis. (a) N-capping by uronium salt. (b) Trans amidation derived from the primary amine: A. Acyl migration of the base acetyl segment: B. N-terminal detachment of the monomer during neutralization.

4.4.3 Synthesis of *aepone*- and *aep*-PNA oligomers

4.4.3a Homopyrimidine sequences

The polypyrimidine (polythymine octamers) sequences of PNAs containing *aepone/aep* units were synthesized, following the Boc-protection strategy, as outlined above. This was used to examine the effect of the *aepone/aep* unit on triplex-forming ability with the complementary DNA A_8 oligomer in a 2:1 PNA:DNA stoichiometry. The unmodified aminoethylglycyl (*aeg*) PNA-T_8 oligomer control was also synthesized by following the same strategy. The *aep*-T or *aepone*-PNA-T units were incorporated at one or more pre-determined positions within the *aeg*-PNA oligomer sequence to obtain mixed

backbone PNAs as modified PNAs. The sequences are shown in Tables 1 and 2. The capping step at the end of each coupling cycle was not deemed necessary, as the coupling reaction as monitored by Kaiser's test indicated a high coupling efficiency, > 90%.

One *aep or aepone* unit was introduced at either the 'N' or 'C' terminus in sequences (Table 1) to obtain PNAs **2-3/11/13-16**. To study of the effect of introduction of increasing numbers of *aepone/aep* units on the stability and selectivity of DNA, complexation was done with sequences having more than one *aepone/aep* units (Table 1, PNA **4/7-10**). Further, octamers bearing eight modified units (homooligomers of *aep/aepone*) were also synthesized (Table 1, PNA **1-16**) to see the effect of only modified backbone over control *aeg*-PNA (**1**) backbone.

Table 1: Polypyrimidine and Complementary Sequences

Entry	Sequence Composition	Modified PNA
1	BocHN–T–T–T–T–T–T–T–T-*b*-ala-MF	*aeg*-(Control)
2	BocHN–T–T–T–T–t–T–T–T-*b*-ala- MF	one (2*S*,4*S*)-*aepone*-PNA
3	BocHN–t–T–T–T–T–T–T–T-*b*-ala- MF	one (2*S*,4*S*)-*aepone*-PNA
4	BocHN–T–T–T-t-T–T–T-t-*b*-ala-MF	two (2*S*,4*S*)-*aepone* PNA
5	BocHN-t-t-t-t-t-t-t-t-*b*-ala-MF	homo oligo of 8 (2S,4*S*) *aepone*-PNA
6	BocHN-t-t-t-t-t-t-t-t-*b*-ala-MF	homo oligo of 8 (2*S*,4*S*) *aep*-PNA
7	BocHN-T-T-t-T-T-t-T-T- *b*-ala-MF	two (2S,4*R*)-*aep*-PNA
8	BocHN-T-T-t-T-T-t-T-T- *b*-ala-MF	two (2*S*,4*S*)-*aepone*- PNA
9	BocHN-T-T-t-T-T-t-T-T- *b*-ala-MF	two (2S,4*R*)-*aepone*-PNA
10	BocHN-T-T-t-T-T-t-T-T- *b*-ala-MF	two -(2*S*,4*S*)-*aep*-PNA
11	BocHN–T–T–T–t–T–T–T-T-*b*-ala-MF	one (2*S*,4*R*)-*aepone*-PNA
12	BocHN–T–T–T–t–T–T–T-t-*b*-ala-MF	one-(2*S*,4*R*)*aepone*-PNA
13	BocHN –T–t–T–T–T–T–T–T–T-*b*-ala -MF	two (2*S*,4*R*)-*aepone*-PNA
14	BocHN –T–t–T–T–T–T–T–T–T-*b*-ala -MF	one (2*S*,4*S*)-*aep*-PNA
15	BocHN –T–t–T–T–T–T–T–T–T-*b*-ala -MF	one (2*S*,4*R*)-*aepone*-PNA
16	BocHN –T–t–T–T–T–T–T–T–T-*b*-ala -MF	one (2*S*,4*R*)-*aep*-PNA

4.4.3a Mixed purine-pyrimidine sequences

In order to study the duplex formation potential of the *aepone/aep* PNA backbone, it is necessary to synthesize mixed sequences incorporating both purines and pyrimidine units of *aepone/aep* PNA. Therefore, the *aepone/aep* PNA-T/A/C/G monomers

were incorporated into decamers of unmodified PNA at different desired positions (Table 2, entry 17-33).

Table 2: Mixed Base PNA Comprising A, T, G and C Nucleobases

Entry	Sequence Composition	Modified PNA
17	BocHN–t–T–T–T–t–T–T–T-*b*-ala-MF	*aeg*-(Control)-PNA
18	BocNH-G-T-A-G-A-T-C-A-C-T-*b*-ala-MF	one (2*S*,4*S*)-*aep*-PNA
19	BocNH-g-T-A-G-A-T-C-A-C-T-*b*-ala-MF	one (2*S*,4*S*)-a*epone*-PNA
20	BocNH-g-T-A-G-A-T-C-A-C-T-*b*-ala-MF	one (2*S*,4*R*)-a*ep*-PNA
21	BocNH-g-T-A-G-A-T-C-A-C-T-*b*-ala-MF	one (2*S*,4*S*)-*aepone*-PNA
22	BocNH-G-T-A-G-A-T-C-A-c-T-*b*-ala-MF	one (2*S*,4*R*)-*aepone*-PNA
23	BocNH-G-T-A-G-A-T-C-A-c-T-*b*-ala-MF	one (2*S*,4*R*)-*aepone*-PNA
24	BocNH-G-t-A-G-A-T-C-A-C-T-*b*-ala-MF	two (2*S*,4*R*)-*aepone*-PNA
25	BocNH-G-T-A-G-A-t-C-A-C-t-*b*-ala-MF	one (2*S*,4S)-*aep*-PNA
26	BocNH-G-T-A-G-A-t-C-A-C-T-*b*-ala-MF	one (2S,4*R*) *aep*-PNA
27	BocNH-G-T-A-G-A-t-C-A-C-T-*b*-ala-MF	one (2*S*, 4*S*)-*aepone*-PNA
28	BocNH-G-T-A-G-A-t-C-A-C-T-*b*-ala-MF	one (2*S*, 4*R*)-*aepone*-PNA
29	BocNH-G-T-A-G-A-t-C-A-C-T-*b*-ala-MF	one (2S,4*S*)-*aep*-PNA
30	BocNH-G-T-A-G-A-T-C-a-C-T-*b*-ala-MF	one (2S,4*R*)-*aep*-PNA
31	BocNH-G-T-A-G-A-T-C-a-C-T-*b*-ala-MF	one (2*S*, 4*S*) *aepone*-PNA
32	BocNH-G-T-A-G-A-T-C-a-C-T-*b*-ala-MF	one (2*S*, 4*R*) *aepone*-PNA
33	BocNH-G-T-A-G-A-T-C-a-C-T-*b*-ala-MF	one (2*S*, 4*R*) *aepone*-PNA

4.4.4 Cleavage of the PNA oligomers from the solid support

The cleavage of peptides from the Merrifield resin by strong acids like trifluoromethane sulphonic acid (TFMSA)-trifluoroacetic acid (TFA) yields peptides with free carboxylic acids at their 'C' termini.[31] The synthesized PNA oligomers were cleaved from the resin using TFA-TFMSA to obtain sequences bearing *b*-alanine free carboxylic acids at their 'C' termini (Table 3 and 4 PNA **34-66**). After commencing the cleavage reaction, aliquots were removed after 30min, the peptides isolated by gel filtration using Sephadex G 25 gel matrix (see in experimental section) and then analyzed by HPLC. A cleavage time of ~ 2h at room temperature was found to be optimum for complete deprotection cleavage. The exocyclic amino groups of cytosine protected as benzyloxycarbonyl, was also cleaved during this process. When the N^6-exocyclic amino group of adenine is protected as a benzoyl group, deprotection is carried out under alkaline conditions employing ammonia or *N*-methylamine with MeOH (1:4) or ethylenediamine

with ethanol (1:4) at room temperature in 5-12 hr (depends upon no of incorporated protected adenine unit). These conditions sometimes lead to degradation of the peptide by successive 'N'-terminal cleavage. The relatively milder condition for deprotection was optimized involving treatment with N-methylamine in MeOH (1:4) at room temperature for 5 hr. This protocol was followed for oligomers containing N^6-benzoyl adenine *aepone/aep* monomeric units and was carried out prior to their cleavage with TFMSA-TFA.

Table 3: Polypyrimidine oligomer

PNA	Sequence Composition	Modified PNA
34	H_2N–T–T–T–T–T–T–T–T-*b*-ala	*aeg*-(Control)
35	H_2N–T–T–T–T–t–T–T–T-*b*-ala	one (2*S*,4*S*)-*aepone*-PNA
36	H_2N–t–T–T–T–T–T–T–T-*b*-ala	one (2*S*,4*S*)-*aepone*-PNA
37	H_2N–T–T–T-t-T–T–T-t-*b*-ala	two (2*S*,4*S*)-*aepone* PNA
38	H_2N-t-t-t-t-t-t-t-t-*b*-ala	homo oligo of 8 (2S,4*S*) *aepone*-PNA
39	H_2N-t-t-t-t-t-t-t-t-*b*-ala	homo oligo of 8 (2*S*,4*S*) *aep*-PNA
40	H_2N-T-T-t-T-T-t-T-T-*b*-ala	two (2S,4*R*)-*aep*-PNA
41	H_2N-T-T-t-T-T-t-T-T-*b*-ala	two (2*S*,4*S*)-*aepone*- PNA
42	H_2N-T-T-t-T-T-t-T-T-*b*-ala	two (2S,4*R*)-*aepone*-PNA
43	H_2N-T-T-t-T-T-t-T-T-*b*-ala	two -(2*S*,4*S*)-*aep*-PNA
44	H_2N–T–T–T–t–T–T–T-T-*b*-ala	one (2*S*,4*R*)-*aepone*-PNA
45	H_2N–t–T–T–T–T–T–T-*b*-ala	one-(2*S*,4*R*)*aepone*-PNA
46	H_2N–T–T–T–t–T–T–T-t-*b*-ala	two (2*S*,4*R*)-*aepone*-PNA
47	H_2N–T–t–T–T–T–T–T–T-*b*-ala	one (2*S*,4*S*)*aep*-PNA
48	H_2N–T–t–T–T–T–T–T–T-*b*-ala	one (2*S*,4*S*)-*aepone*-PNA
49	H_2N–T–t–T–T–T–T–T–T-*b*-ala	one (2*S*,4*R*)-*aep*-PNA
50	H_2N–T–t–T–T–T–T–T–T-*b*-ala	one (2*S*,4*R*) *aepone*-PNA
	Mixed Base PNA Comprising A, T, G, C	
51	H_2N-G-T-A-G-A-T-C-A-C-T-*b*-ala	*aeg*-(Control) -PNA
52	H_2N-g-T-A-G-A-T-C-A-C-T-*b*-ala	one (2*S*,4*S*)-*aep*-PNA
53	H_2N-g-T-A-G-A-T-C-A-C-T-*b*-ala	one (2*S*,4*S*)-a*epone*-PNA
54	H_2N-g-T-A-G-A-T-C-A-C-T-β-ala	one (2*S*,4*R*)-a*ep*-PNA
55	N_2H-G-T-A-G-A-T-C-A-c-T-β-ala	one (2*S*,4*S*)-*aepone*-PNA
56	N_2H-G-T-A-G-A-T-C-A-c-T-*b*-ala	one (2*S*,4*R*)-*aepone*-PNA
57	H_2N -G-t-A-G-A-T-C-A-C-T-*b*-ala	one (2*S*,4*R*)-*aepone*-PNA
58	H_2N -G-T-A-G-A-t-C-A-C-t-*b*-ala	two (2*S*,4*R*)-*aepone*-PNA
59	H_2N-G-T-A-G-A-t-C-A-C-T--*b*-ala	one (2*S*,4S)-*aep*-PNA
60	H_2N-G-T-A-G-A-t-C-A-C-T--β-ala	one (2S,4*R*) *aep*-PNA
61	H_2N-G-T-A-G-A-t-C-A-C-T-*b*-ala	one (2*S*, 4*S*)-*aepone* -PNA
62	H_2N-G-T-A-G-A-t-C-A-C-T-*b*-ala	one (2*S*, 4*R*)-*aepone*-PNA
63	H_2N-G-T-A-G-A-T-C-a-C-T-*b*-ala	one (2S,4*S*)-*aep*-PNA
64	H_2N-G-T-A-G-A-T-C-a-C-T-*b*-ala	one (2S,4*R*)-*aep*-PNA
65	H_2N-G-T-A-G-A-T-C-a-C-T-*b*-ala	one (2*S*, 4*S*) *aepone*-PNA
66	H_2N-G-T-A-G-A-T-C-a-C-T-*b*-ala	one (2*S*, 4*R*) *aepone*-PNA

4.4.5 Purification of the PNA oligomers

All the cleaved oligomers were subjected to initial gel filtration to remove small molecule impurities. These were subsequently purified by reverse phase HPLC (high pressure liquid chromatography)[30] on a semi-preparative C8 RP column by gradient elution using an acetonitrile in water or by isocratic elution in 10% acetonitrile-water on a semi- preparative HPLC RP C4 column. In some cases, HPLC did not produce a clean single peak profile. Hence, the sample was heated at ~80 ^{o}C for 4-5 min to destroy any secondary structure that might exist before injection. PNA oligomers containing many *aep*-PNA units carry multiple positive charges due to protonation and these were suspended in buffer containing 0.1%TFA and allowed to stand for 2-3h prior to injection. The purity of the oligomers was then checked by reverse phase HPLC on a C18 RP column and confirmed by MALDI-TOF mass spectroscopic analysis.[31] Some representative HPLC profiles and mass spectra are shown in appendix of this chapter. The purified PNA **34-66** sequences obtained are listed in Table 3.

4.4.6 Synthesis of complementary DNA oligonucleotides

The oligodeoxynucleotides (Table 4, DNA **67-72**) required to form PNA-DNA hybrids were synthesized on an automated DNA synthesizer using the standard *b*-cyanoethyl phosphoramidite chemistry.[32] The oligomers were synthesized in the 3' ? 5' direction on a CPG solid support, followed by ammonia treatment. The oligonucleotides were de-salted by gel filtration and their purity ascertained by RP HPLC on a C18 column

Table 4: DNA Oligonucleotide Sequences

DNA	Oligomer Sequences (5' ® 3')	
	For the Homopyrimidine PNA Sequences	
67	G C A A A A A A A A C G	complementary to PNA-T_8 **34-50** with CG clamps
68	G C A A A T A A A A C G	one mismatch DNA for PNAs **34-50**
69	G C A A T A A T A A C G	two mismatch DNA for PNAs **34-50**
70	Poly r(A)	complementary to PNA-T_8 **34-50**
	For Mixed Base PNA Sequences Comprising A, T, G & C Bases	
71	A G T G A T C T A C	antiparallel DNA to PNAs **51-66**
72	C A T C T A G T G A	parallel DNA to PNAs **51-66**

was found to be more than 98%. The DNAs were used without further purification in the biophysical studies.

4.5 RESULT: HYBRIDIZATION STUDIES OF *aepone*- AND *aep*-PNA WITH DNA/RNA

In the present Chapter, studies on PNA-DNA interactions investigated by UV and CD spectroscopic techniques are presented with discussion on the effect of PNA modification on duplex/triplex formation.

4.5.1 L-*cis*-(2*S*,4*S*)-*aepone*-PNA:DNA binding stoichiometry

The UV and CD based Jobs plots were used to find the binding stoichiometry of L-*cis*-(2*S*,4*S*)-*aepone*-PNA:DNA complexes. In UV Jobs plot experiment, the absorbance at 268 nm of differing relative molar ratios (0%-100%) of L-*cis*-(2*S*,4*S*)-*aepone*-PNA-t_8 (**38**) and DNA (**67**) were recorded, maintaining a constant total concentration of PNA and DNA. Figure 6 shows data from these experiments and it is seen that addition of DNA lead to an initial decrease in UV absorbance followed by a crossover point around 2:1 stoichiometry after which the absorbance increased again. This suggested the formation of a PNA_2: DNA complex for *aepone*-PNA (**38**) with DNA (**67**).

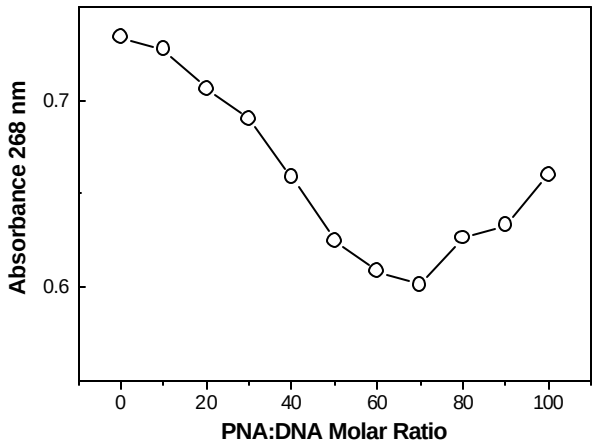

Figure 6: Job's plot for *aepone*-PNA **38**: DNA **67**, indicating 2:1 binding.

A similar CD-Jobs plot[32] was performed to determine the binding stoichiometry of PNA:DNA. In this experiment, the ellipticity of different molar ratios (0%-100%) of L-*cis*-(2*S*,4*S*)-*aepone*-PNA **38** : DNA **67** was recorded at 217 nm and 248 nm by maintaining overall concentration constant (Figure 7A). Figure 7B shows the result of experiments wherein a decrease in CD-ellipticity at 248 nm and an increase CD-ellipticity at 217 nm were observed for the complex. The profile showed a breakpoint around 2:1 stoichiometry at both wavelengths 217 nm and 246 nm, confirming the formation of PNA_2:DNA triplex.

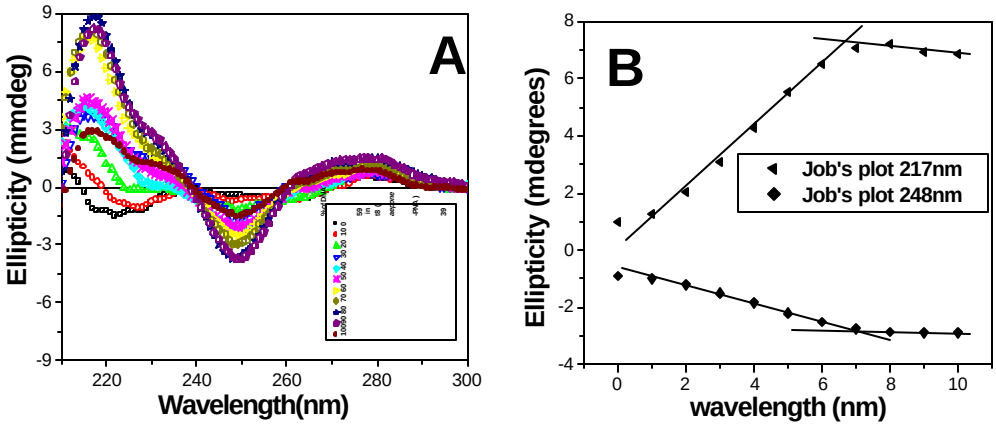

Figure 7:A. CD-spectra of *aepone*-PNA (**38**):DNA (**67**) of different molar ratio and B. CD-Job's plot of wavelength of 217 nm and 248 nm.

4.5.2 PNA_2:DNA Triplexes: UV-Tm studies

The single strands of PNA (**34**-**66**) showed little (<2%) change in absorbance at 260 nm upon heating from 5 to 85 ^{o}C due to self-melting which also leads to sigmoidal transition. The A_8 complementary DNA (**67**) showed a slightly higher increase in absorbance at 260nm (~3%).

4.5.3 [(L-*cis*-(2*S*,4*S*)-*aepone*-PNA)]$_2$:DNA triplexes

Table 5 shows the Tm values for triplexes (PNA **34**-**38**)$_2$:DNA **67** derived from *aeg*-PNA **34** and L-*cis*-(2*S*,4*S*)-*aepone*-PNA sequences with different degrees of

modification (**35**-**38**). Generally, the UV-Tm values obtained for PNA (**34**-**38**):DNA **67** complexes in both 1:1 & 2:1 stoichiometries were almost identical and the plots of absorbance or percent hyperchromicity at 260 nm vs temperature were sigmoidal, indicative of a two-state co-operative transition in UV-melting profiles (Figure 7A1). First derivative curves used for extraction of Tm of all complexes are also shown in (Figure 7A2). The Tm values (Table 5) of these complexes show that

(i) one L-*cis*-(2*S*,4*S*)-*aepone*-PNA-T unit incorporated in unmodified PNA **35**-**36** caused a stabilization of triplex (PNA **36**)$_2$:DNA **67** over control (PNA **34**)$_2$:DNA **67** by ΔTm = +15.9 ^{o}C (Table 5, entry 1 & 3), when present at the 'N' terminus of oligomer. In comparison, when the modification is present in the middle of the oligomer (PNA **35**)$_2$:DNA **67,** stabilization of the complex was enhanced by ΔTm = +12.6^{o}C (Table 5, entry 3).

(ii) increasing the number of L-*cis*-(2*S*,4*S*)-*aepone*-PNA units increased the stability of the triplexes [(PNA **37**)$_2$:DNA **67**, formed by two L-*cis*-(2*S*,4*S*)-*aepone*-PNA units in unmodified PNA] over control (PNA **34**)$_2$:DNA (**67**) by ΔTm= +16.1^{o}C (Table5, entry 4).

Table 5: Tm of PNA$_2$: DNA triplexes

Entry	(PNA)$_2$:DNA 67	Description of PNA	Tm (^{o}C)	DTm (^{o}C) PNA-control **34**
1	**34** H_2N–T–T–T–T–T–T–T–T-β-ala	*Aeg*-(Control)	34.8 (14)	0.0
2	1 x t_{cis}; **35** H_2N–T–T–T–T–t–T–T–T-β-ala	(2*S*,4*S*)-*aepone*	47.4 (10)	12.6
3	1 x t_{cis}; **36** H_2N–t–T–T–T–T–T–T–T-β-ala	(2*S*,4*S*)-*aepon*-	50.7 (12)	15.9
4	2 x t_{cis}; **37** H_2N–T–T–T-t-T–T–T-t-β-ala	(2*S*,4*S*)-*aepone*	50.9 (12)	16.1
5	8 x t_{cis}; **38** H_2N-t-t-t-t-t-t-t-t-β-ala	(2*S*,4*S*)-*aepone*	53.3 (10)	18.5
6	8 x t_{cis}; **39** H_2N-t-t-t-t-t-t-t-t-β-ala	(2*S*,4*S*)-*aep*	>80^{o}C	-
7	1 x t_{trans}; **44** H_2N–T–T–T–t–T–T–T-T-β-ala	(2*S*,4*R*)-*aepone*	45.2	10.7
8	1 x t_{trans}; **45** H_2N–t–T–T–T–T–T–T-β-ala	(2*S*,4*R*)-*aepone*	52.2	17.7
9	2 x t_{trans}; **46** H_2N–T–T–T–t–T–T–T-t-β-ala	(2*S*,4*R*)-*aepone*	60.1	25.6
10	1 x t_{cis}; **48** H_2N–T–t–T–T–T–T–T–T-β-ala	(2*S*,4*S*)-*aepone*	41.2	6.7
11	1 x t_{trans}; **50** H_2N–T–t–T–T–T–T–T–T-β-ala	(2*S*,4*R*)-*aepone*	40.3	5.8
12	2 x t_{cis}; **41** H_2N-T-T-t-T-T-t-T-T-β-ala	(2*S*,4*S*)-*aepone*	59.0	14.5
13	2 x t_{trans}; **42** H_2N-T-T-t-T-T-t-T-T-β-ala	(2*S*,4*R*)-*aepone*	59.5	15.0

**Buffer:10 mM Sodium Phosphate, 100mM NaCl, 0.1% EDTA The values quoted are average of three experiments and are accurate to ±.5oC. Values in bracket indicate % hyperchromicities*

(iii) the UV-melting plots of the (PNA **38**)$_2$:DNA **67** complexes formed by fully modified oligomer of L-*cis*-(2*S*,4*S*)-*aepone*-PNA **38** also indicated the stabilization of this triplex over the control triplex (PNA **34**)$_2$:DNA **67** by ΔTm = +18.5 ^{o}C (Table 5, entry 5).

4.5.4 L-*trans*-(2*S*,4*R*)-*aepone*-PNA and DNA triplexes

In view of the above encouraging results of *aepone* modified PNAs with different stereochemistry at C4 of *aepone*-PNA were studied. Figures 8B1 and 8B2 show the melting profiles and their derivative curves of triplexes (PNA **44-46**)$_2$:DNA **67** formed by one and two units of L-*trans*-(2*S*,4*R*)-*aepone*-PNA-T incorporated into PNA at different positions. The Tm of these triplexes (PNA **44-46**)$_2$:DNA **67** are given in Table 5 and the results indicate that these triplexes are also stabilized like *cis*-(2*S*,4*S*)-*aepone,* over the control triplex (PNA **34**)$_2$:DNA **67** (i) by ΔTm = +10.7 ^{o}C (Table 6, entry 7) for one modification in middle, (ii) by ΔTm = +17.7 ^{o}C (Table 6, entry 8) for one modification at *N*-terminus (PNA **45)** and (iii) by ΔTm = 25.6 ^{o}C (Table 6, entry 9) for two modifications as in PNA **46**.

4.5.5 Comparison between L-*cis*-(2*S*,4*S*)- and L-*trans*-(2*S*,4*R*)-*aepone*-PNA

For systematic comparative study between L-*cis*- and *L-trans*-(2*S*,4*S/R*)-*aepone*-PNA-T oligomers with DNA **67,** the PNAs **41/42/48/50** were designed by incorporation of one and two units of both L-*cis*- and *L-trans*-(2*S*,4*S/R*)-*aepone*-PNA-T in unmodified PNA. Figure 8C1 *and* Figure 82 show melting profiles and derivative curves of triplexes having modifications of L-*cis*- *and L-trans*-(2*S*,4*S/R*)-*aepone*-PNA-T at N-terminus in triplexes (PNA **48/50**)$_2$**:**DNA **67** respectively and their melting profiles are given in (Table 5; entry 10 & 11). The results indicate that their binding affinity with complementary DNA are almost equal and stabilized over control triplexes (PNA **34**)$_2$:DNA **67** by ΔTm ~ 5.8-6.7 (Table 5 entry 12 & 13). Figure 8D1 and Figure 8D2 show melting profiles and

derivative curves respectively of triplexes (PNA **41/42**)$_2$**:**DNA **67** containing two modifications of L-*cis*- *and L-trans*-(2*S*,4*S/R*)-*aepone*-PNA-T, and their melting temperatures are given in Table 5 (entry 3 & 4). The data indicates that they are also equally stabilized over control triplexes (PNA**34**)$_2$:DNA **67** , but by a higher magnitude of ΔTm ~14-15 ºC (Table 5, entry 12 & 13) compared to single substituted *aepone* PNAs.

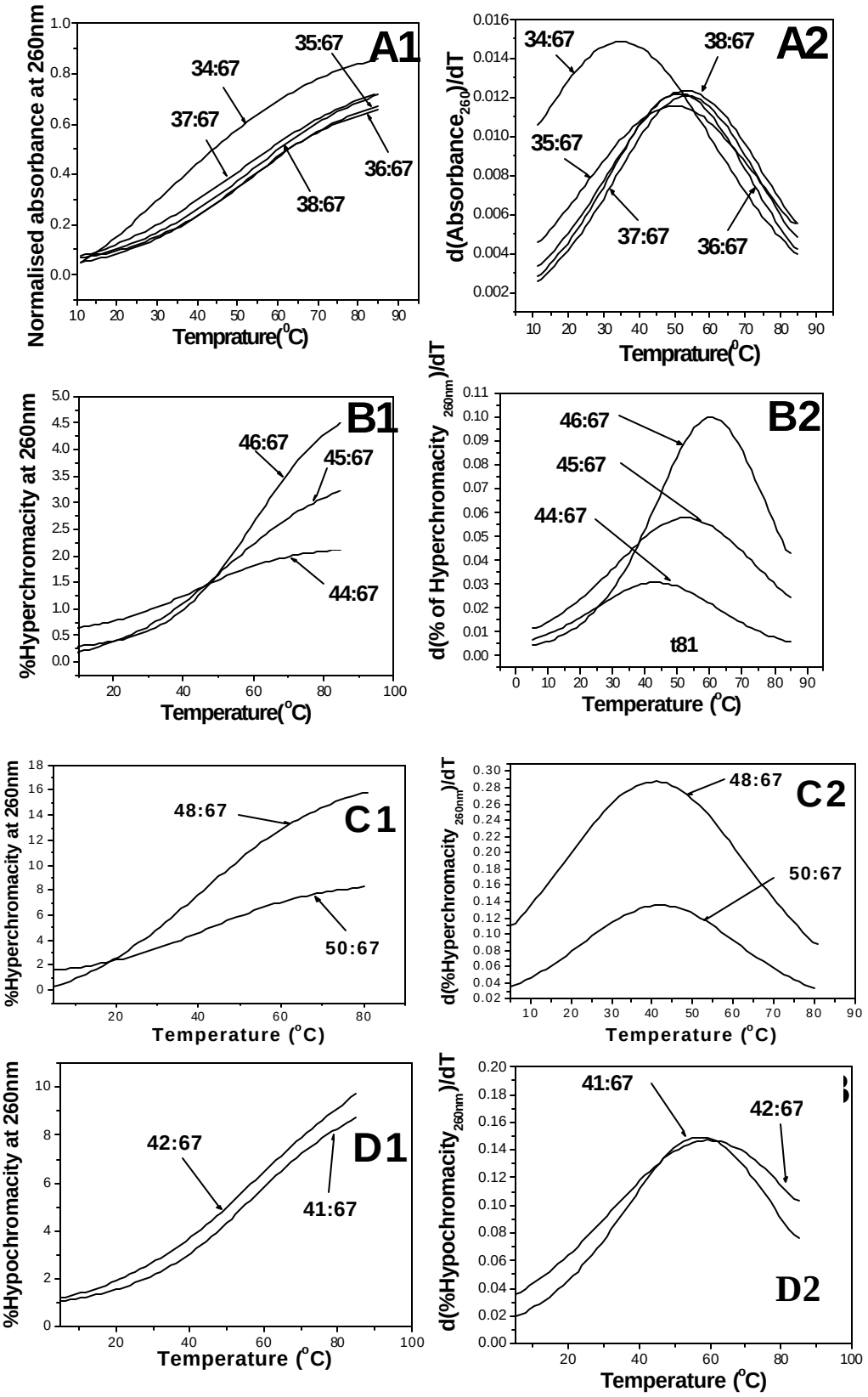

Figure 8: UV-melting profile PNA **51**, **65** and **66** with DNA **71-72** and their derivatives curve

4.5.6 [(L-*cis*-(2*S*,4*S*)-*aepone*-PNA)]$_2$:RNA triplexes

Unmodified *aeg*-PNA binds to DNA and RNA equally well without appreciable selectivity among these nucleic acids. To see if there is any binding selectivity for *aepone*-PNA between DNA and RNA, (PNA **34**-**38**)$_2$:poly r(A) (RNA **70**) complexes were constituted from *aeg*-PNA-T$_8$ **34,** mixed backbone *aeg*-/*aepone*-PNA (**35**-**37**) and homooligomer L-*cis*-(2*S*,4*S*)-*aepone*-PNA (**38**) with RNA **70**. The melting profiles of these complexes and their derivative curves are given in Figure 9. Tm values derived from various *aeg*-PNA and L-*cis*-(2*S*,4*S*)-*aepone*-PNA sequences with different degrees of modifications are in listed in Table 6.

(i) Single modification of L-*cis*-(2*S*,4*S*)-*aepone*-PNA in the middle induced destabilization of (PNA **35**)$_2$:RNA **70** complex over the control triplex (PNA **34**)$_2$:RNA **70** by ΔTm = -15.9 ^{o}C (Table 6, entry 2).

(ii) Single modification of L-*cis*-(2*S*,4*S*)-*aepone*-PNA at N-terminus in PNA caused a destabilization of triplex (PNA **36**)$_2$:RNA **70** over the control (PNA **34**)$_2$:RNA **70** by ΔTm = -17.8 ^{o}C (Table 6, entry 1 and 3).

Table 6: Tm of (PNA)$_2$: poly r(A) triplexes

Entry	(PNA)$_2$: poly r(A) 70	Description of PNA	Tm (^{o}C)	DTm (^{o}C) PNA-control 34
1	**34** H_2N–T–T–T–T–T–T–T–T-*b*-ala	*Aeg*-(Control)	58.0 (39)	0.0
2	1 x $t_{cis;}$ **35** H_2N–T–T–T–T–t–T–T–T-*b*-ala	(2*S*,4*S*)-*aepone*	43.1 (19)	-15.9
3	1 x $t_{cis;}$ **36** H_2N–t–T–T–T–T–T–T–T-*b*-ala	(2*S*,4*S*)-*aepone*	41.2 (27)	-17.8
4	2 x $t_{cis;}$ **37** H_2N–T–T–T-t-T–T–T-t-*b*-ala	(2*S*,4*S*)-*aepone*	41.8 (14)	-17.2
5	8 x $t_{cis;}$ **38** H_2N-t-t-t-t-t-t-t-t-*b*-ala	(2S,4S)-*aepone*	45.6 (8)	-13.4
6	8 x $t_{cis;}$ **39** H_2N-t-t-t-t-t-t-t-t-*b*-ala	(2*S*,4*S*)-*aep*	35.1	-22.9

**Buffer: 10 mM Sodium Phosphate, 100 mM NaCl, 0.1% EDTA. The values quoted are average of three experiments and are accurate to ±5^{o}C. Values in bracket indicate % hyperchromicities*

(iii) Increasing the number of L-*cis*-(2*S*,4*S*)-*aepone*-PNA units to two also destabilized the derived triplex (PNA **37**)$_2$: RNA **70**, over control (PNA **34**)$_2$: RNA **70** by ΔTm = -17.2 ^{o}C (Table 6, entry 4).

(iv) the triplex of the homooligomer of L-*cis*-(2*S*,4*S*)-*aepone*-PNA-T (PNA **38**)$_2$:RNA **70** also indicated destabilization of over control triplexes (PNA **34**)$_2$: RNA **70** by ΔTm = -13.4 ^{o}C (Table 6, entry 5).

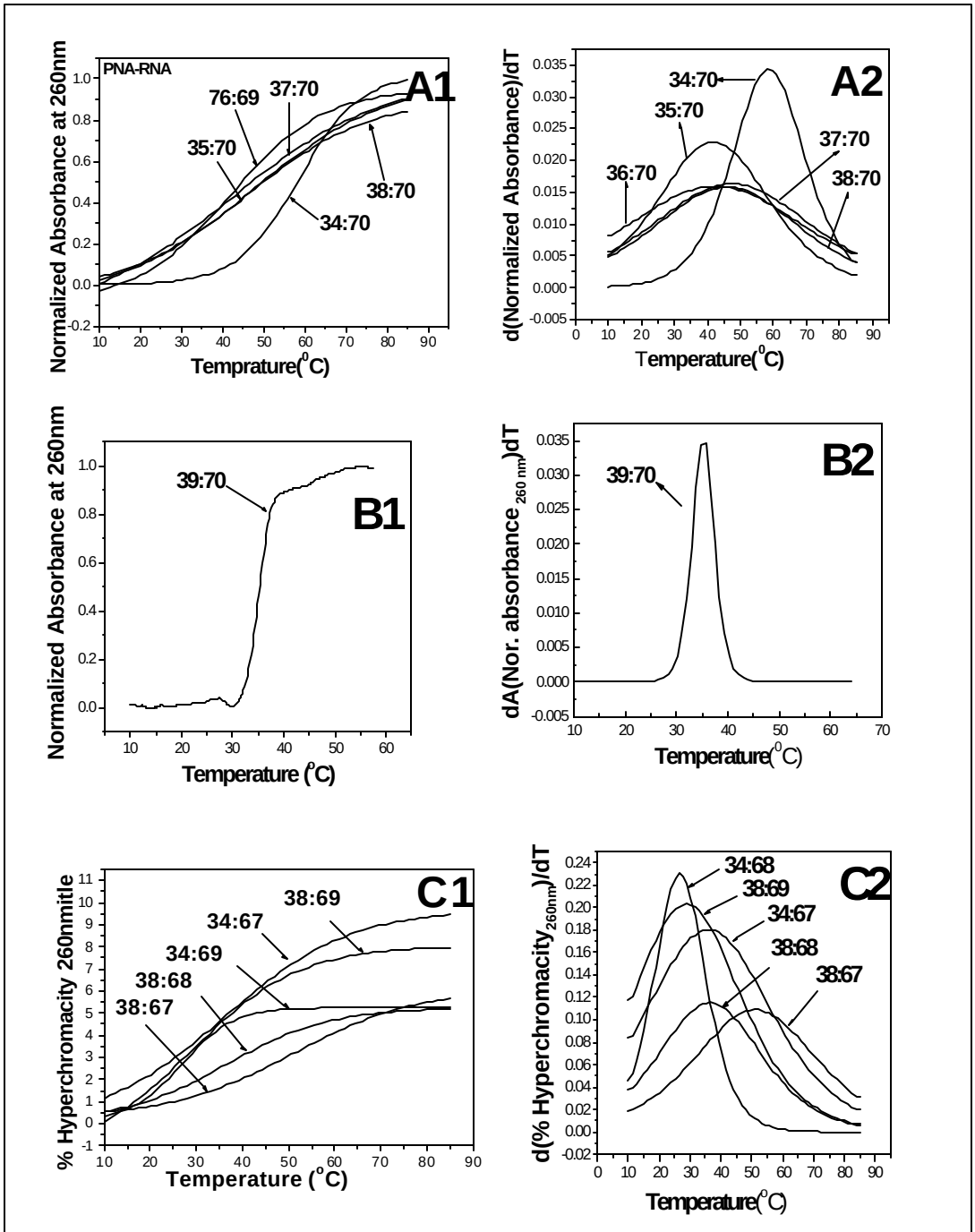

Figure 9: UV-melting profiles (left) and their corresponding 1st derivative curves (right) of *aep*-PNA (**34**-**38**)$_2$: RNA **70** as triplexes. UV-melting profile DNA: RNA *Left*: UV-melting and *right*: derivative curve of PNA **38** with one thymine mismatch DNA **68** and two thymine mismatch DNA **69**

4.5.7 L-*cis*-(2*S*,4*S*)-*aep*-PNA and RNA triplexes

To delineate the contribution of C5-carbonyl group in influencing the binding selectivity of modified PNA among DNA and RNA, the triplexes *aep*-PNA (39):poly r(A) and L-*cis*-(2*S*,4*S*)-*aep*-PNA-T_8 (**39**) lacking C5 carbonyl in PNA was subjected for UV-melting studies. The results were compared with that of *aepone*-PNA complex (L-*cis*-(2*S*,4*S*)-*aepone*-PNA **38**):poly r(A). The melting profiles and their derivative curves of triplexes (PNA **39**)$_2$:RNA **70** are shown in Figure 9 and the Tm values given in Table 6. It is seen that this complex was destabilized over control (PNA **34**)$_2$:(RNA **67)** by ΔTm = -22.9 ^{o}C and also destabilized the RNA hybrid (PNA **39**)$_2$:RNA **70** of fully modified *aepone*-PNA by ΔTm = -10.5 ^{o}C.

4.5.8 Mismatch studies of PNA with DNA

The complexes of PNAs **34** and **38** were constituted with DNA **68** containing one mismatch base and DNA **69** with two mismatch bases (Figure 10) and the melting profiles are given in Figure 9. The Tm values (Table 7) indicate that fully modified *aepone*-PNA (**34**) complex with mismatch DNAs **68** and **69** decrease by 15.0 ^{o}C and 24.1 ^{o}C respectively**,** while the Tm of unmodified *aeg*-PNA with DNA **68** having one mismatch decreases by 9.1 ^{o}C. Two mismatches in DNA further destabilized the derived triplexes.

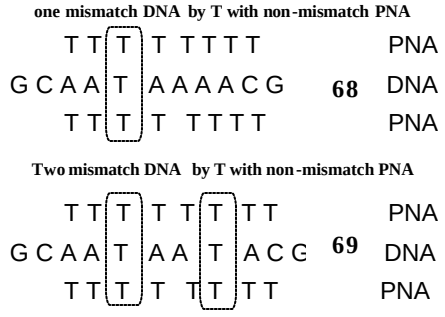

Figure 10: One and two mismatch DNA with non-mismatch triplexes complexes

Table 7: Tm values of PNA with complementary mismatch DNA*

Entry	$(PNA)_2$:DNA	Tm	D Tm (A-B)[a]
1	**34** (H_2N–T–T–T-T-T–T–T-T-*b*-ala):DNA **67** (complementary)	38.1	-
2	**34** (H_2N–T–T–T-T-T–T–T-T-*b*-ala):DNA **68** (one mismatch)	27.2	9.1
3	**38** (H_2N-t-t-t-t-t-t-t-t-*b*-ala):DNA **67** (complementary)	53.5	-
4	**38** (H_2N-t-t-t-t-t-t-t-t-*b*-ala):DNA **68** (one mismatch)	38.5	15.0
5	**38** (H_2N-t-t-t-t-t-t-t-t-*b*-ala):**69** (two mismatch)	29.4	24.1

t= *L-cis*-(2S,4*S*)-*aepone*-PNA

[a]*A: non-mismatch; B: Mismatch*

**Buffer: 10 mM Sodium Phosphate, 100mM NaCl, 0.1% EDTA. The values quoted are average of three experiments and are accurate to* $\pm.5^{o}C$.

Thus *aepone*-PNA modifications induce higher destabilization of mismatches compared to unmodified PNA and this suggests a greater discrimination of DNA mismatches by *aepone*-PNAs.

4.5.9 UV-Tm Studies in PNA:DNA duplexes

The oligothymine sequences described above form triplexes in which the binding orientation (parallel-antiparallel) of the two PNA strands involved in complex formation remains indistinguishable. Mixed purine-pyrimidine sequences exclusively form PNA:DNA duplexes. The effect of *aepone*-PNA modifications in duplexes were hence examined and these studies also permit investigatation of the orientational preferences (parallel/antiparallel) induced by chiral *aepone* units in binding complementary DNA.

4.5.10 (*aepone*-PNA):DNA duplexes

Modified L-*cis/trans-aepone*-PNA unit incorporated into mixed PNA sequences (PNA **57/58/65/67)** were targeted to bind complementary antiparallel DNA **71** and parallel DNA **72** to constitute both types duplexes. For comparison, unmodified PNA **51** was used**.**

4.5.10a Antiparallel (aepone-PNA:DNA) duplex

(*aepone*-PNA):DNA The melting profiles (Figure 11A1) and derivative curves (Figure11A2) for *antiparallel* duplexes L-*cis*-*aepone*-PNA **57:**DNA **71** and L-*cis*-*aepone*

PNA **58:**DNA**71** formed by one and two modifications respectively (Figure 10C and 10C2) were used to derive the Tm values of duplexes given in Table 8. The data indicate that duplex 1 x *aepone*PNA **57:**DNA **71** is stable over control duplex of unmodified PNA **51:**DNA**71** by ΔTm = +14.1 (Table 8, entry 2) formed by fully unmodified PNA **51** with DNA **71.** The Tm value of the duplex 2 x *aepone*PNA **58:**DNA **71** formed by incorporation of two modifications of L-*cis*-(2*S*,4*S*)-*aepone*-PNA-T are more stabilized over control duplex by ΔTm = +25.1 (Table 8, entry 3).

Table 8: Tm value *parallel and antiparallel* duplexes of PNA:DNA*

Entry	PNA	Tm (°C) DNA71 (ap)	Tm (°C) DNA 72 (p)	ap-p	DTm (°C) *ap-p*
1	**51** H_2N-G-T-A-G-A-T-C-A-C-T-*b*-ala	45.9	40.0	ap > p	5.9
2	1 x t_{cis} **57** H_2N -G-t-A-G-A-T-C-A-C-T-*b*-ala	60.4	36.2	ap > p	24.2
3	2x t_{cis} **58** H_2N-G-T-A-G-A-t-C-A-C-t-*b*-ala	71.0	28.3	ap > p	42.7
4	1x a_{cis} **65** H_2N-G-T-A-G-A-T-C-a-C-T-*b*-ala	58.6	44.0	ap > p	14.6
5	1x a_{trans} **66** H_2N-G-T-A-G-A-T-C-a-C-T-*b*-ala	51.9	39.1	ap > p	12.8

**cis*: (2S,4S); trans: (2S,4R); ap: antiparllel; p: parallel; Buffer:*10 mM Sodium Phosphate,100 mM NaCl, 0.1% EDTA*. The values quoted are average of three experiments and are accurate to ±5oC.

4.5.10b Parallel (aepone-PNA:DNA) duplex

(*aepone*-PNA):DNA: Figure11B shows melting profiles (Figure11B1) and derivative curves (Figure11B2) of *parallel* duplexes L-*cis*-*aepone*-PNA **57:**DNA **72** and L-*cis*-*aepone*-PNA **58:**DNA **72**. The Tm values are given in Table 8 (entry, 2 and 3) which indicate that the parallel duplex 1 x *aepone*PNA **57:**DNA **72** was destabilized with respect to parallel duplex of control PNA **51:**DNA**72** by ΔTm = -3.8 ^{o}C**.** The parallel duplex formed by two modifications of L-*cis*-(2*S*,4*S*)-*aepone*-PNA-T as in PNA **58:**DNA **72** was further destabilized over control parallel duplex PNA **51:**DNA**72** by ΔTm = -11.7 ^{o}C.

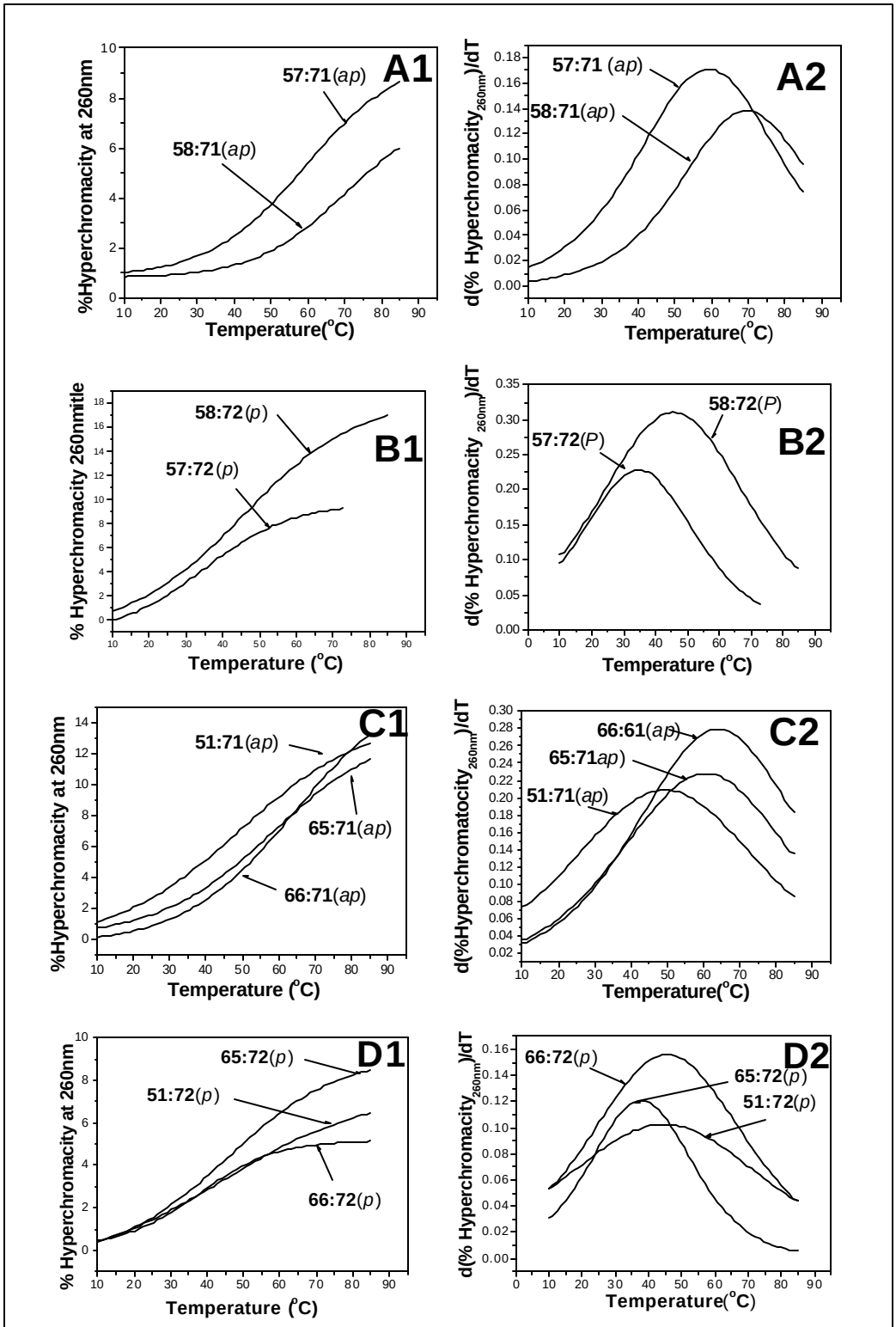

Figure 11: UV-melting profile PNA **51**, **65** and **66** with DNA **71-72** and their derivatives curve

4.5.10c Parallel vs Antiparallel

Tm values of (Table 8) indicate that antiparallel duplex formed by incorporation of L-*cis*-(2*S*,4*R*)-*aepone*PNA-T (PNA **51**)are significantly stabilized over that of parallel duplex by ΔTm = +24.2 ^{o}C for one modifiation and ΔTm = +42.7 ^{o}C for two modifications in L-*cis*-(2*S*,4*R*)-*aepone*PNA-T (PNA **57**). The Tm value also indicated stabilization of antiparallel duplex of L-*cis*-(2*S*,4*R*)-*aepone*-PNA-A (PNA **66**) over the corresponding parallel duplex by ΔTm = +14.6 ^{o}C for one modification and ΔTm = +12.8 ^{o}C for two modifications in (PNA **57**) of over parallel duplex.

4.5.11 Comparison of duplex stability between L-*cis*-(2*S*,4*S*)- and L-*trans*-(2*S*,4*R*)-*aepone*-PNA

The effect of stereochemistry at C4 of prolyl ring on DNA hybridization in *aepone*-PNAs **63** and **65** was studied with complementary DNAs **71** and **72** in both anti-parallel and parallel duplexes.

4.5.11a Comparison between antiparallel duplexes

The Figure 11C1 shows the melting profiles and derivative curves (Figure 11C2) of *antiparallel* duplexes L-*cis*-(2*S*,4*S*)-*aepone*-PNA-A **65:**DNA **71** and L-*cis*-(2*S*,4*S*)-*aepone*PNA-A **66:**DNA **71** formed by of incorporation of one modifications in mix sequence of unmodified decamer. The Tm values of these duplexes along with control duplex shown in Table 8 (entry 1-5), indicates that duplexes from both PNAs having L-*cis*-(2*S*,4*S*)-*aepone*-A (PNA **65**) and L-*trans*-(2*S*,4*R*)-*aepone*-A (PNA **66**) modifications are stabilized over the duplexes formed by control (PNA **51:**DNA**71**) by ΔTm = +12.7 ^{o}C (Table 8, entry 4-entry1) and 16.0 ^{o}C for L-*trans*-*aepone*-PNA-T (Table 8, entry 5-entry1) respectively.

4.5.11b Comparison between parallel duplexes

Figure 11D1 and 10D2 are the melting profiles and derivative curves of *parallel* duplexes (PNA **65/66**):(DNA **72)** formed by PNA **66/67** with DNA **72** have exhibited respectively and their Tm values are given in Table 8. The Tm values of these duplexes indicate that duplex with 1 x L-*cis*-(2*S*,4*S*)-*aepone*-A PNA **65:**DNA **72** is slightly stabilized over unmodified PNA duplex PNA **51:**DNA **72** by ΔTm = +4.0 ^{o}C. The duplex of 1 x L *trans*-(2*S*,4*S*)-*aepone*-PNA-A PNA **66:**DNA **72** is not stabilized to that extent over control duplex PNA **51:**DNA **72** (ΔTm = +0.9 ^{o}C). Thus relative Tm values of both duplexes reveal narrow difference between L-*cis* and *trans*- *aepon*e-PNA-A.

4.5.12 *aep*-PNA and DNA triplexes

4.5.12a [L-cis-(2S,4S/R)-aep-PNA)]$_2$:DNA triplexes

For comparative study, the triplex [L-*cis*-(2*S*,4*S*)-*aep*-PNA **39**)]$_2$:DNA **67** formed by fully modified backbone PNA was studied and it was observed that the Tm value of this triplex was more than 80 ^{o}C (Table 6, entry 6).[20]

The binding affinities of L-*cis/trans-aep*-PNAs **40**, **43**, **47** and **49** with DNA **67** was measured to compare with triplexe (*aep*-PNA 34)$_2$:DNA **67**. The melting profiles and derivative curves of L-*cis*-(2*S*,4*S*)-*aep* PNA-T triplex PNA **47**$_2$**:**DNA **67** and L-*trans*-(2*S*,4*R*)-*aep*-PNA-T (PNA **49)**$_2$**:**DNA **67** are shown in Figure 12A and Figure 12A2 respectively. The Tm values of these triplexes given in Table 9, indicate that the *trans-aep* triplex (PNA **49)**$_2$**:**DNA **67** is more stable over the control triplex (PNA **34**)$_2$:DNA **67** by ΔTm ~+7.6 ^{o}C (Table 9, entry 2) while the *cis-aep* triplex (PNA **47)**$_2$**:**DNA **67** was stabler by ΔTm of only +3.3 ^{o}C (Table 9, entry 2). The triplexes PNA **40**$_2$**:**DNA **67** incorporating two *trans-aep*-PNA-T modifications and PNA **43**$_2$**:** DNA **67** with two *cis-aep*-PNA-T modifications showed enhanced stability over control PNA **34**$_2$:DNA **67** by ΔTm of +35.9

^{o}C and +18.6 ^{o}C respectively (Table 9, entry 3). The results show that triplexes formed by *trans*-(2*S*,4*R*)-*aep* PNAs are significantly more stable than triplexes from *cis*-(2*S*,4*S*)-*aep*-PNAs.

Table 9: Tm value of $(PNA)_2$:DNA triplex*

Entry	$(PNA)_2$:DNA 67		Tm (^{o}C)	DTm (^{o}C) (PNA-Control)
1	1x t; **47** H_2N–T–t–T–T–T–T–T–T–T-*b*-ala	(2*S*,4*S*)-*aep*-PNA	39.1	+4.3
2	1x t; **49** H_2N–T–t–T–T–T–T–T–T–T-*b*-ala	(2*S*,4*R*)-*aep*-PNA	42.4	+7.6
2	2x t; **40** H_2N-T-T-t-T-T-t-T-T- *b*-ala	(2*S*,4*R*)-*aep*-PNA	60.7	+35.9
4	2x t; **43** H_2N-T-T-t-T-T-t-T-T- *b*-ala	(2*S*,4*S*)-*aep*-PNA	53.4	+18.6

**Buffer: 10 mM Sodium Phosphate, 100mM NaCl, 0.1% EDTA. The values quoted are average of three experiments and are accurate to ±.5^{o}C.*

4.5.13 *aep*-PNA and DNA duplexes

A comparative study of *aepone*-PNA:DNA duplexes, with same sequences of *aep* PNA (**63** and **64**) were made to study as parallel and antiparallel duplexes with complementary DNA **71** and DNA **72** respectively.

4.5.13a Antiparallel (aep-PNA:DNA) duplexes

The melting profiles and corresponding derivative curves of *antiparallel* duplex of L-*cis/trans*-(2*S*,4*S*/*R*)-PNA-A (PNA **63/64**):DNA **71** are shown in Figure 12C1 and 12C2 respectively. The Tm values of the duplexes are given in Table 10, which indicate that the duplex L-*cis*-*aep*-PNA **63**:DNA **71** is remarkably stabilized over control duplex PNA **51:**DNA **71** by ΔTm = +18.8 ^{o}C (Table 10, entry 1) and L-*trans*-*aep*-PNA duplex **64:**DNA **71** is stabilized over control duplex by ΔTm = +15.4 ^{o}C (Table 10, entry 2).

Table 10: Tm data for the (2*S*,4*R*/*S*)-*aepone-and aep*-PNA mixed base PNA:DNA duplexes*

Entry	PNA	Tm (^{o}C) DNA 71	Tm (^{o}C) DNA 72	*ap-p*	DTm(^{o}C) *ap-p*
1	1 x $a_{cis;}$ **63** H_2N-G-T-A-G-A-T-C-a-C-T-*b*-ala	64.7	45.2	ap > p	19.5
2	1 x $a_{trans;}$ **64** H_2N-G-T-A-G-A-T-C-a-C-T-*b*-ala	61.3	45.0	ap > p	16.3

**cis*: (2*S*,4*S*); *trans*: (2*S*,4*R*); ap: antiparallel; p: parallel; *Buffer: 10 mM Sodium Phosphate,100mM NaCl, 0.1% EDTA. The values quoted are average of three experiments and are accurate to ±.5^{o}C.*

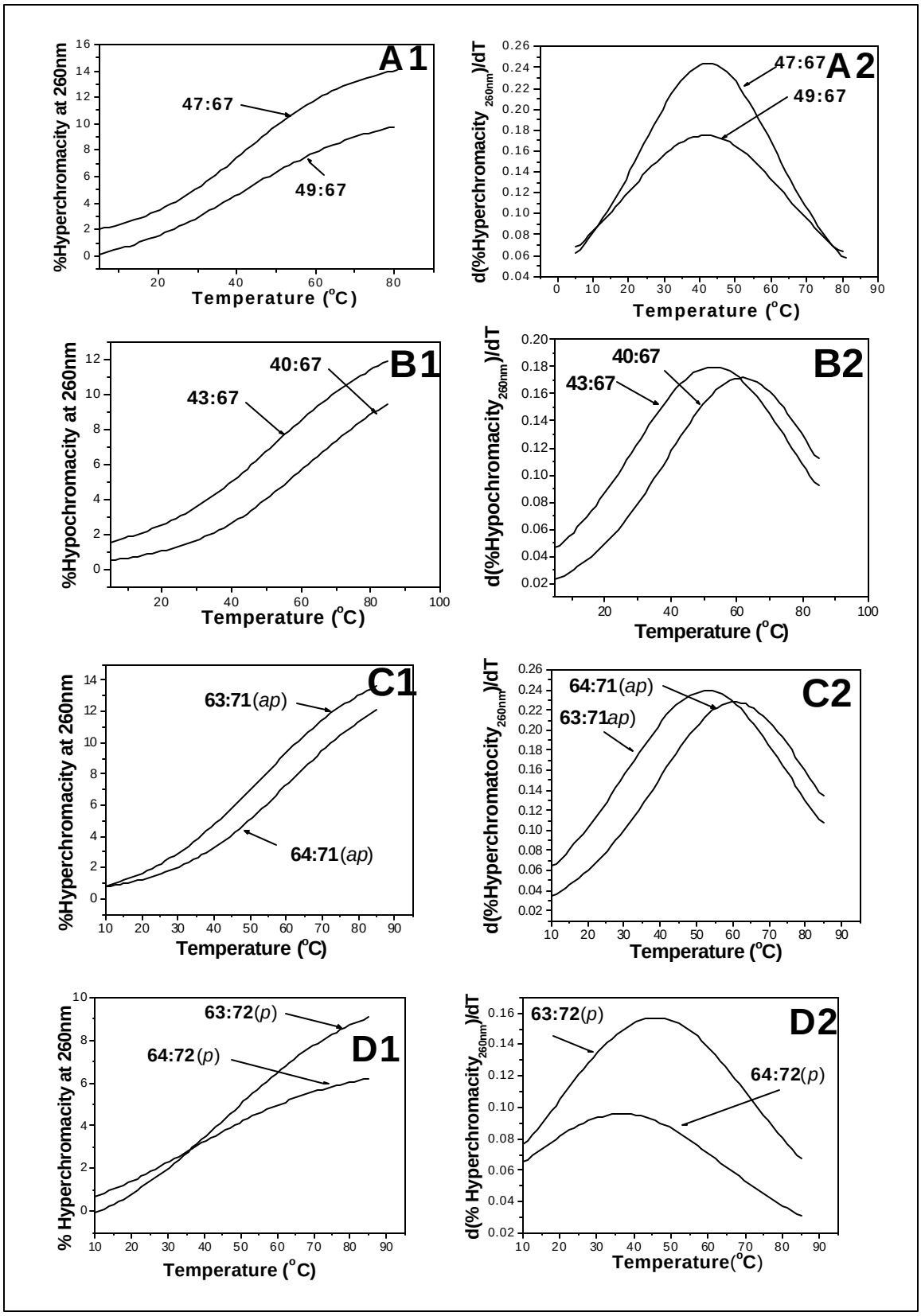

Figure 12: A and B UV-melting profiles (left) and their corresponding 1st derivative curves (right) of *aep*-PNA (**47**/**49**/**40**/**43**)$_2$:DNA **67** as triplexes. C. *aep*-PNA (**63**-**64**):DNA **71** as *antiparallel* duplexes and D. *aep*-PNA (**63**-**64**):DNA **72** as *parallel* duplexes.

4.5.13b Parallel (aep-PNA:DNA) duplexes

Figure 12D1 and 12D2 shows the melting profiles and their derivative curves for parallel duplex L-*cis/trans*-(2*S*,4*S/R*)-PNA-A **63/64**):DNA **72** respectively and the Tm values are given in Table 10. The data indicate that L-*cis*-*aep*-containing parallel duplex PNA **63:**DNA **72** is slightly stabilized over the control parallel duplex PNA **51**:DNA**72** by ΔTm = +5.2 ^{o}C for *cis*-*aep*-PNA **63** and by ΔTm = +5.0 ^{o}C for L-*trans*-*aep*PNA **64:**DNA **72**.

4.5.14 Comparison of triplex stability between *aep*- and *aepone*-PNA

Comparison between L-cis-(2S,4S)-aep- and aepone-PNA: The comparative study of triplex stability between L-*cis*-(2*S*,4*S*)-*aep*- and *aepone*-PNA$_2$:DNA was done on the basis of observed UV-Tm values from preceding Section. The Tm of triplexes formed by L-*trans*-(2*S*,4*R*)-*aep*- and *aepone*-PNA-T with DNA are summarized in Table 11, which indicate that the *aep*-PNA triplex (PNA **47**)$_2$:DNA **67** was slightly destabilized compared to corresponding *aepone*-PNA triplex (PNA **48**)$_2$:DNA **67** formed with DNA **67** by ΔTm = -2.1 ^{o}C (Table 11, entry1, 2) in *cis* series. With two modifications, the *aepone*-PNA triplex PNA **41**$_2$:DNA **67** was also more stabilized over the corresponding *aep*-PNA triplex formed (PNA **43**)$_2$:DNA **67** formed by two unit of L-*cis*-(2*S*,4*S*)-*aep*-PNA-T incorporated in unmodified by ΔTm = +6.6 ^{o}C [(Table 11, (Entry 3-Entry 4)]. Hence, stability of triplexes formed by one unit of L-*cis*-(2*S*,4*S*)-*aep*-PNA-T less stable than L-*cis*-(2*S*,4*S*)-*aepone*-PNA-T while triplexes formed by two units of L-*cis*-(2*S*,4*S*)-*aep*-PNA-T is more stable than that of two units of L-*cis*-(2*S*,4*S*)-*aepone*-PNA-T.

Table 11: Summary of Tm value of (L-***cis***-(2***S***,4***S***)-*aep*- and *aepone*-PNA)$_2$:DNA triplex

Entry	(PNA)$_2$:DNA 67	Modified PNA unit	Tm (^{o}C)	DTm (^{o}C) *aep*-*aepone*
1	**47** H_2N–T–t–T–T–T–T–T–T–T-*b*-ala	one (2*S*,4*S*)-*aep*-PNA	39.1	0.0
2	**48** H_2N–T–t–T–T–T–T–T–T–T-*b*-ala	one-(2*S*,4*S*)-*aepone*-PNA	41.2	-2.1
3	**41** H_2N-T-T-t-T-T-t-T-T-*b*-ala	two (2S,4*S*)-*aepone*- PNA	59.0	0.0
4	**43** H_2N-T-T-t-T-T-t-T-T-*b*-ala	two -(2*S*,4*S*)-*aep*-PNA	53.4	-6.6

Comparison between L-trans-(2S,4R)-aep- and aepone-PNA: The summarized Tm values (Table 12) of triplexex formed by L-*trans*-(2*S*,4*R*)-*aep*- and *aepone*-PNA-T with DNA indicates that triplex (PNA **49**)$_2$:DNA **67,** formed by one unit L-*trans*-(2*S*,4*R*)-*aep*-PNA incorporated in unmodified PNA, slightly more stable than triplex (PNA **50**)$_2$:DNA **67,** formed by single unit L-*trans*-(2*S*,4*R*)-*aepone*-PNA incorporated in unmodified PNA **50** with DNA **67** by ΔTm = +2.1 ^{o}C [(Table 12, (Entry1-Entry2)]. Almost similar result is also observed by triplexes (PNA **40**)$_2$:DNA **67** and (PNA **42**)$_2$:DNA **67** formed by two unit of L-*trans*-(2*S*,4*R*)-*aep*- and *aepone*-PNA-T incorporated in unmodified PNA respectively. The Tm values of these triplexes show that L-*trans*-(2*S*,4*R*)-*aep*-PNA-T is stable than that of L-*trans*-(2*S*,4*R*)-*aepone*-PNA-T only by ΔTm = 1.2 ^{o}C [(Table 12, (Entry 3-Entry 4)] L-*trans*-(2*S*,4*R*)-*aep*- and *aepone*-PNA-T. Therefore, stability of triplexes formed by one and two unit of L-*trans*-(2*S*,4*R*)-*aep*- and *aepone*-PNA-T in unmodified PNA are almost same.

Table 12: Summary of Tm value of **[**(L-*trans*-(2***S,4R***)-*aep*- /*aepone*-PNA)$_2$:DNA triplex

Entry	(PNA)$_2$:DNA 67		Modified PNA unit	Tm (^{o}C)	D**Tm (^{o}C)** *aep-aepone*
1	**49**	H_2N–T–t–T–T–T–T–T–T-*b*-ala	one (2*S*,4*R*)-*aep*-PNA	42.4	-
2	**50**	H_2N–T–t–T–T–T–T–T–T-*b*-ala	one (2*S*,4*R*)-*aepone*-PNA	40.3	2.1
3	**40**	H_2N-T-T-t-T-T-t-T-T-*b*-ala	two (2*S*,4*R*)-*aep*-PNA	60.7	-
4	**42**	H_2N-T-T-t-T-T-t-T-T-*b*-ala	two (2*S*,4*R*)-*aepone*-PNA	59.5	1.2

4.5.15 Comparison of duplex stability between *aepone*- and *aep*-PNA

4.5.15a Comparison of duplex stability between L-cis-(2S,4S)-aep/aepone-PNA

In Table 13, the Tm values of antiparallel duplex (PNA **63**)**:**(DNA **71**) formed by L-*cis*-(2*S*,4*S*)-*aep*-PNA-A containing unmodified PNA **63** indicate that this duplex is more stable than same kind of duplex (PNA **65**)**:**(DNA **71**) formed L-*cis*-(2*S*,4*S*)-*aep*-PNA containing PNA **65** formed by L-*cis*-(2*S*,4*S*)-*aepone*-PNA-A by ΔTm = 6.1 ^{o}C [(Table 13, (entry 1-entry 2)]. While the Tm values of parallel duplex (PNA **63**)**:**(DNA **72**), formed by

L-*cis*-(2*S*,4*S*)-*aep*-PNA-A (PNA **63**) and duplex (PNA **65**):(DNA **72**), formed by L-*cis*-(2*S*,4*S*)-*aepone*-PNA-A (PNA **65**) indicate that these duplexes are showing same almost same stability.

Table 13: Tm values of Duplexes (PNA):(DNA)*

Entry	PNA	Tm (°C) DNA 71	DTm(°C) cis-trans	Tm (°C) DNA 72	DTm (°C) cis-trans
1	1x 1x a_{cis} **63** H_2N-G-T-A-G-A-T-C-a-C-T-*b*-ala	64.7	-	45.2	-
3	1x $a_{cis\text{-}aepone}$ **65** H_2N-G-T-A-G-A-T-C-a-C-T-*b*-ala	58.6	6.1	44.0	+1.2
2	1x $a_{trans\text{-}aep}$ **64** H_2N-G-T-A-G-A-T-C-a-C-T-*b*-ala	61.3	-	45.0	-
4	1x $a_{trans\text{-}aepone}$ **66** H_2N-G-T-A-G-A-T-C-a-C-T-*b*-ala	51.9	9.4	39.1	+5.9

cis: (2*S*,4*S*); *trans*: (2*S*,4*R*);

4.5.15b Comparison duplex between L-trans-(2S,4R)-aep/aepone-PNA

In Table 13, the Tm values of antiparallel duplex (PNA **64**):(DNA **71**) formed by L-*trans*-(2*S*,4*R*)-*aep*-PNA-A containing unmodified PNA **66** indicate that this duplex is more stable than same kind of duplex (PNA **66**):(DNA **71**) formed L-*trans*-(2*S*,4*R*)-*aep*-PNA containing PNA **66** formed by L-*cis*-(2*S*,4*S*)-*aepone*-PNA-A by ΔTm = +9.4 °C [(Table 13, (entry 3-entry 4)]. While the Tm values of parallel duplex (PNA **64**):(DNA **72**), formed by L-*transs*-(2*S*,4*S*)-*aep*-PNA-A (PNA **64**) and duplex (PNA **66**):(DNA **72**), formed by L-*trans*-(2*S*,4*S*)-*aepone*-PNA-A (PNA **66**) indicate that L-*transs*-(2*S*,4*S*)-*aep* duplex (PNA **64**):(DNA **72**), also stable than L-*trans*-(2*S*,4*S*)-*aepone*-PNA duplexes (PNA **66**):(DNA **72**) by ΔTm = +5.9 °C [(Table 13, (entry 3-entry 4)].

4.5.16 Hyperchromicity observations

A useful parameter of interest is the hyperchromicity changes accompanying the melting transitions which can be measured from UV-melting curves.[34] This data suggests two ranges of hyperchromicity values for various *aepone*-PNAs, 6-9% and 9-12%. The duplexes of *aepone*-PNAs having purines generally exhibited higher hyperchromicity than

those containing pyrimidines. Same trends are also observed for *aep*-PNA. Generally, higher Tms were accompanied by larger % hyperchromicities although the hyperchromicity changes could not always be directly correlated with the thermal stabilities in some cases.

4.5.17 Circular dichorism studies

4.5.17a aepone-PNA monomers

The CD-spectra of aqueous solutions of thymine monomers of L-*cis/trans*-(2*S*,4*S*/*R*)-*aepone*-PNA **34**/**38** are shown in Figure 13. A positive ellipticity was observed at 268 nm for L-*trans*-(2*S*,4*R*)-*aepone*-PNA monomer (**38**) nm in water while a negative ellipticity was observed at wavelength 270 nm for L-*cis*-(2*S*,4*S*)-*aepone*-PNA monomer (**34**), which is almost opposite to the *trans*-monomer.

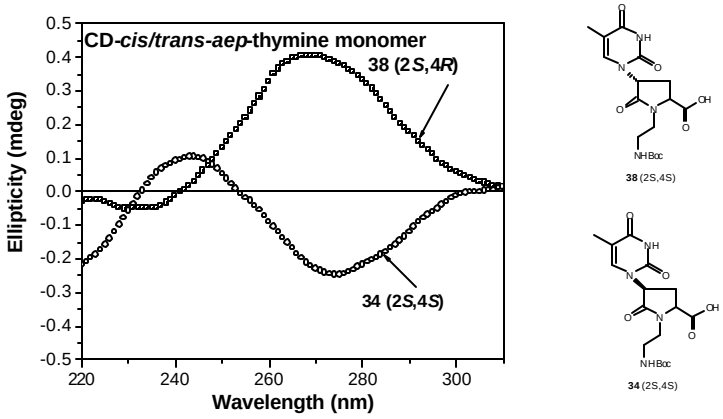

Figure 13: CD profiles L-*cis*-(2*S*,4*S*)-*aepone*-PNA thymine acid monomer **37** and L-*trans*-(2*R*,4*S*)-*aepone*-PNA thymine acid **38** monomer at 10 ^{o}C.

4.5.17b CD-studies for (aepone-PNA)$_2$:DNA triplexes

The complexation between DNA and PNA was also studied by CD-spectroscopy. The CD-spectra of single stranded PNAs (**34**-**38**), DNA **67** and the derived triplexes *(aep/aepone*-PNA-**34**-**38**)$_2$:DNA **67** scanned at 10^{o}C are shown in Figure 14. The CD

spectra of single stranded *aepone*PNAs showed a positive band in the region 220 nm with a very weak signal in 260-280 nm region.

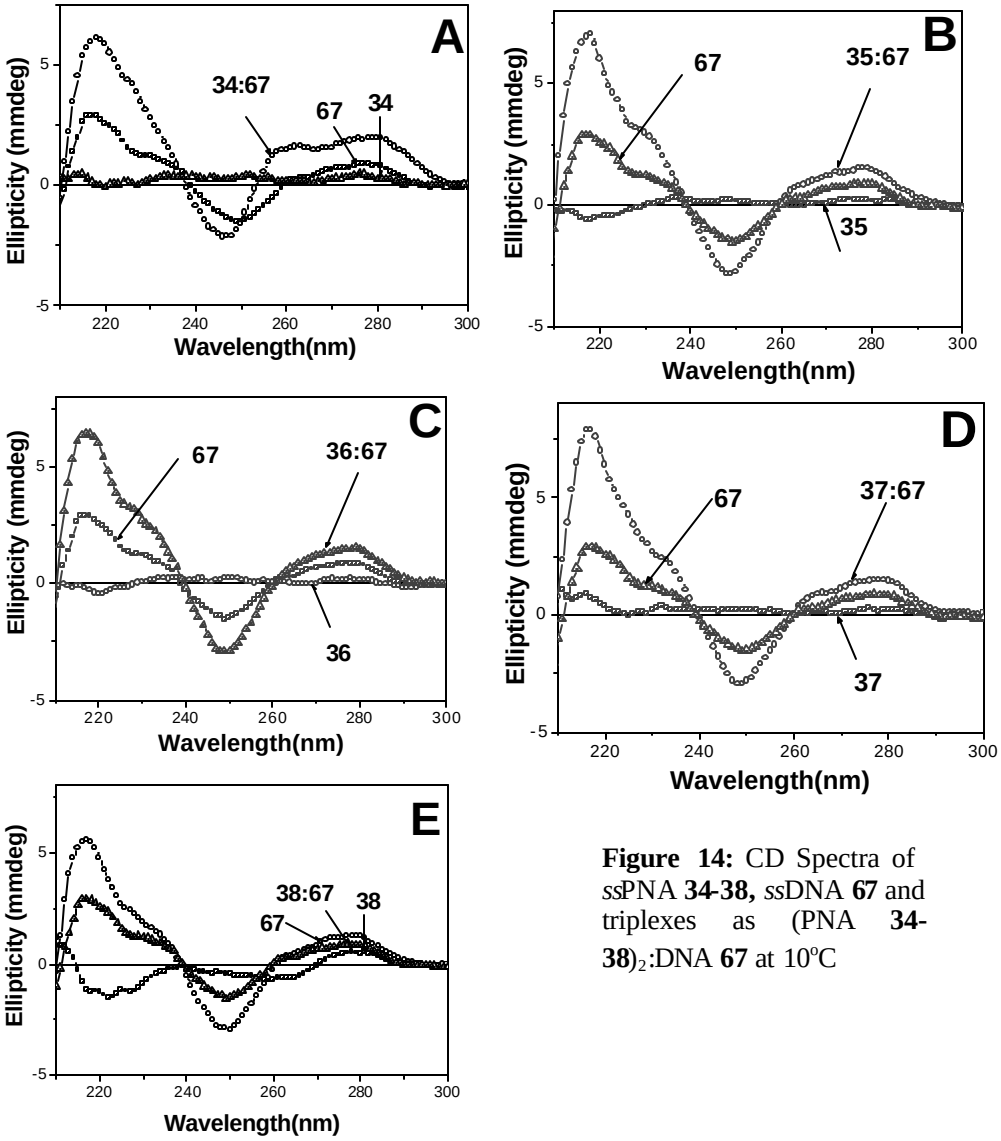

Figure 14: CD Spectra of *ss*PNA **34-38,** *ss*DNA **67** and triplexes as (PNA **34-38**)$_2$:DNA **67** at 10^{o}C

The CD-signature of triplexes with one *cis-aepone*-PNA modification (**35/36**)$_2$:DNA **67** (Figure 14B, 14C) at either N-terminus (PNA **36**) or middle (PNA **35**) and with two modifications of *cis-aepone*-PNA (**37**)$_2$:DNA **67** (Figure 14D) at C-terminus and in middle are quite similar to the CD of control triplex (PNA-**34**)$_2$:DNA **67** (Figure 14A). These exhibited characteristic positive double hump patterns at 260 and 280 nm,

although broad. The CD spectra of triplex derived from full modification with *cis-aepone*-PNA-T (**38**)$_2$:DNA **67** (Figure 14E) was slightly different, having a weak signal at 260 nm compared to control *aeg*-PNA triplexes (PNA **35**)$_2$:DNA **67** (Figure 14A).

In all the cases, the CD spectra were not simply a sum of the spectra of single stranded constituents but showed additional attributes, indicating true hybridization.

4.5.17c CD-studies for (aepone-PNA)$_2$:RNA triplexes

The triplex formation by *aepone*-PNAs with RNA was also studied by CD-spectroscopy. Figure 15 shows the CD-spectra of single stranded of *aepone*-PNAs, RNA

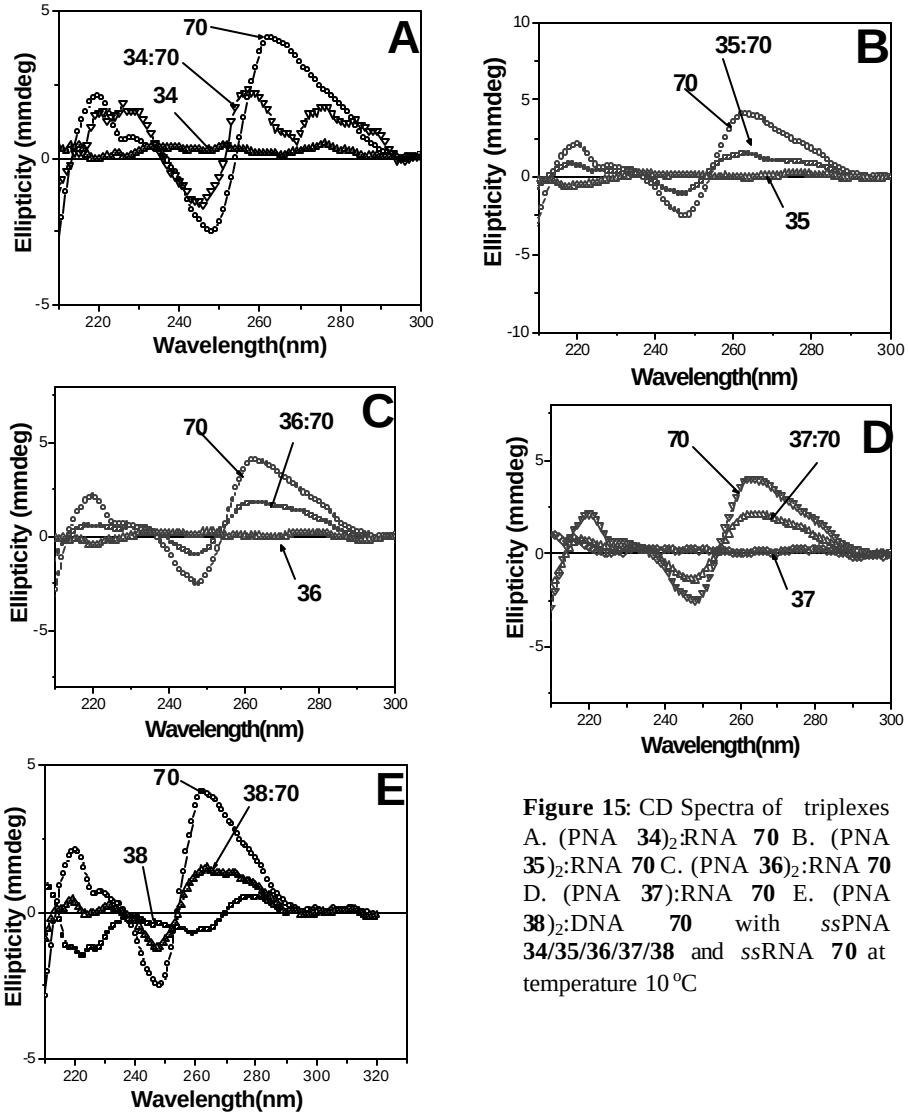

Figure 15: CD Spectra of triplexes A. (PNA **34**)$_2$:RNA **70** B. (PNA **35**)$_2$:RNA **70** C. (PNA **36**)$_2$:RNA **70** D. (PNA **37**):RNA **70** E. (PNA **38**)$_2$:DNA **70** with *ss*PNA **34/35/36/37/38** and *ss*RNA **70** at temperature 10 ^{o}C

and their triplexes as *(aepone*-PNA)$_2$:RNA scanned at 10 ^oC. The CD profiles of all *aepone* triplexes *aepone*-PNA (**35**-**38**)$_2$:RNA(**70**) (Figure 15 B-E) showed broad positive signal in 260-280 nm with ill resolved bands at 260 and 280 nm, in comparison to that of control triplex *(aeg*-PNA **34**)$_2$:RNA(**70**) (Figure 15A), which showed well resolved double humped positive bands at 260 and 280 nm. In all the cases, the positive band at 270 nm of RNA was significantly reduced in triplexes.

4.5.17d CD-melting for (aepone-PNA)$_2$:DNA triplexes

The thermal stability of triplexes of *aeg*-PNA-T$_8$ (**34**) and *aepone*-PNA-T$_8$ (**38**) with complementary DNA dA$_8$ as (PNA **34)**$_2$:DNA **67** and (PNA **38**)$_2$:DNA **67** was also studied by CD-melting experiments. The CD-spectra of triplexes (PNA **34)**$_2$:DNA **67** and (PNA **38**)$_2$:DNA **67** at different temperature (5-85^oC) are given in Figure 16A and 16C

Table 14: Tm value of CD-melting of PNA with DNA

Entry	(PNA)$_2$:DNA 67	Description of PNA	Tm (^oC)	D**Tm (^oC) PNA-control**
1	**34** H$_2$N–T–T–T–T–T–T–T–T-*b*-ala	*Aeg*-(Control)	36.2	0.0
5	1x 8; **38** H$_2$N-t-t-t-t-t-t-t-t-*b*-ala	8 *cis*-(2S,4S)-*aepone*	53.5	+17.3

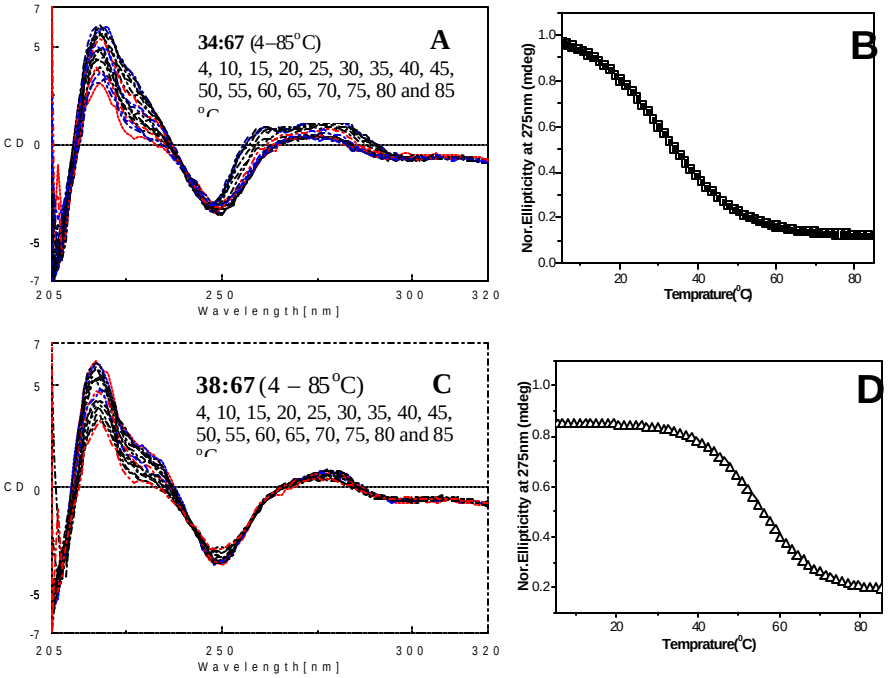

Figure 16: *Left***.** CD Spectra of PNA **38,** PNA **34** with DNA **67** at different Temperature 5-85^oC; *Right*. Melting profiles of (PNA **34**/**38**)$_2$:DNA **67** at 275

respectively. The melting profile of ellipticity vs temperature at wavelength 267 nm was obtained from CD-spectra of these triplexes are shown in Figure 16B and 16D. The melting temperature (Tm) was obtained from first derivative curves of Figure 16B and 15D. The measured Tm (53.5 ^{o}C) of (*aepone*-PNA **38**)$_2$:DNA **67** is higher than that of control (*aeg*-PNA **34)**$_2$:DNA **67** (36.2 ^{o}C) by ΔTm = +17.3 ^{o}C (Table 14, entry 2-entry1), which is supporting result from UV-melting studies.

4.5.17e CD-studies for (aep/aepone-PNA):DNA duplexes

Due to achiral nature of *aeg*-PNA, no characteristic signal is observed for single stranded unmodified PNA **51** (Figure 17). The CD signal of single modified *cis/trans-aepone*-PNA **65/66** and *aep*-PNA **64** which are chiral, exhibited weak profiles (Figure 17).

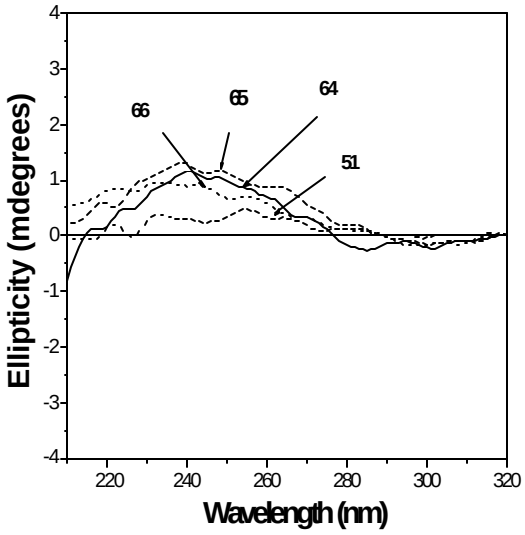

Figure 17: CD Spectra of single strand of PNA **51/64/65/66.**

The CD signatures of duplexes of *cis*-(2*S*,4*S*)-*aepone*-PNA-T **57** having pyrimidine modification, with *antiparallel* DNA **71** and *parallel* DNA **72** (Figure 18B) showed very weak signals compared to that of the CD of control duplexes PNA **51:**DNA **71** (*antiparallel*) and PNA **51:**DNA **72** (parallel) (Figure 18A).

The CD patterns of *antiparallel* and *parallel* duplexes from the purine modifications as in *cis*-(2*S*,4*S*)-*aepone*-PNA-A **65** and *trans*-(2*S*,4*S*)-*aepone*-PNA-A **66** with DNA **71** and DNA **72** respectively, (Figure 18C-D), are quite similar to CD of control duplexes PNA **51:**DNA **71**) (antiparallel) and PNA **51:** DNA**72** (parallel) (Figure 18A). However slight shift of bands among *antiparallel* and *parallel* duplexes PNA (**66**):DNA (**71**/**72)** were noticed.

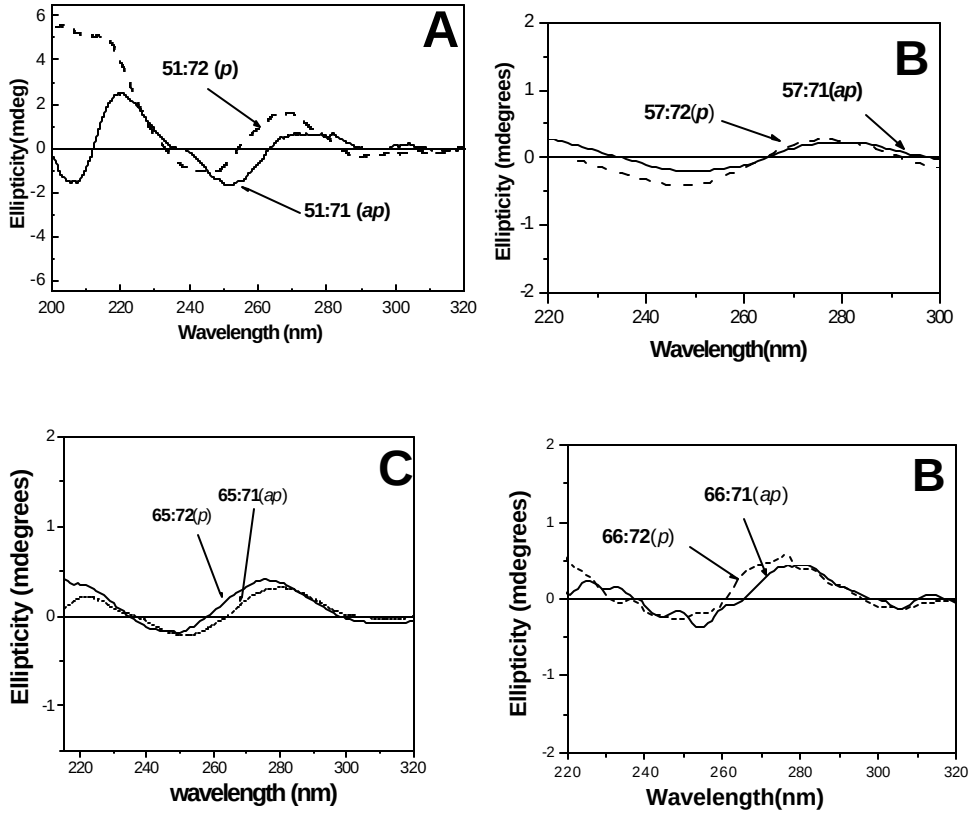

Figure: 18: CD Spectra: A. control antiparallel duplex PNA **51**:DNA **71** and parallel duplexes PNA **51**:DNA **72**; B. antiparallel duplex PNA **57**:DNA **71** and parallel duplexes PNA **57**:DNA **72**.; C. antiparallel duplex PNA **65**:DNA **71** and parallel duplexes PNA **65**:DNA **72**. D. antiparallel duplex PNA **66**:DNA **71** and parallel duplexes PNA **65**:DNA **72** at temperature 10 ℃.

4.5.17f aep-PNA:DNA duplexes

The CD spectra of *aep*PNA duplexes with single modification *cis*-(2*S*,4*S*)-*aep*-PNA-A **63** and *trans*-(2*S*,4*S*)-*aep*-PNA-A **64** with antiparallel DNA **71** and parallel DNA **72** respectively, (Figure 19A-B), exhibited weaker intensity signals in 260-280 nm region

compared to that of control unmodified duplexes PNA **51:**DNA **71** and PNA **51:**DNA **72** (Figure 19A).

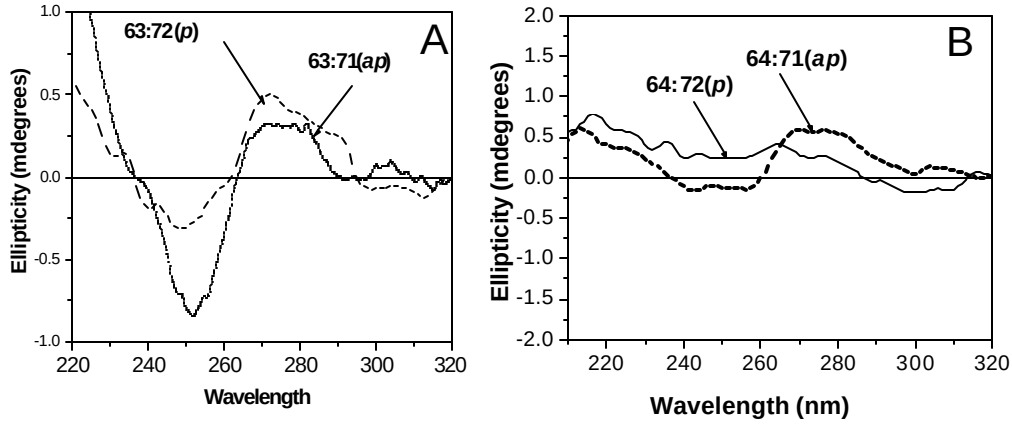

Figure 19: CD Spectra of PNA **5**, parallel and *antiparallel* PNA: DNA duplexes at 10 ^{o}C

4.6 DISCUSSION

The effect of PNA backbone modification in the form of *aep*PNA is expected to significantly affect the PNA:DNA thermal stability. The UV-Tm, CD and presented in the last section suggests that the *aepone*-PNA:DNA interaction is significantly modulated.

aeg-PNA homopyrimidine sequences comprising thymine units are known to form PNA_2:DNA triplexes.[35] Both UV- and CD-Jobs plot data indicated a 2:1 binding stoichiometry (PNA_2:DNA) for PNA oligomers of *aepone*-PNA modifications. The percent hyperchromicity vs temperature plots derived from the UV-melting data indicated a single transition, characteristic of PNA_2:DNA triplex melting, wherein both the PNA strands dissociate from the DNA strand simultaneously in a single step.

Triplexes: The PNA/DNA single strands, upon heating exhibited <3% change in absorbance compared to 6-12% absorbance change for duplexes and triplexes. This ruled out any significant contribution from PNA single stranded ordering to the sigmoidal transition observed for the PNA_2:DNA triplexes.

The *aepone* PNAs **35** (1x L-*cis*-(2*S*,4*R*)-*aepone*-PNA-T at the C-terminus) and **36** (1x L-*cis*-(2*S*,4*R*)-*aepone*-PNA-T in centre), **37** (2 x L-*cis*-(2*S*,4*R*)-*aepone*-PNA-T) and PNA **38** [*cis*-(2*S*,4*R*)-*aepone*-PNA-T_8] and the unmodified *aeg*PNA **34** were hybridized with the complementary DNA **67** (GCA_8CG) that has GC and CG locks at the 5' and 3'-ends to avoid slippage in complexes. The T_m's of different triplexes indicated that L-*cis*-(2*S*,4*R*)-*aepone*-PNA-T in oligomers **35-38** significantly stabilize the derived triplexes with DNA **67** over triplexes of unmodified PNA **34** (ΔT_m 16-19 ^oC). In comparison, the *aepone*–PNAs **35-38** effected destabilization of the triplexes formed with RNA poly r(A), as compared to the triplex from unmodified PNA **34** (ΔT_m 12-15 ^oC). What is significant is that even the completely modified *aepone*-PNA-T_8 oligomer **38** forms successful complexes with DNA **67** and poly r(A)**70** with well defined transitions.

The preference for DNA hybridization of *aepone*-PNAs (Figure 20a) **35-38** and lowering stability of RNA hybrids in contrast to behaviour of *aeg*PNA is opposite of the previously selectivity observed for pyrrolidinone-A_8[36] PNA (Figure 20a) having reverse

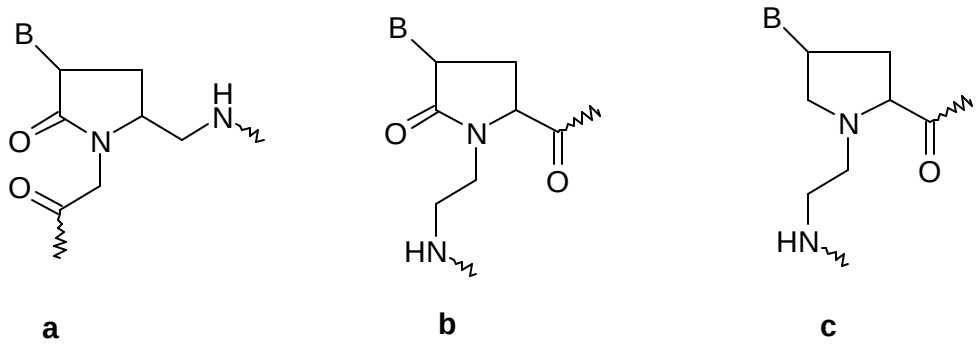

Figure 20: a. *pyrr*-PNA; b. *aepone*-PNA; c. *aep*-PNA

polarity. The trend observed in the Tm of the *aepone*PNA:RNA complexes was the reverse of that observed with the PNA:DNA triplexes. A successive increase in the number of

aep-PNA (Figure 20c) units in the PNA oligomer led to a progressive decrease in the melting temperature as well as in the hyperchromicity during melting. Thus, increasing the number of *aep*-PNA units caused PNA:DNA complexation to be favoured, but PNA:RNA complexation to be disfavoured.

The *aepone*-PNA analogues are more akin to the recently reported pyrrolidinyl PNAs in terms of the observed selectivities.[20] The *aep*-PNA oligomer **39** devoid of C5 carbonyl, bound DNA with a very high T_m with incomplete melting even at 80 ^oC. The strong binding of *aep*PNA **39** with DNA **67** is not entirely due to the electrostatic interactions as it showed a lower binding with poly rA as compared to *aeg*PNA **34**. This suggests that the conformational preorganization plays an important role in determining the binding strengths.

The triplexes formed by L-*trans*-(2*S*,4*R*)-*aepone*-PNA-T substituted PNAs **44**-**46** and DNA **67** were stabilized over unsubstituted control triplexes PNA **34**:DNA **67** by ΔTm = 10-17 ^oC for single modification and ΔTm = 25.6 ^oC for double modifications. The triplexes of L-*cis* and *trans*-*aepone*-PNAs are almost of same stability.

The Tm values of triplexes formed by single/double substitutions of L-*cis*/*trans*-*aep*-PNA-T (**47**/**49**/**40**/**43**) with DNA **67** indicated that triplexes (PNA **47**/**49**)$_2$:DNA **67** were marginally stable over the unmodified triplex (PNA **34**)$_2$:DNA **67** by ΔTm = 4.3-7.6 ^oC; triplexes L-*cis*-*aep* (PNA **40**)$_2$:DNA **67** and L-*trans*-*aep*-(PNA **43**)$_2$:DNA **67** had significantly enhanced ΔTm's of 35.9 ^oC and 18.6 ^oC respectively over control. These results show that triplexes formed by L-*cis*-*aep*-PNA have higher stability over L-*cis*-*aep*-PNA triplexes.

In comparison, L-*cis*/*trans*-*aepone*/*aep*-PNA triplexes derived from PNAs **41**/**43**/**47**/**48** had almost equal stabilities. Single substituted L-*cis*-*aep*-PNA-T triplex is marginally stabler than L-*cis*-*aepone*-PNA-T (ΔTm = 2.1 ^oC) and doubly substituted L-

cis-*aep*-PNA-T triplex is slightly more stable than L-*cis*-*aepone*-PNA-T (ΔTm = 6.6 ^{o}C). In case of L-*trans*-*aep*-PNA and L-*trans*-*aepone*-PNA-T, both had almost equal stabilities for single (ΔTm = 2.1 ^{o}C) and double substitutions (ΔTm = 1.2 ^{o}C).

The binding pattern of the presently designed *aepone*-PNA is interesting; it has affinity to DNA more than that of PNA, but lower than that of *aep*-PNA, affinity to RNA less than that of PNA and more than that of *aep*-PNA. The tetrahedral nature of pyrrolidine nitrogen in *aep*-PNA is switched back to the planar amide in *aepone*-PNA, as in unmodified PNA with consequent influence on the backbone conformation. Importantly, the side-chain *syn*/*anti* rotameric equilibrium present in unmodified PNA is avoided in *aepone*-PNA, inspite of the ring nitrogen retaining the amide character. Thus *aepone*-PNA is an evolved structure by design, combining the features of both *aeg*-PNA and *aep*-PNA. It also emerges from the present data that *aep*-PNA has a selectivity to bind DNA over RNA, and this aspect needs to be further confirmed with studies using mixed RNA sequences. The CD spectral features of *aepone*-PNA:DNA/RNA hybrids were similar to that of PNA:DNA/RNA hybrids, suggesting no major differences in base stacking patterns.

The effect of backbone chirality of *aepone*-PNA while binding to complementary DNA sequences to form triplexes seems to be unimportant in homopyrimidine (T_8) sequences, since these bind to complementary DNA in both parallel (HG) and antiparallel (WC) orientations. The mixed purine-pyrimidine sequences (**51**-**66**) were constructed to explore the effect of the *aepone/aep* backbone chirality on the directionality of binding in duplexes.

In *aepone*-PNA:DNA recognition, like *aeg*-PNA specific hydrogen bonding between the complementary nucleobases of PNA(*aep*/*aeg*) and DNA occurs, since even a single mismatch in the middle of the sequence was found to inhibit *aepone*-PNA:DNA

complexation. The homooligomer of *aepone*-PNA studied here have similar spatial disposition of the nucleobase attached to the proline ring at C4, equivalent to the nucleobase attachment at C1' of ribose ring in DNA. Changing the stereochemistry at the C4, does not appreciably affect the stability of the *aepone*-PNA_2:DNA complexes. The structural changes caused by the difference in stereochemistry at C4 are probably accommodated within the flexibility imparted to the backbone by the aminoethyl moiety flanking the proline ring. Such flexibility is lost when the proline nitrogen is part of an exocyclic amide moiety.

The inclusion of single L-*cis*/*trans*-(2*S*,4*S*/*R*)-*aepoene/aep*-PNA-A modification within a mixed sequence *aeg*PNA oligomer **51** bearing all four nucleobases led to interesting nucleobase- and stereochemistry-dependent stabilization effects. The stabilization was also at least partly due to electrostatic interactions for *aep*-PNA, which are removed in *aepone* PNA.

Duplex: The L-*cis/trans*-(2*S*,4*S*/*R*)-*aepone*-PNA-A units in their corresponding positions in PNA **51** uniformLy stabilized the *antiparallel* duplexes by 5-13 ^{o}C and the duplex formed by L-*cis/trans*-(2*S*,4*S*/*R*)-*aep*-PNA-A was stabilized by larger magnitude 15-20 ^{o}C over the control **51**:**71**. The *parallel* duplexes formed by purine (L-*cis/trans*-(2*S*,4*S*/*R*)-*aepone/aep*-PNA-A modified PNA (**63-66**) with DNA **72** were stabilized over the control **51**:**72** by only by 1-7 ^{o}C.

The presence of single and double L-*trans*-(2*S*,4*R*)-*aepoene*-PNA-T units within a mixed sequence of all four bases A/T/G/C e.g., **57** & **58** (ΔTm $\approx$15 ^{o}C) were more efficient in differentiating between the *antiparallel* and *parallel* binding orientations than the *aeg*-PNA **51** (ΔTm $\approx$5 ^{o}C).

The duplexes formed by the purines, L-*cis/trans*-(2*S*,4*S*/*R*)-*aepone/aep*-PNA-A exhibited hyperchromicity upon melting that was as good as the control duplexes (8-12%).

The pyrimidines L-*cis/trans*-(2*S*,4*S*/*R*)-*aepone*-PNA-A, on the other hand, showed a lower hyperchromicity (6-9%) than L-*cis/trans*-(2*S*,4*S*/*R*)-*aep*-PNA-A, which could be a consequence of less efficient nucleobase stacking. The pyrrolidine ring pucker and/or *syn*/*anti* orientation of the nucleobases that are directly attached to the ring may dictate the individual parallel/antiparallel preferences observed for the nucleobases on chiral *aep* units while this puckering was underplayed in *aepone*-PNA due to presence of planar amide carbonyl at C5 of prolyl ring. It is known that the nature of the 4-substituent plays an important role in defining the pucker of the pyrrolidine ring in 4-substituted prolines (see Chapter 3). The individual purines or pyrimidines at C4-position in *aep*PNA perhaps causes different pyrrolidine ring puckers and consequent backbone conformational changes. The relatively better stabilizing effect of purines over the pyrimidines may arise from a better stacking effect in the resulting duplexes compared to the control.

The introduction of chiral monomers in the backbone allows the investigation of effect of stereogenic centers in the achiral PNA oligomer. Thus, it is of interest to examine the cumulative effect of stereogenic centers inserted into a PNA oligomer in inducing a preferred handedness and if such eventual stereochemical preorganization of PNAs can influence the selectivity of the DNA/RNA recognition process. It has been conjectured that effective mechanisms of inducing chirality/binding selectivity would involve some immobilization of the rotation around the bonds of the α-carbon of the amino acid. A comparison of the structures of the complexes formed by PNA with complementary DNA/RNA and the corresponding DNA:DNA and DNA:RNA complexes suggested that PNA hybrids are right handed helices with a base-pair geometry not too much different from 'A' or 'B' form DNA. The preferred handedness of the PNA:DNA duplexes seems to be dictated by the DNA and the CD spectra of *parallel* and *antiparallel* DNA:PNA duplexes were distinctly different.

Of the two stereocenters in each chiral *aepone*-PNA unit, the C2-stereocenter is present directly in the backbone (Figure 21) and hence expected to exert a greater influence in inducing chirality in the oligomer backbone. The C4 stereocenter carrying the nucleobase may mostly affect the base stacking. However, since both are part of the pyrrolidine ring, the two roles may be correlated.

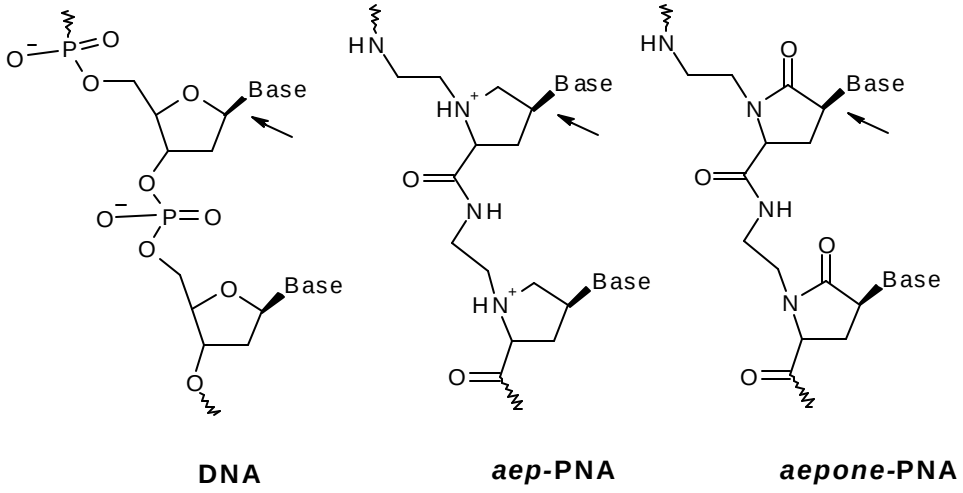

Figure 21: The similar spatial disposition of the nucleobase to the ring structure in DNA, *aep*-PNA and *aepone*-PNA

PNA-T_8 oligomers were demonstrated to form PNA_2:DNA triplexes with the DNA polypurine strand as the central strand. In such cases, CD supported the fact that a triplex is formed as the only PNA:DNA complex, and that it is a right-handed helix[37] The conformation of bases in the PNA_2:DNA triplex was found to be very similar to that of the conventional DNA_2:DNA T*A:T triplex. The differences in the CD spectra of the PNA_2:DNA and the DNA_2:DNA triplexes suggest that the helical winding may somewhat differ between the two types of triplexes.

The CD induced by the *aepone*-PNA units in the PNA single strands seemed to be inconsequential, since the *aep*-PNA:DNA duplexes/triplexes gave very similar CD signals and not very different from that of the control achiral *aeg*PNA complexes. This is perhaps

a consequence of the fact in PNA:DNA complexes, the CD contribution of the DNA dominates over any inherent CD of the PNA involved in the structure.

The CD signals of the duplexes of the *aepone*-PNA oligomers **63-66** with complementary DNA **71**/**72** were also similar to those of the control *aep*-PNA **51**. The backbone geometry (2*S*,4*S*/*R*) did not have any dramatic effect on the geometry of either *parallel* or *antiparallel* PNA:DNA duplexes.

4.7 CONCLUSIONS

The *aepone*PNA substitutions were shown to possess very interesting DNA-binding properties. The ability of PNAs containing these units in differentiating between *parallel* and *antiparallel* binding modes, which is incongruous in PNA_2:DNA triplexes, becomes obvious in PNA:DNA duplexes. The introduction of carbonyl group into the prolyl ring as in *aepone*-PNA remarkably lowers the Tm value of equivalent prolyl PNA devoid of ring carbonyl group i.e. *aep*-PNA, from high to intermediate range and better than the *aeg*-PNA:DNA complex. Due to the absence of positive charge on the pyrrolidine nitrogen resulting from incorporation of C5 carbonyl group into prolyl ring partly reduces the binding affinity. The main contributing factor to the stability remains the specific hydrogen bonding between the A-T and G-C nucleobases. The *aepone* units (Figure 22) in

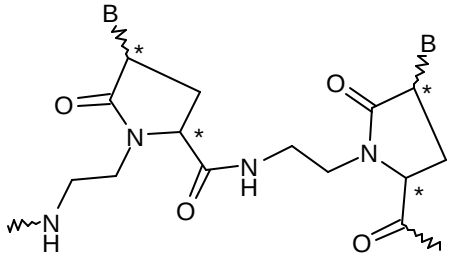

Figure 22: The *aepone*-PNA backbone showing the two chiral centers of each *aepone*-PNA unit.

mixed sequence duplexes exhibit stabilization effects that are dependent on the nucleobase type and backbone chirality. Thus, besides the positive charge and inter-nucleobase hydrogen bonding, other factors like the pyrrolidine ring pucker and/or *syn*/*anti* orientation of the nucleobases may play an important role. In order to explain all the observed results, more work needs to be carried out, including conformational analysis of the pyrrolidine ring, etc. To investigate the undiluted effect of the aminoethylprolyl backbone, homooligomeric *aepone*PNA sequences need to be studied at length.

4.8 EXPERIMENTAL

4.8.1 Solid phase peptide synthesis

4.8.1a Picric acid estimation of resin functionalizations

The typical procedure for estimation of the loading value of the resin was carried out with 5mg of the resin and comprised the following steps:

The resin was swollen in dry CH_2Cl_2 for at least 30 min. The CH_2Cl_2 was drained off and a 50% solution of TFA in CH_2Cl_2 was added (1 mL x 2), 15 min each. After washing thoroughly with CH_2Cl_2, The TFA salt was neutralized with a 5% solution of DIPEA in CH_2Cl_2 (1 mL x 3, 2 min each). The free amine was treated with a 0.1M picric acid solution in CH_2Cl_2 (2 mL x 2, 3 min each). The excess picric acid was eliminated by extensively washing the resin with CH_2Cl_2. The adsorbed picric acid was displaced form the resin by adding a solution of 5% DIPEA in CH_2Cl_2. The eluant was collected and the volume was made up to 10 mL with CH_2Cl_2 in a volumetric flask. The absorbance was recorded at 358nm in ethanol and the concentration of the amine groups on the resin was calculated using the molar extinction coefficient of picric acid as 14,500 $cm^{-1}M^{-1}$ at 358 nm.

4.8.1b Kaiser's Test

Kaiser's test was used to monitor the Boc-deprotection and amide coupling steps in the solid phase peptide synthesis. Three solutions were used, viz. (1) Ninhydrin (5.0 g) dissolved in ethanol (100 mL), (2) Phenol (80 g dissolved in ethanol (20 mL) and (3) KCN: 2 mL of a 0.001M aqueous solution of KCN in 98 mL pyridine).

To a few beads of the resin to be tested taken in a test tube, were added 3-4 drops of each of the three solutions desribed above. The tube was heated at 100 ^{o}C for ~5 min, and the colour of the beads was noted. A blue colour on the beads and in the solution

indicated successful deprotection, while colourless beads were observed upon completion of the amide coupling reaction. The blank solution should remain yellow.

4.8.1c Cleavage of the PNA oligomers from the solid support

A typical cleavage reaction was carried out with 5 or 10mg of resin-bound PNA oligomer. The resin-bound PNA oligomer (10 mg) was stirred in an ice-bath with thioanisole (20 μL) and 1,2-ethanedithiol (8 μL) for 10min, TFA (120 μL) was added and stirring was continued for another 10 min. TFMSA (16 μL) was added and stirring continued for 2 h. The reaction mixture was filtered through a sintered funnel. The residue was washed with TFA (3 x 2 mL) and the combined filtrate and washings were evaporated under vacuum and co-evaporated with ether, avoiding heating during this process. The residue was precipitated using dry ether and centrifuged to obtain a white pellet. The pellet was re-dissolved in methanol (~0.1 mL) and re-precipitated by adding ether. The pellet collected after centrifugation was subjected to this re-precipitation process at least thrice, when a white precipitate was obtained of the crude PNA oligomer.

4.8.1d Gel Filtration

The crude PNA oligomer obtained after ether precipitation was dissolved in water (~0.5 mL) and loaded on a gel filtration column.[38] This column consisted of G25 Sephadex and had a void volume of 1mL. The oligomer was eluted with water and ten fractions of 1mL volume each were collected. The presence of the PNA oligomer was detected by measuring the absorbance at 260 nm. The fractions containing the oligomer were freeze-dried. RP HPLC determined the purity of the cleaved crude PNA oligomer on a C18 column. If found to be above 90%, the oligomers were sued as such for experiments without further purification. If the purity was not satisfactory, the oligomers were purified by HPLC/FPLC.

4.8.1e FPLC

The crude PNA oligomers were dissolved in water containing 0.1% TFA, the starting buffer for injection. The polypyrimidine T8 sequences were purified using a gradient of 0 to 50% buffer B in 30 min at a flow rate of 1.0 mL/min, where buffer A = water with 0.1% TFA and buffer B = 60% CH3CN in water containing 0.1% TFA. The mixed sequence PNAs eluted earlier and hence had to be purified using a gradient of 0 to 30% B in 30 min at a flow rate of 1.0 mL/min, when good resolution of the peaks was obtained. The purity of the oligomer after FPLC was ascertained by HPLC on a C18 RP column.

4.8.1f HPLC

The purity of the PNA oligomers was ascertained on an analytical RP C18 column using a gradient of 5 to 80% CH_3CN in water containing 0.1% TFA at a flow rate of 1.5 mL/min. HPLC purification of the mixed sequence decamers was carried out on a semi-preparative RP C4 column using isocratic elution at a flow rate of 6.0 mL/min. The eluent was varied between 8 to 12% CH3CN in water containing 0.1% TFA to obtain optimum separation of the constituent peaks. The oligomers so collected were re-checked for purity by analytical HPLC as described above.

4.8.1g MALDI-TOF Mass Spectrometry

Literature reports the analysis of PNA purity by MALDI-TOF mass spectrometry[52] in which several matrices have been explored, *viz.* sinapinic acid (3,5-dimethoxy-4-hydroxycinnamic acid), CHCA (α-cyano-4-hydroxycinnamic acid) and DHB (2,5-dihydroxybenzoic acid). Of these, sinapinic acid was found to give the best signal to noise ratio with all the other matrices typically producing higher molecular ion signals.

For all the MALDI-TOF spectra recorded for the *aep*PNAs reported in this Chapter, sinapinic acid was used as the matrix and was found to give satisfactory results.

4.8.1h UV-T_m experiments

UV melting experiments were performed on Lambda -35 UV Spectrometer (Perkin-Elmer) equipped with a thermal melt system, PTP-6 Peltier Temperature Programmer with water circulator Thermoshake K20. The sample for Tm measurement was prepared by mixing calculated amount of stock oligonucleotide and PNA solutions together in 2 mL of sodium phosphate buffer (pH 7.1). The samples 2 mL were transferred to quartz cell, sealed with Teflon stopper after degassing with nitrogen gas for 15 min, and equilibrated at the starting temperature for at least 30 min. The OD at 260 nm was recorded in steps from 10-85 ^{o}C with temperature increment of 0.2 ^{o}C/min. The results were normalized and analysis of data was performed on using Origin 5.0 (Microsoft Corp.).

3.8.1i UV studies

All the UV spectrophotometric studies were performed on a Perkin Elmer λ15 UV-VIS spectrophotometer equipped with a Julabo temperature programmer and a Julabo water circulator to maintain the temperature. The samples were degassed by purging nitrogen or argon gas through the solution for 2-3 min prior to the start of the experiments. Nitrogen gas was purged through the cuvette chamber below 15 ^{o}C to prevent the condensation of moisture on the cuvette walls.

3.8.1j UV-Jobs plot

To a solution of DNA **67** in 0.01M sodium phosphate at pH 7.4, were added portions of the complementary PNA oligomer **38** to make 10 different fraction with mole ratio from 0-100% with fixed concentration. Then UV of each fraction was scanned at the temperature of the circulating water was maintained at 10 ^{o}C (i. e., well below the melting

temperature of the complexes) and the absorbance at was recorded at 268 This was plotted as a function of the PNA mole fraction.

3.8.2 UV-Tm

The PNA oligomers and the appropriate DNA **67** oligomers were mixed together in stoichiometric amounts (2:1 PNA:DNA for oligothymine-T_8 PNAs or 1:1 for the duplex forming PNAs, *viz*., the mixed base sequences) in 0.01M sodium phosphate buffer, pH 7.4 to achieve a final strand concentration of either 0.5 or 1μM each strand. Extinction coefficient C = 6.6, T = 8.6, A = 13.7 and G = 11.7 [$(\mu mol)^{-1}$ cm^{-1}] was used to calculate the concentration of PNA by follow Lambert Beer's Law: $A = \hat{I} cl$.

The antiparallel complexes involving the PNAs containing all the four nucleobases were constituted using DNA **71**, while DNA **72** was used to get the parallel complexes. The samples were heated at 85 ^{o}C for 5 min followed by slow cooling to room temperature. They were allowed to remain at room temperature for at least half an hour and refrigerated overnight prior to running the melting experiments. Each melting experiment was repeated at least thrice. The absorbance or the percent hyperchromicity at 260 nm was plotted as a function of the temperature. The Tm was determined from the peaks in the first derivative plots and is accurate to ± 1 ^{o}C.

4.8.3 Mismatch studies

DNA **68-69** was used to probe the specificity of the L-*cis*-(2*S*,4*S*)-*aepone*-PNA-oligothymine-t_8 interaction with DNA. The relevant PNA and DNA strands were mixed together in a 2:1 molar ratio and subjected to UV-melting.

4.8.4 Circular dichorism (CD)

CD spectra were recorded on a Jasco J-715 spectropolarimeter. The CD spectra of the PNA: DNA complexes and the relevant single strands were recorded in 0.01M sodium phosphate buffer, pH 7.4. The temperature of the circulating water was kept below the melting temperature of the PNA:DNA complexes, i. e., at 10 ^{o}C.

CD-Job's plot: Similarly, the CD-Job's plot experiment was done by scanning CD-spectra of each fraction of PNA **38** and DNA **67**. Then Ellipticity was recorded for each one and plotted as function of the PNA mole fraction.

CD-Melting: CD-melting of homo oligo of *aepone*-PNA **38** and *aeg*-PNA **34** with complementary DNA **67** was done by scanning the CD-spectra of $(PNA)_2$:DNA complexese at different temperature from 4 ^{o}C – 85 ^{o}C on interval of 5 ^{o}C.

The CD spectra of the oligothymine T_8 single strands and mixed sequences were recorded as an accumulation of 8 scans from 320 to 195 nm using a 1cm cell, a resolution of 0.1 nm, band-width of 1.0 nm, sensitivity of 2 mdegrees, response 2 sec and a scan speed of 50 nm/min. For the PNA_2:DNA complexes, spectra were recorded as an accumulation of 4 scans, response of 1 sec and a scan speed of 200 nm/min.

The CD spectra of the mixed base PNAs and the derived PNA:DNA duplexes were also recorded as an accumulation of 3 scans and a scan speed of 200 nm/min.

The PNA:DNA/RNA complexes were constituted by mixing appropriate strands in a 2:1 stoichiometry in buffer followed by heating to 90 ^{o}C and annealed by slow cooling to 4 ^{o}C to obtain PNA_2:DNA triplexes.

1.9 REFERENCES

1. Milligan, J.; Matteucci, M. D.; Martin, J. C. Current concepts in antisense drug design. *J. Med. Chem.* **1993**, *36*, 1921-1937.
2. Woolf, T.; Jennings, C.; Rebagliati, M.; Melton, D. The stability, toxicity and effectiveness of unmodified and phosphorothioate antisense oligodeoxynucleotides in xenopus oocytes and embryos. *Nucleic Acid Res.* **1990**, *18*, 1763-1769
3. Skorski, T.; Perrotti, D.; Nieborowska-Skorska, M.; Gryaznov, S. M.; Calabretta, B. Antileukemia effect of G-myc N3'-P5' phosphoramidate antisense oligonucleotide *in vivo*. *Proc. Natl. Acad. Sci.* USA **1997**, *94*, 3966-3971.
4. Eckstein, F. Phosphorothioates oligonucleotides : What is their origin and what is unique about them? *Antisense Nucleic Acid Drug Dev*. **2000**, *10*, 117-121
5. (a) Summerton, J.; Weller, D. Morpholino antisense oligomer: Design, preparation and properties. *Antisense nucleic Acid Drug Dev*. **1997,** *7*, 187-190. Marwick, C. (b) First "antisense'' drug will treat CMV retinitis. *J. Am. Med. Assoc*. **1998**, *280*, 871.
6. (a) Uhlmann, E.; Peyman, A.; Breipont, G.; Will, W. D. PNA: Synthetic polyamide nucleic acids with unusual binding properties. *Angew. Chem. Int. Ed.* **1998**, *37*, 2796-2823. Good, L.; (b) Awasthi, S. K.; Dryselius, R.; Larsson, O.; Nielsen, P. E. Bacterisidal antisense effects of peptide–PNA conjugates. *Nature Biotech.* **2001**, *19*, 360-364. (c) Braash, D. A.; Corey, D. R. Novel antisense and peptide nucleic acid strategies for controlling gene expression. *Biochemistry* **2002,** *41*, 4503-4510.(c) Hanvey, J. C.; Peffer, N. J.; Bissi, J. E.; Thomson, S. A.; Cadilla, R.; Josey, J. A.; Ricca, D. J.; Hassman, C. F.; Bonham, M. A.; Au, K. G. Antisense and antigene properties of peptide nucleic acids. *Science* **1992**, *258*, 1481-1485.
7. (a) Kurreck, J.; Wyszko, E.; Gillen, C.; Erdmann, V. A. Design of antisense oligonucleotides by locked nucleic acids. *Nucleic Acid Res*. **2002**, *30*, 1911-1918. (b) Herdewijn, P. Heterocyclic modifications of oligonucleotides and antisense technology. *Antisense Nucleic Acid Drug Dev*. **2000**, *10*, 297-310. (c) Mickelfield, J. Backbone modification of nucleic acids: Synthesis, structure and therapeutic applications. *Current Med. Chem*. **2001**, *8*, 1157-1179. (d) Soomets, U.; Hallbrink, M.; Langel, U. Antisense properties of peptide nucleic acids. *Front. Biosci.* **1999**, *4*:D 782-786.
8. Wilfinger, W. W.; Mackey, K.; Chomczynski, P. Effect of pH and ionic strength on the spectrophotometric assessment of nucleic acid purity. *Biotechniques* **1997**, *22*, 474-6, 478-81.
9. Lober, G.; Zimmer, C. pH Induced changes in the UV-absorption band of deoxyribonucleic acid. *Biochem. Biophys. Res. Commun.* **1968**, *31*, 641-645.
10. Puglisi, J. D. Tinocco, Jr., I. absorbance melting curves of RNA. *Meth*. *Enzym*. **1989**, 180.
11. (a) Giesen, U., Kleider, W., Berding, C., Ørum, H., and Nielsen, P. E. (1998) A formula for thermal stability (Tm) prediction of PNA/DNA duplexes. *Nucleic Acids Res.* **1998,** *26***,** 1601–1620. (b) Xia, T.; SantaLucia J. Jr.; Burkard, M. E.; Kierzek R.; Schroeder S. J.; Jiao X., Cox C.; and Turner D. H. Thermodynamic parameters for an expanded nearest-neighbor model for form ation of RNA duplexes with Watson-Crick base pairs. *Biochemistry* **1998**, *37*, 14719-14735. (c) SantaLucia, J. Jr.; A unified view of polymer, dumbbell, and oligonucleotide DNA nearest-neighbor thermodynamics, *Proc. Natl. Acad. Sci. USA.* **1998**, *95*, 1460-1465.

12. Calloway, Dean. Beer-Lambert Law *J. Chem. Educ.* **1997**, *74*, 744.

13. (a) Job, P. *Ann. Chim* . **1928**, *11,* 3-203. b) Cantor C. R.; Schhimmel, P. R. The behavior of biological macromolecules. *Biophysical Chem.* Part III **1980**, 62

14. Hoff, A. J.; Roos, A. L. Hysteresis of denaturation of DNA in the melting range. *Biopolymers* . **1972**, *11*, 1289-94.

15. Hoffman, P. D.; Wang, H.; Lawrence, C. W.; Iwai, S.; Hanaoka, F.; Hays, J. B. Binding of MutS mismatch repair protein to DNA containing UV photoproducts, "mismatched" opposite Watson-Crick and novel nucleotides, in different DNA sequence contexts. *DNA Repair (Amst)*. **2005**, *4*, 983-93. (b) Igloi, G. L. Variability in the stability of DNA-peptide nucleic acid (PNA) single-base mismatched duplexes: real-time hybridization during affinity electrophoresis in PNA containing gels. *Proc. Natl. Acad. Sci. USA* **1998**, *95*, 8562–8567.

16. Egholm, M.; Buchardt, O.; Christensen, L.; Beherns, C.; Freier, S. M.; Driver, D. A.; Berg, R. H.; Kim, S. K.; Norden, B.; Nielsen, P. E. PNA hybridizes to complementary oligonucleotides obeying the Watson-Crick hydrogen bonding rules. *Nature* **1993**, *365*, 566-568.

17. (a) Egholm, M.; Nielsen, P. E.; Buchardt, O.; Berg, R. H. Recognition of guanine and adenine in DNA by thymine and cytosine containing peptide nucleic acids. *J. Am. Chem. Soc.* **1992**, *114*, 9677–9678. (b) Leijon, M.; Gra¨slund, A.; Nielsen, P. E.; Buchardt, O.; Norde´n, B. Kristensen S. M.; Erickson, M. Structural characterization of PNA-DNA duplexes by NMR. Evidence for DNA in a B-like conformation. *Biochemistry* **1994**, *33*, 9820 -9825.

18. Nordén, B.; Kurucsev, T. Analysing DNA complexes by circular and linear dichroism. *J Mol Recognit* **1994**, *7*, 141-155.

19. Wittung, P.; Nielsen, P.; Norde´n, B. Extended DNA-recognition repertoire of PNA. *Biochemistry* **1997**, *36*, 7993–7979. Wittung, P., Eriksson, M., Lyng, R., Nielsen, P. E., and Norde´n,B. Induced chirality in PNA-PNA duplexes. *J. Am. Chem. Soc.* **1995**, *117*, 10167–10173.

20. Eriksson, M.; Nielsen, P. E. PNA-nucleic acid complexes: Structure, stability and dynamics. *Q. Rev. Biophys*. **1996**, *29*, 369–394.

21. D'Costa, M.; Kumar, V. A.; Ganesh, K. N. Aminoethylprolyl (*aep*PNA): mixed purine, pyrimidine oligomers and binding orientation preferences for PNA:DNA duplex formation. *Org. Lett*. **2001**, *3*, 1281-1284.

22. (a) Erickson, B. W.; Merrifield, R. B. Solid phase peptide synthesis In the proteins Vol. Ii, 3rd ed.; Neyrath, H. and Hill, R.L. eds., **1976**, Academic Press, New York, pp 255. (b) Merrifield, R. B.; Stewart, J. M.; Jernberg, N. Instrument for automated synthesis of peptides. **1966,** *Anal. Chem*. *38*, 1905. (c) *Oligonucleotide Synthesis. A Practical Approach* Ed. M. J. Gait, IRL Press, **1984,** Oxford, Washington D. C.

23. (a) Christensen, L.; Fitzpatrick, R.; Gildea, B.; Petersen, K.; Hansen, H. F.; Koch, C.; Egholm, M.; Buchardt, O.; Nielsen, P. E.; Coull, J.; Berg, R. H. *J. Peptide Sci.* **1995**, *3*, 175-183. (b) Dueholm, K., Egholm, M., Behrens, C., Christensen, L.; Hansen, H. F.; Vulpius, T.; Petersen, K. H.; Berg, R. H.; Nielsen, P. E.; Buchardt, O. Synthesis of peptide nucleicacid monomers containing the 4 natural nucleobases—thymine, cytosine, adenine, and guanine and their oligomerization. *J. Org. Chem.* **1994**,

59, 5767–5773. (c) Uhlmann, E.; Peyman, A.; Breipohl, G.; Will, D. W. PNA: synthetic polyamide nucleic acids with unusual binding properties. *Angew. Chem. Int. Ed.* **1998**, *37*, 2796–2823.

24. (a) Thomson, S. A.; Josey, J. A.; Cadilla, R.; Gaul, M. D.; Hassman, C. F.; Luzzio, M. J. Fmoc mediated synthesis of peptide nucleic acids. *Tetrahedron* **1995**, *51*, 6179-6194. (b) Goodnow, R. A.; Jr., Richou, A-. R.; Tam, S. Synthesis of thymine, cytosine, adenine, and guanine containing *N*-Fmoc protected amino acids: building blocks for construction of novel oligonucleotide backbone analogs. *Tetrahedron Lett.* **1997**, *38*, 3195-3198. (c) Egholm, M.; Christensen, L., Dueholm, K. L.; Buchardt, O., Coull, J.; Nielsen, P. E. Efficient pH-independent sequence-specific DNA-binding by pseudoisocytosine-containing bis-PNA. *Nucleic Acids Res.* **1995**, *23*, 217–222.
25. Gisin, B. F. The preparation of Merrifield resins through total esterification with cesium salt. *a. Helv. Chim. Acta.* **1970**, *56*, 1476-1482.
26. Erickson, B. W.; Merrifield, R. B. *Solid Phase Peptide Synthesis. In the Proteins* Vol. II, 3rd ed.; Neurath, H. and Hill, R. L. eds., **1976,** Academic Press, New York, pp 255.
27. (a) Hodges, R. S.; Merrifield, R. B. Monitoring of solid phase peptide synthesis by an automated spectrophotometric picrate method. *Anal. Biochem.* **1975**, *65*, 241-272.
28. (a) Angell, Y. M.; Alsina, J.; Albericio, F.; Barany, G. Practical protocols for stepwise solid-phase synthesis of cysteine-containing peptides. *J. Pept. Res.* **2002,** *60*, 292-9. (b) Mc Murray, J. S.; Lewis, C. A.; Obeyesekere, N. U. Influence of solid support, solvent and coupling reagent on the head-to-tail cyclization of resin-bound peptides. *Pept. Res.* **1994**, *7*, 195-206.
29. Kaiser, E.; Colescott, R. L.; Bossinger, C. D.; Cook, P. I. Colour test for the detection of free terminal amino groups in the solid phase synthesis of peptides. *Anal. Biochem.* **1970**, *34*, 595.
30. Koch, T.; Hansen, H. F. Andersen, P.; Larsen, T.; Batz, H. G. Ottesen, K.; Ørum, H. Improvement in automated PNA synthesis using Boc/Z monomers Peptide nucleic acid (PNA). *J. Peptide Res.* **1997**, *49*, 80-88.
31. (a) Butler, J. M.; Jiang-Baucom, P.; Huang, M.; Belgrader, P.; Girard, J, Peptide nucleic Acid Characterization by MALDI-TOF Mass Spectrometry. *Analytical Chemistry* **1996**, *68*: 3283-3287. (b) Ross, P. L.; Lee, K.; Belgrader, P Discrimination of Single-Nucleotide Polymorphisms in Human DNA using Peptide Nucleic Acid Probes detected by MALDI-TOF mass spectrometry. *Analytical Chemistry* **1997**, *69*: 4197-4202. Jiang-Baucom P, Girard JE: DNA typing of Human Leukocyte Antigen Sequence Polymorphisms by Peptide Nucleic Acid Probes and MALDI-TOF mass Spectrometry. *Analytical Chemistry* **1997**, *69*: 4894-4898
32. Sojka, B.; Piunno, P.A.E.; Wust, C.C.; Krull, U.J. A novel phosphoramidite method for automated synthesis of oligonucleotides on lass supports for biosensor development. *ppl Biochem. Biotechnol.* **2000**, *1*, 103.
33. (a) Lowe, G.; Vilaivan, T. Solid phase synthesis of novel peptide nucleic acids. *J. Chem. Soc., Perkin Trans I* **1997**, 555-560. (b) Lowe, G.; Vilaivan, T.; Westwell, M. S. Hybridization studies with chiral peptide nucleic acids. *Bioorg. Chem.* **1997,** *25*, 321-329 (c) Vilaivan, T.; Khongdeesameor, C.; Harnyuttanokam, P.; Lowe, G. Synthesis and properties of novel pyrrolidinyl PNA carrying β amino acid spacers. *Tetrahedron Lett.* **2001**, *42*, 5533-5536. (d) (d) Hickman, D. T.; Samuel, T.; Morral, J. King, P. M.; Cooper, M. A.; Mickelfield, J. Design, synthesis, conformational analysis and nucleic acid

hybridization properties of thymidyl pyrrolidine-oligonucleotide mimics (POM) *Org. Biomol. Chem*. **2003**, *1*, 3277-3292. (e) Gangamani, B. P.; Kumar, V. A.; Ganesh, K. N. Chiral analogues of peptide nucleic acids:synthesis of 4-aminoprolyl nucleic acids and DNA complementation studies using UV-CD spectroscopy. *Tetrahedron* **1999**, *55*, 177-192.

34. Wittung, P.; Nielsen, P. E.; Norden, B., Observation of a PNA-PNA-PNA Triplex *J. Am. Chem. Soc*. **1997,** *119*, 3189-3190.
35. Riccelli, P. V.; Hall, T. S.; Pancoska, P.; Mandell, K. E.; Benight, A. S. DNA sequence context and multiplex hybridization reactions: melting studies of heteromorphic duplex DNA complexes. *J. Am. Chem. Soc*. **2003**, *125*, 141-50.
36. Lowe, G.; Vilaivan, T. A novel pyrrolidinyl PNA showing hi gh sequence specificity and preferential binding to DNA over RNA. *J. Am. Chem. Soc*. **2002**, *124*, 9326-9327.
37. Puschl, A.; Boesn, G.; Zuccarello, G.; Dahl, O.; Pitsch, S.; Nielsen, P. E. Synthesis of pyrrolidinone PNA: A novel conformationally restricted peptide nucleic acid analogues. *J. Org. Chem.* **2001**, *66*, 707-712.
38. (a) Kim, S. K., Nielsen, P. E., Egholm, M., Buchardt, O., Berg, R. H., and Norde´n, B. (1993) Right-handed triplex formed between peptide nucleic acid PNA-T8 and poly(dA) shown by linear and circular dichroism spectroscopy. *J. Am. Chem. Soc.* **1993**, *115*, 6477–6481. (b) Tedeschi, T.; Sforza, S.; Dossena, A.; Corradini, R.; Marchelli.; R. Lysine-based peptide nucleic acids (PNAs) with strong chiral constraint: control of helix handedness and DNA binding by chirality. *Chirality* **2005**, *17 Suppl*, S196-204.
39. (a) Porath, J.; Flodin, P.; Gel Filtration: A method for desalting and group separation. *Nature*, **1959**, *183*, 1657–1659. (b) Gel Filtration: Principles and Methods, 7:th edition, Pharmacia Biotech, **1997**.

4.10 APPENDIX

1. HPLC of PNA **36**, **37, 38** and **45**

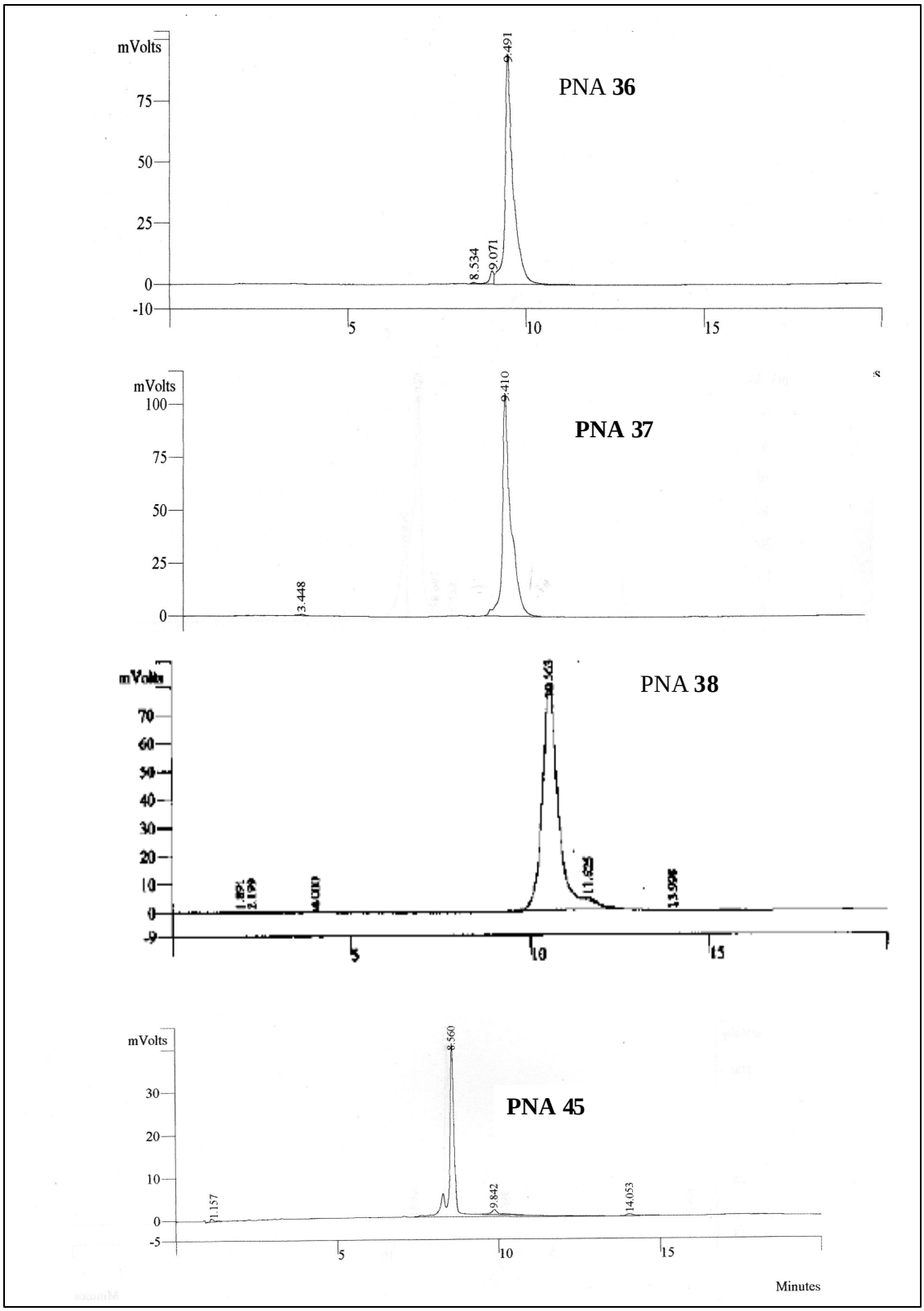

2. HPLC of PNA **46, 51** and **58**

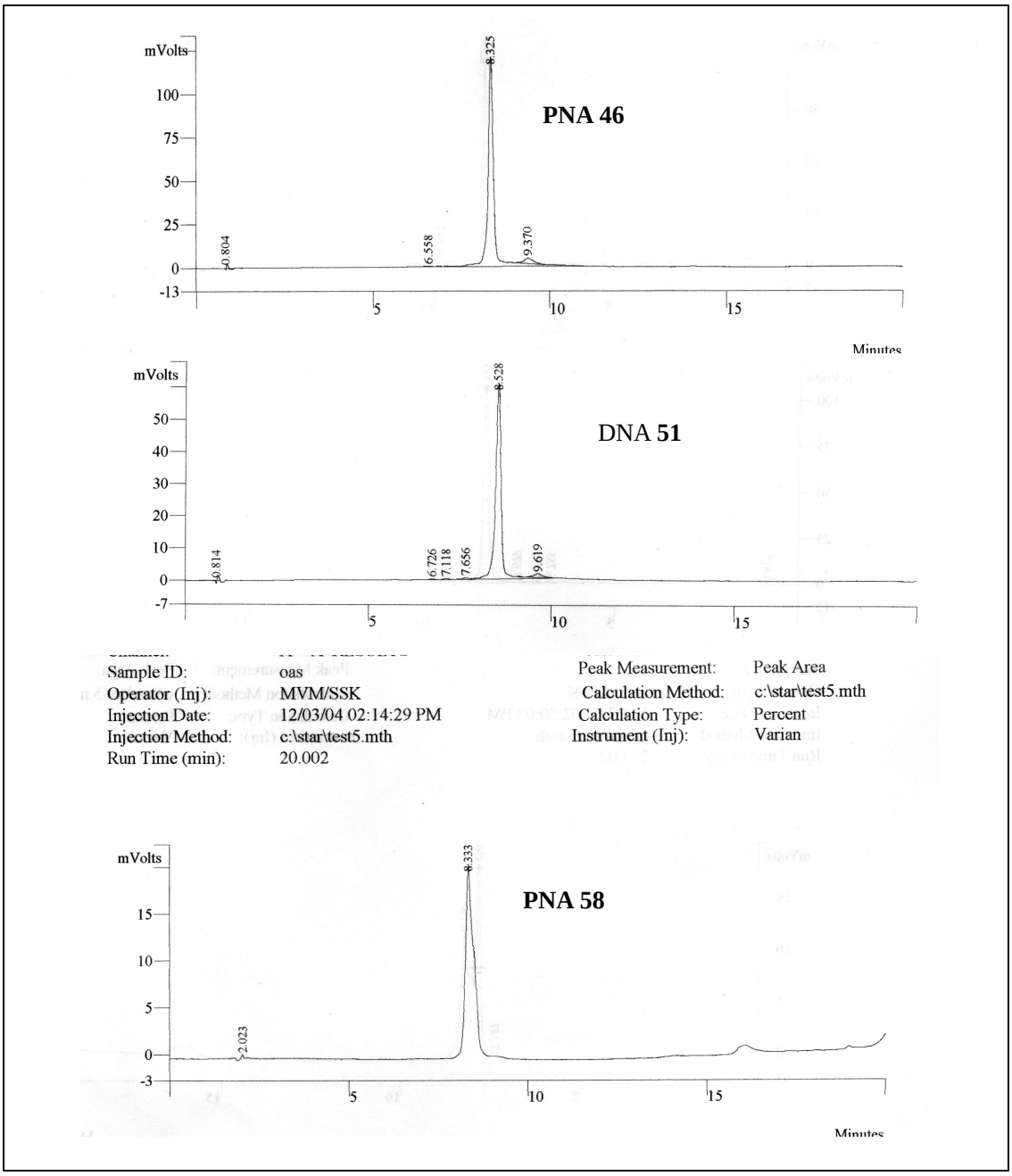

3. HPLC of DNA **67-69**

Method Notes
COLUMN-HP C18,125 x 4 mm ID ,5 micron.
MOBILE PHASE-A=5%ACN IN 0.1M TEAA , B=30%ACN IN 0.1MTEAA , A TO B IN 20 MINS.
FLOW 1.5 ML/MIN
DETECTOR-UV AT 254NM

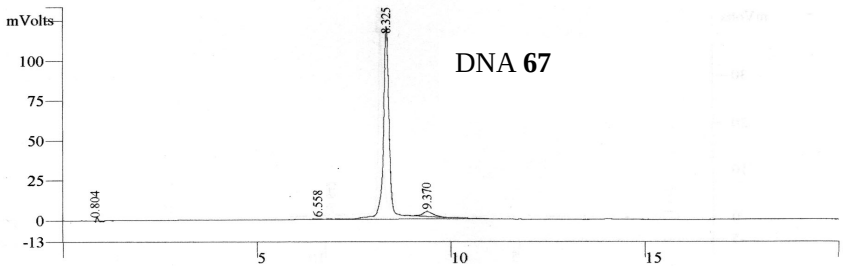

DNA **67**

Method Notes
COLUMN-HP C18,125 x 4 mm ID ,5 micron.
MOBILE PHASE-A=5%ACN IN 0.1M TEAA , B=30%ACN IN 0.1MTEAA , A TO B IN 20 MINS.
FLOW 1.5 ML/MIN
DETECTOR-UV AT 254NM

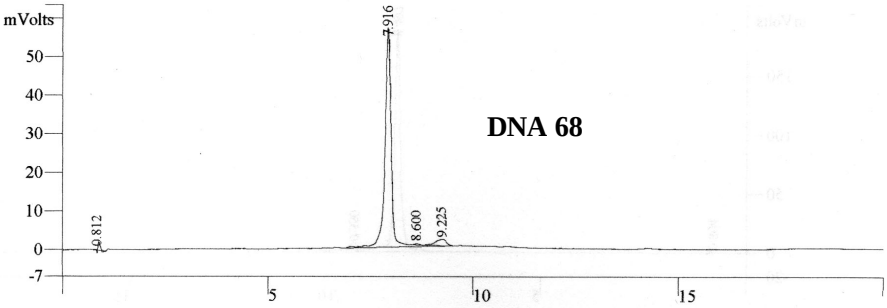

DNA 68

Peak No	Result ()	Ret Time (min)	Peak Area (counts)	Width 1/2 (sec)

Method Notes
COLUMN-HP C18,125 x 4 mm ID ,5 micron.
MOBILE PHASE-A=5%ACN IN 0.1M TEAA , B=30%ACN IN 0.1MTEAA , A TO B IN 20 MINS.
FLOW 1.5 ML/MIN
DETECTOR-UV AT 254NM

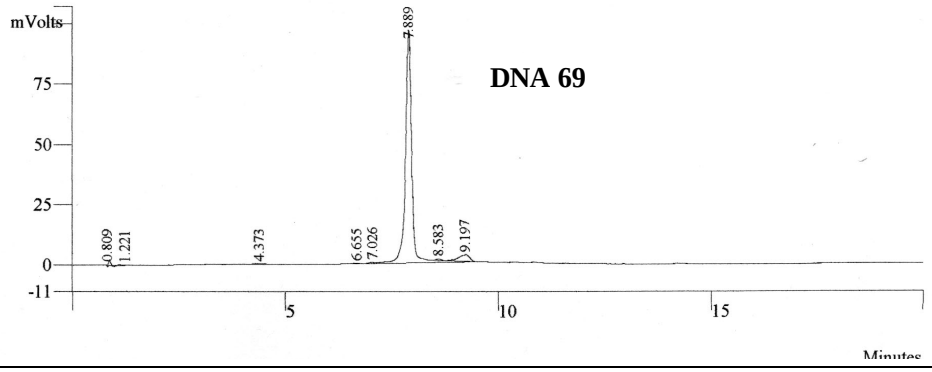

DNA 69

4. MALDI-TOF Mass Spectra of PNA **35** and **37**

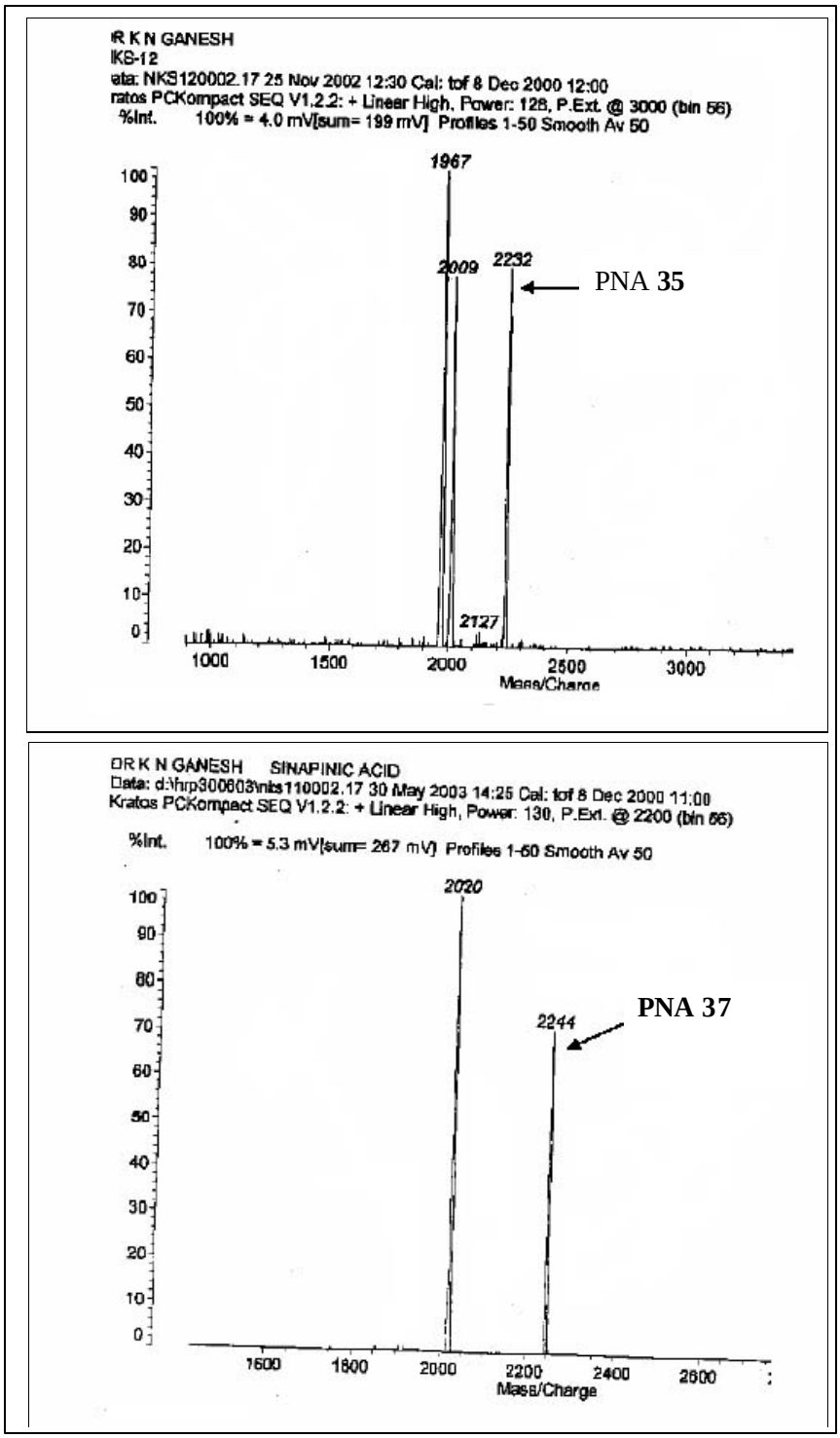

5. MALDI TOF-Mass spectra of PNA **38, 41** and **42**

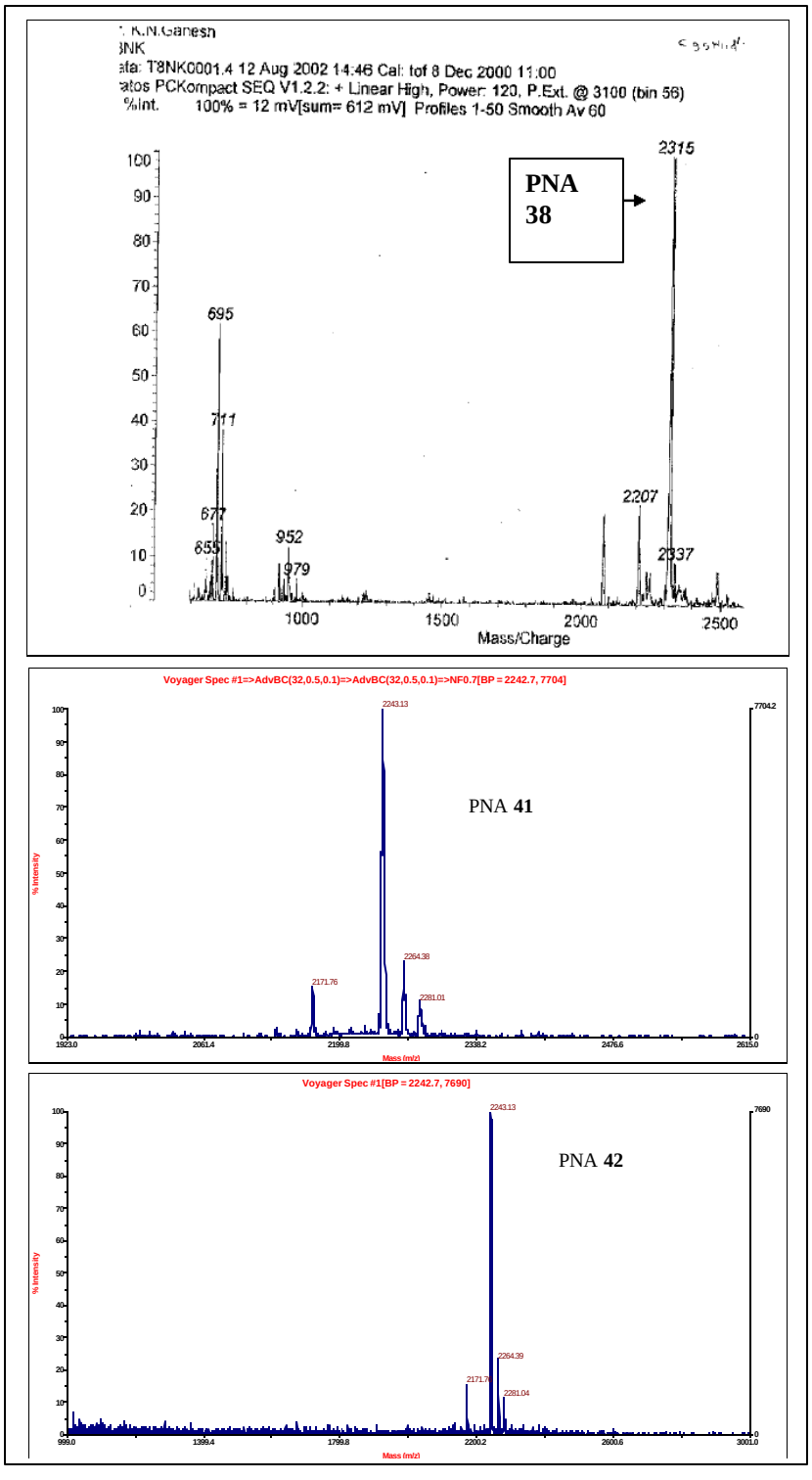

6. MALDI TOF-Mass spectra of PNA **50** and

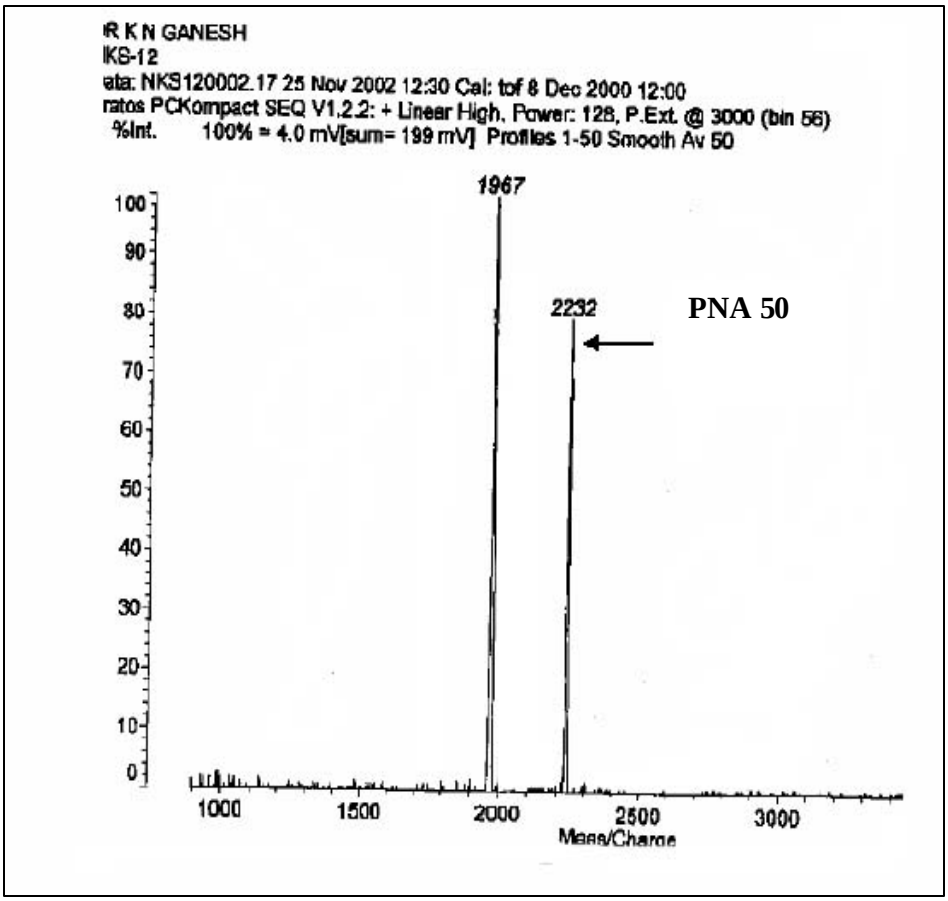

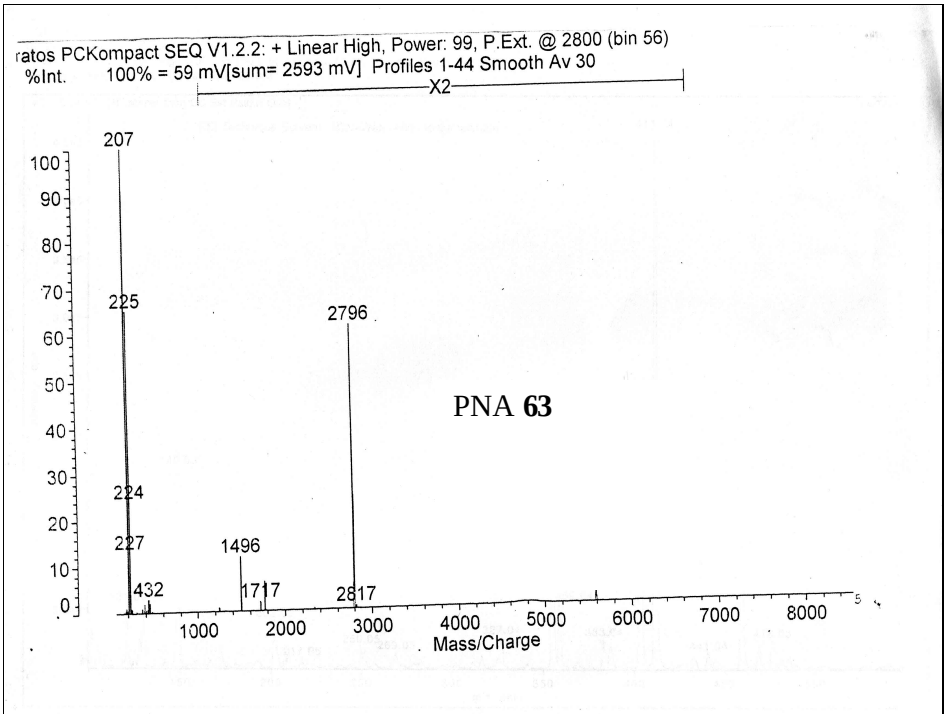

CHAPTER 5

CHAPTER 5A: PNA TETRAPLEXES: BIOPHYSICAL STUDIES OF G-TETRAD OF *aep*-PNA

CHAPTER 5B: PNA TETRAPLEXES: BIOPHYSICAL STUDIES OF *i*-MOTIF OF *aeg*-PNA

CHAPTER 5B

PNA TETRAPLEXES: BIOPHYSICAL STUDIES OF *i*-MOTIF OF *aeg*-PNA

CHAPTER 5A: PNA TETRAPLEXES: BIOPHYSICAL STUDIES OF G-TETRAD OF *aep*-PNA

5A.1 INTRODUCTION

Nucleic acids are versatile in forming self-assembled structures. One of the most important class of these are the quadruplexes, specifically derived from self association of G-bases observed in DNA/RNA telomeres (Figure 1a).[1-3] Telomere is a repeating structure in DNA sequences associated with proteins at the termini of eukaryotic chromosomes (Figure 1b)[4] and has an important role in replication of the end regions of the chromosomes within the cell nucleus. The basic structure of telomeres is formed by repeated occurrence of G nucleotides of DNA.[5] The guanine-rich sequences of DNA are known to have an ability to form G-tetrads leading to four-stranded secondary structure.[6] The inventory of sequences forming telomeric structures correspond to d(TTTTGGGG), d(TTGGGG) and d(TTAGGG) present in sequences from *Oxytrieha, Tetrahymena,* and *humans* respectively.[7] The regular short repeat sequences leading to G-quadruplexes of DNA fall into the general motif d(T_3-(T/A)-G_{3-4}).[8]

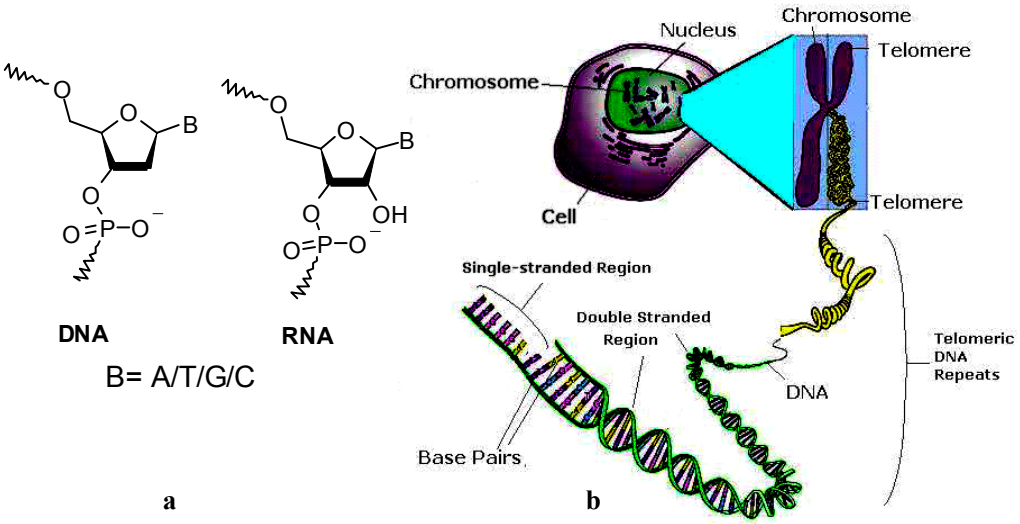

Figure 1: (a) Chemical structure of DNA and RNA. (b) Typical structure of cell nucleus.[6c]

The secondary structural inventory of DNA related to or derived from Watson-Crick base-pairing include structures such as hairpins and cruciforms.[9] Higher order DNA structures such as triplexes and quadruplexes are stabilized by cyclic Hoogsteen (HG) hydrogen bonding arising from association of four guanines (Figure 2).[10] It is reported that the G-rich sequences in DNA may adopt non-B folded, quadruplex structures shown in Figure 2 in the presence of monovalent ions (K^+, Na^+ etc) at physiological conditions.[11] The crystal structure of DNA sequence 5′-TGGGGT-3′, corresponding to telomere of *Tetrahymena*, was shown to form parallel stranded G-tetrads in presence of Na^+, Ca^+, K^+ or Tl^+ in crystals and in solution.[12]

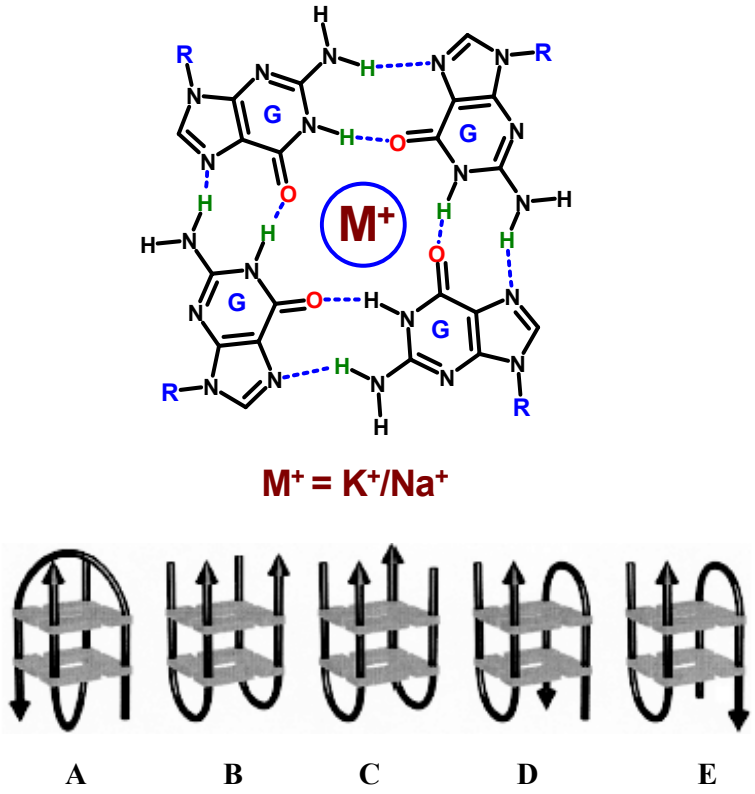

Figure 2: *above*: Hydrogen pattern in G-tetrad and a monovalent cation (Na^+/K^+) occupies the central position. *below*: (A) Diagonal loops; (B) Two parallel edgewise loops. (C) Two antiparallel edgewise loops; (D) Adjacent parallel strands with edgewise loops; (E) Alternating antiparallel strands with edgewise loops.[17]

Like DNA, the elements of G-tetrad formation are also evident in RNA. For example, RNA G-tetrad structure is observed in filamentous *bacteriaphage fd*.[13] Recently, the fragile X mental retardation protein (FMRP) has been shown to bind RNA structures formed by G-tetrads.[14] The RNA tetrads of $r(UGGGGU)_4$ also form parallel stranded structures like DNA in presence of Sr^{+}.[15] The G-repetitive units in long sequences of DNA give different types of folded tetraplex structures. Folding topology of G-tetrads in solution critically depends on the number of G-rich repetitive units, the nature of sequence and the concentration of metal ions. The well-established folding topology in DNA G-quadruplexes are given in Figure 2 as (A) diagonal loops protruding on either side of the guanine tetrad core, (B) two parallel edgewise loops protruding on the same side, (C) two antiparallel edgewise loops protruding on the same side, (D) adjacent parallel strands with edgewise loops protruding on opposite sides and (E) alternating antiparallel strands with edgewise loops protruding on opposite sides.[15]

5A.1.1 Characterization of G-tetrad formation in DNA

The G-tetrad structures of DNA are very much important in biology. A number of techniques and established methodologies have been applied to characterize their structures. These include chemical probing, NMR, crystallography, circular dichroism, Raman spectroscopy, gel electrophoresis, ultraviolet absorption and ESI-mass spectroscopy and are widely used to characterize the G-tetrad formed structures in nucleic acids.

5A.1.1a Chemical and Enzymatic Probes

Chemical and enzymatic probes are useful tools for the study of telomeric DNAs. The guanine base in a G-quartet is nearly saturated with hydrogen bonds, and therefore the G-quartet structure is particularly sensitive to these types of perturbations. In the absence

of detailed NMR or crystallographic data, chemical probing methods offer the best diagnostic evidence for G-quartet formation.

(1) *Nuclease Sensitivity*. The G-quartet structures are resistant to hydrolysis by both endo- and exo-nucleases.[16]

(2) *UV Crosslinking*. The ultraviolet light (UV)-induced covalent crosslinking of thymines is characteristic of the folded G-quartet form. Thymidine residues from different repeats brought into proximity by folded structures may be detected via photo crosslinking to form T-T dimers by 2+2 cycloaddition.[17]

(3) *Chemical Protection*. The most characteristic signature of G-quartet formation is the strong steric protection conferred by the structure to methylation of the guanine N7 by dimethyl sulfate (DMS). This is caused by their involvement in hydrogen bonds. Thus DMS can used to distinguish telomeric and non-telomeric G-rich DNA sequences. N7 of guanines in G-quartet are also resistant to chemical modification by diethylpyrocarbonate (DEPC).[18]

5A.1.1b Nuclear Magnetic Resonance

Nuclear magnetic resonance (NMR) is an invaluable tool for the study of nucleic acid structures and enables elucidation of folded conformations. Initial NMR studies of telomeric DNA sequences did not provide detailed structural information except indicating the presence of unusual structures. The NMR study of $d(TTGGGG)_4$ revealed the presence of nonstandard G-G base pairs and the existence of guanines in the unusual *syn* conformation.[19] Th first detailed NMR study of a G-quartet structure was done on the oligomer d(GGTTTTTGG), which was shown to form a tetramolecular complex by calorimetric analysis.[20] The significant finding of these studies was that the glycosidic torsion angle alternated between *syn* and *anti* for each adjacent pair of Gs along the strand (Figure 3). Such alternation of glycosidic torsion angles was also observed in the similar

sequence d(GGTTTTCGG).[21] The second significant result from NMR studies of d(GGTTTTTGG) was the existence of multiple conformers that were in slow exchange on the NMR timescale. Qualitative NMR studies also revealed that the nature of the tetraplexes formed by telomeric DNAs differed according to the presence of Na^+ or K^+ as the counterion[22] and that the stability of the structures depended on the monovalent cation present. Both $d(TTGGGG)_4$ and $d(TTAGGG)_4$ were studied in Na^+-phosphate or K^+-phosphate buffers and showed a complexity of the imino proton spectrum indicating presence of multiple species at the high substrate concentrations required for NMR studies.[23] The imino proton spectrum was markedly different for both oligomers in Na^+ and K^+ buffers. Temperature dependent imino proton spectra also revealed that the K^+ quadruplex were more stable than the Na^+ tetraplexes with imino protons still observable for the K^+ quadruplex of d $(TTGGGG)_4$ even at 90 °C.

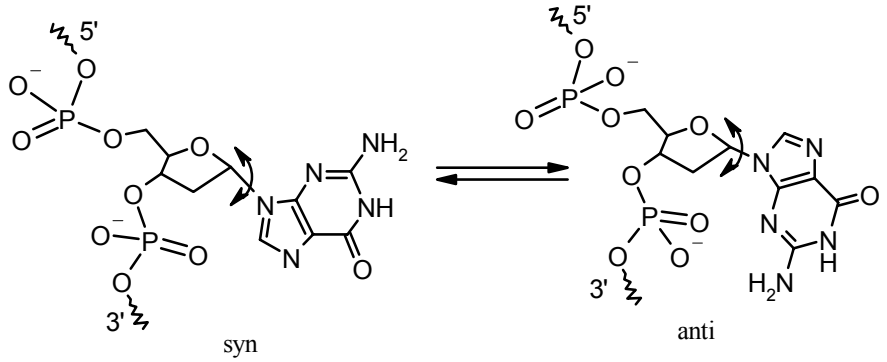

Figure 3: *Syn* and *anti* conformation of nucleoside

5A.1.1c X-Ray Crystallography

X-ray crystallographic analysis of d(GGGGTTTTGGGG) supported the general features postulated for the G-quartet core structure.[24] The glycosidic torsion angles alternate *syn-anti-syn-anti* along the strand and around in any given G-quartet. The thymidine loops are located on opposite ends of the G-quartet core in head-to-tail fashion,

unlike the structure suggested by NMR. The crystal structure exposes the detail structural features in G-quartets, which are difficult to observe with NMR. It was seen that the base geometry is often distorted from the ideal square planar arrangement of guanines that are somewhat buckled out of the plane of the G-quartet. The crystal structure of DNA sequence 5′-TGGGT-3′, corresponding to telomere of *Tetrahymena* was shown to form parallel stranded G-tetrads in presence of Na^+, Ca^+, K^+ or Tl^+ in crystals and in solution (Figure 4).[26]The central channel of this entities have also shown the considerable charge density resulting from bound potassium ion located between the second and third G-quartets at the center of the core structure.

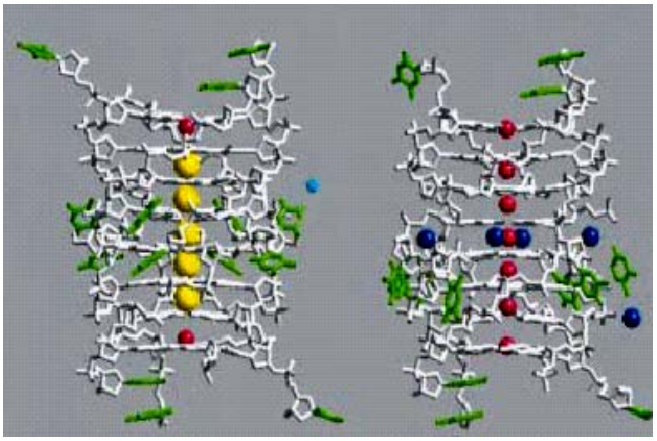

Figure 4: Crystal structure of d(TG_4T) in presence of monovalent ion.[26]

5A.1.2 Polymorphism in DNA G-quartet

The contrast between the structures derived from X-ray crystallography and NMR spectroscopy for the same oligomeric sequence adequately illustrated polymorphic nature of telomeric DNAs. The numerous structures possible for telomeric DNAs make it difficult to determine a priori, as to which of these structures are formed under a given set of conditions. The interesting aspect of telomeric DNA structures is that the same bases can be assembled in many different ways with similar basic hydrogen-bonding structures

and this flexibility lead to polymorphism in telomeric DNA. The following classes of polymorphism are observed in DNA (Figure 5a-d).

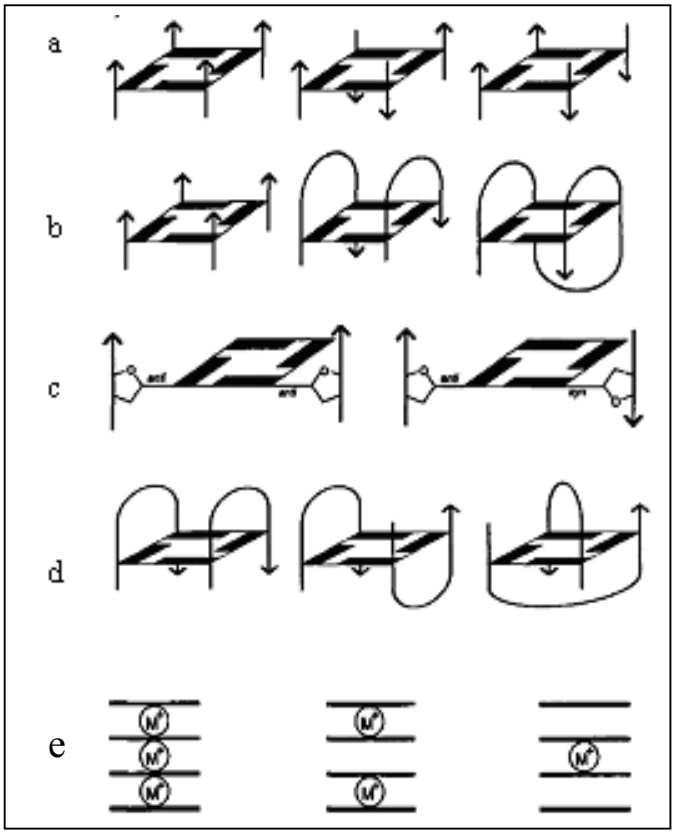

Figure 5: Geometry arrangement of polymorphism; (a) Parallel vs Antiparallel Strands; (b) Strand Stoichiometry; (c) Glycosidic Conformation; (d) Loop Geometry; (e) Ion-Binding. [9]

***(1) Parallel vs Antiparallel Strands*:** One fundamental source of structural variation is the possibility of forming different G-quartets in which the strands have different polarities. Four strands can come together in a tetrameric complex in at least three different ways as shown in Figure 5a.[27]There are two permutations: all four strands can be parallel or two parallel-two antiparallel strands. In principle, three parallel strands and one *anti*-parallel strand could form a tetraplex, but this type of structure has not yet been observed. G-

quartet structures can be formed with the relative arrangement of adjacent backbones that are all parallel, alternate with antiparallel, or adjacent antiparallel combination.[27]

(2) ***Strand Stoichiometry***: The same oligomer can form different types of structures by association of one or more molecules. For example, a telomeric DNA sequence containing four repeats can form an intramolecular quadruplex, a dimer, or a telomeric quadruplex, as shown in Figure 5b.[27] This type of polymorphism depends on the concentration of the DNA. Representative members for each of these three classes have been characterized structurally and are illustrated in Figure 5b. Thus, the association of one, two or four strands can form G-quartet structures.

(3) ***Glycosidic Conformation***: Guanines in G-quartets are observed in both *syn* and *anti* conformation. In principle, a string of four G residues can adopt different combinations of glycosidic conformations. The only observed patterns thus far are *all-anti* and alternating *syn-anti.* Guanines involved in the same quartet that are on parallel strands have the same glycosidic torsion, while guanines on antiparallel strands have opposite glycosidic torsions, as illustrated in Figure 5c.[28] The glycosidic conformation changes the relative orientations of the bases on adjacent G-quartets, and thus can affect the stacking energy between G-quartets. Thus adjacent Gs in the same G-quartet can have the same or the opposite glycosidic torsion angle depending on whether their constituent strands are parallel or antiparallel.

(4) ***Loop Geometry***: Depending on whether the G-quartet formation is unimolecular or bimolecular, the G-strings can be connected by a variety of combinations of loop crossings. For example, in dimeric species, loops can join adjacent or diagonal strands, with the two loops oriented in a head-to-tail or head-to-head fashion. Figure 5d[29] illustrates these types of polymorphism.

(5) ***Ion-Binding Geometry***: The metal ions may interact with the G-quartet structures in different ways and with different stoichiometries. The ion binding geometry is known from its crystal structure with certainty only for d(GGGGTTTTGGGG) in the potassium (K^+) form,. The electron density for the positive ion is found in between the second and third G-quartet levels. Other ion stoichiometries are possible, with ions binding to every G-quartet, or to every other G-quartet, as shown in Figure 5e.[30]

5A.1.3 Nondenaturing electrophoresis

Nondenaturing polyacrylamide gel is used for the separation and purification of fragments of double-stranded DNA while *denaturing polyacrylamide gel* is used for the separation and purification of single stranded fragments of DNA.[31] Nondenaturing (native) gel electrophoresis is a simple but powerful method for the analysis of telomeric DNA structures. Electrophoretic mobility is dependent on the size, shape, and charge of the molecule as it passes through the gel matrix. In denaturing gels, DNA fragments exist primarily as single strands that migrate according to their molecular weights. In nondenaturing gels, DNA fragments that adopt particular structures migrate differently from single stranded DNAs of the same length. This technique is therefore useful for distinguishing different topological structures adopted by oligonucleotides such as multiple or oligomeric structures and ion dependent structures and these are also temperature dependent.

***Assay for Structure formation*:** Unusual gel mobilities were obtained for telomeric DNA structure. Multimerization of telomeric DNA sequence occurs by interaction of the terminal fragments, and the stability of the oligomers formed depends strongly on whether Na^+ or K^+ is present. Different telomeric oligonucleotides assume compact high mobility forms on native gels[22] at low temperatures (5 °C). In contrast, oligonucleotides from telomeric C-strands, or oligonucleotides without G-strings, did not form such high

mobility species. This simple assay is routinely used for analysing structures in telomeric DNA sequences.

Assay for multiple or oligomeric structures: Native gels are particularly useful for detection of multiple species in an oligonucleotide, due to alternate conformers or higher-order structures. Telomeric DNAs are polymorphic in that they form both multiple conformers and oligomeric species. Alternate conformers typically have similar, yet distinct, mobilities, while dimers and other structures exhibit quite different mobilities. G-quartet structures, frequently detected as thermodynamic mixtures of forms by native gel electrophoresis can be formed by dimerization or tetramerization of oligonucleotides.[31] Also, higher-order structures formed by the end-to-end association of quadruplexes has been studied by using native gels.[32]

Strand stoichiometry: A simple and elegant method for determining the stoichiometry of a complex involves mixing oligonucleotides that have tails of different lengths that do not perturb the ability to form G-quartet structures. If equimolar amounts of an oligonucleotide "A" are mixed with oligonucleotide "B", then the stoichiometry of a given complex can be determined from the number of mixed species (dimers "AA", "AB" and "BB" and tetramers "AAAA", "AAAB", "AABB", "ABBB", and "BBBB") that are produced. This simple technique has been used to demonstrate dimer formation by telomeric oligonucleotides[33] and tetramer formation in nontelomeric and telomeric oligonucleotides.[34]

Ion-dependent structure formation: Telomeric DNAs exhibit a strong preference for binding certain cations. Consequently, the counterion used in a native gel experiment can change the stability of structured forms. Dimerization of macronuclear DNA from *Oxytricha* is preferentially stabilized by K^+ in native gels.[35] *Oxytricha* telomeric oligonucleotides do not form a structure in the absence of added counterions or in the

presence of Li^+ but readily form a structure in the presence of Na^+ or K^+ added to the gel running buffer. K^+ stabilized the quadruplex formed by r(UGGGGU) better than Na^+, and Sr_2^+ also stabilizes quadruplex formation.[36]

***Temperature dependent structure formation*:** Because the dissociation of G-quartet structures is often slow, native gels can be used to monitor the temperature dependence of structure formation. *Oxytricha* telomeric DNA dimers are stable in K^+ up to 70 °C. Gels run at different temperatures have been used to compare the relative stabilities of a set of related sequences or simply to monitor structure formation.[27]

5A.1.4 Thermal denaturation by UV and CD spectroscopy

5A.1.4a UV-Spectra

The UV spectra of telomeric DNAs typically exhibit two overlapping peaks in the 260 to 280 nm range. Characteristic absorption changes are observed upon folding of telomeric DNAs. The absorbance at 275 nm typically decreases by ~10%, and the absorbance at 295 nm increases by ~100%.[38] Consequently, these wavelengths can be used to monitor folding or unfolding processes.

Several studies have used thermal denaturation monitored by changes in UV or CD to obtain thermodynamic information on telomeric DNAs. In general, telomeric sequences are very stable, and their stability depends strongly on the monovalent cation present and the nature of sequence.[39] Telomeric DNA sequences also undergo slow folding and unfolding kinetics and this presents experimental difficulties in optimizing conditions and comparing results. The parallel quadruplexes formed by d(TTTTGGG) in solution are extremely stable, with a $\Delta G°$ of -47 kcal/mol at 25 °C. In contrast, the quadruplex formed by d (TGGGT) exhibits a $\Delta G°$ of - 7 kcal/mol.[40] The main difference between these two

sequences is the presence of a 3' terminal T residue that can greatly affect the stability of the quadruplex structure. The difference in stability of a parallel and antiparallel hairpin dimer structure adopted by same sequences has been determined using thermal denaturation. The antiparallel structure formed by d(GGGGTTTTGGGG) is -5 kcal/mol less stable than the parallel structure adopted by d(3′-GGGGTT-5′-5′-TTGGGG-3′).[41] This difference represents the net change between forcing glycosidic torsion angles to the *syn* conformation, the differential stacking and ionic interaction energies in the two structures.

5A.1.4c CD-Spectra

The circular dichroism (CD) spectra of telomeric DNAs are very much dependent on the conformation and sensitive to base stacking geometry. Two basic forms of CD spectra are typically observed for telomeric DNAs: type 1 with a positive CD band at 265 nm and a negative band at 240 nm and type II showing a positive band at 295 nm and a negative band at 260 nm.[42] The two types of CD spectra are strongly correlated to the conformation of the G-quartet core. The parallel quadruplex structure formed by d(3'-GGGGTT-5') where all guanines are in the *anti* conformation exhibits a type I CD spectrum.[43] The antiparallel quadruplex formed by d(GGGGTTTTGGGG) where the guanines have alternate *syn-anti* conformation exhibits a type II CD spectrum.[44] Presence of multiple conformations and mixture of parallel and antiparallel quadruplexes often make it difficult to assign structures by CD data alone.

5A.1.5 Application of quadruplexes

Quadruplex structural motif is adopted by the chromosome telomeres, immunoglobulin switch region and regulatory region of oncogenes.[45] Thus the G-quadruplex is seen as a promising target for anticancer drug design with ever-increasing

discoveries of G-quadruplex structure binding proteins, such as human DNA topoisomerase I, BLM (Bloom's syndrome protein), WRN (Werner's syndrome protein), in the *Recq* family of helicases, SV40 large tumor antigen helicase and so forth.[46] The novel supramolecular architecture of G-quartets has also led to the development of interesting and functional non-covalent assemblies such as G-wire, ion-channels and self-assembled ionophores.[47] In recent years, considerable efforts have been directed towards the synthesis and investigation of new DNA analogs with improved binding properties with nucleic acids other than the natural canonical counterparts. Search for more stable quadruplexes from modified analogs compared to natural DNA may also help in understanding the complex mechanism of quadruplex formation.

5A.2 RATIONALE AND OBJECTIVE OF PRESENT WORK

The quadruplex formation by many modified oligonucleotides,[48] for examples LNA[49] (Locked Nucleic acid) and PNA[50-52] have been well studied. Since, PNA was developed to mimic Watson-Crick and Hoogsteen base pairing, they also ideally participate in G-quartet formation in mainly two-ways: (1) G-rich PNAs forming hybrid quadruplexes alone or in presence of DNA templates and (2) Self-assembly of G-rich sequences of PNA-DNA chimeras. Armitage, *et. al*.[53] have discussed the formation of PNA_2-DNA_2 hybrid quadruplexes by strand invasion and overhang effect. The quadruplex formation by PNA-DNA chimeras – $^{5'}$TGGG$^{3'}$-t, $^{5'}$TGG$^{3'}$-gt, t-$^{5'}$GGGT$^{3'}$ and tg-5'GGT3' where lower and upper case letters indicate PNA and DNA residues respectively, have been reported.[54] Recently, TG_3 homo oligomer PNA was also shown to form quadruplex at pH 7.4 in presence of cations[55] by electrospray ionization mass spectrometry (ESI-MS)[55] and confirmed by ^{1}H NMR and thermal stability measurements by UV absorbance change at 305 nm with temperature experiment.

During previous studies of PNA properties by chemical modification in this laboratory, the aminoethyl prolyl (*aep*) PNA[56] emerged as one of the useful analogues (Figure 6). This PNA analog is positively charged and has constrained chiral backbone as a ring, instead of the linear achiral backbone of *aeg*-PNA (Figure 6).[57] This part of the Chapter describes the tetraplexing properties in G-rich sequences of *aeg*-*aep* mixed backbone and *aep*-PNA oligomers to understand the effect of chirality and conformational rigidity on the tetraplexing stability of PNA.

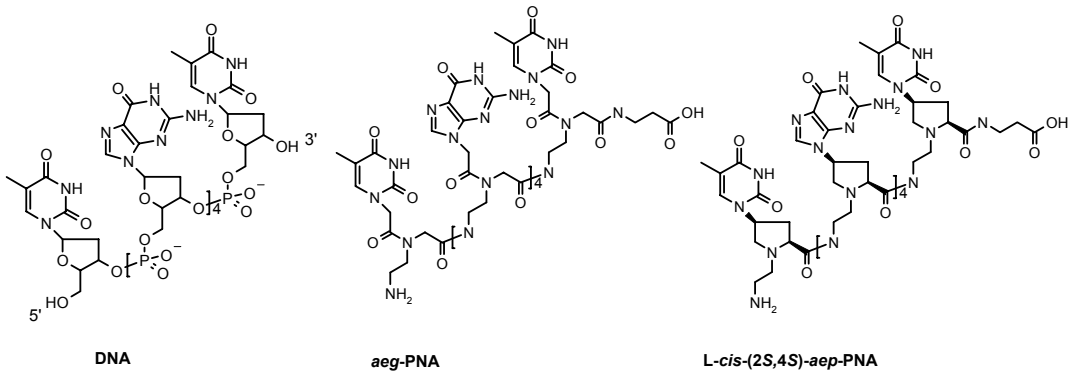

Figure 6: Chemical configuration of DNA *aeg*-PNA and *aep*-PNA in TG_4T

The specific objectives of this chapter are

(i) Synthesis of T and G monomers of L-*cis*-(2S,4S)-*aep*-PNA and *aeg*-PNA.

(ii) Synthesis of G-rich sequences of *aep*- and *aeg*-PNA oligomers

(iii) Comparative study of G-tetrad forming properties in *aep*-PNA, *aeg*-PNA and DNA (figure 6).

5A.3 PRESENT WORK

5A.3.1 Synthesis of *aep*-PNA-(T/G) monomers

1-(N-Boc-aminoethyl)-4*S*-(N3-benzoylthymine-1-yl)-2*S*-proline methyl ester **8** was synthesized from 4*R*-hydroxy compound **6** by N1-alkylation of N3-Benzoyl protected thymine at C-4 of prolyl ring under Mitsunobu reaction conditions as described brfore

(Scheme 1). The reaction was accompanied by inversion at C4 lead to the 4*S* isomer. The ester compound **8** upon treatment with NaOH in aqueous methanol for 24h got hydrolysed with the cleavage of the N3-benzoyl group. Neutralization of the excess alkali with Dowex 50 H^+ and work-up gave 1-*N*-(Boc-aminoethyl)-4*S*-(N3-benzoylthymine-1-yl)-2*S*-proline carboxylic acid **9** in quantitative yield.

1-*N*-(Boc-aminoethyl)-4*S*-(2-amino-6-chloropurine-9-yl)-2*S*-proline methyl ester **11** was prepared by N9-alkylation of 2-amino-6-chloropurine with 1-*N*-(Boc-aminoethy)-4*R*-(*O*-mesyl)-2*S*-proline methyl ester compound **10** in presence of base (K_2CO_3) and catalytic amount 18-crown-6 in DMF by as reported procdure.[57]

The aminoethyprolyl (*aep*) guanine monomer **12** was obtained by simultaneous hydrolysis and oxidation of 1-*N*-(Boc-aminoethyl)-4*S*-(2-amino-6-chloropurine-9-yl)-2S-proline methyl ester **11** using NaOH in aqueous methanol. The initial ester hydrolysis was

Scheme 1: Synthesis of *aep*-PNA-(T/G) monomers

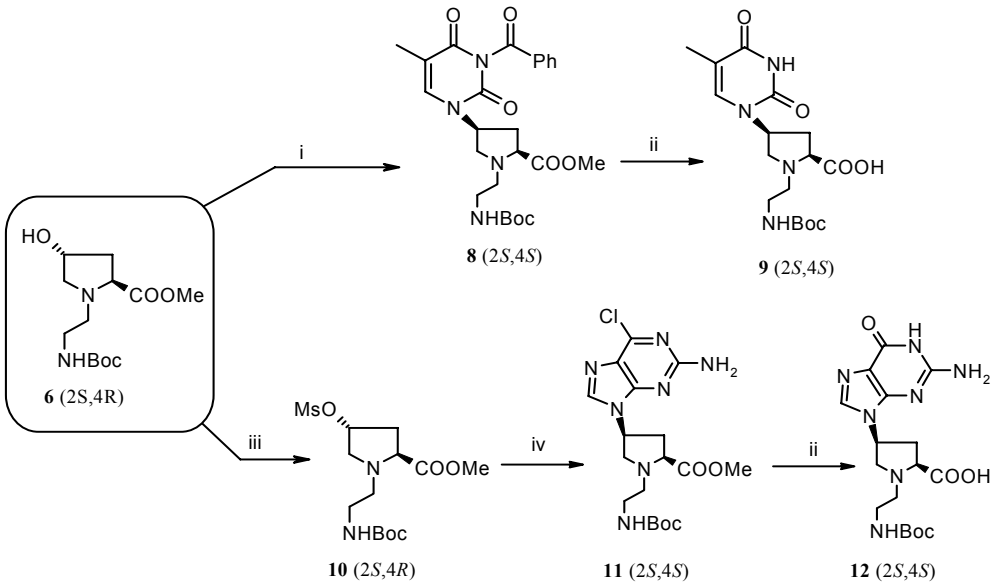

Reagents: (i) N3-Bz-Thymine, DIAD, PPh_3, dry THF, 55%.; (ii) 1N NaOH, CH_3OH:H_2O (1:1) overnight, 90%.; (iii) $MeSO_2Cl$, dry Et_3N, dry DCM, 0 ^{0}C, 3 hr, 80%.; (iv) 2-Amino-6-chloropurine, K_2CO_3, 18-crown-6, DMF, 70^{0}C, overnight, 65%.

completed within 10 minutes, followed by complete conversion of the 6-chloro to the 6-oxo-function after 75h (Scheme 1).

The *N*-(Boc-aminoethyl)-(thymin-1-yl)-glycine (T) and N-(Boc-aminoethyl)-(guanin-9-yl)-glycine (G) monomer (Figure 7) were synthesized from reported procedures (see chapter 2).

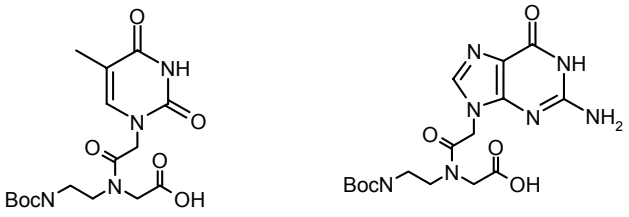

aeg-Thymine (T) *aeg*-Guanine (G)

Figure 7: Chemical structure of *aeg*-PNA

5A.3.2 Synthesis of *aep*-PNA and *aeg*-PNA oligomers

The syntheisis of following PNA oligomers was carried out by solid phase synthesis method following Boc-Chemisty of peptide synthesis.

1. H_2N-T-G-G-G-G-T-*β*-ala-MF
2. H_2N-T-G-G-G-G-G-*β*-ala-MF
3. H_2N-T-G-G-g-G-T-*β*-ala-MF
4. H_2N-T-G-G-G-G-t-*β*-ala-MF
5. H_2N-t-g-g-g-g-t-*β*-ala-MF
6. H_2N-t-g-g-g-g-*β*-ala-MF
7. H_2N-t-g-g-g-*β*-ala-MF
8. H_2N-t-g-g-*β*-ala-MF
9. H_2N-t-g-*β*-ala-MF

[a] G, T = *aeg*-PNA; g, t = L-*cis*-(2*S*,4*S*)-*aep*-PNA and MF=Merrifield resin.

The *aep*-PNA oligomers were cleaved from the solid support using TFMSA to yeild oligomers with 'C' terminal carboxylic acids. The cleaved oligomers were initially desalted by size exclusion chromatography over G25 sephadex and subsequently purified by FPLC on a reverrse phase C column. The purity of the oligomers was re-checked by reverse phase analytical HPLC on C18 column and confirmed by MALDI-TOF and ESI

mass spectrometry. Some representative HPLC profiles and mass spectra are shown in appendix.

5A.3.3 Characterization of PNA

The pure oligomers PNA **1-9** were characterized by MALDI-TOF and ESI mass spectroscopy and their spectral data is given in Table 1.

Table 1: *aeg*-PNA and L-*cis*-(2*S*,4*S*)-*aep*-PNA sequences.[a]

PNA/DNA	Sequences PNA/DNA	Molecular Formula	Calculated Molecular Mass	Observed Mass
1	H_2N-T-G-G-G-G-T-*β*-ala	$C_{69}H_{87}N_{37}O_{22}$	1786.70	3664.03, 2469.36, 2096, 1299.36
2	H_2N-T-G-G-G-G-*β-ala*	$C_{58}H_{74}N_{32}O_{19}$	1520.58	1520.40
3	H_2N-T-G-G-g-G-T-*β-ala*	$C_{70}H_{89}N_{37}O_{21}$	1784.73	1787.70
4	H_2N-T-G-G-G-G-t-*β-ala*	$C_{70}H_{89}N_{37}O_{21}$	1784.73	1786.20
5	H_2N-t-g-g-g-g-t-*β-ala*	$C_{75}H_{99}N_{37}O_{16}$	1774.86	1778
6	H_2N-g-g-g-g-t*β-ala*	$C_{63}H_{83}N_{33}O_{13}$	1510.58	1593, 1555.48, 1510,
7	H_2N-g-g-g-t-*β-ala*	$C_{51}H_{68}N_{26}O_{11}$	1221.28	1263
8	H_2N-g-g-t-*β-ala*	$C_{39}H_{53}N_{19}O_9$	931.98	1011.86, 995.88, 973.88, 931.9
9	H_2N-g-t-*β-ala*			643
10	d(3'-T-G-G-G-G-T-5')	*Synthesized on ABI DNA synthesizer*		

[a] G, T = *aeg*-PNA and g, t = L-*cis*-(2*S*,4*S*)-*aep*-PNA.

5A.4 G-Quartet formation by *aep*-G/*aeg*-G-PNA and DNA: Comparative Study

The efficacy of the *aep*-G quartet formation under physiological conditions by *aeg*-G- PNA and DNA was studied using UVand CD spectroscopies, isothermal titration calorimetry and mass spectroscopy techniques.

5A.4 RESULTS

5A.4.1 UV-Tm Studies

The UV-spectrum of *aeg*- and *aep*-PNAs recorded in 10mmol potassium phosphate buffer and 100mmol of KCl is shown in Figure 8. Two broad peaks in the range at 253-273 nm were seen in spectra of both *aeg*- and *aep*-PNA. This suggests the formation of G-tetrad in *aeg*-PNA well as in *aep*-PNA. The UV spectrum of control DNA TG_4T (**10**) in same buffer condition exhibited broad overlapping of two peaks in this range.[5]

The stabilities of G-tetrad complexes of *aeg*-, *aep*-PNA and DNA were studied by temperature dependent UV absorbance changes. The UV-thermal denaturation experiments were performed by following absorbance at 295 nm where the characteristic change occur due to disruption in tetrad structure.[58] It is reported that the UV hypochromicity at 285-300 nm decreases with increase in temperature for DNA G-quadruplexes. The negative sigmoidal transition at 295 nm resulting from melting of quadruplexes suggests a cooperative effect.[59] Tetraplex stability is dependent on the nature and concentration of metal ion (Na^+/K^+) and pH 7.0-7.4, and hence thermal stability of G-tetrads of *aep*-, *aeg*-PNA and DNA under different physiological conditions were studied at 295 nm. The results are discussed in following paragraphs.

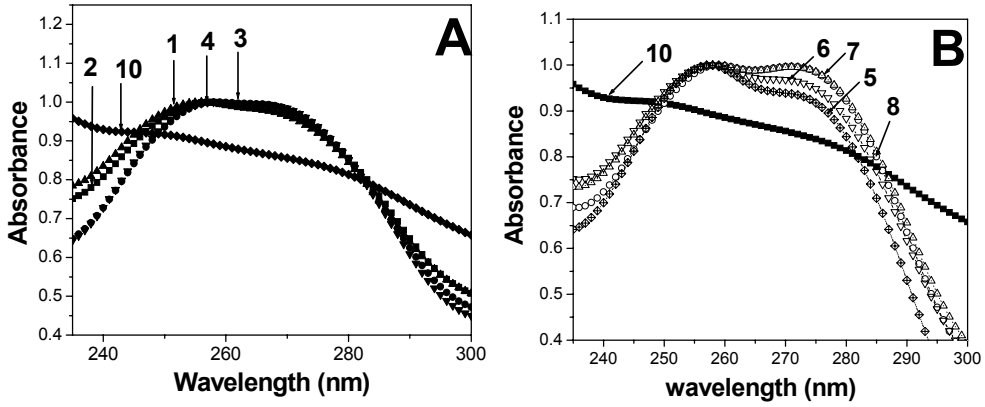

Figure 8: A. UV-spectra of *aeg*-PNA **1-2**, *aeg-aep*-PNA **3-4**.; B. *aep*-PNA (**5-8**) and DNA **10** at 10 ^oC

5A.4.1a Salt concentration dependent stability of G-tetrads in PNA

Figure 9 shows the UV-melting profiles of PNAs **1** and **3-5** at 295 nm in sodium phosphate buffer (10 mM) and NaCl (100 mM) at pH 7.4. These profiles show inverse-sigmoidal curves at 295 nm, characteristic of UV melting of G-quartets. The tetraplex melting temperature of *aeg*- and *aep*-PNAs extracted from first derivative curves (see appendix) of the melting profiles are given in Table 2. Figure 9A, shows the melting of PNAs **1-5** in 10mm sodium phosphate and 100 mM NaCl ($[Na^+]$). The Tm values indicate that single *aep*-PNA modification (g) at C-terminus or in the middle enhance Tm by 1 to 1.5 ^oC, while all modified *aep*-(g) PNA **5** only slightly destabilized ($\Delta Tm \approx -0.8\ ^oC$) the tetraplexes compared to control. Interestingly, the *aep* modification led to enhancements in hypochromicity, with maximum effect (20 %) seen with all-modified *aep*-PNA-**5**.

To see the effect of different metal ions in tetraplexing nature of PNA, UV-melting experiments with PNA **1**, PNA **3**, PNA **6** and DNA **10** were performed in potassium phosphate (10 mM) buffer devoid of any Na^+ ion at same pH (7.4). The melting profiles of these PNA are shown in Figure 9B and their Tm values are given in Table 2. The Tm values indicate that K^+ induces significant stabilization of *aeg*-*aep*-PNA tetraplex ($\Delta Tm = +5.8\ ^oC$) compared to Na^+, while show that either no effect of salt or slight stabilized.

The Tm values (Figure 9B) suggest that 10 mM K^+ in phosphate buffer significantly stabilizes the control *aeg*-PNA ($Tm = +5.8\ ^oC$) while destabilizing the *aep* modified PNAs and DNA. However increasing $[K^+]$ at higher buffer concentration (100 mM) enhanced the Tm of both *aeg* and *aep*-PNAs by 13 ^oC and 9 ^oC respectively. Addition of 100 mM KCl further enhanced the Tm by 1-2 ^oC. Thus G-quartet formation in *aeg*-PNA **1**, *aep*-PNA **5** and PNA **3** (chimarae of *aeg*- and *aep*-PNA) is more preferable in presence of K^+ than Na^+. The overall hypochromicity at 295 nm also generally increased

with all PNAs (8-20%). The overall results of salt effects indicate that K^+ stabilized PNA tetraplexes much more than Na^+.

5A.4.1b pH-Dependent studies

Since *aep*-PNAs are protonatable at ring nitrogen at physiological pH, tetraplexing properties in *aep*-PNAs were examined at different pHs. The melting profiles of PNAs in 10mM potassium phosphate buffer having 100 mM KCl at pH's 5.8, 6.4 and 7.8 were determined (Figure 10) and results are shown in Table 3. At higher pH of 7.8, the melting profiles of PNA **2**, PNA **5** and PNA **6** (Figure 10A) monitored at same wavelength are similar to the characteristic melting profile of tetraplexes of DNA. The Tm values of all modified *aep*-G PNAs **5** and **6** were slightly destabilized compared to unmodified *aeg*-PNA by ΔTm of 2-4 ^oC.

At slightly lower of pHs 7.0, (Figure 10B and Table 3) and pH 6.4 (Figure 10C and Table 3) the stability of quadruplexes marginally increased to that at pH 7.8 and for the different PNAs, the stabilities were similar. All the different PNAs were more stable than the corresponding DNA sequence 10 by 6-7 ^oC.

Table 2: UV-melting temperature (Tm) of PNAs at different concentration of metal ion*

Figure of UV-Melting curve at λ_{max} = 295nm	PNA/DNA	List of PNA and DNA Sequence	Buffer Condition	Tm (^{0}C)
9A	**1**	H_2N-T-G-G-G-G-T-β-ala	10mmol. Sodium Phosphate with 100 mmol NaCl	46.5
	3	H_2N-T-G-G-g-G-T-β-ala		48.0
	4	H_2N-T-G-G-G-G-t-β-ala		47.6
	5	H_2N-t-g-g-g-g-t-β-ala		45.7
9B	**1**	H_2N-T-G-G-G-G-T-β-ala	10mmol. Potassium-Phosphate	52.3
	3	H_2N-T-G-G-g-G-T-β-ala		48.0
	5	H_2N-t-g-g-g-g-t-β-ala		46.3
	10	d(3'-T-G-G-G-G-T-5')		44.5
9C	**1**	H_2N-T-G-G-G-G-Tβ-ala	100mmol. Potassium-Phosphate	65.9
	3	H_2N-T-G-G-g-G-T-β-ala		57.2
9D	**1**	H_2N-T-G-G-G-G-Tβ-ala	100mmol. Potassium-Phosphate with 100mmol KCl	67.8
	3	H_2N-T-G-G-g-G-T-β-ala		58.2

*All Tm's average2/3 measurement and accurate with in ±0.5 ^{o}C. All experiments aer done at pH 7.4

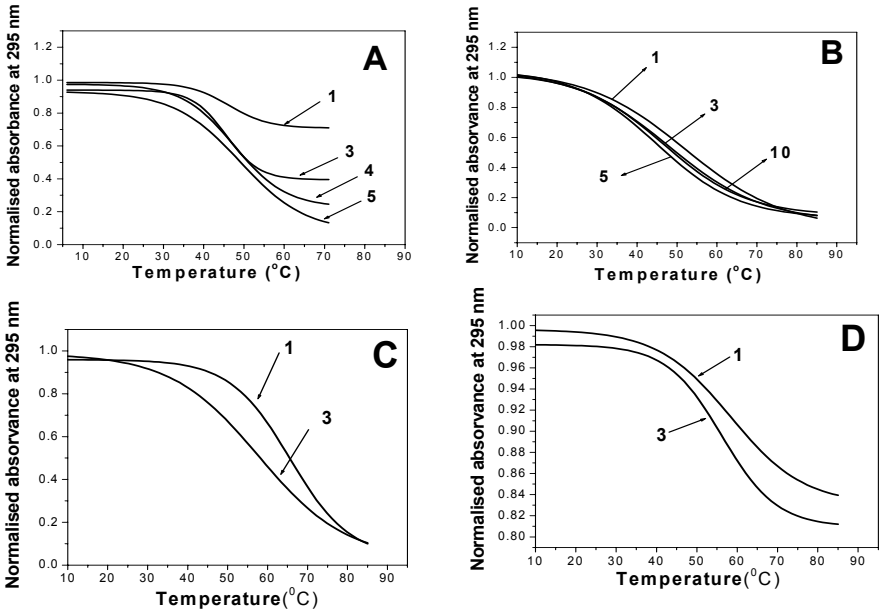

Figure 9: UV-melting profile of *aeg*-PNA and *aep*-PNAs A. PNA **1**, **3-5**.; **B.** PNA 1, **3, 5** and **10**.; C. PNA **1** and PNA **3**.; D. PNA **1** and PNA **3** at different concentration of metal ion. Derivatives curves are given in appendix.

At slightly acidic pH 6.4 (Figure 10C), *aeg*- and *aep*-PNA **2**, **5** and **6** generally show the signature of G-tetrad formation, with the melting profiles showing complicated

pattern perhaps due to multiple transitions. At acidic pH 5.4 (Figure 10D), the negative sigmoidal signature of G-quadruplex disappeared completely and interestingly was replaced by patterns of typical double helix transitions.

Table 3: UV-melting temperature (Tm) of PNAs at different pHs

Figure of UV-Melting curve at λ_{max} = 295nm	PNA/DNA	List of PNA and DNA Sequence	pH of Buffer	Tm (^{0}C)
10A	**2**	H_2N-T-G-G-G-G-β-ala	7.8	63.1
	5	H_2N-t-g-g-g-g-tβ-ala		61.0
	6	H_2N-g-g-g-g-t-β-ala		59.2
10B	**1**	H_2N-T-G-G-G-G-Tβ-ala	7.0	64.0
	2	H_2N-T-G-G-G-G-β-ala		63.4
	5	H_2N-g-g-g-g-tβ-ala		64.8
	10	d(3'-T-G-G-G-G-T-5')		57.2
10C	**2**	H_2N-T-G-G-G-G-β-ala	6.4	Multiple transition
	5	H_2N-t-g-g-g-g-t-β-ala		
	6	H_2N-g-g-g-g-tβ-ala		
10D	**2**	H_2N-T-G-G-G-G-β-ala	5.8	Non - characteristic transition
	6	H_2N-g-g-g-g-t-β-ala		
	3	H_2N-T-G-G-g-G-T-β-ala		

All Tm's average2/3 measurement and accurate with in ±0.5 ^{o}C. All experiments aer done in 10 mM Potassium Phosphate containing 100 mM KCl.

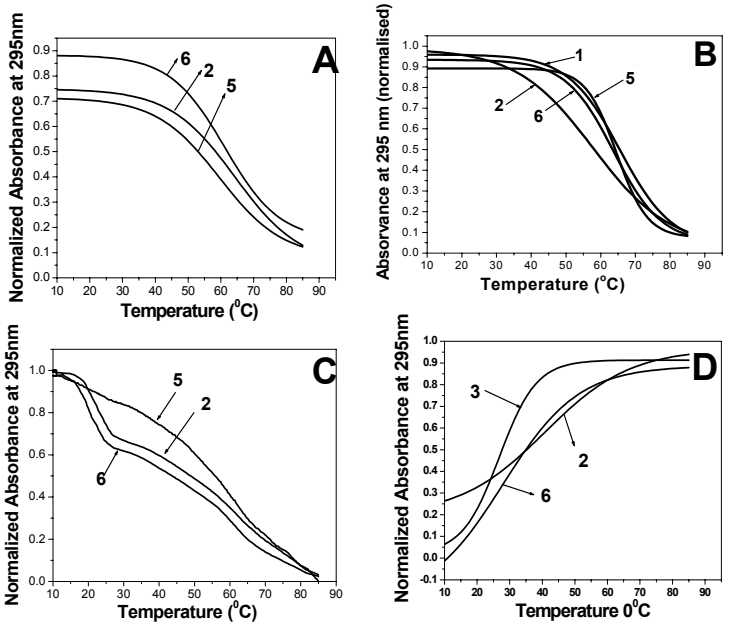

Figure 10: UV-melting profile of PNAs at different pH: A. PNA **2**, **6** and **5.**; B. PNA **1-2** and **5**.; C. PNA **2**, **5** and **6**.; D. PNA **2**, **3** and **6** in same concentration of K^+ metal ions 110mM. Derivatives curves are given appendix.

5A.4.1c Length Dependent study of G-quartet in *aep*-PNA

The UV melting curves of all modified *aep*-PNAs **5**-**9** corresponding to different lengths were recorded in potassium phosphate (100mM) containing 100 mM of KCl. Monitored at 295 nm, only PNAs **5, 6** and **7** exhibited characteristic tetraplex melting profiles (Figure 11A). The Tm values (Table 4) of all PNAs **5** and **6** were higher than DNA **10** while that of PNA **7** was slighter lower than DNA **10**. The shorter *aep*-PNAs **8** and **9** did not form any tetraplexes under these conditions. Although PNA **8** exhibited duplex type transition, PNA **9** failed to show any transition (Figure 11B). The Tm of *aeg*-PNA **1** in these conditions is 61.0 (Table 4).

Table 4: UV-melting temperature (Tm) of at different length of *aep*-PNAs Sequences*

Figure	PNA/ DNA	List of PNA Sequence	Tm (^{0}C)
11A	**5**	H_2N-t-g-g-g-g-t-β-ala	59.3
	6	H_2N-g-g-g-g-tβ-ala	56.4
	7	H_2N-g-g-g-tβ-ala	50.1
	10	d (3'-T-G-G-G-G-T-5')	54.0
11B	**1**	H_2N-T-G-G-G-G-T-β-ala	61.0
	8	H_2N-g-g-tβ-ala	nd
	9	H_2N-g-tβ-ala	nd

* All Tm's average2/3 measurement and accurate with in ±0.5 ^{o}C. All experiments aer done at pH 7.4.

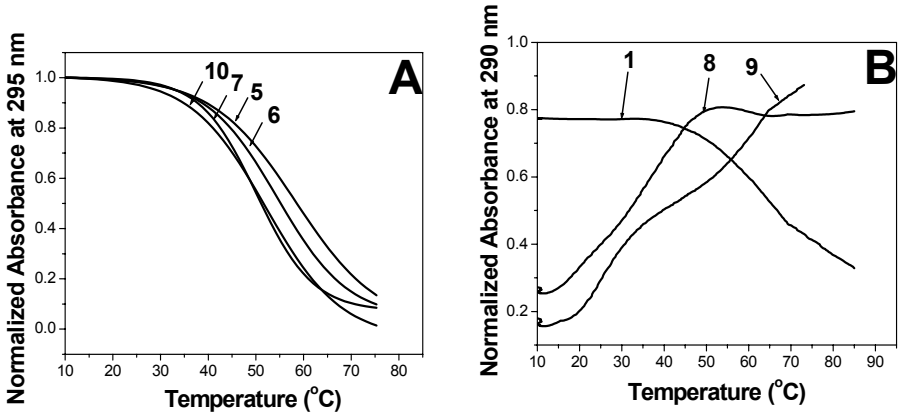

Figure 11. UV-Melting profile of *aep*-PNA A. PNA **5**, **6**, **7** and DNA **10**; B. *aep*-PNA **1**, **8** and **9**. Derivatives curves are given appendix.

5A.4.2 Additional results on G-tetraplexes of PNA

5A.4.2a Hysteresis: Intramolecular vs Intermolecular folding

Two types of G-quartets have been observed in DNA: *inter*molecular and *intra*molecular. These can often be distinguished by hysterisis experiments: dissociation upon heating leads to a decrease in absorbance resulting in a inverse-sigmoidal curve, characteristics of tetraplexes[60] and upon cooling at same rate, re-association should lead to an increase of absorbance, characteristic of intermolecular quadruplexes. The heating and cooling curves of UV-profile of *aep*-PNA **5** and PNA **6** are given in Figure 12, which suggest that PNA **5** and PNA **6** perhaps form intermolecular quartet.

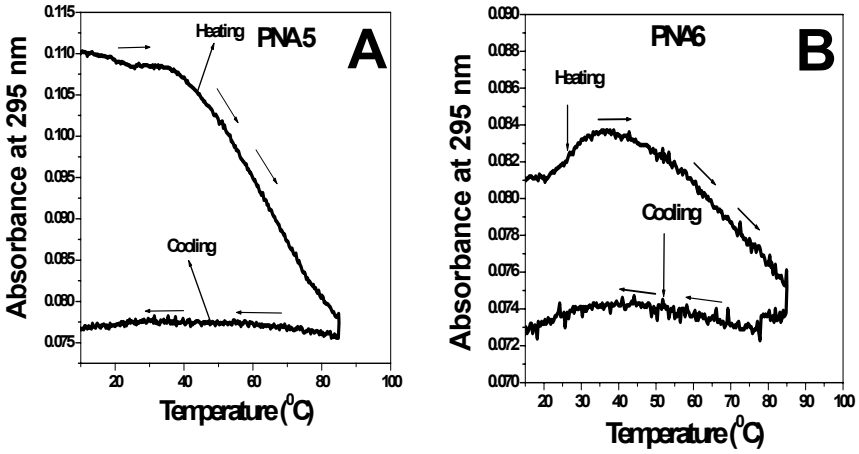

Figure 12: UV-melting profile of A. PNA **5** and B. PNA **6** in 10mM Potassium Phosphate and 100mM KCl at pH 7.4 and wavelength 295nm.

5A.4.2b Circular Dichroism spectroscopy

The CD-spectra of *aep*-PNAs of different lengths and DNA **10** are shown in Figure 13. The CD spectrum of DNA **10** has one maxima at 262 nm and one minima at 238.5 nm, which is characteristic of G-quadruplex. The CD-spectra of L-*cis*-(2*S*,4S)-*aep*-PNAs **5-8** also show one maxima (271 nm) and one minima (223.5 nm), but location of both maxima and minima in these PNAs are different from DNA.

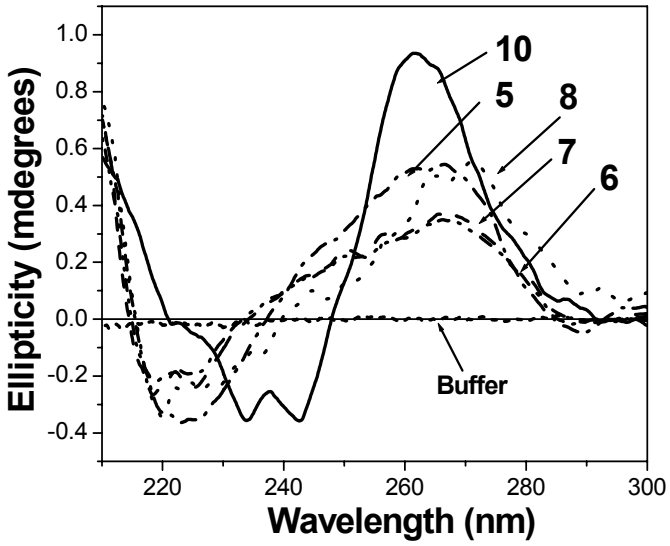

Figure 13: CD-spectra of *aep*-PNAs in 100 mmol potassium phosphate and 100 mM KCL.

5A.4.2c Mass Spectral Data

Recently Ghosh, *et. al*.[55] has reported the characterization of a PNA_4 quadruplex by electrospray ionization mass spectrometry (ESI-MS) to study the molecularity of the PNA species and seek evidence for Q-PNA. ESI-MS has been used to observe noncovalent intermolecular complexes of DNA and PNA-DNA hybrids.[54] G-rich sequences of PNA as in **TG3** has been analyzed by positive ion nano electrospray ionization mass spectrometry (nano-ESI-MS). Analysis at a cone voltage of 60 V and source temperature of 30 °C showed peaks corresponding to a triply charged species at *m*/*z* 1716.9 and a doubly charged species at *m*/*z* 2575.2.10 The associated molecular weight (MW) for these peaks was 5148, consistent with tetramer formation by PNA **TG3** (MW of PNA **TG3**) 1287 (0.5 Da). Peaks corresponding to $(M4 + 2H + Na)^{3+}$, $(M4 + 2H + K+)^{3+}$, and $(M4 + H + 2K)^{3+}$ were also seen, which supports that **TG3** forms tetramers by ESI-MS.[55]

Table 5: *aeg*-PNA and L-*cis*-(2*S*,4*S*)-*aep*-PNA sequences*

PNA	Calculated Molecular Mass	ESI mass spectra	MALDI-TOF mass spectra
1	1786.70	3664.03, 2469.36, 2096, 1299.36	M^+ = 1787.3
2	1518.58	-	M^+ = 1518 $(4M+3K+Na+H)^{5+}$ = 1242; $(4M+Na+K+3H)^{5+}$ = 1227.6;
3	1784.73	1787.70	1782, $(4M+3Na+6K+H)^{10+}$ = 743.1 and $(4M+3Na+K+3H)^{7+}$ = 1034.10
4	1784.73	1786.20	
5	1774.86	M^+ = 1774.86, $(4M+8K+H)^{10+}$ = 741.4, $(4M+7K)^{7+}$ = 1056.49, $(4M+K+8H)^{9+}$ = 794.04 $(4M+6K+Na+2H)^{9+}$ = 817.59.	M^+ = 1774.86; $(M^+ + 2Na^+ + 2K^+)^+$ = 7223.44
6	1510.58	1593, 1555.48, 1510,	$(M+K^++4H)^+$ = 1553.58; $(4M+K+3H)^{4+}$ = 1564.08; $(4M+2Na+K+H)^{4+}$ = 1575.08; $(4M+Na+3K)^{4+}$ = 1588.58; $(M+2K+Na+H)^+$ = 1547.08
7	1221.28	1263	1263
8	931.98	1011.86, 995.88, 973.88, 931.9	973.88-
9	643	643	643

*G, T = *aeg*-PNA and g, t = L-*cis*-(2*S*,4*S*)-*aep*-PNA.

The MALDI-TOF PNA **1-9**, *aeg*-PNA **2**, single modified *aep*-PNA **3** and homo-oligomer *aep*-PNAs **5-6** are listed in Table 5. The expected mass peaks exhibited along with additional peaks derived from addition of Na^+ and K^+ ions. The observed M^+ from MALDI-TOF could be fitted into mass compositions as shown in Table 5. $(4M+3K+Na+H)^{5+}$ for PNA **1**, $(4M+3Na+6K+H)^{10+}$ for PNA **2**, $(M^+ + 2Na^+ + 2K^+)^+$ for PNA **3** and $(4M+K+3H)^{4+}$ are evidence for tetraplex.

5A.4.2d Iso thermal titration calorimetry

The stability of G-tetrad depends both upon the concentration of metal ion and the concentration of DNA oligomer. The structure of tetraplexes will be disrupted by dilution, which was studied by "Isothermal titration calorimetry" (ITC) experiment.[61-63] In this experiment the annealed and the unannealed PNA tetraplexes were separately titrated (diluted) with buffer and the rate of change in heat of dilution (dq/dt) was recorded at 20 ^oC. The ITC plot of dq/dt vs volume of titrant for PNA **1**, PNA **3** and PNA **5** given in

Figure 14. It is seen that the plots of annealed samples of *aeg*-PNA **1**, *aeg-aep*-PNA **3** and *aep*-PNA **5** show characteristic titration curves indicating heat evolved during the dilution of tetraplexed PNA, while ITC plots of PNA **1** and PNA **5** without annealing do not show the any ordered curves, expected for tetraplex formation. The data shown have been corrected for buffer dilution effects. These experiments, gave further proof for tetraplex formation by PNA, though the data are insufficient to obtain any thermodymanmic information.

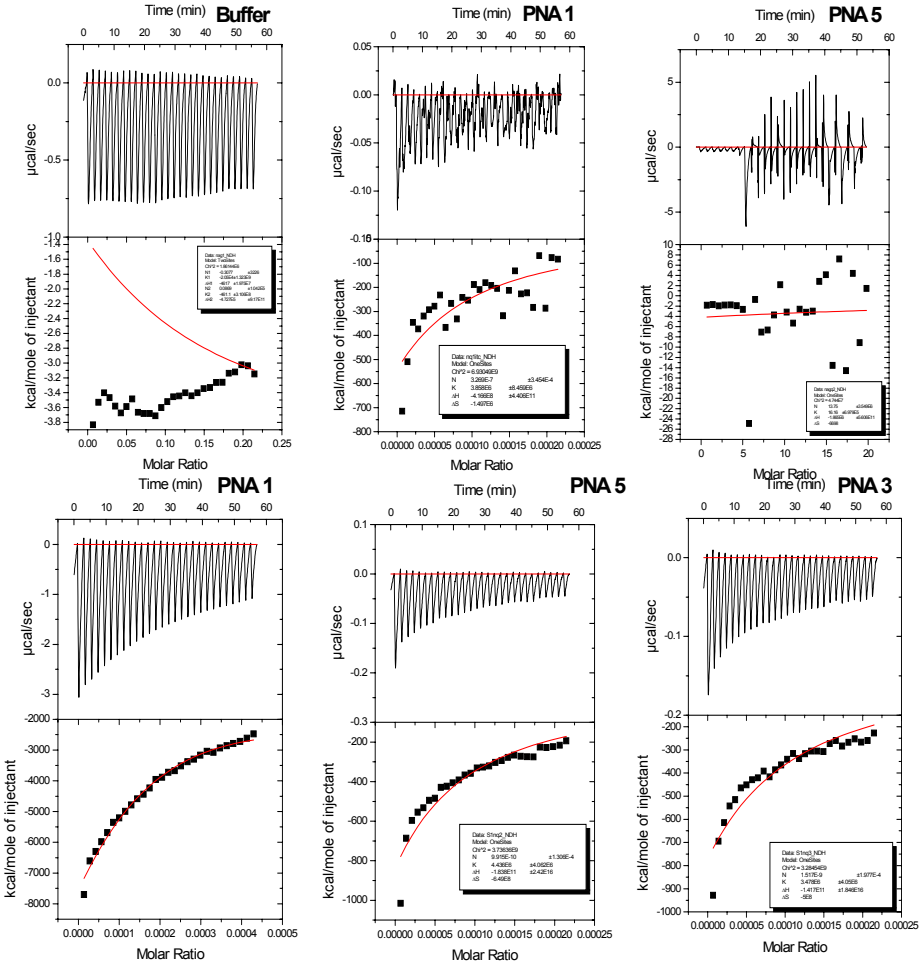

Figure 14: ITC Graph of PNAs in Buffer Soution unannealed and annealed

5A.5 DISCUSSION

The effect of PNA backbone modification as in *aep*-PNA is expected to significantly affect the stability of the G_4-quadruplexes. The UV, UV-Tm, CD and Mass spectral data presented in last section suggests that formation G_4-quadruplexes by *aep*-PNA is significantly modulated according to conditions.

G-rich *aeg*-PNA sequences are known to form G_4-tetraplexes in the presence of monovalent metal cation. The UV-spectra of *aeg*-PNAs (**1** and **2)**, *aeg*-*aep*PNAs (**3** and **4**) and *aep*-PNAs (**5-9**) are quite similar having two broad peaks in 260-280 nm range, suggesting tetraplex formation by these PNAs. The UV-absorbance vs temperature plot derived from UV-melting shows negative sigmoidal curves, characteristic of tetraplex formation. The stability of G_4-tetraplexes of *aeg*- and *aep*-PNA units is almost same in presence of Na^+ at pH 7.4. G_4-tetraplexes formed by the *aeg*-PNA **1** in presence of K^+ at pH 7.4 are more stable than *aep*-PNA **6** (ΔTm = 2-6 ^oC). On further, increasing the concentration of [K^+] upto 100 mM, the stability of tetraplexes is significantly changed. Since the prolyl ring nitrogen of *aep*-PNA is protonated even at neutral pH, the thermal stability of *aep*-PNA were measured at different pHs in the range (7.8-5.8). The formation of tetraplexes is restricted to the pH range 7.8-6.4 and the stability of *aeg* and *aep*-PNAs in phosphate buffer is almost similar at pH 7.8, 7.4 and 7.0. The Tm values of these PNAs at pH 6.4 could not be determined due to appearance of multiple transitions. The formation of tetraplexes in *aeg*- and *aep*-PNA at the acidic pH 5.8 is seriously disfavored and their melting profiles correspond to typical duplex transition in agreement with previous literature.

To find the required minimum length in *aep*-PNA for formation of stable tetraplexes, length dependent study in *aep*-PNAs (**5-9**) was done in the presence of [K^+] = 110 mM at pH 7.4. The results indicated that only tetramer or longer PNAs tg_4t, tg_4 and tg_3

formed stable G-quartets. The shorter sequences like tg_2 and tg did not show any signature of G_4-tetraplex in UV-thermal experiments.

The study of *intrastrand* vs *interstrand* G-quadruplex formation of PNA was carried out by heating-cooling experiments. Interstrand association is kinetically slower than intrastrand association. The heating and cooling melting profiles of PNAs **4** and **5** indicated slower re-association than dissociation, which suggested formation *inter*-molecular rather than *intra*-molecular quartets.

The CD-spectra of *aep*-PNAs (**5-9**) are slightly different from that of known quadruplex forming DNA **10**. In *aep*-PNAs (**5-9**) the maxima is observed at wavelength 265-270 nm, similar to that of DNA **10.** The minima at 220nm in PNAs is slightly different than that of DNA **10** at 238-243 nm. The difference in minima of CD-spectra of *aep*-PNAs may be due to unusual conformation of its prolyl ring. The ring nitrogen being protonatable even at neutral pH, may alter the puckering of the prolyl ring, affecting the secondary structure of *aep*-PNA.

The formation of G-tetraplexes was also observed in mass spectra (MALDI-TOF and ESI) of *aeg*- and *aep*-PNA. The presence of ion peaks at expected tetrameric molecular mass composition of PNA **1-6** suggests the formation of G-quadruplexes.

From the above results of UV-thermal denaturation experiments, it is seen that the stability of the G_4-quartets is highly dependent upon the concentration of monovalent metal ions. To examine the role of metal ion ($[M^+]$, the tetaraplexes of PNA in buffer solution contains salt was diluted with same buffer and measuring the evolved heat of dilution with substraction of values (buffer dilution) by ITC experiment. These ITC results for tetraplexed PNAs qualitatively showing that dilution disrupts the tetraplexes.

5A.6 CONCLUSIONS

The synthesis and characterization G-rich sequences of *aeg*-PNA and *aep*-PNA are reported. The formation of G-tetrad structures in *aep*- and *aeg*-PNA is observed under different conditions of pH, salt and metal ions K^+ and Na^+. The stability of G-tetrad structure in *aep*- and *aeg*-PNAs are almost similar and both of them stabilize the G-tetrad structures better than in DNA. The formation of quadruplexes is also supported by mass spectroscopy, CD-spectra and ITC.

5A.7 EXPERIMENTAL

5A.7.1 Synthesis of *aeg*- and *aep*-PNA monomer and oligomer

The synthesis of thymine and guanine monomers of *aeg*- and *aep*-PNA was achieved by following the same procedures as reported in Chapter 1. These monomers were used to synthesize the corresponding PNA oligomers by *solid phase synthesis procedure* reported in Chapter 4.

5A.7.2 UV-Melting Experiment

The concentrations of the synthesized PNAs were determined spectrophotometrically at λ 260 nm at 80 °C, by use of the molar extinction coefficient calculated for unstacked oligonucleotides [11700 cm^{-1} M^{-1} (G); 8800 cm^{-1} M^{-1} (T)] in buffer solution, used for the melting experiments. UV melting experiments were performed on Lambda-35 UV Spectrometer (Perkin-Elmer) equipped with a thermal melt system, PTP-6 Peltier Temperature Programmer with water circulator Thermohake K20.

Melting curves were recorded with a concentration of approximately 10 μM of single strand PNAs in 2 mL of the buffer solution in Teflon-sealed quartz cuvettes of 1 cm optical path length. The resulting solutions were then heated at 80 °C for 15 min, then slowly cooled and kept at 20 °C for 20 min. After thermal equilibration at 20 °C, the UV

absorption at λ 295 was monitored as a function of the temperature, increasing at a rate of 0.5 °C/min. UV-thermal denaturation method was used to study the change in UV-absorbance, which was recorded with respect to increase in temperature at constant wavelength. The results were normalized and the data was analysed using Origin 5.0 (Microsoft Corp.).

5A.7.3 Circular Dichroism spectral studies

5-10 μM stock solution of each PNA (**5-8)** and DNA **10** strands taken in 2 mL of 100mM potassium phosphate buffer with salt 100mM KCl was annealed by heating at 90 ^{o}C for 5min, followed by slow cooling to room temperature and kept at room temperature for 30 min then, refrigerate in for 72 h. The CD spectra of the refrigerated samples of all PNA were recorded on a Jasco J-715 spectropolarimeter at temperature 10 ^{o}C by accumulation 5 scans and a scan speed of 200nm/min.

5A.7.4 ITC-Measurements

The VP-ITC micro Calorimeter was used to study dilution effect on G-quartet structure of PNA. In this experiment, annealed sample was diluted with the same buffer in which sample was prepared. The dilution was done by successive injection of 10 μL PNA samples to 1.5 mL of buffer in cell at interval of 20 seconds at 15 ^{o}C.

5A.7.5 Mass Spectroscopy

Electron spray ionization mass spectrometer (QSTAR MultiView1.5.0 TOF-MS-IN) was used for characterization of G-quartet formation. The 2 μM solution of PNA in 1mL of methanol was used for recording mass spectra. ABI-MALDI-TOF spectrometer was used to record mass of PNA by using *Voyager spec* electronic software. The mass of neat PNA was recorded in presence of matrices CHCA (α-cyano-4-hydoxycinnamic acid).

5A.8 REFERENCES

1. (a) Shida, T.; Yokoyama, K.; Tamai, S.; Sekiguchi, J.; Self-association of telomeric short oligodcoxyribonucleotides containing a dG cluster. *Chem. Pharm. Bull*. **1991**, 39, 2207-11. (b) Xu, X.; Hamhouyia, F.; Thomas, S. D.; Burke, T. J.; Girvan, A. C.; McGregor, W. G.; Trent, J. O. Miller, D. M.; Bates, P. J. Inhibition of DNA replication and induction of S phase cell cycle arrest by G-rich oligonucleotides. *J. Biol. Chem*. **2001**, *276*, 43221-30.
2. Patel, D. J.; Bouaziz, S.; Kettani, A.; Wang, Y. Structures of guanine-rich and cytosine-rich quadruplexes formed *in vitro* by telomeric, centromeric, and triplet repeat disease DNA sequences. In *Oxford Handbook of Nucleic Acid Structures.* Edited by Neidle S. New York: Oxford University Press; 1999:389-453.
3. (a) Jin, R.; Breslauer, K. J.; Jones, R. A.; Gaffney, B. L. Tetraplex formation of a guanine-containing nonameric DNA fragment. *Science* **1990**, *250*, 543-46. (b) Guschlbauer, W.; Chantot, J. F.; Thiele, D. Four-stranded nucleic acid structures 25 years later: from guanosine gels to telomer DNA. *J. Biomol. Struct. Dyn*. **1990**, *8*, 491-511.
4. (a) Sundquist, W. I. The structures of telomeric DNA. *Nucleic Acids Mol. Biol.* **1991**, *5*, 1-24. (b) Xu, X.; Hamhouyia, F.; Thomas, S. D.; Burke, T. J.; Girvan, A. C.; Mc Gregor, W. G.; Trent, J.O.; Miller, D. M.; Bates, P. J. Inhibition of DNA replication and induction of S phase cell cycle arrest by G-rich oligonucleotides. *J. Biol. Chem*. **2001,** *276*, 43221-43230.
5. Blackburn, E. H.; Szostak, J. W. The Molecular Structure of Centromeres and Telomeres. *Annu. Rev. Biochem.* **1984**, *53*, 164-94.
6. Williamson, J. R. G-quartet structures in telomeric DNA. *Annu*. *Rev*. *Biophys*. *Biomol*. *Struct*. **1994**, *23*, 703-730.
7. (a) Balagurumoorthy, P.; Brahmachari, S. K.; Mohanty, D.; Bansal, M.; Sasisekharan, V. Hairpin and parallel quartet structures for telomeric sequences. *Nucleic Acids Res*. **1992,** *20*, 4061-67. (b) Mohanty D.; Bansal, M. Conformational polymorphism in G-tetraplex structures: strand reversal by base flipover or sugar flipover. *Nucleic Acids Res*. **1993**, *21*, 1767-74.
8. (a) Blackburn, E. H.; Szostak, J. W. The Molecular Structure of Centromeresand Telomeres. *Annu. Rev. Biochem.* **1984**, *53,* 164-94. (b) Williamson, J. R. Guanine quartets. *Curr*. *Opin. Struct. Biol*. **1993**, *3*, 357-362.
9. (a) Scaria, P. V.; Shire, S. J.; Shafer, R. H. Quadruplex structure of d(G3T4G3) stabilized by K^+ or Na^+ is an asymmetric hairpin dimer. *Proc. Natl Acad. Sci. USA* **1992***, 89*, 10336-10340. (b) Chen, F. M. Sr2+ facilitates intermolecular G-quadruplex formation of telomeric sequences. *Biochemistry* **1992,** *31*, 3769-76
10. Ren, J.; Qu, X.; Trent, J. O.; Chaires, J. B. Tiny telomere DNA. *Nucleic Acids Res*. **2002,** *30*, 2307-2315.
11. Sen, D.; Gilbert, W. A sodium-potassium switch in the formation of four stranded G_4-DNA. *Nature* **1990**, *344*, 410-14.
12. Lu, M.; Guo, Q.; Kallenbach, N. R. Structure and stability of sodium and potassium complexes of dT_4G_4 and dT_4G_4T. *Biochemistry* **1992**, *31*, 2455-2459.

13. Venczel, E.A.; Sen, D. Parallel and antiparallel G-DNA structures from a complex telomeric sequence. *Biochemistry* **1993**, *32*, 6220-28.
14. Zakian, V. A. Structure and function of telomeres. *Annu. Rev. Genet*. **1989**, *23*, 579-604.
15. Schultze, P.; Hud, N. V.; Smith, F. W.; Feigon, J. The effect of sodium, potassium and ammonium ions on the conformation of the dimeric quadruplex formed by the Oxytricha nova telomere repeat oligonucleotide d($G_4T_4G_4$). *Nucleic Acids Res*. **1999**, *27*, 3018-3028.
16. (a) Deng, J.; Xiong, Y.; Sundaralingam, M. X-ray analysis of an RNA tetraplex $(UGGGGU)_4$ with divalent Sr2+ ions at subatomic resolution (0.61A). *Proc. Natl Acad. Sci. USA* **2001**, *98*, 13665-13670. (b) Liu, H.; Kugimiya, A.; Sakurai, T.; Katahira, M.; Uesugi, S. A comparison of the properties and the solution structure for RNA and DNA quadruplexes which contain two GGAGG sequences joined with a tetranucleotide linker. *Nucleosides Nucleotides Nucleic Acids* **2002** *21*, 785–801. (c) Sugimoto, N.; Ohmichi, T.; Sasaki, M. The stability of DNA and RNA G-quartets. *Nucleosides Nucleotides* **1996**, *15*, 559–567. (d) Cheong, C. J.; Moore, P. B. Solution structure of an unusually stable RNA tetraplex containing G-Quartet and U-Quartet structures. *Biochemistry* **1992**, *31*, 8406–8414. (d) Chen, F. M. Sr^{2+} facilitates intermolecular G-quadruplex formation of telomeric sequences. *Biochemistry* **1992,** *31*, 3769-76.
17. (a) Williamson, J. R.; Raghuraman, M. K.; Ceeh, T. R. Monovalent cation-induced structure of telomeric DNA: the G-quartet model. *Cell* **1989**, *59*, 871-80. (b) Lu, M.; Guo, Q.; Kallenbach, N. R. Thermodynamics of G-tetraplex formation by telomeric DNAs. *Biochemistry* **1993**, *32*, 598-601.
18. Jin, R.; Gaffney, B. L.; Wang, C.; Jones, R. A.; Breslauer, K. J. Thermodynamics and structure of a DNA tetraplex: a spectroscopy and calorimetric study of the tetramolecular complexes of d(TG3T) and d(TG3T:GsT). *Proc. Natl. Acad. Sci. USA* **1992,** *89*, 8832-8836.
19. Aboul-ela, F.; Murchie, A. I. H.; Norman, D. G.; Lilley, D. M. J. Solution structure of a parallel-stranded tetraplex formed by d(TG_4T) in the presence of sodium ions by nuclear magnetic resonance spectroscopy. *J. Mol. Biol*. **1994**, *243*, 458-471.
20. Smith, F.W.; Schultze, P.; Feigon, J. Solution structures of unimolecular quadruplexes formed by oligonucleotides containing Oxytricha telomere repeats. *Structure* **1995**, *3*, 997-1008.
21. Aboul-ela, F.; Murchie, A. I.; Lilley, D. M. NMR study of parallel-stranded tetraplex formation by the hexadeoxynucleotide d(TG4T). *Nature* **1992**, *360*, 280-282.
22. Gavathiotis, E.; Searle, M. S. Structure of the parallel-stranded DNA quadruplex $d(TTAGGGT)_4$ containing the human telomeric repeat: evidence for A-tetrad formation from NMR and molecular dynamics simulations. *Org. Biomol. Chem*. **2003**, *1*, 1650–1656.
23. (a) Wang, Y.; Jin, R.; Gaffney, B.; Jones, R. A. Breslauer, K. J. Characterization by ^1H NMR of glycosidic conformations in the tetramolecular complex formed by d(GGTTTTTGG). *Nucleic Acids Res.* **1991**, *19*, 4619-4622.
24. Wang, Y.; Patel, D. J. Guanine residues in d(T_2AG_3) and d(T_2G_4) form parallel-stranded potassium cation stabilized G-quadruplexes with antiglycosidic torsion angles in solution. *Biochemistry* **1992**, *31*, 8112-8119.
25. Sket, P.; Crnugelj, M.; Plavec, J. d(G3T4G4) forms unusual dimeric G-quadruplex structure with the same general fold in the presence of K+, Na+ or NH4+ ions *Bioorg. Med. Chem.* **2004**, *12*, 5735-5744.

26. Caceres, C.; Wright, G.; Gouyette, C.; Parkinson, G.; Subirana, J. A. Thymine tetrad in d(TGGGGT) quadruplexes stabilized with Tl+/Na+ ions. *Nucleic Acids Research* **2004**, *32*, 1097-1102.
27. Padmanabhan, K.; and Tulinsky, A.; An ambiguous structure of a DNA 15-mer thrombin complex. *Acta Crystallogr. D* **1996**, *52*, 272-282.
28. Marathias, V. M.; Bolton, P. H. Determinants of DNA quadruplex structural type: sequence and potassium binding. *Biochemistry* **1999**, *38*, 4355-4364.
29. Kang, C.; Zhang, X.; Ratliff, R.; Moyzis, R.; Rich, A. Crystal structure of four-stranded Oxytricha telomeric DNA. *Nature* **1992**, *356*, 126-131.
30. Sen, D.; Gilbert, W. The structure of telomeric DNA: DNA quadraplex formation. *Curr. Opin. Struct. Biol.* **1991**, *1*, 435-438.
31. Wang, Y.; de los Santos, C.; Gao, X.; Greene, K.; Live, D.; Patel D. J. Multinuclear nuclear magnetic resonance studies of Na^+ cation-stabilized complex formed by d(GGTTTTCGG) in solution. *J. Mol. Biol*. **1991**, 222, 819-832.
32. Shippen-Lentz, D.; Blackburn, E. H. Functional evidence for an RNA template in telomerase. *Science* **1990,** *247,* 546-552.
33. Sen, D.; Gilbert, W. Formation of parallel four-stranded complexes by guanine-rich motifs for meiosis. *Nature* **1988**, *334*, 364-366.
34. Sen. D.; Gilbert, W. Novel DNA superstructures formed by telomereo like oligomers. *Biochemistry* **1992**, *31*, 65-70.
35. Haider, S.; Parkinson, G. N.; Neidle, S. Crystal structure of the potassium form of an Oxytricha nova G-quadruplex. *J. Mol. Biol*. **2002**, *320*, 189-200.
36. Leonard, G. A.; Zhang, S.; Peterson, M. R.; Harrop, S. J.; Helliwell, J. R.; Cruse, W. B.; d'Estaintot, B. L.; Kennard, O.; Brown, T.; Hunter, W. N. Self-association of a DNA loop creates a quadruplex: crystal structure of d(GCATGCT) at 1.8 A Ê resolution. *Structure* **1995**, *3*, 335-340.
37. Phillips, K.; Dauter, Z.; Murchie, A. I. H.; Lilley; D. M.; Luisi; B. The crystal structure of a parallel-stranded guanine tetraplex at 0.95A resolution. *J. Mol. Biol*. **1993**, *273*, 171-182.
38. Kelly, J. A.; Feigon, J.; Yeates, T. O. Reconciliation of the X-ray and NMR structures of the thrombin-binding aptamer d(GGTTGGTGTGGTTGG). *J. Mol. Biol*. **1996**, *256*, 417-422.
39. Kim, J.; Cheong, C.; Moore, P. B. Tetramerization of an RNA oligonucleotide containing a GGGG sequence. *Nature* **1991**, *351*, 331–332.
40. Smith, F. W.; Feigon, J. Strand orientation in the DNA quadruplex formed from the Oxytricha telomere repeat oligonucleotide d($G_4T_4G_4$) in solution. *Biochemistry* **1993**, *32*, 8682-8692.
41. Ishikawa, F.; Matunis, M. J.; Dreyfuss, G.; Cech, T.R. Nuclear proteins that bind the pre-mRNA 3' splice site sequence r(UUAG/G) and the human telomeric DNA sequence d(TTAGGG)n. *Mol. Cell. Biol*. **1993**, *13*, 4301-4310.
42. (a) Marquet, R.; Baudin, F.; Gabus, C.; Darlix, J-L.; Mougel, M. et al. Dimerization of human immunodeficiency virus (type 1) RNA: stimulation by cations and possible mechanism. *Nucleic Acids Res.* **1991**, *19*, 2349-2357. (b) Shafer, R.H.; Smirnov, I. Biological aspects of DNA/RNA quadruplexes. *Biopolymers* **2000**, *56*, 209–227.

43. (a) Cantor, C. R.; Warshaw, M. M.; Shapiro, H. Oligonucleotide interactions. 3. Circular dichroism (CD) studies of the conformation of deoxyoligonucleotides. *Biopolymers* **1970**, *9*, 1059-1077. (b) Porumb, H.; Monnot, M.; Fermandjian, S. Circular dichroism signatures of features simultaneously present in structured guanine-rich oligonucleotides: a combined spectroscopic and electrophoretic approach. *Electrophoresis*, **2002**, *23*, 1013-1020.
44. (a) Hanakahi, L. A.; Sun, H. Maizels, N.; High affinity interactions of nucleolin with G-G-paired rDNA. *J. Biol. Chem*. **1999**, *274*, 15908-15912. (b) Bates, P. J.; Kahlon, J. B.; Thomas, S. D.; Trent, J. O.; Miller, D. M. Antiproliferative activity of G-rich oligonucleotides correlates with protein binding. *J. Biol*. *Chem*. **1999**, *274*, 26369-26377.
45. A. W.; Bogdarina, I.; Schroeder, E.; Taylor, I. A.; Kneale, G. G. *J. Mol. Biol.* **2000**, *301*, 575-584. Gaffney BL, Wang C, Jones R A. Nitrogen- 15-labeled oligodeoxynucleotides.4. Tetraplex formation ofd[G(^{15}N7)GTITITGG and d[T(^{15}N7)-GGGT] monitored by proton detected nitrogen-15 NMR. *J. Am. Chem. Soc*. **1992**, *114*, 4047-4050.
46. (a) Guo, Q.; Lu, M.; Kallenbach, N. R. Effect of thymine tract length on the structure and stability of model telomeric sequences. *Biochemistry* **1993**, *32*, 3596-3603. (b) Darnell, j. C.; Jensen, K. B.; Jin, P.; Brown, V.; Warren, S. T.; Darnell, R. B. *Cell* **2001**, *107*, 489-499.
47. (a) White, L. K.; Wright, W. E.; Shay, J. W. Telomerase inhibitors. *Trends Biotechnol*. **2001**, *19*, 114-120. .(b) Bearss, D.J.; Hurley, L.H.; Von Hoff, D. D. Telomere maintenance mechanisms as a target for drug development. *Oncogene* **2000**, *19*, 6632-6641. (c) Mergny, J. L.; Mailliet, P.; Lavelle, F.; Riou, J. F.; Laoui, A. Helene, C. The development of telomerase inhibitors: the G-quartet approach. *Anticancer Drug Des*. **1999,** *14*, 327-339. (d) Simonsson, T.; Pecinka, P.; Kubista, M. DNA tetraplex formation in the control region of c-myc. *Nucleic Acids Res*. **1998**, *26*, 1167-1172. (e) Kettani, A.; Kumar, R. A.; Patel, D. J. Solution structure of a DNA quadruplex containing the fragile X syndrome triplet repeat. *J. Mol. Biol*. **1995**, *254*, 638-656.
48. Dominick, P. K.; Jarstfer, M. B. A conformationally constrained nucleotide analogue controls the folding topology of a DNA G-quadruplex. *J. Am. Chem. Soc*. **2004,** *126*, 5050–5051.
49. Randazzo, A.; Esposito, V.; Ohlenschläger, O.; Ramachandran, R; Mayol, L. NMR solution structure of a parallel LNA Quadruplex. *Nucleic Acids Res.* **2004**, *32*, 3083-3092.
50. Nielsen, P. E.; Egholm, O.; Berg, R. H. & Buchardt, O. Sequence selective recognition of DNA by strand displacement with a thymine substituted ployamide. *Science* **1991**, *254*, 1497-1500.
51. Egholm, M.; Buchardt, O.; Christensen, L.; Beherns, C.; Freier, S. M.; Driver, D. A.; Berg, R. H.; Kim, S. K.; Norden, B.; Nielsen, P. E. PNA hybridizes to complementary oligonucleotides obeying the Watson-Crick hydrogen bonding rules. *Nature* **1993**, *365*, 566-568.
52. Esposito, V.; Galeone, A.; Mayol, L.; Messere, A.; Piccialli, G.; Randazz, A. A PNA-DNA chimeras forming quadruplex structures. *Nucleosides Nucleotides Nucleic Acids* **2003**, *22*, 1681-4.
53. (a) Datta, B.; Schmitt, C; Armiatage, B. A. Formation of a PNA_2-DNA_2 hybrid quadruplex. *J Am. Chem. Soc*. **2003**, *125*, 4111-8. (b) Armiatage, B. A. The impact of nucleic acid secondary structure on PNA hybridization. *Drug Discov Today* **2003**, *8*, 222-228.

54. Esposito, V.; Randazzo, A.; Messere, A.; Galeone, A.; Petraccone, L.; Giancola, C.; Piccialli, G.; Mayol, L. Synthesis and Structural Characterization of PNA-DNA Quadruplex-Forming Chimeras. *Eur. J. Org. Chem.* **2003**, 3364-3371.

55. Ghosh, Y. K.; Balasubramanian, S. A. PNA G_4 Quadruplex. *J. Am. Chem. Soc*. **2004**, *126*, 5944-5945.

56. (a) Vairamani, M.; Gross, M. L.; G-quadruplex formation of thrombin-binding aptamer detected by electrospray ionization mass spectroscopy *J. Am. Chem. Soc.* **2003**, *125*, 42-43. (b) Rosu, F.; Gabelica, V.; Houssier, C.; Colson, P.; De Pauw, E. Triplex and quadruplex DNA structures studied by electrospray mass spectrometry *Rapid Commun. Mass Spectrom*. **2002**, *16*, 1729-1736.

57. (a) D'Costa, M.; Kumar, V. A.; Ganesh, K. N. Aminoethylprolyl peptide nucleic acids (*aep*-PNA): chiral PNA analogues that forms highly stable DNA:*aep*PNA_2 triplexes. *Org. Lett.* **1999**, *1*, 1513-1516. (b) D'Costa, M.; Kumar, V. A.; Ganesh, K. N. Aminoethylprolyl (*aep*) PNA: mixed purine, pyrimidine oligomers and binding orientation preferences for PNA:DNA duplex formation. *Org. Lett*. **2001**, *3*, 1281-1284.

58. (a) Perry, P. J.; Jenkins, T. C. Recent advances in the development of telomerase inhibitors for the treatment of cancer. *Expert Opin*. *Invest*. *Drugs* **1999,** *8*, 1981-2008. (b) Catasti, P.; Chen, X.; Moyzis, R. K.; Bradbury, E. M.; Gupta, G. Structure-function correlations of the insulin-linked polymorphic region. *J. Mol. Biol.* **1996**, *264*, 534-545.

59. Mergny, J. L.; Phan, A. T.; Lacroix, L. Following G-quartet formation by UV spectroscopy. *FEBS Lett*. **1998,** *435*, 74-78.

60. Murchie, A. I. H.; Lilley, D. M. J. Retinoblastoma susceptibility genes contain 5' sequences with a high propensity to form guanine-tetrad structures. *Nucleic Acids Res.* **1992**, *20*, 49-53.

61. Dempsey, L. A.; Sun, H.; Hanakahi, L. A. Maizels, N. G_4 DNA binding by LR1 and its subunits, nucleolin and hnRNP D. A role for G-G pairing in immunoglobulin switch recombination. *J. Biol. Chem*. **1999**, *274*, 1066-1071.

62. Zahler, A. M.; Williamson, J. R.; Cecla, T. R.; Prescott, D.M. Inhibition of telomerase by G-quartet DNA structures. *Nature* **1991**, *350,* 718-20.

63. Siddiqui-Jain, A.; Grand, C. L.; Bearss, D. J.; Hurley, L. H. Direct evidence for a G-quadruplex in a promoter region and its targeting with a small molecule to repress c-MYC transcription. *Proc. Natl Acad. Sci. USA*, **2002**, *99*, 11593-11598.

5A.9 APPENDIX

1. HPLC of PNA 1-6

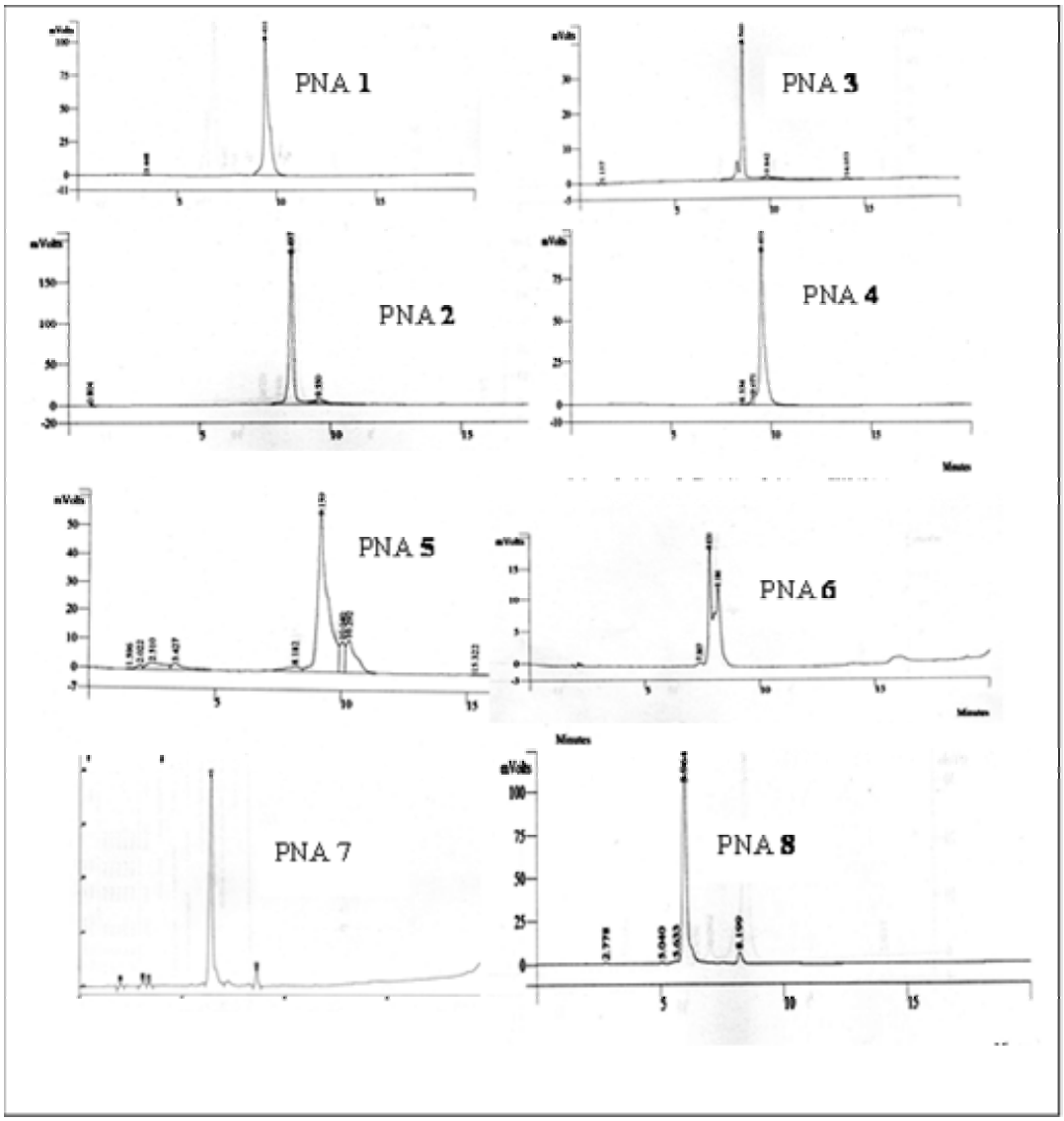

2. Derivative curves of UV-Melting profiles *aeg*-/aep-PNA **1-6** and DNA **10**

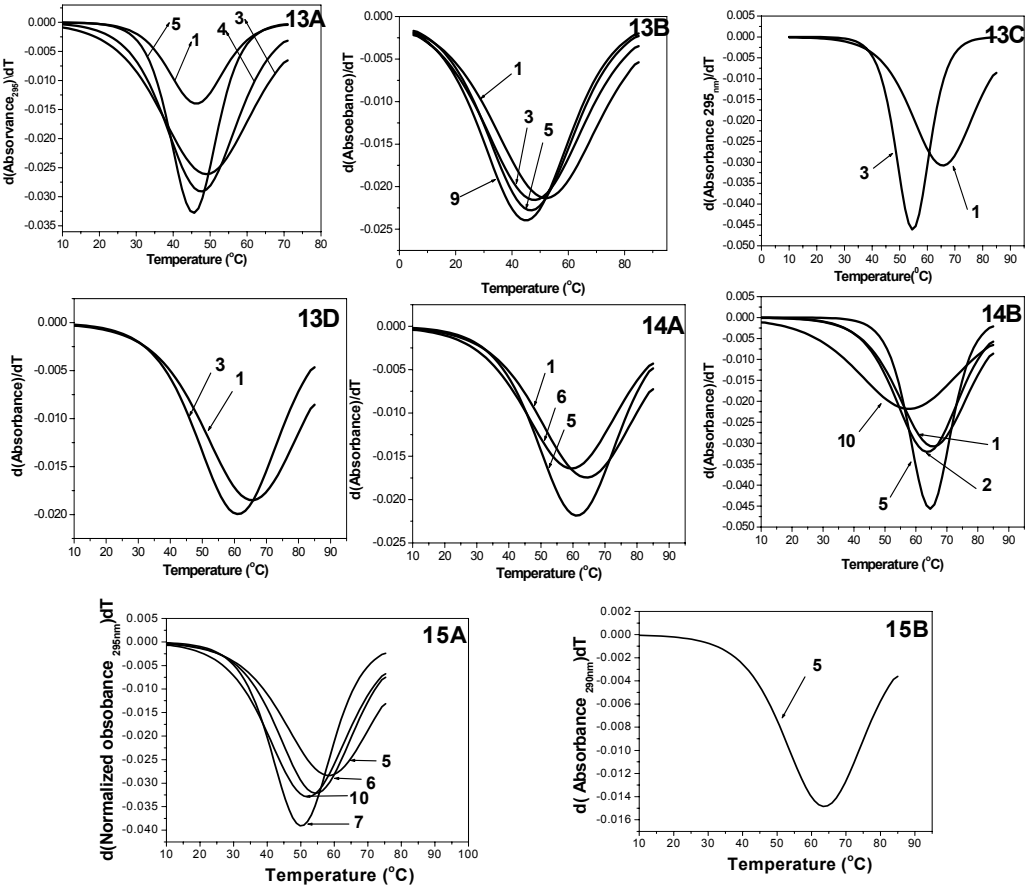

3. MALDI-TOF of PNA **1-2** and **4**

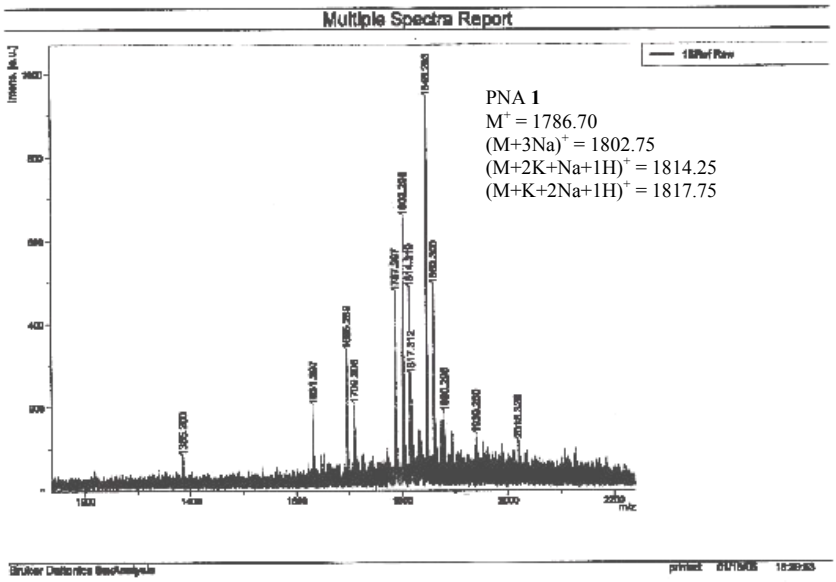

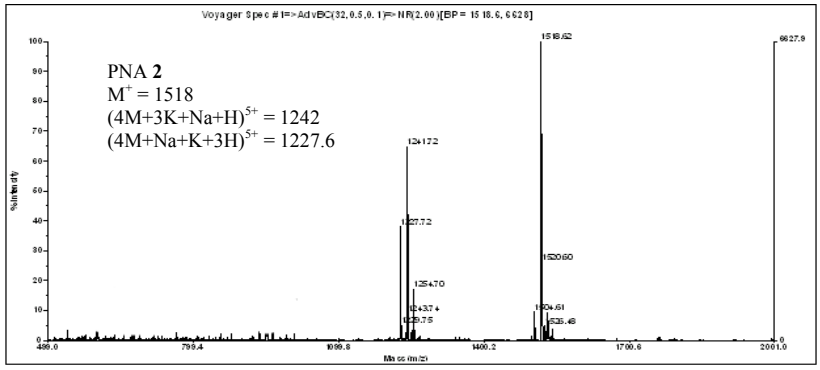

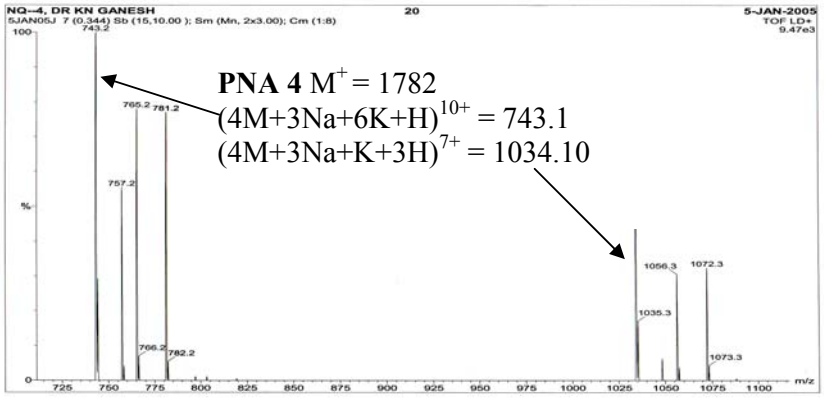

4. ESI mass of PNA **3** and **5**

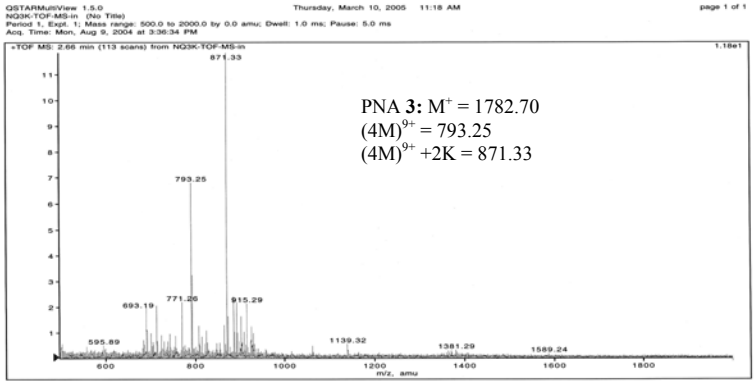

PNA **3:** $M^+ = 1782.70$
$(4M)^{9+} = 793.25$
$(4M)^{9+} + 2K = 871.33$

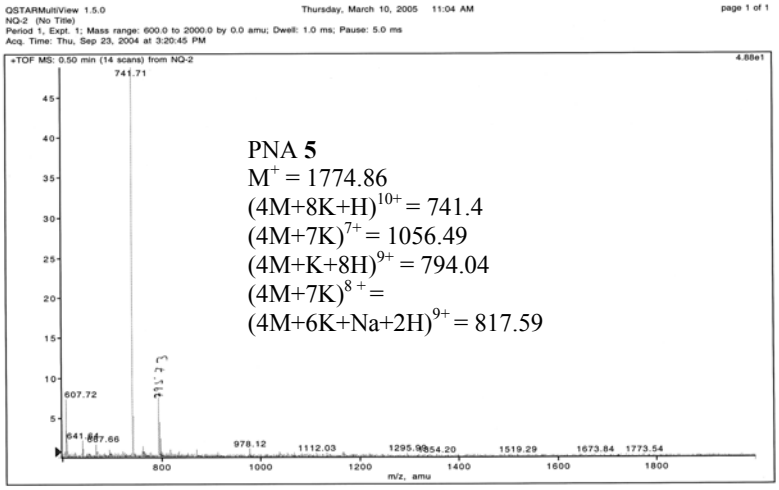

PNA **5**
$M^+ = 1774.86$
$(4M+8K+H)^{10+} = 741.4$
$(4M+7K)^{7+} = 1056.49$
$(4M+K+8H)^{9+} = 794.04$
$(4M+7K)^{8+} =$
$(4M+6K+Na+2H)^{9+} = 817.59$

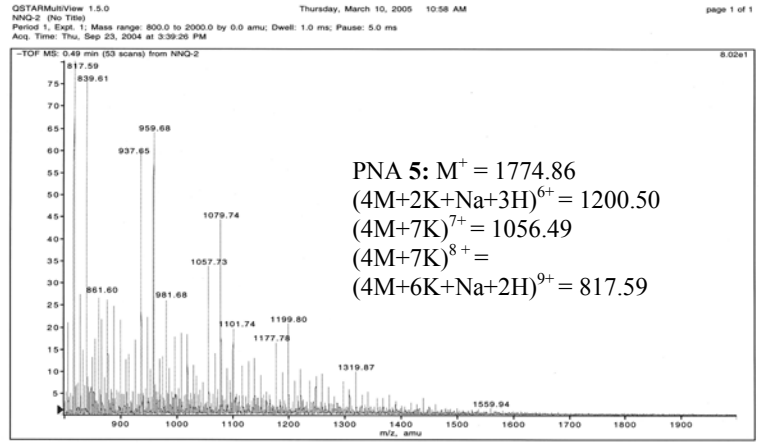

PNA **5:** $M^+ = 1774.86$
$(4M+2K+Na+3H)^{6+} = 1200.50$
$(4M+7K)^{7+} = 1056.49$
$(4M+7K)^{8+} =$
$(4M+6K+Na+2H)^{9+} = 817.59$

5. MALDI-TOF of PNA 5 (with salt Na^+)

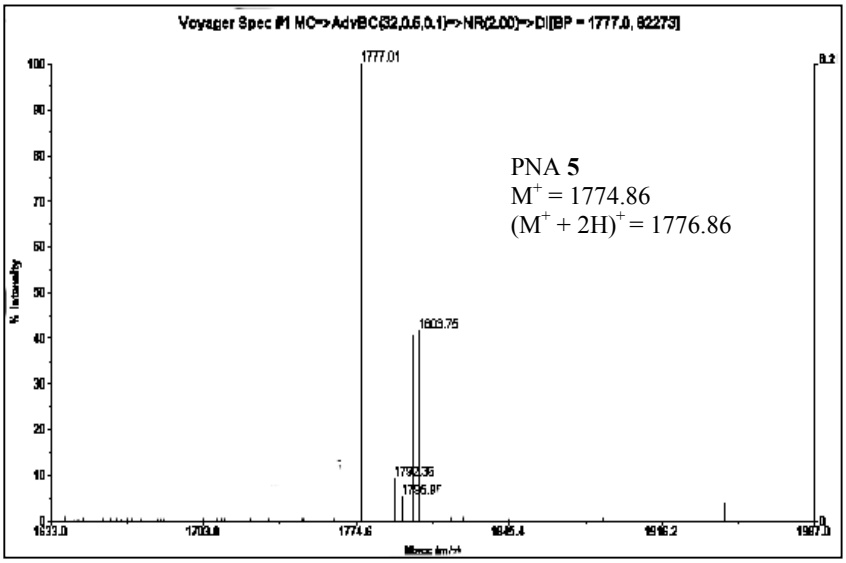

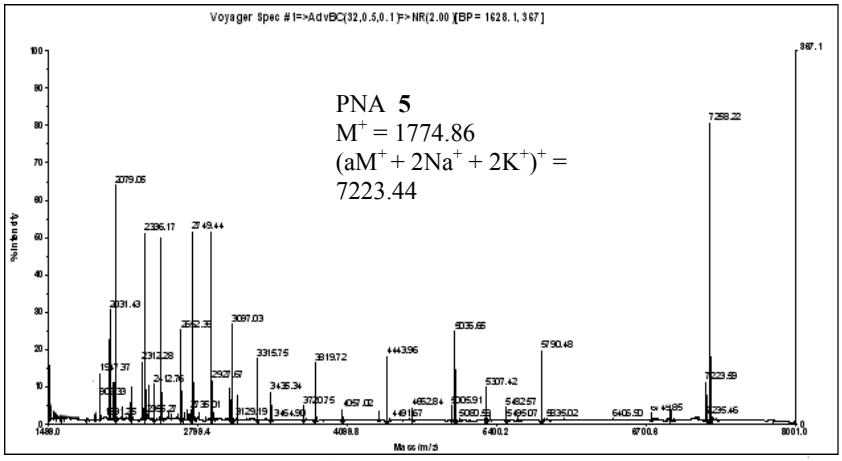

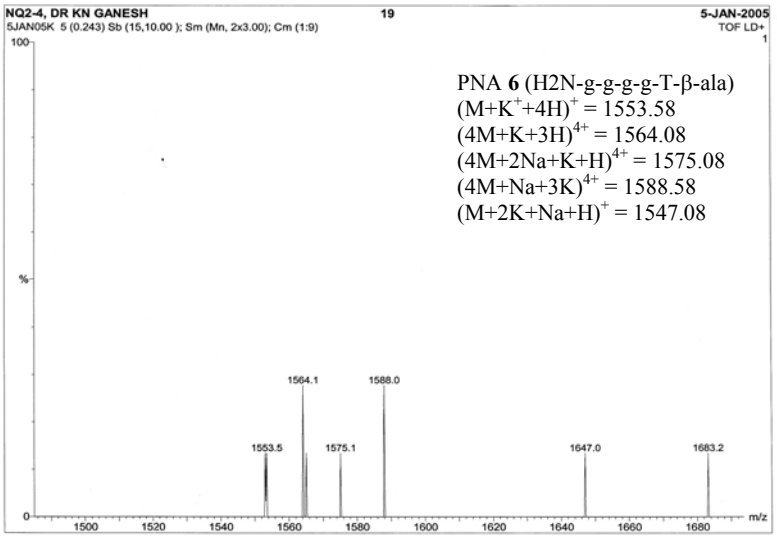

6. ESI mass of PNA **5-6**

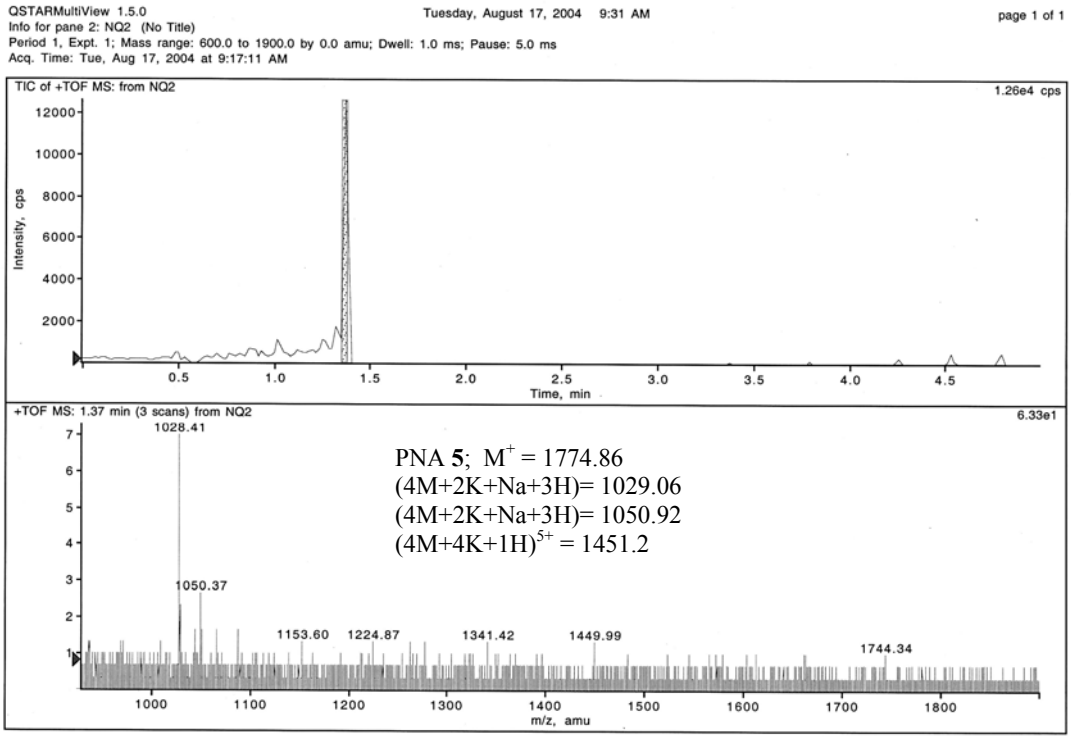

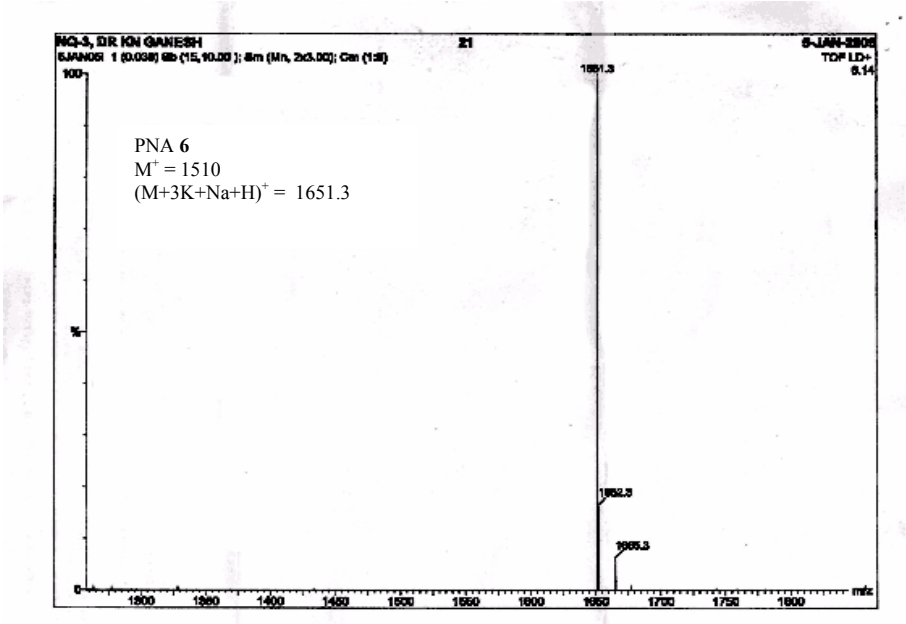

7. ESI mass spectra of PNA **5**

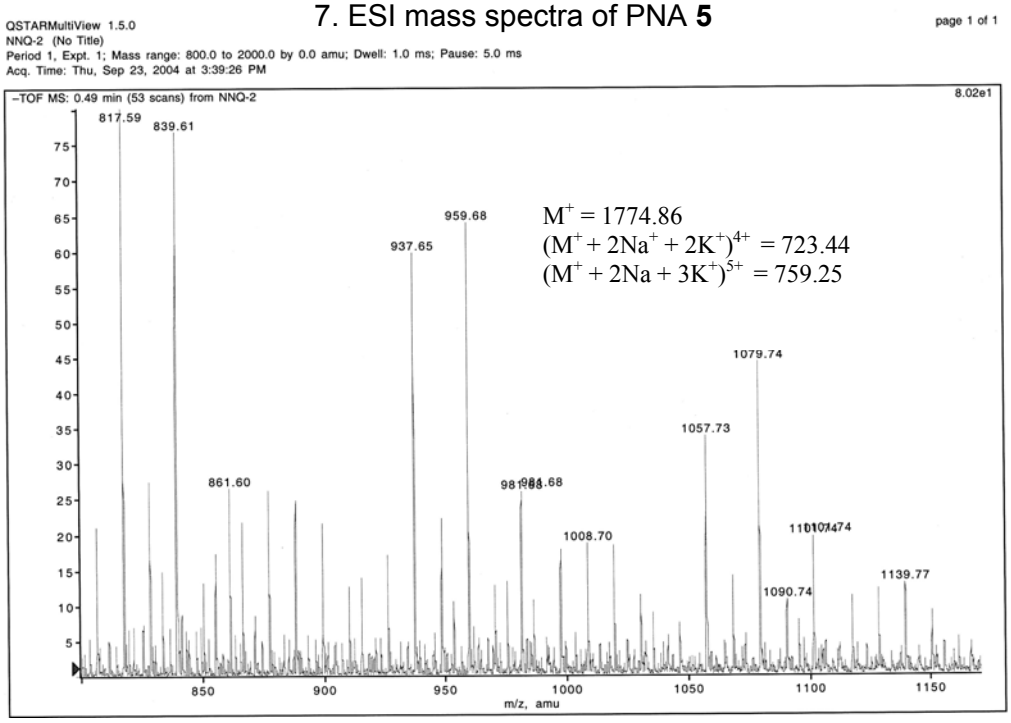

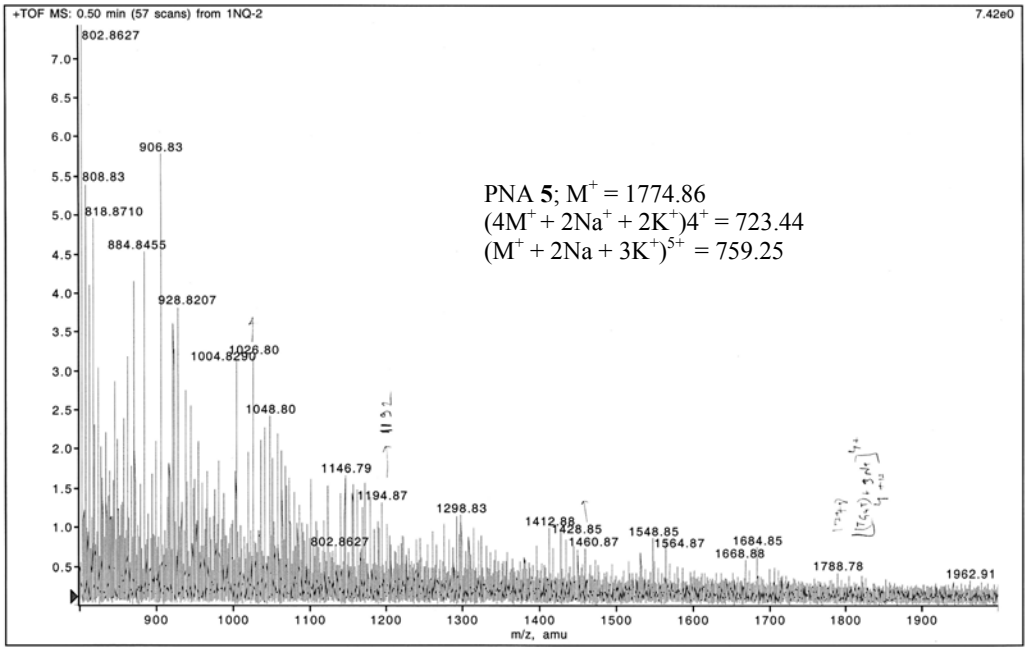

8. MALDI-TOF of PNA **1**

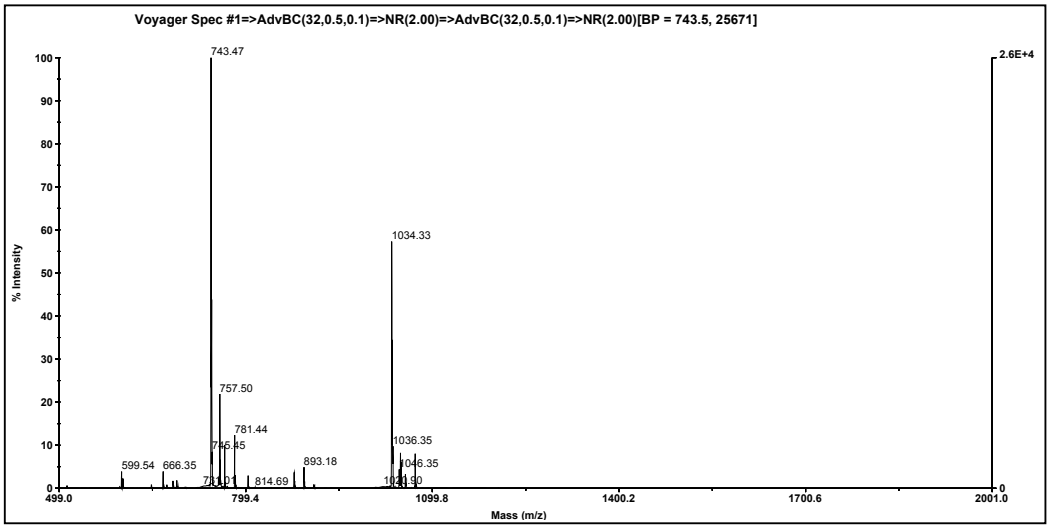

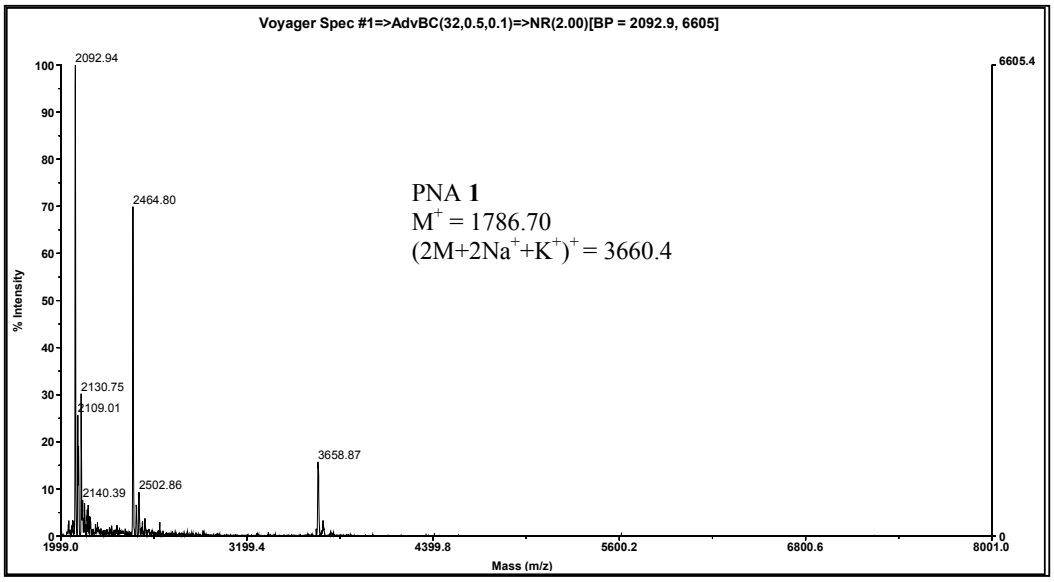

PNA **1**
$M^+ = 1786.70$
$(2M+2Na^+ + K^+)^+ = 3660.4$

9. MALDI-TOF of PNA **7-9**

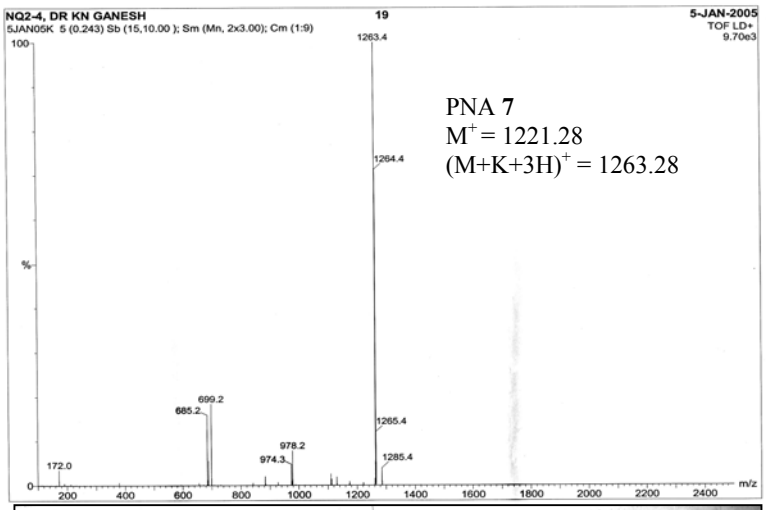

PNA **7**
M^+ = 1221.28
$(M+K+3H)^+$ = 1263.28

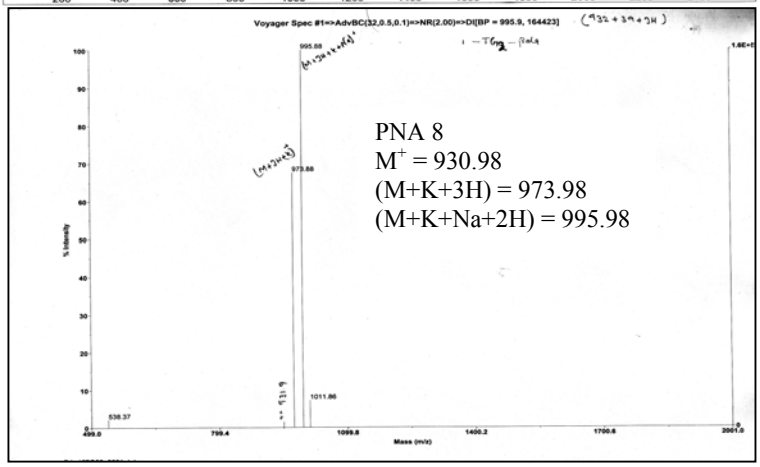

PNA 8
M^+ = 930.98
(M+K+3H) = 973.98
(M+K+Na+2H) = 995.98

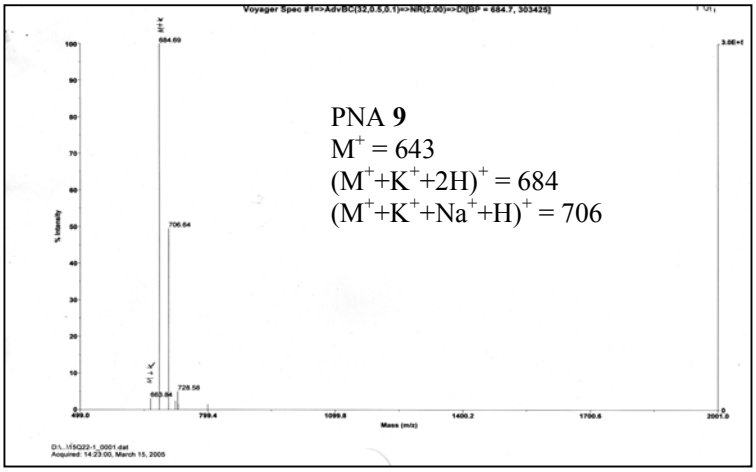

PNA **9**
M^+ = 643
$(M^+ + K^+ + 2H)^+$ = 684
$(M^+ + K^+ + Na^+ + H)^+$ = 706

10. MALDI-TOF of PNA **3**

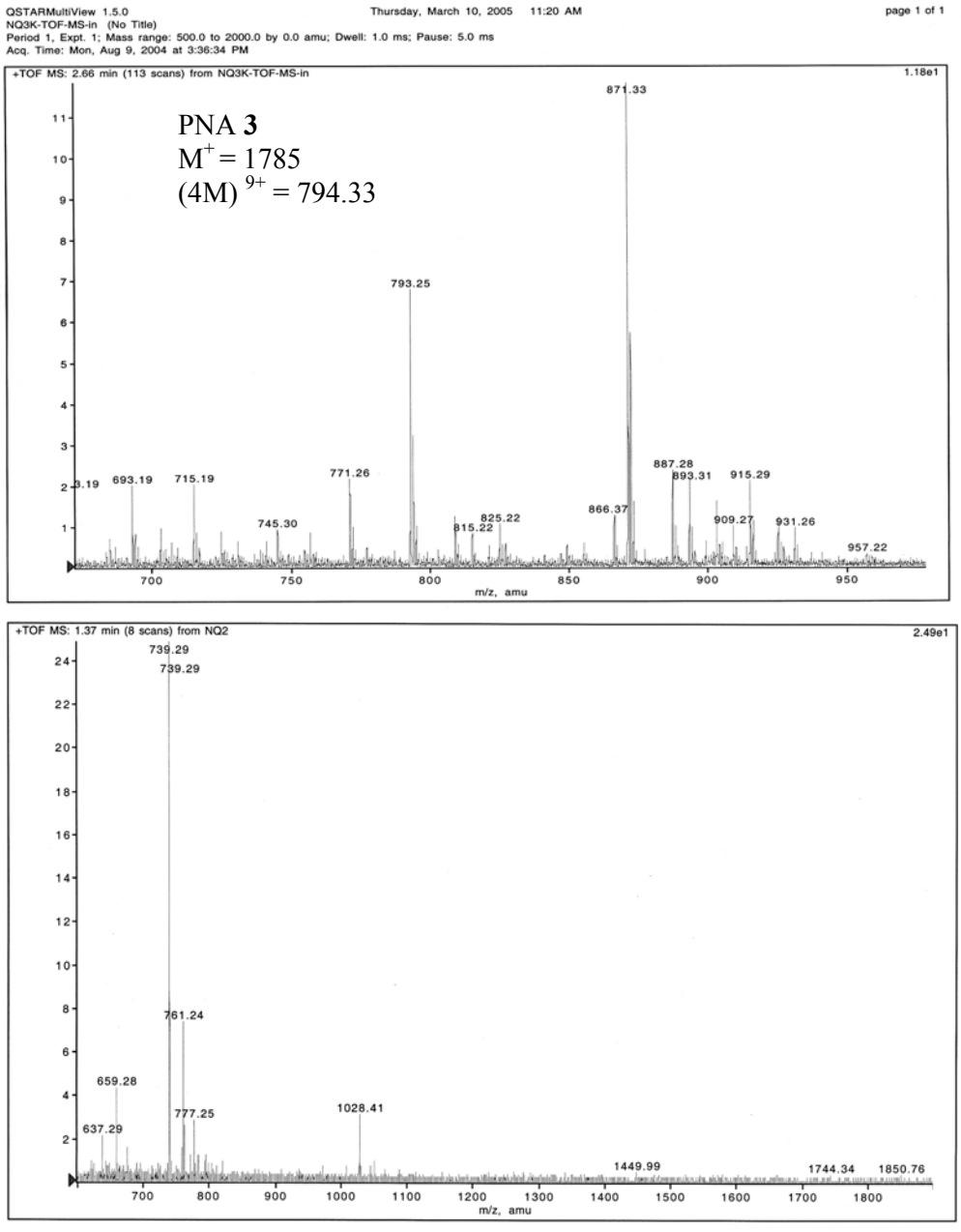

CHAPTER 5B: PNA TETRAPLEXES: BIOPHYSICAL STUDIES OF *i*-MOTIF OF *aeg*-PNA

5B.1 INTRODUCTION

In continuation of the previous section, the study of other class of tetraplexes namely the *i*-motif in nucleic acids is described in this section. The telomeric DNA has guanine (G) and cytosine (C) rich DNA sequence regime[1] and G-rich DNA oligomers are well known to form G_4-tetrads via combination of Watson-Crick and Hoogsteen hydrogen bond mediated cyclic structures, as elaborated in the earlier Section.[2] In comparison, the C-rich sequences form tetramers via the semi protonated C-C^+ base pairs held by three hydrogen bonds to form parallel double strands.[3] Two such double strands interdigitating through C:C^+ base pairs lead to the four-stranded *i*-motif structure (Figure 1).[4] The opposed dipoles of exocyclic C2-carbonyl and N4-amino groups favour such an interaction of consecutive base pairs by alternate stacking of the amino and carbonyl groups.[5]

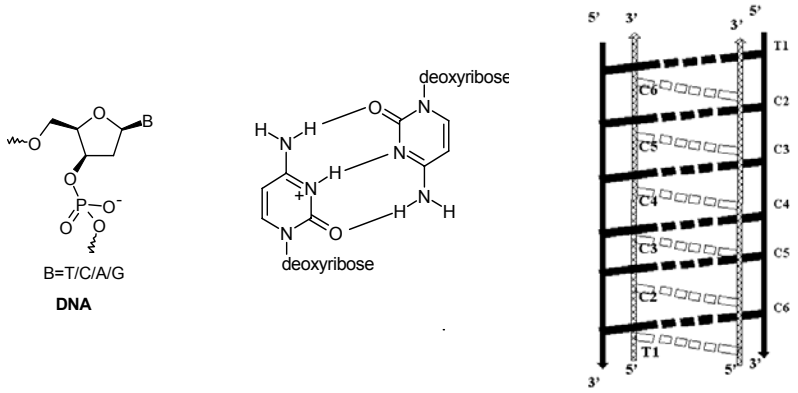

Figure 1: (a) Chemical structures of DNA; (b) Schematic diagram of *i*-motif in DNA.

Recently, the discovery of *i*-motif structures and investigation of their properties in context to possible biological relevance is extensively described within the framework on quadruplexes of DNA/RNA.[6] The structure of the DNA oligomer with continuous C-stretch (5′-TC_6-3′) at acidic pH formed a four-stranded complex, in which two base-paired parallel-stranded duplexes are intimately associated via their base pairs, which are fully intercalated.[7] The relative orientation of the duplex pairs is anti-parallel so that each base

pair is face-to-face with its neighbour. The possibility of forming *i*-motif structure with C-rich ribonucleic acids (RNA) has been investigated.[8] The C-rich sequence of RNAs as r(UC_5), r(C_5), r(C_5U) and r(UC_3) associate into multiple intercalated structures at acidic pH. The conformational differences between RNA *i*-motif and the DNA *i*-motif arise from the C3′-endo pucker of the RNA sugars. The orientations of the intercalated C:C^+ pairs in RNA result in a slight widening of the narrow grooves at the steps where the hydroxyl groups come in close contact. Two types of *i*-motif structures are postulated in RNA sequence r(UC_5). The major one is the *i*-motif similar to DNA and the minor one is different with respect to stacking topology due to 2′-OH/2′-OH, repulsive contacts in the fully intercalated structure. The free energy of the RNA *i*-motif (on average -4 kJ mol^{-1} per C·C^+ pair) is half the value of DNA *i*-motif structures.[5,9]

5B.2 RATIONALE OF PRESENT WORK

5B.2.1 Structural characterization of the *i*-motif structure in DNA/RNA

The structure of *i*-motif in nucleic acid is characterized by many known techniques like NMR-spectroscopy, X-ray crystallography, Raman spectroscopy, CD and UV-spectroscopies.

5B.2.1a NMR-Spectroscopy

A tetrameric DNA structure with protonated C:C^+ base pairs has been studied by NMR.[10] Oligomers containing continuous tracts of cytidine form hemiprotonated base pairs at acidic pH and are double-stranded. The structure of the DNA oligomer 5'-d(TCCCCC)[11] at acidic pH is found to be a four-stranded complex in which two base-paired parallel-stranded duplexes are intimately associated, with their base pairs fully intercalated. The NMR spectrum indicates the structure to be highly symmetrical with the

four strands being equivalent. A model derived by energy minimization with constrained molecular dynamics shows excellent compatibility with the observed nuclear Overhauser effects (NOEs) such as inter-residue sugar-sugar NOEs H1'-H1', H1'-H2" and H1'-H4', which are diagnostic for such tetrameric structures.[12] Proton exchange transfer occurs easily from a donor hydrogen (DH) to an acceptor (A) via hydrogen-bonded complex (DH-A). Exchange requires the disruption of the base pair, followed by chemical exchange from the open pair and it occurs even at neutral pH in the absence of added catalyst. The formation of *i*-motif in d(TC_8), d(TC_3) and d($T_2C_8T_2$) has also been characterized by NMR.[14]

5B.2.1b Characterization of i-motif Structure by Crystallography

i-Motif structure in C-rich sequences of DNA has also been characterized by single crystal X-ray diffraction.[15] The *i*-motif structure assigned by NMR and X-ray are not quite similar, but show some gross similarities. The X-ray structure reveals much more microheterogeneity that can be visualized in the NMR structure. Differences are found in phosphate orientations and the relative positioning of the adjacent chains. There is a great similarity in the interactions of the bases and the overall packing of the sugar phosphate backbones. Both analyses show a large number of C4'-exo puckers, with minor differences in the helical twist.[5] This organization, termed as the intercalation motif (*i*-motif), is distinctly different from either the DNA duplexes or the G_4-DNA quadruplexes in which four planar guanine residues are found in cyclic hydrogen bonding. Gehring *et. al.*[6,10,] attribute the stability to van der Waals stabilization between the sugar phosphate backbones across the narrow groove and the opposite dipole orientations of the carbonyl and amino groups. The closer stacking of the bases of 3.1 Å, instead of the more familiar 3.4 Å arising from the exocyclic residue overlapping with the local n-electron clouds, is

also known to impart additional contribution to stability. The crystal structure of a four intercalated DNA sequence d(C4) is also reported (Figure 2).[16]

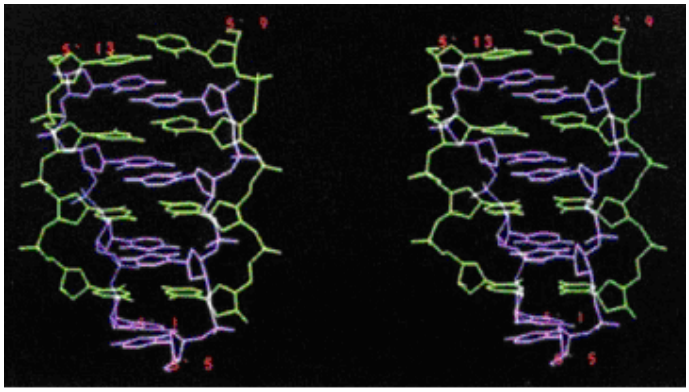

Figure 2: Crystal structure of d (C4)[16]

5B.2.1c Raman spectroscopy

Raman spectroscopy is an effective probe of nucleic acid secondary structure determination in both solution and crystalline samples.[17] Raman spectra of solutions of 5′-dCMP, d(CCCT), and d(C_8) were excited at 514.5 nm. Raman frequencies of well-resolved bands are accurate to within (1.5 cm^{-1}). For d(CCCT) and d(C_8), spectral intensities were normalized to the phosphodioxy stretching band at 1092 cm^{-1}, which is essentially invariant to pH change in the range of present interest. Raman spectra of single crystals of d(CCCT) were obtained at 514.5 nm excitation. The nucleic acid *i*-motif, which results from antiparallel intercalation of two parallel-stranded duplexes containing hemiprotonated cytosine base pairs [$(C:C)^+$], is characterized by a unique Raman signature. Both thermostability (Tm) and the extent of cytosine protonation (pKC) in *i* motif quadruplexes of d(CCCT) and d(C8) have been monitored. The crystal structure is conserved in aqueous solution, despite the fact that C3′-*endo* conformation is rarely seen in deoxynucleosides. Stabilization of the *i* motif by cytosine base pairing and stacking, estimated here as <0.17 kcal/mol of $(C:C)^+$, is apparently sufficient to compensate for the

incorporation of C3′-*endo* sugars in the backbone of the solution quadruplex. In the d(CCCT) crystal, the four phosphodiester strands are not conformationally identical, leading to an asymmetric quadruplex. The Raman signature of hemiprotonated cytosine base pairs is distinct from the signatures of unprotonated and protonated cytosines, making it useful as marker for protonated cytosines. This should be of value in assessing the extent of cytosine protonation/hemiprotonation in duplex, triplex, and quadruplex structures of DNA.

5B.2.1d Characterization of i-motif structure by CD

The structural characterization of *i*-motif in DNA by CD of $d(C_3TA_2)_3C_3$ indicated little dependence on the cation species.[18] In CD profiles with either Na^+ or K^+, a positive band around 275 nm and a negative one near 250 nm existed at neutral pH, whereas a peak near 288 nm and a trough near 256 nm appeared at pH 5.5.[19] The red-shift in the CD bands as the pH is lowered to 5.5, which are attributed to the *i*-motif structure.

5B.2.1e Thermal denaturation study by UV

In UV spectra, protonated cytosines show characteristic absorption at 295 nm.[20] Hence UV-thermal transitions monitored at 295 nm show a reverse sigmoidal pattern characteristic of formation of $C\text{-}C^+$ tetraplexes like G-quartet structure.[21] The kinetic and thermodynamic aspects of *i*-motif formation in modified oligonucleotides has been studied by UV at 295 nm.[22]

DNA and RNA have very versatile auto-association properties,[8] the range of which extends from formation of duplexes to triplexes and tetraplexes. RNA lacks ability to form *i*-motif structures in some sequences.[23] Considerable interest is now growing in the study of tetraplexing properties of mimics of natural oligonucleotides such as phosphorothioates,[24] LNA,[25] and PNA.[26-27] While G_4 tetraplex formation was successfully

demonstrated recently in *aeg*-PNA,[28] it was reported that the PNA H-$C_4A_4C_4$-Lys-NH_2 did not form C-C^+ tetraplexes at pH 7.0. However, The *i*-motif formation in *alanine*-PNA was observed by Diedersen, *et*. *al*.[29] Based on steric factors, it was shown that *ala*-PNA forms C-C^+ complexes in C_4 tetramer, but not in C_8-octamer (Figure 3). The successful confirmation of *i*-motif structure by UV and NMR in TC_4 sequences of *ala*-PNA encourages us to trace tetraplexing properties in 1-*N*-aminoethylglycine peptide nucleic acid (*aeg*-PNA). As described in the preceding Chapters, PNA is one of most promising mimic of nucleic acid with remarkable thermal stability over DNA as both in duplex and G-quadruplexes. However, no report exists so far on successful tetraplexing properties of unmodified PNA.

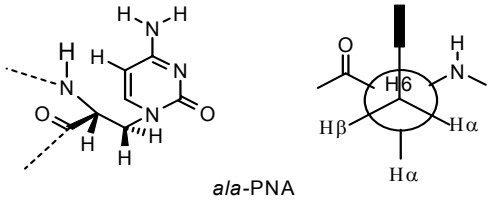

ala-PNA

Figure 3: Chemical structure of alanine PNA

5B.2.2 Objective

Recently, a large number of nucleic acid mimics have been developed, for antisense therapeutics, but few reports exist on *i*-motif formation by them. Due to the interesting result of *ala*-PNA, we chose to examine *aeg*-PNAs with C-rich sequences TCn (n = 2, 3, 4, 8) to study the pH dependent tetraplex formation by temperature dependent UV-spectroscopy (Figure 4).

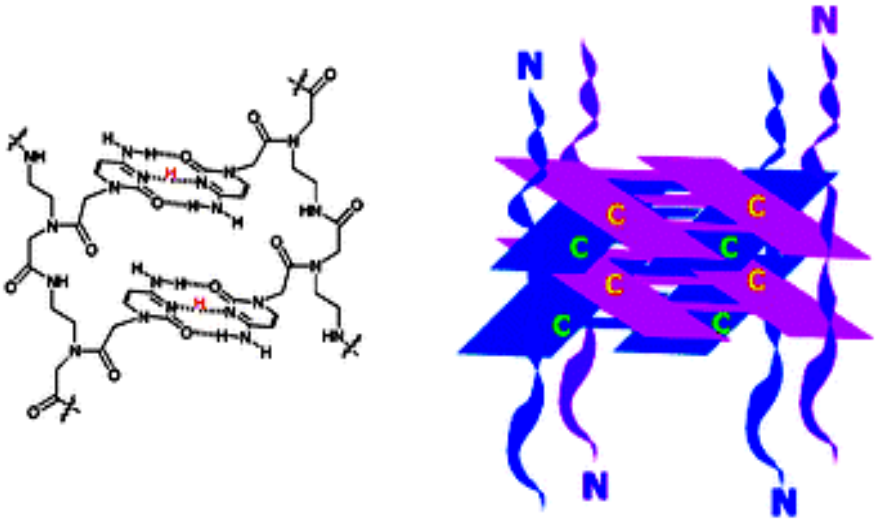

Figure 4: Schematic presentation of PNA *i*-motif

5B.3 PRESENT WORK

5B.3.1 Synthesis and characterization of *aeg*-PNA oligomers

The cytosine (C) and thymine (T) monomer (Figure 5) of aminoethylglycine-(*aeg*)-PNA monomers were synthesized by using synthetic procedures described earlier.[30-31] For *i*-motif study in PNA, the following oligomers of PNA TCn were synthesized on solid support Merrifield resin, using *t*-Boc chemistry using similar procedure as described in Chapter 4.

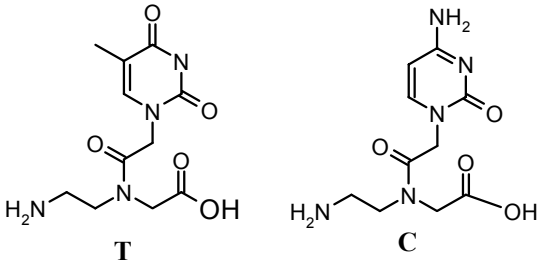

Figure 5: Chemical structure of Thmine and Cytosine monomer of *aeg*-PNA

1. H_2N-T-C-C-*β-ala*-MF; (TC_2)
2. H_2N-T-C-C-C-*β-ala*-MF; (TC_3)
3. H_2N-T-C-C-C-C-*β-ala*-MF; (TC_4)
4. AcHN-Lys-T-C-C-C-C-C-C-C-C-CONH-MBHA; (TC_8)

All these PNAs sequences were cleaved from resin using TFA-TFMSA and they were purified to homogeneity by HPLC and characterized by MALDI-TOF mass spectroscopy.[32] MALDI-TOF mass spectra of TC_2 (PNA **1**), TC_3 (PNA **2**), TC_4 (PNA **3**) and TC_8 (PNA **4**) pure PNA **1-4** (Table 1) are Shown in Table 1. The HPLC chromatogram and mass spectra of PNA **1-4** are given in an appendix to this Chapter. For comparative study, the DNA sequences d(TC_8) and d(TC_8) were synthesisized on *ABI*-DNA synthesizer. A typical mass spectra of TC_4 (PNA **3**) and TC_8 (PNA **4**) are shown in Figure 6.

Table 1: Oligomers for the study of *i-motif* of PNA

PNA	Sequences of PNA	Molecular Formula	Molecular weight (Calculated)
1	H_2N-T-C-C-*β-ala*	$C_{34}H_{49}N_{15}O_{12}$	859.86
2	H_2N-T-C-C-C-*β-ala*	$C_{44}H_{62}N_{20}O_{15}$	1111.11
3	H_2N-T-C-C-C-C-*β-ala*	$C_{54}H_{75}N_{25}O_{18}$	1361.36
4	AcHN-Lys-T-C-C-C-C-C-C-C-C-$CONH_2$	$C_{99}H_{137}N_{47}O_{30}$	2465.49

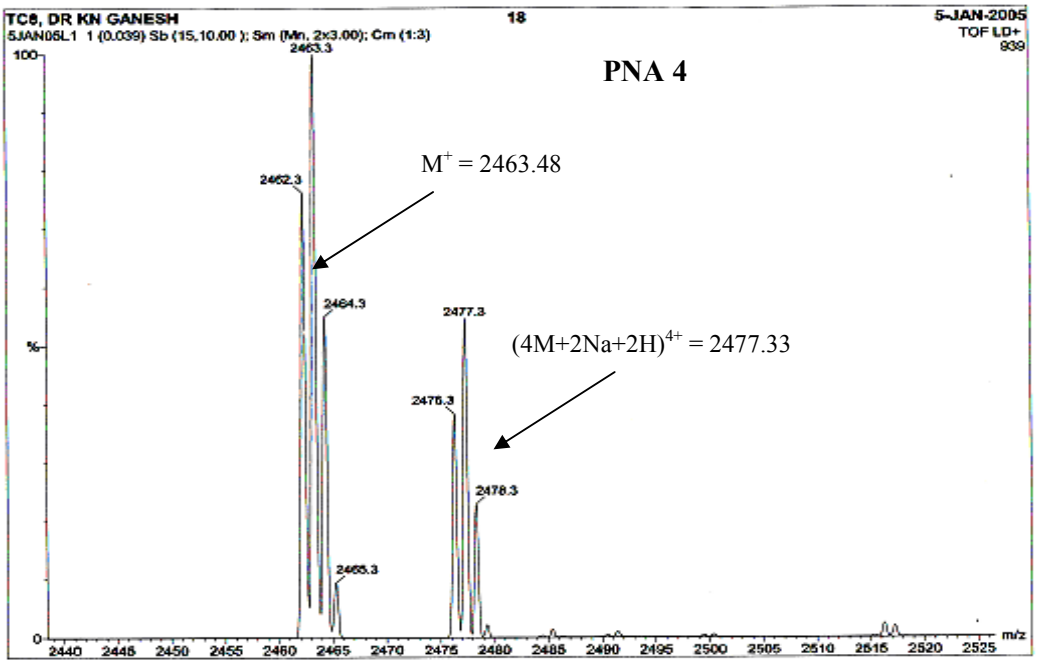

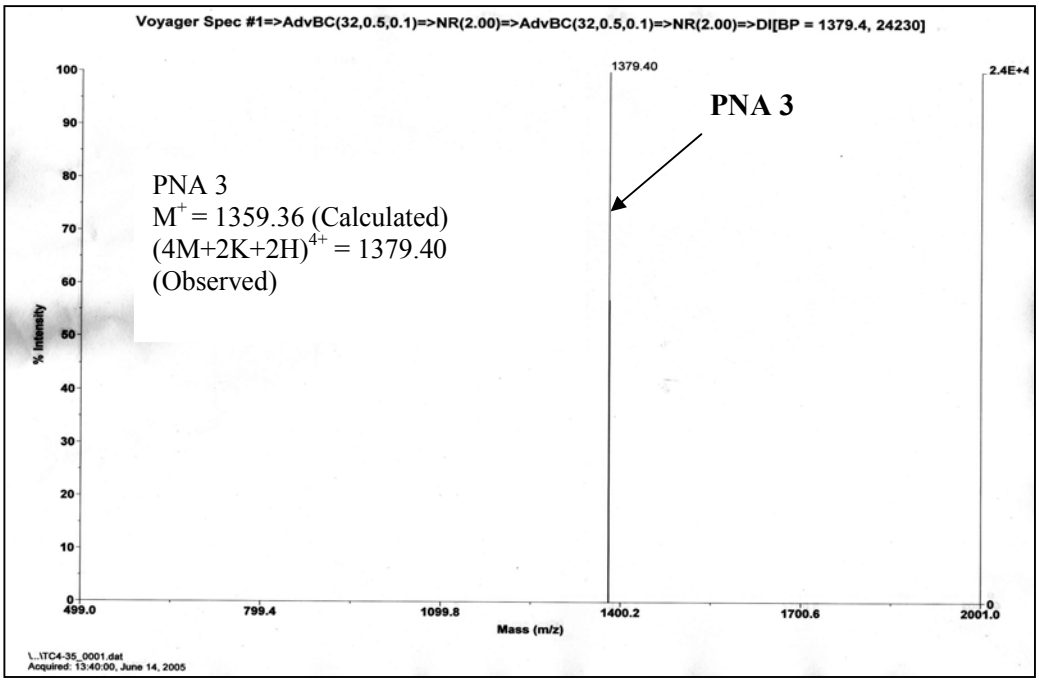

Figure 6: MALDI-TOF mass spectrum of PNA **3** and PNA**4**

5B.4 RESULTS

5B.4.1 Biophysical study of i-motif in PNA by UV spectrophotometer

In the following section, the structures of G-tetrad in *aeg*-PNA and *aep*-PNA have been studied by use of temperature dependent UV-spectroscopy.

5B.4.1a Determination the pK_a for N3 of cytosine

Determination of the pK_a for N3 of cytosine (C)[5,17,23] in monomer and oligomer PNA **4** is determined by their UV-spectra. The UV spectra of PNA **4** were recorded at different pHs in the range 2.8-5.1, at 25°C. The band at 275 nm found at acidic pH 2.8 slowly decreased in intensity and shifted to the lower wavelength 260 nm as the pH is increased. Earlier, it has been observed that the difference in absorbance spectra of protonated and non-protonated cytosine in DNA/RNA is maximum in the region 290-295 nm.[34] Figure 7 shows a plot of UV absorbance at 275 and 295 nm in PNA **4** and in

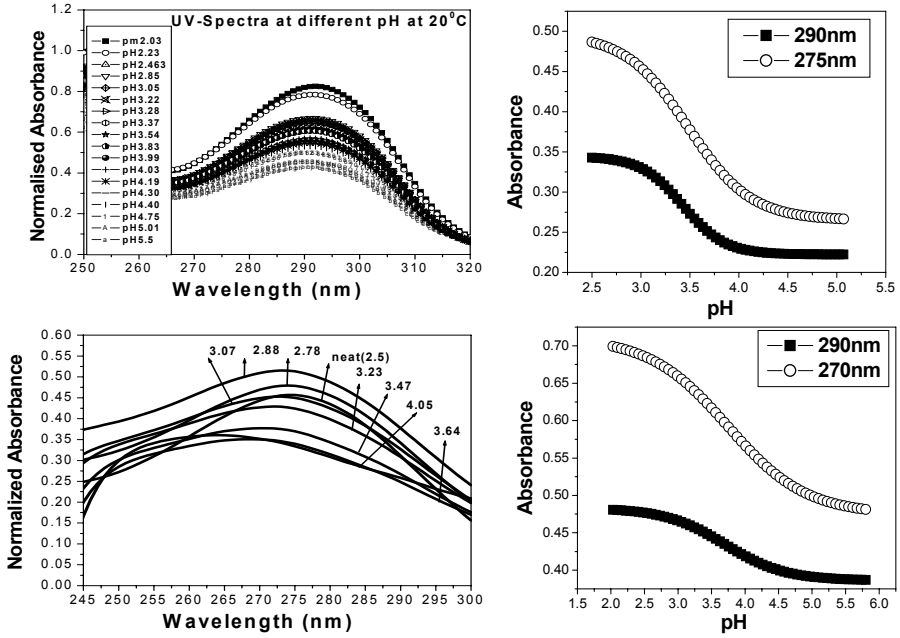

Figure 7: *Left*. The UV-spectra of cytosine monomer and PNA **4**. *Right*. The plot of UV-absorbance vs. pH at 275 and 295 nm.

cytosine monomer as a function of pH and it is seen that the spectral differences between protonated and non-protonated C in PNA are more at 275 nm. From these data, the pK_a for N3 of C in PNA is obtained as 3.42 for PNA **4** and 3.72 for PNA C-monomer, which is significantly lower than that seen for N3 of C in DNA/RNA, which is about 4.8.[37] The formation of C-C^+ tetraplexes in PNA **3**, **4** and $d(TC)_8$ **6** at pHs 3.0, 4.5, 5.0, 6.5 and 7.0 were monitored at 295 nm, for a true comparison with the established tetraplex formation in $d(TC)_n$ by following absorption at 295 nm.[35]

5B.4.2 *i*-motif formation in *aeg*-PNA at different pHs

At pH 3.0: The UV melting profiles (absorbance vs. temperature) of PNAs **3,4** and DNA **5, 6** followed at 295 nm are given in Figure 8A. The observed inverse sigmoidal plots of melting profiles are characteristics for *i*-motif and G-quartets.[22] This preliminary observation of tetraplexes in these sequences suggested the formation of *i*-motif in PNA at low pH 3.0. The Tm values of PNA **3**, PNA **4** and DNA **5** were extracted from the first derivative of their respective melting curves and given in Table 2.

At pH 4.5: The UV melting profile (absorbance vs. temperature) of PNA **3**,**4** and DNA **5**,**6** monitored at 295 nm are given in Figure 8B and these are also show similar type of negative sigmoidal curves. Hence, the PNA **3**,**4** and DNA **5**,**6** are also forming *i*-motif structure at this acidic pH 4.5 and the Tm values extracted from first derivatives plot are given in Table 2.

At pH 5.0: The UV-melting profiles of PNA **1-4** and DNA **6** at pH 5.0 are shown in Figure 8C, which suggests successful formation of *i*-motif in PNA **3**,**4** and DNA **6** 295 nm. The Tm value of PNA **3,** PNA **4** and DNA **6** shows presence of *i*-motif at this pH. PNAs **1-2** do not have negative sigmoidal transition characteristic of *i*-motif under these conditions.

At pH 6.0 and 6.5: The melting profiles of PNA **4** and DNA **6** at pH 6.0 are shown in Figure 8D and at pH 6.5 in Figure 8E. The results indicate absence of i-motif structure in PNA **4** and retention of *i*-motif in DNA **6**.

Table 2: Tm of PNA and DNA *i*-motif at different pH

PNA/ DNA	Sequences of PNA	Tm at different pH (^{0}C) *				
		3.0	**4.5**	**5.0**	**6.0**	**6.5**
1	H_2N-T-C-C-β-ala	nf	nf	nf	-	-
2	H_2N-T-C-C-C-C-β-ala	nf	nf	nf	-	-
3	H_2N-T-C-C-C-C-C-C-β-ala	67.3	40.0	40.5	-	-
4	H_2N-lysT-C-C-C-C-C-C-C-C-C-$CONH_2$	67.4	55.0	46.0	nf	nf
5	d (5'-T-C-C-C-3') DNA	47.5	43.0	ns	-	-
6	d (5'-T-C-C-C-C-C-C-C-C-C-3') DNA	58.4	58.7	55.7	50.4	52.0

* *nf: i-motif is not formed; ns: not studied*

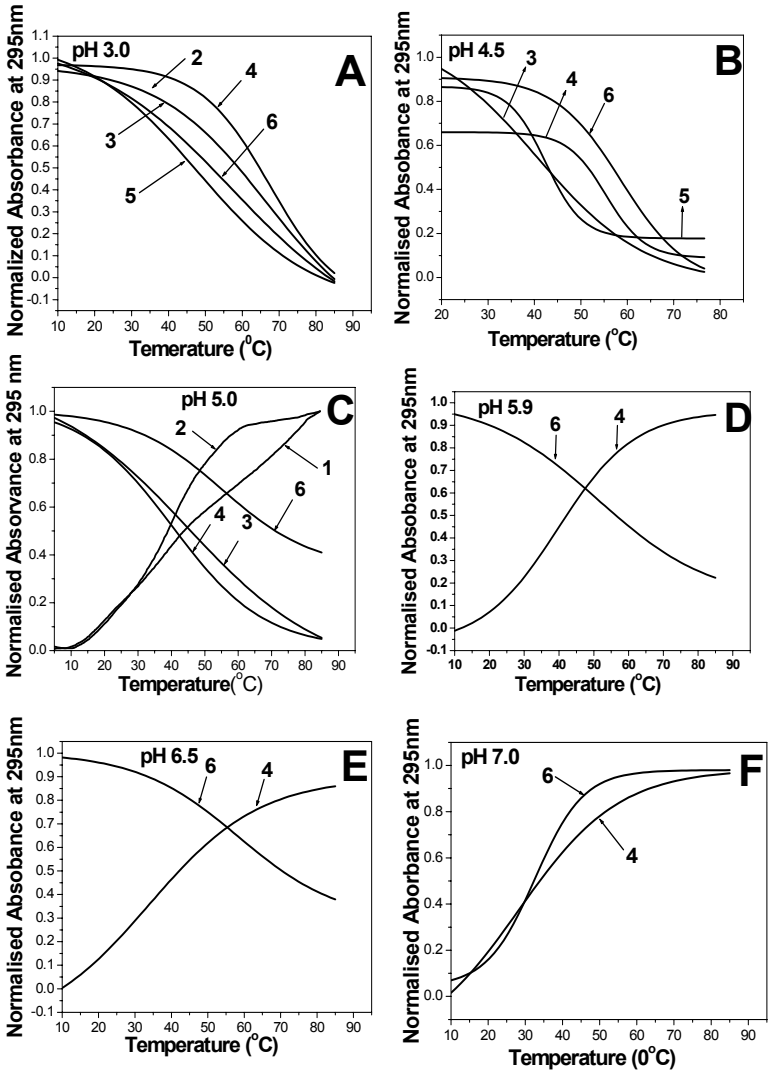

Figure 8: UV melting profile of *aeg*-PNA TCn series

At neutral pH 7.0: In Figure 8F, the melting profiles of both DNA **6** and PNA **4** suggest complete absence of *i*-motif in both cases. On the otherhand, the profile indicates duplex formation. Tms of these duplex transions are obtained 28.8 ^{o}C for PNA **4** and 39.9 ^{o}C for PNA **6**.

5B.4.3 Isothermal Titration Calorimetry (ITC)

ITC was also used to study the dissociation of tetraplex of PNAs **3** and **4** and DNA **5** and **6** (see in appendix). In ITC, the enthalpic change associated with dissociation was measured incrementally as a function of dilution by buffer. In both cases, the titration

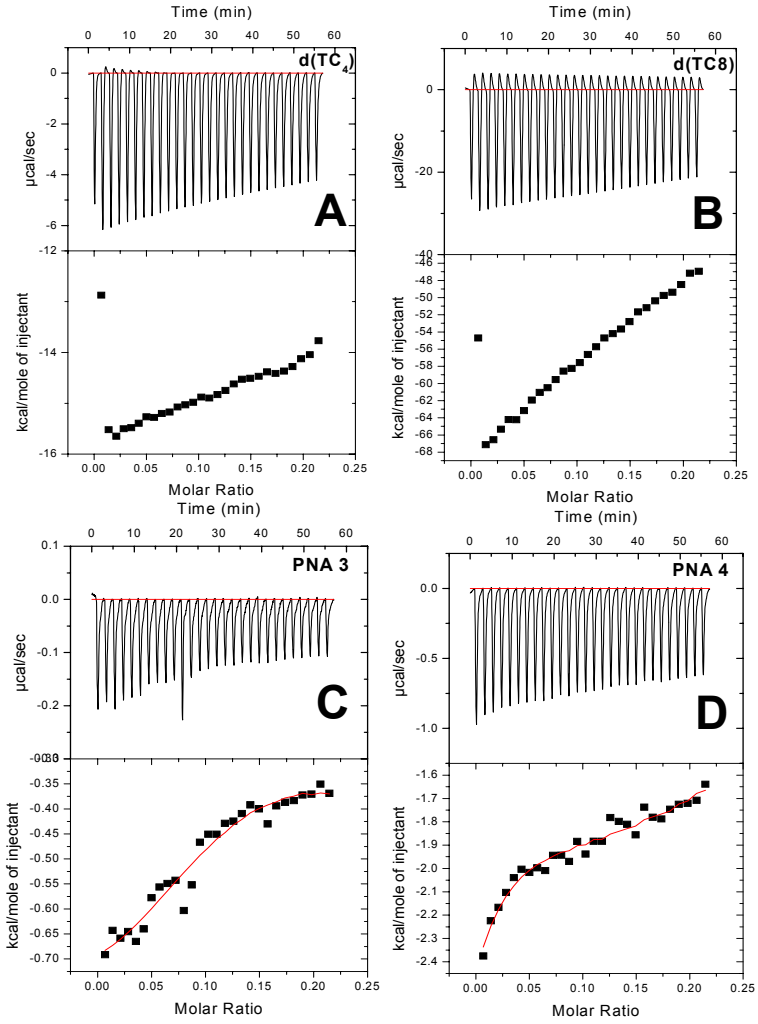

Figure 9: A. ITC profile of DNA **5**, B. DNA **6,** C. PNA **3** and PNA **4.**

profile corresponded to classical saturation isotherms, with the liberated heat slowly leveling off after the dissociation event. The data were corrected for solvent dilution effects by subtraction of the blank buffer titration data. The total enthalpy computed from the integrated area of the isotherms indicated that the enthalpy change in dissociation of TC_8 was about twice that of TC_4 (Figures 8A-8D)

5B.5 DISCUSSION

The temperature dependent UV-absorbance results on C-rich PNA and DNA sequences are shown in Figure 8. The melting experiments were done in 100 mM sodium acetate buffer for the pH range 3.0-5.0 and 10 mM phosphate buffer for the pH range 6.0-7.0. The successful formation of tetraplexes in different PNA/DNA sequences was indicated by observance of negative sigmoidal transitions (Figure 8). The accurate Tm values obtained from the first derivative curves and the Tm data for PNA **4** and DNA **6** are shown in Table 2. The PNAs **1** (TC_2) and **2** (TC_3) failed to show tetraplex formation at any of the pH conditions. The PNA **3** and PNA **4** showed formation of strong C-C^+ tetraplexes at pHs 3 and 4. Significantly, these PNA C-C^+ tetraplexes were much more stabilized compared to the analogous DNA C-C^+ tetraplexes by 10-20^{o}C at low pH. The stability of PNA C-C^+ tetraplexes was also dependent on pH. A comparison of pH dependent Tm of different PNA and DNA C-oligomers (Table 2) reveals that PNAs **3** and **4** form tetraplexes only in the acidic regime, upto pH 5.5. At pH 5.0, the PNA C-oligomers **3** and **4** form tetraplexes while at pH 6.0, no tetraplex formation is observed for these oligomers. This is seen from the reversal of melting curves for PNA oligomers at higher pH 6 (Figure 3). In comparison, the isosequential DNA C-oligomers **5** and **6** shows tetraplex formation upto pH 6.5. Both PNA and DNA C-oligomers fail to form tetraplexes at pH 7.0. The pH effect on tetraplex stability is more drastic for PNA C-oligomers with ∂Tm/ ∂pH being 10,

while that for DNA is only about 3. The difference in the cut-off pH in PNA (6.0) and DNA (6.5) for tetraplex formation is perhaps a reflection of the lower pK_a of N3-C in PNA (Figure 2) compared to that in d $(TC)_n$. The lower pK_a of N3-C in PNA compared to that in DNA is due to electronic effects: C in DNA is linked to glycosidic carbon while not so in PNA. These cause alterations of pK_a of N-3 C in PNA compared to DNA. Such differences in nucleobase properties due to electronic effects may partly explain other important biophysical effects displayed by Pans, different from those of DNA.

5B.6 CONCLUSIONS

While *i*-motif in C-rich sequences of DNA is well established, a similar motif in PNA was hitherto unknown. The synthesis and characterization of PNA TC_n (n = 2, 3, 4 and 8) were done to study *i*-motif in these PNA by UV-spectroscopy. The results clearly demonstrate formation of *i*-motif in PNA via C-C^+ base pairing in acidic pH 3.0-5.0 range. PNA C-C^+ tetraplexes possess significantly higher stability compared to analogous DNA C-C^+-tetraplexes. The absence of *i*-motif at higher pH in PNA in contrast to DNA arises from the lower pKa of N-3 of C in PNA compared to DNA.

5B.7 EXPERIMENTAL

5B.7.1 Synthesis of *aeg*- PNA monomers and oligomer

The synthesis of thymine (T) and cytosine (C) monomer of *aeg*-PNA was done by following the same procedure as in Chapter 1. These monomers were used to synthesize the PNA oligomers by solid phase synthesis procedure described in Chapter 4.

5B.7.2 UV-Melting Experiments

UV melting experiments were performed on Lambda-35 UV Spectrometer (Perkin-Elmer) equipped with a thermal melt system, PTP-6 Peltier Temperature Programmer with water circulator Thermohake K20. The samples 2 mL were transferred to quartz cell and sealed with Teflon stopper after degassing with nitrogen gas for 15 min and equilibrated at the starting temperature for at least 30 min. The OD at 260 nm was recorded in steps from 10-85 ^{o}C with temperature increment of 0.2 ^{o}C/min. The results were normalized and analysis of the data was performed on using Origin 5.0 (Microsoft Corp.).

The concentrations of the synthesized PNAs were determined spectrophotometrically at λ 260 nm at 80 °C, by use of the molar extinction coefficients calculated for unstacked oligonucleotides [6700 (C); 8800 (T) cm^{-1} M^{-1}] in buffer solution. Melting curves were recorded with a concentration of approximately 10 μM of single strand in 2 mL of the tested solution in Teflon-sealed quartz cuvettes of 1 cm optical path length. The resulting solutions were then heated at 80 °C for 15 min, then slowly cooled and kept at 20 °C for 20 min. After thermal equilibration at 20 °C, the UV absorption at λ 295 nm was monitored as a function of the temperature, increasing at a rate of 0.5 °C/min. Temperature dependent UV-absorbance was recorded at constant wavelength 290 nm. A plot of absorbance vs. temperature was obtained to determine the thermal melting point. In

this case shape of melting curve is negative sigmoidal due to decreased hypochroism at 295 nm.

5B.7.3 ITC Experiments

The VP-ITC micro Calorimeter was used to study dilution effect on G-quartet structure of PNA. In this experiment, annealed sample was diluted with same buffer in which sample was prepared. The dilution was done by successive injection of 10μL PNA sample in 1.5mL of buffer in cell at interval of 20 seconds at 15^{o}C.

5B.7.4 Mass Spectroscopy

5B.7.4a ESI- Mass spectroscopy

Electron spray ionization mass spectrometer (QSTARMultiView1.5.0 TOF-MS-IN) was used for characterization of G-quartet formation. The 2 μM solution of PNA in 1mL of methanol was used for recording mass spectra.

5B.7.4b MALDI-TOF- Mass spectroscopy

ABI-MALDI-TOF spectrometer was used to record mass of PNA by using *Voyager spec* electronic software. The mass of neat PNA was recorded in presence of matrices CHCA (α-cyano-4-hydroxycinnamic acid).

5B.8 REFERENCES

1. Ferrer, N.; Azorin, F.; Villasante, A.; Gutierrez, C.; Abad, J. P. Centromeric dodeca-satellite DNA sequences form fold-back structures. *J. Mol. Biol*. **1995**, *245*, 8-21.
2. Phan, A. T.; Mergny, J. L. Human telomeric DNA: G-quadruplex, i-motif and Watson-Crick double helix. *Nucleic Acids Res*. **2002,** *30*, 4618-4625
3. (a) Mills, M.; Lacroix, L.; Arimondo, P. B.; Leroy, J. L.; Francois, J. C.; Klump, H.; Mergny, J. L. Unusual DNA conformations: implications for telomeres. *Curr. Med. Chem. Anti-Canc. Agents*. **2002**, *2*, 627-44. (b) Ahmed, S.; Kintanar, A.; Henderson, E. Human telomeric C-strand tetraplexes. *Nat Struct Biol*. **1994**, *1*, 83-8. (c) Mathur, V.; Verma, A.; Maiti, S.; Chowdhury, S. Thermodynamics of i-tetraplex formation in the nuclease hypersensitive element of human c-myc promoter. *Biochem. Biophys. Res. Commun*. **2004,** *320*, 1220-1227.
4. Patel, D. J; Bouaziz, S.; Kettani, A.; Wang, Y. Structures of guanine-rich and cytosine-rich quadruplexes formed *in vitro* by telomeric, centromeric, and triplet repeat disease DNA sequences**.** In *Oxford Handbook of Nucleic Acid Structures.* Edited by Neidle S. New York: *Oxford University Press* **1999**, 389-453.
5. Gueron, M.; Leroy, J. L. The *i*-motif in nucleic acids. *Curr. Opin. Struct. Biol*. **2000**, *10*, 326-331.
6. Leroy, J. L. Cytidine protonation and base-pair intercalation in nucleic acid structures: the *i*-motif. *Nucleic Acids Res. Suppl*. **2002**, 7-8.
7. Robidoux, S.; Klinck, R.; Gehring, K.; Damha, M. J. Association of branched oligonucleotides into the *i*-motif. *J. Biomol. Struct. Dyn*. **1997**, *15*, 517-527.
8. Snoussi, K.; Nonin-Lecomte, S.; Leroy, J. L. The RNA i-motif. *J. Mol. Biol*. **2001,** *25*, 139-153.
9. Deng, J.; Sundaralingam, M. Synthesis and crystal structure of an octamer RNA r(guguuuac)/r(guaggcac) with G.G/U.U tandem wobble base pairs: comparison with other tandem G.U pairs. *Nucleic Acids Res*. **2000**, *28*, 4376-4381.
10. Esmaili, N.; Leroy J. L. i-motif solution structure and dynamics of the d(AACCCC) and d(CCCCAA) tetrahymena telomeric repeats. *Nucleic Acids Res***. 2005**, *33*, 213-24.
11. Kanaori, K.; Maeda, A.; Kanehara, H.; Tajima, K.; Makino, K. ^{1}H nuclear magnetic resonance study on equilibrium between two four stranded solution conformations of short d(CnT). *Biochemistry* **1998**, *37*, 12979-12986.
12. Gehring, K.; Leroy, J. L.; Guéron, M. A. Tetrameric DNA structure with protonated cytosine:cytosine base pairs. *Nature* **1993**, *363,* 561-564.
13. Leroy, J. L.; Guéron, M. Solution structures of the *i*-motif tetramers of d(TCC), d(5methylCCT) and d(T5methylCC): novel NOE connections between amino protons and sugar protons. *Structure* **1995**, *3*, 101-120.
14. Nonin, S; Leroy, J. L. Structure and conversion kinetics of a bi-stable DNA *i*-motif: broken symmetry in the $[d(5mCCTCC)]_4$ tetramer. *J. Mol. Biol*. **1996**, *261*, 399-414.
15. Wei, L.; W.; Wua, P.; Ohmichia, T.; Sugimotoa, N. A tetrameric DNA structure with protonated cytosine.cytosine base pairs.Characterization and thermodynamic properties of quadruplex/duplex competition. *FEBS Lett,* **2002**, 77-81

16. Chen, L.; Cai, L.; Zhang, X.; Rich, R.; Crystal Structure of a Four-Stranded Intercalated DNA: d(C_4). *Biochemistry* **1994**, *33*, 13540-13546.
17. Benevides, J. M.; Kang, C.; Thomas, G. J. Jr. Raman signature of the four-stranded intercalated cytosine motif in crystal and solution structures of DNA deoxycytidylates d(CCCT) and d(C_8). *Biochemistry* **1996**, 35, 5747-5755.
18. Miyoshi D.; Matsumura S.; Li. W.; Sugimoto, N.; Structural polymorphism of telomeric DNA regulated by pH and divalent cation. *Nucleosides Nucleotides Nucleic Acids* **2003**, *22*, 203-221.
19. Weil, J.; Min, T.; Yang, C.; Wang, S.; Sutherland, C.; Sinha, N.; Kang, C. Stabilization of the *i*-motif by intramolecular adenine-adeninethymine base triple in the structure of d(ACCCT). *Acta Crystallogr*. *D Biol Crystallogr* **1999**, *55*, 422-429.
20. Li. W.; Wu, P.; Ohmichi, T.; Sugimoto, N. Characterization and thermodynamic properties of quadruplex/duplex competition. *FEBS Lett*. **2002**, *526,* 77-81.
21. Malliavin, T. E.; Gau, J.; Snoussi, K.; Leroy, J. L. Stability of the i-motif structure is related to the interactions between phosphodiester backbones. *Biophys. J*. **2003**, *84*, 3838-3847.
22. Lacroix, L.; Mergny, J. L.; Leroy, J. L; Helene C. Inability of RNA to form the *i*-motif: implications for triplex formation. *Biochemistry* **1996**, *35*, 8715-8722.
23. Mergny, J-. L.; Phan, A-. T.; Lacroix, L. Following G-quartet formation by UV-spectroscopy. *FEBS letters* **1998**, *435*, 74-78.
24. (a) Kanehara, H.; Mizuguchi, M.; Tajima, K.; Kanaori, K.; Makino, K. Spectroscopic evidence for the formation of four-stranded solution structure of oligo-deoxycytidine phosphorothioate. *Biochemistry* **1997**, *36*, 1790-1797. (b) Kanaori, K.; Sakamoto, S.; Yoshida, H.; Guga, P.; Stec, W.; Tajima, K.; Makino, K. Effect of phosphorothioate chirality on *i*-motif structure and stability. *Biochemistry* **2004**, *43*, 5672-5672.
25. (a) Petersen, M.; Wengel. J. LNA: a versatile tool for therapeutics and genomics. *Trends in Biotechnology* **2003**, *21*, 74-81. (b) Randazzo A, Esposito, V.; Ohlenschlager, O.; Ramachandran, R.; Mayola, L. NMR solution structure of a parallel LNA quadruplex. *Nucleic Acids Res.* **2004**, *32*, 3083-3092.
26. Nielsen P. E.; Egholm, O.; Berg R. H.; Buchardt, O. Sequence selective recognition of DNA by strand displacement with a thymine substituted ployamide. *Science* **1991**, *254*, 1497-1500.
27. Ganesh, K. N.; Nielsen, P. E. Peptide nucleic acids: analogs and derivatives. *Current Org. Chem.* **2000**, 931-943. (b) Kumar, V. A.; Ganesh, K. N. Conformationally constrained PNA analogues: structural evolution toward DNA/RNA binding selectivity. *Acc. Chem. Res*. **2005**, *38*, 404-12.
28. (a) Datta, B.; Bier, M. E.; Roy, S.; Armitage, B. A. Quadruplex formation by a guanine-rich PNA oligomer. *J. Am. Chem. Soc*. **2005**, *127*, 4199-4207. (b) Ghosh, Y. K.; Stephens, E.; Balasubramanian, S. A. PNA G_4 Quadruplex. *J. Am. Chem. Soc*. **2004**, *126*, 5944-5945.
29. Diederichsen, U. Oligomers with intercalating cytosine-cytosine$^+$ base pairs and peptide backbone: DNA *i*-motif analogs. *Angew Chem*., *Int*. *Ed*. *Engl*. **1998**, *37*, 2273-2276.
30. Dueholm, K. L.; Egholm, M.; Beherns, C.; Christensen, L.; Hansen, H. F.; Vulpius, T.; Petersen, K. H.; Berg. R. H.; Nielsen, P. E.; Buchardt, O. Synthesis of peptide nucleic acid monomers containing

the four natural nucleobases: Thymine, Cytosine, Adenine, and Guanine and their oligomerization. *J. Org. Chem*. **1994,** *59*, 5767-5773.

31. (a) Gisin, B. F. The preparation of Merrifield resins through total esterification with cesium salt. *a. Helv. Chim. Acta.* **1970**, *56*, 1476-1482. (b) Erickson, B. W.; Merrifield, R. B. **1976**, *Solid Phase Peptide Synthesis. In the Proteins* Vol. II, 3rd ed.; Neurath, H. and Hill, R. L. eds., Academic Press, New York, pp 255.
32. Dick, L. W. Jr.; McGown, L. B. Aptamer-enhanced laser desorption/ionization for affinity mass spectrometry. *Anal. Chem*. **2004**, *76*, 3037-3041.
33. (a) Rosu, F.; Gabelica, V.; Shin-ya, K.; DePauw, E.; Telomestatin induced stabilization of the human telomeric DNA quadruplex monitored by electrospray mass spectrometry. *Chem. Commun*. **2003**, *34*, 2702–2703. (b) Vairamani, M.; Gross, M. L; G-quadruplex formation of thrombin-binding aptamer detected by electrospray ionization mass spectroscopy *J. Am. Chem. Soc.* **2003**, *125*, 42-43.
34. Mergny, J. L.; Lacroix, L. Kinetics and thermodynamics of *i*-DNA formation: phosphodiester versus modified oligodeoxynucleotides. *Nucleic Acids Res*. **1998**, *26*, 4797-4803.

5B.9 APPENDIX

1. HPLC of PNA

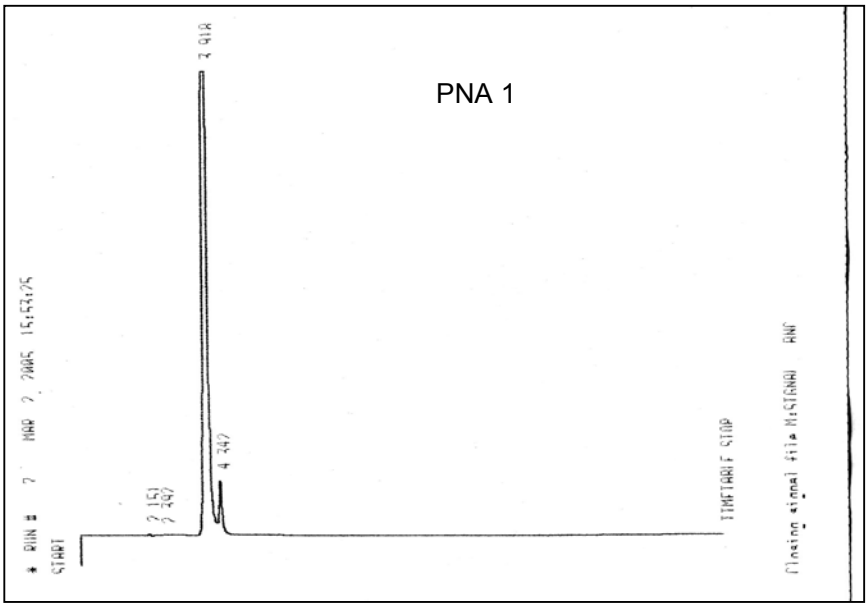
PNA 1
2.151
2.497
4.347
2.918
START
TIMETABLE STOP

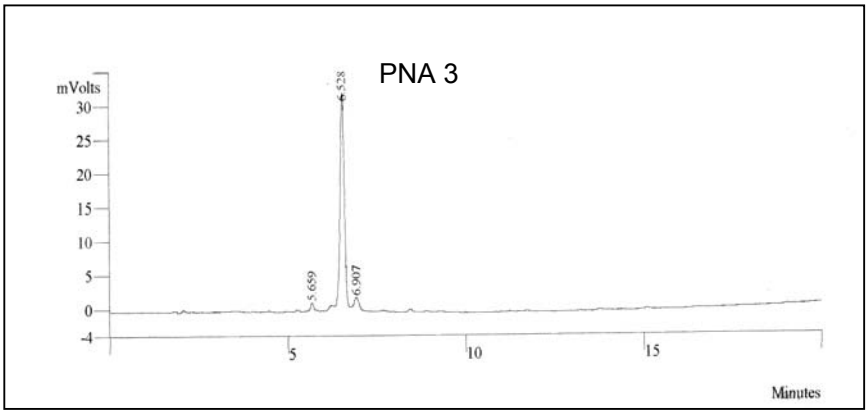
PNA 3
mVolts
30
25
20
15
10
5
0
-4
5.659
6.528
6.907
5
10
15
Minutes

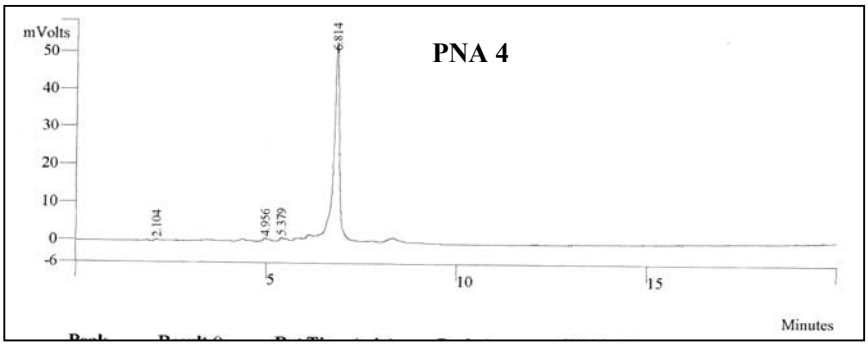
PNA 4
mVolts
50
40
30
20
10
0
-6
2.104
4.996
5.379
6.814
5
10
15
Minutes

2. MALDI-TOF spectra of PNA **1** and PNA **2**

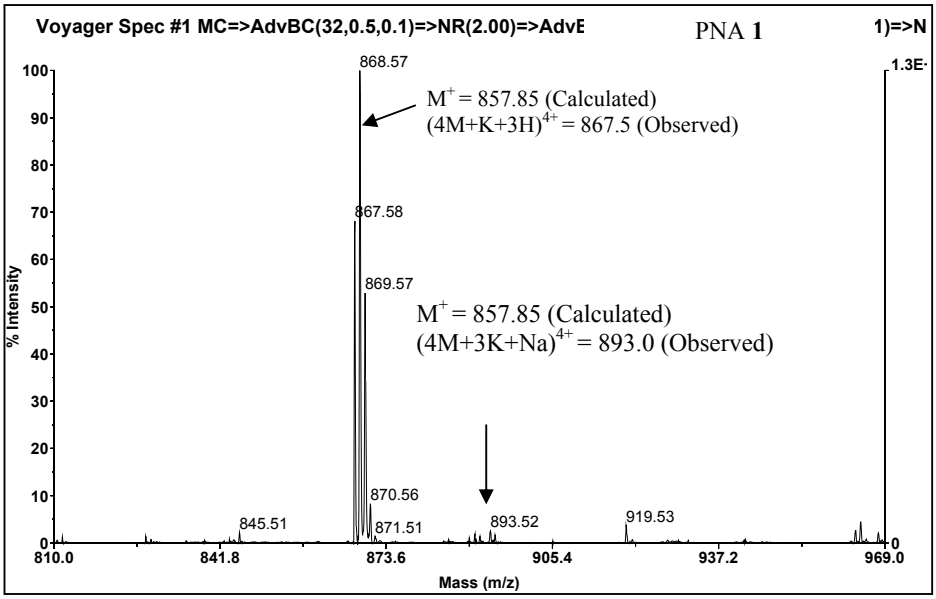

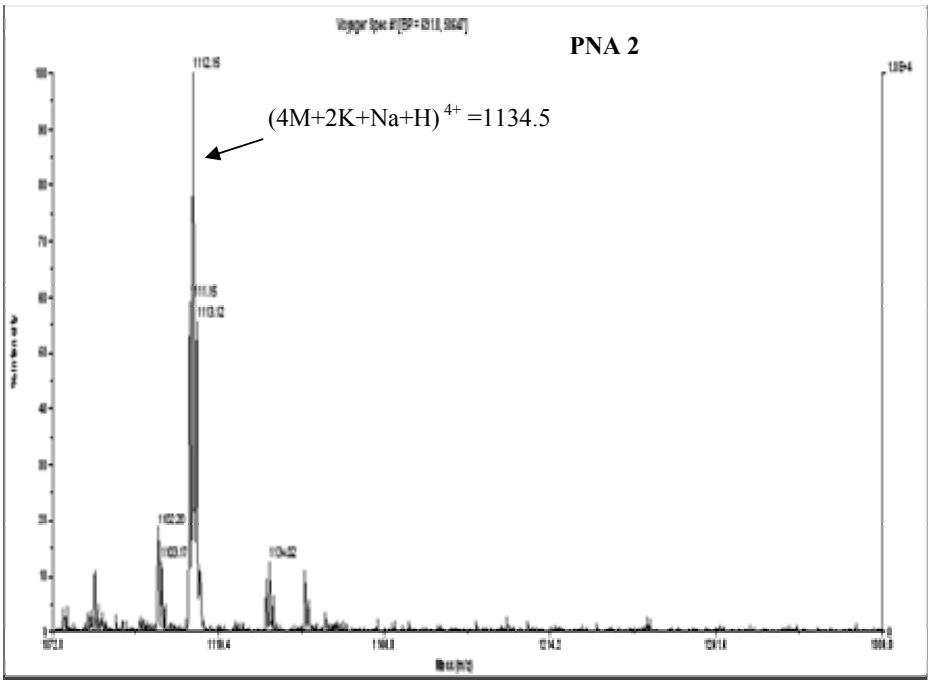

4. MALDI-TOF spectra of PNA **1** and PNA **2**

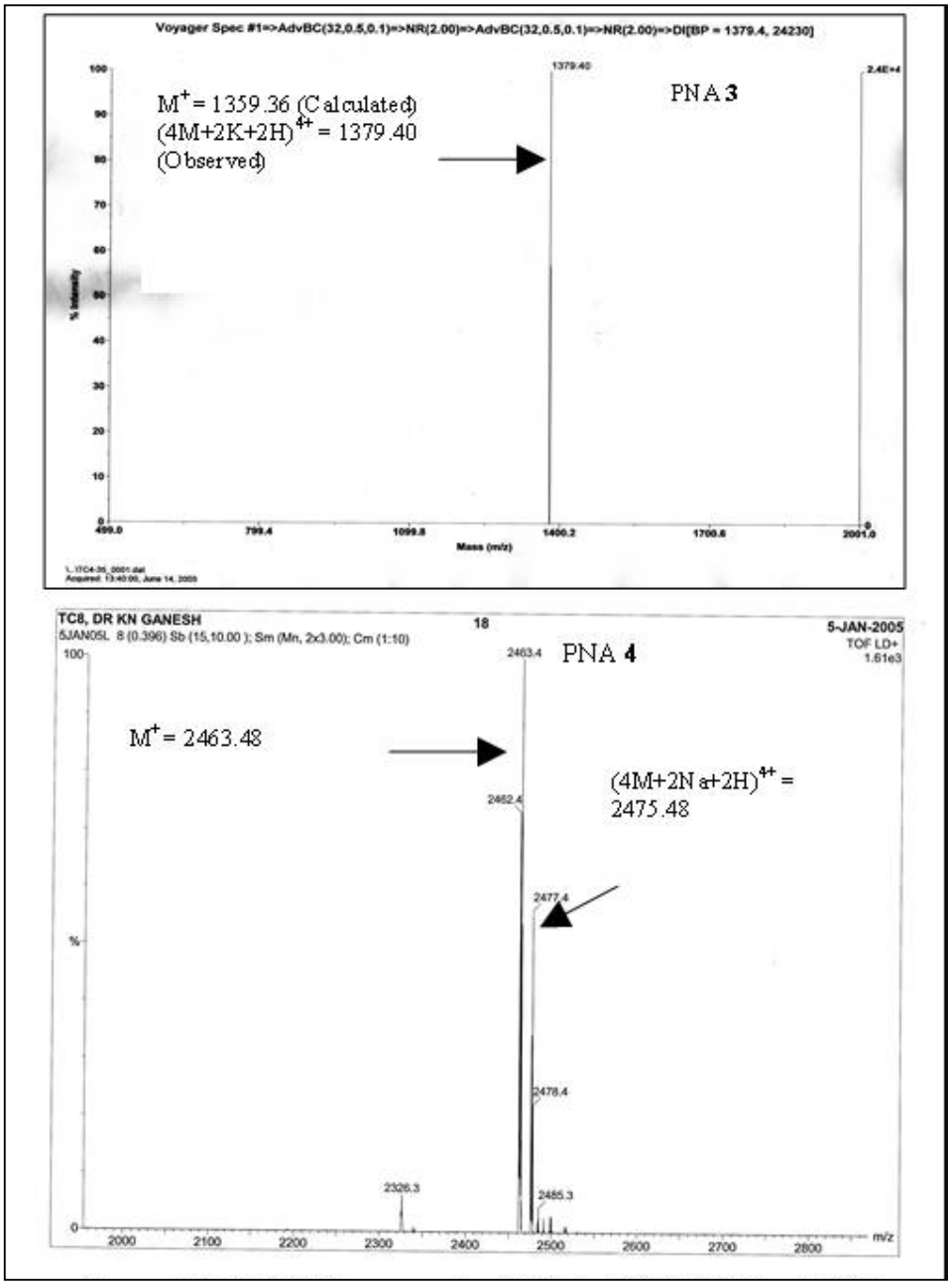

5. UV-Spectra of PNA **4** and cytosine monomer of *aeg*-PNA

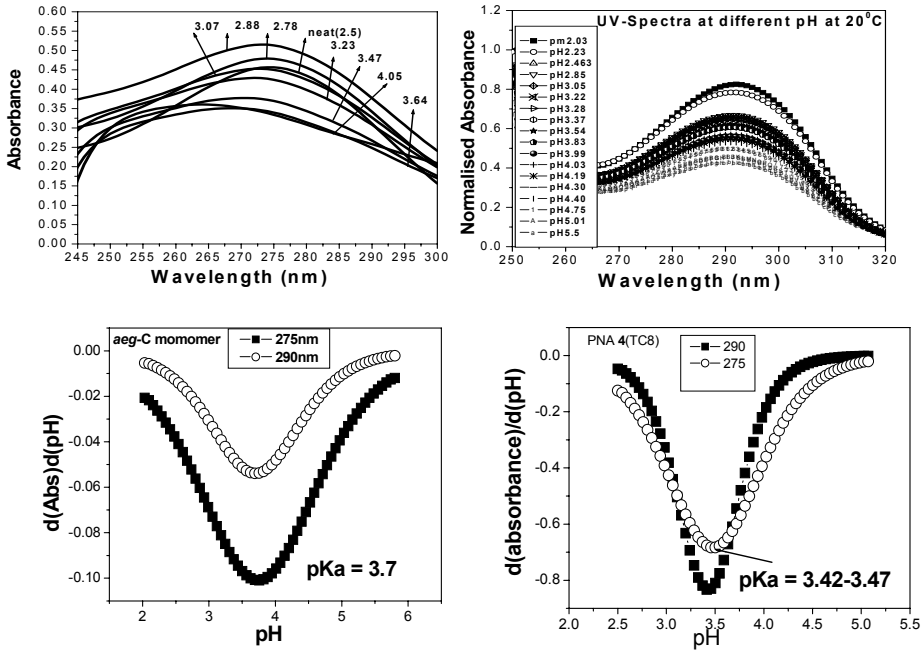

First derivative of UVmelting curves of PNA at different pH

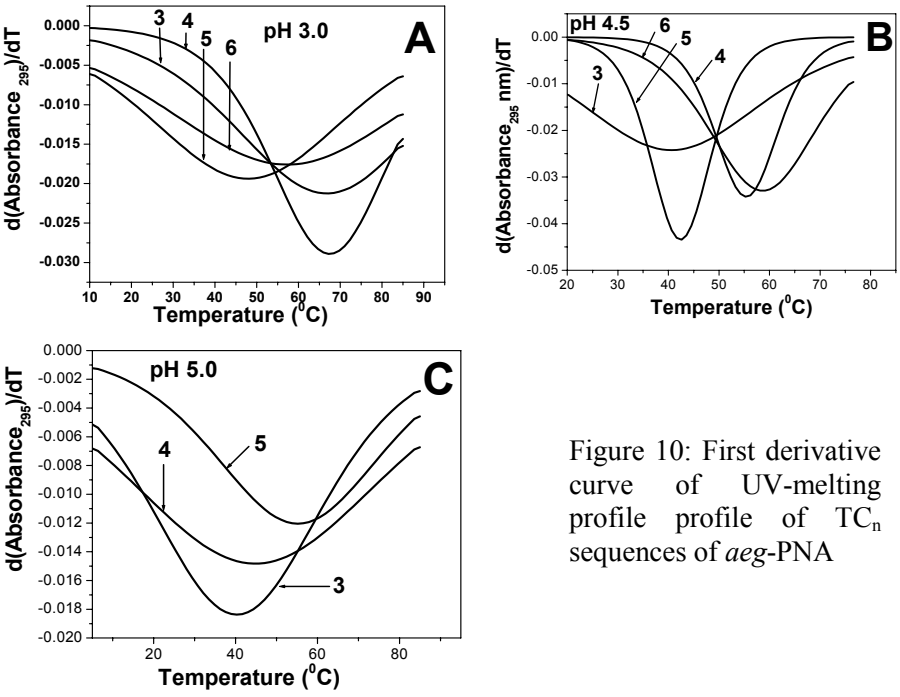

Figure 10: First derivative curve of UV-melting profile profile of TC_n sequences of *aeg*-PNA

CHAPTER 6

SYNTHESIS AND STUDY OF FOLDAMER PROPERTIES OF UNNATURAL *δ-N*-AMINOETHYL PYRROLIDINE ACID & PEPTIDES

CHAPTER 6: SYNTHESIS AND STUDY OF FOLDAMER PROPERTIES OF UNNATURAL*d*-*N*-AMINOETHYL PYRROLIDINE ACID & PEPTIDES

6.1 INTRODUCTION

The proteins and ribonucleic acids (RNA) are unique natural polymers with ability to adopt compact secondary and tertiary structures in well-ordered conformations (Figure 1).[1] Naturally occurring peptides are polymers of *a*-amino acids (Figure 1b) and their secondary structures are determined by sequence of amino acids i.e. nature of side chains.[1b] The most regular secondary structures in protein are the *a*-helix, 3_{10}-helix and *b*-sheet.[2] Generally, oligomers of substituted α-amino acids adopt 3_{10}-helix, which is very common in oligomers of *alanine* (Figure 1c).[3] These structures display characteristic hydrogen-bonding pattern in the backbone, which depends on the hydrogen bond forming ability of their amide groups. These amide groups serve as both donors and acceptors of hydrogen bonds. A number of synthetic designs have been reported to study the structural diversity and functional characteristics of polypeptides and many of the structural analogues mimic the molecular functions of natural peptides.[2b,4]

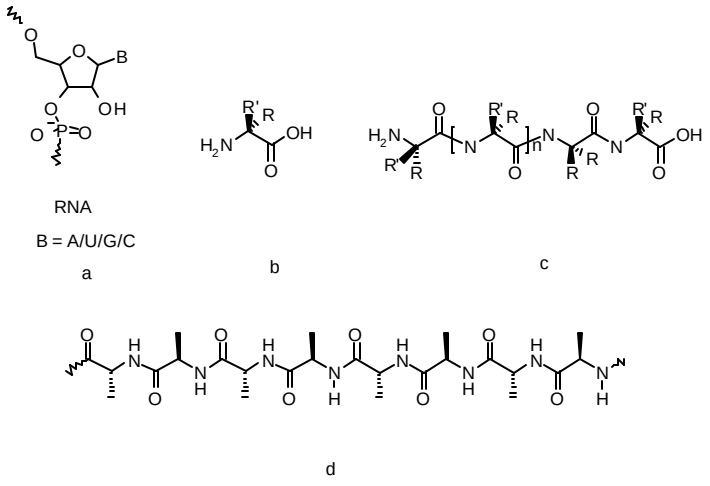

Figure 1: Chemical structure of (a) RNA, (b) *a*-amino acid, (c) disubstituted alanine and (d) monosubstituted oligomer oligomers

6.1.1 Structural organization in protein

Figure 2 shows the hierarchy in structural organization of proteins, where the *primary* sequence of amino acids leads to *structure* of protein[5] which are mostly of three

types *helix*, *strand* and *b-turn*. These secondary structures adopt supersecondary structures in form of *b-hairpin*, *a-hairpin* and *b-a-b motif*. Finally, the supersecondary structures of same peptides assemble into the most stable and well-ordered *tertiary* and *quaternary* functional structures.

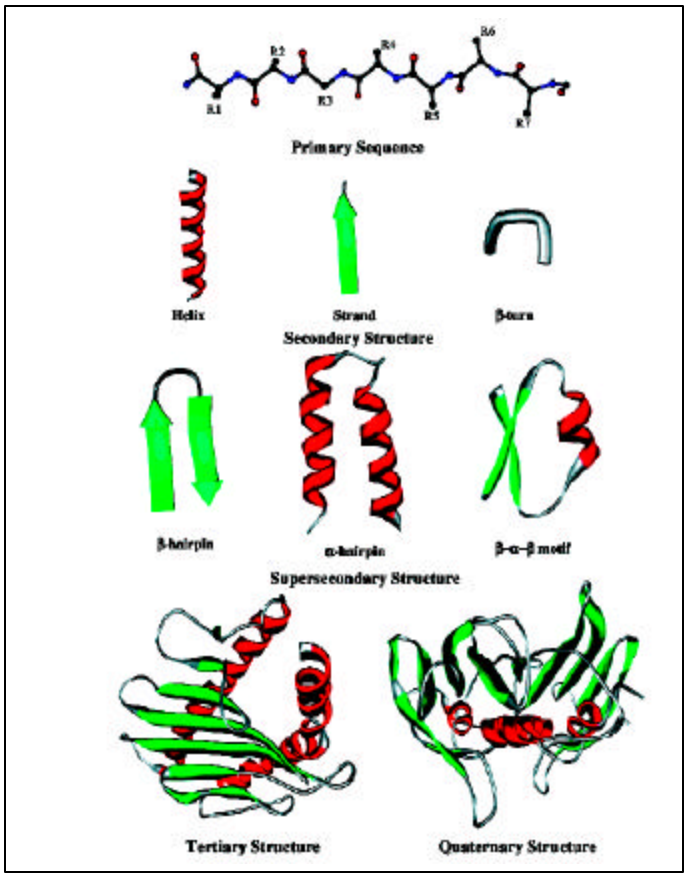

Figure 2: Hierarchy in structural organization of protein.[5]

6.1.2 Conformational properties of *b*-amino acids

Conformational properties of *b*-amino acids can be analyzed in terms of the main chain *torsional angles* in convention of Balram as *w*, *f*, *q* and *y* (Figure 3a).[6] The folded helical or turn-like conformation of *b*-peptides requires a gauche conformation about the *q* defined by C^2-C^3 bond. A *trans*-rotamer lead to a fully extended conformation, when the

appropriate value of *f* and *y* are provided (figure 3a). The effects of substituents on the conformation of *b*-amino acids have also been studied and described in Figure 3b.[7] The unsubstituted *b*-amino acid e.g. *b*-alanine, is highly flexible and similar to glysine in the α-amino acid. In Figure 3b, The alkyl substituents at position 2 and 3 in *b*-amino acid favor *gauche* conformation about the C^2-C^3 bond.[8] The C^2, C^3 disubstituted amino acids are even more conformationally restricted and favor *gauche* conformations when the substituents are *anti*.[8] The *gauche*-type torsional angles are even more strongly favor in cyclohexane and cyclopentane ring as in *trans*-2-aminocyclohexancarboxylic acid (ACHC)[9] and *trans*-2-aminocyclopentancarboxylic acid (ACPC).[10] When substituents at C^2 and C^3 are *syn*, a trans conformation of about C^2-C^3 bond is favored, which encourages the formation of *sheetlike* structure (Figure 3e).[11]

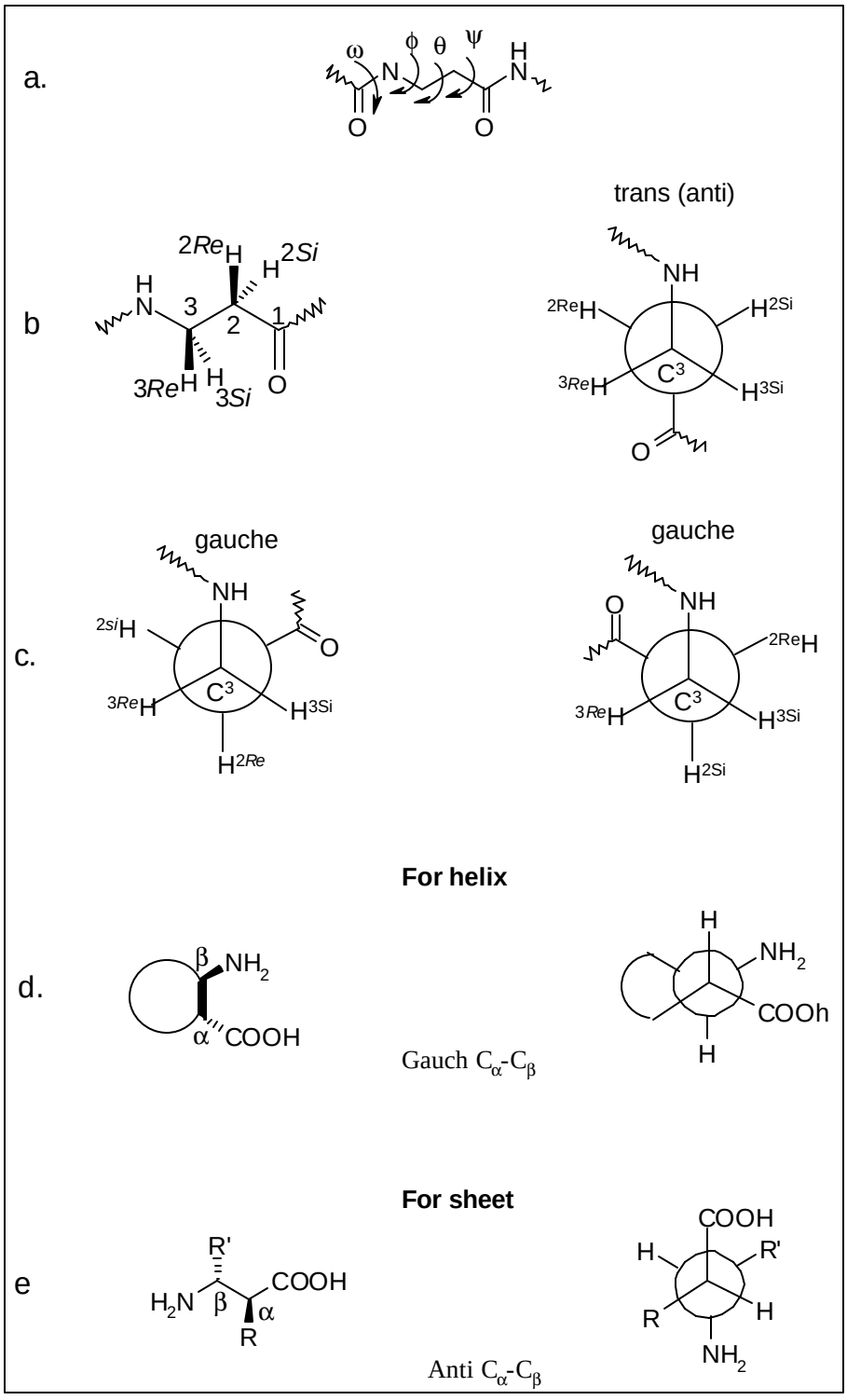

Figure 3: (a) Representation of torsional angles in *b*-peptide Conformation of *b*-peptide. (b), (c), (d) and (e) Rotamers for *b*-alanine regarding the ϕ dihaderal angle.

6.1.2a 14-Helix

b-peptides containing the conformationally constrained cyclic amino acid ACHC have shown that these peptide adopt *14*-helices in the solid state as well as in organic solvents (Figure 4d). Seebach *et al*[12] found that a series of *b*-peptides prepared from acyclic residue with a diverse collection of side chains adopt 14-helix in organic solvents (Figure 4b). Depending on the stereochemistry of substituted *b*-amino acids, either a left-handed or right handed *14*-helix is formed. The peptides of *b*-amino acids, which are derived from the naturally occurring L-amino acids adopt left-handed *14*-helices.

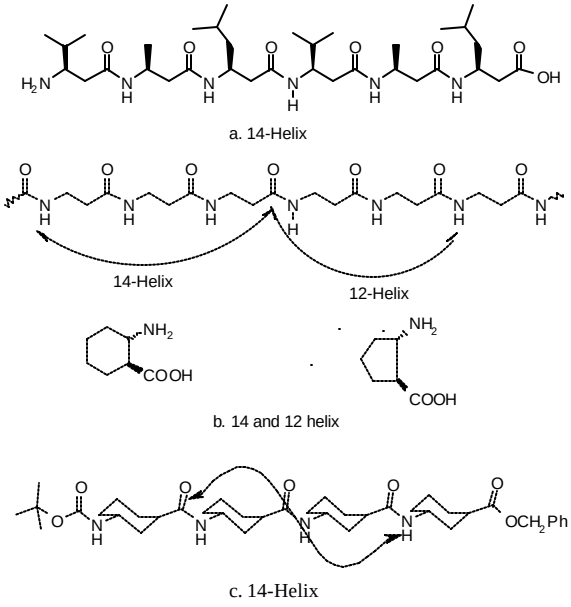

Figure 4: 14-Helices are in *b*-peptides.

6.1.2b 12-Helix

Systematic conformational study and molecular dynamics calculation of the cyclopentane-containing amino acid *trans*-2-cyclopentancarboxylic acid (ACPC) (Figure 5) versus the *trans*-2-aminocyclohexancarboxylic acid (ACHC) have suggested the inherent preferences for different helical conformation.[13] The structure of the 12-helix is stabilized by a series of hydrogen bonds between amides carbonyl groups at *i* position and

an amide portion at *i+3* position. The helix repeats at approximately every 2.5 residues with the polarity of α-helix and the amide protons exposed from *N*-terminal end of the helix.

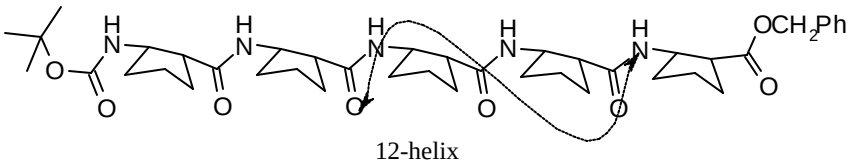

Figure 5: *12*-Helices are in *b*-peptides (ACPC)

6.1.2c 10/12-Helix

The *b*-peptides with alternating b^2- and b^3- monosubstituted residues (Figure 6) can adopt the 10/12-helix conformation.[5,14] The characteristic feature of this helix is the inter-winded network of 10- and 12-membered hydrogen bonded rings. In this helix, the amide is surrounded by methylene on one side of the hydrogen bond (*i*, *i+2*) forming the 10-membered rings, while in the 12-atom rings are formed between amides surrounded by side chain (i+*1*, *i+3*).

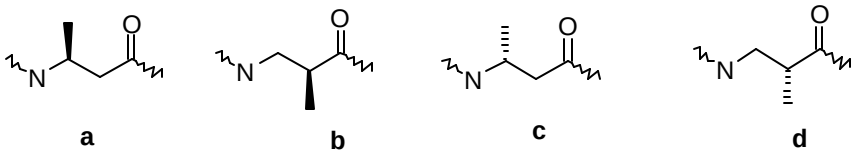

Figure 6: 10/12-helix formation by dipeptides of (a); (*S*)-β^3-homoalanine; (b) (*S*)-β^2-homoalanine; (c) (*R*)-β^3-homoalanine and (d) (*R*)-β^2-homoalanine.

6.1.2d 10-Helix

Recently Fleet *et. al.*[15] prepared peptides from a monomer of four-membered ring constrained *b*-amino acid and these peptides display an unprecedented 10-helix secondary structure (Figure 7). The constituent of these *b*-amino acids contains an oxetane ring (four-membered ring ether). The amino and carboxyl substituents are *cis* on the four-membered ring, in contrast to the *trans* of cyclohexane-, cyclopentane-, and pyrrolidine

ring containing *b*-amino peptides. *10*-helical folding in nonpolar solvents (chloroform or benzene) was established by two-dimensional NMR analysis.

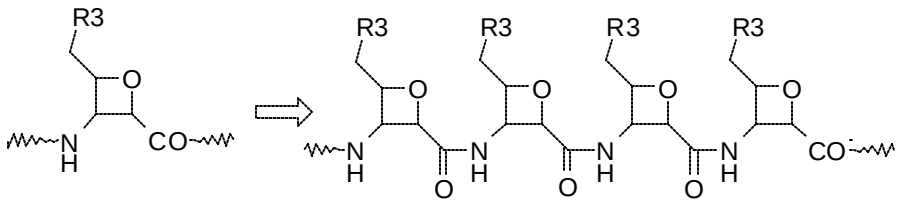

Figure 7: Structure of β-amino acids contain an oxetane

6.1.2e 8-Helix

This type of helix formation is rarely observed in polypeptides. But, the crystal structure of short oligomers of the achiral monomer 1-(aminomethyl)-cyclopropancarboxylic acid (Figure 8a) and 1-(aminomethyl)-cyclohexancarboxylic acid (Figure 8b) of disclose a propensity for this *b*-amino acid residue to form eight-membered ring hydrogen bonds (Figure 8).[16] These observations led Abele *et al.*,[16] to suggest that longer oligomers of this type may adopt a regular 8-helix, which would have approximately two residues per turn.

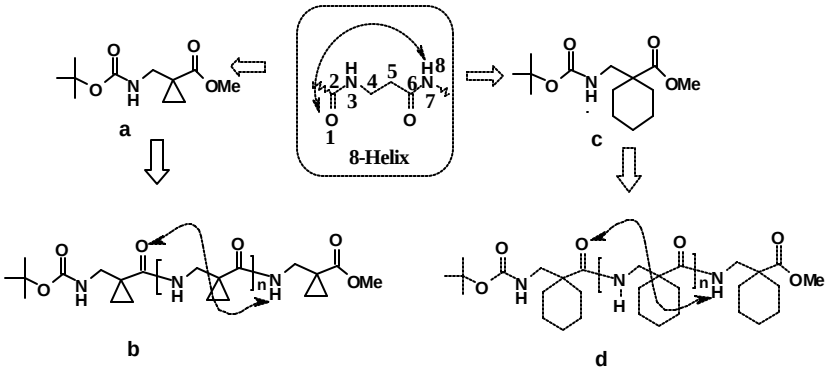

Figure 8: Structure of cyclopropane (a) and cyclohexane (c) ring containing organization of *b*-peptide*b*-peptides

6.1.2f *b*-Sheet-like structure

There are in principle two types of sheet like secondary structures available for *b*-peptides, one in which each residue has an *anti* C^2-C^3 torsion angle and another in which each residue has *gauche* C^2-C^3 torsion angle. The *anti* type of *b*-peptide sheet is distinctive since all backbone carbonyls are oriented in approximately the same direction (Figure 9),[17] which would endow the resulting sheet with a net dipole. In contrast, *b*-sheet formed by α-peptides has little or no net dipole because the backbone carbonyl alternate in direction along each strand. [18]

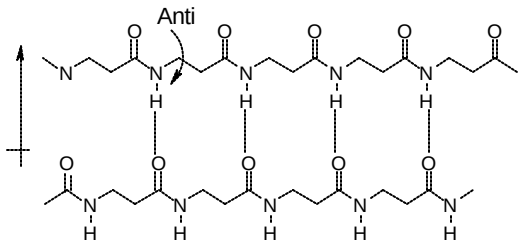

Figure 9: A typical *b*-Sheet-like structure

6.1.2g Twisted strand

Twisted strand conformation exhibits bifurcated hydrogen bonds in intra-strand fashion involving backbone and chain conformation (Figure 10). Furthermore, the residue adopts a *gauche* conformation for this twisted strand, resulting in a 13-residue repeating structure.[19]

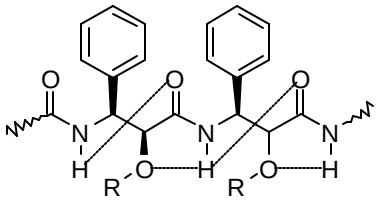

Figure 10: Bifurcated hydrogen bonds

6.1.2h Non-hydrogenbonded secondary structure

Oligo-PCA, oligo-NIP and oligo-β^3-homoproline β-peptides (Figure 11)[20] form another set of secondary structures in methanol which adopted by non hydrogen bonded as *b*-turn.

Figure 11: Secondary structures as *b*-turn formed by non-hydrogen bonding

6.1.2i Non-*b*-synthetic peptides

The *g*-,[21] *d*-[22] amino acids and α-aminoxy acid[23] homologues of α-peptides adopt helical or linear conformations mimicking the structures and potential functions of their natural counterparts. *g*-Peptide (Figure 12, 3a and 3b) was well explored by Seebach *et al.*[21] and shown to have tendency to form 14-membered hydrogen bonding in helix formation. In literature,[22] *d*-homologue is not very much explored: aliphatic (Figure 12, 3c) and aromatic (Figure 12, 3d) *d*-peptides have been studied for formation of secondary

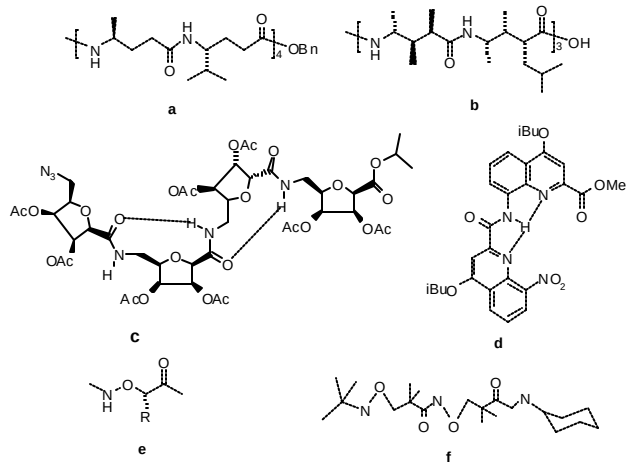

Figure 12. Chemical structure of γ- (**a** and **b**), *d*-(**c** and **d**), α-aminoxy (**e**) and *b*-aminoxy peptides (**f**)

(Figure 12). The predictability of the folding of an oligomeric molecule largely depends upon intramolecular interaction (eg., hydrogen bond) taking place between two consecutive units. Yang *et al.*[23] have described a new class of synthetic peptides - homooligomeric α-aminoxy acid (Figure 12, 3e), wherein addition of one oxy group at N-terminus in α-amino acids leads to 1.8_8 (or a twisted 2_8 helix with two residues per turn). Recently, *b*-aminoxy oligomers and their secondary structures (Figure 12, 3f) have also been reported.[24]

6.1.3 Structural study of (*d-aep*) peptides by CD/IR spectroscopy

Since, circular Dichroism (CD) spectroscopy has played a pioneering role in secondary structural analysis of polypeptides. Greenfield and Fasman[25] first proposed a quantitative method of determining protein secondary structure from CD spectra of a synthetic polypeptides, $(Lys)_n$, which can adopt three conformations under different conditions.

6.1.3a Circular Dichroism Spectroscopy

Greenfield and Fasman[25] have proposed a quantitative method of determining protein secondary structure from CD spectra of a synthetic polypeptides $(Lys)_n$, that adopts three conformations under different conditions. A typical CD spectra of poly-L-lysine in the α-helical, antiparallel β-pleated sheet and random coil conformation are illustrated in Figure 14. A polypeptide, which is random, has CD spectrum, which is similar to that of a simple amide, but larger in magnitude. The spectrum displays a small positive transition n-π* transition at approximately 230 nm and a negative large transition single π-π* at ca. 195 nm. The spectrum of α-helix shows a large negative n-π* transition at 222 nm. The π-π* transition is split into two transitions because of exciton coupling. One transition has negative band at ca. 208 nm and a positive band at approximately 192

nm. The CD spectrum of *antiparallel b*-pleated sheet also shows evidence of exciton coupling in π-π^* transition. However the splitting of the transition is different than in case of the α-helix. The spectrum of the *antiparallel* β-structure shows a negative band at 218 nm and a positive band at 195 nm.

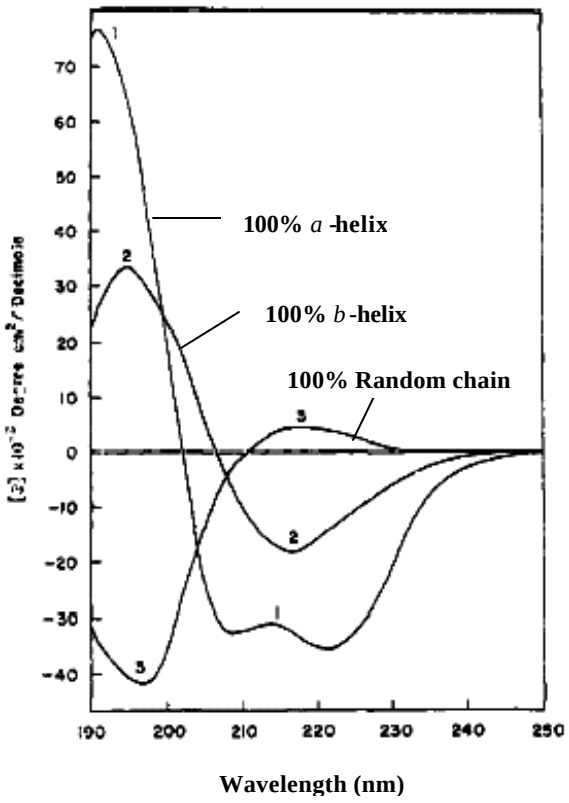

Figure 13: Typical CD spectra of poly-L-lysine peptides.[27]

6.1.3b FT-IR Spectroscopy

From the variety of fast time-scale methods, CD spectroscopy was first used for conformational characterization of midsize peptides. Vibrational spectroscopy (infrared and Raman) was applied from late 1960s as a complementary approach to CD in determining polypeptide and protein structures.[26] Like CD; vibrational spectroscopy has a fast time scale (10^{-13} s). Amide vibration is highly sensitive to H-bonding. *Amide A* (NH stretching) region indicates populations of free (characterized by the 3460-3410 cm-1

band) and hydrogen-bonded (characterized by the 3380-3300 cm^{-1} bands) NH. However *Amide I* band (carbonyl stretching coupled with in-plane NH bending and CN stretching modes, around 1695-1610 cm^{-1}) which are shifted to lower wavenumber during the formation of hydrogen bonds. While amide II (NH bending and CN stretching, around 1575-1480 cm^{-1} band shift to higher wavenumber. Generally, IR bands appearing between 1690 and 1660 cm^{-1} in the spectrum of polypeptides in D_2O or H_2O have been assigned to *b*-turns.

6.2 RATIONALE AND OBJECTIVES OF PRESENT WORK

As we know, the chemists think like an artist and always try to synthesize some unnatural things, which behave almost like natural one. The exploiting of these features, a number of compounds is generated with new properties such as interesting biological activity. Recently, non-natural peptides as *b*-peptides, which is polymers of synthetic *b*-amino acid amino acid, have emerged as the most prominent class of synthetics mimics of protein architecture. A many different types of secondary structural elements such as *helices, turns* and *pleated sheets* of *b*-peptides have been discovered. Till now, three different types of well-ordered secondary structures were observed in *b*-peptides as (1) 3_{14}-helix, (2) 2.6_{12}-helical conformation and (3) the helix comprises alternating 10- and 12-membered hydrogen-bonded rings. These helical structures based on different substitution patterns of the constituent of *b*-amino acids and some of them have identified and elaborated.

The specific objectives of this chapter are (1) the synthesis of *d*- aep and *d*- aep one the monomer and (2) structural study of *d*- aep peptides by CD-spectroscopy and FT-IR spectroscopy (Figure 14). The chemical structure of *d*- aep and *d*- aep one are given in Figure 14.

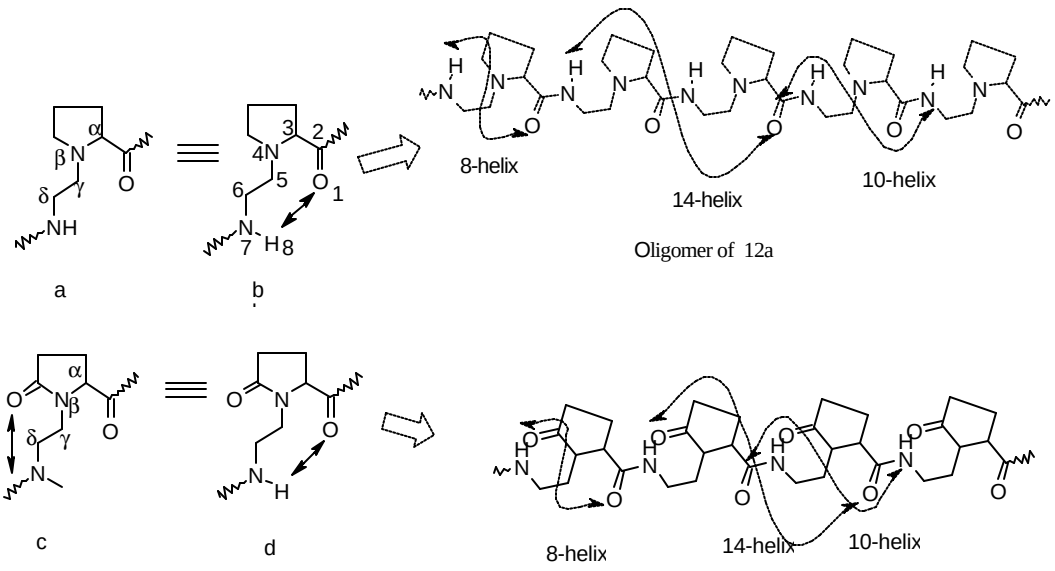

Figure 14: *Left*. Chemical structure of *d-aep* and (*d-aepone*); *Right*. Their proposed secondary structure.

6.3 PRESENT WORK

6.3.1 Monomer synthesis of *d-aep* and *d-aepone* acid

Methyl ester of δ-aminoethyl pyrrolidine amino acid (**6**): The methyl ester of *d*-aminoethyl pyrrolidine acid (*d*-aep) **6** was synthesized from naturally occurring amino acid, L-proline **4** (Scheme 1) by esterification of **4** with thionyl chloride (SO_2Cl_2)/MeOH, followed by *N*-alkylation of proline ring by *O*-mesylate **3** of compound **2** prepared by *N*-Boc protection of 2-aminoethanol **1**.

Methyl ester of *d*-aminoethyl pyrrolidinone amino acid (**7**): The methyl ester of *aep one* **7** was achieved by direct oxidation of compound **6** with the versatile oxidizing agent $RuCl_3/NaIO_4$. The synthetic procedure was discussed in detail of chapter 2. $RuCl_3/NaIO_4$.

Scheme 1: Synthesis of *d*-aminoethyl prolyl amino acid (*d-aep*)

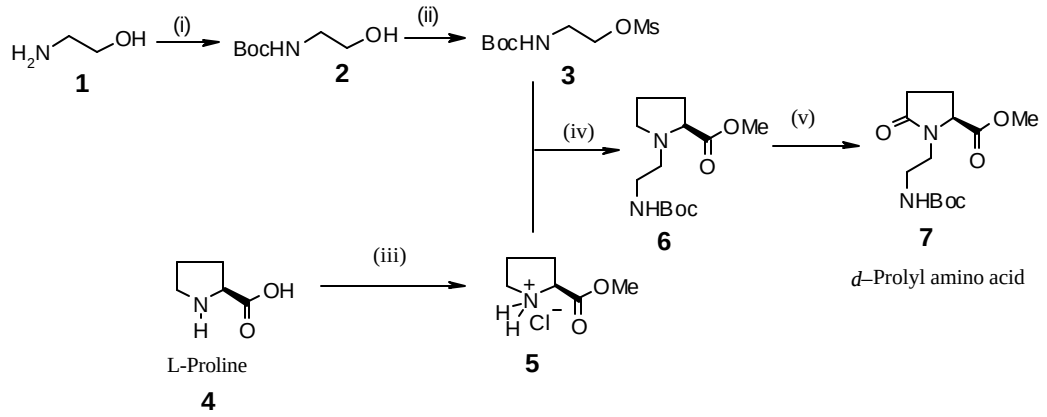

Reagents and conditions: (i) $(Boc)_2O$, Et_3N, dioxane:water (1:1), 0^0C-rt1, 18h, 90%; (ii) $MeSO_2Cl$, Et_3N, DCM, 0^0C, 2h, 80%; (ii) $SOCl_2$, MeOH, 0^0C-rt, 2h then reflux for 5h, quantitative; (iv) DIEA, DMAP, DMF:CH_3CN (1:1), rt-50^0C, 48h, 65%; (v) $NaIO_4/RuCl_3$, EtOAc:H_2O, rt, 1h, 45%.

6.3.2 Synthesis and purification of (*d-aep*) oligomers

Synthesis: The carboxylic acid of **6** was obtained by hydrolysis of ester with aqueous NaOH and the acid was used for the synthesis of *d- aep* peptides. The *d- aep* peptides (**1-5**) were synthesized by standard procedure of solid phase synthesis by using Boc-chemistry on MBHA resin and *b*-alanine as linker (for details see in Chapter 4).

Table 1: *d-aep* peptides*

Entry	***d*-AEP peptides**
1	H_2N-(*d- aep*)$_2$-*b-ala*-CO-MB
2	H_2N-(*d- aep*)$_3$-*b-ala*-CO-MB
3	H_2N-(*d- aep*)$_4$-*b-ala*-CO-MB
4	H_2N-(*d- aep*)$_6$-*b-ala*-CO-MB
5	H_2N-(*d- aep*$_7$-*b-ala*-CO-MB

*Whereas MB is MBHA resin.

Purification and characterization: *d*-Aminoethyl pyrrolidine amino acid (*d-aep*) peptides **1**-**5** (Table 2) were obtained by cleaving the oligomers from the above resins by using the standard protocol of TFA-TFMSA reagent. The purity of these peptides was checked by analytical reverse phase HPLC at wavelength (215 nm) in using water and acetonitrile with 1% TFA. The impure peptides were purified by C-4 column by HPLC and the purity was checked analytical HPLC on C-18 column. Finally, all peptides were characterized by MALDI-TOF mass spectroscopy as are given in Table 2.

Table 2: *d*- aminoethyl pyrrolidine amino acid (*d*-AEP)*

Entry	*d*-Proly amino acid (*d*-APA)	Molecular Formula	Molecular Mass
1	H_2N-(*d*- *aep*)$_2$-*b*-ala $CONH_2$	$C_{19}H_{34}N_6O_4$	410.52
2	H_2N-(*d aep*)$_3$-*b*-ala- $CONH_2$	$C_{26}H_{46}N_8O_5$	550.71
3	H_2N-(*d*- *aep*)$_4$-*b*-ala- $CONH_2$	$C_{33}H_{58}N_{10}O_6$	690.89
4	H_2N-(*d*- *aep*)$_6$-*b*-ala- $CONH_2$	$C_{47}H_{82}N_{14}O_8$	971.27
5	H_2N-(*d*- *aep*)$_7$ -βala-$CONH_2$	$C_{54}H_{94}N_{16}O_9$	1111.45

6.3.3 Results and Discussion: Structural study of (*d-aep*) peptides by CD/IR spectroscopy

The most common stable structures of peptides are *a*-helix and antiparallel *b*-pleated sheet and these have characteristic signatures in CD and IR spectra. In this section, the secondary structure of (*d-aep*) peptides is elucidated by CD and FT IR-spectroscopy. The secondary structures are formed by intramolecular structure are formed by intramolecular H-bonding which is favoured in organic solvents such as chloroform ($CHCl_3$). Hence all CD/ IR spectra were done in $CHCl_3$. For comparison in some cases, spectra were done in MeOH.

6.3.3a CD spectroscopy

The CD-spectra of *d*- *aep* monomer **6** in $CHCl_3$ (Figure 15A) and *d*- *aep* peptides (**1**-**5**) in MeOH (Figure 15B) were recorded at room temperature. The CD-signature of monomer exhibited a weak maxima at 245 nm and strong minima at 230. While the CD-

signature of *d- aep* heptamer **5** and hexamer **4** peptides exhibited a same similar strong minima at 217 nm, but are different from that of dimer (*d-aep* **1)**, trimer (*d-aep* **2**) and tetramer (*d-aep* **4**). However, the CD patterns for of *d- aep* **1-3** are almost of similar pattern among themselves.

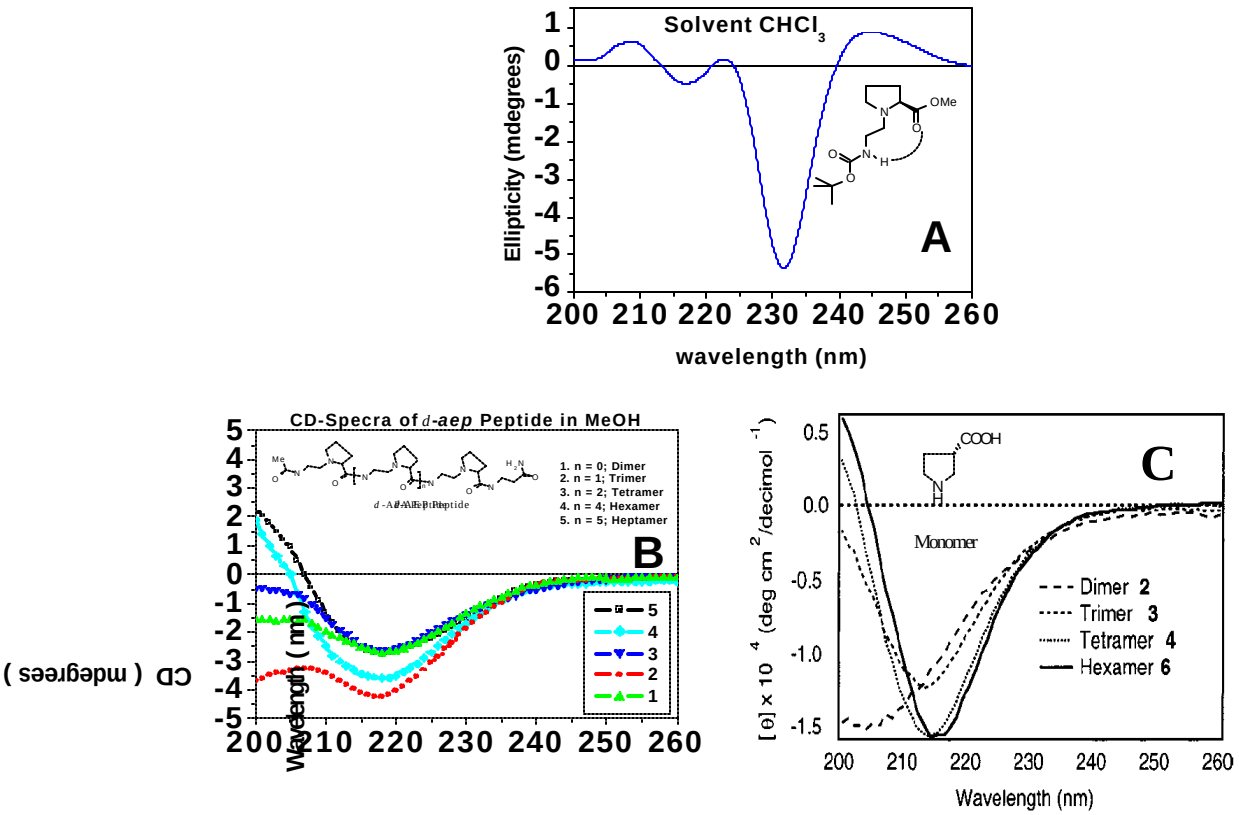

Figure 15: *Left*. CD-Spectra of monomer 6, *Right*. CD-spectra of *d*-APA acid in MeOH at 25 ^{o}C
CD of PCA in MeOH[20b]

From the literature,[20] the CD spectra of non-hydrogen bonded *b*-peptide helices display characteristic CD signatures of regular secondary structure. Figure 15C shows the reported CD-spectra in methanol for the *R*-pyrrolidine-3-carboxylic acid (PCA) series.[20b] The tetramer, pentamer and hexamer of PCA display nearly identical CD spectra, with a

minimum at ca. 214 nm and a zero crossing at ca. 203 nm. This signature is slightly different from that of the lower members of the PCA series, monomer, dimer and trimer, which is characteristic of a regular secondary structure and the extent of secondary structure formation is maximal beyond *four* PCA residues.

The CD spectra of *d- aep* peptides in $CHCl_3$ and MeOH are showing similar minima. The *d- aep* peptides (dimer **1**, trimer **2** and tetramer **3**) also show almost a similar kind of CD pattern in MeOH as that of PCA peptides. While CD of hexamer **4** and heptamer **5** *d- aep* peptides are similar to the pentamer and hexamer of PCA peptides. Thus, the length-dependent CD patterns of *d- aep* peptides suggest that larger size peptides show regular secondary structures similar to PCA which is *b*-helix.

6.3.3b FT-IR Spectroscopy

In the course systematic structural studies of *d- aep* peptides, FT-IR spectroscopy studies were carried out on the monomer and oligomers.

FT-IR of monomers: FT IR spectra of *d- aep* (**6**) and *d- aep* one (**7**) in MeOH are shown in Figure 16. From the IR spectrum of compound **6**, the derived NH-stretching frequency and C=O frequencies seen are given in Table 3. The observed NH-stretching is frequency for compound **6** is 3300 cm^{-1} and C=O stretching frequency is 1658 cm^{-1} (Table 3, entry 1). The FT IR spectra of compound **7** shows two NH frequencies 3328 cm^{-1} and 3422 cm^{-1}(Table 3, entry 2) in $CHCl_3$, while the compound **6** has only one at 3300 cm^{-1} (Table 3, entry 1). This suggests that compound **6** possesses showing stronger intra-molecular hydrogen bonding compared to compound **7.** Thus**,** the compound **6** is an appropriate candidate for forming 8-helix structure.

Table 3: FT-IR spectroscopic studied of *d- aep* amino acid

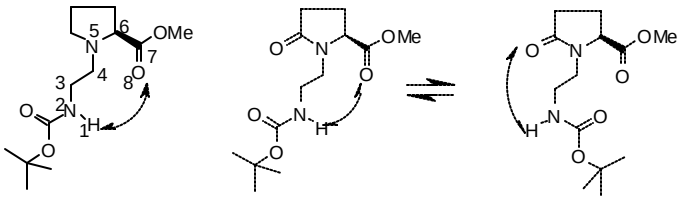

Entry	*d*-AEP	Frequency used for assignment (cm^{-1})	
1	**6**	1658, 1753	3300
2	**7**	1673, 1686, 1751	3328, 3452

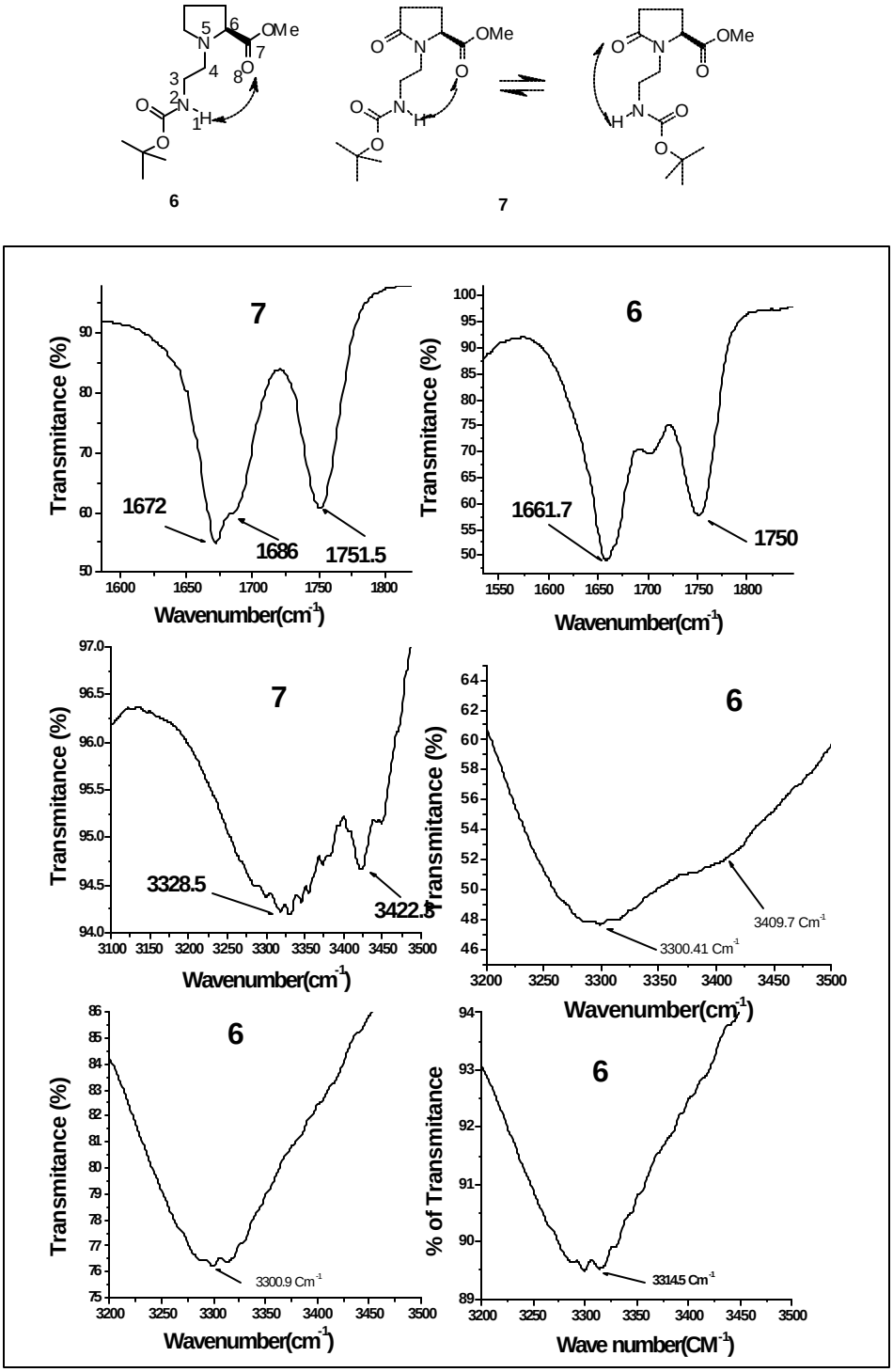

Figure 16: IR-spectra of *d- aep* s monomer **6** and AEPone **7** in $CHCl_3$

It is reported in literature[27] that *N*-methylacetamide (**8**) displays a solvent-exposed NH band at 3460 cm^{-1} in $CHCl_3$ (Table 4, entry 1). In addition to non-hydrogen-bonded amide absorption at 3460 cm^{-1} the oxopiperidinylacetamide (**9)** shows minor intramolecular hydrogen bonding seen by presence of a broad absorption at 3350 cm-1 (Table 4, entry 2). The formation of a seven-membered-ring hydrogen bond resulting from endocyclic carbonyl and side chain NH is generally not favoured. In peptidomimetic (**10**)**,** the major NH stretch band at 3350 cm^{-1} (Table 4, entry 2) indicates strong internal hydrogen bonding which may be due to either 7-membered (endocyclic carbonyl and exocyclic NH) or 11-membered ring interaction as shown below. The compound **11**, (Table 4, entry 4), show a substantial tendency for reverse turn formation via 11-membered intramolecular H-bonding.

Table 4: The reported FT IR data following reported compound **8-11**

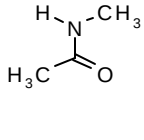

8

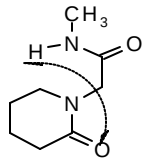

9

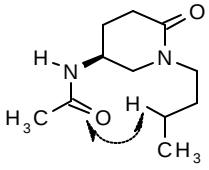

10

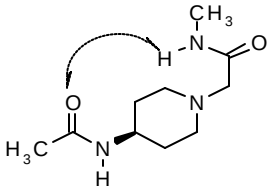

11

Entry	Compound	Frequency used for assignment (cm^{-1})
		Amide A (NH stretch)
1	**8**	3460
2	**9**	3460 (max); 3350 (min)
3	**10**	3460 (min); 3350 (max)
4	**11**	3460 (max); 3350 (min)

* IR spectra are scanned in $CHCl_3$[29]

In comparison, the IR NH frequencies of *d- aep* monomer **6** and *d- aep* one monomer are almost similar to that of reported compound **10.** This indicates that these peptides have the capability to form intramolecular hydrogen bonding with 8-membered

ring, which leads to *b*-turn at monomer level. Since *d*- *aep* monomer **6** has one strong IR peak at 3300 cm^{-1} compared to two peaks *d*- *aep* one monomer **7**, it appears that 8-membered intramolecular H-bonding in that *d*- *aep* monomer **6** is more favourable than that of *d*- *aep* one monomer **7**.

FT-IR of Peptides: The FT IR spectra of all *d*- *aep* s peptides (**1**-**5**) in MeOH were recorded at room temperature (Figures 17 and 18) in transmittance mode. The spectra shows the C=O stretching (Figure 17) and the NH stretching frequency (Figure 18) in all *d*- *aep* peptides and the data is given in Table 5 (entry 1-6). The C=O stretching and the NH stretching frequency of *d*- *aep* monomer **6** are at 1657, 1752 cm^{-1} (C=O) and 3300 cm^{-1} (NH, Table 5, entry 1) respectively. The NH stretching frequency of dimer was at 3499 cm^{-1} while the oligomers (trimers to heptamer) exhibited the NH stretching at a slightly lower frequency (3435 cm^{-1}). In contrast to the monomer **6** that showed two bands for amide –C=O, the dimer to heptamer oligomers exhibited only one band in the region 1663-1675 cm^{-1}. These results suggest that the *d*- *aep* peptides **1**-**6** form *b*-turn.

Table 5: FT-IR spectroscopic data of *d*-AEP peptide from Figure 18 and 19*

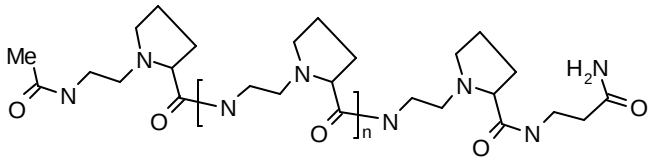

Entry	*d*-Aminoethyl Proly amino acid (*d*-AEP)	Frequency used for assignment (cm^{-1})	
		Amide A NH strech	AmideI -C=O
1	**6**. BocNH-(*d*- *aep*)COOMe (monomer)	3300; 3409	1657; 1752
2	**1.** H_2N-βala-(*d*- *aep*)$_2$$CONH_2$; dimer	3499	1669
3	**2**. H_2N -βala-(*d*- *aep*)$_3$$CONH_2$; trimer	3435	1663
4	**3**. H_2N -βala-(*d*- *aep*)$_4$$CONH_2$; tetramer	3433	1675
5	**4**. H_2N -βala-(*d*- *aep*)$_6$$CONH_2$; Hexamer	3435	1663
6	**5**. H_2N -βala-(*d*- *aep*)$_7$$CONH_2$; Heptamer	3436	1663

*IR spectra of all peptides scanned in MeOH.

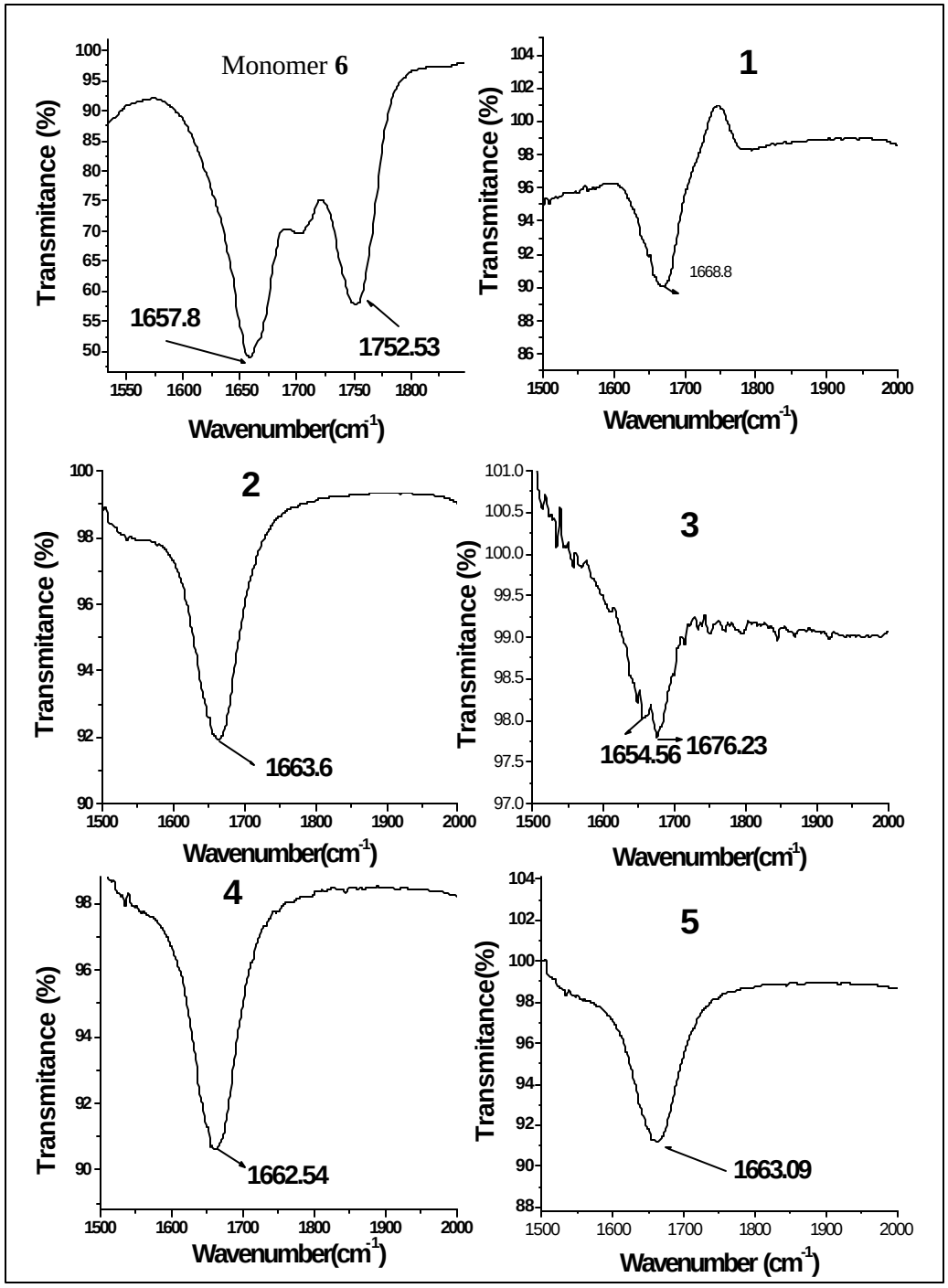

Figure 17: FT IR -spectra of *d- aep* peptides in MeOH in range 1500-2000 cm^{-1}
(Amide 1; -C=O stretch)

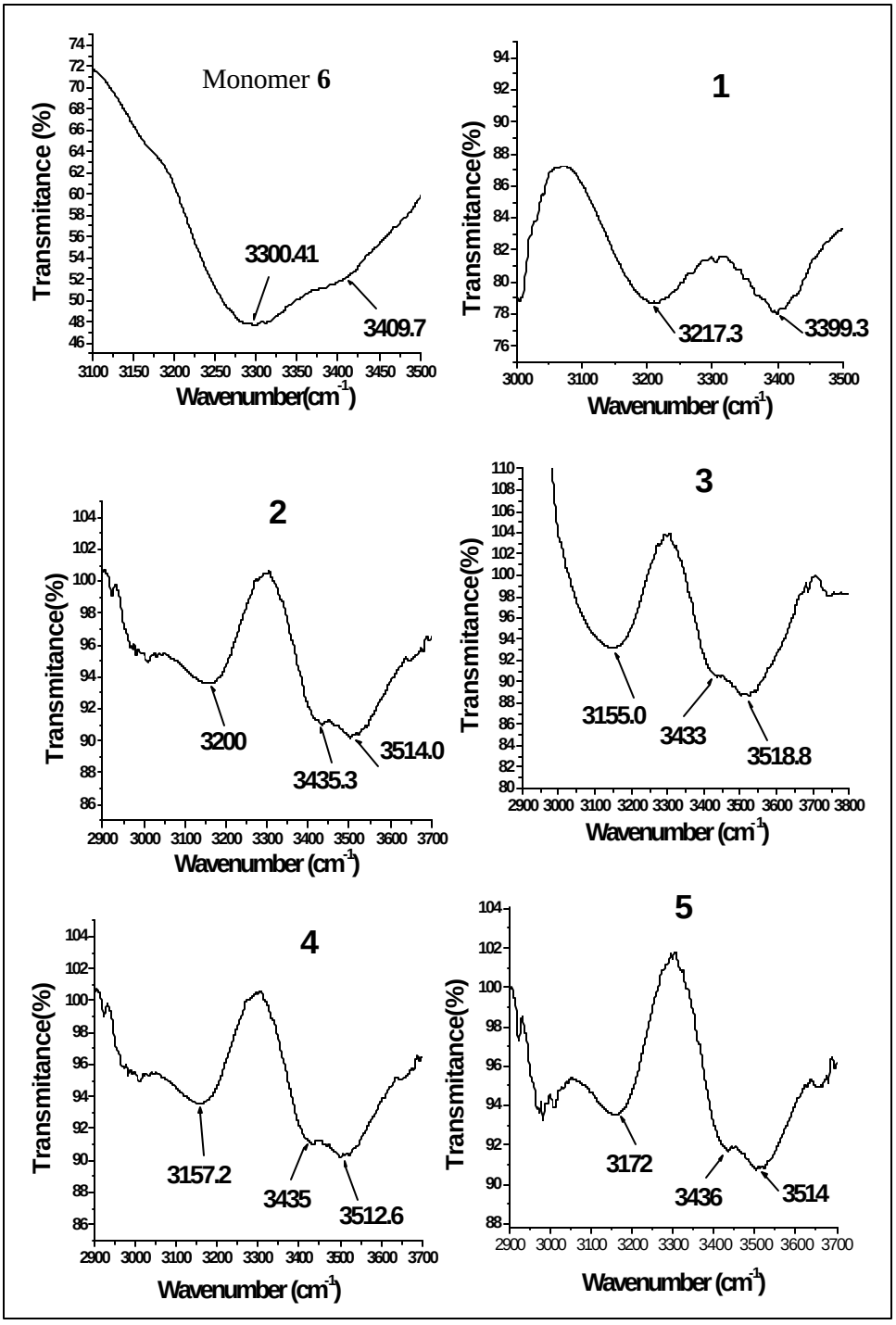

Figure 18: FT IR-spectra of *d- aep* peptides in MeOH in range 2900-3700 cm^{-1} (Amide A; NH stretch)

6.4 CONCLUSIONS

This short Chapter reports the synthesis of *d- aep* monomer and oligomers of peptides and structural characterization CD and FT IR. The preliminary studies done indicates longer *d- aep*s (**4** and **5**) peptides (longer than tetramer) adopt a specific secondary structure in methanol like *b*-helix type, while showing *b*-turn type in the monomer. Further investigations are necessary to confirm these preliminary results observations.

6.5 REFERENCES

1. Kirshenbaum, K.; Zuckermann, R.N.; Dill, K. A. Designing polymers that mimic biomolecules. *Curr. Opin. Struct. Biol.* **1999**, *9*, 530–535. (b) Armitage, B. A. Bioinspired organic chemistry. *Annu. Rep. Prog. Chem. Sect B: Org. Chem.* **2000**, *96*, 187–229.
2. Hill D. J.; Mio, M. J.; Prince, R. B.; Hughes, T. S.; Moore, J. S. A field guide to foldamers. *Chem. Rev.* **2001**, *101*, 3893-4012. (b) Cheng R, P. Beyond de novo protein design de novo design of non-natural folded oligomers. *Curr. Opin. Struct. Biol.* **2004**, *14*, 512-20.
3. (a) Gellman, S. H. Foldamers: a manifesto. *Acc. Chem. Res.* **1998**, *31*, 173-180. (b) Cheng, R. P.; Gellman, S. H.; De Grado, W. F. *b*-Peptides: From structure to function. *Chem. Rev.* **2001**, *101*, 3219-3232.
4. Seebach, D.; Matthews, J. ß-peptides: a surprise at every turn. *Chem. Commun.* **1997**, 2015-2022. Gademann, K.; Hintermann, T.; Schreiber, J. V. Beta-peptides:twisting and turning. *Current medicinal Chemistry* **1999**, *6*, 905-925.
5. Venkatraman, J.; Shankaraman, S. C.; Balaram, P. Design of folded peptides. *Chem. Rev.* **2001**, *101*, 3131-3152.
6. Banerjee, A.; Balaram, P. Stereochemistry of peptides and polypeptides containing omega amino acids *Curr. Science* **1997**, *73*, 1067.
7. Appella D. H.; Christiansen, L. A.; Klein, D. A.; Powell, D. R, Huang, X.; Barchi, J. J. Jr, Gellman, S. H. Residue-based control of helix shape in beta-peptide oligomers. *Nature* **1997**, *387*, 381-384.
8. Wang, X.; Espinosa, J. F.; Gellman, S. H. 12-Helix formation in aqueous solution with short beta-peptides containing pyrrolidine-based residues. *J. Am. Chem. Soc.* **2000**, *122*, 4821.
9. (a) Appella, D. H.; Christiansen, L. A.; Karle, I. L.; Powell, D. R.; Gellman, S. H. Beta-peptide foldamers: robust helix formation in a new family of beta-amino acid oligomers. *J. Am. Chem. Soc.* **1996**, *118*, 13071. (b) Appella, D. H.; Christiansen, L. A.; Karle, I. L.; Powell, D. R.; Gellman, S. H. Synthesis and characterization of trans-2-aminocycloexanecarboxylic acid oligomers: An unnatural secondary structure, and implications for beta-peptide tertiary structure. *J. Am. Chem. Soc.* **1999**, *121*, 6206-6212.
10. Applequist, J.; Bode, K. A.; Appella, D. H.; Christiansen, L. A.; Gellman, S. A. Theoretical and experimental circular dichroic spectra of the novel helical foldamer Poly[(1R,2R)-trans-2-aminocyclopentanecarboxylic acid]. *J. Am. Chem. Soc.* **1998**, *120*, 4891.
11. (a) Hintermann, T.; Gademann, K.; Jaun, B.; Seebach, D. Gamma-peptides forming more stable secondary structures than alpha-peptides: synthesis and helical NMR-solution structure of the gamma-hexapeptide analog of H-(Val-Ala-Leu)$_2$-OH *Helv. Chim. Acta* **1998**, *81*, 983. (b) Krauthauser, S.; Christianson, L. A.; Powell, D. R.; Gellman, S. H. Antiparallel sheet formation in beta-peptide foldamers: effects of beta-amino acid substitution on conformational preference. *J. Am. Chem. Soc.* **1997**, *119*, 11719. (c) Seebach, D.; Abele, S.; Gademann, K.; Jaun, B. *Angew. Chem. Int. Ed.* **1999**, *38*, 1595.
12. (a) Seebach, D.; Ciceri, P.E.; Overhand, M.; Jaun, B.; Rigo, D.; Obrist, L.; Hammel, U.; Amstutz, R.; Widmer, H. "Probing the helical secundary structure of short-chain *b*-peptides", *Helv. Chim. Acta*,

1996, *79*, 2043-2066. (b) Seebach, D.; Overhand, M.; Kuhnle, F. N. M.; Martinoni, B.; Oberer, L.; Hommel, U.; Widmer, H. *Helv. Chim. Acta* **1996**, *79*, 913.

13. Christiansen, L. A.; Lucero, M. J.; Appella, D. H.; Klein, D. A.; Gellman, S. H. Improved treatment of cyclic beta-amino acids and successful prediction of beta-peptide secondary structure using a modified force field: AMBER*C. *J. Comput. Chem.* **2000**, *21*, 763.
14. (a) Seebach, D.; Abele, S.; Gademann, K.; Guichard, G.; Hintermann, T.; Jaun, B.; Matthews, J. L.; Schreiber, J. V.; Oberer, L; Hommel, U.; Widmer, H. Beta(2)- and beta(3)-peptides with proteinaceous side-chains-synthesis and solution structures of constitutional isomers, a novel helical secondary structure and the role of hydrophobic interactions on folding. *Helv. Chim. Acta*. **1998**, *81*, 932. (b) Seebach, D.; Gademann, K.; Schreiber, J. V.; Matthews, J. L.; Hintermann, T.; Jaun, B.; Oberer, L.; Hommel, U.; Widmer, H. 'Mixed' Beta-Peptides: A unique helical secondary structure in solution *Helv. Chim. Acta* **1997**, *80*, 2033.
15. Claridge, T. D. W.; Goodman, J. M.; Moreno, A.; Angus, D.; Barker, S. F.; Taillefumier, C.; Watterson, M. P.; Fleet, G. W. J. 10-Helical conformations in oxetane *b*-amino acid hexamers. *Tetrahedron Lett.* **2001**, *42*, 4251-4255.
16. (a) Yang, D.; Qu, J.; Li, B.; Ng, F.-F.; Wang, X.-C.; Cheung, K.-K.; Wang, D.-P.; Wu, Y.-D. "Novel turns and helices in peptides of chiral-aminoxy acids". *J. Am. Chem. Soc.* **1999**, *121*, 589. (b) Abele, S.; Seebach, D. *Helv. Chim. Acta* **1999**, *82*, 1559.
17. (a) Bestian, H. *Angew. Chem., Int. Ed. Engl.* **1968**, *7*, 278. (b) Huck, R.; Fisk, J.D. Gellman, S. H. Promotion of sheet formation in *a*-peptide strands by a *ß*-peptide reverse turn. *Org. Lett.* **2000**, *2*, 2607–2610. (c) Das, C.; Raghothama, S.; Balaram, P. Four-stranded β-sheet structure in a designed, synthetic polypeptide. *J. Chem. Soc., Chem. Commun.* **1999**, 967-968.
18. Masamoto, J.; Sasaguri, K.; Ohizumi, C.; Kobayashi, H. *J. Polym. Sci. A-2* **1970**, *8*, 1703.
19. Motorina, I. A.; Huel, C.; Quiniou, E.; Mispelter, J.; Adjadj, E.; Grierson, D. S. *J. Am. Chem. Soc.* **2001**, *123*, 8.
20. Huck, B. R.; Langenhan, J. M.; Gellman, S. H. Non-hydrogen-bonded secondary structure in beta-peptides: evidence from circular dichroism of (S)-pyrrolidine-3-carboxylic acid oligomers and (S)-nipecotic acid oligomers. *Org. Lett.* **1999**, *1*, 1717-1720. (c) Huck, B. R.; Fisk, J. D.; Guzei, I. A.; Carlson, H. A.; Gellman, S. H. Secondary structural preferences of 2,2-disubstituted pyrrolidine-4-carboxylic acid oligomers: beta-peptide foldamers that cannot form internal hydrogen bonds. *J. Am. Chem. Soc.* **2003**, *125*, 9035-9037.
21. (a) Hanessian, S.; Luo, X.; Schaum, R.; Michnick, S. Design of secondary structures in unnatural peptides: stable helical ?tetra-, hexa-, and octapeptides and consequences of a-substitution. *J. Am. Chem. Soc.* **1998**, *120*, 8569-8570. (b) Baldauf, C.; Gunther, R.; Hofmann, H. J. Control of helix formation in vinylogous gamma-peptides by (E)- and (Z)-double bonds: a way to ion channels and monomolecular nanotubes. *J. Org. Chem.* **2005**, *70*, 5351-5361
22. (a) Baldauf, C.; Gunther, R.; Hofmann, H. J. Delta-peptides and delta-amino acids as tools for peptide structure design a theoretical study. *J. Org. Chem.* **2004**, *69*, 6214-20. (b) Huc, I. Aromatic oligoamide foldamers. *Eur. J. Org. Chem.* **2004**, 17-29.

23. Yang, D.; Zhang, Y. H.; Li. B.; Zhang, D. W. Synthesis of Chiral beta 3-aminoxy peptides. *J. Org. Chem*. **2004**, *69*, 7577-81

24. Gademann, K.; Hane, A.; Rueping, M.; Jaun, B.; Seebach, D. The fourth helical secondary structure of β-peptides: The (P)-2_8-helix of a β-hexapeptide consisting of (2R,3S)-3 amino-2-hydroxy acid residues. *Angew. Chem. Int. Ed. Engl.* **2003**, *42*, 1534-1537.

25. (a) Adler, A. J.; Greenfield, N. J.; Fasman, G. D. Circular dichroism and optical rotatory dispersion of proteins and polypeptides. *Methods Enzymol*. **1973**, *27*, 675-735. (b) Greenfield, N.; Fasman, G. D. Computed circular dichroism spectra for the evaluation of protein conformation. *Biochemistry* **1969**, *8*, 4108-4116. (c) Greenfield, N.; Davidson, B.; Fasman, G. D. The use of computed optical rotatory dispersion curves for the evaluation of protein conformation. *Biochemistry* **1967**, 1630-7. (d) Stone, M. T.; Fox, J. M.; Moore, J. S. A helicene-containing foldamer displaying highly solvent-dependent CD spectra. *Org. Lett*. **2004**, *6*, 3317-3320.

26. Vass, E.; Hollósi, M.; Besson, F.; Buchet, R. Vibrational spectroscopic detection of beta- and gamma-turns in synthetic and natural peptides and proteins. *Chem. Rev.* **2003**, *103*, 1917-1954.

27. Weber, K.; Ohnmacht, U.; Peter Gmeiner, P. Enantiopure 4- and 5-aminopiperidin-2-ones: regiocontrolled synthesis and conformational characterization as bioactive beta-turn mimetics. *J. Org. Chem*. **2000**, *65*, 7406-7416.

28. Cheng, R. P.; Gellman, S. H.; De Grado, W. F. *b*-Peptides: from structure to function. *Chem. Rev*. **2001**, *101*, 3219-3232.

29. Park, J. S.; Lee, H. S.; Lai, J. R.; Kim, B. M.; Gellman, S. H. Accommodation of alpha-substituted residues in the beta-peptide 12-helix: expanding the range of substitution patterns available to a foldamer scaffold. *J. Am. Chem. Soc*. **2003**, *125*, 8539-8545.

6.6 APPENDIX

1. ^{1}H-NMR, ^{13}C, and ^{13}CDEPT spectra of monomer (**6**)

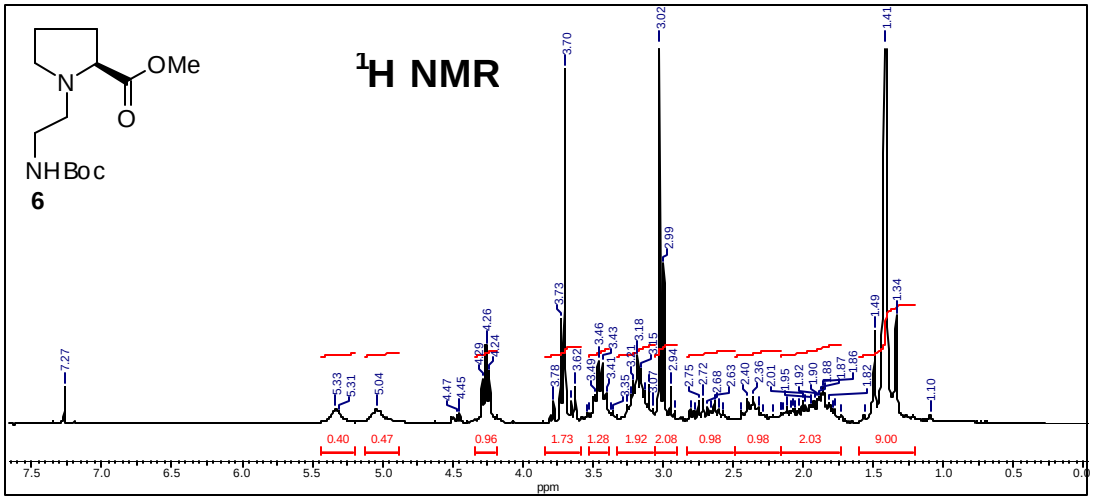

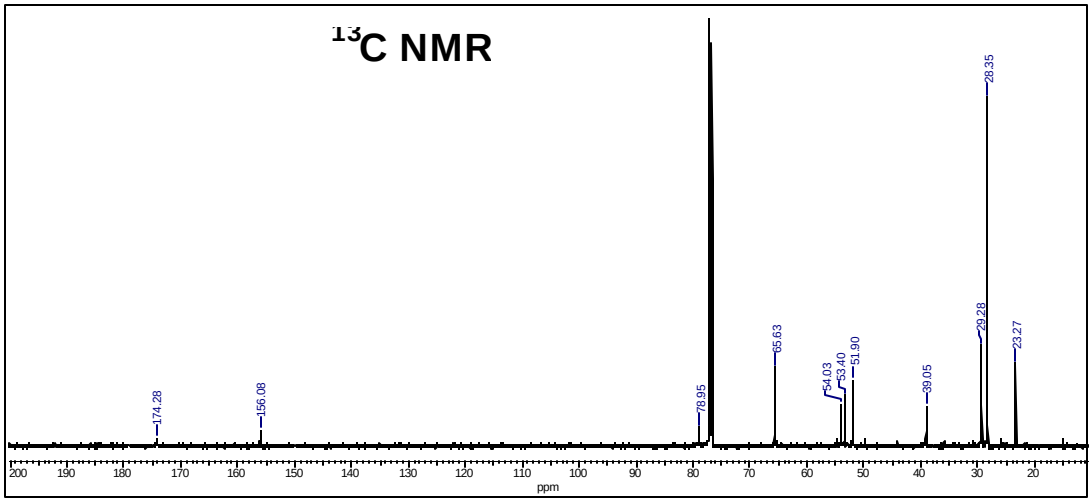

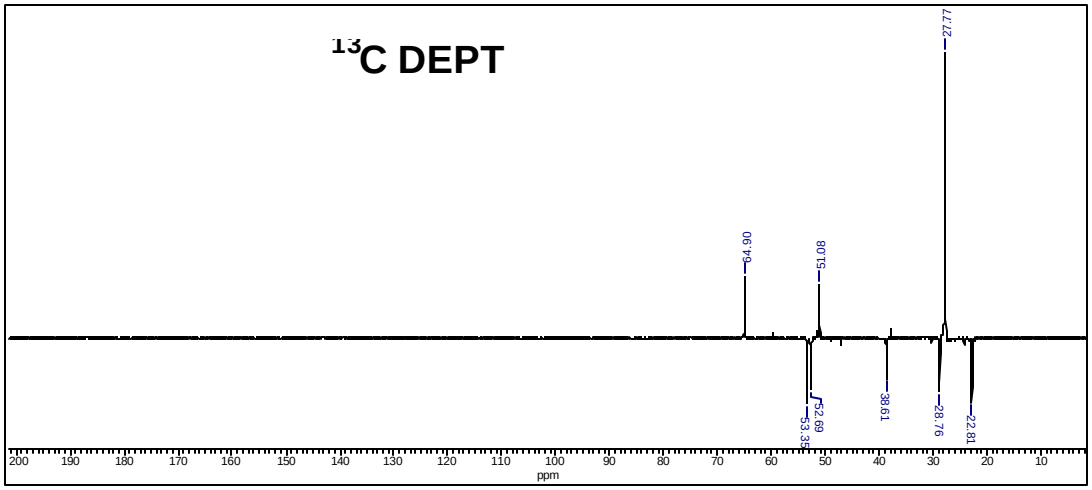

2. ^{1}H-^{1}H COSEY & ^{1}H-^{13}H HETCOR 2D NMR spectra of *aep* monomer (**6**)

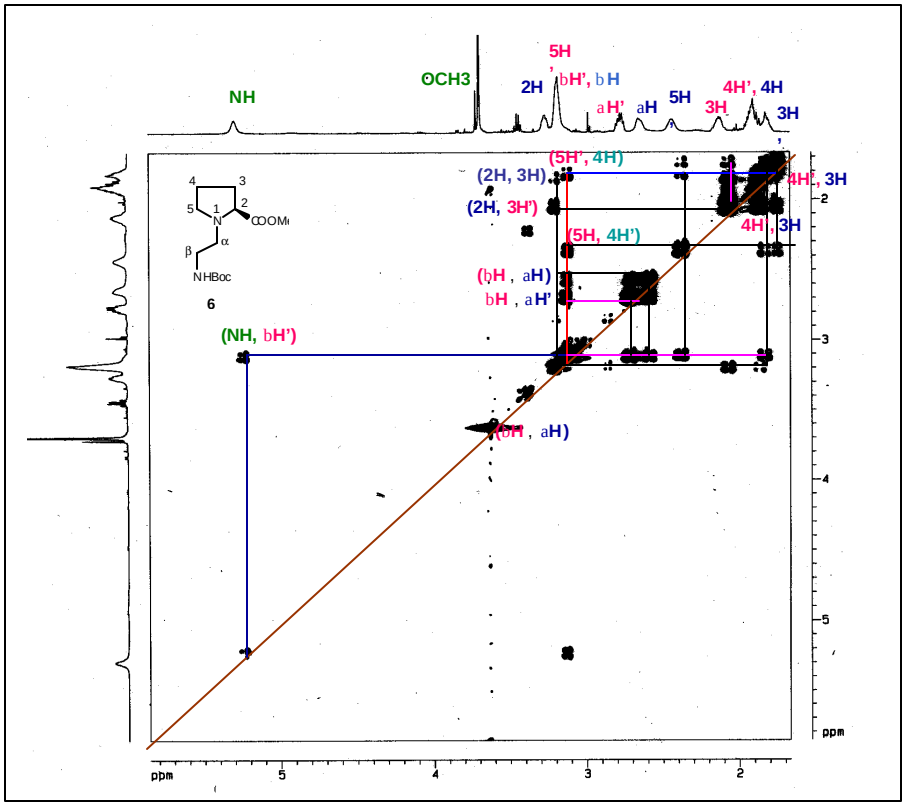

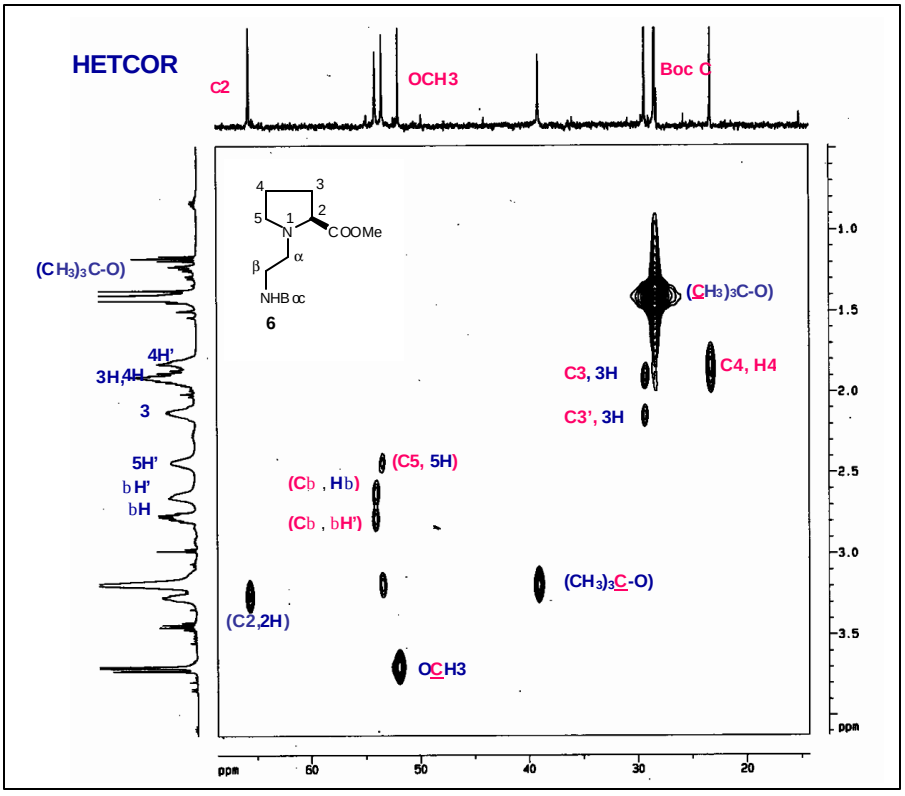

3. ^{1}H-^{1}H NOESY spectra *d*-AEP **6**

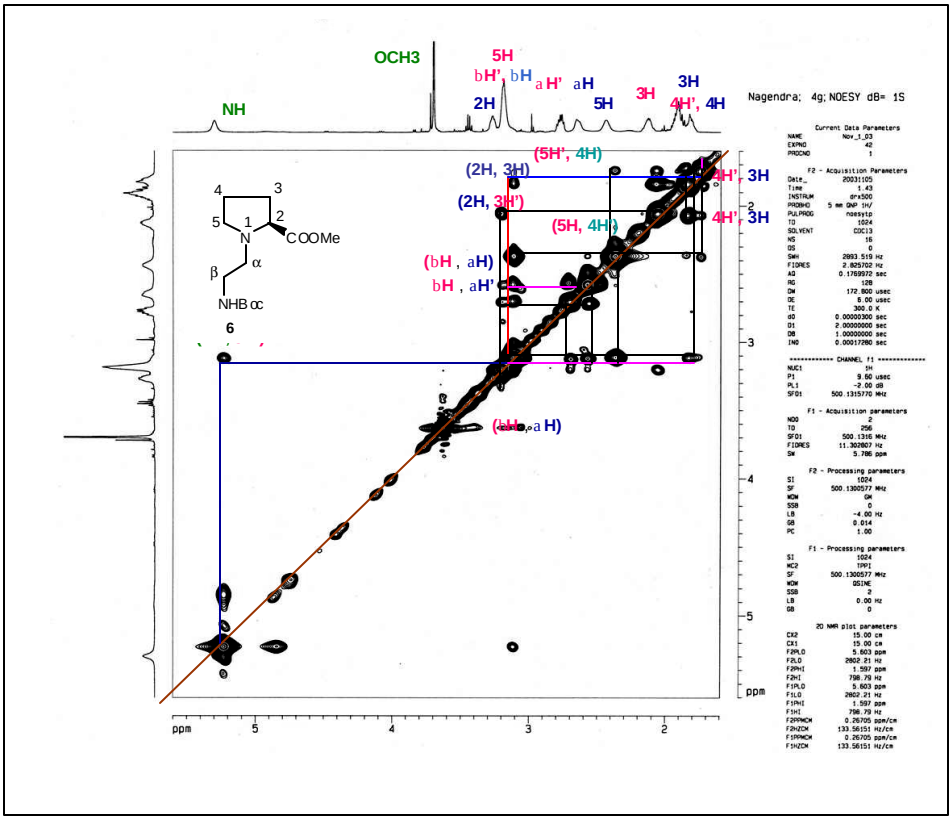

Mass spectra of compound **6**

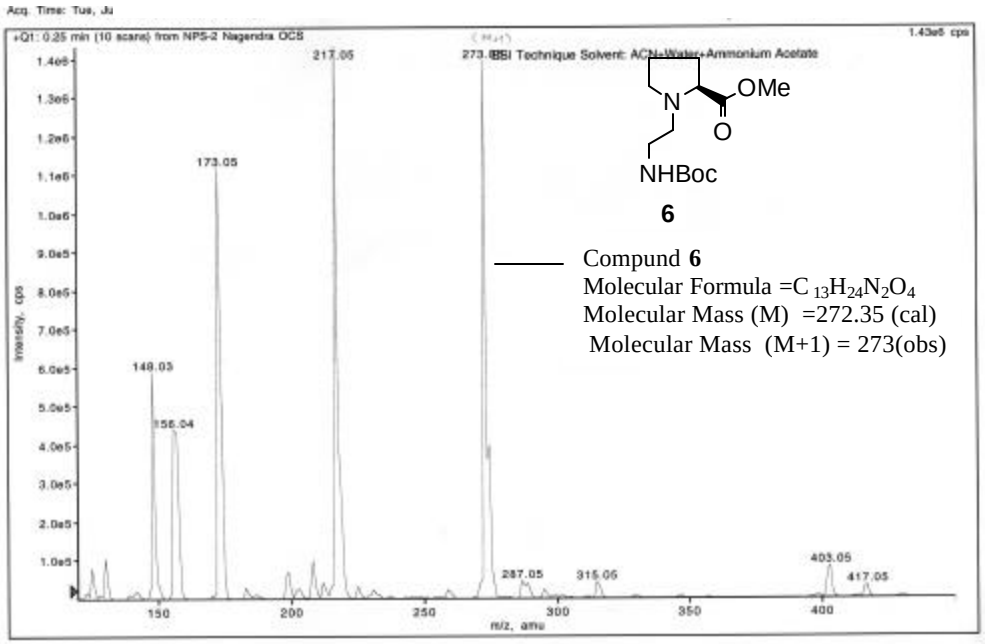

4. HPLC of *d-aep* **2**, *d-aep* **3**, *d-aep* **4** and *d-aep* **5**

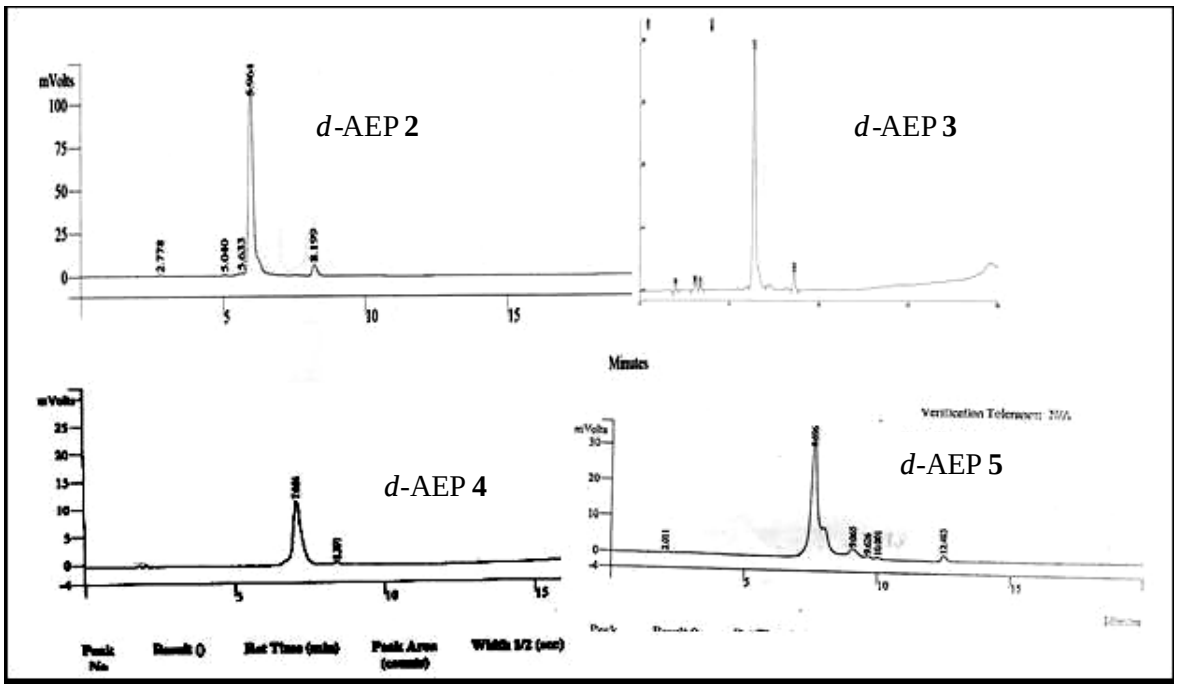

5. MALDI-TOF mass spectra of *d-aep* **2**

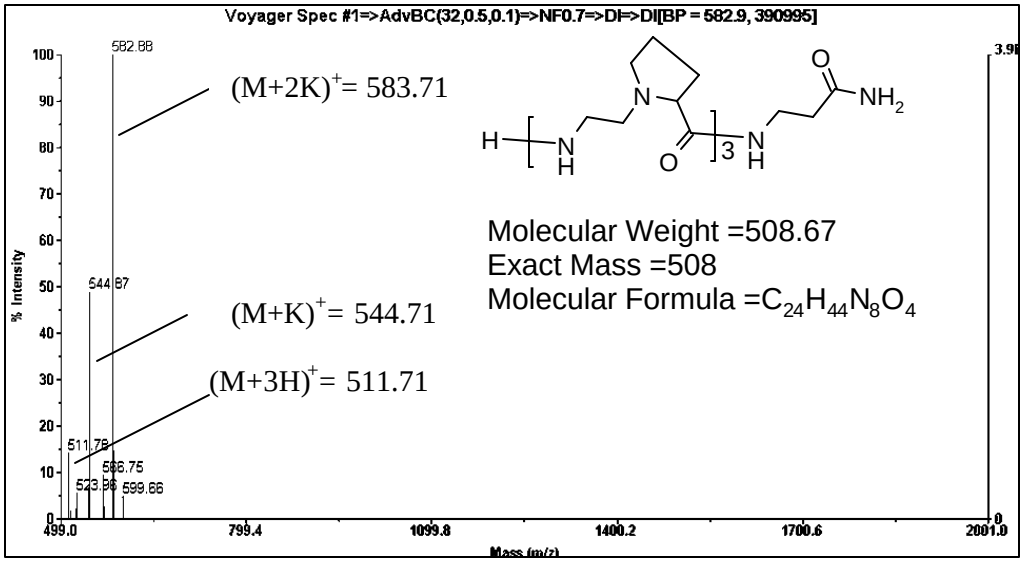

MALDI-TOF mass spectra of *d-aep* **3**

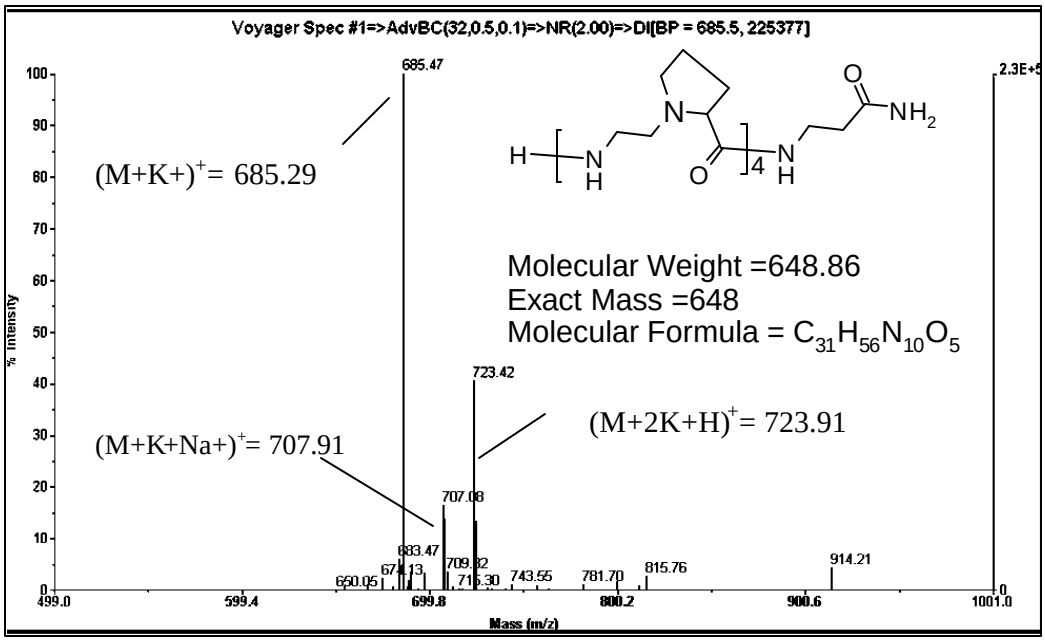

6. MALDI-TOF Mass spectra of *d-aep* **4**

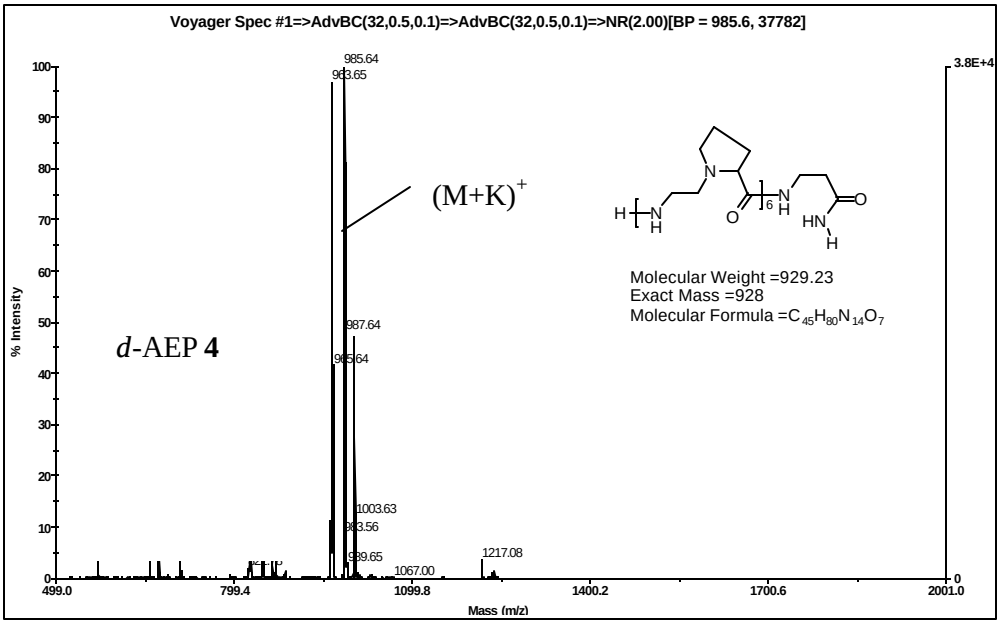

MALDI-TOF Mass spectra of *d-aep* **5**

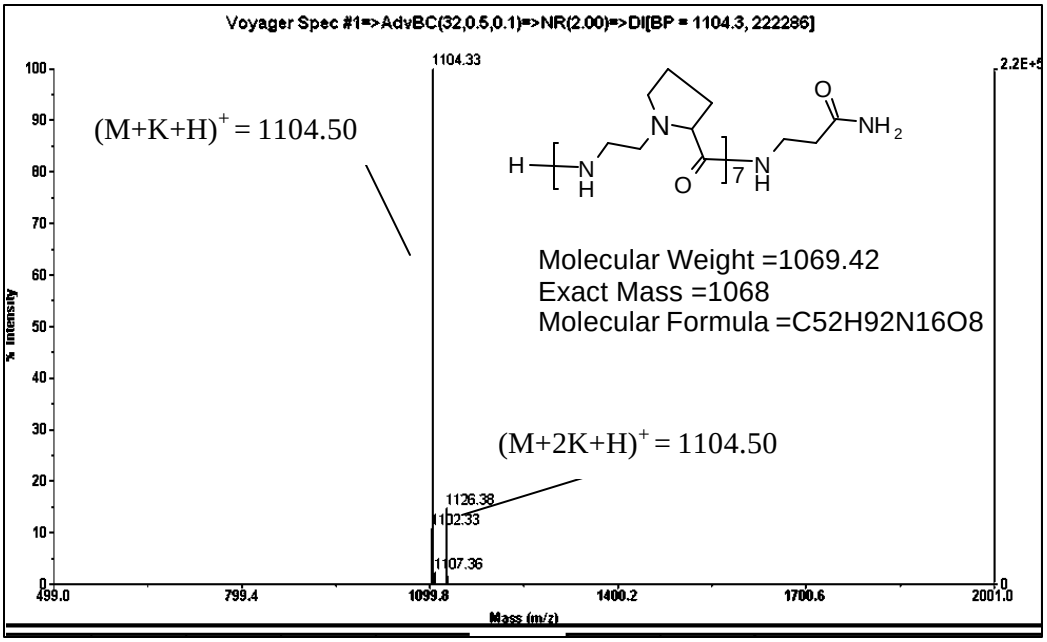

ERRATUM

COMMUNICATION

ChemComm
www.rsc.org/chemcomm

Expanding the repertoire of pyrrolidyl PNA analogues for DNA/RNA hybridization selectivity: aminoethylpyrrolidinone PNA (*aepone*-PNA)†

Nagendra K. Sharma and Krishna N. Ganesh*

Division of Organic Chemistry (Synthesis), National Chemical Laboratory, Pune 411008, India. E-mail: kng@ems.ncl.res.in; Fax: 91 20 589 3153; Tel: 91 20 589 3153

Received (in Cambridge, UK) 30th June 2003, Accepted 7th August 2003
First published as an Advance Article on the web 20th August 2003

New PNA analogues derived from aminoethylpyrrolidin-5-one backbone show stabilization of *aepone*-PNA:DNA hybrids and destabilization of the corresponding RNA hybrids compared to unmodified PNA.

Peptide Nucleic Acids (PNA, **I**) are one of the most prominent findings of the search for structural analogues of DNA/RNA for antigene/antisense therapeutics.[1] The binding of PNA to the target DNA/RNA sequences occurs with high sequence specificity and this attribute of PNAs for biological and medicinal applications has not yet been fully realized due to poor aqueous solubility, ambiguity in binding orientation specificity (parallel/antiparallel) and lack of sufficient discrimination in binding between target DNA and RNA.[1b,2] Classical PNA is conformationally very flexible and can attain different conformations to accommodate binding to both DNA and RNA. NMR study of PNA oligomers has indicated it to be a complex mixture (up to 2^n) of conformational isomers arising from *cis* and *trans* tertiary amide bonds with a significant barrier to rotational interconversion.[3] PNA hybridization to DNA/RNA is dependent on the tertiary amide conformation and hence affected by the slow rotamer equilibrium. Examination of the crystal structures of PNA/DNA, PNA/RNA, PNA/PNA and PNA_2/DNA triplexes reveal that the linker carbonyl is pointing towards the carboxyl end of PNA.[4]

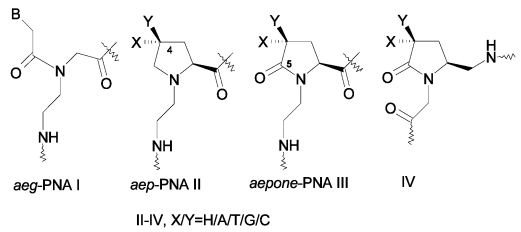

One way to study the criticality of such structural features is to design structures with frozen rotation of the side chain by locking them into rings as exemplified by the different pyrrolidene based PNA analogues.[5] In one of our earlier modifications, remarkable stabilization of the derived PNA:DNA hybrids was achieved in the chiral and cationic aminoethylprolyl PNA (*aep*-PNA, **II**), having the neutral tertiary amide group of PNA **I** replaced by a protonatable cyclic tertiary amine.[6] In order to avoid the dominance of the non-sequence specific electrostatic component in *aep*-PNA:DNA binding and to get the best characteristics from both the normal PNA and the *aep*-PNA, we resorted to restoring the amide character to the pyrrolidene ring nitrogen. Herein we report the synthesis and evaluation of aminoethylpyrrolidin-5-one PNA (*aepone*-PNA, **III**) having the endocyclic amide CO at C5. The synthesis of all four nucleobase protected monomers (**4,5**) and incorporation of the *aepone*-T monomer **4** into *aeg*-PNA backbone to examine the selectivity in hybridization stability with DNA and RNA is reported. Our present modification with a pyrrolidine-*N*1–CH_2CH_2NH– backbone is quite different from the previously known[7] pyrrolidine-*N*1–CH_2CO backbone (**IV**) as it leads to different C and N termini for the derived PNAs. The chemical synthesis of the target pyrrolidin-5-one system was done *via* selective C5-oxidation of *N*-(aminoethyl-)prolines, wherein despite the available choice of endo- and exo-cyclic N_α–CH_2 groups, the endocyclic 5-CH_2 is preferentially oxidized as confirmed by the reported crystal structure.

The literature methods for the synthesis of 4-substituted pyrrolidin-5-one consist of reaction of proline substrates with RuO_4 generated *in situ* by oxidation of RuO_2 with $NaIO_4$.[8] In these examples, the ring imino nitrogen is protected with a Boc group. In our examples, N1 has an ethylamino substituent that has competing N_α-methylene groups susceptible to oxidation. The reaction of (4*R*)-O-mesyl-N1(ethylamino-N-boc) proline ester **2** with $RuCl_3/NaIO_4$, in a biphasic solvent system, was complete within 1 h and led to a product mixture from which only the major C5-one product **3** could be isolated in 45% yield and successfully characterized (Scheme 1). The identity of the oxidation site in **3** as C5 was unambiguously deduced from its crystal structure (Fig. 1).‡ The oxidation of the C5 endocyclic methylene seems to be preferred over that of exocyclic methylenes, in spite of C5 having an electronegative α-substituent. This compound was used to alkylate N1 of pyrimidines T and C and N9 of purines A and 2-amino-6-chloropurine (precursor for G) which are suitably protected at exocyclic amino groups (Scheme 1) to obtain the (2*S*,4*S*)-*aepone*-PNA monomer esters (**4a–7a**). Upon hydrolysis with LiOH/MeOH esters yielded the monomers (**4b–7b**) suitable for solid phase synthesis of *aepone*-PNA oligomers. It should be pointed out that the synthetic strategy for pyrrolidinone PNA monomers reported here involving prior N-alkylation followed by C5 oxidation is much shorter than the one previously reported[7] for similar analogues.

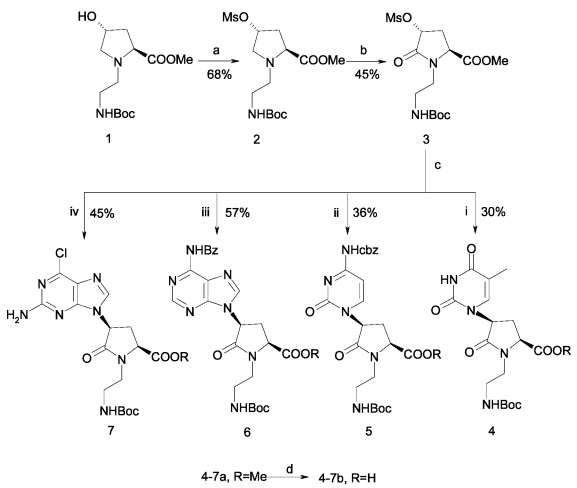

Scheme 1 Synthesis of aepone-PNA monomers. a) $MeSO_2Cl$, Et_3N in DCM at 0 °C; b) $NaIO_4$, $RuCl_3{\cdot}xH_2O$, CH_3CN–CCl_4–H_2O (1 : 1 : 1.5), 20 min; c) K_2CO_3, 18-crown-6 ether, DMF, 70 °C; i) thymine; ii) N4-cbz-cytosine; iii) N^6-bz-adenine; iv) 2-amino-6-chloropurine.

† Electronic supplementary information (ESI) available: ^1H NMR of **3–7**, mass spectra of **3–7**, **9–11**, HPLC, UV-melting curves and experimental details. See http://www.rsc.org/suppdata/cc/b3/b307362a/

DOI: 10.1039/b307362a

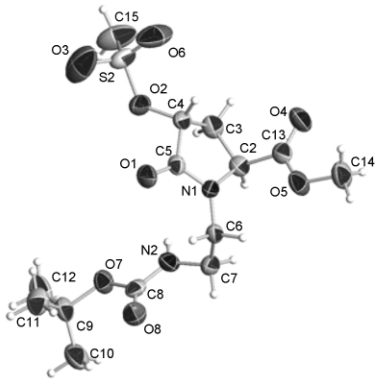

Fig. 1 ORTEP diagram of the crystal structure of **3**.

PNA T_8 oligomers **9–12** incorporating the modified monomers were synthesized using Boc chemistry on β-alanine derivatized Merrifield resin followed by cleavage from the resin with TFA/TFMSA, purification of PNA oligomers by reverse phase HPLC and characterized by MALDI-TOF. The modified *aepone*-T monomer **4b** was incorporated at the C-terminus in PNA **9**, at the C-terminus and centre in PNA **10** and at all positions in PNA **11**. The complementary DNA sequence **13** (GCA_8CG) had GC and CG locks at the 5′- and 3′-ends to avoid slippage of duplexes. The PNA:DNA/RNA complexes were constituted by mixing appropriate strands in a 2 : 1 stoichiometry in buffer followed by heating to 90 °C and annealed by slow cooling to 4 °C to obtain PNA_2:DNA triplexes.

The T_ms of different triplexes as extracted from the derivative plot of temperature dependent UV absorbance (Fig. 2) at 260 nm is shown in Table 1. It is seen that *aepone*-PNA oligomers **9–11** significantly stabilise the derived triplexes with DNA **14** as compared to that from the unmodified PNA oligomer **8** (ΔT_m 16–19 °C) (Fig. 2A). In comparison, the *aepone*-PNAs **9–11** effected destabilization of the triplexes formed with poly(rA), compared to the triplex from unmodified PNA **8** (ΔT_m 12–15 °C) (Fig. 2B). What is significant is that even the completely modified PNA oligomer **11** binds DNA and poly(rA) with a well defined T_m. This result on specificity of hybridization of *aepone*-PNAs **9–11** with preference for significant stabilization of DNA hybrids over RNA hybrids of unmodified PNA **8** is opposite to the selectivity observed for pyrrolidinone-A_8 PNA with opposite polarity;[7] these analogues stabilised RNA hybrids more than the DNA hybrids. The *aepone*-PNA analogues are more akin to the recently reported[9] pyrrolidinyl PNAs in terms of observed selectivities.

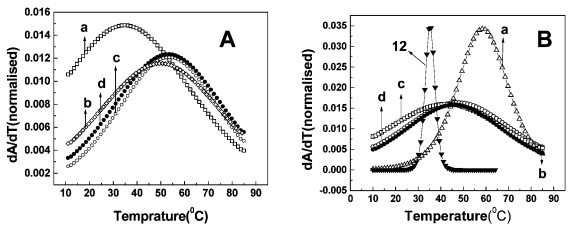

Fig. 2 Derivative UV absorbance (260 nm)–temperature profiles. A) PNA:DNA**13** hybrids and B) PNA:poly(rA) hybrids: a) **8**, b) **9**, c) **10**, d) **11**.

Table 1 UV-T_m (°C) of PNA-DNA/RNA hybrids[a]

Entry	PNA	DNA **13**	poly(rA)
1	**8**	34.8 (14)	58.0 (39)
2	**9**	50.7 (12)	43.1 (19)
3	**10**	50.9 (12)	41.8 (14)
5	**11**	53.3 (10)	45.6 (8)
6	**12**	> 80	35.1

[a] Buffer: 10 mM sodium phosphate, 100 mM NaCl, 0.1 mM EDTA. The values quoted are the average of three experiments and are accurate to ±0.5 °C. Values in parentheses indicate %hyperchromicities.

8. H_2N–T–T–T–T–T–T–T–T-β-ala-COOH (*aeg*-T_8)
9. H_2N–T–T–T–T–T–T–T-**t**-β-ala-COOH
10. H_2N–T–T–T-**t**-T–T–T-**t**-β-ala-COOH
11. H_2N-**t-t-t-t-t-t-t-t**-β-ala-COOH (*aepone*-$\mathbf{t}_8$)
12 H_2N-***t-t-t-t-t-t-t-t***-β-ala-COOH (*aep*-$\boldsymbol{t}_8$)
13 d(GCAAAAAAAACG) (DNA)

The *aep*-PNA oligomer **12** devoid of C5 carbonyl, bound DNA with a very high T_m, melting incompletely even at 80 °C. The strong binding of **12** with DNA is not entirely due to the electrostatic interactions as it showed a lower binding with poly(rA) as compared to PNA **8**. This suggests that the conformational preorganization plays an important role in determining the binding strengths. In this context, the binding pattern of the presently designed *aepone*-PNA is interesting; it has affinity to DNA more than that of PNA, but lower than that of *aep*-PNA and affinity to RNA less than that of PNA and more than that of *aep*-PNA. The tetrahedral nature of pyrrolidine nitrogen in *aep*-PNA is switched back to the planar amide in *aepone*-PNA, as in unmodified PNA with a consequent influence on the backbone conformation. Importantly, the side-chain *syn*/*anti* rotameric equilibrium present in unmodified PNA is not possible in *aepone*-PNA, although the ring nitrogen retains the amide character. Thus *aepone*-PNA (**III**) is an evolved structure by design, combining the features of both PNA (**I**) and *aep*-PNA (**II**). It also emerges from the present data that *aep*-PNA has a selectivity to bind DNA over RNA, and this aspect needs to be confirmed with studies using mixed RNA sequences. The CD spectral features of *aepone*-PNA:DNA/RNA hybrids were similar to that of PNA:DNA/RNA hybrids, suggesting no major differences in base stacking patterns.

In summary, we have reported the synthesis of (2*S*,4*S*)-*aepone*-PNA monomers (**4–7**) as new PNA analogues *via* selective C5 oxidation of *aep*-proline derivatised intermediate **2**. The *aepone*-poly T_8 oligomers (**9–11**) show reverse selectivity in DNA/RNA binding compared with the reported glycylaminomethyl pyrrolidinone[7] and are a useful addition to the growing library of proline/pyrrolidine based PNA analogues[5] to fine tune the binding selectivities. Further studies to delineate the sequence dependent effects of *aepone*-PNA and its stereomers are in progress.

N. K. S. thanks UGC, New Delhi for a research fellowship. We thank Dr M. Bhadbhade and Mr R. Gonnade for crystal data.

Notes and references

‡ *Crystal data* for **3**: Crystallised from CH_2Cl_2–MeOH, $C_{14}H_{24}N_2O_8S$, M = 380.41, crystal dimensions 0.61 × 0.09 × 0.05 mm, crystal system: monoclinic, space group $P2_1$, a = 12.739(5), b = 9.294(4), c = 15.994(6) Å, β = 103.419(8)°, V = 1841.9(13) Å^3, Z = 4, D_c = 1.372 g cm^{-3}, μ(Mo-Kα) = 0.219 mm^{-1}, T = 293(2) K, F(000) = 808, max. and min. transmission 0.9885 and 0.8780, 9094 reflections collected, 6134 unique [$I > 2\sigma(I)$], S = 1.109, R value 0.0652, $wR2$ = 0.1213 (all data R = 0.0816, $wR2$ = 0.1283). CCDC 213533. See http://www.rsc.org/suppdata/cc/b3/b307362a/ for crystallographic data in CIF or other electronic format.

1 (*a*) P. E. Nielsen and G. Haaima, *Chem. Soc. Rev.*, 1997, 73 and references cited therein (*b*) P. E. Nielsen and K. N. Ganesh, *Curr. Org. Chem.*, 2000, **4**, 931.
2 D. A. Braasch and D. R. Corey, *Biochemistry*, 2002, **41**, 4503.
3 S. C. Brown, S. A. Thomson, J. M. Veal and D. G. Davis, *Science*, 1994, **265**, 777.
4 L. Betts, J. A. Josey, J. M. Veal and S. R. Jordan, *Science*, 1995, **270**, 1838.
5 V. A. Kumar, *Eur. J. Org. Chem.*, 2002, 2021–2032.
6 (*a*) M. D'Costa, V. A. Kumar and K. N. Ganesh, *Org. Lett.*, 1999, **1**, 1513; (*b*) M. D'Costa, V. A. Kumar and K. N. Ganesh, *Org. Lett.*, 2001, **3**, 1281.
7 A. Puschl, T. Boesen, G. Zuccarello, O. Dahl, S. Pitsch and P. E. Nielsen, *J. Org. Chem.*, 2001, **66**, 707.
8 (*a*) X. Zhang, A. C. Schmitt and W. Jiang, *Tetrahedron Lett.*, 2001, **42**, 5335; (*b*) X.-L. Qiu and F.-L. Qing, *J. Org. Chem.*, 2003, **68**, 3614.
9 T. Vilaivan and G. Lowe, *J. Am. Chem. Soc.*, 2002, **124**, 9326.

Available online at www.sciencedirect.com
SCIENCE DIRECT®
Tetrahedron Letters 45 (2004) 1403–1406
Tetrahedron Letters

Regioselective oxidation of *N*-alkylpyrrolidines to pyrrolidin-5-ones by $RuCl_3/NaIO_4$ ☆

Nagendra K. Sharma and Krishna N. Ganesh*

Division of Organic Chemistry (Synthesis), National Chemical Laboratory, Pashan Road, Pune 411008, India

Received 12 October 2003; revised 22 November 2003; accepted 11 December 2003

Abstract—$RuCl_3/NaIO_4$ under EtOAc/H_2O biphasic conditions, selectively oxidizes the Nα-*endo*-methylene group of pyrrolidine derivatives, without affecting the *exo*-methylene group adjacent to the N-heteroatom.

Functionalized pyrrolidinone derivatives are key intermediates for the synthesis of many biologically active compounds.[1] Pyroglutamic acids are known to introduce unique structural constraints into peptide chains[2] and derivatives functionalized at C4 have important biological activities.[3,4] Most reported methods to obtain C4-functionalized pyroglutamates involve asymmetric 1,3-dipolar cycloadditions[5] or N-alkylation using lithium enolates derived from pyroglutamic esters.[6] In a recent report, C4-substituted *N*-Boc pyrrolidin-5-one derivatives were synthesized from 4-(*R*)-hydroxy-L-proline through oxidation of 4-substituted-*N*-Boc proline[7,8] using the versatile oxidizing agent RuO_4 generated in situ from $RuO_2/NaIO_4$ in a biphasic solvent system.[9] Our intention was to prepare C4-functionalized N-alkylated pyroglutamate derivatives **5** (Scheme 2) as intermediates for the synthesis of modified peptide nucleic acids (PNA). This can be achieved by N-alkylation of suitable pyroglutamates; however, the use of strong bases in N-alkylation is accompanied by a facile opening of the pyrrolidine ring. To overcome this, we attempted a hitherto unknown direct oxidation of various N-alkylated C4-substituted pyrrolidine derivatives **4** (Scheme 2) using the oxidizing agent $RuCl_3/NaIO_4$. Herein we report the interesting results observed on regioselective oxidation of the endocyclic Nα-methylene (C5), in preference to oxidation of other Nα-methylenes such as the exocyclic N-CH_2 or CH_2-NHBoc, which yield the desired monomers for *aepone*-PNA synthesis.[10]

To test the efficiency of $RuCl_3/NaIO_4$, *N*-Boc-4-acetoxy and 4-*O*-TBDMS proline methyl esters **1** were treated with the reagent in two different biphasic solvent systems $CCl_4/CH_3CN/H_2O$ (1:1:1.5) and EtOAc/H_2O (1:1) (Scheme 1). The reaction gave the corresponding C5-one products **2** in 70–75% yield. The structures of the compounds were confirmed from the spectral data. Thus $RuCl_3/NaIO_4$ is as efficient as $RuO_2/NaIO_4$ for oxidation of the present substrates.

Various *N*-(Boc-aminoethyl)-4-(*R*/*S*)-substituted proline methyl esters **4** (Scheme 2) prepared from 4-(*R*)-hydroxyproline derivative **3** directly or via a Mitsunobu reaction,[11] at C4 were then subjected to oxidation using $RuCl_3/NaIO_4$ in either $CCl_4/CH_3CN/H_2O$ (1:1:1.5) or EtOAc/H_2O (1:1) at room temperature and, as followed by TLC analysis, the starting materials disappeared with the appearance of a major product during a 30 min to 1 h period. Isolation of the product after aqueous

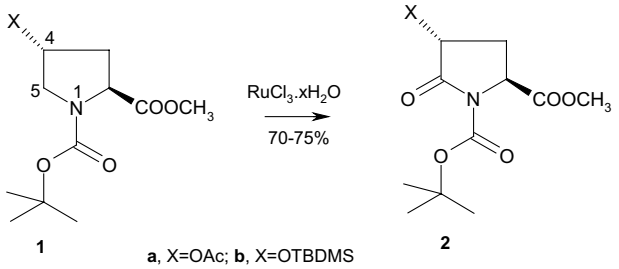

Scheme 1.

Keywords: $RuCl_3/NaIO_4$; Oxidation; *N*-Alkyl pyrrolidinones.
☆ Supplementary data associated with this article can be found, in the online version, at doi:10.1016/j.tetlet.2003.12.072
* Corresponding author. Tel./fax: +91-20-589-3153; e-mail: kng@ems.ncl.res.in

0040-4039/$ - see front matter © 2003 Elsevier Ltd. All rights reserved.
doi:10.1016/j.tetlet.2003.12.072

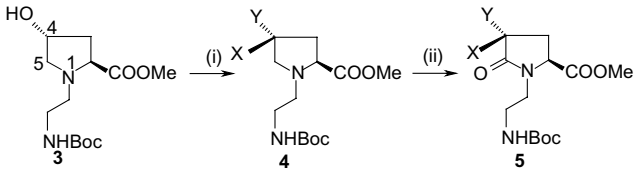

Scheme 2. Reagents and conditions: (i) Ac_2O, Py, rt, 5 h for **4b**, 80%; TBDMSCl, DMF, imidazole 6 h for **4c**, 70%; Ph_3P, DIAD, PhCOOH for **4d**, THF, 5 h, 80%; Ph_3P, DIAD, methyl tosylate for **4e**, THF, 8 h, 65%; Ph_3P, DIAD, 4-nitrobenzoic acid for **4f**, THF, 10 h, 70%; (ii) $NaIO_4/RuCl_3{\cdot}xH_2O$, AcOEt/$H_2O$, rt, 30 min to 1 h, yields 30–45%. Details of **a**–**f** are given in the footnote of Table 1.

work-up and characterization indicated the structures to be **5**, with oxidation occurring at C5. The isolated yields of the products were in the range 30–45% and the solvent system EtOAc/H_2O (1:1) gave the best yield (Table 1). There was no particular dependence of the yields on the stereochemistry of the C4-substituents, with *R* and *S* isomers behaving similarly. Among the different C4-substituents OMs, OBz, OAc, TBDMS, OTs and OPNB, the reaction gave the best yield with the 4-OMs derivative. A comparable C5-one product was obtained even with the proline substrate **4g** lacking any C4-substituents.[5] The reactions of *N*-alkyl substrates **4** were also found to be faster than those of *N*-Boc analogues **1**. All products were characterized by appropriate spectral data.

RuO_4 generated in situ from $RuCl_3/NaIO_4$ is well known to oxidize methylene groups α to N or O heteroatoms into carbonyl groups.[12] In the case of tertiary amines present as a part of polycyclic systems with *N*-benzyl substitution, the first oxidation occurs at the exocyclic benzylic methylene followed by the endocyclic methylene.[13] In the substrates used here (**4a**–**4g**), there are three Nα-methylene groups—endocyclic C5, exocyclic N-CH_2 and NHBoc-CH_2. Of the different possible oxidation products including N-oxide formation, it was found that the major products (**5a**–**5g**) obtained from a regioselective oxidation of the endocyclic CH_2 resulted at C5 of the pyrrolidine ring to give the lactam derivatives. The identity of the oxidation product was unambiguously confirmed by single crystal X-ray data for **5a**[10] and **5d** (Fig. 1). The present approach is therefore convenient as it gave intermediates for transformation into other C4-substituted pyrrolidin-5-ones, particularly the *aepone*-PNA analogues.[10]

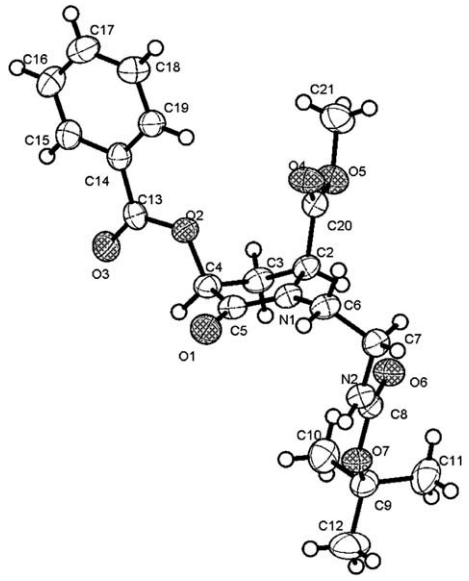

Figure 1. ORTEP diagram of the crystal structure[15] of **5d**.

Spectroscopic characterization. In the absence of any crystallographic data, it is necessary to unambiguously identify the site of oxidation and this was done using ^1H and ^{13}C NMR data (Table 2). In view of the similar chemical shifts of different Nα-methylene protons, the ^1H NMR was completely assigned using ^1H–^1H DQF COSY. While assignment of H5 is straightforward due to coupling with H4, assignment of βH′H″ were done via the connectivity with NH followed by assignment of αH′H″. The different carbons were assigned from the ^1H–^{13}C HETCOR experiment.

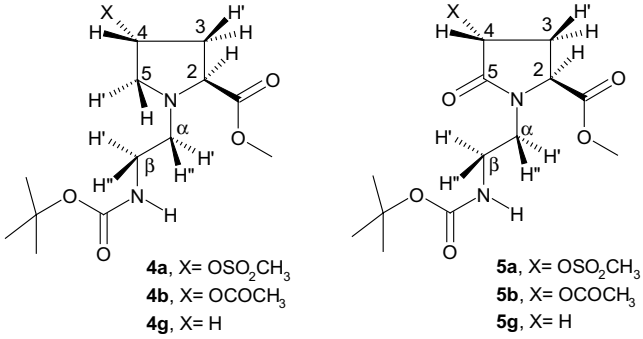

Table 1. Reaction yields for $RuCl_3/NaIO_4$ oxidation of substrates **4**[a]

Entry	Substrate	Product	EtOAc/H_2O (% yield)	$CH_3CN/CCl_4/H_2O$ (1:1:1.5)	Time (min)
1	**4a**	**5a**	45	45	60
2	**4b**	**5b**	38	30	30
3	**4c**	**5c**	39	32	45
4	**4d**	**5d**	45	36	30
5	**4e**	**5e**	35	30	75
6	**4f**	**5f**	40	37	45
7	**4g**	**5g**	35	41	45

[a] For **a**–**c**, X = H; **d**–**f**, Y = H; **a**, Y = OMs; **b**, Y = OAc; **c**, Y = OTBDMS; **d**, X = OBz; **e**, X = OTs; **f**, X = OPNB; **g**, X = H; Y = H. For a typical reaction procedure, see Ref. 14.

Table 2. Selected ^{1}H and ^{13}C chemical shifts (δ ppm)[a]

Compound	4a	5a	4b	5b	4g	5g
H4	5.2	5.3	5.3	5.4	1.8, 1.9	2.1
H5′	2.8	—	2.6	—	2.4	—
H5″	3.4	—	3.5	—	3.1	—
αH′	2.6	3.0	2.6	3.1	2.6	3.1
αH″	2.7	3.1	2.7	3.1	2.7	3.2
βH′	3.1	3.5	3.1	3.5	3.1	3.1
βH″	3.1	3.7	3.2	3.7	3.1	3.4
NH	5.1	4.8	5.2	4.9	5.2	4.9
C4	79.0	75.6	73.0	69.6	23.3	23.0
C5	58.4	169.8	58.6	171.2	53.4	172.4
Cα	53.5	42.0	53.2	42.9	54.8	42.1
Cβ	39.0	37.4	39.0	37.5	39.0	38.2

[a] All spectra were recorded at 500 MHz for ^{1}H and 125 MHz for ^{13}C in $CDCl_3$.

The oxidized products **5** exhibited characteristic similarities in their ^{1}H and ^{13}C NMR data compared to the reaction substrates **4** as seen from the selected data shown in Table 2. In the ^{13}C NMR, the signal around 68.0 ppm due to C5 in substrates **4** disappeared after oxidation giving rise to a new signal at around 170.0 ppm characteristic of C=O. The C4-signal was shifted upfield by 3.4 ppm in **5a**–**5b** upon oxidation, while that of Cα was shifted upfield by 10–12 ppm. In contrast, the chemical shift of Cβ was not affected much. In the ^{1}H NMR of **4**, the multiplets arising from the nonequivalent H5′5″ protons around 2.6 and 3.4 ppm disappeared in product **5**, while signals due to αH and βH were retained with a downfield shift of ca. 0.3 ppm perhaps due to anisotropic effects of the C5-carbonyl. Interestingly, no significant changes were seen for H4, except for a change of the multiplet to a triplet. The spectral data shown in Table 2 are for **5a** whose crystal structure is known[10] along with **5b** and **5g** whose crystal structures are not available. All three compounds showed similar patterns in NMR, strongly supporting the regiospecificity of the reaction.

In summary, we have observed that the endocyclic methylene group at C5 of pyrrolidine derivatives is more susceptible to oxidation with $RuCl_3/NaIO_4$ than the other two exocyclic methylene groups α to heteroatom N. These derivatives could be useful for synthesis of N-alkylated pyrrolidinones and unnatural amino acids.

Supplementary material

Experimental procedures, NMR (^{1}H–^{1}H COSY and ^{13}C–^{1}H HETCOR) and mass spectra of **5a**, **5d**, **5e** and **5g** are available in the supplementary material.

Acknowledgements

N.K.S. thanks the UGC–CSIR, New Delhi, for a fellowship. K.N.G. is an Honorary Professor of the Jawaharlal Nehru Centre for Advanced Scientific Research, Bangalore. Special thanks are due to Dr. M. M. Bhadbade and Mr. R. G. Gonnade for crystal data and Dr. P. Rajamohan for NMR spectra.

References and notes

1. (a) Najera, C.; Miguel, Y. *Tetrahedron: Asymmetry* **1999**, *10*, 2245–2303, and references cited therein; (b) Barco, A.; Benetti, S.; Pollini, G. P.; Baraldi, P. G.; Guarneri, M.; Gandolfi, C.; Ceserani, R.; Longiave, D. *J. Med. Chem.* **1981**, *24*, 625–628.
2. Bernardi, F.; Garavelli, M.; Scatizzi, M.; Tomasini, C.; Trigari, V.; Crisma, M.; Formaggio, F.; Peggion, C.; Toniolo, C. *Chem. Eur. J.* **2002**, *8*, 2516–2525.
3. Hon, Y.-S.; Chang, Y.-C.; Gong, M. I. *Heterocycles* **1990**, *31*, 191–195.
4. (a) Dinsmore, A.; Doyle, P. M.; Steger, M.; Young, D. W. *J. Chem. Soc., Perkin Trans. 1* **2002**, 613–621; (b) Bourry, A.; Pitard, F.; Rigo, B.; Sanz, G.; Camus, F.; Norberg, B.; Durant, F.; Couturier, D. *J. Heterocycl. Chem.* **2002**, *39*, 109–114; (c) Goswami, L. N.; Srivastava, S.; Panday, S. K.; Dikshit, D. K. *Tetrahedron Lett.* **2001**, *42*, 7891–7892; (d) Tomasini, C.; Villa, M. *Tetrahedron Lett.* **2001**, *42*, 5211–5214; (e) Bragg, R. A.; Clayden, J.; Bladon, M.; Ichihara, O. *Tetrahedron Lett.* **2001**, *42*, 3411–3414; (f) Acevedo, C. M.; Kogut, E. F.; Lipton, M. A. *Tetrahedron* **2001**, *57*, 6353–6359; (g) Konas, D. W.; Coward, J. K. *J. Org. Chem.* **2001**, *66*, 8831–8842.
5. Merino, P.; Revuelta, J.; Tejero, T.; Chiacchio, U.; Rescifina, A.; Piperno, A.; Romeo, G. *Tetrahedron: Asymmetry* **2002**, *13*, 167–172.
6. (a) Ezquerra, J.; Pedregal, C.; Rubio, A.; Yruretagoyena, B.; Escribano, A.; Ferrando, S. S. *Tetrahedron* **1993**, *49*, 8665–8678; (b) Ezquerra, J.; Pedregal, C.; Rubio, A. *J. Org. Chem.* **1994**, *59*, 4327–4331; (c) Dikshit, D. K.; Panday, S. K. *J. Org. Chem.* **1992**, *57*, 1920–1924.
7. Zhang, X.; Schmitt, A. C.; Jiang, W. *Tetrahedron Lett.* **2001**, *42*, 5335–5338.
8. Qiu, X. L.; Qing, F. L. *J. Org. Chem.* **2003**, *68*, 3614–3617.
9. Nakata, H. *Tetrahedron* **1963**, *19*, 1959–1963.
10. Sharma, N. K.; Ganesh, K. N. *Chem. Commun.* **2003**, *19*, 2484–2485.
11. (a) D'Costa, M.; Kumar, V. A.; Ganesh, K. N. *Org. Lett.* **1999**, *1*, 1513–1516; (b) Vidal, J. A. G.; Silverman, R. B. *Org. Lett.* **2001**, *3*, 2481–2484.
12. Sheehan, J. C.; Tulis, R. W. *J. Org. Chem.* **1974**, *39*, 2264–2267.
13. Bettoni, G.; Carbonara, G.; Franchini, C.; Tortorella, V. *Tetrahedron* **1981**, *37*, 4159–4164.
14. Typical general procedure: To a vigorously stirred solution of compound **4** (2.3 mmol) in AcOEt (20 mL), an aqueous solution (20 mL) of $NaIO_4$ (9.08 mmol) and $RuCl_3{\cdot}xH_2O$ (catalytic amount, 0.02 mmol) was added. After 30 min, the reaction was quenched by the addition of isopropyl alcohol and stirred for another 20 min and then the reaction mixture was concentrated in vacuo. The residue was taken into ethyl acetate (20 mL) and washed with water, the organic extract dried over Na_2SO_4 and concentrated to dryness. The crude product was purified by column chromatography to give **5** as a white foam. Yield 30–45%.
15. Single crystals of the compound **5d** were obtained from a mixture of CH_2Cl_2 and CH_3OH and a good quality crystal was selected using a Leica Polarizing Microscope. X-ray intensity data were collected on a Bruker SMART APEX

CCD diffractometer at room temperature. Crystal data: $C_{20}H_{26}N_2O_7$, $M = 406.43$, crystal dimensions $0.61 \times 0.59 \times 0.14$ mm, crystal system monoclinic, space group $P2_1$, $a = 9.2779(15)$, $b = 8.9289(14)$, $c = 13.239(2)$ Å, $\beta = 96.512(3)°$, $V = 1089.7(3)$ Å^3, $Z = 2$, $D_c = 1.239$ g cm^{-3}, μ(Mo-K$_\alpha$) $= 0.094$ mm^{-1}, $T = 293(2)$ K, $F(000) = 432$, 5493 reflections collected, 3634 unique [$I > 2\sigma(I)$], S = 1.053, R value 0.0393, $wR2 = 0.1116$ (all data $R = 0.0416$, $wR2 = 0.1135$). CCDC no 221794: *cis*-1-(*N*-Boc-amino-ethyl)-4(*S*)-*O*-benzoyl-5-one-2(*S*)-proline methyl **5d**. All the data were corrected for Lorentzian, polarization and absorption effects using Bruker's SAINT and SADABS programs. SHELX-97 (G. M. Sheldrick, SHELX-97 program for crystal structure solution and refinement, University of Gottingen, Germany, 1997) was used for structure solution and full matrix least squares refinement on F^2. Hydrogen atoms were included in the refinement as per the riding model.

PNA C–C$^+$ *i*-motif: superior stability of PNA TC_8 tetraplexes compared to DNA TC_8 tetraplexes at low pH†

Nagendra K. Sharma and Krishna N. Ganesh*

Received (in Cambridge, UK) 17th May 2005, Accepted 20th June 2005
First published as an Advance Article on the web 13th July 2005
DOI: 10.1039/b506870c

Study of self-assembly of PNA TC_8 monitored by UV thermal transition at 295 nm indicates formation of a C–C$^+$ tetraplex (*i*-motif) in acidic pH, with higher stability than the analogous dTC_8.

Telomeric DNA has guanine (G) and cytosine (C) rich DNA sequence regimes. G-rich DNA oligomers are well known to form G_4-tetrads *via* WC and HG hydrogen bond mediated cyclic structures.[1] The complementary C-rich sequences form tetramers *via* the semiprotonated C–C$^+$ base pairs held by three hydrogen bonds to form parallel double strands.[2] Two such double strands interdigitating through C–C$^+$ base pairs lead to a four-stranded *i*-motif structure (Fig. 1(a)). The opposed dipoles of exocyclic C2-carbonyl and N4-amino groups favour interaction of consecutive base pairs by alternate stacking of the amino and carbonyl groups.[3]

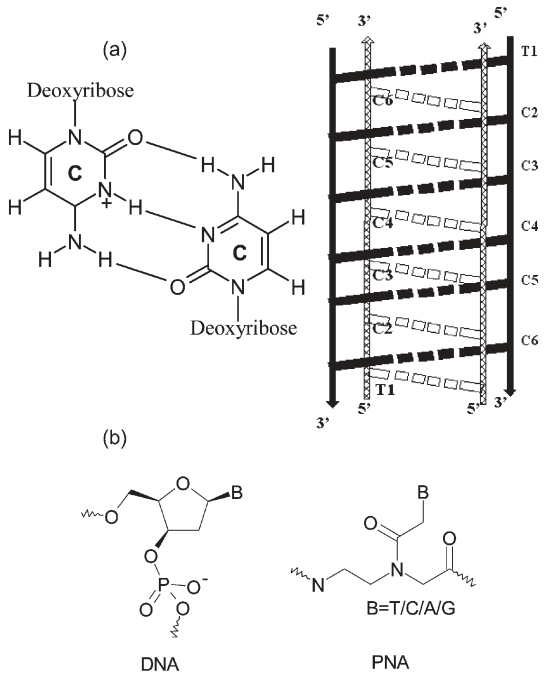

Fig. 1 (a) Schematic diagram of the *i*-motif in DNA. (b) Chemical structures of DNA and PNA.

NMR spectroscopy[3,4] has been extensively used to characterise the solution structure of the *i*-motif in oligonucleotides $d(TC_5)$, $d(T_2C_8T_2)$, dA_2C_4 and dC_4A_2. Rich and co-workers[5] have the solved the *i*-motif structure in several C-rich oligonucleotides by X-ray crystallography, while Raman spectroscopy[6] was used to characterise the *i*-motif in DNAs dTC_3 and dTC_8. In UV spectra, C and protonated C$^+$ show a large absorption difference at 295 nm.[7] Hence UV-thermal transitions monitored at 295 nm, show a reverse sigmoidal pattern, which is characteristic of C–C$^+$ tetraplex formation.[7] The thermodynamics and kinetics of *i*-motif formation in modified oligonucleotides has also been studied by UV at 295 nm.[8]

DNA and RNA have very versatile auto-association properties, the range of which extends from formation of duplexes to triplexes and tetraplexes.[9] RNA has been shown to lack the ability to form *i*-motif structures.[10] Considerable interest is now growing in the study of tetraplexing properties of mimics of natural oligonucleotides such as phosphorothioates,[8a] LNA[11] and PNA.[12] While G_4 tetraplex formation was successfully demonstrated recently in PNA,[13,14] it was reported that the PNA H–$C_4A_4C_4$–Lys–NH_2 did not form C–C$^+$ tetraplexes at pH 7.0.[14] Owing to favourable steric factors, it was shown that a PNA analogue gly-ala-PNA forms C–C$^+$ complexes in a C_4-tetramer, but not in a C_8-octamer.[15] Thus, *no* reports exist so far on successful C–C$^+$ tetraplexing properties of unmodified *aeg*-PNA. We herein present the first observation on C–C$^+$ tetraplexing properties of unmodified PNA sequences TC_4 and TC_8, analogous to the isosequential DNA, but with higher thermal stability in the acidic pH range.

To study the *i*-motif in PNAs, we synthesised PNAs TC_n corresponding to different lengths (Table 1). TC_2 (PNA **1**), TC_3 (PNA **2**), TC_4 (PNA **3**) and TC_8 (PNA **4**) were synthesized by standard procedures on solid phase method using Boc-chemistry (for details see ESI†). For comparative study, the DNA sequences $d(TC_8)$ and $d(TC_8)$ were synthesized on an *ABI*-DNA synthesizer. All sequences were purified by HPLC to homogeneity and characterized by mass spectrometry.

Table 1 Oligomers for the study of the *i-motif* of PNA

	Sequences of PNA/DNA
1	H_2N–T–C–C–βala–COOH
2	H_2N–T–C–C–C–βala–COOH
3	H_2N–T–C–C–C–C–βala–COOH
4	AcHN–Lys–T–C–C–C–C–C–C–C–C–$CONH_2$
5	d(TCCCC)
6	d(TCCCCCCCC)

Division of Organic Chemistry, National Chemical Laboratory, Pune, 411008, India. E-mail: kng@ems.ncl.res.in; Fax: 9120589153; Tel: 9120589153

† Electronic supplementary information (ESI) available: Experimental procedures, HPLC and mass spectra of PNAs **1–4**, pH dependent UV spectra and UV–T_m measurements. See http://dx.doi.org/10.1039/b506870c

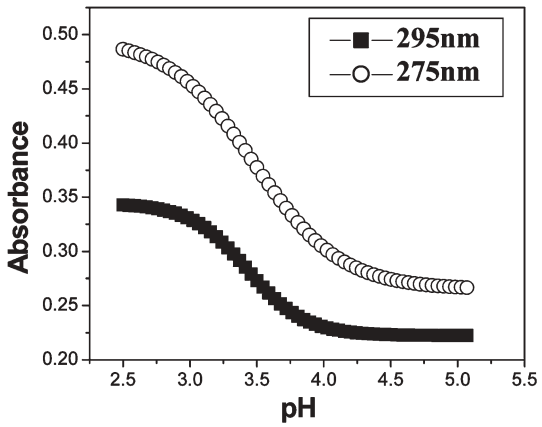

Fig. 2 UV absorbance at 275 and 295 nm of PNA **4** as a function of pH.

The UV spectra of PNA **4** were recorded at different pH values in the range 2.8–5.1 at 25 °C. The band at 275 nm found at acidic pH 2.8 slowly decreased in intensity and shifted to lower wavelength at 260 nm, with increase in pH (see ESI†). Earlier, it had been observed that the difference in absorbance spectra of protonated and non-protonated cytosine in DNA/RNA is maximum in the region 290–295 nm.[10] Fig. 2 shows a plot of UV absorbance at 275 and 295 nm in PNA **4** as a function of pH and the absorbance differences between protonated and non-protonated C in PNA are greater at 275 nm. From these data, the pK_a for N3 of C in PNA is obtained as 3.45, which is significantly lower than the pK_a of 4.8 reported for N3 of C in DNA/RNA.[10]

The formation of C–C$^+$ tetraplexes from PNAs **3**, **4** and d(TC)$_8$ **6** at pH 3.0, 4.5, 5.0, 6.5 and 7.0 were monitored at 295 nm, for a true comparison with the tetraplex formation in d(TC)$_n$ as per the reported procedures.[7,10] The temperature dependent UV-absorbance results obtained are shown in Fig. 3.

Table 2 pH Dependent T_m of TC$_8$ in PNA and DNA[a]

	T_m (°C) at varying pH					
pH	3.0	4.5	5.0	6.0	6.5	7.0
PNA **4**	67.4	55.0	46.0	nf	nf	nf
DNA **6**	58.4	58.7	55.7	50.4	52.0	nf

[a] nf indicates not formed.

The melting experiments were done in 100 mM sodium acetate buffer for the pH range 3.0–5.0 and 10 mM phosphate buffer for the pH range 6.0–7.0. The successful formation of tetraplexes in different sequences was indicated by observance of negative sigmoidal transitions (Fig. 3). Accurate T_m values were obtained from the first derivative curves and the T_m data for PNA **4** and DNA **6** are shown in Table 2. The PNAs **1** (TC$_2$) and **2** (TC$_3$) failed to show tetraplex formation at any of the pH conditions. PNAs **3** and **4** showed formation of strong C–C$^+$ tetraplexes at pH 3 and 4.5, respectively. Significantly, these PNA C–C$^+$ tetraplexes were much more stabilised (by 10–20 °C) compared to the analogous DNA C–C$^+$ tetraplexes. The stability of PNA C–C$^+$ tetraplexes were also dependent on pH. A comparison of pH dependent T_m of different PNA and DNA C-oligomers (Table 2) reveals that PNAs **3** and **4** form tetraplexes only in the acidic regime, up to pH 5.5. At pH 5.0, the PNA C-oligomers **3** and **4** form tetraplexes while at pH 6.0, no tetraplex formation is observed for these oligomers. This is seen from the reversal of melting curves for PNA oligomers at pH higher than 6 (Fig. 3). In comparison, the isosequential DNA C-oligomers **5** and **6** show tetraplex formation up to pH 6.5. Both PNA and DNA C-oligomers fail to form tetraplexes at pH 7.0. The pH effect on tetraplex stability is more drastic for PNA C-oligomers with $\partial T_m/\partial$pH being 10, while that for DNA is only about 3. The difference in the cut-off pH for tetraplex formation in PNA (5.5)

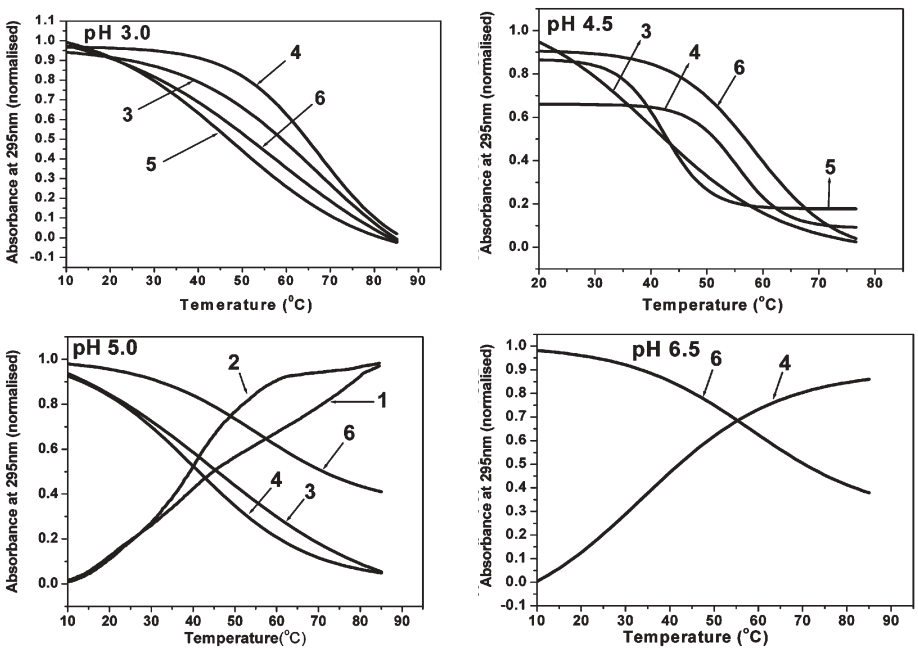

Fig. 3 UV–T_m of PNA and DNA at different pH values.

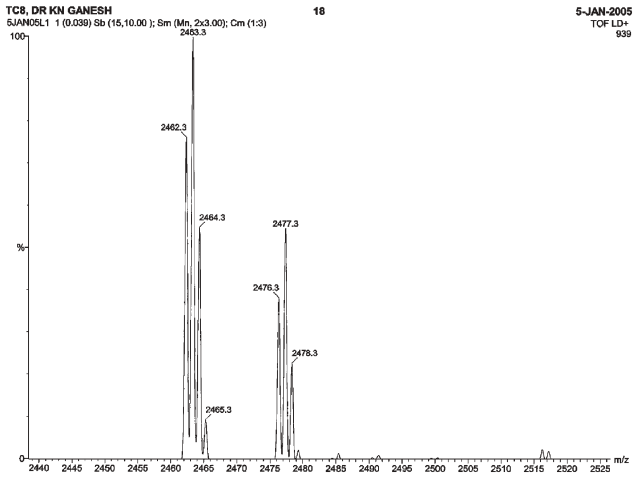

Fig. 4 MALDI-TOF mass spectrum of PNA **4**.

and DNA (6.5) is perhaps a reflection of the lower pK_a of N3-C in PNA (Fig. 2) compared to that in d(TC)$_n$.[10]

The identity of PNA C-oligomers, is supported by mass spectral data (Fig. 4). The MALDI-TOF mass spectra of PNA **4** TC_8 oligomer exhibited two sets of peaks separated by 14 mass units. While the cluster at *m*/*z* 2463 corresponds to the calculated ($C_{99}H_{137}N_{47}O_{30}$) mass of M^+, the cluster at *m*/*z* 2477 corresponds to $(4M + 2H^+ + 2Na^+)^{4+}$.

In summary, this communication demonstrates the hitherto unknown formation of the C–C$^+$ tetraplex in unmodified C-oligomeric PNAs. It is shown that in the acidic pH 3.0–5.0 range, PNA C–C$^+$ tetraplexes possess significantly higher stability compared to analogous DNA C–C$^+$ tetraplexes. Recently, it was reported[14] that the PNA $C_4A_4C_4$–Lys–NH_2 did not show formation of C–C$^+$ tetraplexes at pH 7.0. Up to now, no modified DNAs or their analogues have been known to form a more stable *i*-motif than natural DNA.[2,7] In light of this and the current interest in modified peptide nucleic acid analogues,[16] the first observation and characterization of C–C$^+$ tetraplexes reported here, holds promise to further examine the role of the PNA backbone structure in tetraplex formation.‡ The effect of modified backbones and sequences on influencing the self-assembling properties of nucleic acids has current importance in the development of practical applications for therapeutics and diagnostics.[11,12]

N. K. S. thanks UGC-CSIR, New Delhi for a research fellowship. K. N. G. is an Honorary Professor of the Jawaharlal Nehru Centre for Advanced Scientific Research, Bangalore.

Notes and references

‡ Though the present results do not give a direct evidence for interdigitation of base pairs, the UV characteristics similar to that of DNA C–C$^+$ tetraplexes, suggest that PNA TC_8 may have a similar arrangement. A similar structure is proposed for gly-ala PNA[15]

1 S. Neidle and G. N. Parkinson, *Curr. Opin. Struct. Biol.*, 2003, **13**, 275–283.
2 M. Guéron and J.-L. Leroy, *Curr. Opin. Struct. Biol.*, 2000, **10**, 326–331.
3 K. Gehring, J.-L. Leroy and M. Gueron, *Nature*, 1993, **363**, 561–564.
4 N. Esmaili and J.-L. Leroy, *Nucleic Acids Res.*, 2005, **33**, 213–224.
5 (*a*) L. Chen, L. Cai, X. Zhang and A. Rich, *Biochemistry*, 1994, **33**, 13540–13546; (*b*) C. H. Kang, I. Berger, C. Lockshin, R. Ratiff, R. Moyzis and A. Rich, *Proc. Natl. Acad. Sci. USA*, 1995, **92**, 3874–3878; (*c*) L. Cai, L. Chen, S. Raghavan, R. Ratliff, R. Moyzis and A. Rich, *Nucleic Acids Res.*, 1998, **26**, 4696–4705.
6 J. M. Benevides, C. H. Kang and G. J. Thomas, Jr., *Biochemistry*, 1996, **35**, 5747–5755.
7 A. T. Phan and J.- L. Mergny, *Nucleic Acids Res.*, 2002, **30**, 4618.
8 (*a*) J. L. Mergny and L. Lacroix, *Nucleic Acids Res.*, 1998, **26**, 4797–4803; (*b*) W. Lia, P. Wua, T. Ohmichia and N. Sugimotoa, *FEBS Lett.*, 2002, **526**, 77–81.
9 D. E. Gilbert and J. Feigon, *Curr. Opin. Struct. Biol.*, 1999, **9**, 305–314.
10 L. Lacroix, J. L. Mergny, J. L. Leroy and C. Helene, *Biochemistry*, 1996, **35**, 8715.
11 J. Wengel, *Chem. Commun.*, 2001, 1419–1924.
12 P. E. Nielsen and K. N. Ganesh, *Curr. Org. Chem.*, 2000, **4**, 1931–1941.
13 Y. Krishnan-Ghosh, E. Stephens and S. Balasubramanian, *J. Am. Chem. Soc.*, 2004, **125**, 11009–11016.
14 B. Datta, M. E. Bier, S. Roy and B. A. Armitage, *J. Am. Chem. Soc.*, 2005, **127**, 4199–4207.
15 U. Diederichsen, *Angew. Chem., Int. Ed.*, 1998, **37**, 2273–2276.
16 V. A. Kumar and K. N. Ganesh, *Acc. Chem. Res.*, 2005, **38**, 404–412.

